Vol. 65 February, 1961 No. 2

THE JOURNAL OF PHYSICAL CHEMISTRY

(Registered in U. S. Patent Office)

CONTENTS

NOTES

THE JOURNAL OF PHYSICAL CHEMISTRY

(Registered in U. S. Patent Office)

W. ALBERT NOYES, JR., EDITOR

ALLEN D. BLISS — ASSISTANT EDITORS — A. B. F. DUNCAN

EDITORIAL BOARD

A. O. ALLEN	D. H. EVERETT	J. E. RICCI	E. R. VAN ARTSDALEN
C. E. H. BAWN	S. C. LIND	R. E. RUNDLE	M. B. WALLENSTEIN
J. BIGELEISEN	F. A. LONG	W. H. STOCKMAYER	W. WEST
D. D. ELEY	K. J. MYSELS	A. R. UBBELOHDE	EDGAR F. WESTRUM, JR.

Published monthly by the American Chemical Society at 20th and Northampton Sts., Easton, Pa.

Second-class mail privileges authorized at Easton, Pa. This publication is authorized to be mailed at the special rates of postage prescribed by Section 131.122.

The *Journal of Physical Chemistry* is devoted to the publication of selected symposia in the broad field of physical chemistry and to other contributed papers.

Manuscripts originating in the British Isles, Europe and Africa should be sent to F. C. Tompkins, The Faraday Society, 6 Gray's Inn Square, London W. C. 1, England.

Manuscripts originating elsewhere should be sent to W. Albert Noyes, Jr., Department of Chemistry, University of Rochester, Rochester 20, N. Y.

Correspondence regarding accepted copy, proofs and reprints should be directed to Assistant Editor, Allen D. Bliss, Department of Chemistry, Simmons College, 300 The Fenway, Boston 15, Mass.

Business Office: Alden H. Emery, Executive Secretary, American Chemical Society, 1155 Sixteenth St., N. W., Washington 6, D. C.

Advertising Office: Reinhold Publishing Corporation, 430 Park Avenue, New York 22, N. Y.

Articles must be submitted in duplicate, typed and double spaced. They should have at the beginning a brief Abstract, in no case exceeding 300 words. Original drawings should accompany the manuscript. Lettering at the sides of graphs (black on white or blue) may be pencilled in and will be typeset. Figures and tables should be held to a minimum consistent with adequate presentation of information. Photographs will not be printed on glossy paper except by special arrangement. All footnotes and references to the literature should be numbered consecutively and placed in the manuscript at the proper places. Initials of authors referred to in citations should be given. Nomenclature should conform to that used in *Chemical Abstracts*, mathematical characters be marked for italic, Greek letters carefully made or annotated, and subscripts and superscripts clearly shown. Articles should be written as briefly as possible consistent with clarity and should avoid historical background unnecessary for specialists.

Notes describe fragmentary or incomplete studies but do not otherwise differ fundamentally from articles and are subjected to the same editorial appraisal as are articles. In their preparation particular attention should be paid to brevity and conciseness. Material included in Notes must be definitive and may not be republished subsequently.

Communications to the Editor are designed to afford prompt preliminary publication of observations or discoveries whose value to science is so great that immediate publication is imperative. The appearance of related work from other laboratories is in itself not considered sufficient justification for the publication of a Communication, which must in addition meet special requirements of timeliness and significance. Their total length may in no case exceed 1000 words or their equivalent. They differ from Articles and Notes in that their subject matter may be republished.

Remittances and orders for subscriptions and for single copies, notices of changes of address and new professional connections, and claims for missing numbers should be sent to the American Chemical Society, 1155 Sixteenth St., N. W., Washington 6, D. C. Changes of address for the *Journal of Physical Chemistry* must be received on or before the 30th of the preceding month.

Claims for missing numbers will not be allowed (1) if received more than sixty days from date of issue (because of delivery hazards, no claims can be honored from subscribers in Central Europe, Asia, or Pacific Islands other than Hawaii), (2) if loss was due to failure of notice of change of address to be received before the date specified in the preceding paragraph, or (3) if the reason for the claim is "missing from files."

Subscription rates (1961): members of American Chemical Society, $12.00 for 1 year; to non-members, $24.00 for 1 year. Postage to countries in the Pan-American Union $0.80; Canada, $0.40; all other countries, $1.20. Single copies, current volume, $2.50; foreign postage, $0.15; Canadian postage $0.10; Pan-American Union, $0.10. Back volumes (Vol. 56–64) $30.00 per volume; foreign postage, per volume $1.20, Canadian, $0.40; Pan-American Union, $0.80. Single copies: back issues, $3.00; for current year, $2.50; postage, single copies: foreign, $0.15; Canadian, $0.10; Pan-American Union, $0.10.

The American Chemical Society and the Editors of the *Journal of Physical Chemistry* assume no responsibility for the statements and opinions advanced by contributors to THIS JOURNAL.

The American Chemical Society also publishes *Journal of the American Chemical Society, Chemical Abstracts, Industrial and Engineering Chemistry,* International Edition of *Industrial and Engineering Chemistry, Chemical and Engineering News, Analytical Chemistry, Journal of Agricultural and Food Chemistry, Journal of Organic Chemistry, Journal of Chemical and Engineering Data, Chemical Reviews, Chemical Titles* and *Journal of Chemical Documentation.* Rates on request

25.LIBR.2504

THE JOURNAL OF
PHYSICAL CHEMISTRY

(Registered in U. S. Patent Office) (© Copyright, 1961, by the American Chemical Society)

VOLUME 65 FEBRUARY 24, 1961 NUMBER 2

THE PRIMARY SOLVATION OF THE PROTON IN THE SOLVENT EXTRACTION OF STRONG ACIDS[1]

BY D. G. TUCK AND

Department of Chemistry, University of Nottingham, Nottingham, England

RICHARD M. DIAMOND

Lawrence Radiation Laboratory, University of California, Berkeley, California

Received October 16, 1959

Evidence is reported for the presence of the trihydrated hydronium ion, $H_3O(H_2O)_3^+$, in extracts from aqueous solutions into basic organic solvents of the strong acids $HClO_4$, HBr and HCl. In the organic phase, this species is further solvated by (hydrogen-bonded) coördination to the basic organic molecules, and so the degree of extraction depends partly upon the coördinating ability of the solvent molecules. With the somewhat weaker acids, HNO_3 and CCl_3CO_2H, the proton coördinates preferentially in the low-dielectric-constant organic phase with the more basic (charged) anion than with water. The molecule formed is solvated by water and (or) organic solvent molecules, depending upon the solvent basicity. For solvents such as the ethers and ketones, the resulting species is $HNO_3 \cdot H_2O$(sol), and with the more basic tributyl phosphate, an anhydrous species, HNO_3·TBP(sol), results.

Introduction

Since the early years of the ionic theory, attempts have been made to measure the number of water molecules associated with an ion in aqueous solution. Various properties of solvated ions have been studied with this end in view, but the measurements do not give concordant results because they are concerned with different aspects of solvation. Much of the progress made in recent years can be ascribed to the differentiation now made between primary, *i.e.*, first-shell or coördinate, and secondary solution.[2-5] A review by Bockris discusses the various experimental techniques that have been employed,[6] and Stokes and Robinson give a more recent survey.[2b]

A great deal of attention has been directed to the hydration of the hydrogen ion. Because of its very small size, the bare proton has a much higher charge density than any other ion. This charge density makes the existence of the free proton in any solvating medium very improbable and, in particular, explains the strong binding of the proton to a water molecule to form the hydronium ion, H_3O^+. There is already evidence from X-ray,[7] nuclear magnetic resonance,[8] infrared[9] and Raman[10] studies for the existence of this species in the solid state, and it must certainly exist as a more highly hydrated species in aqueous solution. An accumulation of indirect evidence now available suggests that in not too concentrated aqueous solution the H_3O^+ group behaves as an ion that can be further solvated by a "primary" shell of three water molecules to give as a predominant species the symmetrical structure shown in Fig. 1a. Because of the unique charge distribution of the H_3O^+ ion, with approximately $^1/_3$ of the positive charge concentrated on each proton, the hydrogen bonding of the three water molecules is much stronger than that between water molecules in bulk water. This results in much stronger coördinate solvation

(1) This work was supported in part by the U. S. Atomic Energy Commission. The early part was performed at the Laboratory of Nuclear Studies and the Chemistry Department, Cornell University, Ithaca, New York.

(2) (a) N. Bjerrum, *Z. anorg. Chem.*, **109**, 275 (1920); (b) R. A. Robinson and R. H. Stokes, "Electrolyte Solutions," Butterworths Scientific Publications, London, 1955.

(3) J. D. Bernall and R. H. Fowler, *J. Chem. Phys.*, **1**, 515 (1933).

(4) D. D. Eley and M. G. Evans, *Trans. Faraday Soc.*, **34**, 1093 (1938).

(5) J. P. Hunt and H. Taube, *J. Chem. Phys.*, **18**, 757 (1950).

(6) J. O'M. Bockris, *Quart. Revs.*, **3**, 173 (1949).

(7) F. S. Lee and G. B. Carpenter, THIS JOURNAL, **63**, 279 (1959).

(8) (a) R. E. Richards and J. A. S. Smith, *Trans. Faraday Soc.*, **47**, 1261 (1951); (b) Y. Kakiuchi, H. Shono, H. Komatsu and K. Kigoshi, *J. Chem. Phys.*, **19**, 1069 (1951).

(9) D. E. Bethell and N. Sheppard, *ibid.*, **21**, 1421 (1953).

(10) R. C. Taylor and G. L. Vidale, *J. Am. Chem. Soc.*, **78**, 5999 (1956).

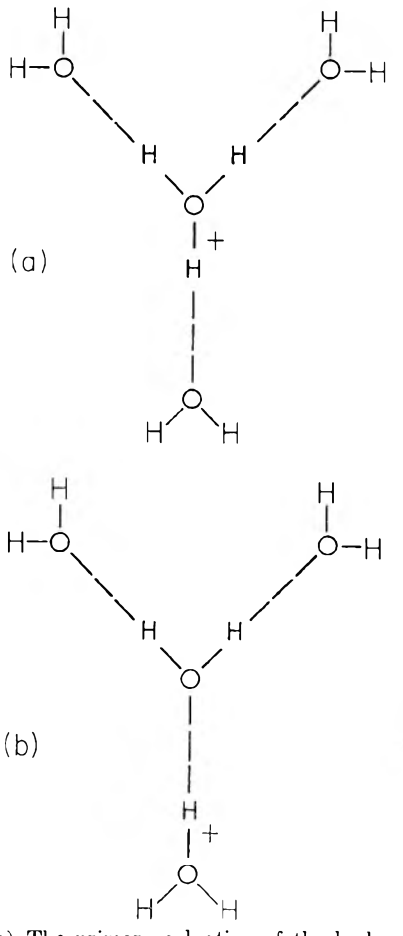

Fig. 1.—(a) The primary solvation of the hydronium ion; (b) charge transfer in $H_9O_4^+$.

than exists for other univalent positive ions of the same size, *e.g.*, K^+. With the latter ion, the charge can be regarded as being spread over the whole surface of the ion, and hydrogen bonding to the hydrating molecules is not possible.[11,12] Just as the limiting tetrahedral ice structure is partially broken down in water by the kinetic energy of the water molecules, so to a lesser extent (because of the stronger bonding) the trihydrated hydronium ion must also be in equilibrium with lower hydrate species. But a number of studies suggests the predominant existence of a trihydrated hydronium ion in solution. For example, Robinson and Stokes have calculated hydration numbers from activity coefficient data,[13] and a more refined treatment by Glueckauf[14] leads to a value of 3.9 for the primary hydration number of the proton. Isopiestic measurements of the water vapor pressure over ion-exchange resins give a similar result.[15,16] The interpretation by Bascombe and Bell[17] of the acidity function of mineral acids in terms of ion–solvent interaction indicates the coordination of four water molecules to each proton, as do similar calculations by Wyatt.[18] One must note particularly the work of Wicke, Eigen and Ackermann on the specific heats of aqueous solutions, and their interpretation of a variety of data in terms of the $H_3O(H_2O)_3^+$ ion shown in Fig. 1a.[19]

The study of the extraction of strong acids into organic solvents provides yet another and possibly more direct measurement of the primary hydration of the proton, especially if the anion is large enough to be unhydrated so that all the water carried into the organic phase is associated with the proton. The amount of water extracting into ethers with complex metal acids has been found to be four to five molecules per molecule of acid,[20–23] and electrolysis of ether extracts of $HFeCl_4$ showed that this water is associated with the H^+ ion only.[24] Spectral studies have also indicated that the extracted water is not coördinated to the tetrachloroferrate anion.[25] The present work arose out of studies of the extraction of the mineral acids into basic organic solvents and provides a further test of the degree of primary solvation of the proton. A preliminary account of these results already has been published.[26]

Experimental

Reagents.—Analytical grade perchloric, nitric, hydrochloric, hydrobromic and trichloroacetic acids were suitably diluted some time before use. Commercial tri-*n*-butyl phosphate was purified by a procedure described previously,[27] and dibutyl Cellosolve (ethylene glycol dibutyl ether) was shaken with 5% sodium carbonate solution, dried with anhydrous magnesium sulfate and stored over chromatographic alumina to prevent peroxide formation.[28]

Volume Change Measurements.—The procedure followed closely that described earlier by one of us.[29] Five ml. of aqueous acid of known strength and an equal volume of solvent were pipetted carefully into a calibrated, stoppered measuring cylinder and gently shaken until equilibrium was reached. The increase in volume of the organic phase caused by the extraction of a measured quantity of acid gives, by a simple calculation, the composition of the extracted species. Acid concentrations were determined by titration with standard alkali; aliquots of the organic phase were dissolved in neutralized water–acetone mixture before titration.

The main supposition implicit in this method is that the total volume of the two-phase system shall remain constant throughout an experiment, and this has been confirmed in all our experiments unless otherwise noted in the text. One needs to be sure that the solvent is effectively as insoluble in

(11) R. M. Diamond, THIS JOURNAL, **63**, 659 (1959).

(12) R. M. Diamond and D. G. Tuck, "Progress in Inorg. Chem.," Vol. II, Interscience Publishers, Inc., New York, 1960.

(13) R. H. Stokes and R. A. Robinson, *J. Am. Chem. Soc.*, **70**, 1870 (1948).

(14) E. Glueckauf, *Trans. Faraday Soc.*, **51**, 1235 (1955).

(15) E. Glueckauf and G. P. Kitt, *Proc. Roy. Soc. (London)*, **A228**, 322 (1955).

(16) M. H. Waxman, Thesis, Brooklyn Polytechnic Institute, 1952; quoted in ref. 14.

(17) K. N. Bascombe and R. P. Bell, *Disc. Faraday Soc.*, **24**, 158 (1957).

(18) P. A. H. Wyatt, *ibid.*, **24**, 162 (1957).

(19) E. Wicke, M. Eigen and T. Ackermann, *Z. physik. Chem. (N.F.)*, **1**, 340 (1954).

(20) S. Kato and R. Ishii, *Sci. Papers Inst. Phys. Chem. Research, Tokyo*, **36**, 82 (1939).

(21) J. Axelrod and E. H. Swift, *J. Am. Chem. Soc.*, **62**, 33 (1940).

(22) A. H. Laurene, D. E. Campbell, S. E. Wiberley and H. M. Clark, THIS JOURNAL, **60**, 901 (1956).

(23) R. J. Myers, D. E. Metzler and E. H. Swift, *J. Am. Chem. Soc.*, **72**, 3767 (1950).

(24) (a) J. E. Savolainen, unpublished results, quoted in ref. 22. (b) E. J. Goon, Ph.D. dissertation, Rensselaer Polytechnic Institute, New York, 1953.

(25) (a) A. H. Laurene, Ph.D. dissertation, Rensselaer Polytechnic Institute, New York, 1952. (b) H. E. Friedman, *J. Am. Chem. Soc.*, **74**, 5 (1952).

(26) D. G. Tuck and R. M. Diamond, *Proc. Chem. Soc.*, 236 (1958).

(27) D. G. Tuck, *J. Chem. Soc.*, 2783 (1958).

(28) W. Dasler and C. D. Bauer, *Ind. Eng. Chem., Anal. Ed.*, **18**, 52 (1946).

(29) D. G. Tuck, *J. Chem. Soc.* 3202 (1957).

mineral-acid solution as it is in water; this has been checked by a technique described elsewhere.[30]

Volumetric Determination of Water.—For the system perchloric acid–dibutyl Cellosolve, the water content of the organic phase was determined volumetrically in a number of cases by the Karl Fischer method,[31] using a deadstop end-point technique. One modification to the normal procedure was found to be necessary. In methyl alcohol (the titration medium), perchloric acid is strongly dissociated, so that the conductivity of the solution is high throughout the titration, making the end-point difficult to determine. This problem was overcome by the addition of 5 ml. of A. R. grade pyridine, which complexes the perchloric acid by salt formation and thus reduces the initial conductivity. Under these conditions the end-point can be found accurately in the usual way.

Results

Perchloric Acid–Dibutyl Cellosolve.—Dibutyl Cellosolve (DBS) was chosen as a typical solvent of medium basicity and of relatively low solubility in and for water. Perchloric acid is extracted quite well by this solvent, as shown by the results in Table I.

TABLE I

EXTRACTION OF $HClO_4$ INTO DIBUTYL CELLOSOLVE

$HClO_4$ concn., aq. phase (M)	4.15	4.92	5.90	6.49	7.48	8.37
$HClO_4$ concn., org. phase (M)	0.15	1.10	1.91	2.33	3.02	3.79
D_{HClO_4}	0.036	0.222	0.324	0.359	0.404	0.441

The experimental results for the increase in volume of the organic phase as a result of the extraction of perchloric acid are shown in Fig. 2. Up to approximately 2.2 M $HClO_4$ in the organic phase, there is a linear dependence of Δv on total acid extracted, with a slope over this portion of the curve of 8.4 mmoles $HClO_4$ extracted per 1 ml. increase in volume. This corresponds to the extraction of an aqueous solution of 845 g. of $HClO_4$ per liter, or 56.5% $HClO_4$, so that the H_2O:$HClO_4$ ratio is 4.3. Similar experiments with perchloric acid and diisopropyl ketone give a precisely analogous straight line of slope 8.65 mmoles/ml., corresponding to a H_2O:$HClO_4$ ratio of 4.1. For this system the experiments were not carried to the point at which deviations from linearity in the plot became noticeable (see Fig. 2).

The Karl Fischer determinations of water extracted into dibutyl Cellosolve from perchloric acid solutions give the results in Table II, after correction for the solubility of water in the pure solvent.

TABLE II

VOLUMETRIC DETERMINATION OF WATER CONTENT OF EXTRACT SOLUTIONS OF $HClO_4$ IN DBS

$HClO_4$ concn., org. phase (M)	$HClO_4$ concn., equil. aq. phase (M) (interpolated)	H_2O concn., org. phase (M)	Ratio $H_2O/HClO_4$
0.53	4.2	2.33	4.4
1.00	4.8	4.30	4.3
1.58	5.5	6.31	4.0
2.10	6.2	7.52	3.6

The Extraction of Strong Acids into Tri-*n*-butyl Phosphate.—The extraction of the hydrogen halides into solvents such as ethers and ketones is too poor to permit one to carry out volume-change experiments on such systems. With strongly basic solvents such as the phosphate esters, however, there is significant extraction of these acids, as well as of $HClO_4$. The solvent volume changes found in the extraction of HCl, HBr and $HClO_4$ into tri-*n*-butyl phosphate (TBP) are shown in Fig. 3. The results obtained from these experiments are summarized in Table III.

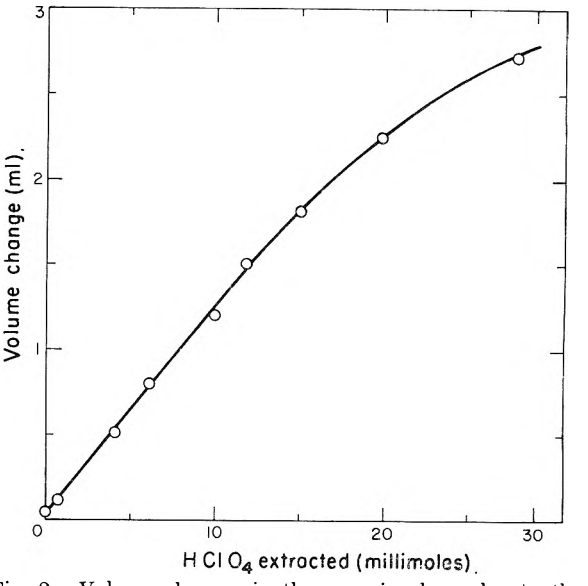

Fig. 2.—Volume changes in the organic phase due to the extraction of perchloric acid into dibutyl Cellosolve.

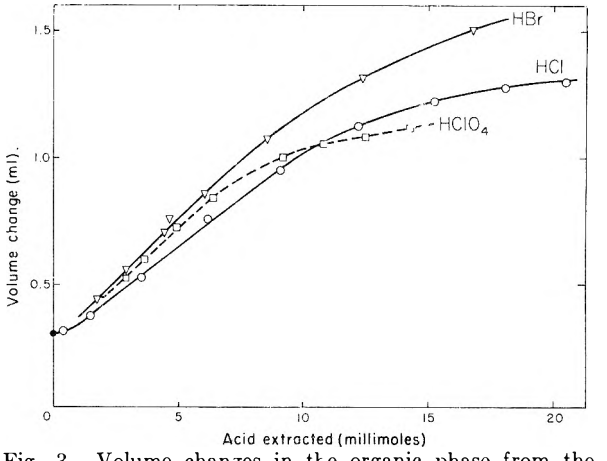

Fig. 3.—Volume changes in the organic phase from the extraction of HCl, HBr and $HClO_4$ into tributyl phosphate.

TABLE III

VOLUME CHANGES IN THE EXTRACTION OF HCl, $HClO_4$ AND HBr IN TBP

Acid	Slope of straight line portion (mmoles/ml.)	H_2O:acid ratio	Approximate beginning of deviations from linearity: Mmoles extracted	Organic phase molarity	Aq. phase molarity
HCl	13.1	3.1 ± 0.2	9.5	1.58	5.4
$HClO_4$	10.6	2.9 ± 0.3	6.3	1.09	2.73
HBr	11.1	3.5 ± 0.2	8.5	1.41	4.5

At high $HClO_4$ concentrations there is an increase in the total volume of the two-phase system after equilibration amounting to about 2% of the original

(30) D. G. Tuck, *Anal. Chim. Acta*, **20**, 159 (1959).

(31) J. Mitchell and D. M. Smith, "Aquametry," Interscience Publishers, Inc., New York, 1948.

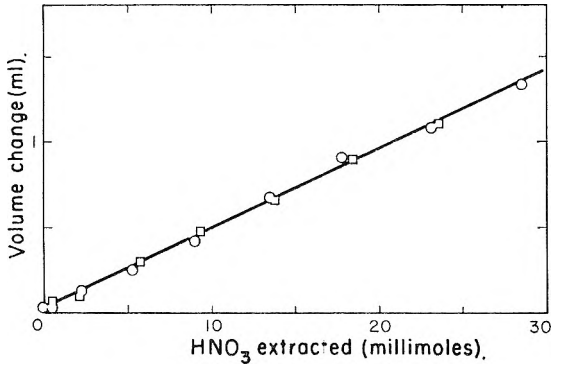

Fig. 4.—Volume changes in the organic phase from the extraction of HNO_3 into dibutyl Cellosolve.

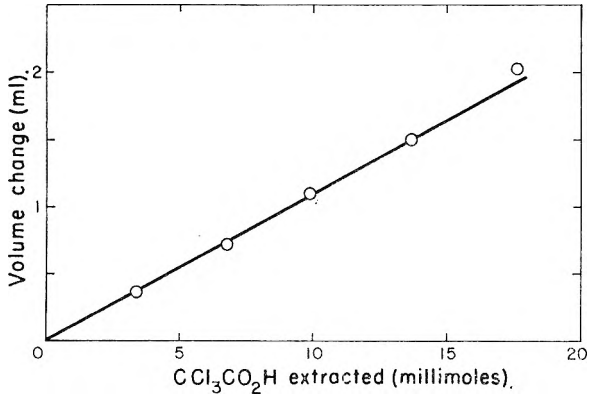

Fig. 5.—Volume changes in the organic phase from the extraction of CCl_3COOH into dibutyl Cellosolve.

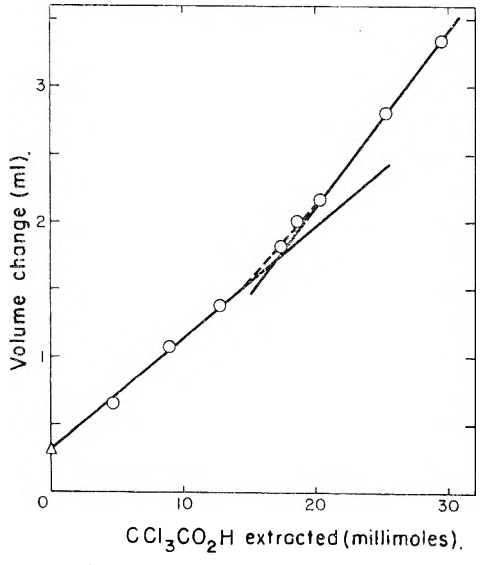

Fig. 6.—Volume changes in the organic phase from the extraction of CCl_3COOH into tributyl phosphate; ΔV at zero acid is taken from previous work.[27]

volume. Under these conditions it is not possible to interpret the volume change results. No reason for this effect is immediately forthcoming.

Nitric and Trichloroacetic Acids.—Nitric acid extracts well into dibutyl Cellosolve, as it does into other similar solvents (see ref. 12). The extraction data are given in Table IV.

The solvent volume-change results from this system (Fig. 4) show a linear dependence of ΔV on total HNO_3 extracted over the whole range studied. The slope of 20.6 mmoles per ml. of solvent volume increase is to be compared with a value of 18.1 mmoles/ml. found for the higher analog dibutyl carbitol[29]; this latter value corresponds to extraction of the species $HNO_3 \cdot H_2O$.

TABLE IV

EXTRACTION OF HNO_3 INTO DIBUTYL CELLOSOLVE

HNO_3 concn., aq. phase (M)	HNO_3 concn., org. phase (M)	D_{HNO_3}
1.60	0.09	0.055
3.02	0.41	.136
4.30	1.09	.253
5.34	1.74	.326
6.58	2.51	.382
7.65	3.22	.421
8.82	3.96	.450
9.92	4.68	.472
11.04	5.33	.483
12.23	6.14	.502

It is possible that the present (larger) value arises as a result of the two processes

$$R_2O(org) + HNO_3(aq) \longrightarrow R_2O \cdot H_2O \cdot HNO_3(org)$$

and

$$R_2O(org) + HNO_3(aq) \longrightarrow R_2O \cdot HNO_3(org)$$

The solvent volume-change arising from the latter process yields a value of 42.5 mmoles/ml., so that the first process must predominate. Trichloroacetic acid extracts even better into dibutyl Cellosolve than HNO_3, as shown by the results given in Table V. The plots of ΔV *vs.* trichloroacetic acid extracted into DBS and into TBP are given in Figs. 5 and 6.

TABLE V

EXTRACTION OF CCl_3COOH INTO DIBUTYL CELLOSOLVE

CCl_3COOH concn., aq. phase (M)	0.10	0.20	0.28	0.37	0.52
CCl_3COOH concn., org. phase (M)	0.63	1.18	1.33	2.10	2.51
CCl_3COOH	6.3	5.9	5.8	5.6	4.8

Discussion

The result of the volume-change method for the ratio of H_2O to $HClO_4$ for extraction into DBS to yield organic phase solutions varying from 0.15 to 2.0 M in acid is 4.3 ± 0.2. Similarly, for extraction into DIPK, the ratio is 4.1 ± 0.2. These results are the same within their experimental errors. The results given in Table II for the direct Karl Fischer determinations of water extracted into DBS from $HClO_4$ solutions are very similar, but show a slightly larger decreasing trend by 2M $HClO_4$ in the acid phase.[32]

(32) The reason for this difference is mainly that the Karl Fischer titrations determine the water content at a particular acid concentration, while the volume-change method, as applied, gives an average value over the range of concentration where the plot is linear. The mere fact that the initial portion of the plot is linear means that the individual deviations from the average value (tangents to the curve at the appropriate point) are small, and the volume-change results should fall in between the extreme values of the Karl Fischer method over the same concentration range. Also, in correcting the experimental titration results for the normal water solubility in the solvent, it has been assumed that this correction is constant over the range of acid concentrations studied and is equal to that of pure water. Actually, however,

The ratio H_2O:$HClO_4$ found by the volume-change method for extraction into TBP to yield solutions up to 1.2 M in acid is 2.9 ± 0.3. This is actually in good agreement with the values 4.3 and 4.1 obtained with DBS and DIPK, as the following discussion indicates. It has been shown that the solubility of H_2O in TBP at ~25° is equivalent to one mole of water per mole of TBP.[27,33,34] There is evidence that this solubility is the result of the formation of a weakly hydrogen-bonded complex TBP·H_2O.[33] The solvent volume change at any given acidity represents the effect of extracting both H_2O and $HX(H_2O)_h$ in a proportion that depends on their respective activities in the aqueous phase and on the formation constants of the species TBP·H_2O and TBP·$HX(H_2O)_h$. As the aqueous acid concentration is increased, the over-all effect in the organic phase is the increasing replacement of H_2O by $HX(H_2O)_h$. The result can be written as

$$TBP{\cdot}H_2O(org) + H^+(H_2O)_h(aq) + X^-(aq) \longrightarrow H_2O(aq) + TBP{\cdot}H^+(H_2O)_hX^-(org)$$

Therefore the volume change associated with this process corresponds to a slope for the linear part of the curves in Fig. 3 equivalent to $h - 1$. Thus the experimental results again indicate that the acid is essentially tetrahydrated in the solvent with a ratio of H_2O:$HClO_4$ of 3.9 ± 0.3.

Similarly the studies on HCl and HBr extraction into TBP yield (corrected) values of H_2O:acid of 4.1 ± 0.2 and 4.5 ± 0.2, respectively, for organic phase acid concentrations up to 1.5 M. At higher acid concentrations the plots of ΔV *vs.* acid concentration yield lower values; the start of the non-linear portions of the plots for TBP come progressively at a lower aqueous and organic phase acid concentration for HCl, HBr and $HClO_4$.[35] It should be noted that the work of Baldwin, Higgins and Soldano[36] on the extraction of HCl, HBr and HI into TBP also can be similarly corrected for the water already present in the TBP and leads to a hydration value for the acids of approximately four. They find, by Karl Fischer titration of the organic phase, water to acid ratios of 4.1 and 4.6 for HCl and HBr, respectively, in comparison with the values 4.1 and 4.5 found by the volume-change method. This again demonstrates the agreement of the two independent types of water measurement.

These results indicate that when the strong acids $HClO_4$, HBr and HCl extract into the typical basic organic solvents DBS, DIPK and TBP, 4.0 to 4.5 moles of water accompany one mole of acid. Similar results have been obtained for the extraction of the strong acid $HFeCl_4$ into diisopropyl ether, and in this case it has been shown that the water is associated with the H^+ ion and not with the anion.[24,25] This is certainly reasonable, as univalent anions larger than Cl^- and without specific hydrophilic groups are not usually considered to have much primary (coördinate) hydration.[37] Also, the fact that acids as diverse as HCl, HBr, $HClO_4$ and $HFeCl_4$ all show extraction into several basic solvents with the same H_2O:acid ratio strongly suggests a common hydrated species, and the only ion common to these acids is the H_3O^+ ion.[38] In dilute aqueous solution the hydronium ion must be highly hydrated. But even in moderately concentrated aqueous solution, there may be insufficient water to provide secondary solvation for all the hydronium, and other ions present. It is this inability of the aqueous acid phase to provide secondary solvation for the hydronium ion that forces the latter across into the basic solvent to solvate there. Ample evidence is available that coördination with the solvent is involved, since these strong acids show no significant extraction into non-basic organic solvents and show lowered extraction if the coördinating group in the solvent molecule is blocked.[11,12,39]

The results of the present work, then, suggest that the strong acids extract from aqueous solutions of less than about 7 M acid into organic solvents of moderate basicity (ethers, ketones, esters, but not the amines) with the hydronium ion retaining a primary hydration shell of three water molecules. The solvent molecules coördinate to this shell of water, and are not involved in direct coördination to the proton, that is, in displacement of the primary hydration shell.[40] But as the aqueous acid concentration is increased, there will be a decreasing amount of water available to solvate

the organic phase water solubility decreases with an increase in the aqueous phase acidity, both because more solvent molecules are involved in secondary solvation of the proton and because the aqueous phase water activity decreases. For these reasons we have increasingly over-corrected for water solubility in the organic phase.

(33) K. Alcock, S. S. Grimley, T. V. Healey, J. Kennedy and H. A. C. McKay, *Trans. Faraday Soc.*, **52**, 39 (1956).

(34) R. L. Moore, "The Mechanism of Extraction of Uranium by Tributyl Phosphate," U.S.A.E.C. Report AECD-3196 (n.d.).

(35) Such a curvature in the volume-change plots could arise because of an increase in solubility of the organic solvent in the aqueous phase with increasing acid concentration. But it was shown that the solubility of DBS in 8M $HClO_4$ is still quite small and essentially the same as in pure water.

(36) W. H. Baldwin, C. E. Higgins and B. A. Soldano, THIS JOURNAL, **63**, 118 (1959).

(37) For example, one may compare the limiting equivalent conductivities of Br^-, I^- and ClO_4^-, which decrease in that order, with the limiting equivalent conductivities of the alkali or alkaline earth ions, or even of F^- and Cl^-. The values of the cations and small anions increase with increasing atomic weight, that is, in the inverse order of their ionic radii. This indicates that they are hydrated, and that the degree of hydration, and hence effective hydrated radius, decreases in the order $Li^+ > \ldots > Cs^+$, $Be^{++} > \ldots > Ba^{++}$, $F^- > Cl^-$. But for the larger anions, Br^-, I^- and ClO_4^-, and the larger cations, NMe_4^+, NEt_4^+, NPr_4^+, NBu_4^+, the effective aqueous radii go in the same order as the ionic radii, suggesting that these large ions do not drag a shell of water molecules with them, that is, they do not have a primary hydration shell. Or, one may consider the activity coefficient calculations of Glueckauf (ref. 14) which indicate little primary hydration of the larger anions.

(38) Such an assumption of a trihydrated hydronium ion, $H_3O^+(H_2O)_3$, as the extracting cation in strong acid extraction systems involving moderately basic solvents such as ethers, ketones, esters, etc., but not amines, has been used to explain why the acids extract an order of magnitude or more better than the corresponding lithium salts, which have comparable activities in aqueous solution (ref. 11).

(39) I. Nelidow and R. M. Diamond, THIS JOURNAL, **59**, 710 (1955).

(40) Organic molecules do not, in general, replace the primary-shell water molecules because the H_2O molecule is small and possesses a relatively high dipole moment. The ion–water interactions are stronger than the corresponding ion–solvent interactions, and the water molecules can pack around the hydronium ion in a primary solvation shell much more easily than can the bulkier organic molecules. These considerations do not apply, however, to the very basic amine extractant systems, nor to any but the very strong acids. (See the discussion later in this paper for HNO_3 and CCl_3CO_2H.)

each ion, and even the primary hydration shell of the extracted hydronium ion will be disturbed. The plots of solvent volume change *vs.* acid extracted all show an initially linear region where the hydronium ion extracts with three water molecules. Eventually, with increasing acid concentration, they all begin to curve toward lower hydration numbers as the scarcity of "free" water interferes with even the primary hydration shell. For example, the deviation from linearity shown in Fig. 2 for $HClO_4$ into DBS becomes significant above ~15 mmoles $HClO_4$ extracted per 5 ml. of solvent; the equilibrium aqueous phase is approximately 6.3 *M* in perchloric acid, arising from an initial aqueous solution of 7 *M* $HClO_4$. Such an initial solution corresponds to 50% $HClO_4$, or a water to acid ratio of about 5.5. The fact that with TBP extractions the acid concentration at which the volume change plots begin to deviate from a straight line is progressively lower in the order HCl, HBr, $HClO_4$, indicates the correctness of this explanation, as this is the order of decreasing water activity for aqueous solutions of these acids at a fixed concentration.

A very different situation exists in the extraction of acids weaker than HCl, HBr, $HClO_4$, $HFeCl_4$ (and other metal complex acids) into organic solvents of moderate basicity. Acids as weak as nitric and trichloroacetic do not show the extraction of a tri-hydrated hydronium ion. It seems that the hydration number of nitric acid extracted into organic solvents is seldom above unity, and in only one case does a value near four appear. (For pentaether,[41] the hydration number found by direct titration is 6.6, but the solubility of water in this solvent is high, and the possibility of inter- and intra-molecular interactions of the basic groups rather confuses the issue.) For example, in extraction into TBP, the acid is present as HNO_3·TBP,[27,33] and the process can be represented as

$$TBP{\cdot}H_2O + HNO_3(aq) \rightleftharpoons TBP{\cdot}HNO_3 + H_2O(aq)$$

Thus, in extract solutions of HNO_3 in a basic solvent, the proton is essentially different in its chemical bonding and environment from its state in similar extract solutions of strong acids such as $HClO_4$, HI, HBr and HCl. We believe that the reason lies in the comparatively low ionization constant of nitric acid ($K_i = 23$)[42] relative to those of HCl, HBr and $HClO_4$, for which values of $pK = -7$ and higher have been estimated.[43,44] That is, the small primary hydration numbers of HNO_3 in organic solvents ($0 \rightarrow 1$) are due to the ability of NO_3^- to compete successfully with H_2O for the proton in a low dielectric constant medium. This results in the extraction of the HNO_3 molecule rather than of the hydrated hydronium ion. Whether the hydration number is 0 or 1 or something between, indicating a mixture, depends upon the basic strength of the solvent molecule, that is, upon its ability to compete with H_2O for hydrogen-bonded coördination to the HNO_3 molecule. If the solvent is not too basic, a water molecule will hydrogen-bond to the HNO_3 molecule and will in turn be similarly bonded to by an organic molecule. This behavior has been observed with extraction into ethers, polyethers and ketones.[29,45,46] However, a more basic solvent such as TBP can compete favorably with water for coördination to the HNO_3 molecule, and so leads to the anhydrous species, TBP·HNO_3.

Evidence that the low hydration numbers of HNO_3 are really due to its weakness as an acid and consequent extraction as a molecule, that is, evidence for the importance of acid strength in determining the extent of proton hydration in the solvent phase, is clearly shown by the extractive behavior of trichloroacetic acid ($pK = 0.7$).[47] The results of the volume-change measurements (Fig. 5 and 6) are remarkably similar to those for nitric acid. For DBS the slope of 9.95 mmoles/ml. corresponds to a solution in which the CCl_3·COOH:H_2O ratio is 1:0.9. For TBP, the analogy with HNO_3 is even closer. Up to a TBP:CCl_3-COOH ratio of approximately one (18.1 mmoles CCl_3COOH extracted), the reciprocal of the volume change is 12.5 mmoles/ml. Taking the extrapolated density of CCl_3CO_2H as 1.62,[48] one finds that the volume change for the process

$$TBP{\cdot}H_2O(org) + CCl_3COOH(aq) \longrightarrow TBP{\cdot}CCl_3COOH(org) + H_2O(aq)$$

is (101–18) ml./mole, corresponding to 12.1 mmoles/ml. The excellence of the agreement with the experimental result is perhaps rather fortuitous, because the density of liquid CCl_3COOH is an extrapolated value. However, there seems to be little doubt possible about the conclusion. Above a CCl_3CO_2H:TBP ratio of 1.0 in the organic phase, the phosphoryl group is completely saturated, and the volume-change slope changes to approximately 7.9 mmoles/ml. Here again then, there is rather less than one molecule of H_2O per acid in the region in which extraction is due to the basic oxygen of the P–O–C bond; nitric acid behaves in precisely the same way.[27] It seems, then, that as far as hydration in the organic phase of solvent extraction systems, the weaker strong acids, nitric and trichloroacetic, have very similar behavior and this is also borne out by results on the extraction of these acids into diisopropyl ketone.[46]

Acknowledgment.—We wish to thank R. P. Bell, F.R.S., for helpful discussions of this problem.

(41) E. Glueckauf and H. A. C. McKay, unpublished results, quoted by H. A. C. McKay, *J. Inorg. Nuclear Chem.*, **4**, 375 (1957).

(42) O. Redlich and G. C. Hood, *Disc. Faraday Soc.*, **24**, 87 (1957).

(43) J. C. McCoubrey, *Trans. Faraday Soc.*, **51**, 743 (1955).

(44) R. P. Bell, "Acids and Bases," Methuen and Co., London, 1952, p. 59.

(45) J. Sutton, "Distribution of Nitric Acid Between Water and Ether," U. K. A. E. A. Report AERE C/R 438, November, 1949.

(46) D. G. Tuck, unpublished work.

(47) R. P. Bell, ref. 44, p. 63.

(48) J. Kendall and E. Brackeley, *J. Am. Chem. Soc.*, **43**, 1826 (1921).

NITRIC ACID EQUILIBRIA IN WATER–SULFURIC ACID[1]

BY N. C. DENO, HENRY J. PETERSON AND EDWARD SACHER

College of Chemistry and Physics, the Pennsylvania State University, University Park, Penna.

Received February 11, 1960

Absorption spectra (220–400 mμ) were measured for solutions of HNO_3 in 0–99% aqueous sulfuric acid. On the basis of nitration kinetics, it had been concluded previously that concentrations of NO_3^- and HNO_3 were equal in 44% H_2SO_4 and that the shift of equilibrium from HNO_3 to NO_2^+ was complete in 90% H_2SO_4. The spectroscopic data confirm both conclusions. A species more strongly absorbing than HNO_3 or NO_2^+ appears in 85–99% H_2SO_4. It is tentatively identified as the mixed anhydride, O_2NOSO_3H. It is calculated that its relative concentration maximizes at 90% H_2SO_4 where it accounts for about 9% of the added HNO_3.

On the basis of rates of nitration of aromatic compounds, it was concluded that the maximum in the rates of nitration at 90% H_2SO_4 was due to the dominant conversion of HNO_3 to the active nitrating agent, NO_2^+.[2] It had also been concluded on the basis of the rates of nitration of anisole that concentrations of HNO_3 and NO_3^- were equal in about 46% H_2SO_4.[3] The simple expedient of checking these conclusions by spectroscopic measurements has not been reported and this work was designed to accomplish this objective.

In water, HNO_3 is completely dissociated to NO_3^-. Of a number of studies reported on the absorption of NO_3^- in water,[4–8] the values of λ_{max} 303 mμ and ϵ 6.9 reported by v. Halban[4] were exactly reproduced in this work and are close to the most recently reported values.[5] A report of a λ_{max} at 385 mμ for NO_3^-[8] was not substantiated.

The behavior of HNO_3 in 100% H_2SO_4 has been studied extensively by Raman spectra and cryoscopic measurements. The Raman spectra of HNO_3 in several strong acids has a single characteristic emission at 1400 cm.$^{-1}$.[9,10] The simplicity of the spectrum as well as other arguments have identified this species as NO_2^+.[9] This identification is entirely in accord with the freezing point depression of HNO_3 in 100% H_2SO_4, which was four times that of a non-electrolyte.[11] The presence of the nitrogen as a cation as shown by transference experiments further supports NO_2^+.[12]

Experimental

The absorption spectra of solutions of nitric acid in sulfuric acid were examined from 220–400 mμ and from 0–99% H_2SO_4. A Beckman DU spectrophotometer was used. The absorption cells were thermostated at 25 ± 1°. The absorption from 320–400 mμ was negligible. A brief summary of the data from 220–310 mμ is recorded in Table I. The detailed data are presented elsewhere.[13]

The solutions were 10^{-2} to 10^{-4} molar in HNO_3 and were prepared by adding through a micropipet 0.01 ml. of a freshly prepared one molar stock solution of HNO_3 to the appropriate % H_2SO_4. Urea was added to the HNO_3 stock solution in an amount which ultimately resulted in a 10^{-4} to 10^{-6} molar solution of urea in the solutions spectroscopically studied. With this expedient, the reported extinction coefficients for NO_3^- in water[4,5] were reproduced easily, and the data were more reproducible than when purification of the HNO_3 alone was used. The urea presumably destroys lower oxidation states of nitrogen which continuously form by the light-catalyzed decomposition of HNO_3. The stock solution of HNO_3 must be freshly prepared. In the region 80–99% H_2SO_4, identical results were obtained with or without added urea. Presumably the strong acid converts HNO_2 and/or NO_2 to NO plus HNO_3.

TABLE I

EXTINCTION COEFFICIENTS (ϵ) FOR SOLUTIONS OF HNO_3 IN 0–99% AQUEOUS SULFURIC ACID

% H_2SO_4	Extinction coefficients at mμ listed[a] 220	250	270	290	310
0.0[b]	33 × 10²	9.37	1.85	5.34	6.06
20.0[c]	33 × 10²	8.75	3.08	6.45	5.8f
41.6	20 × 10²	6.77	5.90	6.80	3.8
69.0[d]	2.7 × 10²	7.30	8.76	4.45	0.7
80.3	2.7 × 10²	8.05	8.90	4.10	.7
83.9	2.7 × 10²	9.53	9.35	4.16	.7
89.4	7.1 × 10²	54	16.7	4.02	.7
94.5	3.1 × 10²	33	7.12	1.8	.4
99.4	1.3 × 10²	12	1.9	0.4	.2

[a] The extinction coefficient is the ratio of optical density to concentration in moles/l. In computing the numbers in this Table, the total stoichiometric concentration of HNO_3 was used without regard for the form in which the HNO_3 existed. [b] λ_{max} 303 mμ, ϵ 6.90. [c] λ_{max} 301 mμ, ϵ 7.19. [d] λ_{max} 265 mμ, ϵ 9.05.

For picrate ion in water solution, $10^{-3}\epsilon$ = 8.38, 11.6, 13.2, and 13.1 at 320, 340, 350 and 360 mμ, respectively. These values were assumed to obtain in 0–30% H_2SO_4.

For picric acid, $10^{-3}\epsilon$ exhibited a small increase from 40–70% H_2SO_4 at 320–360 mμ. The increase was linear with % H_2SO_4 and ϵ had the following respective values at 40.5 and 69.0 % H_2SO_4: 3.38 and 3.59 (320 mμ), 4.00 and 4.17 (340 mμ), 3.53 and 3.71 (350 mμ), and 2.51 and 2.67 (360 mμ). The values of ϵ for picric acid at 5–30% H_2SO_4 were obtained by extrapolation of these linear plots.

The absorption spectra of solutions of picric acid in 0–69% H_2SO_4 were measured and are published in detail elsewhere.[14] Values of the ratio of concentrations of picrate anion to picric acid were the same whether calculated from data at 340, 350 or 360 mμ and nearly the same for data at 320 mμ. These ratios are recorded in Table II.

(1) This research was supported in part by a grant from the Petroleum Research Fund administered by the American Chemical Society. Grateful acknowledgment is hereby made to the donors of this fund. This research also was supported in part by a grant from the National Science Foundation. Grateful acknowledgment is hereby made of this support.

(2) F. H. Westheimer and M. Kharasch, *J. Am. Chem. Soc.*, **68**, 1871 (1946); R. J. Gillespie and D. G. Norton, *J. Chem. Soc.*, 971 (1953). The latter reference summarizes much of the earlier literature.

(3) N. Deno and R. Stein, *J. Am. Chem. Soc.*, **78**, 578 (1956).

(4) H. v. Halban, *Trans. Faraday Soc.*, **21**, 620 (1925).

(5) R. N. Jones and G. D. Thorn, *Can. J. Research*, **27B**, 580 (1949).

(6) R. A. Morton and R. W. Riding, *Proc. Roy. Soc. (London)*, **A113**, 717 (1926).

(7) E. Siegler-Soru, *Arch. phys. Biol.*, **5**, 237 (1927).

(8) K. Schaefer, *Z. anorg. Chem.*, **97**, 285 (1916); K. Schaefer and H. Niggerman, *ibid.*, **98**, 77 (1916).

(9) C. K. Ingold, D. J. Millen and H. G. Poole, *J. Chem. Soc.*, 2576 (1950); D. J. Millen, *ibid.*, 2589 (1950).

(10) J. Chédin, *Ann. chim.*, **8**, 302 (1937).

(11) R. J. Gillespie, J. Graham, E. D. Hughes, C. K. Ingold and E. R. Peeling, *J. Chem. Soc.*, 2504 (1950).

(12) G. M. Bennett, J. C. Brand and G. Williams, *ibid.*, 869 (1946).

(13) Ph. D. Thesis of Edward Sacher, Pennsylvania State Univ., 1960.

(14) Ph. D. Thesis of Henry J. Peterson, Pennsylvania State Univ., 1960.

Table II

Values of $c_{NO_3^-}/c_{HNO_3}$ and c_{P^-}/c_{HP} (HP = Picric Acid) as a Function of % H_2SO_4

% H_2SO_4	Derivative in respect to % H_2SO_4 of: (Log $c_{NO_3^-}/c_{HNO_3}$)[a]	(Log $c_{NO_3^-}/c_{HNO_3}$)	$-H_0$[b]
30	0.76	0.068	0.068
34	.49	.054	.073
38	.31	.046	.080
42	.12	.052	.088
46	− .09	.056	.098
50	− .32	.057	.106
54	− .54	.060	.110
58	− .81	.072	.110
	(Log c_{P^-}/c_{HP})[c]	(Log c_{P^-}/c_{HP})	
4.8	−0.01	0.03	
9.8	− .356	.070	0.078
18.2	− .95	.070	.069
29.6	−1.8	.070	.068

[a] Calculated from data presented in ref. 13, an abbreviated portion of which appears in Table I. [b] H_0 is the acidity function introduced by L. P. Hammett, which has been found to correlate the shift of B/BH$^+$ equilibria with acidity for a wide variety of bases (F. A. Long and M. A. Paul, *Chem. Revs.*, 57, 1, 935 (1957)). The last two columns demonstrate that H_0 shows a fair correlation with the NO_3^-/HNO_3 and P^-/HP equilibria. [c] Data on the P^-/HP equilibria have been reported briefly (D. J. Shepherd quoted in a footnote by C. D. Coryell and R. C. Fix, *J. Inorg. Nuclear Chem.*, 1, 119 (1955)).

Discussion

The Equilibrium between HNO_3 and NO_3^-.—The spectrum of NO_3^- in water is characterized by a weak maximum at 303 mμ and a strong maximum below 220 mμ. A convincing argument has been advanced identifying the 303 band as an n → π* transition.[15] The strong maximum below 220 is probably a π → π* transition as judged by ε 3280 at 220 mμ.

From 0–20% H_2SO_4 there are small changes in the spectra which can be related to the changing properties of the solvent system. In particular, the n → π* transition at 303 shifts to 301 mμ. This is related to the increased hydrogen bonding ability of the solvent. From 0–20% H_2SO_4, H_3O^+ is increasingly introduced and by virtue of its greater acidity it will more strongly hydrogen bond to the non-bonding electrons on the oxygen of the NO_3^- ion. The effect of this bonding to the n-electrons is to produce a blue shift of the n → π* band.[15,16]

From 20–60% H_2SO_4 a large spectral shift occurs due to the shift of equilibrium from NO_3^- to HNO_3. The identification of the spectrum in 60% H_2SO_4 as due to molecular HNO_3 rests most simply on the fact that the spectrum is nearly identical with that reported for 100% HNO_3[5], which is known to consist principally of molecular HNO_3. The spectrum of HNO_3 exhibits a maximum at 265 mμ. This is the n → π* band which has undergone a pronounced blue shift as the n-electrons in NO_3^- become more localized when the proton is added to form HNO_3.[15,16]

Values for the relative concentrations of NO_3^- and HNO_3 (Table II) were calculated from 20–60% H_2SO_4 and were independent of the wave length used in their computation. This is compelling evidence that the equilibrium was between only two species.

From 65–82% H_2SO_4 the spectra between 220 and 400 mμ are virtually invariant. In this region the added HNO_3 exists as molecular HNO_3.

The Equilibrium between HNO_3, NO_2^+ and O_2NOSO_3H.—From 85% H_2SO_4, where HNO_3 predominates, to 99% H_2SO_4 where NO_2^+ predominates, marked changes occur in the absorption spectra. Throughout the 220–270 mμ region, the extinction coefficients increase sharply from 85–90% H_2SO_4 and subsequently fall to low values at 99% H_2SO_4. It is evident that a spectroscopic species other than HNO_3 or NO_2^+ has appeared. This species (I) is tentatively identified as the mixed anhydride, O_2NOSO_3H, on the basis of the following arguments.

From 89–100% H_2SO_4, the Raman spectra data of Chédin[10] are used to calculate the % HNO_3 converted to NO_2^+, and these estimates are summarized in Table III. After correcting for the water produced by the reaction

$$HNO_3 + H_2SO_4 = H_2O + NO_2^+ + HSO_4^- \quad (1)$$

it is evident that over 90% of the added HNO_3 is converted to NO_2^+ from 92–100% H_2SO_4.

From 92–98% H_2SO_4, the absorption between 220–310 mμ must be due to the new spectroscopic species (I) plus a small contribution from NO_2^+. In particular, HNO_3 cannot significantly contribute. One example will suffice to show this. At 94.5% H_2SO_4, all but a few per cent. of the added HNO_3 is converted to NO_2^+ (Table III). Even if 5% remained as HNO_3, it would contribute only 0.5 to the total extinction coefficient at 250 mμ whereas the observed value was 33 (Table I).

Table III

% HNO_3 Converted to NO_2^+ as Calculated from the Intensity of the 1400 Cm.$^{-1}$ Raman Line[a]

% H_2SO_4 added[b]	% HNO_3 converted to NO_2^+	Effective[c] % H_2SO_4
100	100	98.5
97.5	100	96.0
95	100	93.6
92.5	70	91.3
90	60	89.2

[a] Calculated from the data in ref. 10. [b] The solutions were made up by adding 95 parts of the sulfuric acid listed in this column to 5 parts of 100% HNO_3. [c] The conversion of HNO_3 to NO_2^+ produces H_2O which effectively reduces the concentration of H_2SO_4 below that listed in the first column.

Since the concentration of NO_2^+ is sensibly constant from 92–99% H_2SO_4 (Table III), a constant amount can be subtracted from the observed ε values to give the component of ε due solely to the new spectroscopic species (I). These values appear as ϵ_I in Table IV.

It is attractive at this point to attempt to identify I by relating ϵ_I to expectations based on equilibrium constant expressions. To make such an attempt, we are forced to use concentrations in place of activities from lack of data on activity coefficients. The validity of such an assumption is difficult to justify because of the lack of a satis-

(15) H. McConnell, *J. Chem. Phys.*, 20, 700 (1952).

(16) M. Kasha, *Disc. Faraday Soc.*, 9, 14 (1950); G. J. Brealey and M. Kasha, *J. Am. Chem. Soc.*, 77, 4462 (1955).

TABLE IV

DEMONSTRATION OF THE CONSTANCY OF $\epsilon_I/c_{HSO_4^-}$ AND THE LACK OF CONSTANCY OF ϵ_I/a_{H_2O}

% H_2SO_4	ϵ^a 260 mμ	ϵ_I [b]	$\epsilon_I/c_{HSO_4^-}$ [c]	ϵ_I/a_{H_2O} [d]
99	6.3	3.2	3.2	
98	9.4	6.3	3.1	12.0
96	14.0	11.0	2.8	4.5
94	21.8	18.7	3.1	3.1
92	30.0	26.9	3.2	2.2

[a] Extinction coefficients calculated from the total stoichiometric concentration of HNO_3, which was 0.0649 molar. [b] Corrected for the absorption due to NO_2^+ by subtracting the ϵ at 100% H_2SO_4, estimated by extrapolation, from ϵ in the previous column. [c] Other values of $\epsilon_I/c_{HSO_4^-}$ were 1.5 at 270 mμ, 0.68 at 280 mμ, and 0.34 at 290 mμ. No trends were shown at any of these three wave lengths. The values of $c_{HSO_4^-}$ were estimated by the method of J. Brand (ref. 19) which treats the reaction of $H_2O + H_2SO_4$ to form $H_3O^+ + HSO_4^-$ as complete. From 90–100% H_2SO_4, values estimated on this basis and values of $c_{HSO_4^-}$ estimated from Raman spectra (T. F. Young, L. F. Maranville and H. M. Smith in W. J. Hamer, "The Structure of Electrolytic Solutions," John Wiley and Sons, New York, N. Y., 1959, p. 51) are in agreement. [d] Values of a_{H_2O} were taken from ref. 18.

factory theory relating activity coefficients to structure and media. However, such an assumption has been used successfully to calculate the solubility of $BaSO_4$ in 94–100% H_2SO_4,[17] the activity of H_2O in 81–98% H_2SO_4,[18] values of the H_0 acidity function from 83–99% H_2SO_4,[18,19] and the approximate freezing point depressions of a wide variety of inorganic and organic compounds in 97–100% H_2SO_4.[17,20,21]

The most glaring example of concentrations not paralleling activities in concentrated sulfuric acids is the large increase in solubility of nitrobenzene from 85–95% H_2SO_4, but this behavior is conceivably the result of compound formation.[22] Further examples of concentrations not paralleling activities have been observed in precise freezing point experiments in 98–100% H_2SO_4.[21] The deviations reported do not appear large enough to affect the following discussion.

The argument will thus proceed using concentrations in place of activities. Equation 2

$$NO_2^+ + HSO_4^- = O_2NOSO_3H(I) \qquad (2)$$

expresses the equilibrium between NO_2^+ and the mixed anhydride (I). From 92–99% H_2SO_4, ϵ_I would be proportional to the concentration of I. Since $c_{NO_2^+}$ is constant from 92–99% acid, equation 2 would require that $c_I/c_{HSO_4^-}$ be constant and thus $\epsilon_I/c_{HSO_4^-}$ also be constant. This was found to be true (Table IV).

Two other observations support the identification of I as O_2NOSO_3H. First, according to eq. 2, addition of HSO_4^- should increase c_I and this increase should be proportional to the added HSO_4^- in 92–99% H_2SO_4, where $c_{NO_2^+}$ is sensibly constant. This effect was qualitatively observed in 98% H_2SO_4 where $c_{HSO_4^-}$ is 2.0 molar.[23] Addition of 120 and 240 g. of $NaHSO_4$ per liter increases $c_{HSO_4^-}$ to about 3 and 4 molar. These additions should increase c_I and thus ϵ_I by factors of 1.5 and 2. Experimentally, it was observed that from 260–290 mμ, ϵ_I increased by factors of 1.9 and 3.4. This is regarded as satisfactory agreement in view of the large amounts of $NaHSO_4$ added.

Secondly, from a qualitative comparison of the absorption spectra of HNO_3, I and N_2O_5 (Table I), it is evident that I must have larger extinction coefficients than HNO_3. Although it is not evident why the anhydride (I) should absorb more, the same effect appears with nitric anhydride, N_2O_5. The extinction coefficients for N_2O_5 in CCl_4 at 270, 290 and 310 mμ are 90, 30 and 12.[5] These may be compared with the values for HNO_3 in 69% H_2SO_4 (Table I), which are 8.8, 4.5 and 0.7 at the same respective wave lengths.

The most plausible alternative structure for I is $H_2NO_3^+$. This would equilibrate with NO_2^+ according to the equation

$$NO_2^+ + H_2O = H_2NO_3^+ \qquad (3)$$

In 92–99% H_2SO_4 where $c_{NO_2^+}$ is constant, eq. 3 requires that ϵ_I/a_{H_2O} would be constant if I were $H_2NO_3^+$. The data in Table IV do not support such an assumption.

If the value of K_{eq} ($K_{eq} = c_I/c_{NO_2^+}c_{HSO_4^-}$) for eq. 2 were known, the extinction coefficients and concentrations of HNO_3, NO_2^+ and O_2NOSO_3H could be computed from the spectroscopic data. The results of a number of such calculations using provisional values for K showed that values of K much below 0.01 gave calculated values of $c_{NO_2^+}$ larger than those in Table III. Values of K much above 0.01 gave $c_I + c_{NO_2^+}$ greater than the HNO_3 added which is impossible. A value of $K = 0.01$ is certainly not precise, but it can be used to estimate the order of magnitude of the relative concentrations. The results of such estimates are as follows. The % HNO_3 existing as O_2NOSO_3H is about 1% in 85% H_2SO_4, increases to a maximum of 9% in 90% acid, and decreases to 5 and 1% in 95 and 99% H_2SO_4. The % HNO_3 existing as NO_2^+ follows the values in Table III ultimately declining to about 10% in 85% H_2SO_4. The % HNO_3 remaining as HNO_3 decreases from 90% in 85% H_2SO_4 to zero in 90% acid.

(17) L. P. Hammett and A. J. Deyrup, *J. Am. Chem. Soc.*, **55**, 1900 (1933).

(18) N. Deno and R. W. Taft, Jr., *ibid.*, **76**, 244 (1954).

(19) J. C. D. Brand, *J. Chem. Soc.*, 1002 (1950).

(20) M. S. Newman, H. G. Kuivila and A. B. Garrett, *J. Am. Chem. Soc.*, **67**, 704 (1945); M. S. Newman and N. Deno, *ibid.*, **73**, 3644, 3651 (1951); R. J. Gillespie and associates, *J. Chem. Soc.*, 2473 (1950).

(21) S. J. Bass, R. J. Gillespie and J. V. Oubridge, *ibid.*, 837 (1960).

(22) N. Deno and C. Perrizzolo, *J. Am. Chem. Soc.*, **79**, 1345 (1957).

(23) Footnote c of Table IV.

THERMODYNAMIC STUDIES ON LIQUID TERNARY ZINC SOLUTIONS[1]

BY TOSHIO YOKOKAWA, AKIRA DOI AND KICHIZO NIWA

Department of Chemistry, Faculty of Science, Hokkaido University, Sapporo, Japan

Received April 9, 1960

Vapor pressure of zinc has been measured as to three ternary metallic solutions: tin–zinc–bismuth, indium–zinc–bismuth and tin–zinc–indium in the range 0 to 0.3 in zinc mole fraction at the neighborhood of 625°K. by Knudsen's effusion method. The results show that the excess partial molar free energy of mixing of zinc in the indium–zinc–bismuth system gives a maximum, when plotted against concentration of bismuth, mole fraction of zinc being kept constant at 0.1. This fact is concordant with the calculation, which is based upon the assumption of a simple pair bond model. In the other two systems the above comparison is not successful. It has been suggested that this may be attributed to the influence of the third component on pair interaction.

Recently much effort has been made toward the theoretical interpretation of electro-magnetic and thermodynamic properties of metallic solutions. Thermodynamic properties have been established for a wide variety of binary solutions. On the other hand, only a few studies have been carried out on ternary systems except multi-component systems in high dilution. It would be interesting to find any new character in ternary systems beyond what is expected from three separate binary systems. In the case of multi-valent B-metals in the periodic table, the comparison of a ternary system with a binary one is especially interesting because in these metals the electronic state and accordingly ionic radius show complex behavior on alloying. Thus in the present work the vapor pressure of zinc in ternary liquid solutions of Sn–Zn–Bi, In–Zn–Bi and Sn–Zn–In was measured by means of Knudsen's effusion method. The results are discussed in comparison with those found in binary solutions.

Experimental

Knudsen's effusion method was employed. Experimental apparatus and procedure have been described in the previous paper.[2] A Pyrex crucible, on the lid of which an orifice is ground, is hung by platinum wire from a thermobalance. Effusion velocity is determined by current change of a linear differential transformer, the central core of which is attached to the beam of the balance through platinum wire. The effective area of the orifice is determined by combining the effusion velocity of solid pure zinc and its vapor pressure, the latter having been established by Barrow, *et al.*[3]

The applicability of this method to zinc liquid alloys has been tested in the system.[2] Vaporization velocity is great enough compared with effusion loss in spite of disturbance of oxide film and diffusion of zinc through bulk phase to surface is great enough to keep the surface concentration constant.

Purities of metals used are 99.9% (zinc), chemical pure (tin), 99.9% (bismuth), and 99.999% (indium). Alloys were prepared in the following way: pure metals of desired composition were sealed in small Pyrex tubes under vacuum and kept at about 450° for about ten hours, then quenched. For the case of ternary alloys, a binary alloy without zinc was made at first and then zinc was added.

For the sources of error of determining vapor pressures by the present method, there should be taken into consideration temperature, sensitivity of the thermobalance, the rate of current change in the linear differential transformer, and the orifice area. Then the fractional average deviation of vapor pressure amounts to 3.24%. The relative error of activity is estimated to be 4%.

Experimental Results

Sn–Zn–Bi System.—Mother liquid metals or alloys, to which zinc was added, were prepared from tin and bismuth, the atomic ratio being 0, 0.33, 0.5, 0.66 and ∞. Concentration of zinc ranged 0.05 to 0.2. At each concentration vapor pressures of zinc were measured ten times over the temperature range of about 70° in two or three runs. Experimental results are summarized in Table I in the form of temperature equations, though the temperature coefficients are not as reliable as the absolute values on account of the rather narrow temperature range. Activity of zinc at 625°K. is shown as a function of concentration in Fig. 1. Activity in tin–zinc alloy has been measured already by Taylor[4] by e.m.f. method. Present data are slightly lower than the value extrapolated from Taylor's data. As for the bismuth–zinc binary system, the activity value of the present measurement agrees well with the previous data[5]. Activity of zinc monotonously increases as tin is replaced by bismuth.

TABLE I

VAPOR PRESSURE OF ZINC IN TIN–ZINC–BISMUTH SYSTEM[a]

$\log P = -A/T + B$

X_{Bi}/X_{Sn}	X_{Zn}	A	B
0	0.027	5206	5.546
	.104	5432	6.286
	.150	5976	7.312
	.252	5822	7.249
	.364	5769	7.273
0.499	.050	4225	4.051
	.149	5246	6.161
	.294	6966	9.197
0.998	.066	4508	4.776
	.102	4957	5.666
	.201	5249	6.286
	.284	5630	7.079
2.00	.050	5395	6.041
	.100	4957	5.652
	.151	5867	7.299
	.199	5666	7.095
∞	.056	4195	4.355
	.100	5986	7.467
	.149	5206	6.290

[a] The effective areas of orifices: 0.5795, 0.2433, 0.3579 and 0.2765 mm.^{2}.

(1) (a) Presented at the 44th annual meeting of the Japan Institute of Metals in Tokyo, April, 1959; (b) this paper is a part of the thesis presented by T. Yokokawa to Hokkaido University in partial fulfillment of the requirements for a D.Sc. degree.

(2) K. Niwa, T. Yokokawa and H. Wada, *J. Chem. Soc. Japan* **33**, 1345 (1960).

(3) R. F. Barrow, *et al.*, *Trans. Faraday Soc.*, **51**, 1354 (1955).

(4) N. F. Taylor, *J. Am. Chem. Soc.*, **45**, 2865 (1923).

(5) O. J. Kleppa, *J. Am. Chem. Soc.*, **74**, 6052 (1952).

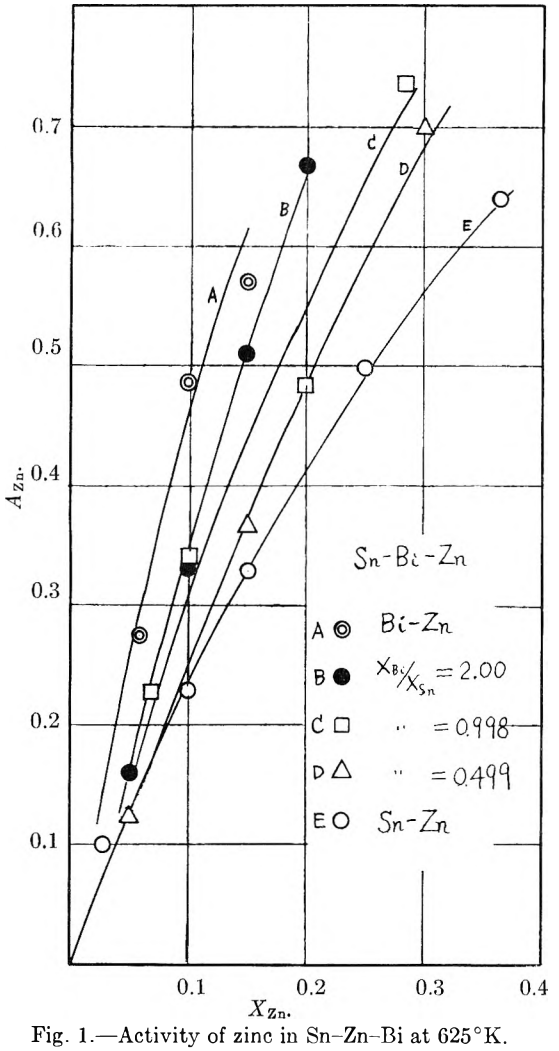

Fig. 1.—Activity of zinc in Sn–Zn–Bi at 625°K.

In–Zn–Bi System.—Measurements have been made in the same way as for Sn–Zn–Bi. Vapor pressure and activity at 625°K. are shown in Table II and Fig. 2, respectively. Activity of zinc in In–Zn has been measured by Svirbely and Selis.[6] The present data agree with theirs within the range of experimental error. As is seen in Fig. 2, activity of zinc increases with bismuth content and has a maximum on the bismuth-rich side of the equiatomic point with respect to indium and bismuth.

TABLE II

VAPOR PRESSURE OF ZINC IN INDIUM–ZINC–BISMUTH SYSTEM[a]

X_{Bi}/X_{In}	X_{Zn}	A	B
0	0.052	4894	5.354
	.085	5874	7.117
	.151	6394	8.153
0.501	.040	6521	8.070
	.109	4989	5.906
0.999	.049	4319	4.711
	.101	4924	5.875
2.01	.033	6909	8.805
	.087	5523	6.755
∞	Table I		

[a] The effective area of the orifice: 0.2765 mm.².

(6) W. J. Svirbely and S. M. Selis, *ibid.*, **75**, 1532 (1953).

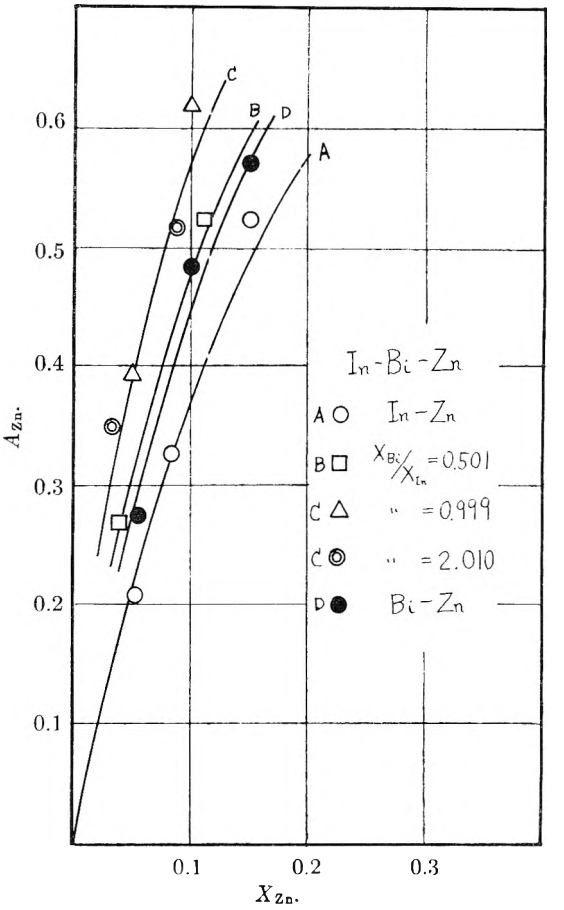

Fig. 2—Activity of zinc in In–Zn–Bi at 625°K.

Sn–Zn–In System.—Master alloys of tin and indium with atomic ratios of 0.33, 1 and 3 were prepared to which zinc was added to the concentration of 0.05 and 0.1 mole fraction. Vapor pressure equations and the activity at 625°K. are shown in Table III and Fig. 3. The activity of zinc at its definite content increases with addition of indium.

TABLE III

VAPOR PRESSURE OF ZINC IN TIN–ZINC–INDIUM SYSTEM[a]

$\log P = -A/T + B$

X_{In}/X_{Sn}	X_{Zn}	A	B
0	Table I		
0.334	0.049	3557	3.003
	.099	4693	5.009
	.153	6172	7.684
0.920	.049	4789	4.950
	.100	5747	6.847
	.151	6367	7.973
3.00	.045	5426	6.155
	.100	5228	5.997
	.149	4999	5.828

[a] The effective area of the orifice: 0.2765 mm.².

TABLE IV

PARAMETERS OF SUB-REGULAR SOLUTIONS (EQUATION 7)

		A_{12}^0	A_{23}^0	A_{31}^0	A_{12}'	A_{23}'	A_{31}'
(a)	Sn(1)–Zn(2)–Bi(3)	1660	3100	−275	−430	1280	−125
(b)	In(1)–Zn(2)–Bi(3)	2320	3100	−700	−420	1280	0
(c)	Sn(1)–Zn(2)–In(3)	2320	1660	0	−430	420	0

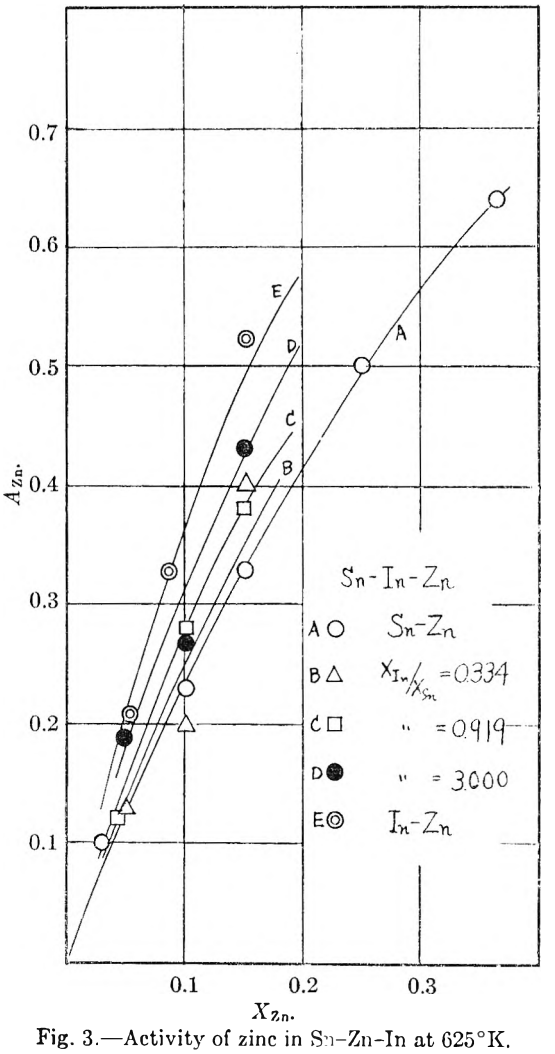

Fig. 3.—Activity of zinc in Sn-Zn-In at 625°K.

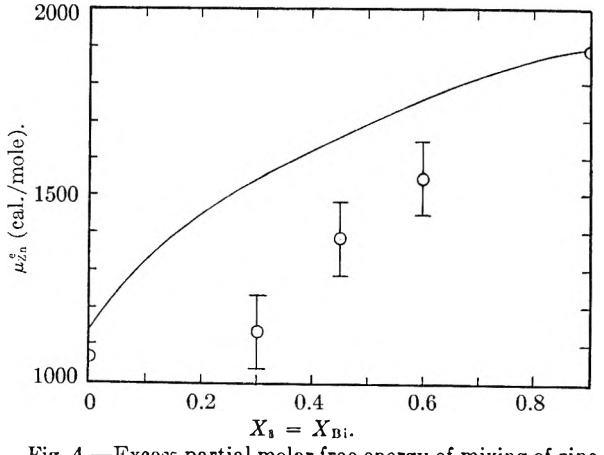

Fig. 4.—Excess partial molar free energy of mixing of zinc in Sn-Zn-Bi at $X_{Zn} = 0.1$ at 625°K., experimental values and calculated one from equation 8.

Discussion

Thermodynamic properties of alloys can be appropriately given in terms of excess functions. In Figs. 4, 5 and 6 are shown the trends of excess chemical potential of zinc, $\mu_{Zn}{}^e$, defined as the difference of the partial molar free energy of solution of zinc from that of ideal solution, at mole fraction of zinc of 0.1 in the three solutions, respectively. The value of $\mu_{Zn}{}^e$ changes almost linearly in Sn-Zn-Bi and Sn-Zn-In systems, while it shows a maximum in the In-Zn-Bi system. The meaning of these behaviors is to be examined on the basis of the facts known about binary solutions. Assuming that $\mu_2{}^e$ in a ternary solution is a function of second order of the mole fraction of the third component, $\mu_2{}^e$ is expressed in general as

$$\mu_2{}^e = A + BX_3 + CX_3{}^2 \qquad (1)$$

where A, B and C are constants independent of concentration. Differentiating equation 1 with respect to X_3, there is obtained

$$\frac{d\mu_2{}^e}{dx_3} = B + 2CX_3 \qquad (2)$$

Then $d\mu_2{}^e/dX_3 = B$ when X_3 is taken as zero, and $d\mu_2{}^e/dX_3 = B + 1.8B$ when X_3 is taken as 0.9. That is to say, B and $B + 1.8C$ give the slopes of $\mu_2{}^e$ at $X_3 = 0$ and $X_1 = 0$, respectively. Therefore, the $\mu_2{}^e$-curve becomes linear, concave or convex to abscissa, according as $C = 0$, $C < 0$ or $C > 0$, respectively.

The physical significances of B and C are not known as simple functions of mole fraction of each component. But one can approximately derive explicit formulas of B and C, provided that these solutions obey the pair-bond model as in the case of non-metallic solutions and further are regarded as regular solutions. In that case the excess molar free energy of solution is given by

$$F^e = X_1X_2A_{12} + X_2X_3A_{23} + X_3X_1A_{31} \qquad (3)$$

where A_{ij} is a constant determined for the i-j pair and independent of the third component. Equation 3 yields an expression for $\mu_2{}^e$

$$\mu_2{}^e = (X_1{}^2 + X_1X_3)A_{12} + (X_3{}^2 + X_1X_3)A_{23} - X_3X_1A_{31} \qquad (4)$$

Putting $X_2 = 0.1$ and differentiating equation 4 with respect to X_3

$$\frac{d\mu_3{}^e}{dX_3} = 0.9(A_{23} - A_{12} - A_{31}) + 2X_3A_{31} \qquad (5)$$

By comparing equation 2 with 5 one obtains

$$B = 0.9(A_{23} - A_{12} - A_{31}), \text{ and } C = A_{31}$$

The above calculation shows that curvature of $\mu_2{}^e$ in a 1-2-3 ternary system is determined by A_{31} or the interaction of the 1-3 binary system. If, here, the following notations are employed to represent the orders of the components of the three systems, 3-1 pairs are Bi-Sn, Bi-In and In-Sn.

(a) Sn(1)-Zn(2)-Bi(3)
(b) In(1)-Zn(2)-Bi(3)
(c) Sn(1)-Zn(2)-In(3)

Bi-Sn and In-Sn systems behave almost as ideal solutions, while the Bi-In system shows a negative deviation from ideality. Then, this analysis predicts that the $\mu_2{}^e$-X_3 curve is linear in (a) and (c) solutions and concave to the abscissa in the (b) solution. This prediction may be qualitatively concordant with experimental results graphed in Figs. 4, 5 and 6.

A more quantitative treatment is tried under the assumption of the "sub-regular" character for each binary system, since most metals behave as

sub-regular solutions on mixing rather than as regular ones. A sub-regular solution[7] is defined as a solution in which the excess free energy of mixing in a binary solution is a function of concentration as expressed by

$$F^e = X_1X_2[A_{12}^0 + (X_1 - X_2)A_{12}'] \qquad (6)$$

By extension of this treatment to ternary systems, the expression may be obtained

$$F^e = X_1X_2A_{12}^0 + X_2X_3A_{23}^0 + X_3X_1A_{31}^0 + X_1X_2\frac{X_1 - X_2}{X_1 + X_2}A_{12}' + X_2X_3\frac{X_2 - X_3}{X_2 + X_3}A_{23}' + X_3X_1\frac{X_3 - X_1}{X_3 + X_1}A_{31}' \qquad (7)$$

It is to be noted that denominators in this equation are introduced in order to evaluate $(X_i - X_j)$ as would be the case when the system under study is reduced to a binary system under the condition of keeping the ratio X_i/X_j constant. Making use of equation 7, one can secure the value of μ_2^e

$$\mu_2^e = X_1(X_1 + X_3)A_{12}^0 + X_3(X_1 + X_3)A_{23}^0 - X_3X_1A_{31}^0 + \frac{X_1}{(X_1 + X_2)^2}[(X_1 - X_2)(X_2 + X_1)(X_3 + X_1) - 2X_1X_2]A_{12}' + \frac{X_3}{(X_2 + X_3)^2}[(X_2 - X_3)(X_3 + X_1)(X_2 + X_3) + 2X_2X_3]A_{23}' - \frac{X_3X_1}{X_3 + X_1}(X_3 - X_1)A_{31}' \qquad (8)$$

Thus one can calculate μ_2^e if A_{ij}^0 and A_{ij}' are known with regard to three separate binary systems. These constants of the binary systems concerned are summarized in Table IV. Sn–Zn, Bi–Zn and In–Zn systems behave as sub-regular solutions only within a limited range of composition. Recently, Wittig and his co-workers[8] measured the heat of mixing (ΔH) of these systems as the functions of composition and found sub-regularity (as far as heat term was concerned) in these systems except in the zinc-rich portion, where an exponential deviation of $\Delta H/X_1X_2$ from linearity was found. Then A^0 and A' of these systems are evaluated from the data in the zinc-dilute portion. Sn–Bi system shows sub-regularity over the whole composition range. As F^e is not measured in Bi–In system, the excess chemical potential of Bi has been calculated from the liquidus curve of the phase diagram. Assuming this system to obey the relation F^e/X_1X_2 = constant (as is found in ΔH by Wittig[8]), A_{12}^0 can be calculated. In Sn–In system F^e is also not measured and calculation from the phase diagram is not possible, because of the appreciable solid solubility of tin in solid indium and conversely of indium in solid tin. Wittig measured the heat of mixing of this system and found it to be nearly zero. Then this system has been assumed to be ideal. By the use of these values of A_{ij}s, μ_{Zn}^es values are calculated for the three systems at $X_{Zn} = 0.1$, as shown in Figs. 10, 11 and 12 (solid lines). As is seen from these figures, the calculated line agrees well with experimental points in In–Zn–Bi system, while the other two lines show a little discrepancy. It is of much interest to find this discrepancy because Sn–Bi and Sn–In systems are nearly ideal or $A_{31}^0 = A_{31}' = 0$. Therefore, one may attribute this effect to A_{12}' and A_{23}' in equation 8. In the derivation it has been assumed that pair interaction (A_{12}) was independent of the third component,[9] which seems not to be the case. It is supposed that the 1-2 interaction may gradually change with addition of the third component and become quite different from that in the case of absence of the third component. It may be so especially when the atomic diameter and electronegativity of the third component are different from those of either or both of the first and second components. In other words, properties of solutions, such as the average radius and electronic behavior which are closely related to the free energy, are substantially determined by the most concentrated component, say, the third component. In In–Zn–Bi system, the strong In–Bi (1–3) interaction seems to mask this rather smaller effect, resulting in agreement of the experiment with calculation. When the accurate energetics of alloy systems become established in the future, the above-mentioned abnormality may be explained.

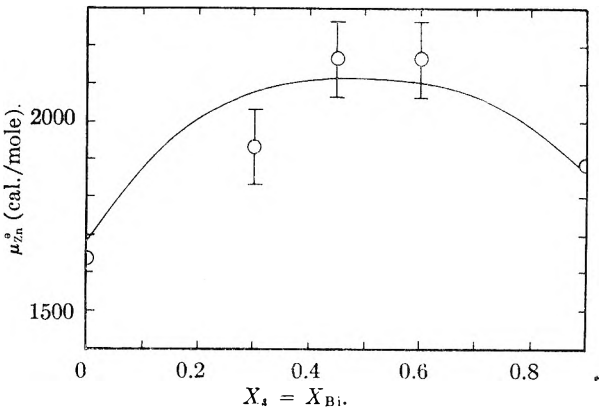

Fig. 5.—Excess partial molar free energy of mixing of zinc in In–Zn–Bi at $X_{Zn} = 0.1$ at 625°K., experimental values and calculated curve from equation 8.

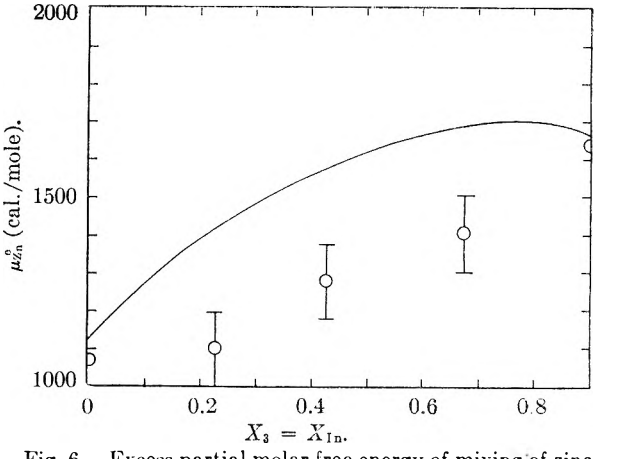

Fig. 6.—Excess partial molar free energy of mixing of zinc in Sn–Zn–In at $X_{Zn} = 0.1$ at 625°K., experimental values and calculated curve from equation 8.

Acknowledgment.—The authors are indebted to Dr. M. Shimoji for his valuable discussion.

(7) H. K. Hardy, *Acta Met.*, **1**, 202 (1952).

(8) F. E. Wittig, *Z. Elektrochem.*, **63**, 327 (1959).

(9) This assumption is not unreasonable from the viewpoint of pair interaction for metal bonding.

INTRAMOLECULAR HYDROGEN BONDING TO π-ELECTRONS IN *ortho*-SUBSTITUTED PHENOLS

BY W. BECKERING

Grand Forks Lignite Research Laboratory, Region III, U. S. Bureau of Mines, Grand Forks, N. Dak.

Received May 14, 1960

Intramolecular hydrogen bonds between hydroxyl groups and aromatic π-electrons are examined in phenols that have an aromatic group attached to the *ortho*-position. The strength of the hydrogen to π-electron bond is varied by placing different substituents on the primed aromatic ring. The strength of the intramolecular bond is related to the planarity of the two aromatic rings in a biphenyl system.

The formation of the hydrogen bond through intermolecular and intramolecular association has been investigated extensively in recent years.[1-7] Intermolecular hydrogen bonding may occur either between solute and solvent or between two solute molecules. The latter is a concentration-dependent phenomenon. Intramolecular hydrogen bonding occurs in those phenolics that have a proton-acceptor group attached to the molecule. The steric configuration of the proton-acceptor group must be such that the internuclear distance between it and the proton will permit the formation of a hydrogen bond. This kind of bonding does not depend on the concentration of the solution. Lüttke and Mecke[8] classified those compounds that exhibit intramolecular hydrogen-bonding into two types. In type I compounds, the substituent X may be either a halogen, alkoxy, hydroxy, cyanide, aromatic or an olefinic group. These compounds generally display two well-defined OH bands. The long wave length band results from the *cis*-form of the molecule and the short wave length band from the *trans*-form. In

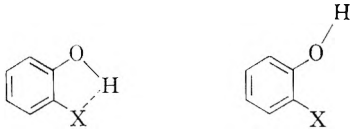

solution an equilibrium exists between these two structures. In type II compounds where X = NO_2, CHO, COOR or COR, the OH band displays a single, broad, diffuse absorption which is shifted considerably to longer wave lengths. In these compounds, the increased strength of the hydrogen bond can be attributed to the increased stability of the six-membered ring which is in contrast to the compounds found in type I, where a five-membered ring is present.

In type I compounds, the *ortho* substituent may be an electronegative atom or it may be a π-electron system arising from an olefinic group or an aromatic ring. Recently West[7] and Baker and Shulgin[9] have investigated type I compounds in which the proton-acceptor group consisted of olefinic π-electrons. In this paper intramolecular hydrogen bonding in type I compounds will be discussed where the proton-acceptor group *ortho* to the hydroxyl group consists of aromatic π-electrons. The effective concentration of the π-electrons will be varied by placing different substituents on the aromatic ring.

Experimental

A Perkin–Elmer model 112 double-pass spectrophotometer was used for determining the fundamental hydroxyl stretching frequencies in the 3,600 $cm.^{-1}$ region. The instrument was equipped with calcium fluoride optics and had a slit width of 75μ at 3,600 $cm.^{-1}$. The spectrophotometer was purged with dry air prior to use. Calibration was accomplished by drawing a smooth curve through the points obtained from the absorption peaks of ammonia and the atmosphere water vapor bands. Absorption peak values were taken from the literature.[10] All samples except 4′-nitro-2-hydroxybiphenyl were run in reagent grade carbon tetrachloride at concentrations of 5.0 g./liter. The 4′-nitro-2-hydroxybiphenyl compound was a saturated solution in CCl_4 of approximately 4.0 g./liter. The path length of the cell was 1.0 mm. All spectra were recorded at room temperature. The reproducibility of the spectra was ±2 $cm.^{-1}$ or better.

The 4′-chloro-2-hydroxybiphenyl, 4′-bromo-2-hydroxybiphenyl, 4′-iodo-2-hydroxybiphenyl and 4′-nitro-2-hydroxybiphenyl were synthesized in this Laboratory according to standard procedures recorded in the literature. 2′-Hydroxy-1-phenylnaphthalene was synthesized at the Bureau of Mines. 2-Propenylphenol, 2-phenylphenol and 2,2′-dihydroxybiphenyl were obtained from commercial sources. The above compounds were purified by either recrystallization, distillation or gas–liquid chromatography.

Results and Discussion

Table I lists the hydroxyl frequencies of the *cis* and *trans* form. Phenol is included in the table for comparison purposes. The high-frequency band is due to the unassociated OH-group found in the *trans* form of the molecule, and the low-frequency band is produced by the *cis* configuration.[11]

There has been considerable discussion in the literature about the planarity of the two aromatic rings in a biphenyl system.[12-14] Although the exact angle between the two planes has not been established, the consensus is that the aromatic rings are neither coplanar nor perpendicular to

(1) N. D. Coggeshall, *J. Am. Chem. Soc.*, **69**, 1620 (1947).
(2) W. Lüttke and R. Mecke, *Z. Elektrochem.*, **53**, 241 (1949).
(3) N. D. Coggeshall and E. L. Saier, *J. Am. Chem. Soc.*, **73**, 5414 (1951).
(4) F. A. Smith and E. C. Creitz, *J. Research Natl. Bur. Standards*, **46**, 145 (1951).
(5) R. A. Friedel, *J. Am. Chem. Soc.*, **73**, 2881 (1951).
(6) D. S. Trifan, J. L. Weinmann and L. P. Kuhn, *ibid.*, **79**, 6566 (1957).
(7) R. West, *ibid.*, **81**, 1614 (1959).
(8) W. Lüttke and R. Mecke, *Z. physik. Chem.*, **196**, 56 (1950).
(9) A. W. Baker and A. T. Shulgin, *ibid.*, **80**, 5358 (1958).
(10) A. R. Downie, M. C. Magoon, T. Purcell and B. Crawford, Sr., *J. Opt. Soc. Am.*, **43**, 941 (1953).
(11) L. Pauling, "The Nature of the Chemical Bond," Cornell Univ. Press, Ithaca, N. Y., 2nd ed., 1948, pp. 320–27.
(12) G. W. Wheland, "Resonance in Organic Chemistry," John Wiley and Sons, Inc., New York, N. Y., 1955, p. 157 ff.
(13) I. L. Karle and L. O. Brockway, *J. Am. Chem. Soc.*, **66**, 1974 (1944).
(14) V. P. Kreiter, W. A. Bonner and R. H. Eastman, *ibid.*, **76**, 5770 (1954).

TABLE I

ABSORPTION PEAK VALUES FOR THE *cis* AND *trans* BANDS IN CM.$^{-1}$

Compound	*cis* band	*trans* band
2-Phenylphenol	3568	3609
2,2′-Dihydroxybiphenyl	3556	3599
2′-Hydroxy-1-phenylnaphthalene	3560	..
4′-Chloro-2-hydroxybiphenyl	3575	3610
4′-Bromo-2-hydroxybiphenyl	3573	3607
4′-Iodo-2-hydroxybiphenyl	3572	3609
4′-Nitro-2-hydroxybiphenyl	3587	3604
2-Propenylphenol	3550	3607
Phenol	..	3610

one another but rather are at some intermediate angle. This angle can be increased by placing bulky groups in the 2- and 6-position, thus forcing the two rings to approach a perpendicular configuration[15-17]; or it can be decreased by placing on the ring certain groups which tend to promote conjugation between the two rings. As the amount of double-bond character of the 1–1′ carbon bond increases, the degree of coplanarity increases also.

2-Phenylphenol.—2-Phenylphenol will be treated first, because it is the simplest aromatic substituted phenol with no functional groups on the primed ring. It displays a strong, sharp band at 3568 cm.$^{-1}$ which is due to the *cis* form of the hydroxyl

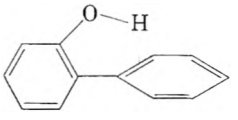

group. The absorption energy is 42 cm.$^{-1}$ lower than the OH-group in phenol. The proton-acceptor group in 2-phenylphenol is the aromatic π-electron system of the primed benzene ring. These π-electron orbitals are perpendicular to the plane of the aromatic ring. Therefore, one anticipates that the strength of the hydrogen to π-electron bond should increase as the degree of noncoplanarity increases. The increase is represented by the angle ω in Fig. 1. Correspondingly, the

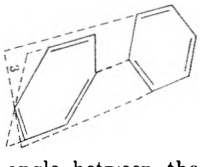

Fig. 1.—ω is the angle between the planes of the two aromatic rings in biphenyl.

strength of the OH-bond should decrease with increasing strength of the proton to π-electron bond. This stabilization of the molecule through the formation of the hydrogen bond will tend to increase the angle ω in Fig. 1 from that of the unsubstituted biphenyl. The absorption frequency of the *trans* hydroxyl group in 2-phenylphenol is 3609 cm.$^{-1}$, which is approximately the same as that of phenol. The intensity of the band in the *trans* form is considerably weaker than that of the *cis* form.[18]

(15) E. Marcus, W. M. Lauer and R. T. Arnold, *ibid.*, **80**, 3742 (1958).

(16) E. Williamson and W. H. Rodebush, *ibid.*, **63**, 3018 (1941).

(17) G. H. Beaven, D. M. Hall, M. S. Lesslie and E. E. Turner, *ibid.*, **74**, 854 (1952).

2,2′-Dihydroxybiphenyl.—In this compound the two hydroxyl groups are favorably located so that both of the protons can "reach over" and form a hydrogen bond with the adjacent π-electrons of the aromatic ring. A twofold twisting effect is now present because both of the hydrogen to

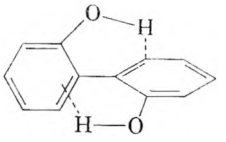

π-electron bonds tend to rotate the two aromatic rings perpendicular to each other. This rotation should produce a stronger hydrogen to π-electron bond than in 2-phenylphenol. The *cis* form has its absorption peak at 3556 cm.$^{-1}$, which is a decrease in energy of 12 cm.$^{-1}$ from that of 2-phenylphenol.

It may be questioned whether this decrease in energy of the absorption band can be ascribed solely to the increase in the non-coplanarity of the two rings. It must be recognized that there is also an increase in the π-electron charge of each of the rings because of the resonance effect of the non-bonding π-electrons on the oxygen atom with the π-electrons on the aromatic ring. This increase in the π-electron concentration also will favor a strengthening of the proton to π-electron bond which would result in a lowering of the OH-frequency.

The absorption frequency of the *trans* form in 2,2′-dihydroxybiphenyl is 3599 cm.$^{-1}$. This represents a drop of 11 cm.$^{-1}$ below that of phenol and is the lowest frequency for the *trans* form of the compounds listed in Table I. An explanation for this drop can be found in the decreased basicity of the oxygen atom of the *trans* OH-group. The drop in basicity is produced by the hydrogen to π-electron bond of the *cis* OH-group. The proton to π-electron bond decreases the effective π-electron concentration of the ring containing the *trans* OH-group, which, in turn, transmits its effect to the oxygen atom through resonance. This lowers the force constant of the *trans* OH-bond, and therefore, a drop in frequency results according to the equation

$$\nu = \frac{1}{2\pi}\sqrt{\frac{k}{\mu}}$$

where ν is the frequency, k the force constant, and μ the reduced mass of the atoms involved in the vibration.

One is led to believe that any resonance that might exist between the two rings must be small because the hydroxyl group normally produces an increase in the electron density of the carbon atoms at the *ortho* and *para* positions. This increase in π-electron density should be transmitted across the 1–1′ carbon bond of the two rings and hence to the *ortho* carbon atom attached to the *trans* OH-group. The resulting increase in basicity of the oxygen atoms should increase the frequency of the *trans* OH-group. Since a drop in the frequency is observed it can be concluded either that

(18) O. R. Wulf, U. Liddel and S. B. Hendricks, *J. Am. Chem. Soc.*, **58**, 2287 (1936).

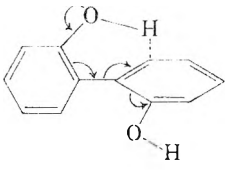

there is little resonance between the two aromatic rings or that the effect of the electron depletion due to the hydrogen to π-electron bond of the *cis* group counteracts any increase resulting from conjugation between the two aromatic rings, so that the over-all observed effect is a lowering of the basicity of the oxygen atom.

2′-Hydroxy-1-phenylnaphthalene.—Ultraviolet spectra of catacondensed aromatics show a red shift with increasing size of the hydrocarbon,[19] indicating a corresponding increase in the π-electron system. The greater π-electron system in naphthalene compared to benzene should result in a stronger proton to π-electron bond in 2′-hydroxy-1-phenylnaphthalene than in 2-phenylphenol. This difference is observed in the spectra of 2′-hydroxy-1-phenylnaphthalene where a strong band occurs at 3560 cm.$^{-1}$, representing a drop of 8 cm.$^{-1}$ from that of 2-phenylphenol. The absence of the *trans* form in this compound probably is due to a shift in the thermal *cis–trans* equilibrium because of the added stabilization of the *cis* form. Other factors such as the size of the molecule undoubtedly enter also in order to account for the existence of the *trans* form in 2,2′-dihydroxybiphenyl.

4′-Halo-2-hydroxybiphenyl.—The halo-substituted compounds display absorption frequencies of the same order of magnitude; therefore, these three compounds will be treated as a group. The values of the *cis*-frequencies are all higher than that of 2-phenylphenol. The halogens can release electrons by resonance and can withdraw electrons by the inductive effect. The energy values indicate that the inductive effect outweighs the resonance effect, so that the net result is a decrease in the π-electron density compared to 2-phenylphenol. The OH-frequency of the *cis* form increases in the order Cl > Br > I, which is in accordance with the electronegativities of the halogens.

The *trans* OH-frequencies in the halo-substituted compounds are slightly below the value for phenol. The bromo compound has the lowest value of the three compounds.

4′-Nitro-2-hydroxybiphenyl.—The nitro group serves as an electron sink for the π-electron density of the nitro-substituted aromatic ring. The resulting decrease in the π-electron concentration is reflected in the weak proton to π-electron bond and a stronger *cis* OH-bond. The energy of the *cis* OH-bond in this compound is the strongest of the compounds examined. With the weakened proton to π-electron bond is a shift in the *cis–trans* equilibrium in favor of the *trans* form of the molecule. This shift is observed in the equivalent intensities of the two peaks—assuming equal extinction coefficients. The other compounds, except 2′-hydroxy-1-phenylnaphthalene which has no *trans* band, display a weak *trans*-absorption band and a strong *cis*-absorption band. This is in contrast to 2-allylphenol[9] and 2-propenylphenol[9] which have weak *cis*-absorption bands and strong *trans*-absorption bands.

From the above results, a relationship is observed between the strength of the hydrogen to π-electron bond and the π-electron concentration on the aromatic ring. Furthermore, there seems to be a relationship between the degree of non-coplanarity and the strength of the hydrogen-π-electron bond. By a careful examination of the hydroxyl frequency, the type of bonding present in the molecule frequently can be determined.

(19) J. R. Platt, *J. Chem. Phys.*, **17**, 484 (1949).

(9) A. W. Baker and A. T. Shulgin, *J. Am. Chem. Soc.*, **80**, 5358 (1958).

THE THERMAL DECOMPOSITION OF BARIUM PERMANGANATE

BY E. G. PROUT AND P. J. HERLEY

Rhodes University, Grahamstown, South Africa

Received May 24, 1960

The thermal decomposition of whole and ground crystals of $Ba(MnO_4)_2$ has been investigated in the temperature range 140–190°. Activation energies for the acceleratory and decay coefficients have been measured. Reaction during the main acceleratory period is presumed to proceed by the mechanism proposed for the decomposition of $KMnO_4$. The decay period follows the unimolecular law. Pre-irradiation in a γ-ray source accelerates the thermal decomposition and the results are interpreted by a mechanism similar to that suggested for pre-irradiated $KMnO_4$.

Roginskiĭ, *et al.*,[1] studied the topography of the thermal decomposition of barium permanganate and suggested that decomposition commenced from a number of surface nuclei and formed an amorphous film which spread into the crystal by way of multiplication of grains of product. Roginskiĭ, *et al.*,[2] also showed that the kinetic curves are sigmoid and that the acceleration of the reaction velocity conforms to $X_t^{2/3}$, where X_t is the mass of solid product at time t, and the deceleration to $m_t^{2/3}$, where m_t is the mass of unchanged permanganate. The reaction is presumed to be autocatalytic.

However no fully developed theory for the decomposition of $Ba(MnO_4)_2$ has been presented and no activation energies determined. The topographical examination suggests that the decomposition

(1) S. Z. Roginskiĭ, E. I. Shmuk and M. Kushnerev, *Izvest. Akad. Nauk S.S.S.R., Otdel. Khim. Nauk*, 573 (1950).

(2) S. Z. Roginskiĭ, S. Y. Elovich and E. I. Smuk, *ibid.*, 469 (1950).

might occur in a manner similar to that of potassium,[3] rubidium[4] and cesium[5] permanganates which disintegrate into a number of small grains during decomposition.

The present study was undertaken in an attempt to investigate this possibility and to extend the study of the effect of pre-irradiation by γ-rays on the thermal decomposition of permanganates to barium permanganate.

Experimental

The apparatus and procedure were similar to that previously used,[3] except for the use of an improved constant temperature decomposition vessel, which is described elsewhere.[6]

Rhombic crystals of $Ba(MnO_4)_2$ (1 × 0.5 × 0.5 mm.) were prepared by the addition of 50 ml. of an aqueous solution containing 4.31 g. of $BaCl_2 \cdot 2H_2O$ to a solution of 8.0 g. of $AgMnO_4$ in 800 ml. of water. Both solutions were at 50°. The precipitated silver chloride was filtered off and evaporation carried out *in vacuo* at 40°. The resulting crystals were recrystallized from aqueous solution. Approximately 16.0 mg. of $Ba(MnO_4)_2$ was decomposed in a run. In the plots shown the pressures are normalized to a common final pressure for comparative purposes.

Pre-irradiations were performed in the spent fuel facility at Harwell. The γ-ray dose rate was ~4 Mrad. hr.$^{-1}$. Pre-irradiations by cathode rays and ultraviolet light were done under conditions previously described.[7]

Results

Unirradiated $Ba(MnO_4)_2$.—The p–t plots for the decomposition of whole crystals are sigmoid, showing an initial burst of gas up to $\alpha \approx 0.04$, followed by a period of acceleration which changes at $\alpha \approx 0.5$ into a period of decay (Fig. 1). There is no induction period between the first evolution of gas and the main acceleration of the reaction. Visual observation of a decomposing crystal (3 × 1 × 1 mm.) showed that during the initial reaction the crystal breaks down into thin flat plates having dimensions in the range (0.5 × 0.5 mm.)-(0.1 × 0.1 mm.). It was not possible to detect any disintegration over the acceleratory and decay periods. The surfaces of the fragments were steel-blue in color at the end of the disintegration and remained so until the end of the reaction.

The decomposition of crystals which had been ground in an agate mortar yielded p–t plots of the same general form as those for whole crystals (Fig. 2). The main differences were a shift of the acceleratory and decay periods to shorter times as a result of a decrease in the duration of the initial reaction.

Reproducibility of results for the isothermal decomposition of whole and ground crystals was satisfactory. For three consecutive runs at 175° with whole crystals the values of k_2 (equation 2) were 2.66, 2.58, 2.68 × 10^{-2} min.$^{-1}$, and k_3 (equation 3) were 1.70, 1.60, 1.78 × 10^{-2} cm. min.$^{-1}$.

Interruption of the decomposition had no effect on the decomposition after reaction was recommenced. Admixture of whole and ground crystals with the products of the decomposition of ground crystals also had no effect. The percentage decomposition calculated in terms of the equation

$$2Ba(MnO_4)_2 \longrightarrow 2BaO + 4MnO_2 + 3O_2$$

was 90 and 88, for whole and ground crystals, respectively.

The initial reaction with whole crystals was not reproducible except in the general form of the p–t plot and the study of this part of the decomposition was confined to ground crystals. The total pressure of gas liberated over this period for ground crystals was directly proportional to the mass of material decomposed. A typical p–t plot is given in Fig. 3. The plot shows an initial evolution of gas ($\alpha \approx 0.02$ of the total decomposition) up to $t \approx 70$ min.

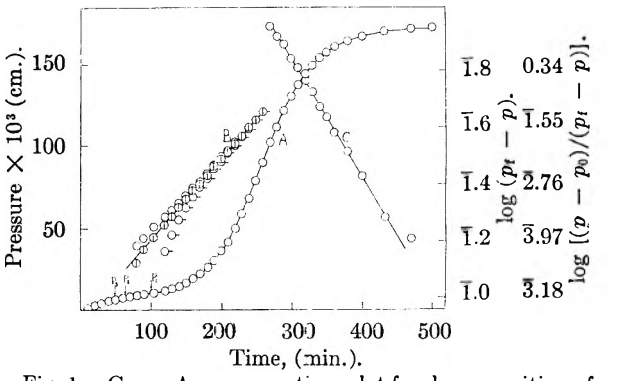

Fig. 1.—Curve A, pressure–time plot for decomposition of whole crystals of $Ba(MnO_4)_2$ at 165°; curves B, effect of varying p_0 in plot of log $[(p - p_0)/(p_f - p)]$ against t; ○, $p_0 = p_1$; ⊙, $p_0 = p_2$; ○, $p_0 = p_3$. Line C: plot of log $(p_f - p)$ against t.

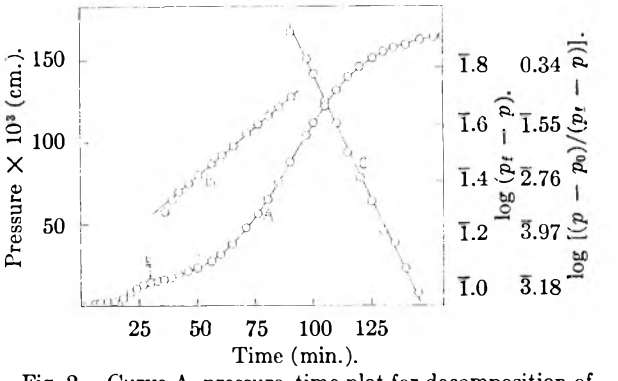

Fig. 2.—Curve A, pressure–time plot for decomposition of ground crystals of $Ba(MnO_4)_2$ at 175°; lines B and C, plots of Prout–Tompkins equation and log $(p_f - p)$ against t, respectively.

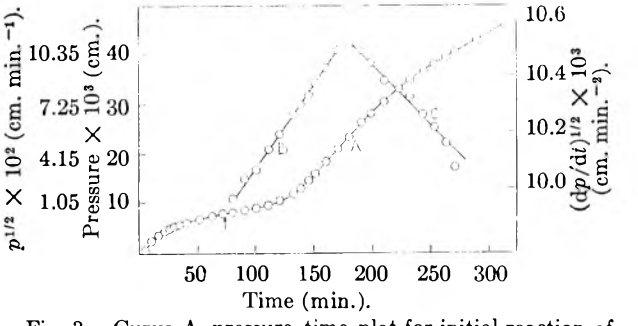

Fig. 3.—Curve A, pressure–time plot for initial reaction of 28 mg. of ground crystals of $Ba(MnO_4)_2$ at 145°; line B, plot of $p^{1/2}$ against t with origin at arrow; line C, plot of $(dp/dt)^{1/2}$ against t.

(3) E. G. Prout and F. C. Tompkins, *Trans. Faraday Soc.*, **40**, 488 (1944).

(4) P. J. Herley and E. G. Prout, THIS JOURNAL, **64**, 675 (1960).

(5) P. J. Herley and E. G. Prout, *J. Chem. Soc.*, 3300 (1959).

(6) E. G. Prout and P. J. Herley, *J. Chem. Educ.*, in press.

(7) E. G. Prout and F. C. Tompkins, *Trans. Faraday Soc.*, **43**, 148 (1947).

TABLE I

REACTION CONSTANTS FOR MAIN ACCELERATORY AND DECAY PERIODS

(All k values $\times 10^{-2}$ min.$^{-1}$)

Temp., °C.	Whole crystals: Unirradiated k_2	Whole crystals: Unirradiated k_3	Whole crystals: Irradiated 211 Mrad. k_2	Whole crystals: Irradiated 211 Mrad. k_3	Whole crystals: Irradiated 111 Mrad. k_2	Whole crystals: Irradiated 111 Mrad. k_3	Ground crystals: Unirradiated k_2	Ground crystals: Unirradiated k_3	Ground crystals: Irradiated 211 Mrad. k_2	Ground crystals: Irradiated 211 Mrad. k_3	Ground crystals: Irradiated 111 Mrad. k_2	Ground crystals: Irradiated 111 Mrad. k_3
190	12.40	5.33					8.30	5.65				
185	6.35	3.20			10.70	14.46	5.88	4.15				
180	4.50	2.02	9.87	10.85	7.13	8.25	4.20	2.90	7.00	9.21		
175	2.58	1.60	5.53	8.24	3.72	5.23	2.88	1.79	4.95	6.38		
170	1.82	1.13	2.93	4.25	2.24	3.63	1.59	1.16	3.11	4.06	2.46	3.67
165	1.11	0.76	2.10	2.66	1.48	2.09	..	..	2.05	2.54		
160	0.80	0.49	1.10	1.71	0.92	1.28	..	..	1.34	1.45		
155			0.89	1.19					0.72	0.89		

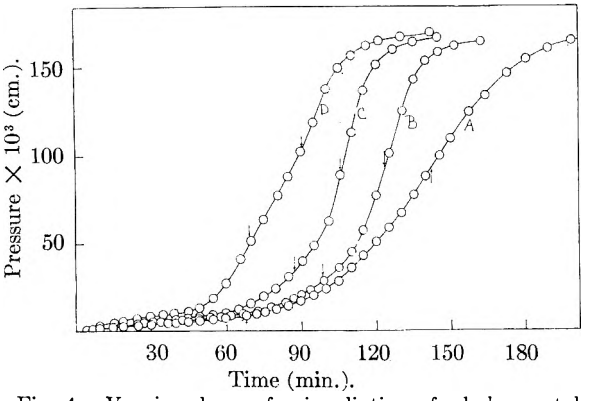

Fig. 4.—Varying doses of γ-irradiation of whole crystals of $Ba(MnO_4)_2$, decomposition temperature 170°. Dose: A, 0 Mrad.; B, 30 Mrad.; C, 111 Mrad.; D, 211 Mrad. → = fit of Prout–Tompkins equation.

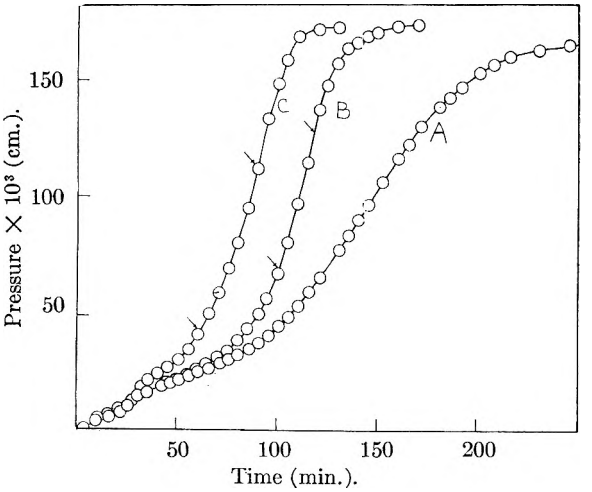

Fig. 5.—Varying doses of γ-irradiation of ground crystals of $Ba(MnO_4)_2$, decomposition temperature 160°. Dose: A, 0 Mrad.; B, 111 Mrad.; C, 211 Mrad. → = fit of Prout–Tompkins equation.

which is not reproducible in that the pressure of gas liberated varied from run to run. The remainder of the plot is sigmoid and reproducible if the origin is taken as the end of the first reaction.

Mathematical Analysis of p–t Plots.—The power law

$$p^{1/n} = k_1 t \qquad (1)$$

does not describe the acceleratory periods of whole or ground crystals when the origin is taken at $t = 0 = p$ or at the p, t values corresponding to the commencement of the acceleration. The method of determining this point is described below. However, the Prout–Tompkins equation[3]

$$\log p/(p_f - p) = k_2 t + c_2 \qquad (2)$$

where p_f = the final pressure, gives a satisfactory fit if the end of the initial reaction is determined, and the origin taken as this point. Difficulty was experienced in this, but a first approximation was made by subtracting from the pressure a value for the initial evolution, p_0, taken near the point at which acceleration begins and plotting log $[(p - p_0)/(p_f - p)]$ against time. This gave a good straight line in the upper part of the accelerating decomposition, but departed from linearity in the early stages. The value of p_0 then was changed until the best straight line was obtained. Figure 1 shows the effect of changing p_0 on the Prout–Tompkins plot for whole crystals. Figure 2 illustrates the plot for ground crystals.

The decay period of the p–t plots for both whole and ground crystals does not conform to equation 2 but obeys the unimolecular decay law

$$\log (p_f - p) = k_3 t + c_3 \qquad (3)$$

Typical analyses are shown in Figs. 1 and 2.

The sigmoid curve of the initial reaction for ground crystals (Fig. 3) is fitted over the acceleration by equation 1 when $n = 2$ and the origin transferred to the commencement of acceleration. The "decay" portion obeys the equation

$$(dp/dt)^{1/2} = k_4 t + c_4 \qquad (4)$$

An example of this analysis is shown in Fig. 3.

Activation energies were calculated from the plots of log $k_{1,2,3}$ or $_4$ against $1/T$(°K.). The values of the constants are given in Tables I and II and derived energies in Table III.

TABLE II

REACTION CONSTANTS FOR INITIAL DECOMPOSITION OF GROUND CRYSTALS

Temp., °C.	$k_1 \times 10^3$, cm. min.$^{-1}$	$k_4 \times 10^4$, min.$^{-1}$
165	4.58	3.56
160	3.52	2.43
155	1.86	1.66
150	1.10	0.80
145	0.75	0.51
140	0.56	0.33

Pre-irradiated $Ba(MnO_4)_2$.—Pre-irradiation with ultraviolet light for 3 hr. at 10 cm. distance, and cathode rays for 10 min., had no effect on the ther-

TABLE III

ACTIVATION ENERGIES (KCAL./MOLE^{-1})

	Whole crystals			Ground crystals	
	Unirradiated	Irradiated 211 Mrad.	Irradiated 111 Mrad.	Unirradiated	Irradiated 211 Mrad.
E_1	..	..	..	33.1	..
E_2	36.1	37.0	39.2	36.9	33.1
E_3	29.6	37.9	37.2	34.2	40.7
E_4	..	..	..	24.9	..

mal decomposition. However, exposure to γ-rays caused an acceleration of the reaction. The effect of varying doses on whole crystals is shown in Fig. 4. Visual observation of a decomposing pre-irradiated crystal (dose 211 Mrad.) yielded the same information as for unirradiated crystals. No fracture took place during the acceleratory and decay periods.

Similar changes which occurred with pre-irradiated ground $Ba(MnO_4)_2$ are shown in Fig. 5.

The decomposition of unirradiated crystals was interrupted, the crystals irradiated, and then the decomposition continued. The resulting p–t plots are shown in Fig. 6.

Activation energies were calculated for whole crystals from the plot of log I *vs.* $1/T$(°K.), where I = time of commencement of the acceleratory period. The plots are shown in Fig. 7. The energies are 32.2 and 30.0 kcal./mole for doses of 211 and 111 Mrad., respectively.

Equation 3 was applicable to all the decay periods. The Prout–Tompkins equation, however, fitted over a limited region (Figs. 4 and 5). The values of the constants k_2 and k_3 are given in Table I. The activation energies calculated from these constants are given in Table III.

Discussion

Unirradiated $Ba(MnO_4)_2$.—The applicability of equation 2 over the acceleratory period for whole crystals suggests that during this stage reaction proceeds by the Prout–Tompkins mechanism.[3] As with $KMnO_4$ and $RbMnO_4$ it is assumed that prior to the commencement of acceleration surfaces of product material are formed, and when a critical thickness has been reached the lateral strains are sufficient to initiate acceleration of the reaction by the Prout–Tompkins mechanism. The flaking of the crystal probably is due to fracture along cleavage planes opened up when the crystal is suddenly raised from room temperature to 170°. The description of the decay period by the unimolecular law indicates that during this stage the probability of reaction is proportional to the mass of undecomposed material.

The study of the initial decomposition of ground $Ba(MnO_4)_2$ shows that acceleration of the reaction in the initial stage occurs by the growth of two-dimensional nuclei, since $n = 2$ in the power law. This probably takes place over the free surfaces and down grain boundaries. At the commencement of the decay period the nuclei interfere and reaction proceeds inwards on approximately spherical particles. Griffiths and Groocock[8] have shown that with such a reaction equation 4 should be applicable and that the activation energy calculated from the plot

(8) P. J. Griffiths and J. M. Groocock, *J. Chem. Soc.*, 3380 (1957).

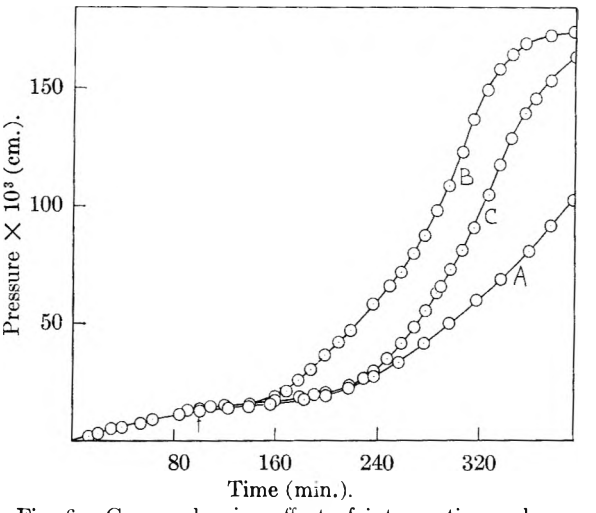

Fig. 6.—Curves showing effect of interrupting a decomposition and irradiating. Whole crystals of $Ba(MnO_4)_2$, decomposition temperature 160°. A, unirradiated; B, irradiated at t = 0, dose 111 Mrad.; C, interrupted at arrow, irradiated 111 Mrad. and decomposition continued with original t = 0 min. After interruption the time interval before C diverges from A is approximately the same as the "induction period" of B.

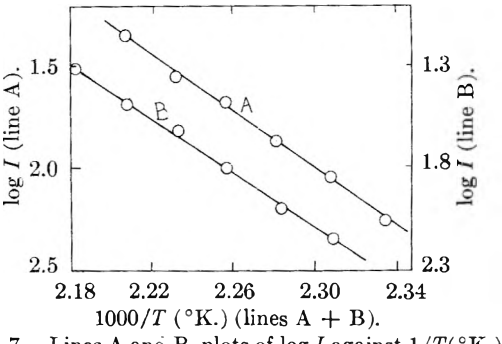

Fig. 7.—Lines A and B, plots of log I against $1/T$(°K.) for whole crystals of $Ba(MnO_4)_2$ pre-irradiated with doses of 211 and 111 Mrad., respectively.

of log k_4 *vs.* $1/T$(°K.) is equal to $^2/_3E_4$, where E_4 is the activation energy associated with the reaction. The value given in Table III is E_4. The main acceleratory reaction begins when a layer of product of critical thickness has been formed. Grinding the crystals causes artificial nucleation of the surfaces and the critical thickness is reached earlier than with whole crystals. This would explain the earlier commencement of the acceleration.

Using the value of 38.6 kcal./mole for the activation energy for whole crystals of $KMnO_4$ and Roginskii's[2] values for the temperatures at which maximum velocity is reached in the same time ($KMnO_4$, 255°; $Ba(MnO_4)_2$, 170°), the calculated heat of activation for $Ba(MnO_4)_2$ is 32.4 kcal./mole. The mean activation energy obtained here is 32.9 kcal./mole.

Pre-irradiated $Ba(MnO_4)_2$.—The thermal decomposition of pre-irradiated crystals of $Ba(MnO_4)_2$ resembles the decompositions of pre-irradiated permanganates of potassium,[9] rubidium[10] and silver,[11] except that the magnitude of the effect

(9) E. G. Prout, *J. Inorg. Nucl. Chem.*, **7**, 368 (1958).
(10) P. J. Herley and E. G. Prout, *ibid.*, in press.
(11) E. G. Prout and M. J. Sole, *ibid.*, **9**, 232 (1959).

แผนกหอสมุด กรมวิทยาศาสตร์

for a given dose is considerably less and no fracture occurs during the main acceleratory period. The irradiation effects for $KMnO_4$, $RbMnO_4$ and $AgMnO_4$ have been explained by assuming that the γ-rays produce displaced cations by the Compton and photoelectric effects, and by photoelectrons. Prior to acceleration of the reaction the point defects anneal and the energy released at the site of recombination of the interstitial and vacancy produces a center of decomposed material. Growth of this center creates strain in the crystal which ultimately causes fracture with the production of fresh surfaces over which reaction occurs and accelerates in a branching manner by the Prout–Tompkins mechanism.

The threshold energy for the displacement of barium atoms is less than the mean energy of the irradiation source ($\sim$ 1.1 Mev.)[12] and it is suggested that a mechanism similar to that proposed for the irradiated permanganates is applicable. Displacement would occur mainly by the photoelectric effect and by photoelectrons. The "irradiation nuclei" will grow by further interstitial-vacancy combination at their boundaries and/or by a reaction at the reactant/product interface. The activation energies obtained from the plots of log I *vs.* $1/T$(°K.) are close to the values of E_3 and E_4 for the interface reactions of ground crystals. This suggests that the growth of irradiation nuclei occurs mainly by an interface reaction. When the nuclei are of a critical size the strain at the interface will be sufficient to produce cracks in the reactant surface at the interface and reaction will accelerate by the Prout–Tompkins mechanism. The absence of fracture over the acceleratory period indicates that the irradiation nuclei do not create sufficient strain in the crystal to disrupt it. Thus the irradiation effect with $Ba(MnO_4)_2$ is due to the production of extra branching planes of reaction initiated at the nuclei, and not to the creation of new surfaces by fracture of the crystal. The former would produce the smallest irradiation effect and would explain why such massive irradiation doses are required.

The pressure of gas liberated prior to acceleration is slightly greater with irradiated than with unirradiated crystals, especially for the heaviest dose. This indicates the growth of additional centers of decomposition. The plots of Fig. 6 show that irradiation and thermal nuclei act independently. A similar result was found for the other permanganates.

For a given dose all the irradiation nuclei will not be formed at the same time since the combination of interstitials and vacancies will occur over the induction period in a manner described by Fletcher and Brown.[13] Consequently during the initial part of the acceleratory period new primary centers for the initiation of branching planes will become operative. Therefore the Prout–Tompkins equation should not be applicable over this time. This probably explains the limited fit of the equation to the p–t plots of all irradiated specimens.

The acceleratory regions of the p–t plots for whole and ground crystals with the same dose should be similar, since approximately the same number of irradiation nuclei are involved. The plots for these regions for doses of 211 and 111 Mrad. at 170° are practically superimposable after a shift of the origin. This is shown too by the agreement of the relevant values of k_2 in Table I.

Acknowledgment.—The authors wish to thank the C.S.I.R.(S.A.) for a grant to cover the cost of irradiations and for a scholarship held by P.J.H. during the investigation.

(12) G. H. Kinchin and R. S. Pease, *Rep. on Progr. Phys.*, **18**, 1, Physical Society, London (1955).

(13) R. C. Fletcher and W. L. Brown, *Phys. Rev.*, **92**, 585 (1953).

THE MERCURY-SENSITIZED RADIOLYSIS AND PHOTOLYSIS OF METHANE[1]

BY GILBERT J. MAINS AND AMOS S. NEWTON

Lawrence Radiation Laboratory, University of California, Berkeley, California

Received June 2, 1960

The radiation chemistry of methane at 260° using 4.5 Mev. electrons was studied in the absence and presence of mercury vapor. The mercury-sensitized photolysis of methane at 260° and the radiolysis of methane at 25° were studied for comparison. The condensation products were analyzed by mass spectrometry and the yields of H_2, C_2H_4, C_2H_6, C_3H_8, iso-C_4H_{10}, n-C_4H_{10}, iso-C_5H_{12}, neo-C_5H_{12} and neo-C_6H_{14} are reported in each case. The failure of mercury vapor to alter the product distribution by ion scavenging is taken as evidence for little contribution of ion–molecule reactions in methane radiolysis at 260°. The temperature coefficient of methane radiolysis was found too small to be accounted for in terms of thermal free radical reactions. A mechanism involving "hot" hydrogen atoms is proposed. A mechanism involving both ion–radicals and radicals also is consistent with the data.

I. Introduction

The condensation of hydrocarbons using ionizing radiation has been studied from early times.[2,3] In 1926, S. C. Lind[4] reported the α-particle radiolysis of methane to yield hydrogen and hydrocarbons as high as pentanes. Lind and Glockler[5] initiated a series of studies of the cathode ray radiolysis of

(1) This work was performed under the auspices of the U. S. Atomic Energy Commission.

(2) M. Berthelot, *Compt. rend.*, **68**, 1035 (1869).

(3) M. Berthelot, *ibid.*, **82**, 1357 (1876).

(4) S. C. Lind and D. C. Bardwell, *J. Am. Chem. Soc.*, **48**, 2335 (1926).

(5) For a review of this work, S. C. Lind and G. Glockler, "The Electrochemistry of Gases," John Wiley and Sons, Inc., New York, N. Y., 1939.

methane in 1927 and reported the production of saturated hydrocarbon liquids. Honig and Sheppard[6] reported similar products using deuterons as ionizing radiation. In 1957, Lampe[7] studied the radiolysis of methane using 2 Mev. electrons and determined the "*G*"-yields for hydrogen, ethane, ethylene, propane and butane.

A number of other studies concerning the mechanism of methane radiolysis have been made. Gevantman and Williams,[8] Meisels, Hamill and Williams,[9,10] and Yang and Manno[11] report studies using iodine and nitric oxide as free radical scavengers. The use of inert gases to sensitize the radiolysis of methane has been described.[9,10]

The photolysis of methane in the vacuum ultraviolet region has been reported to yield hydrogen and acetylene as major products, with smaller yields of ethane, ethylene and higher hydrocarbons.[12] The mercury-sensitized photolysis of methane was studied by Morikawa, Benedict and Taylor[13] who, noting the formation of higher hydrocarbons, proposed free radical reactions for the formation of propane.

These previous radiation studies have generally been carried out at a single temperature. Some have been concerned with the use of free radical scavengers. In this paper we report the radiation chemistry of methane in the presence of mercury vapor which is expected to behave as an ion scavenger through reactions similar to reaction 1.

$$RH^+ + Hg \longrightarrow Hg^+ + RH \qquad (1)$$

These asymmetric charge-transfer reactions[14] proceed with cross sections comparable to those for ion–molecule reactions[15] provided, of course, the ionization potential of RH exceeds 10.43 volts, the first ionization potential of mercury. The neutralization of Hg^+ results in the formation of excited states of mercury, Hg*, which would be expected to sensitize the free radical decomposition of methane by chemical quenching reactions

$$Hg^* + CH_4 \longrightarrow Hg + CH_3 + H \qquad (2)$$

as in the mercury-sensitized photolysis of methane. In order to compare directly the radiolysis experiments with photolysis results, the mercury sensitized photolysis of methane was also studied. Inasmuch as Yang and Manno[11] reported that higher hydrocarbons arose from radical processes, the radiolysis of methane at 25° was studied so that temperature coefficients of the product formation could be ascertained. The present study is an attempt to evaluate the importance of ion–molecule reactions which have been emphasized recently by many authors.[7,9,15]

II. Experimental

Phillips Research Grade methane was used without further purification. The principal impurity, ethane, constituted 0.13% of the total gas and a small amount of CO_2 was present. Instrument Grade mercury, Bethlehem Apparatus Company batch No. 290, was used without further purification.

In the radiolysis experiments 10 mm. of methane was loaded into a Pyrex bombardment cell which had been previously cleaned, baked and evacuated. If mercury was to be present in the experiment, about one ml. of liquid mercury was added prior to evacuation and methane addition. The Pyrex bombardment cell was a cylinder, 4.4 cm. in diameter and 7.6 cm. long. One end of the cell was a thin concave window through which the electron beam was directed; the other was fitted with a glass break-seal to facilitate analysis of the gaseous products. The methane-containing bombardment cell was inserted into an oven made by boring a 10.2-cm. diameter aluminum cylinder to an inside diameter slightly larger than the cell. This was heated by four 100 watt cartridge heating elements and was surrounded by a 5-liter heating mantle to minimize heat leaks. A Hallikainen resistance thermometer and control maintained the temperature of the aluminum oven to ± 1° at 260°. The oven-target cell system was positioned such that the electron beam from the accelerator snout would pass through a 0.0025 cm. aluminum foil window in the aluminum oven and through the thin glass window into the target cell. The entire assembly was electrically isolated for measurement of the electron current impingent on the cell. The electron source was a 4.5 Mev. microwave linear accelerator which produced 50 ma. square wave electron pulses of 5 microsecond duration at selected repetition rates of 7.5 to 30 pulses/second. After the bombardment the products were analyzed using a Consolidated Electrodynamics Corporation Model 21-103A mass spectrometer. The identities of all products from the butanes through the hexanes were checked by the mass spectra of the material collected in each of the respective peaks of a gas chromatographic separation of the condensable products. The 25° experiments were identical with the 260° experiments except the heating was omitted and an air jet cooled the aluminum cylinder during bombardment.

In the photolysis experiments 0.52 microliter of mercury was added to a quartz cell, 2.5 cm. in diameter and 15.2 cm. long. One end of the cell was fitted with a Pyrex break-seal for removal of the products. After the addition of liquid mercury the cell was evacuated, 10 mm. of methane added, and the cell sealed off. The methane-filled cell was inserted into an unsilvered quartz Dewar which was fitted internally with a 250 watt Nichrome coil heating element. The same resistance thermometer used in the radiolysis experiments controlled the temperature of the cell to ± 1° at 260°. Six 4-watt low pressure mercury lamps, located about the quartz Dewar, were used to irradiate the heated photolysis cell.

Blanks were run using both the radiolysis and photolysis procedures to show that pyrolysis in both the sealing-off operation and the heating operation was negligible.

III. Results and Discussion

1. General.—The results of the radiolysis experiments are given in Tables I, II and III. The results of the photolysis experiments are given in Table IV. The yields of products are in agreement with those reported by other investigators[7,10,11,16] when dose rates are considered. However, we cannot confirm the large yield of *n*-butane reported by Manno and Yang.[11] Since most vapor chromatographic columns do not resolve *n*-butane and neopentane it is possible that the peak reported by these authors as *n*-butane was actually a mixture. The product identification and yields at 25° are in good agreement with those reported by Wolfgang[16] from recoil tritium with the exception

(6) R. E. Honig and W. C. Sheppard, THIS JOURNAL, **50**, 119 (1946).

(7) F. W. Lampe, *J. Am. Chem. Soc.*, **79**, 1055 (1957).

(8) L. H. Gevantman and R. R. Williams, Jr., THIS JOURNAL, **56**, 569 (1952).

(9) G. G. Meisels, W. H. Hamill and R. R. Williams, Jr., *J. Chem. Phys.*, **25**, 790 (1956).

(10) G. G. Meisels, W. H. Hamill and R. R. Williams, Jr., THIS JOURNAL, **61**, 1456 (1957).

(11) K. Yang and P. J. Manno, *J. Am. Chem. Soc.*, **81**, 3507 (1959).

(12) W. F. Groth, *Z. physik. Chem.*, **B38**, 366 (1937).

(13) K. Morikawa, W. S. Benedict and H. S. Taylor, *J. Chem. Phys.*, **5**, 212 (1937).

(14) For example, see S. B. Karmopatro and T. P. Das, *ibid.*, **29**, 240 (1958).

(15) D. P. Stevenson and D. D. Schissler, *ibid.*, **23**, 1353 (1955).

(16) M. A. El-Sayed, P. J. Estrup and R. Wolfgang, THIS JOURNAL, **62**, 1356 (1958).

of *n*-pentane which we did not observe. Although no dosimetry was performed, a reasonable approximation of the *G*-yield of a product may be calculated by assuming $G_{H_2} = 5.7$ as found by Lampe.[7] The data of Lampe[7] and others[6] indicate that the yield of hydrogen is essentially linearly dependent upon the total dose in the region of 0–18% H_2. Although the microwave accelerator current drift during bombardment caused some error in estimating the total current passing through the sample, our data also indicate a linear dependence of hydrogen yield on total dose. Except for the fourth run in Table I and the third runs in Tables II and III, the yield of hydrogen varies linearly with the number of electron pulses to which the sample was exposed. It is significant that the yields of hydrogen observed in the high temperature experiments (Tables I, II and IV) are less than the yields calculated by a material balance. In the room temperature experiments, Table III, the reverse is observed. The production of unobserved liquid products in small amounts could account for the failure to attain a material balance at room temperature. Traces of these liquid products being bombarded on the walls of the reaction vessel could account for the excess hydrogen. However, the lack of hydrogen in the high temperature runs is more difficult to explain. It would be tempting to attribute the loss of hydrogen to diffusion into the glass walls of the reaction cells since similar hydrogen losses are observed in hydrogen discharge lamps. It also has been shown by Wolfgang[16] that recoil hydrogen is driven into the walls of the reaction vessel and only partially recovered by heating. This explanation of the hydrogen balance is not very satisfying but alternatives seem more untenable.

TABLE I

METHANE[a] RADIOLYSIS AT 260°

Total electron pulses	Percentage yield of products			
	3.6×10^4	7.2×10^4	21.6×10^4	21.6×10^4
H_2	1.14	3.94	6.41	8.38
C_2H_6	0.56	1.26	1.95	2.42
C_3H_8	.25	0.41	0.73	0.86
n-C_4H_{10}	.03	.05	.10	.12
Iso-C_4H_{10}	.11	.10	.24	.29
Neo-C_5H_{12}	.05	.12	.26	.25
Iso-C_5H_{12}	.03	.04	.07	.09
Neohexane	.03	.03	.12	.09
Diisopropyl	..	.01	..	.02
Heptane	..	.01	.03	.03
Ethylene	.19	.15	.21	.30
Isobutene	.04	.03	.02	.08
Isopentene	.02	.01	.02	.04
H_2 (calcd.)	2.55	3.90	7.13	8.78

[a] Initial pressure of methane was 10 mm. at 25° in all experiments.

2. Comparison of Radiolysis and Photolysis at 260°.—A very striking feature of the data is that the radiolysis of methane and the mercury-sensitized photolysis of methane yield identical products. Indeed, as was noted previously,[17] the nature and distribution of the products for these two different types of radiation were nearly identical. A more complete study indicates that the dose dependence

(17) Gilbert J. Mains and Amos S. Newton, *ibid.*, **64**, 511 (1960).

TABLE II

METHANE–MERCURY[a] RADIOLYSIS AT 260°

Total electron pulses	Percentage yield of product				
	2.7 $\times 10^3$	8.1 $\times 10^3$	8.1 $\times 10^3$	27 $\times 10^3$	36 $\times 10^3$
H_2	1.28	4.37	6.00	11.00	16.46
C_2H_6	0.81	2.10	2.65	3.64	5.07
C_3H_8	.22	0.47	0.54	1.03	1.41
n-C_4H_{10}	.04	.05	.06	0.19	0.22
Iso-C_4H_{10}	.06	.14	.12	.46	.52
Neo-C_5H_{12}	.02	.12	.22	.39	.59
Iso-C_5H_{12}	.03	.03	.04	.05	.18
Neohexane	.01	.04	.07	.20	.28
Biisopropyl	.01	..	..	.09	...
Heptane	<.01	.01	.02	.06	.11
Ethylene	.06	.20	.06	.24	.25
Isobutene	.02	.02	.04	.01	.19
Isopentene	.02	.01	..	.03	...
H_2 (calcd.)	2.15	5.00	6.08	11.89	16.55

[a] Initial pressure of methane was 10 mm. at 25° in all experiments. About one cc. of liquid mercury was added in all experiments.

TABLE III

METHANE[a] RADIOLYSIS AT 25°

Total electron pulses	Percentage yield of product				
	3.6 $\times 10^4$	10.8 $\times 10^4$	10.8 $\times 10^4$	21.6 $\times 10^4$	43.2 $\times 10^4$
H_2	1.00	3.22	4.49	7.63	16.29
C_2H_6	0.46	1.25	1.62	2.53	4.98
C_3H_8	.09	0.23	0.31	0.50	0.94
n-C_4H_{10}	< .01	.05	.05	.06	.17
Iso-C_4H_{10}	.02	.03	.05	.09	.17
Neo-C_5H_{12}	< .01	.02	.03	.04	.06
Iso-C_5H_{12}	....	.02	.03	.04	.11
Neohexane	.01	.03	.05	.06	.12
Biisopropyl	....	.04	..	.02	.13
Heptane	....	.02	.01	.03	.08
Ethylene	.02	.04	.04	.06	.10
Isobutene	....	<.01	.03	.01	.04
Isopentene	....	....	..	.03	.07
H_2 (calcd.)	0.86	2.70	3.40	5.04	11.05

[a] Initial pressure of methane was 10 mm. at 25° in all experiments.

TABLE IV

METHANE–MERCURY[a] PHOTOLYSIS AT 260°

Irradiation time (lamp-min.)	Percentage yield of product				
	3	12	12	24	90
H_2	2.08	4.83	7.30	10.61	16.83
C_2H_6	1.17	1.48	1.79	1.53	1.59
C_3H_8	0.18	0.27	0.32	0.18	0.26
n-C_4H_{10}	.02	.02	.02	.02	...
Iso-C_4H_{10}	.04	.13	.20	.20	.52
Neo-C_5H_{12}	.10	.58	.84	1.90	3.32
Iso-C_5H_{12}	<.01	.02	.02	.02	.06
Neohexane	.02	.09	.11	.27	.40
Heptane	<.01	.02	.02	.03	.07
Ethylene	.06	.07	..	...	.08
Isobutene	<.01	.01	.02	...	...
Isopentene	<.01	.01	.02	...	.05
H_2 (calcd.)	2.38	5.68	7.36	11.76	19.83

[a] Initial pressure of methane was 10 mm. at 25° in all experiments. 0.52 microliter of liquid mercury was added in each experiment.

of the products resulting from radiolysis differs significantly from the dose dependence of the products resulting from photolysis. It is evident from a consideration of Table IV that a steady state apparently is attained in the photolysis experiments and the concentrations of the lower hydrocarbon products are independent of the extent of decomposition after a few per cent. hydrogen is formed. The net effect of extended photolysis is to build up only higher hydrocarbon products. It is further evident from Tables I and II that a steady state is not attained in the radiolysis experiments and extended radiolysis continues to build up all condensation products. Significantly, no difference in the nature of the products of photolysis and radiolysis was observed in the range of decompositions studied.

A free radical mechanism has been proposed[13] for the formation of ethane and propane in the mercury-sensitized photolysis of methane. It seems reasonable to generalize this mechanism to account for higher hydrocarbon products. The relative rates

Free radical formation in photolysis

Primary	$Hg^*(^3P_1) + CH_4 \longrightarrow Hg + CH_3 + H$	(2)
	$Hg^*(^3P_1) + RH \longrightarrow Hg + R + H$	(3)
	$Hg^*(^3P_1) + H_2 \longrightarrow Hg + H + H$	(4)
Secondary	$H + CH_4 \longrightarrow H_2 + CH_3$	(5)
	$H + RH \longrightarrow H_2 + R$	(6)
	$CH_3 + RH \longrightarrow CH_4 + R$	(7)

Product formation in photolysis

$2CH_3 \longrightarrow C_2H_6$	(8)
$H + H \xrightarrow{M} H_2$	(8a)
$CH_3 + R \longrightarrow RCH_3$	(9)
$C_2H_5 + R \longrightarrow RC_2H_5$	(10)

of reaction 2, 3 and 4 may be estimated from the cross-sections for chemical quenching.[18] Because the cross-section for reaction 4 is about a factor of one hundred larger than the cross-section for reaction 2, it is clear that reaction 4 will be more important than reaction 2 after one per cent. hydrogen has been formed. Reaction 3 also becomes competitive with reaction 2 in these studies because, in some cases, sufficient products are built up for this to occur. Since the secondary reactions 5, 6 and 7, totally or partially involve activation energies of the order of 8 to 10 kcal./mole whereas the chemical quenching reactions involve little or no activation energy, reaction 3 initially must be faster than reaction 6.[19] This is especially true in the experiments reported here because of the very high relative concentration of $^3P_1$ Hg atoms near the walls of the reaction vessel. However, because the quantum yield of methane decomposition exceeds unity[13] at 260° it is clear that reaction 5 must become important very rapidly. The steady state concentrations of ethane, propane and *n*-butane are therefore expected to depend upon both the concentration of hydrogen atoms and upon the concentration of excited mercury atoms. The conclusion that reaction 6 is appreciable compared to reaction 3 requires that the rapid build up of neopentane must be ascribed to a low cross-section for hydrogen abstraction from neopentane as well as a low cross-section for chemical quenching by neopentane. Inasmuch as neither cross-section is known absolutely with accuracy, it is impossible to decide whether reaction 3 or reaction 6 predominates in these experiments. Steady state calculations assuming reaction 3 to predominate indicate the ratio of ethyl radicals to methyl radicals to be 0.16, a value which is consistent with the steady state concentration of ethane, propane and *n*-butane.

From the nature and distribution of the photolysis products we conclude that the mechanism of product build-up must proceed primarily by one carbon additions. However, the presence of *n*-butane and isopentane may be evidence for a two carbon branching step at the ethane, with possible branching at propane or isobutane. An overall mechanism could be represented as

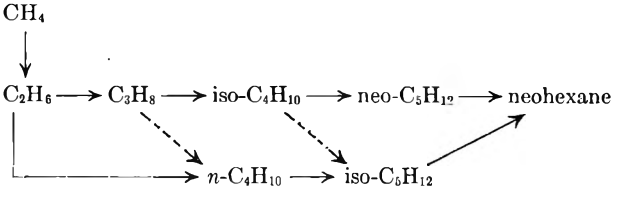

The build up of olefins can be attributed to radical disproportionation reactions, 11, 12 and 13. A

$H + C_2H_5 \longrightarrow C_2H_4 + H_2$	(11)
$CH_3 + C_2H_5 \longrightarrow C_2H_4 + CH_4$	(12)
$C_2H_5 + C_2H_5 \longrightarrow C_2H_4 + C_2H_6$	(13)

consideration of the ratio of the rates of combination to disproportionation,[20] leads to the conclusion that most of the ethylene arises from reactions 11 and 12 with reaction 11 being the most important. Rabinovitch[21] has recently reported the ratio of the rate constant for reaction 11 to the rate constant for the corresponding combination to form excited ethane to be 0.05. Inasmuch as the yield of ethane from the reaction of an ethyl radical and a hydrogen atom is not known, in the experiments reported here, the yield of ethylene from reaction 11 cannot be estimated from this ratio of rate constants.

It may be concluded that free radical processes, as noted above, can account for all of the products of the photolysis. Furthermore, the higher products are built up more rapidly in the photolysis system than in the radiolysis system at 260°. Therefore, we cannot agree with statements[7,10] which are based upon reaction rate considerations, that free radical processes cannot account for the radiolysis of methane. It is clear that the radiation chemistry of methane at 260° can be accounted for by free radical processes. It is not possible to exclude a free radical mechanism for the radiolysis of methane at 260° by means of arguments based upon the nature and distribution of the products.

3. Mercury-sensitized Radiolysis at 260°.—

(18) K. J. Laidler, "Chemical Kinetics of Excited States," Oxford Univ. Press, New York, N. Y., 1955.

(19) Some of the hydrogen atoms may be translationally "hot." Reaction 4 is exothermic by 9 kcal./mole and most of this energy will be carried by the hydrogen atoms.

(20) A. F. Trotman-Dickenson, "Free Radicals," Methuen, London, 1959.

(21) B. S. Rabinovitch, D. H. Dills, W. H. McLain and J. H. Current, *J. Chem. Phys.*, **32**, 493 (1960).

A comparison of Tables I and II indicates that the presence of excess mercury vapor (~100 mm. at 260°) did not alter the distribution of products in the radiolysis of methane. That the mercury transferred its absorbed energy to the methane is obvious from a comparison of the first column of Table I with the last column of Table II. In both experiments the reaction vessels were subjected to approximately the same amount of radiation. In the absence of mercury only 1.14% hydrogen was obtained; in the presence of mercury 16.46% hydrogen was obtained. Inasmuch as the ionization potential of mercury is considerably less than the ionization potential of methane (and higher hydrocarbon products up to isobutane), the mechanism of energy transfer cannot involve charge transfer. Multiply-charged mercury ions, Hg^{+2}, Hg^{+3}, etc., and excited ions, $(Hg^{+})^*$, are expected to be removed by collision with unexcited mercury atoms. Therefore, it would appear that reactions 2, 3 and 4, and possibly analogous reactions involving higher excited states of atomic mercury, are the mechanism of energy transfer from the mercury to the methane or to reaction products.

Because of the low ionization potential of mercury and because the ratio of mercury to methane was over five in these experiments, it is reasonable to conclude that the mercury vapor would effectively scavenge H_2^+, H^+, CH_4^+, $C_3H_8^+$ and $C_4H_{10}^+$ formed in the system. Rudolph and Melton[22] have shown that energy alone is an insufficient criterion for charge transfer reactions in competition with ion–molecule reactions. However in the systems studied by Rudolph and Melton both charge transfer and ion–molecule reactions could occur as the result of the collision. In the systems reported here an ion must survive an average of five collisions with mercury atoms before the possibility of an ion–molecule reaction with methane presents itself. Inasmuch as the probable removal of these ions does not alter the nature or distribution of radiolysis products it would appear that these intermediates are either unimportant in the radiolysis of methane at 260°, or that they undergo reactions very similar to free radical reactions. The latter alternative has found recent support in the studies of Martin and Melton.[23] If the principal reaction of CH_4^+ in these systems is

$$CH_4^+ + RH \longrightarrow R + CH_5^+ \qquad (14)$$

and this reaction is chemically similar to the analogous free radical reaction 7, then the small effect of mercury on the product distribution is understandable. The net effect of mercury vapor would be the suppression of reaction 14 and the acceleration of reaction 7. Since these two reactions are presumably chemically similar, the product distribution would be expected to show only small changes owing to the increased dose rate in the presence of mercury.

It must be noted that CH_3^+, an important ion in the mass spectrum of methane, would not be scavenged by mercury. However, this ion is presumably derived in whole or in part from the unimolecular dissociation of CH_4^+ in the mass spectrometer ionization chamber. Since the ion collection time in a mass spectrometer is about 10^{-6} seconds while the calculated lifetime of CH_4^+ in the experiments reported here is about 10^{-9} seconds, it seems reasonable to conclude that CH_3^+ is less abundant than CH_4^+. Should CH_3^+ survive neutralization for an average of five collisions it would be expected to undergo an ion–molecule reaction of the type depicted as reaction 17, *vide infra*, as suggested by Meisels, Hamill and Williams.[10] Inasmuch as $C_2H_5^+$ would also not be scavenged by mercury vapor, the possibility of further ion–molecule reactions involving $C_2H_5^+$ cannot be ruled out. In view of the probable reduced importance of CH_3^+ in these experiments and the ten-fold acceleration of the free radical reaction by the mercury vapor without altering the product distribution, it seems probable that ion–molecule reactions do not significantly contribute to the radiolysis of methane at 260°. Manno and Yang[12] estimate that 15% of the ethane and propane and none of the higher products arise by non-free radical processes. If the free radical mechanism is characterized by a temperature coefficient of 8 kcal./mole (a typical activation energy for hydrogen abstraction) and no temperature coefficient is ascribed to the non-free radical mechanism, the latter, would be expected to constitute less than 0.1% to the reaction at 260°. If such a calculation and its assumptions are accepted, the conclusions of this section are in accord with the results of Manno and Yang.

4. Radiolysis at 25°.—The radiolysis yields of propane and higher hydrocarbons are markedly less in the 25° runs given in Table III than in comparable runs at 260° in Table I. The yields of propane and butanes are reduced by about a factor of two or three at 25°. The yield of neopentane is reduced by a factor of about five. These temperature coefficients are too small to be attributed to a thermal radical mechanism involving hydrogen abstractions such as reactions 5, 6 and 7. It appears necessary to postulate that all or part of the radiolysis of methane must proceed *via* a mechanism with a temperature coefficient corresponding to an activation energy of two kcal./mole or less. As the results of this investigation and the results of Manno and Yang[11] indicate that a significant fraction of the radiolysis reaction proceeds *via* a thermal free radical path, it seems reasonable to propose that two radiolysis mechanisms, a thermal radical mechanism and a temperature independent mechanism, are in competition. The former dominates at 260°; the latter becoming significant only at lower temperatures.

One possible temperature-independent mechanism which requires consideration is the ion-molecule mechanism, *via*

$$CH_4 \rightsquigarrow CH_4^+ + e^- \qquad (15)$$

$$CH_4^+ \longrightarrow CH_3^+ + H \qquad (16)$$

$$CH_3^+ + CH_4 \longrightarrow C_2H_5^+ + H_2 \qquad (17)$$

There are several reasons for questioning the importance of this mechanism. No reactions analogous to reaction 17 have been found which yield hydrocarbon products as high as the pentanes yet

(22) P. S. Rudolph and C. E. Melton, *J. Chem. Phys.*, **32**, 586 (1960).
(23) T. W. Martin and C. E. Melton, *ibid.*, **32**, 700 (1960).

such reactions are required to explain the low temperature coefficients of these higher products. Furthermore, both Meisels, Hamill and Williams[10] and Manno and Yang[11] reject an ion–molecule mechanism for these higher hydrocarbon products. If CH_3^+ arises by unimolecular thermal decomposition of CH_4^+, this mechanism should also exhibit a temperature coefficient. Melton and Rudolph[24] have shown that the relative abundance of CH_3^+ in the mass spectrum of methane is reduced by a factor of two when 5.1 Mev. α-particles are used to ionize methane at room temperature. While reactions 15, 16 and 17 cannot be ruled out as contributing to the production of ethane in the radiolysis of methane, similar ion–molecule sequences cannot account for higher hydrocarbon products.

Another temperature-independent mechanism, proposed by Gevantman and Williams[8] and recently supported by Davison,[25] involves translationally "hot" hydrogen atoms. Thus the sequence of hydrogen abstraction reactions, (5) and (6), can be replaced by their "hot" analogs, *viz.*

$$H^* + CH_4 \longrightarrow CH_3 + H_2 \qquad (5')$$
$$H^* + RH \longrightarrow R + H_2 \qquad (6')$$

The evidence for "hot" hydrogen atoms in systems subjected to ionizing radiation is manifold. The Doppler broadening of atomic hydrogen spectra in hydrogen discharge lamps is well known.[26] The distortion of the mass one peak in the mass spectra of hydrocarbons may be interpreted as evidence for "hot" ions and by inference for "hot" neutral

$$RH^+ + e^- \longrightarrow R + H^* \qquad (18)$$

species. "Hot" hydrogen atoms would be expected from the dissociative neutralization of hydrocarbon ions, *viz.*, especially in methane where little of the 8.5 e.v. liberated could be accommodated in vibrational degrees of freedom. Yang and Gant[27] have postulated that "hot" tritium atoms occur in the β-induced tritium labeling of ethylene and in the recoil labeling of ethylene by neutralization of hydrogen molecule ions. Probably some "hot" hydrogen atoms also arise from direct action of ionizing radiation on the hydrocarbon molecule. Estrup and Wolfgang[28] have shown that translationally hot tritium atoms are responsible for the labeling of methane in the presence of scavengers, I_2, Br_2 and NO. The series of inert gases, He, Ne, Ar, Xe were shown to moderate the hot tritium atoms in the order given.

A "hot" hydrogen atom mechanism seems reasonable based upon the similarities between the radiolysis and photolysis results already discussed. If, for example, 50% of the hydrogen atoms in the room temperature radiolysis are translationally "hot," the failure of Manno and Yang to scavenge them with NO is understood. These "hot" atoms are poorly moderated by H_2, methane and ethane[29] and would not be expected to thermalize rapidly by elastic collisions. If only 10% of these "hot" hydrogen atoms abstract hydrogen from methane, the production of ethane in the presence of NO can be explained. Hamill and Magee[30] have compared "hot" and thermal hydrogen atom abstraction reactions and deduced a "probability factor" of 0.04 and 0.16 for the hydrogen abstraction reaction from methane and ethane, respectively, by an 0.8 e.v. deuterium atom. The equations developed by these authors indicate that a much larger "probability factor" is to be expected for hydrogen atoms arising from reaction 18. Since reactions 5′ and 6′ could effectively occur at almost every collision, the rapid build up of higher hydrocarbon products at room temperature is readily understood. Recently Williams[31] described the radiolysis of methane by electrons of energy near or below the ionization potential of methane. The distribution of products found was similar to that reported here. While Williams did not propose a mechanism, the "hot" hydrogen atom mechanism suggested here is in accordance with his results.

It should be noted that the experiments described here do not eliminate reactions of radical molecule ions such as reaction 14 as possible free radical precursors. Similarly the neutralization of CH_5^+ must result in either a methyl radical and hydrogen, a methyl radical and two hydrogen atoms, or methane and a hydrogen atom. The addition of mercury as an ion scavenger may simply transfer the role of radical precursor from the molecule ion to the excited mercury atom through reactions 1 and 2. A mechanism involving molecule ions as radical precursors can be used to explain the reduction of methane radiolysis in the presence of xenon scavenger[25] and the reduction in higher products by the addition of NO or iodine.[8–10] One can also use reaction 14 to explain the acceleration of methane radiolysis in the presence of argon or krypton.[9,10]

It is clear that further experiments will be necessary to establish uniquely the role of reaction 14 in the radiolysis of methane.

Acknowledgments.—The authors are grateful to Mrs. Sylvia Waters for reading the mass spectra, to Mr. Aldo F. Sciamanna for making the mass spectrometer runs and for carrying out a few photolysis experiments, and to Mr. William Everett for aiding with the electron irradiations.

(24) C. E. Melton and P. S. Rudolph, private communication.

(25) W. H. T. Davison, The Chem. Soc. Special Publication No. 9, 151 (1957).

(26) G. Series, "Spectrum of Atomic Hydrogen," Oxford Univ. Press, New York, N. Y., 1957.

(27) K. Yang and P. L. Gant, *J. Chem. Phys.*, **31**, 1589 (1959).

(28) P. J. Estrup and R. Wolfgang, *J. Am. Chem. Soc.*, **82**, 2661 (1960).

(29) R. J. Carter, W. H. Hamill and R. R. Williams, Jr., *ibid.*, **77**, 6457 (1955).

(30) J. L. Magee and W. H. Hamill, *J. Chem. Phys.*, **31**, 1380 (1959).

(31) R. R. Williams, Jr., THIS JOURNAL, **63**, 776 (1959).

ULTRAVIOLET SPECTRA AND ACID DISSOCIATION CONSTANTS OF SOME PYRAZYLMETHYL KETONES

BY NASEEM NAQVI,[1] E. L. AMMA, QUINTUS FERNANDO[2] AND ROBERT LEVINE

Contribution No. 1074 from the Department of Chemistry, University of Pittsburgh, Pittsburgh 13, Pennsylvania

Received June 10, 1960

The ultraviolet spectra of phenyl pyrazylmethyl ketone (phenacylpyrazine), and the three isomeric pyridyl pyrazylmethyl ketones have been determined in aqueous solutions of varying *p*H and in methanol. Empirical assignments of electronic transitions have been made and used to determine qualitatively the position of the keto–enol equilibrium in each of these compounds. The acid dissociation constants of these compounds have been determined spectrophotometrically and potentiometrically. The concentrations of the keto and enol tautomers of the 2, 3 and 4-pyridyl derivatives in aqueous solutions, in the *p*H range 1–12, have been calculated. The rate constants for keto and enol formation in neutral aqueous solutions have been determined for the three isomeric pyridyl compounds.

In earlier work carried out in this Laboratory a series of ketones containing the pyrazylmethyl group was prepared.[3] Since these ketones are structurally analogous to β-diketones, it is not too surprising that they form chelates with copper(II). It can be seen from structures I and II that a β-diketone I differs from a pyrazylmethyl ketone II, in that a carbonyl group in the former class of compounds is replaced by an azomethine function in the latter. In structure II where R is the 2-

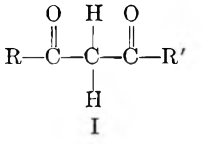

I

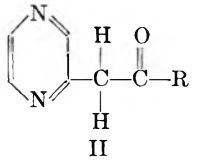

R = C_6H_5; -2, -3 and 4-C_5H_4N

II

pyridyl radical, it is possible for chelation with a metal ion to take place between either the pyridine nitrogen or a pyrazine nitrogen and the enolic hydroxyl group. Two factors would appear to influence whether the pyridine nitrogen or the pyrazine nitrogen is involved in chelate formation. These are (1) a steric factor and (2) the basicities of the nitrogen atoms in the pyridine and pyrazine rings. It was therefore of interest to determine the acid dissociation constants as well as the ultraviolet spectra of the pyrazylmethyl ketones. In this work the various bands in the ultraviolet spectra of these compounds have been assigned empirically to the appropriate molecular species present in solution. Some information concerning the nature of the bonding in the metal complexes of these compounds could be obtained from a qualitative interpretation of the ultraviolet spectra of the ligand molecules along with that of the metal complexes. For example, if π-bonding in the metal complexes is a significant factor, its effect should be readily observable in the spectra of the complexes. It is to be expected just as in the case of the β-diketones, that the compounds having structure II will exist in solution as an equilibrium mixture of the keto and enol forms. The variation of keto and enol concentrations with solvent for each compound can be ascertained by a study of the ultraviolet spectra.

(1) Abstracted from a thesis submitted by N. Naqvi in partial fulfillment of the requirements for the degree of Doctor of Philosophy.

(2) All inquiries about this paper should be addressed to this author.

(3) J. D. Behun and R. Levine, *J. Am. Chem. Soc.*, **81**, 5157 (1959).

Experimental

Preparation and Purification of Compounds.—A detailed description of the preparation of the compounds used in this work has been published.[3] The pure enol form of phenacylpyrazine was prepared by dissolving the substance in 20% aqueous sodium hydroxide and neutralizing rapidly with hydrochloric acid to a *p*H of 7. The freshly precipitated compound was dissolved in benzene, and the solution shaken with Florisil, filtered and cooled. The product thus obtained had a melting point of 82–83°.

The 2-pyridyl and 3-pyridyl pyrazylmethyl ketones were recrystallized from a mixture of ether and petroleum ether and had melting points 87–88° and 129–130°, respectively. The 4-pyridyl compound was recrystallized from a mixture of benzene and petroleum ether and had a melting point of 142–143°. A sample of methylpyrazine was kindly supplied by Wyandotte Chemicals Corporation, Wyandotte, Michigan.

Spectrograde solvents were used in obtaining the ultraviolet spectra. All other compounds used in this work were of reagent grade purity.

Ultraviolet Spectra.—The ultraviolet spectra of all solutions were recorded with a Cary Model 14 spectrophotometer at 25 ± 1°, using a pair of stoppered 1 cm. silica cells. Measurements were made on solutions ranging in concentration from 3×10^{-5} to 5×10^{-5} *M*. Standard solutions of $HClO_4$ were used for solutions of *p*H less than 2 and carbonate-free sodium hydroxide for solutions of *p*H greater than 11. In the intermediate range of *p*H, buffer solutions of constant ionic strength 0.1 were used. The buffer components were CH_3COOH and CH_3COONa, Na_2HPO_4 and KH_2PO_4, H_3BO_3 and NaOH, together with appropriate quantities of KCl.

The *p*H values of the aqueous solutions were measured with a Beckman Model G *p*H meter equipped with an external glass-saturated calomel electrode pair and calibrated with standard buffer solutions at *p*H 4.00 and 7.00.

Potentiometric Titrations.—A weighed quantity of the pyrazylmethyl ketone was transferred to a water-jacketed vessel thermostated at 25.0°, and dissolved in a measured volume of standard $HClO_4$. The resulting solution was degassed with nitrogen and titrated with carbonate-free sodium hydroxide in an atmosphere of nitrogen. A Beckman Model G *p*H meter with a glass-saturated calomel electrode pair, calibrated with buffer solutions at *p*H 4.00 and 7.00, was used for *p*H measurements. In the case of phenacylpyrazine, the titration had to be carried out in a 50% v./v. water–dioxane mixture, since the compound was not sufficiently soluble in aqueous solutions.

Results

Ultraviolet Spectra.—The spectra of acetophenone and methylpyrazine were obtained in various solvents and the results are given in Table IV. The spectrum of acetophenone consists of two main bands at ~240 and 280 mμ. In addition there is a very weak, broad band at 320 mμ. Methylpyrazine shows two principal regions of absorption, ~270

TABLE I

ACID DISSOCIATION CONSTANTS OF PYRAZYLMETHYL KETONES DETERMINED POTENTIOMETRICALLY AT 25°

Compound	pK'	pK_1'
Phenacylpyrazine	..	12[a]
2-Pyridyl pyrazylmethyl ketone	2.98	10.21
3-Pyridyl pyrazylmethyl ketone	3.42	10.53
4-Pyridyl pyrazylmethyl ketone	4.17	9.72

[a] Determined in 50% v./v. water–dioxane.

TABLE II

ACID DISSOCIATION CONSTANTS OF PYRIDYL PYRAZYLMETHYL KETONES DETERMINED SPECTROPHOTOMETRICALLY AT 25 ± 1°

Methyl ketone	K_t	K_t'	pK_{1e}	pK_{1k}	pK_{2e}	pK_{2k}
2-Pyridyl pyrazyl-	0.2	3.8	3.1	1.9	9.4	10.1
3-Pyridyl pyrazyl-	.95	6.3	3.5	2.7	10.2	10.2
4-Pyridyl pyrazyl-	.3	4.6	4.3	3.1	9.1	9.6

TABLE III

RATE CONSTANTS FOR KETO–ENOL FORMATION AT 27 ± 0.5° AND pH 7.0

Compound	k_1 (sec.$^{-1}$)	k_2 (sec.$^{-1}$)
2-Pyridyl pyrazylmethyl ketone	3.8×10^{-3}	8.8×10^{-4}
3-Pyridyl pyrazylmethyl ketone	4.8×10^{-3}	4.4×10^{-3}
4-Pyridyl pyrazylmethyl ketone	3.5×10^{-3}	1.1×10^{-3}

TABLE IV

ULTRAVIOLET SPECTRA OF ACETOPHENONE AND METHYLPYRAZINE[a]

	Acetophenone		Methylpyrazine	
Solvent	Absorption maxima (mμ)	Assignment	Absorption maxima (mμ)	Assignment
95% Methanol	242 (4.09)	π-π_2*	266 (3.79)	π-π*
	280 (2.97)	π-π*	273 (3.74)	(doublet)
	320 (V.W.)	n-π_1*	308 (V.W.)	n-π*
2.0 M $HClO_4$	246 (4.09)	π-π_2*	276 (3.86)	π-π*
	283 (3.07)	π-π*		
1.0 M NaOH	244 (4.11)	π-π_2*	266 (3.83)	π-π*
	290 (B)	π-π_1*	272 (3.82)	(doublet)
			290 (W.S.)	n-π*

[a] The values in parentheses are log molar extinction coefficients. V.W. = very weak; B = broad; S = shoulder.

TABLE V

ULTRAVIOLET SPECTRA OF PHENACYLPYRAZINE[a]

Solvent	Absorption maxima (mμ)	Assignment
95% Methanol	247 (3.99)	π-π_2*
	265 (3.93)	π-π*
	271 (S)	
	310 (3.17)	π-πE_1*
	360 (3.18)	π-πE_2*
1.0 M $HClO_4$	250 (4.11)	π-π_2*
	273 (4.07)	π-π*
1.0 M NaOH	239 (4.43)	π-π_2*
	271 (3.70)	π-π*
	330 (4.03)	π-πE_1*
	383 (4.10)	π-πE_2*

[a] The notation π-π_{E_1}* and π-π_{E_2}* refer to bands of the enol form derived from π-π^*_2 and the π-π* bands of the keto form.

mμ and ~310 mμ. If phenacylpyrazine existed only in the keto form there would be no appreciable interaction between the benzene and pyrazine rings. Hence, the spectrum of phenacylpyrazine would be a composite of the spectra of methylpyrazine and acetophenone. The observed bands at 247, ~270 and 310 mμ in 95% methanol are in agreement with the above conclusion.

The ultraviolet spectrum of the 2-pyridyl derivative in various solvents and at various pH values are given in Table VI. The spectra of phenacylpyrazine and the 2-pyridyl derivative are very similar in 95% methanol and in 1.0 M NaOH, but it is of considerable significance that the spectra are different in 0.1 M $HClO_4$ solution. Indeed a general similarity of the pyrazylmethyl ketones is to be expected, and the purpose of examining phenacylpyrazine was to gain insight into the more complex pyridyl derivatives having more than one basic center.

In 95% methanol, 2-pyridyl pyrazylmethyl ketone exhibits four prominent bands at 234, ~307 and 356 mμ. The spectra of the 3-pyridyl derivative in 95% methanol and in solutions of pH <12 are very similar to the spectra of the 2-pyridyl compound. However, in 1.0 M base the spectra of the two compounds are different, since the 3-pyridyl derivative is cleaved in solutions of pH values greater than 12. This cleavage is readily observable since the absorption at 240 mμ disappears and simultaneously the long wave length enol bands decrease in intensity. The general features of the spectra of the 4-pyridyl compound are quite similar to those of the preceding compounds.

Potentiometric Determination of Acid Dissociation Constants.—The equilibria involving pyrazylmethyl ketones in aqueous solutions is complicated by keto–enol tautomerism. The neutral forms of these compounds which exist as the keto or enol forms are represented by B_k and B_e, respectively. The monoprotonated forms of the 2-, 3- and 4-pyridyl derivatives can also exist as the keto and enol forms and are designated by B_kH^+ and B_eH^+, respectively. The anionic species of any of these compounds can exist in only one form, B^-.

The apparent dissociation constants K' and K_1', which can be measured potentiometrically are defined as follows (all terms in brackets represent molar concentrations).

$$K' = \frac{[B_e + B_k][H^+]}{[B_eH^+ + B_kH^+]} \quad (1) \qquad \text{and} \qquad K_1' = \frac{[B^-][H^+]}{[B_e + B_k]} \quad (2)$$

Values of K' and K_1' were calculated from a number of points on the titration curves using the equations

$$K' = \frac{[T_R - ClO_4^- + H^+ + Na^+][H^+]}{[ClO_4^- - H^+ - Na^+]} \quad (3)$$

$$K_1' = \frac{[Na^+ - OH^- - ClO_4^-][H^+]}{[T_R - Na^+ + OH^- + ClO_4^-]} \quad (4)$$

The terms Na^+, H^+, OH^- and ClO_4^- refer to the molar concentrations of these ions, and T_R is the total molar concentration of the pyrazylmethyl ketone used. Table I gives the average values obtained for pK' and pK_1' from a number of potentiometric titrations and calculations using the above equations. The maximum uncertainty in these pK values is ±0.05.

Spectrophotometric Determination of Acid Dissociation Constants.—In acid solutions containing the 2-, 3- and 4-pyridyl derivatives, the equilibria (5)–(8) must be considered, if the protonation of the pyrazine ring which occurs at high acidities is neglected.

TABLE VI

ULTRAVIOLET SPECTRA OF PYRAZYLMETHYL KETONES

2-Pyridyl		3-Pyridyl		4-Pyridyl		
Solvent	Absorption maxima (mμ)	Solvent	Absorption maxima (mμ)	Solvent	Absorption maxima (mμ)	Assignment
95% Methanol	234 (3.68)	95% Methanol	233 (3.68)	95% Methanol	234 (3.56)	π-π_2^*
	267 (S) }		269 (3.82) }		265 (S) }	π-π^* and
	271 (3.87) }		}		271 (3.73) }	π-π_1^*
	307 (3.61)		305 (3.61)		300 (3 86)	π-$\pi_{E_1}^*$
	358 (3.81)		355 (3.81)		357 (4 11)	π-$\pi_{E_2}^*$
0.1 *M* $HClO_4$	230 (3.62)	0.1 *M* $HClO_4$	222 (3.76)	0.1 *M* $HClO_4$	230 (3 55)	π-π_2^*
			258 (S)		256 (3.86)	
	266 (3.94) }		264 (4.05) }		264 (3.85) }	π-π^* and
	271 (W.S.) }		270 (S = 4.01) }		271 (S) }	π-π_1^*
	320 (3.71)		300 (3.51)		328 (3.68) }	π-$\pi_{E_1}^*$
	368 (4.08)		350 (3.56)		368 (4.10) }	π-$\pi_{E_2}^*$
1.0 *M* NaOH	243 (4.03)	NaOH at *p*H 11.0	236 (3.93)	NaOH at *p*H 12.0	241 (3.93)	π-π_2^*
	325 (B.S.)		320 (3.66)		338 (3.89)	π-$\pi_{E_1}^*$
	388 (4.23)		380 (3.82)		386 (4.16)	π-$\pi_{E_2}^*$
Buffer at *p*H 7.0	233 (3.91)	Buffer at *p*H 7.0	232 (3.98)	Buffer at *p*H 7.0	220 (3.98)	π-π_2^*
	265 (S) }		250 (S) }		}	π-π^* and
	271 (4.12) }		269 (4.05) }		270 (3.94) }	π-π^*
	305 (2.24) V.W.		305 (2.16) V.W.		303 (3.39)	π-$\pi_{E_1}^*$
	355 (2.94) W.				350 (3.24)	π-$\pi_{E_2}^*$

$$B_kH^+ \overset{K_{1k}}{\rightleftharpoons} B_k + H^+ \quad (5)$$

$$B_eH^+ \overset{K_{1e}}{\rightleftharpoons} B_e + H^+ \quad (6)$$

$$B_k \overset{K_t}{\rightleftharpoons} B_e \quad (7)$$

$$B_kH^+ \overset{K_t'}{\rightleftharpoons} B_eH^+ \quad (8)$$

The subscripts k and e refer to the keto and enol forms, respectively, and B represents the organic compound. In the case of phenacylpyrazine, protonated species are not present in the *p*H range investigated since protonation of the pyrazine ring takes place at low *p*H values.

If ϵ is the observed molar absorbance of an aqueous solution of a pyridyl derivative, in acid solution, and $\epsilon_{B_eH^+}$, $\epsilon_{B_kH^+}$, ϵ_{B_e} and ϵ_{B_K} are the molar absorptivities of all the possible species present, then, at wave lengths greater than 270 mμ

$$\epsilon \cdot \{B_eH^+ + B_kH^+ + B_e + B_k\} = \epsilon_{B_eH^+} \cdot [B_eH^+] + \epsilon_{B_e}[B_e] \quad (9)$$

since all keto forms of these compounds do not absorb appreciably at wave lengths greater than 270 mμ. Therefore

$$K_{1e} = \frac{\left\{\epsilon_{B_eH^+} - \epsilon \frac{(B_eH^+ + B_k + B_kH^+)}{B_eH^+}\right\}[H^+]}{(\epsilon - \epsilon_{B_e})} \quad (10)$$

and it follows that

$$(\epsilon - \epsilon_{B_e}) + \frac{\epsilon \cdot [H^+]}{K'} + \frac{(\epsilon + \epsilon \cdot H^+)}{K_t} = \frac{[H^+]\epsilon_{B_eH^+}}{K_{1e}} \quad (11)$$

In equation 11, H^+ and ϵ can be obtained readily; K' already has been determined potentiometrically. Therefore, in order to determine K_{1e}, the values of ϵ_{B_e}, $\epsilon_{B_eH^+}$ and K_t have to be determined.

A reliable value of ϵ_{B_e} can be obtained by measuring the absorbance of a solution containing only the neutral enol form, and $\epsilon_{B_eH^+}$ can be determined by measuring the absorbance of a solution containing only the protonated enol form. However, in most cases keto–enol equilibrium is established rather rapidly and accurate values for ϵ_{B_e} and $\epsilon_{B_eH^+}$ are difficult to obtain. An aqueous solution of the pyridyl derivative containing a calculated amount of NaOH was neutralized rapidly to *p*H 7.0 with a calculated quantity of $HClO_4$; in this solution only the neutral enol form is present initially. The absorbance of this solution at a fixed wave length was followed with time, and extrapolated back to zero time when only the form B_e should have been present. The value of ϵ_{B_e} thus obtained was used in equation 11. A similar procedure was used for determining $\epsilon_{B_eH^+}$. An alkaline solution of the pyridyl compound was acidified and brought to a *p*H of 1.7 at which the protonated pyridine derivative predominated. The absorbance of the solution containing the protonated species was again followed with time and extrapolated back to zero time to give a value for $\epsilon_{B_eH^+}$ which was used in equation 11.

The constants K_t' and K_t were calculated by measuring the absorbance of an equilibrium mixture of the two protonated forms, B_eH^+ and B_kH^+, as well as the absorbance of a mixture of the two neutral forms, B_e and B_k, at a fixed wave length. The time taken for the absorbance to reach a constant value, which implied that equilibrium was attained, varied for each of the pyrazylmethyl ketones. For the pyridyl derivatives, the maximum time required for equilibration of the keto and enol forms was about 30 min. Unfortunately no measurements could be made on the phenacylpyrazine since equilibrium was attained in a few seconds. From the values of $\epsilon_{B_eH^+}$ and ϵ_{B_e} already determined the constants K_t and K_t' readily were obtained.

All spectrophotometric measurements were made at two different wave lengths, both wave lengths being greater than 270 mμ. For the 2-pyridyl derivative the wave lengths used were 340 mμ and 363 mμ; for the 3-pyridyl compound, 340 mμ and

360 mμ and for the 4-pyridyl compound, 335 mμ and 368 mμ.

The keto and enol forms of the neutral species of the 2-, 3- and 4-pyridyl derivatives as well as the phenacylpyrazine can dissociate further

$$B_e \overset{K_{2e}}{\rightleftharpoons} B^- + H^+ \quad (12)$$

$$B_k \overset{K_{2k}}{\rightleftharpoons} B^- + H^+ \quad (13)$$

The dissociation constants K_{2e} and K_{2k} are given by the expressions

$$K_{2e} = \frac{K_1'(K_t + 1)}{K_t} \quad (14)$$

$$K_{2k} = K_t K_{2e} \quad (15)$$

The values of all the acid dissociation constants determined spectrophotometrically depend largely on the accuracy with which K_t and K_t' are known. Unfortunately, because of the rapid attainment of equilibrium between the keto and enol forms of the molecules, these constants can be determined only approximately, and the uncertainty in the pK values reported in Table II is about ±0.2. However, these acid dissociation constants show significant trends, and are discussed later.

Rate Constants.—The time *vs.* absorbance data obtained in the determination of K_t were used to determine the rate constants k_1 and k_2 for the forward and reverse reactions of equation 16. A similar set of data also was obtained for K_t' but the rapid rate of equilibration of the protonated keto and enol forms of all the compounds precluded us from obtaining sufficiently accurate rate constants for the reactions given in equation 8.

The kinetic data obtained satisfied the rate expression 17 for opposing first-order reactions.

$$B_e \overset{k_1}{\underset{k_2}{\rightleftharpoons}} B_k \quad (16)$$

$$(k_1 + k_2) = \frac{1}{t} \ln \frac{x_e}{x_e - x} \quad (17)$$

where t is the time in seconds, x_e the equilibrium concentration of the keto form, and x the concentration of the keto form at any time t. The concentration of the keto form x_e at equilibrium is proportional to the difference between the absorbance at zero time and that at equilibrium. The concentration of the keto form x, at any time t, is proportional to the difference between the absorbance at zero time and that at time t. When values of t are plotted against corresponding values of log $(x_e - x)$, the slope of the straight line obtained will be $-2.303/(k_1 + k_2)$, from which $(k_1 + k_2)$ was calculated.

The equilibrium constant K_t (for reactions in equation 7) is given by

$$K_t = k_2/k_1 \quad (18)$$

From the calculated values of $(k_1 + k_2)$ and equation 18, the individual rate constants k_1 and k_2 were obtained and are shown in Table III.

Reactions with Metal Ions.—Qualitative tests were carried out with approximately 1% ethanol solutions of the pyrazylmethyl ketones and these various metal ions in buffer solutions between pH 2 and 5: silver(I), copper(II), magnesium(II), calcium(II), strontium(II), barium(II), zinc(II), cadmium(II), mercury(II), aluminum(III), indium(III), thallium(I), lead(II), arsenic(III), titanium(IV), chromium(III), manganese(II), iron(II), iron(III), cobalt(II), nickel(II), cerium(III), lanthanum(III), uranyl(VI), zirconyl(IV) and vanadyl (IV).

The 2-, 3- and 4-pyridyl derivatives all gave the reactions: a yellowish-brown precipitate with copper(II) at pH > 2; yellow precipitate with nickel(II) at pH > 4.7; green coloration with iron (III) at pH < 4.7; red coloration or precipitate with vanadyl(II) at pH > 2; phenacylpyrazine formed a yellowish-brown precipitate with copper(II) at pH > 3; a yellow precipitate with nickel(II) at pH > 4.7, and a green coloration with iron(III) at pH < 3.5; vanadyl(II) did not react with phenacylpyrazine. Mercury(II) showed marked differences in its reactions with the pyrazylmethyl ketones. No reaction was obtained with phenacylpyrazine; with the 2- and 3-pyridyl derivatives an orange or yellow precipitate was obtained at pH 2. With an excess of mercury(II), the 4-pyridyl compound gave a white precipitate between pH 1 and 4.7, and the 2-, and 3-pyridyl compounds gave white precipitates at pH 4.7.

Discussion

Ultraviolet Spectra.—The solution spectra of phenacylpyrazine and the three isomeric pyridyl derivatives are rather complex. A simple approach to the interpretation of the spectrum of phenacylpyrazine is to consider that the spectrum is made up of absorption bands from acetophenone and methylpyrazine. An interpretation of the absorption bands present in phenacylpyrazine will facilitate the interpretation of the spectra of the pyridyl derivatives.

The spectrum of acetophenone consists of two main bands at ~240 and 280 mμ and a weak broad band at 320 mμ. The 240 mμ band is sometimes called the "K" band and is a π-π* electronic transition in the benzoyl system while the 280 mμ band is the analog of the symmetry forbidden 260 mμ band of benzene.[4,5] The 320 mμ band in acetophenone has previously been assigned to an n-π* transition.[4] The usual red shifts of the absorption bands with increasing dielectric constants of the solvents are observed. In solvents other than methanol the n-π* transition probably is obscured by the 280 mμ band.

In methylpyrazine which has two main bands at ~270 and ~310 mμ, the band at ~270 mμ is assigned to a π-π* transition by analogy with other monosubstituted pyrazines.[6] The 310 mμ band is assigned to an n-π* transition. The 270 mμ band shifts to the red whereas the 310 mμ band shifts to the blue with increasing dielectric constant of the solvent. This blue shift is characteristic of n-π* transitions.[7,8]

The spectrum of phenacylpyrazine appears to be

(4) H. L. McMurray, *J. Chem. Phys.*, **9**, 241 (1941).
(5) E. A. Braude and F. Sondheimer, *J. Am. Chem. Soc.*, **77**, 3754 (1955).
(6) F. Halverson and R. C. Hirt, *J. Chem. Phys.*, **19**, 711 (1951).
(7) H. M. McConnell, *ibid.*, **20**, 700 (1952).
(8) M. Kasha, *Disc. Faraday Soc.*, **9**, 14 (1950).

a composite of the spectra of methylpyrazine and acetophenone since in 95% methanol there are three bands at 247, ~270 and 310 mμ.

However, the 310 mμ band is more intense than would be expected for an n-π* transition. The broad, flat absorption region between 280 and 310 mμ is probably a composite of the 310 mμ band as well as the 280 mμ band originating from a π-π* transition in acetophenone. Further the broad band at 360 mμ is one that is not observed in either of the parent molecules. The red shift and the increase in intensity, with *p*H and solvent, of both the 310 and 360 mμ bands is the key to their origin (Table V).

In 95% methanol phenacylpyrazine exists as an equilibrium mixture of the keto and enol forms. The enol form corresponds to complete conjugation between the benzene and pyrazine rings and should give a red shift of approximately 90–100 mμ.[9]

In 1 *M* acid solution the 360 mμ band disappears, and there is no shoulder on the 275 mμ band which might indicate the presence of the 310 mμ absorption. Therefore, the absorption at 310 and 360 mμ is characteristic of the enol form of the molecule. Further, the bands at 240 and 270 mμ decrease in intensity going from acid to methanol to alkali while the 310 and 360 mμ intensities increase in the same order of solvents.

In 95% methanol, 2-pyridyl pyrazylmethyl ketone exhibits four prominent bands at 234, ~307 and 356 mμ. The 234 mμ band is analogous to the 240 mμ absorption band in acetophenone. The absorption in the 270 mμ region is the same as that observed in methylpyrazine, but it must also contain the ~270 mμ absorption of isolated pyridyl ketones.[10] The 307 mμ band is the π-π* transition (234 mμ) of the keto form of the 2-pyridyl compound shifted to longer wave lengths due to complete conjugation in the enol form and hereafter referred to as the π-$\pi^*_{E_1}$ band. The 358 mμ absorption originates from the π-π^*_1 and the π-π* transitions in pyridine and pyrazine, but become one transition in the enol form. This interpretation is supported by an analogous behavior of phenacylpyrazine and by the virtual disappearance of these long wave length bands in aqueous solution at *p*H 7. Therefore, at *p*H 7 the molecule appears to exist predominantly in the keto form. Furthermore, at *p*H 7 the 307 mμ band is more intense than the 358 mμ band whereas at every other *p*H value the reverse is true because at these other *p*H values the n-π* transition in pyrazine in the 310 mμ region is completely overwhelmed by the strong enol absorption in this same region.

In 1.0 *M* NaOH solution the 271 mμ band is removed and the band at 388 mμ corresponding to the 360 mμ in methanol is increased considerably in intensity. The 310 mμ band present in methanol solutions shifts to 320 mμ and becomes a more intense broad shoulder of the 388 mμ band. Further, at *p*H 12 a weak absorption appears at 274 mμ while the rest of the bands parallel those in 1.0 *M* NaOH. These facts are all consistent with the presence of keto and enol tautomers present in equilibrium in solution. The band assigned to the enol form of the molecule increases in intensity with increasing *p*H to a maximum value at *p*H 12. The significance of this interpretation is discussed in the section on acid dissociation constants.

The spectra of phenacylpyrazine and the 2-pyridyl derivative are markedly different in acid solution. In 2.0 *M* $HClO_4$ phenacylpyrazine shows no absorption beyond 300 mμ but the 2-pyridyl derivative has two fairly strong bands at 320 and 375 mμ, which are the expected positions for absorption by the enol form of the compound.

The most reasonable structure of the enol form of 2-pyridyl pyrazylmethyl ketone is a *trans*-planar structure since the *cis* form will be sterically hindered. Whereas the 2-pyridyl compound exists as keto and enol tautomers in 1.0 *M* acid, phenacylpyrazine exists predominantly in the keto form. There are two possible reasons for this behavior: (1) hydrogen bonding in the singly protonated species as shown in structure III, (2) the enol form can be stabilized by delocalizing the positive charge on the protonated pyridine nitrogen.

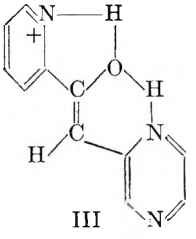

III

The 234 mμ band (π-π_2* transition) is not as strongly affected by acid and base concentration as the 274 band and is perhaps more localized in the pyridine ring.

The spectrum of the 3-pyridyl compound in 0.1 *M* acid also confirms our assignments of the absorption at about 270 mμ. In the 2-pyridyl compound we had assumed that the absorption at ~270 mμ was composed of the π-π_1* band of pyrazine and a π-π* band of pyrazine arising from the keto form of the molecule. In support of this assignment, in the 3-pyridyl derivative the 234 mμ band is shifted to 226 mμ and a corresponding blue shift is to be expected in the π-π_1* (270 mμ) band of pyridine. This shift appears as a shoulder at ~250 mμ in the 270 mμ band of the 3-pyridyl compound.

In the 4-pyridyl compound the bands at 305 and 350 mμ, due to the enol form of the compound have a minimum intensity at *p*H 7. As the *p*H is raised or lowered from *p*H 7, the enol concentration appears to increase and these bands are shifted toward the red. This compound also cleaves in solutions of *p*H greater than 12. One peculiar feature is present in the 4-pyridyl compound in neutral solution, namely, the pyridine band at 230 mμ is shifted to approximately 220 mμ without the π-π_1* band being appreciably affected. A similar behavior has been noted previously in 4-pyridine aldehydes.[10]

Summary of Spectra.—We have used the spectra of pyrazine, acetophenone and phenacylpyrazine to interpret the spectra of the 2-, 3- and 4-pyridyl pyrazylmethyl ketones. In 95% methanol solu-

(9) K. Hausser, *Z. f. tech. Physik*, **15**, 10 (1934).

(10) K. Nakamoto and A. E. Martell, *J. Am. Chem. Soc.*, **81**, 5857 (1959).

tion they all exhibit four principal regions of absorption, ~235, 270, 310 and 360 mμ. The first two are transitions within the isolated pyridine and pyrazine molecules, the last two are absorptions of the completely conjugated enol molecule. The apparent enol concentration of each molecule is a minimum in aqueous solution at *p*H 7, and increases with both increasing and decreasing *p*H. However, this apparent enol concentration is in reality a composite of several enol species, namely, the neutral form B_e, the protonated form B_eH^+ and the enolate anion B^-. This is discussed further in the section on acid dissociation constants. The 3- and 4-pyridyl compounds cleave in basic solutions of *p*H >12. This is seen by the decrease in intensity of the 235, 310 and 360 mμ bands, while the 270 mμ band increases in intensity.

Acid Dissociation Constants.—The substitution of the group R—CH=C(OH)— (where R is a pyrazine ring) in the *meta* position in a pyridine ring decreases the pK_a of pyridine from 5.16 to 3.5 (Table II pK_{1_e} values). Substitution of the same group in the *ortho* position in the pyridine ring causes a further decrease in the base strength of pyridine, and substitution in the *para* position results in an increase in the base strength of pyridine over the *meta* substituted compound. These results can be accounted for readily in terms of an inductive (electron-withdrawing) effect, which decreases with increasing distance from the pyridine nitrogen. If the substituent is a pyrazylmethyl keto group, the same trend is observed, the base strength of the pyridine nitrogen, pK_{1_k}, decreasing in the order 4-pyridyl > 3-pyridyl > 2-pyridyl pyrazylmethyl ketone. All pK_{1_k} values are smaller than the corresponding pK_{1_e} values, as expected, since a carbonyl group exerts a greater base-weakening effect on an acid–base center in an aromatic ring, than a —C(OH)= group substituted in the same position. The identical trends in pK_{1_e} and pK_{1_k} values of the pyridyl derivatives indicate that hydrogen bonding, steric effects and resonance interactions have only a minor effect on the base strength of the pyridine nitrogen. Furthermore, the values of the apparent dissociation constant pK' determined potentiometrically should also show the same trend as pK_{1_e} and pK_{1_k}.

The apparent dissociation constants pK'_1 as well as pK_{2_e} and pK_{2_k} decrease in the order 3-pyridyl > 2-pyridyl > 4-pyridyl pyrazylmethyl ketone. If the benzene ring in phenacylpyrazine is replaced by a pyridine ring it is not surprising that there is a marked decrease in pK'_1 as well as pK_{2_e} and pK_{2_k}. The pyridyl group can stabilize the enolate ion to a greater extent, through resonance interactions, than a phenyl group. Moreover, this stabilization takes place to a greater extent with an *ortho* substituted pyridine and a *para* substituted pyridine, the *meta* substituted pyridine showing the smallest tendency to stabilize the anion. It is of interest that other factors such as hydrogen-bonding, steric and solvation effects seem to have a negligible effect on these acid dissociation constants.

Figure 1 shows the manner in which the sum of the concentrations of the neutral enol B_e, the protonated enol B_eH^+ and the enolate anion B^- varies with *p*H for each of the three pyridyl compounds. These curves were calculated from the values of the equilibrium constants in Table II. The curves in Fig. 1 confirm the assignments made for the enol bands in the ultraviolet spectra of the compounds, and also account for the observation that the total concentration of the enol forms is a minimum in neutral solutions and increases with the addition of either acid or base.

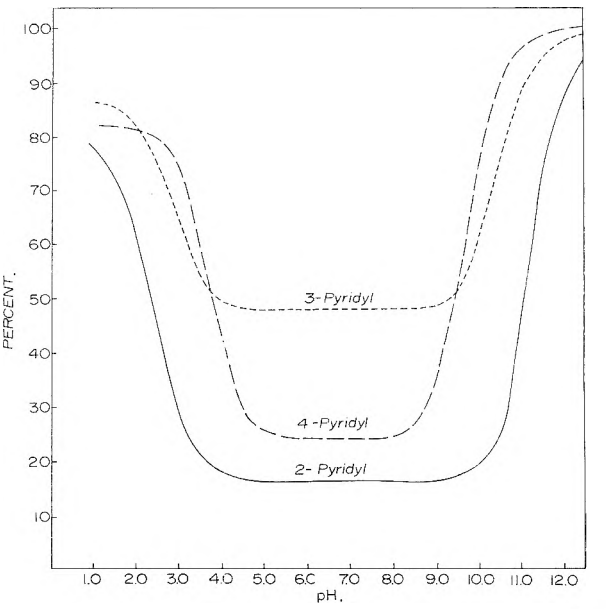

Fig. 1.—Variation of concentration of [Be + BeH^+ + B^-] with *p*H.

The rates of enolization should depend on the acid strengths of the enol, if no other complicating factors are present. The stronger the acid, the more rapidly will enol formation occur, since stronger acids tend to stabilize the enolate anions to a greater extent. The values of the rate constants k_2 (Table III), show that the 4-pyridyl compound which is the strongest acid enolizes most rapidly. But the 2-pyridyl compound, which is a stronger acid than the 3-pyridyl compound has the slowest rate of enolization. This anomaly is possibly due to the steric effect of the pyridine nitrogen in the *ortho* position.

The rate at which the enol form reverts to the keto form will depend to a great extent on the mechanism by means of which this prototropic reactions occurs. If we ignore the minor differences in k_1, the rate constants for keto formation, it appears that the same mechanism is involved in all three cases. If the rate-determining step in keto formation is that in which the enolate anion picks up a proton from the solution, then the rate constant k_1 would be governed primarily by the extent to which the negative charge in the enolate is delocalized. It appears therefore that the delocalization of the negative charge on the enolate anion occurs to practically the same extent in all three compounds. If however we take into account the small differences in k_1, then the rate constant k_1 parallels the pK_{2_e} value. Therefore the

manner in which the base strength increases and the rate of keto formation decreases is: 3-pyridyl > 2-pyridyl > 4-pyridyl pyrazylmethyl ketone.

Acknowledgment.—One of the authors (Q.F.) is grateful to the National Science Foundation for supporting this work with a research grant G-9736.

THE PROTON MAGNETIC RESONANCE SPECTRA OF SOME METAL VINYL COMPOUNDS

BY DONALD W. MOORE AND JAMES A. HAPPE

Michelson Laboratory, U. S. Naval Ordnance Test Station, China Lake, California

Received June 20, 1960

The proton n.m.r. spectra of divinylmercury, tetravinyltin and trivinylaluminum etherate have been studied at 40 mc. Spectral parameters have been determined by solution of the seculiar equations for an ABC-type spin system.

Introduction

Proton magnetic resonance spectra of metal–organic compounds are often characterized by a reduction of the separation between functional groups found in ordinary organic compounds, since the metal tends to increase the electronic shielding around adjacent groups. It is even possible for a strongly electropositive metal to invert the usual order of chemical shifts in the n.m.r. spectrum of an alkyl derivative. The work of Baker[1] with tetraethyllead and Narasimhan and Rogers[2] with diethylmercury illustrate typical results encountered with metal alkyls.

A second and often useful characteristic of metal–organic n.m.r. spectra is the apprearance of satellite lines owing to the normal abundance of magnetic isotopes present. In reference 2, the spectrum of diethylmercury exhibits Hg^{199} satellites which have the effect of expanding the CH_2–CH_3 chemical shift, permitting assignment of spectral parameters for the main spectrum by simple first-order treatment of the satellites. In this case and in tetraethyllead[1] the satellite spectra indicate two unexpected effects: the spin-coupling between CH_3 protons and the metal is stronger than that for the CH_2 protons and, further, these two J-values are of opposite sign.

In the work reported here on divinylmercury and tetravinyltin, the determination of precise chemical shifts and coupling constants was simplified by the presence of strong spin-coupling between all three vinyl protons and the magnetic isotopes Hg^{199}, Sn^{117} and Sn^{119}, all of spin $I = {}^1/_2$. Though the main spectra were badly collapsed owing to the electropositive screening influence of the metal, straightforward determination of approximate spectral parameters was made possible by first-order treatment of satellite lines. The treatment of the proton spectrum of trivinylaluminum etherate was then simplified, since approximate coupling constants were known and chemical shifts could be roughly predicted.

Precise determination of spectral parameters for the three metal–vinyl compounds was accomplished using an IBM 709 computer program which rapidly calculates the required ABC-type vinyl spectrum. Refinement of input δ- and J-values was done by trial-and-error until agreement between calculated and observed spectra was within the limits of observational error, about ± 0.3 c.p.s.

Assignments of lines were based upon the presumed relationship between proton-proton spin-coupling constants in vinyl groups: $J_{trans} > J_{cis} > J_{gem}$. Results indicate that the metal–proton spin-coupling constants do not necessarily obey this rule. They were, however, all of the same sign in the two cases studied.

Experimental

The n.m.r. spectra of all three materials were obtained from vacuum-distilled samples run at 40 mc. A Varian V-4302 spectrometer was used and line position measurements were made by means of the audio sideband modulation technique. Chemical shifts relative to cyclohexane were measured using an external concentric reference sample. The divinylmercury and trivinylaluminum etherate were prepared by the Chemistry Division, Naval Ordnance Laboratory, Corona, California. Tetravinyltin was obtained as a research sample from the Metal and Thermit Corporation, Rahway, New Jersey.

Results

Divinylmercury.—The complete proton n.m.r. spectrum (Fig. 1) shows a strong central spectrum flanked by satellite systems which are typical 12-line ABC-type spectra. The Hg^{199} isotope which produces the satellite lines has a normal abundance of 16.86%. The strong spin-coupling of Hg^{199} nuclei to the three vinyl protons has the effect of producing an expanded set of pseudochemical-shifts in the satellites, while the appearance of the central spectrum is obviously that of a collapsed vinyl system in which δ- and J-values are of comparable magnitude. The problem of assigning spectral parameters was thus simplified by first identifying the line groups in the two satellite systems. This was accomplished readily by invoking the accepted rule for vinyl proton spectra $J_{trans} > J_{cis} > J_{gem}$.

The determination of accurate spectral parameters was initiated with approximate δ- and J-values obtained by first-order treatment of the satellite sets. It was assumed that high- and low-field systems were unmixed, that is, all metal-proton J-values are of the same sign. Subsequent refinement of parameters proved this assumption correct, as well as the assumption that all proton–

(1) E. B. Baker, *J. Chem. Phys.*, **26**, 960 (1957).

(2) P. T. Narasimhan and M. T. Rogers, *J. Am. Chem. Soc.*, **82**, 34 (1960).

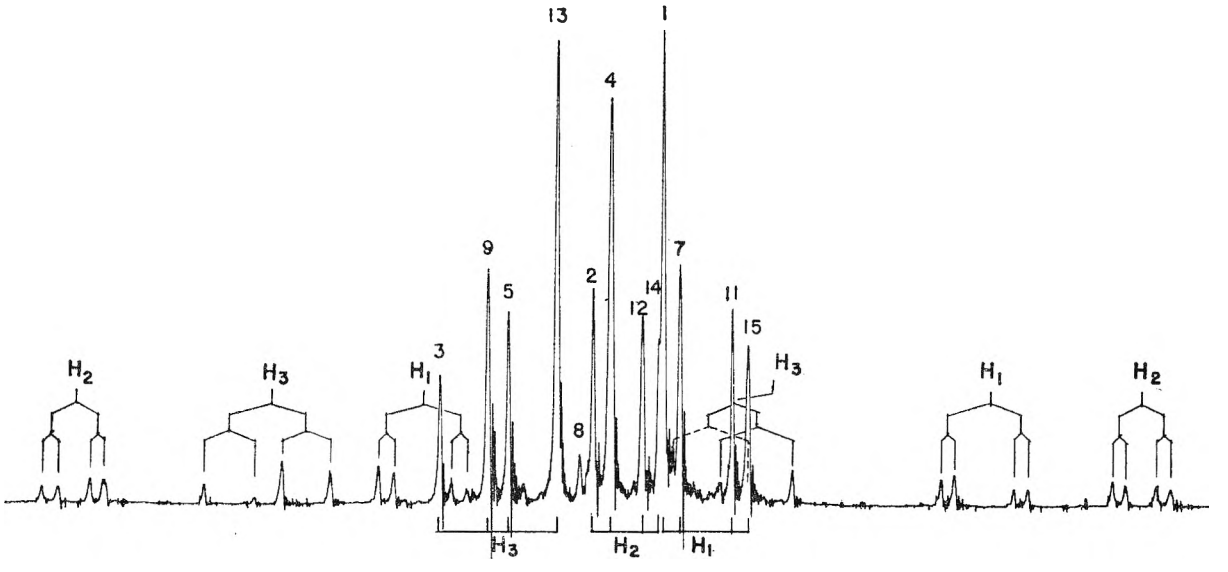

Fig. 1.—Divinylmercury n.m.r. spectrum at 40 mc. showing Hg^{199} satellites.

proton coupling constants were of the same sign. This was tested by computing four sets of spectra using all the possible sign combinations (+++, −++, +−+, ++−). Only the set with all J's positive gave reasonable agreement with the observed spectrum. Final parameters are summarized in Table I. Table II gives calculated and

TABLE I

SUMMARY OF N.M.R. SPECTRAL PARAMETERS[a]

Proton chemical shifts (relative to H_1) at 40 mc., c.p.s.

	H_1	H_2	H_3
Divinylmercury	0	−21.6	−53.7
Tetravinyltin	0	−18.2	−25.7
Trivinylaluminum etherate	0	−14.3	−24.4

Proton chemical shifts (relative to cyclohexane) at 40 mc., c.p.s.

	H_1	H_2	H_3
Divinylmercury	−181.0	−202.6	−234.7
Tetravinyltin	−165.9	−184.1	−191.6
Trivinylaluminum etherate	−167.1	−181.4	−191.5

Proton–proton J-values, c.p.s.

	J_{12} (*gem*)	J_{23} (*cis*)	J_{13} (*trans*)
Divinylmercury	3.5	13.1	21.0
Tetravinyltin	3.7	13.2	20.3
Trivinylaluminum etherate	6.3	15.3	21.4

Metal–proton J-values, c.p.s.

	J_{X1}	J_{X2}	J_{X3}
Divinylmercury	159.6	295.5	128.5
Tetravinyltin	90.6	183.1	98.3

[a] Parameters are numbered according to the diagram

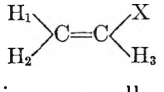

observed line positions, as well as intensities for the main spectrum of divinylmercury. The chemical shifts for the main spectrum and the three metal–proton spin-coupling constants were calculated from the assumed relationships

$$\delta_A' = \delta_A \pm 1/2\, J_{AX}$$
$$\delta_B' = \delta_B \pm 1/2\, J_{BX}$$
$$\delta_C' = \delta_C \pm 1/2\, J_{CX}$$

TABLE II

DIVINYLMERCURY N.M.R. SPECTRUM, 40 MC.[a]

Low-field Hg^{199} lines c.p.s.			High-field Hg^{199} lines, c.p.s.		
	Calcd.	Obsd.		Calcd.	Obsd.
H_2	−359.8	−360.1	H_3	−188.2	−187.3
H_2	−355.6	−356.1	H_3	−175.4	−174.9
H_2	−347.3	−347.1	H_3	−167.1	−167.3
H_2	−343.0	−342.6	H_3	−154.4	−154.7
H_3	−316.5	−316.3	H_1	−112.5	−112.5
H_3	−304.0	−303.2	H_1	−108.7	−108.3
H_3	−295.7	−296.3	H_1	−91.6	−91.5
H_3	−283.1	−283.3	H_1	−87.6	−87.7
H_1	−270.8	−270.6	H_2	−62.9	−63.4
H_1	−266.6	−266.1	H_2	−59.1	−59.2
H_1	−250.0	−250.3	H_2	−50.2	−50.1
H_1	−245.8	−246.0	H_2	−46.4	−46.0

Main spectrum				
Transition	Frequency, c.p.s. Calcd.	Obsd.	Intensity Calcd.	Obsd.
6	−260.7	.....	0.007	..
3	−254.4	−253.6	0.45	0.50
9	−241.3	−241.5	0.82	0.91
5	−234.7	−234.9	0.71	0.74
13	−221.5	−221.7	1.93	1.84
8	−215.2	−214.6	0.08	0.10
2	−210.4	−210.6	0.85	0.82
4	−205.8	−205.7	1.98	1.67
12	−197.3	−197.0	0.75	0.71
14	−192.6	−192.5	0.49	0.61
1	−191.0	−190.7	1.69	1.80
7	−186.4	−185.9	0.95	0.99
11	−171.2	−171.6	0.69	0.80
15	−166.5	−166.9	0.58	0.70
10	−142.4	.....	0.005	..

[a] All frequencies refer to cyclohexane.

where frequencies on the left are those of the satellite groups and those on the right refer to the main spectrum.

Tetravinyltin.—The tetravinyltin spectrum (Fig. 2) exhibits a badly collapsed vinyl group line system with four weak sets of satellites arising from the isotopes Sn^{117} and Sn^{119}, normal abundances 7.67 and 8.68%, respectively. Since the gyromagnetic ratios of these nuclei differ by only 4.61%, their

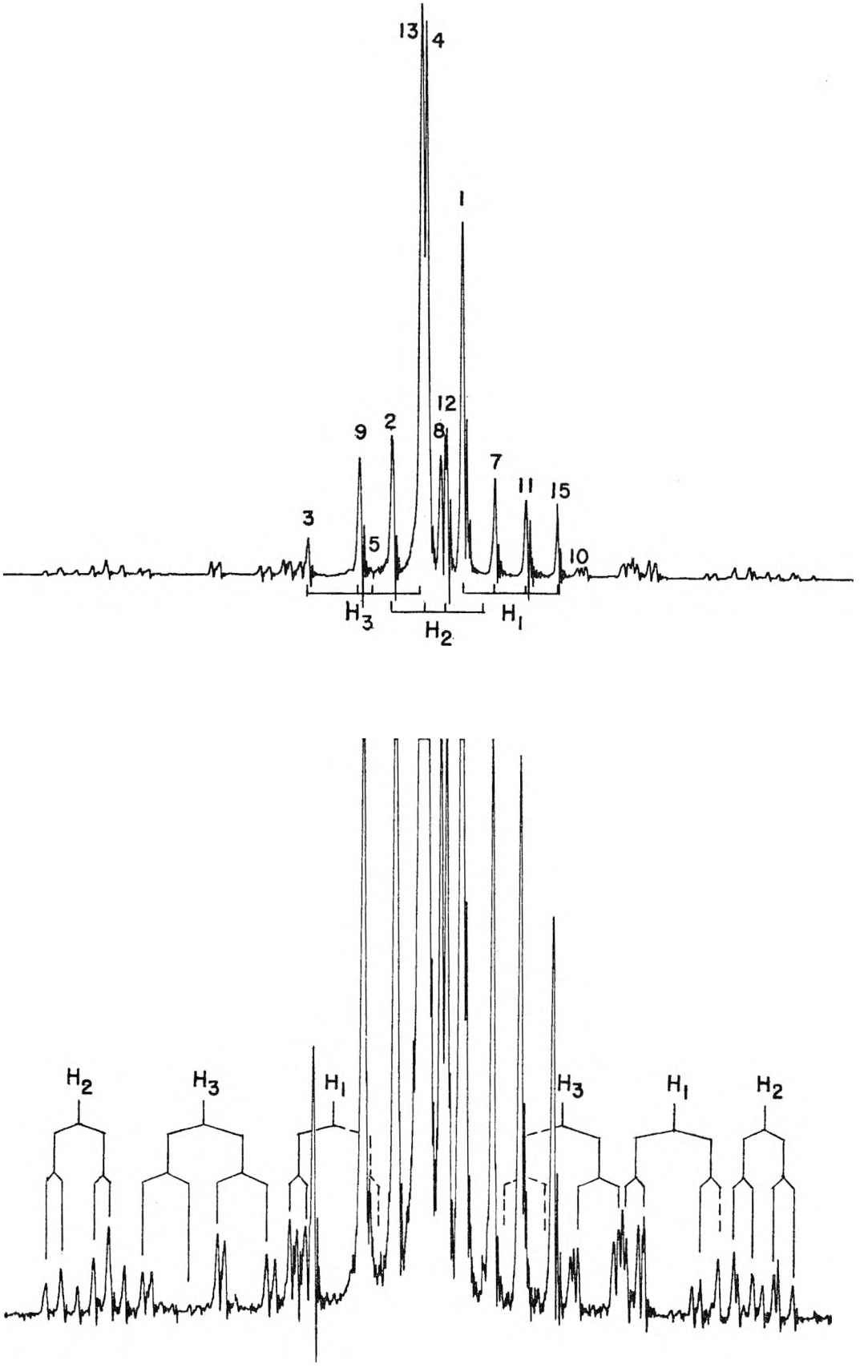

Fig. 2.—Tetravinyltin n.m.r. spectrum at 40 mc. showing Sn^{117} and Sn^{119} satellites: (upper) main spectrum with transitions labeled according to Table V (lower) amplitude increased to show satellites, with Sn^{119} spectra indicated. Sn^{117} spectra appear as a superimposed set with slightly smaller metal-proton coupling values.

corresponding satellite spectra are superimposed as closely spaced doublets with the Sn^{119} line always at a greater separation from the parent peak. Only the Sn^{119} satellites were treated in the determination of spectral parameters. As with the divinylmercury case, the expanded satellite spectra were attacked first using the same group assignments as in the previous case. Refinement was carried to the limit of experimental error before attempting to fit the data to the main peak system. In both cases parameters so determined gave an acceptable fit to the observed main spectrum without further refinement. As in the previous case, all possible combinations of signs of proton–proton coupling constants were tried, and best agreement was achieved with all signs alike. These values are summarized in Table I. Table III summarizes calculated and observed spectral data for tetravinyltin.

TABLE III

TETRAVINYLTIN N.M.R. SPECTRUM, 40 MC.

Low-field Sn^{119} Lines, c.p.s.			High-field Sn^{119} Lines, c.p.s.		
	Calcd.	Obsd.		Calcd.	Obsd.
H_2	−285.6	−285.8	H_3	−163.6	.....
H_2	−280.8	−280.9	H_3	−152.1	.....
H_2	−273.0	−273.1	H_3	−143.2	−142.8
H_2	−268.3	−268.7	H_3	−131.8	−131.8
H_3	−259.1	−259.7	H_1	−129.7	−129.7
H_3	−246.5	−246.4	H_1	−124.3	−124.5
H_3	−239.2	−239.3	H_1	−109.4	−109.0
H_3	−226.6	−226.5	H_1	−104.0	−103.5
H_1	−220.2	−220.1	H_2	−99.9	−100.1
H_1	−215.5	−215.5	H_2	−94.5	−94.5
H_1	−200.3	.....	H_2	−88.4	−88.5
H_1	−195.6	.....	H_2	−83.0	−83.7

Main spectrum				
	Frequency, c.p.s.		Intensity	
Transition	Calcd.	Obsd.	Calcd.	Obsd.
6	−217.7	.....	0.01	..
3	−213.0	−213.4	0.16	0.18
9	−200.1	−200.6	0.64	0.64
5	−197.2	.....	0.04	..
2	−191.7	−191.4	0.75	0.77
13	−184.3	−184.3	2.67	2.83
4	−183.2	−183.2	3.05	3.05
8	−179.6	−179.9	0.53	0.62
12	−178.8	−178.6	0.68	0.66
1	−174.0	−174.4	2.09	2.01
14	−170.3	.....	0.002	..
7	−165.6	−166.0	0.58	0.52
11	−158.2	−158.4	0.43	0.43
15	−149.8	−149.7	0.33	0.27
10	−144.2	−144.1	0.05	0.05

Trivinylaluminum Etherate.—It was necessary to study this vinyl compound as a one-to-one complex with diethyl ether, since pure trivinylaluminum polymerizes rapidly when isolated. It is presumed that the point of attachment of the ether molecule is in the vacant coördination sites around the aluminum atom and that the difference between the vinyl group spectra of pure material and the ether adduct would be small. However, an unexpectedly large spin-coupling value observed between the *gem*-protons may indicate some deformation of the vinyl-group bonds caused by interaction with the ether molecule.

The spectrum observed for this addition compound appears in Fig. 3. Determination of the two chemical shifts and three spin-coupling values was started using approximations based upon the two previous cases. Agreement was obtained with the observed spectrum only by greatly increasing the *gem*-proton coupling constant. Trial spectra with all four possible combinations of signs of J's indicated best agreement when all signs were the same. Observed and calculated spectra are given in Table IV.

TABLE IV

TRIVINYLALUMINUM ETHERATE N.M.R. SPECTRUM, 40 MC.

Transition	Frequency		Intensity	
	Obsd.	Calcd.	Obsd.	Calcd.
6	.....	−215.9	..	0.02
3	−215.1	−215.2	0.15	.15
5	−198.6	−199.3	.64	.07
9		−199.1		.58
2	−192.7	−192.3	.31	.44
13	−183.3	−183.2	4.22	2.71
8		−182.5		0.49
4	−181.8	−181.2	2.71	3.32
12	−176.1	−176.2	2.93	0.67
1		−175.6		2.41
14	.....	−165.2	..	0.01
7	−164.3	−164.5	0.38	.37
11	−159.6	−159.7	.35	.45
15	−148.5	−148.6	.29	.27
10	.....	−141.6	..	.03

Theoretical

Computation of the ABC-type spectra of these materials was accomplished using the IBM 704/709 SPIN program devised by Dr. R. E. von Holdt of the Lawrence Radiation Laboratory, Livermore, California.[3] SPIN is a complete n.m.r. spectrum program for systems of up to five nuclei of $^1/_2$ spin. (Larger systems can, of course, be solved with this program if their spin Hamiltonians can be reduced to submatrices of order 32 × 32 or smaller.) As input SPIN requires the correct form of the Hamiltonian matrix, the matrix of transition probabilities, and a complete set of spectrum parameters. The program then diagonalizes the matrix to obtain stationary state energies and computes transition frequencies and line intensities.

The eight basic spin functions used were the same as those given in Pople, Schneider and Bernstein.[4] The fifteen computed transitions can then be labeled according to Table V (in the limiting case where $\delta >> J$).

In the treatment of the divinylmercury and tetravinyltin spectra it was not actually necessary to make correct assignments of the observed lines in the main spectra, since these spectra could be computed from the parameters determined for the satellites. Refinement of the trivinylaluminum etherate parameters, however, was greatly facili-

(3) The SPIN program is available in binary card form for either IBM 704 or 709 users. Requests should be sent to Dr. Bert E. Holder, Chemistry Division, University of California, Lawrence Radiation Laboratory, P. O. Box 808, Livermore, California, specifying type of computer to be used.

(4) J. A. Pople, W. G. Schneider and H. J. Bernstein, "High Resolution Nuclear Magnetic Resonance," McGraw-Hill Book Co., New York, N. Y., 1959, p. 132.

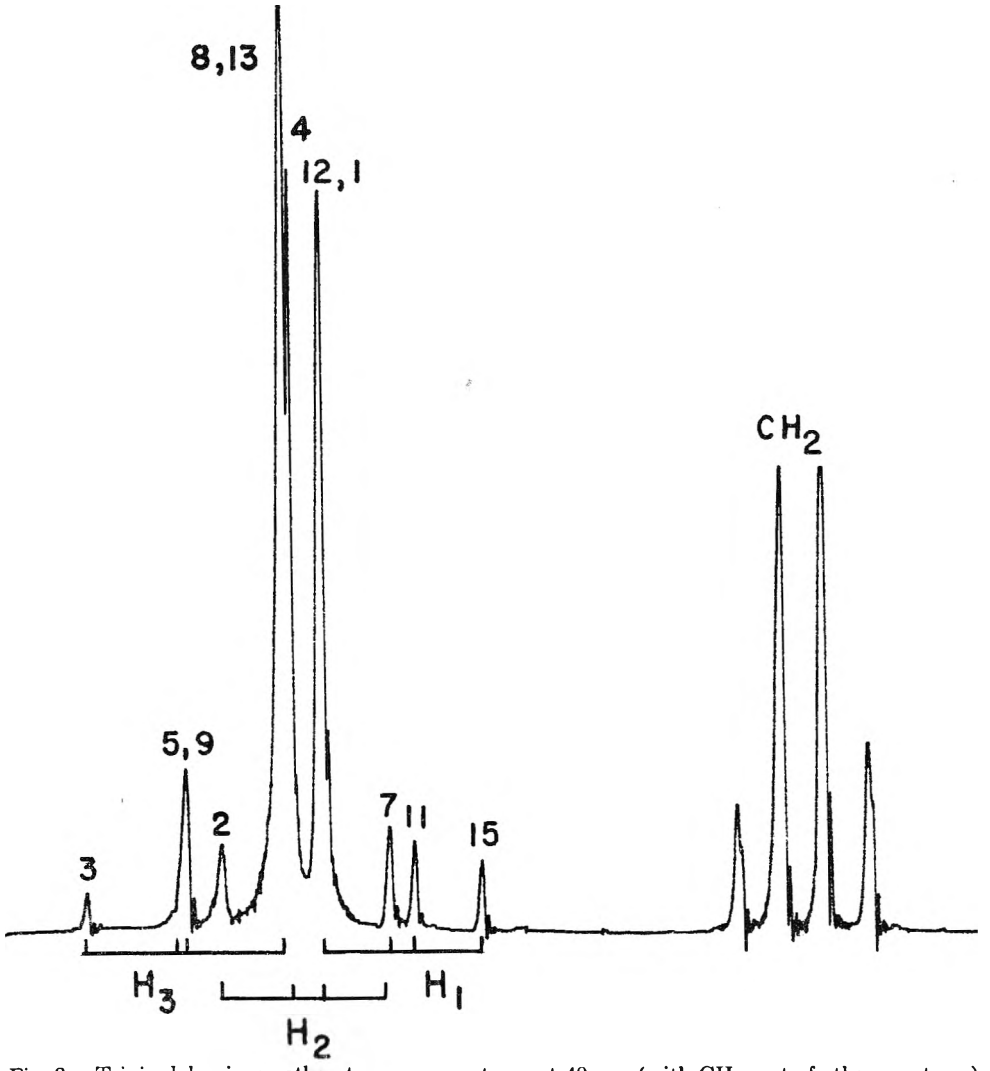

Fig. 3.—Trivinylaluminum etherate n.m.r. spectrum at 40 mc. (with CH_2 part of ether spectrum).

TABLE V

TRANSITION ASSIGNMENTS

	Transition		Nucleus
1	$\alpha\alpha\alpha$	$\beta\alpha\alpha$	1
2	$\alpha\alpha\alpha$	$\alpha\beta\alpha$	2
3	$\alpha\alpha\alpha$	$\alpha\alpha\beta$	3
4	$\beta\alpha\alpha$	$\beta\beta\alpha$	2
5	$\beta\alpha\alpha$	$\beta\alpha\beta$	3
6	$\beta\alpha\alpha$	$\alpha\beta\beta$	Comb.
7	$\alpha\beta\alpha$	$\beta\beta\alpha$	1
8	$\alpha\beta\alpha$	$\beta\alpha\beta$	Comb.
9	$\alpha\beta\alpha$	$\alpha\beta\beta$	3
10	$\alpha\alpha\beta$	$\beta\beta\alpha$	Comb.
11	$\alpha\alpha\beta$	$\beta\alpha\beta$	1
12	$\alpha\alpha\beta$	$\alpha\beta\beta$	2
13	$\beta\beta\alpha$	$\beta\beta\beta$	3
14	$\beta\alpha\beta$	$\beta\beta\beta$	2
15	$\alpha\beta\beta$	$\beta\beta\beta$	1

tated by sorting the observed lines into quartets assigned to each of the three protons using assignments deduced from the tetravinyltin spectrum. The input parameters then were adjusted in successive iterations to bring the computed quartets into coincidence with those observed. Figure 3 shows these groups, and the individual transitions according to Table V. Note the comparative strength of the central combination line (transition 8) in this as well as the preceding spectra. Any attempt at proper assignment of collapsed ABC-type spectra such as these must take into account the appearance of strong combination lines as well as the vanishing intensity of some proper transitions such as 5 and 14 in the spectrum above.

Discussion

Chemical Shifts.—The proton chemical shifts for these three vinyl compounds do not vary in the order which would be predicted from simple electronegativity considerations. Although the strong shielding of vinyl protons by the aluminum is consistent with its low electronegativity, the difference observed for the tin and mercury compounds is unexpectedly large. Since the electronegativity values given by Pauling[5] for Sn^{IV} and Hg^{II} are both 1.9, one would expect little difference in their shielding effects. Some difference might be predicted from the greater number of vinyl groups competing for the available electrons in the carbon–metal orbitals, but this line of reasoning would

(5) L. Pauling, "The Nature of the Chemical Bond," 3rd Ed., Cornell University Press, Ithaca, N. Y., 1960, p. 93.

lead to a reduced shielding in the tin case, contrary to what is observed. A possible explanation lies in the known variation of diamagnetic susceptibilities for the metal ions. According to the self-consistent set of data compiled by Klemm[6] the following values apply

	$-\chi \times 10^{-6}$
Al^{III}	2
Sn^{IV}	16
Hg^{II}	37

The possible additional effects arising from structural differences and possible intermolecular effects await further evaluation in the study of these and other related organo-metallic compounds.

Spin-Coupling Values.—The proton–proton *J*-values observed for the mercury and tin vinyl compounds are consistent with those generally observed for vinyl groups, though some enhancement of all three constants over characteristic values (Pople, Schneider and Bernstein,[4] p. 193) is apparent. In the case of trivinylaluminum etherate the large *gem*-proton *J*-value of 6.3 c.p.s. compared with a normal 1–3 c.p.s. strongly suggests a reduction in the terminal H–C–H bond angle. This conclusion follows from the work of Karplus and Gutowsky,[7,8] who showed the theoretical dependence of the coupling value on the interproton bond angle.

The two sets of metal–proton coupling constants in Table I reveal the expected strength of the *trans*-coupling, but show the *cis*- and *gem*-couplings to be nearly equal. An explanation for this anomaly might be found in structural studies of these molecules, although the previously reported behavior of metal alkyl spin-coupling constants indicates the difficulty of attempting to correlate structure with spin-coupling.

Acknowledgment.—The invaluable assistance of Dr. Bert E. Holder, Dr. Richard E. von Holdt and Mr. Frank Abell of the Lawrence Radiation Laboratory, Livermore, California, in providing us with the SPIN computer program, is gratefully acknowledged.

We are also indebted to Dr. Bodo K. W. Bartocha, Mr. Andrew J. Bilbo and Mrs. Marilee Y. Gray, Naval Ordnance Laboratory, Corona, California for preparation of the divinylmercury and trivinylaluminum etherate samples.

(6) P. W. Selwood, "Magnetochemistry," 2nd Ed., Interscience Publishers, Inc., New York, N. Y., 1956, p. 78.

(7) M. Karplus and H. S. Gutowsky, Abstracts, ACS Meeting, San Francisco, 1958, p. 9-Q.

(8) H. S. Gutowsky, M. Karplus and D. M. Grant, *J. Chem. Phys.*, **31**, 1278 (1959).

QUANTUM EFFICIENCIES OF FLUORESCENCE OF ORGANIC SUBSTANCES: EFFECT OF SOLVENT AND CONCENTRATION OF THE FLUORESCENT SOLUTE[1]

BY W. H. MELHUISH

Institute of Nuclear Sciences, Department of Scientific and Industrial Research, New Zealand[2]

Received June 20, 1960

The absolute quantum efficiencies of fluorescence of deaerated solutions of several organic fluorescent substances in petroleum ether (b.p. 60–80°), ethanol (99%) and benzene at 25° were measured with a rhodamin B quantum counter. An equation was derived for correcting the observed efficiencies of fluorescence for reabsorption of fluorescence and shifts in the region of absorption away from the quantum counter. Absolute quantum efficiencies of fluorescence extrapolated to zero concentration, bimolecular self quenching constants and oxygen-quenching constants were measured at 25°. Quinine bisulfate, 5×10^{-3} *M* in 1 *N* H_2SO_4, is proposed as a standard with an absolute quantum fluorescence efficiency of 0.51 at 25°.

A knowledge of quantum efficiencies and self-quenching constants of fluorescent organic molecules in solution has many important applications in physical chemistry, for example, in the investigation of internal conversion, intersystem crossing (singlet–triplet transitions), fluorescence quenching and the transfer of electronic excitation energy in solution.

The measurement of quantum fluorescence efficiencies has been reviewed recently by Förster.[3] The method of Bowen[4] has the merit of simplicity and if modified,[5] may be used over a wide range of wave lengths. Since 1951 other methods of measuring fluorescence efficiencies have been published. Bowen[6] integrated the fluorescence intensity (quanta $sec.^{-1}$ $m\mu^{-1}$) emerging from a monochromator, over all wave lengths. The apparatus was calibrated with a sample of known absolute quantum efficiency. Gilmore, *et al.*,[7] used a photocell of known wave length response to view the fluorescence. The fluorescence spectrum was measured in a separate experiment and used to correct the photocell output. Forster and Livingston[8] used an integrating sphere and a thermopile as the detector.

Most authors make no correction for reabsorption of fluorescence which can cause anomalously high efficiencies. Budo, Dombi and Szöllösy[9]

(1) Department of Chemistry, University of California, Los Angeles 24, California.

(2) Contribution No. 83.

(3) Th. Förster, "Fluoreszenz Organischer Verbindungen," Vandenhoeck und Ruprecht, Göttingen, 1951, p. 143.

(4) E. J. Bowen, *Proc. Roy. Soc.* (*London*), **154A**, 349 (1936).

(5) W. H. Melhuish, *N. Z. J. Sci. and Tech.*, **37.2B**, 142 (1955).

(6) E. J. Bowen, *Trans. Faraday Soc.*, **50**, 97 (1954).

(7) E. H. Gilmore, G. E. Gibson and D. S. McClure, *J. Chem. Phys.*, **20**, 829 (1952).

(8) L. S. Forster and R. Livingston, *J. Chem. Phys.*, **20**, 1315 (1952).

(9) A. Budo, J. Dombi and L. Szöllösy, *Acta Phys. et Chem. Szeged* (*N. S.*), **2**, 18 (1956).

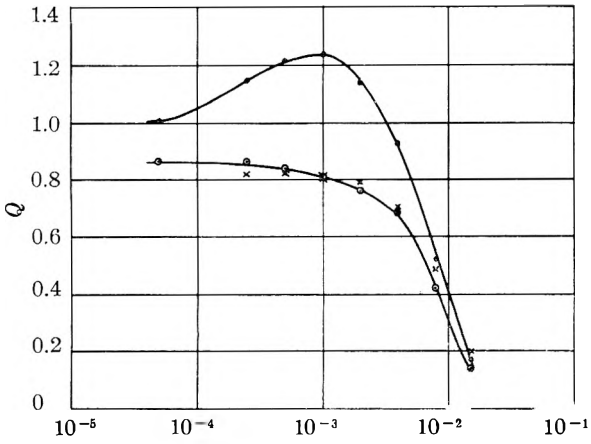

Fig. 1.—Self-quenching of fluorescein in water (*p*H 12.5): ●, observed (Budó, *et al.*); ⊙, corrected (Budó, *et al.*); ×, corrected (method of this paper).

have shown that reabsorption of fluorescence in solutions of the fluorescein anion is such as to give up to 1.5 times the true value (Fig. 1) when the solution is illuminated and observed from the same side.

In this work, absolute quantum efficiencies of fluorescence were measured using the rhodamin B quantum counter and employing existing equations for calculating absolute quantum fluorescence efficiencies, modified to allow for fluorescence reabsorption and shifts in the region of absorption away from the quantum counter at low solute concentrations. The temperature of the solutions was maintained at 25 ± 0.1°.

Experimental

Fluorescent Substances and Solvents.—Anthracene, anthranilic acid, quinine bisulfate, 2-naphthylamine and acridone were purified from stock chemicals by several recrystallizations. 1,6-Diphenyl-1,3,5-hexatriene was of scintillation grade and was used without further purification. Methyl anthranilate was distilled twice at 15 mm. pressure taking the middle cuts in each case. These various anthracene derivatives were prepared by conventional methods: 9-bromo- (m.p. 99°), 9,10-dibromo- (m.p. 219°), 9,10-diphenyl- (m.p. 246°) and 9,10-di-1-naphthyl- (m.p. 408°). The substances were recrystallized from a suitable solvent, purified on activated alumina columns (eluted with a 50/50 mixture by volume of petrol ether and benzene) and finally fractionally sublimed in a stream of nitrogen.[10] Perylene was prepared from 2-bi-naphthol as outlined by Morgan and Mitchell.[11] A yellow substance (m.p. 155°) fluorescing blue in solution also was isolated. This substance is probably 1,1′-dinaphthyl-2,2′-oxide and must not be confused with perylene. Pure perylene (m.p. 276°) was prepared by chromatography and sublimation as described above. 9-Cyanoanthracene was prepared using the method of Bachmann and Kloetzel.[12] The substance was purified as described above (m.p. 178°).

The purity of the samples was checked by comparing the melting points and absorption spectra with those published (where available).

Benzene (British Drug Houses, A.R.) and ethanol (B.D.H., A.R.) 99/100%, were used without further purification. Petrol ether (B.D.H., 60–80°) and heavy paraffin were purified by shaking with successive quantities of 10% fuming sulfuric acid, washing with aqueous caustic soda and finally with water. After drying with calcium chloride, the solvents were passed down 50 cm. columns of silica gel until the transmission extended to 220 mμ.

(10) W. H. Melhuish, *Nature*, **184**, 1933 (1959).

(11) G. T. Morgan and J. G. Mitchell, *J. Chem. Soc.*, 536 (1934).

(12) W. E. Bachmann and M. C. Kloetzel, *J. Org. Chem.*, **3**, 55 (1938).

Irradiation Source.—Solutions were excited with a 125 watt high pressure mercury lamp ("black lamp"). The lamp output was stabilized by connecting it in series with barretters, to a 50 cycle/sec. a.c. supply. The quantum spectrum of the lamp, measured with the spectro-fluorophotometer described below, had a broad band at about 366 mμ (relative quanta = 93%), two lines at 390.6 and 404.6 mμ (each = 1%) and a region between 368 and 385 mμ (= 5%). A 2% correction therefore was made to the quantum efficiencies of those substances which did not absorb in the region of 390 to 405 mμ.

The mean optical density of a solution to heterochromatic radiation may be calculated from an equation given by Kortüm.[13] It was assumed here that the band shape could be approximated by the two lines found at low pressure, 365.0 and 366.3 mμ, the ratios of the intensities being taken as $I(365)/I(366.3) = 0.38$. The mean optical densities of the solutions therefore were calculated from

$$\bar{E} = \epsilon_1 cl + \log 1.38 - \log [1 + 0.38 \times 10^{(\epsilon_1 - \epsilon_2)cl}]$$

where ϵ_1, ϵ_2 are the molecular extinction coefficients of the solute at 366.3 and 365.0 mμ, respectively, c = concentration of the solute (mole/l.) and l = thickness of the solution (cm.). The $\alpha_\lambda x$ term of equation 6 was thus calculated from

$$\alpha_\lambda x = \epsilon_1 c\, 2.303 + 0.323 - 2.303 \log [1 + 0.38 \times 10^{(\epsilon_1 - \epsilon_2)xc}] \quad (1)$$

where

$\alpha_\lambda x$ = the absorption coefficient of the soln. for the exciting radiation
x = 1.14 (45° illumination)

Fluorescence Photometer.—Fluorescence intensities (relative quanta/sec.) were measured with a rhodamin B quantum counter. The fluorescence from the solution fell on the quantum counter and the fluorescence excited in the quantum counter transmitted through a red filter to a photomultiplier. The 100 cycle/sec. component in the fluorescence excited by the mercury lamp was detected by the photomultiplier and the output signal amplified with negative feedback a.c. amplifiers. The signal from the photomultiplier was compared with a standard signal from a photocell, using a difference amplifier and phase detector as a null detector. The photocell was illuminated with light taken from the exciting beam by a plane glass plate. Stability against fluctuations in the intensity of the mercury lamp was good; a 20% change caused less than 0.4% change in the intensity reading. The possibility that photomultiplier noise might affect the linearity of the photometer was tested by injecting noise into the photomultiplier by allowing a small amount of unmodulated light to fall on the photocathode. Deviations were found to be less than 2% with signal to noise ratios down to 0.4.

The cuvette used was disc-shaped (28 mm. diameter and 9.5 mm. thick) whose back and sides were painted with non-reflective black paint to reduce internal reflection. The rhodamin B quantum counter (28 mm. in diameter and 8 mm. thick) was placed 10.5 cm. from the cuvette face. Some tests of the suitability of rhodamin B as a device for measuring quanta has been reported previously.[5,14] The first author (ref. 5) found small deviations at 450 mμ where rhodamin B does not absorb strongly. It was considered that the addition of acriflavin, which absorbs strongly at 450 mμ, might improve the response of the quantum counter since energy absorbed by acriflavin is known to be efficiently transferred to rhodamin B. The quantum counter was a 1 cm. thick solution of rhodamin B (4 g./l.) and acriflavin (1 g./l.) in 90% glycerol and 10% ethanol. The red filter in front of the photomultiplier was a 1 cm. solution of methyl red (indicator solution, 0.75 g./l.) and *o*-nitrophenol (5 g./l.) in 95% ethanol and 5% 2 *N* sulfuric acid.

Fluorescence Spectra.—These were determined using a Hilger wave length spectrometer as the monochromator.[15] Intensities were measured with the electronic apparatus described above and were converted to relative quanta $sec.^{-1}$

(13) G. Kortüm, "Kolorimetrie, Photometrie und Spektrometrie," Springer Verlag, Berlin, 1955, p. 43.

(14) G. Weber and F. J. W. Teale, *Trans. Faraday Soc.*, **53**, 646 (1957).

(15) W. H. Melhuish, *J. Phys. Chem.*, **64**, 762 (1960).

$m\mu^{-1}$. The concentration of the solute ranged from 10^{-2} to 5×10^{-7} M.

Measurement of Absolute Quantum Fluorescence Efficiencies.—A 5×10^{-3} M solution of quinine bisulfate in 1 N H_2SO_4 was used as a standard of fluorescence. The solution showed good stability to radiation, was not quenched by dissolved air and had a very small fluorescence–absorption overlap. However the intensity of fluorescence had a fairly steep temperature dependence, about -0.2 to -0.3% per ° in the range 10 to 40°. The absolute quantum efficiency of fluorescence at 25° was 0.510 (Appendix I). The error in this figure could be as high as 2% as a result of the uncertainty of the reflectivity of magnesium oxide under the conditions of the experiment. Absolute quantum efficiencies of relatively strong air free solutions of some organic substances were determined at 25°, making corrections for stray light scattered from the exciting beam by the cuvette window and the supports and stops in the optical system. A correction also was made for the small amount of stray radiation scattered from the emitted fluorescence by the quantum counter into the photomultiplier.

The effect of the concentration of the solute on its fluorescence efficiency was determined over a wide concentration range using the photocell in place of the quantum counter. The use of a photocell for measuring self-quenching constants did not introduce appreciable errors as little change in the spectral distribution of fluorescence occurred with change in concentration. This was checked for the case of perylene in benzene where overlap between absorption and fluorescence spectra caused a large change in the first maximum of the fluorescence spectrum as the concentration was increased above about 10^{-4} M. Care was taken to minimize the scattering of exciting radiation into the photocell, which was particularly high at low concentrations of solute. Such scattered radiation was reduced further by placing a filter (1 mm. of a solution of ferric alum, 10 g./l. in 2 N H_2SO_4) in front of the photocell. Oxygen-quenching constants were also determined with the photocell by measuring the fluorescence intensities of the solutions before and after de-aeration. Aerated solutions of benzene and ethanol were assumed to contain 1.45×10^{-3} M oxygen and aerated petrol ether (hexane fraction), 2.4×10^{-3} M oxygen. These figures are given by Seidell[16,17] although other values are quoted which differ considerably from these. Consequently there is some uncertainty in the values of the quenching constants given in Table III.

Results

It is first necessary to relate the measured intensity of fluorescence (relative quanta/sec.) to the several variables in the measuring system. Förster (ref. 3, p. 35) has derived an expression giving the intensity of fluorescence $dB'(\lambda')$ in the wave length interval between λ' and $\lambda' + d\lambda'$ falling on a small aperture perpendicular to and at a large distance from a rectangular cuvette, in terms of the absorption coefficients of the solution and the geometry of the cuvette. The equation, however, neglects the possibility of the reabsorption of fluorescence. Errors due to reabsorption followed by re-emission of fluorescence can become high if the exciting radiation is absorbed near the front face of the cuvette. At least 85% of the emitted fluorescence moves back into the solution where a fraction of it may be reabsorbed. The re-emitted radiation adds to the primary fluorescence escaping from the front face of the cuvette. Corrections to Förster's equation for reabsorption of fluorescence have been made by Budo and Ketskeméty[18] and their method with slight modifications was adopted here. Previous workers have also neglected shifts in the region of absorption away from the front face when the solution is diluted. This effect is important if the photocell is placed close to the cuvette. The equation of Budo and Ketskeméty therefore was modified to allow for such shifts

$$dB'(\lambda') = AQf(\lambda')d\lambda'\alpha_\lambda x \int_{z=0}^{l} \frac{d^2}{(d+mz)^2} \Big/ [\exp -(\alpha_\lambda x + \alpha_{\lambda'} z)][1 + QK' + Q^2K'K'' + \ldots]dz \quad (2)$$

where

A = $\rho E_0/4\pi n^2$ (see Förster[1])

Q = absolute quantum efficiency of fluorescence

α = absorption coefficient (= k in Förster[1])
= 2.303 ϵc where ϵ = molecular extinction coefficient and c = concentration, mole/l. Thus α_λ = absorption coefficient at the wave length of the exciting radiation λ; $\alpha_{\lambda'}$ = absorption coefficient at the wave length λ'

l = thickness of the liquid in the cuvette (cm.)

x = $\sec\left[\sin^{-1}\left(\frac{\sin\theta}{n}\right)\right]$ where θ = angle of incidence of the exciting beam on the front face of the cuvette

d = distance from the face of the cuvette to the observing aperture (cm.)

m = 0.65 to 0.75 for the solvents used here (see below and ref. 19)

$K', K'', \ldots = \int_0^\infty f(\lambda')M(\lambda',z,c)d\lambda', \int_0^\infty f(\lambda'')M(\lambda'',z,c)d\lambda'', \ldots$, where $M(\lambda',z,c)$ = fraction of fluorescence reabsorbed at the wave length λ' (secondary fluorescence); $M(\lambda'',z,c)$ = fraction of the secondary fluorescence reabsorbed at λ'' (tertiary fluorescence) .... and so on. (See Budo and Ketskeméty[18]). Note, $\int_0^\infty f(\lambda')d\lambda' = \int_0^\infty f(\lambda'')d\lambda'' = \ldots = 1$

z = distance from the front face (the glass/liquid interface) into the solution (cm.)

Errors caused by shifts in the region of absorption are corrected by the term $d^2/(d + mz)^2$. In the absence of refraction effects, $m = 1$, but with a liquid in the cuvette $m = 0.7$ (for $n = 1.45$). This foreshortening effect has been discussed in ref. 19. Assuming $m = 0$ can give an error up to 10% if the observing aperture is placed 10 cm. from a cuvette 1 cm. thick. The complete neglect of the reabsorption term can result in an error of up to 50% if about 30 to 50% of the absorption spectrum overlaps the fluorescence spectrum and the fluorescence efficiency is high.

The following assumptions have been made: the fluorescence is assumed to be emitted isotropically; the efficiency of fluorescence is assumed to be independent of wave length; the exciting radiation is assumed to fall on a small area of the cuvette, making virtually a point source

The reabsorption factors $M(\lambda',z,c)$, $M(\lambda'',z,c)\ldots$ depend on the wave length λ', $\lambda'' \ldots$, the shape of the cuvette, the concentration of the solute, the direction of the exciting beam and the position of this beam on the cuvette face. Fluorescence measurements were made with disc-shaped cuvettes, focussing the exciting radiation at an angle o-45° on the center of the flat front face. The calculation of the reabsorption of fluorescence for thif case is outlined in Appendix II. The calculation of fluorescence reabsorption also has been made by

(16) A. Seidell, "Solubilities of Inorganic and Metal-organic Compounds," D. Van Nostrand Co., New York, N. Y., Vol. 1, 3rd ed. (1940).

(17) Ref. 10, suppl. (1952).

(18) A. Budo and I. Ketskeméty, *J. Chem. Phys.*, **25**, 595 (1956).

(19) B. A. Brice, M. Halwer and R. Speiser, *J. Opt. Soc. Am.*, 4,0 768 (1950).

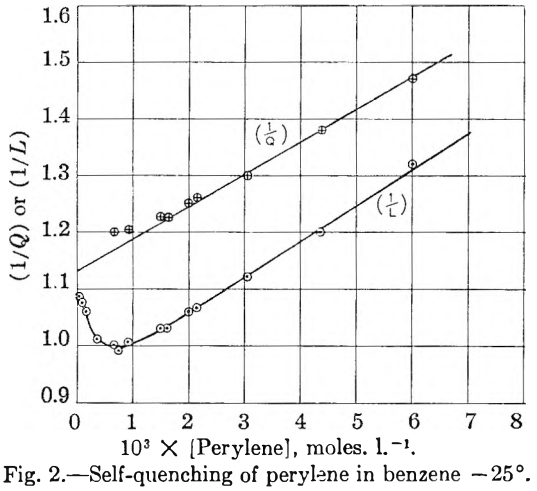

Fig. 2.—Self-quenching of perylene in benzene −25°.

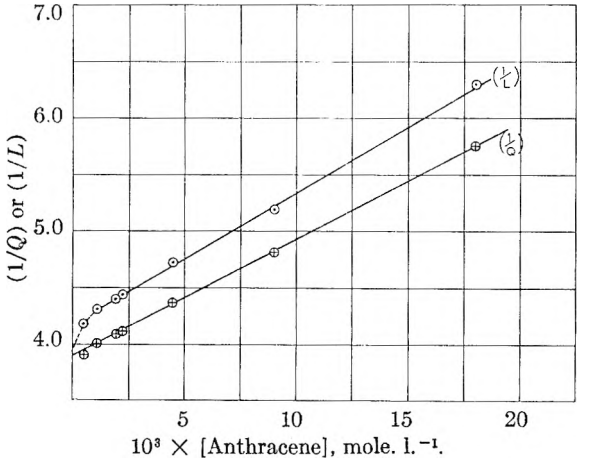

Fig. 3.—Self-quenching of anthracene in benzene −25°.

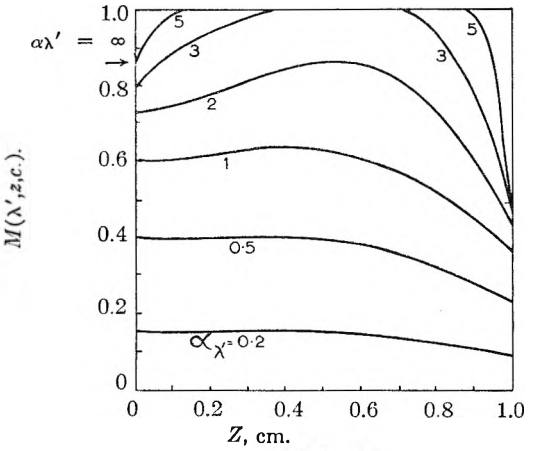

Fig. 4.—Reabsorption factor ($M(\lambda',z,c)$ for a disc-shaped cuvette (3 cm. diam., 1 cm. thick).

Budo and Ketskeméty[16] but the conditions for which their equation holds were not stated clearly.

The observed absolute efficiency L, is obtained if reabsorption is neglected in equation 2 (*i.e.*, $\alpha_{\lambda'} = \alpha_{\lambda''} = \cdots = 0$)

$$dB'(\lambda') = ALf(\lambda')d\lambda'\alpha\lambda x \int_{z=0}^{l} \frac{d^2}{(\alpha + mz)^2}(\exp(-\alpha\lambda x)dz \quad (3)$$

The relation between L and Q can be easily determined for two special cases: (a) when absorption of exciting radiation is virtually complete in the first 1 to 2 mm. Then $M(\lambda',z,c) \approx M(\lambda'',z,c) \approx \cdots \approx 1$ up to a cut-off wave length λ_c, the long wave length edge of the absorption band. Thus $K' \approx K'' \approx \cdots = \int_{\lambda'=0}^{\lambda c} f(\lambda')d\lambda'$. Then on integrating equation 2

$$\int_{\lambda'=0}^{\infty} dB'(\lambda') = AQ(1 - K'Q)^{-1} \Big/ \left\{\int_{\lambda'=0}^{\lambda c} f(\lambda')[\alpha\lambda x/(\alpha\lambda x + \alpha\lambda')]d\lambda' + 1 - K'\right\}$$

Also under the same conditions equation 3 becomes

$$\int_{0=\lambda'}^{\infty} dB'(\lambda') = AL$$

Thus

$$L = Q(1 - K'Q)^{-1}\left\{\int_{z=0}^{\lambda c} f(\lambda')[\alpha\lambda x/(\alpha\lambda x + \alpha\lambda')]d\lambda' + 1 - K'\right\} \quad (4)$$

(b) When the absorption of exciting radiation is small. Then $M(\lambda', z, c) = M(\lambda', 0, c)$ since $M(\lambda', z, c)$ is nearly independent of z when α is small (Fig. 4). Also assuming $M(\lambda', 0, c) \approx M(\lambda', 0, c) \approx \ldots$, etc., and since $K'(0, c) = \int_{\lambda'=0}^{\infty} \Big/ f(\lambda')M(\lambda', 0, c)d\lambda'$, then following the same proceedure as above

$$L = Q(1 + K'(0,c)Q + K'(0,c)^2Q^2 + \ldots) \Big/ \left[\alpha\lambda x \int_{z=0}^{l} \frac{\alpha^2}{(\alpha + 0.7z)^2}(\exp(-\alpha\lambda x)dz\right]$$
$$= Q(1 - K'(0,c)Q)S(\alpha\lambda x) \quad (5)$$

The exciting radiation was assumed to be absorbed more strongly than any of the fluorescence radiation (*i.e.*, $\alpha_\lambda > \alpha_{\lambda'}$). The integral in brackets

$$\alpha\lambda x \int_{z=0}^{l} \frac{d^2}{(d + 0.7z)^2}(\exp(-\alpha\lambda x))dz = S(\alpha\lambda x) \quad (6)$$

has been evaluated for $d = 10.5$ cm. and $b = 1.0$ cm. and is compared with the expression $1 - \exp(-\alpha_\lambda x)$ in Table I.

TABLE I

VALUES OF THE INTEGRAL $S(\alpha_\lambda x)$ (EQUATION 6)

$\alpha_\lambda x$	$S(\alpha_\lambda x)$	$1 - \exp(-\alpha_\lambda x)$
0.02	0.0185	0.0198
.06	.0556	.0582
.10	.0890	.0952
.4	.314	.330
.8	.520	.551
1.0	.595	.632
4	.932	.982
8	.977	1.000
10	.985	1.000
15	.994	1.000

Absolute quantum efficiencies of fluorescence were calculated from equation 4 since the concentrations of the solutions were such as to absorb greater than 99% of the exciting radiation in 10 mm. The fluorescence efficiency of 9,10-diphenylanthracene was, however, determined over a wide concentration range and the measurements corrected by both equations 4 and 5. The corrected efficiencies shown in Table II are remarkably constant over the concentration range 10^{-4} to 10^{-2} M. Self-quench-

TABLE II

CORRECTION OF OBSERVED FLUORESCENCE EFFICIENCIES OF 9,10-DIPHENYLANTHRACENE (25°)

$10^3 \times$ concn. (mole/l.)	Obsd. intensity	$S(\alpha_\lambda x)$	L	Q (cor.) K'	Q (cor.) Eq. 4	Q (cor.) Eq. 5
10.0	1.000					
7.8	1.003					
5.0	1.000	1.000	1.000	0.35	0.84	..
2.0	1.005					
1.5	1.000					
1.11	0.970	0.995	0.975	..	..	..
0.71	.935	.985	.950	..	..	..
.50	.925	.972	.950	..	..	..
.220	.835	.908	.920	0.14	..	0.81
.130	.728	.820	.89	.09	..	.82
.090	.610	.690	.88	.07	..	.83
.050	.418	.480	.87	.05	..	.83
.030	.280	.338	.84	.03	..	.83
.0153	.152	.185	.82	.01	..	.82

ing constants were determined by plotting $1/Q$ against concentration. The deviation from the Stern–Volmer law (equation 7) if reabsorption was neglected was particularly noticeable for perylene where a plot of $1/L$ against concentration actually went through a minimum (Fig. 2). At low concentrations, there was usually a deviation from the simple law which probably was due to the inadequacy of equation 4 at these concentrations. The effect of concentration on the efficiency of fluorescence of anthracene in benzene is shown in Fig. 3 where both $1/L$ and $1/Q$ are plotted against concentration. It is evident that neglect of reabsorption would have led to an error in both k_s and Q_0. The results of similar measurements on several organic substances are given in Table III.

The self-quenching of fluorescein in water (*p*H 12.5) has been measured by Budó, Dombi and Szöllösy[9] who corrected the observed efficiencies for the large amount of fluorescence reabsorption. The observed efficiencies also were corrected using equation 4. It was found that the corrected points fell very close to those of Budó, *et al.* (see Fig. 1). This observation seemed to justify the use of the much simpler equation (equation 4).

Discussion

A decrease in the fluorescence efficiency of a solute as the concentration is increased is due to the quenching of excited solute molecules by unexcited ones (self-quenching). If the quenching requires the close encounter of the two solute molecules, the change in the fluorescence efficiency with concentration should obey the Stern–Volmer law

$$Q_0/Q = 1 + k_s C \qquad (7)$$

Q_0 = efficiency at infinite dilution
Q = efficiency at the concn. c (mole/l.)
k_s = self-quenching constant

It has been considered by many authors notably Förster[3] (p. 176 and 218) that overlap between absorption and fluorescence spectra of a molecule indicates a close coupling between excited and unexcited molecules which can cause quenching even when the molecules are separated over several molecular diameters. Self-quenching by this mechanism obeys the Stern–Volmer law only over a limited concentration range. In the work described here, deviations from the Stern–Volmer law were traced to reabsorption effects (see Figs. 2 and 3).

Bowen and Sahu[20] found the efficiency of 9,10-diphenylanthracene to be 1.0 whereas Bowen and Cook[21] gave the figure 0.80 at low concentrations. As in our work (Table II) these figures may differ as a result of the reabsorption of fluorescence.

The efficiencies of 9-cyanoanthracene and perylene in petrol ether and ethanol at infinite dilution were calculated from equation 7 using these estimates for k_s

9-cyanoanthracene, petroleum ether	$k_s = 300$
9-cyanoanthracene, ethanol	$= 100$
perylene, petroleum ether	$= 200$
perylene, ethanol	$= 80$

Since the solutions are so dilute, large errors in these estimates would not greatly affect Q_0.

The rate constants for self- and oxygen-quenching (Table IV) have been estimated using methods similar to those of Bowen.[6] The fluorescence lifetimes of the substances were calculated from the equation of Förster[3] (p. 158) using the absorption spectra determined in ethanol solution. k_1 is the rate constant for self-quenching, k_2 that for oxygen-quenching. It appears from Table IV that self-quenching is less efficient than oxygen quenching, that is, may not be diffusion controlled, but this question can only be answered satisfactorily by investigating the effect of viscosity on self-quenching.

Acknowledgment.—The author is indebted to Mr. B. J. O'Brien of this Institute for helpful discussions.

Appendix I

Absolute Quantum Fluorescence Efficiency of the Quinine Bisulfate Standard.—The absolute quantum efficiency of fluorescence of a 5×10^{-3} *M* solution of quinine bisulfate in 1 *N* H_2SO_4 at 25° was measured by the method described previously.[5] A more stable a.c. apparatus described above replaced the d.c. method used in ref. 5. Five measurements gave the following results (figures are relative quanta sec.$^{-1}$ cm.$^{-2}$.): (1) exciting radiation scattered from MgO (1 mm.) = 9800 ± 30; (2) radiation scattered into the photomultiplier from MgO with a non-fluorescent red dye in the quantum counter = 40 ± 3; (3) fluorescence from the quinine bisulfate solution = 685 ± 5; (4) radiation scattered into the photomultiplier from the quinine bisulfate solution with a non-fluorescent red dye in the quantum counter = 4 ± 1; (5) radiation scattered from the exciting beam into the quantum counter by the cuvette window = 13 ± 1.

The radiation scattered from a very thick block of MgO which is used for the determination of absolute reflectivities, is about 1.5% higher than from a 1 mm. block; thus (1) must be increased by 1.5%. The previous equation used for calculating absolute quantum efficiencies of fluorescence (ref. 5) is not quite correct; the absolute reflectivity of MgO at 366 mμ is 0.93[22] and not 0.96 which was

(20) E. J. Bowen and J. Sahu, *J. Phys. Chem.*, **63**, 4 (1959).
(21) E. J. Bowen and R. J. Cook, *J. Chem. Soc.*, 3059 (1953).
(22) F. Benford, S. Schwarz and G. P. Lloyd, *J. Opt. Soc. Am.*, **38**, 964 (1948).

TABLE III

ABSOLUTE QUANTUM FLUORESCENCE EFFICIENCIES, SELF- AND OXYGEN-QUENCHING CONSTANTS AT 25°

Substance	Solvent	Concn., M	L	Q	k_s	Q_0	$k(O_2)$[a]
Quinine bisulfate	1 N H_2SO_4	5×10^{-3}	0.510	0.508	14.5	0.546	<5
Anthracene	Benzene	2×10^{-3}	.228	.241	27.5	.256	128
Anthracene	Pet. ether[b]	3×10^{-3}	.220	.241	103	.316	240
Anthracene	Ethanol	3×10^{-3}	.228	.249	28.5	.270	158
Anthracene	H. par.[c]	3×10^{-3}	.295	.323	4 ± 2	.328	..
9-Bromoanthracene	Benzene	1.5×10^{-3}	.048	.050	18 ± 2	.052	25
9-Bromoanthracene	Pet. ether	1.5×10^{-3}	.022	.024	[e]	(.025)	13
9-Bromoanthracene	Ethanol	1.5×10^{-3}	.018	.019	10 ± 5	.020	12
9,10-Dibromoanthracene	Benzene	1.5×10^{-3}	.202	.213	20.5	.220	45
9,10-Dibromoanthracene	Pet. ether	10^{-3}	.081	.088	[e]	(.10)	38 ± 5
9,10-Dibromoanthracene	Ethanol	9×10^{-4}	.096	.103	[e]	(.11)	41
9-Cyanoanthracene	Benzene	1.5×10^{-3}	.885	.796	79	.878	190
9-Cyanoanthracene	Pet. ether	9.2×10^{-4}	.755	.660	[e]	(.85)	140
9-Cyanoanthracene	Ethanol	1.5×10^{-3}	.845	.740	[e]	(.85)	240
9,10-Diphenylanthracene	Benzene	1.5×10^{-3}	1.000	.840	<2	.84	210
9,10-Diphenylanthracene	Pet. ether	10^{-3}	1.002	.83	<2	.83	295
9,10-Diphenylanthracene	Ethanol	10^{-3}	0.975	.81	<2	.81	280
9,10-Di-(1-naphthyl)-anthracene	Benzene	1.5×10^{-3}	.745	.63	[e]	(.61)	140
Perylene	Benzene	2×10^{-3}	.945	.800	52.5	.890	210
Perylene	Pet. ether	5.5×10^{-4}[f]	.913	.790	[e]	(.88)	228
Perylene	Ethanol	3.5×10^{-4}[f]	.990	.840	[e]	(.87)	195
Anthranilic acid	Benzene	8×10^{-3}	.548	.536	10.5	.582	220
Anthranilic acid	Ethanol	1.3×10^{-2}	.575	.558	5.3	.588	290
Methyl anthranilate	Benzene	2.7×10^{-2}	.565	.549	1.0	.565	210
Methyl anthraniliate	Pet. ether	2.7×10^{-2}	.380	.376	2.5	.402	240
Methyl anthranilate	Ethanol	2.7×10^{-2}	.681	.656	1.6	.685	250
2-Naphthylamine	Benzene	2.7×10^{-2}	.497	.486	1 ± 0.3	.50	480
Acridone	Ethanol	1.5×10^{-3}	.845	.780	43	.825	170
Diphenylhexatriene	Benzene	10^{-3}	.796	.750	..	...	225
Diphenylhexatriene	Pet. ether	6×10^{-4}	.640	.610	..	...	490

[a] $k(O_2)$ = oxygen-quenching constant. [b] Unpurified petrol ether gave $k_s = 99$ and $Q_0 = 0.285$. [c] Heavy paraffin, 150 centipoise. [d] Petrol ether, 0.43 centipoise. [e] Not sufficiently soluble to allow the measurement of the self-quenching constant. [f] Exciting radiation not completely absorbed; the fluorescence was corrected by equation 6.

TABLE IV

CALCULATED RATE CONSTANTS FOR SELF- AND OXYGEN-QUENCHING (25°)

Substance	Solvent	$10^9 \times \tau e$[a] (sec.)	$10^9 \times \tau$[b]	$10^{-9} \times k_1$ (l. mole^{-1} sec.$^{-1}$)	$10^{10} \times k_3$
Anthracene	Ethanol	15.5	4.2	7.0	3.8
Anthracene	Pet. ether		4.9	20.9	4.9
Anthracene	Benzene		4.0	6.9	3.2
Quinine bisulfate	1 N H_2SO_4	20.0[c]	10.9	1.3	<0.05
9-Bromoanthracene	Ethanol	13.8	0.28	29	4.2
9-Bromoanthracene	Pet. ether		.35	...	3.7
9-Bromoanthracene	Benzene		.72	14	3.5
9,10-Dibromoanthracene	Ethanol	12.5	1.4	...	2.9
9,10-Dibromoanthracene	Pet. ether		1.3	...	2.9
9,10-Dibromoanthracene	Benzene		2.8	7.3	1.6
9,10-Diphenylanthracene	Ethanol	9.0[d]	7.3	<0.3	4.1
9,10-Diphenylanthracene	Pet. ether		7.5	<0.3	4.2
9,10-Diphenylanthracene	Benzene		7.6	<0.3	3.0
Perylene	Ethanol	5.7[d]	5.0	...	4.0
	Pet. ether		5.1	...	4.5
	Benzene		5.1	7.8	4.2
Acridone	Ethanol	15.2	12.5	3.1	1.3

[a] Solvent, ethanol. [b] $\tau = \tau e/Q_0$ (Q_0 from Table III). [c] Calculated from the spectrum in 1 N H_2SO_4. [d] Bowen[4] gives 7.9 and 6.9 $\times 10^{-9}$ sec., respectively.

the result of a wide extrapolation from earlier data given by these authors. Theoretically determined values of $I_0/I_{av.}$ given previously[5] are not correct since experimentally determined values were found to be closer to unity. The figures used for calculating the absolute quantum fluorescence efficiency of the standard solution were:

$(F/S) = (685 - 17)/(8900 - 40) = 0.075$
$n^2 = 1.81$
$I_0/I_{av.} = 1.005$

R_1 = 0.92 = relative reflectivity of MgO when illuminated at 45° compared with normal illumination
R_2 = 0.93 = absolute reflectivity at MgO at 366 mμ
R_e = 0.050 = exciting light lost by reflection off the cuvette face
R_f = 0.039 = fluorescence light lost by reflection off the cuvette face

R_0 and R_f were determined experimentally. The results agreed closely with those calculated from Fresnel's formula. (F/S) was decreased by 1% to allow for the lower transmission of the cuvette face at 366 mμ compared with longer wave lengths. Thus

$$Q = (F/S)4n^2(I_0/I_{av.})R_1R_2/(1 - R - R_f) = 0.510 \text{ at } 25°$$

The observed absolute efficiencies of other solutions were measured with reference to this standard as

$$Q_x = (x/s)\ 0.282n_x^2$$

where

x = relative quanta/sec. from the unknown
s = relative quanta/sec. from the standard
n_x = refract. index of the soln. containing the unknown x

Appendix II

Reabsorption of Fluorescence in a Disc-shaped Cuvette.—A disc-shaped cuvette of radius R and thickness l is illuminated with a narrow, parallel beam of radiation incident at an angle between 0 and 45° on the flat front face of the cuvette. The thickness of the window is considered negligible compared with l. The sides and back of the cuvette are painted with non-reflecting black paint to prevent internal reflection.

A small volume element, dz, part of the narrow exciting beam causing fluorescence in the solution, is situated a distance z behind the front face. Consider a cone of fluorescence radiation passing through the solution, the axis of the cone coinciding with the axis of the disc and the vertex being at z. The fraction of the radiation of a particular wave length λ' between the cones with vertical half angles θ and $\theta + d\theta$, absorbed by the solution is

$$1 - [\exp(-\alpha_{\lambda'}\, l(\theta)]$$

where

$\alpha_{\lambda'}$ = absorption coefficient of the solution at λ'
$l(\theta)$ = path length (varies with θ)

For the whole cuvette, the fraction absorbed is

$$M(\lambda',z,c) = \int_0^{\pi} \{1 - [\exp(-\alpha_{\lambda'} l(\theta))]\} \sin\theta\, d\theta$$

$l(\theta)$ is not a simple function of θ but behaves as follows: In the hemisphere above the plane of the cuvette window (away from the solution)

θ = 0 to θ_c $l(\theta) = z \sec\theta$ where $\theta_c = \sin^{-1}(1/n)$
= θ_c to $\pi/2$ $= R \operatorname{cosec}\theta$

In the hemisphere below the window (into the solution)

θ = 0 to θ_1 $l(\theta) = (l - z)\sec\theta$ where $\theta_1 = \tan^{-1}/[R/(l - z)]$
= θ_1 to $\pi/2$ $= R \operatorname{cosec}\theta$

The four integrals were evaluated graphically for different values of z and $\alpha_{\lambda'}$ for a cuvette with R = 15 cm. and b = 10 mm. The results are plotted in Fig. 4.

The calculation of $M(\lambda'', z, c)$ (the fraction of secondary fluorescence reabsorbed) is in principle possible using the above method, but would be very laborious and therefore was not attempted here.

CONTINUOUS DISSOLUTION OF COPPER BY NITRIC ACID

BY EDWARD A. TRAVNICEK AND JAMES H. WEBER

University of Nebraska, Lincoln, Nebraska

Received June 20, 1960

The kinetics of the reaction between copper and nitric acid were studied in a flow reactor in which a continuous dissolution process was performed. Experiments were carried out at 20, 30, 40 and 50° over a range of acid concentration of 3 to 5.5 N. The results are consistent with those of previous investigators who believe the nitrous acid produced in one step of the dissolution process acts as an autocatalyst for the reaction. At acid normalities of 4.3 and 5.5, the energy of activations—as defined by Arrhenius—were found to be 9.73 ± 0.30 kcal./g. atom of copper and 7.83 ± 0.14, respectively, over the temperature range of 30–50°.

The continuous dissolution of metals is a phenomenon which has been investigated only infrequently. While the practical applications of this type of process are limited, experimentation in this area can be of scientific interest. In contrast, a number of studies have been made of the batchwise dissolution of metals. This type of experiment often yields the information necessary to determine the rate-controlling step, be it chemical reaction or diffusion, of the process involved. Frequently, however, this is not the case.

Furthermore, the results obtained from experiments conducted batchwise by different groups of investigators are often difficult to compare. The reason is that quite different methods may have been employed. For example, one investigator may rotate a cylindrically shaped metallic sample in the dissolving medium, while another may immerse a thin metallic sheet in an agitated bath of the medium.

On the other hand, in a continuous process the flow rate and, in turn, the flow pattern of the dissolving medium over the surface of the metal can be controlled and reproduced. This, of course, presupposes a properly shaped sample of metal.

In this investigation, which follows the work of Johnson, Hobson and Weber[1] and Kissinger,[2] the

(1) R. L. Johnson, M. Hobson and J. H. Weber, *Ind. Eng. Chem.*, **50**, 1194 (1960).
(2) R. D. Kissinger, Master's Thesis, Univ. of Nebraska, 1958.

continuous dissolution of copper by nitric acid was performed. The purpose was to study the effects of variations in temperature, nitric acid concentration, acid flow rate, and bar length on the rate of dissolution.

The dissolution of copper by nitric acid has been studied previously,[3-12] however, the tests of these workers have been performed batchwise. Various degrees of agitation, different sizes and shapes of copper specimens, and different sized equipment were used. It follows that the flow of the acid over the surface of the metal was not uniform and the rates of dissolution obtained cannot be reduced to a common basis for purposes of comparison.

If the rate of dissolution of copper by nitric acid was controlled by the chemical reaction rate, then the rate of dissolution would not be a function of the acid flow rate over the surface of the metal. However, as numerous authors[8,9,11,13-16] have pointed out, the degree of agitation has an effect on the rate of dissolution. Hence, the rate of dissolution is not controlled entirely by the chemical reaction rate. Buben and Frank-Kamenetskii[14] have proposed that the dissolution of copper is a diffusion controlled reaction and the rate of diffusion depends on the condition of flow past the metallic surface in the same manner as the rate of heat transfer. King and Cathcart[17] have also shown that a diffusion controlled reaction is dependent on the conditions of flow as is the case in heat transfer and suggest that heat transfer rates and dissolution rates may be compared.

The dissolution of copper in nitric acid proceeds in a somewhat unique manner. The nitrous acid which is a reaction product serves as the autocatalyst for the main reaction.[15,16,18-22]

Hedges,[23] as well as Berg,[24] suggest that nitric acid reacts with copper to form cupric oxide. The former proposes that a series of reactions takes place

$$Cu + HNO_3 \longrightarrow CuO + HNO_2 \quad (1)$$

$$CuO + 2HNO_2 \longrightarrow Cu(NO_2)_2 + H_2O \quad (2a)$$

$$CuO + 2HNO_3 \longrightarrow Cu(NO_3)_2 + H_2O \quad (2b)$$

$$Cu(NO_2)_2 + 2HNO_3 \longrightarrow Cu(NO_3) - 2HNO_2 \quad (3)$$

$$3HNO_2 \longrightarrow HNO_3 + 2NO + H_2O \quad (4a)$$

$$HNO_2 + HNO_3 \longrightarrow 2NO_2 + H_2O \quad (4b)$$

Hedges states that dilute nitric acid gives NO as the main product as in reaction 4a, whereas concentrated acid gives mainly NO_2, as in reaction 4b. In most cases a mixture of both NO and NO_2 is produced.

Centnerswer and Heller[7,15] conclude that the copper ions go immediately into the solution as indicated by the equation

$$2HNO_3 + 3Cu + 6H^+ \longrightarrow 2NO + 3Cu^{++} + 4H_2O \quad (5)$$

In either case the NO formed is oxidized by the nitric acid, or the dissolved oxygen, to nitrogen dioxide which is then dissolved in water to form both nitrous and nitric acid.

It is the autocatalytic action of nitrous acid which is often used to explain the fact that an increase in the degree of agitation of the acid solution decreases the speed of dissolution.[7] Increased agitation tends to remove the nitrous acid formed by the reaction from the surface of the metal rapidly and thus decreases the catalytic action.

Berg[25] proposes that the copper reacts with the nitric acid molecules rather than the hydrogen or nitrate ions and has reported the rates of dissolution by copper determined from batch tests as a function of the concentration of the undissociated nitric acid molecules.

$$V(\text{gram-atom/cm.}^{-2}\text{-sec.}) = 147c(1 - \alpha) \quad (6)$$

Later, Berg[4] changed the value of the constant from 147 to 141 to get better agreement with additional data. In another article Berg[3] presented the relationship

$$V(\text{gram atom/cm.}^{-2}\text{-sec.}) = 1.33Tc(1 - \alpha)e^{-8860/RT} \quad (7)$$

This was applied over the temperature range -10 to $+30°$.

One difficulty with obtaining this type of correlation is the lack of reliable dissociation data for nitric acid. In obtaining the original correlation, equation 6, various dissociation data[26-28] were plotted and smoothed. These smoothed data show that the acid is dissociated completely below an acid concentration of 3.3 *N*. It might be pointed out here that in a later paper Berg[24] used only the dissociation data of Chedin.[26] The most recent dissociation data are those of Renner and Theimer[29] and those of Hood and Reilly.[30] The latter determined the degree of dissociation of nitric acid at 0, 25 and 70° over a wide range of concentrations. Previously, the investigations of the degree of dissociation had been restricted to conditions at 20 or 25°. There is not good agreement between the various sets of data.

(3) T. G. Owe Berg, *Z. anorg. allgem. Chem.*, **266**, 118, 130 (1951).
(4) T. G. Owe Berg, *ibid.*, **269**, 210 (1952).
(5) T. G. Owe Berg, *ibid.*, **273**, 101 (1953).
(6) T. G. Owe Berg, *Z. Metallkunde*, **44**, 82 (1953).
(7) M. Centnerszwer and W. Heller, *Roczniki Chem.*, **18**, 425 (1938).
(8) Ya. V. Durdin, *J. Gen. Chem.* (*U.S.S.R.*), **21**, 801 (1951).
(9) J. L. de Hauss, *Chim. anal.*, **34**, 185 (1952).
(10) K. Inamura, *Sci. Rep. Tohoku Univ.*, **16**, 999 (1927).
(11) A. I. Krasilshchikov and I. V. Dedova, *J. Gen. Chem.* (*U.S.S.R.*), **16**, 537 (1946).
(12) Y. Yamamoto, *Bull. Inst. Phys. Chem. Res.* (*Tokyo*), **19**, 281, 437, 587 (1940).
(13) T. G. Owe Berg, *J. chim. phys.*, **53** 109 (1956).
(14) N. Ya. Buben and D. A. Frank-Kamenetskii, *J. Phys. Chem.* (*U.S.S.R.*), **20**, 225 (1946).
(15) M. Centnerszwer and W. Heller, *Metaur et Corrosion*, **14**, 37 (1939).
(16) E. S. Hedges, *J. Chem. Soc.*, 561 (1930).
(17) C. V. King and W. H. Cathcart, *J. Am. Chem. Soc.*, **59**, 63 (1937).
(18) G. V. Akimov and B. P. Batrakov, *J. Phys. Chem.* (*U.S.S.R.*), **13**, 1807 (1939).
(19) G. V. Akimov and I. L. Rosenfeld, *ibid.*, **14**, 1486 (1940).
(20) N. R. Dhar, THIS JOURNAL, **29**, 142 (1925).
(21) N. A. Izgaryschev, *Z. Elektrochem.*, **32**, 281 (1926).
(22) O. H. Veley, *Phil. Trans.*, *A*, 182 (1891).
(23) E. S. Hedges, "Protective Films on Metals," Chapman and Hall, Ltd., London, 1932.
(24) T. G. Owe Berg, *J. chim. phys.*, **50**, 617 (1953).
(25) T. G. Owe Berg, *Z. anorg. allgem. Chem.*, **265**, 332, 338 (1951).
(26) J. Chedin, *Ann. Chim.*, **8**, 243 (1937).
(27) R. Dalmon, *Mem. serv. chim. etat.*, **29**, 141 (1943).
(28) O. Redlich and J. Bigeleisen, *J. Am. Chem. Soc.*, **65**, 1882 (1943).
(29) H. Renner and O. Thiemer, *Acta Phys. Austr.*, **6**, 78 (1952).
(30) G. C. Hood and C. A. Reilly, *J. Chem. Phys.*, **32**, 127 (1960).

Although Berg's experimental work shows no dissolution below 3.3 N, Hauss[9] reports appreciable dissolution by acid of 1.0 N. Buben and Frank-Kamenetskii[14] and Krasilshchikov and Dedova[11] report that the action of nitric acid on copper is not reproducible at an acid concentration of 1 N and below. The results of Johnson, *et al.*,[1] agree with these latter authors.

The formation of the cupric oxide, as indicated by equation 1, is used to explain the passivity of copper toward more dilute nitric acid solutions after being placed in higher normality acid solutions. According to Hauss,[9] the weaker acid is not strong enough to dissolve the cupric oxide formed by the stronger acid and the copper then appears to be passive to the weaker acid.

A = frequency factor, eq. 8
E = energy of activation, eq. 8
G = mass velocity, g./cm.²-sec.
N = normality
R = gas law constant, 1.98 cal./g. mole °K.
T = absolute temperature, °K.
c = concn. moles/l.
k = reaction rate constant, eq. 8
α = degree of dissociation of nitric acid

Apparatus

The reactor consisted of an all glass, water jacketed, vertical tube of 24.4 mm. inside diameter. The copper bar was mounted coaxially in the reactor and retained in position by means of two 1.9 cm. diameter polyethylene rods. The reacting acid passed upward through the annular space between the bar and the reactor wall. The bar was centered between the feed entrance and exit, with calming sections of approximately 15.2 cm. between the ends of the bar and the feed entrance and exit.

Since temperature changes have a large effect upon reaction rates, the temperature of the system must be carefully controlled. A constant temperature bath with a thermostatically controlled electric heater was used. The constant temperature bath was also equipped with a water cooling and steam heating coil. A pump was used to circulate water through the jacket of the reactor.

The feed was brought to the desired temperature by passing it through a stainless steel coil (0.9 cm. o.d., 18–8, type 304) immersed in the constant temperature bath. The flow rate was controlled with a 0.9 cm. stainless steel needle valve and measured with a calibrated flowmeter. The flowmeter was calibrated for each temperature and acid concentration by measuring the amount of acid leaving the reactor in a given period of time.

Temperatures were measured with copper–constantan thermocouples used in conjunction with a Leeds and Northrup semi-precision potentiometer.

Air pressure was used to force the acid from the product receiver to the feed tank at the end of a run. Since the air lines did not come into contact with the acid, they were constructed of copper tubing. All equipment in contact with the acid was either glass, polyethylene or stainless steel.

Experimental Procedure

Preparation of Acid.—The feed tank was partially filled with distilled water and a previously determined amount of concentrated nitric acid added. As the acid was added, air was bubbled through the solution to mix the acid and reduce the concentration of oxides of nitrogen. Samples of the feed were titrated with standardized base. Water, or concentrated acid, as needed, then was added to obtain the desired acid concentration.

Preparation of the Copper Bar.—The condition of the surface of the copper bar is an important factor. To give reproducible results the bars were prepared carefully and in the same manner before use. If the surface of the bar was irregular, the bar was turned down in a lathe; if not, a fine abrasive cloth was used for a preliminary polishing. Finely ground aluminum oxide was used for the final polishing, after which the diameter of the bar was accurately measured at a number of positions.

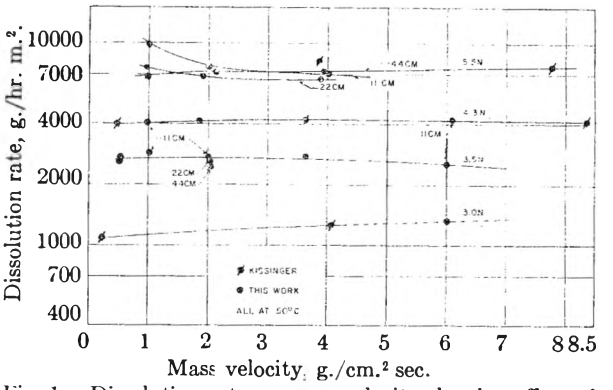

Fig. 1.—Dissolution rate *vs.* mass velocity showing effect of bar length and acid concentration at 50°.

Reaction Procedure.—Before the start of a run the desired flow rate was calculated and the feed adjusted to the proper concentration. After the bath and the water jacket reached the proper temperature, the reactor was filled with acid. The bar was inserted and centered and the acid flow was started immediately at the predetermined rate to prevent oxides of nitrogen from reaching a high concentration.

After the desired acid flow rate was established and a steady state reached, three product samples were taken at approximately five-minute intervals. A feed sample was also taken. Temperatures were measured before each product sampling. Within one minute after taking the last product sample, the bar was withdrawn and washed with tap water. The diameters of the bar were measured at the same positions as before the run. The final average diameter was used for the surface area and mass velocity calculations because the product samples were taken much nearer the end of the run than the start. Duplicate runs were made in a number of instances and the results were found to be reproducible within 10%.

Analytical Procedure.—The methods outlined by Snell[31] were used to determine the amount of copper dissolved. If the copper concentration was below 0.1 mg. per ml. of solution, the sodium diethyldithiocarbamate method was employed and four extractions with 5-ml. portions of carbon tetrachloride per 15-ml. samples were used. The percentage transmission and the absorbance of the copper solutions then were determined.

If the copper concentration in the sample was greater than 0.1 mg. per ml. of solution, concentrated nitric acid was added to the solution until 15 ml. of 6 N acid was obtained and then 10 ml. of concentrated ammonium hydroxide was added to bring out the color of the cupric–ammonium complex. The percentage transmission and the absorbance of the solutions then were determined.

Both systems were found to follow Beer's law; calibration curves also were made. A Beckman Model B spectrophotometer was used to measure the percentage transmission.

Discussion of Results

The continuous dissolution of copper was carried out on an experimental basis. The effects of variations of temperature over the range of 20 to 50°, of mass velocity, G, over the range of 0.2 to 6.5 g./cm.² sec., of acid concentration over the range of 3.0 to 5.5 N and of bar lengths from 11 to 44 cm. were observed. The data are presented in Table I and some are presented graphically (Figs. 1–3) with those of Johnson, *et al.*,[1] and Kissinger.[2]

For 3 N acid at temperatures of 20, 30 and 40° the reaction rate decreased with increasing mass velocity. This would be in agreement with the hypothesis that the gas formed in the reaction has a strong autocatalytic effect. As the mass velocity

(31) F. D. Snell and C. T. Snell, "Colorimetric Methods of Analysis," 3rd Ed., Vol. II, D. Van Nostrand Co., Inc., New York, N. Y., 1953, p. 107.

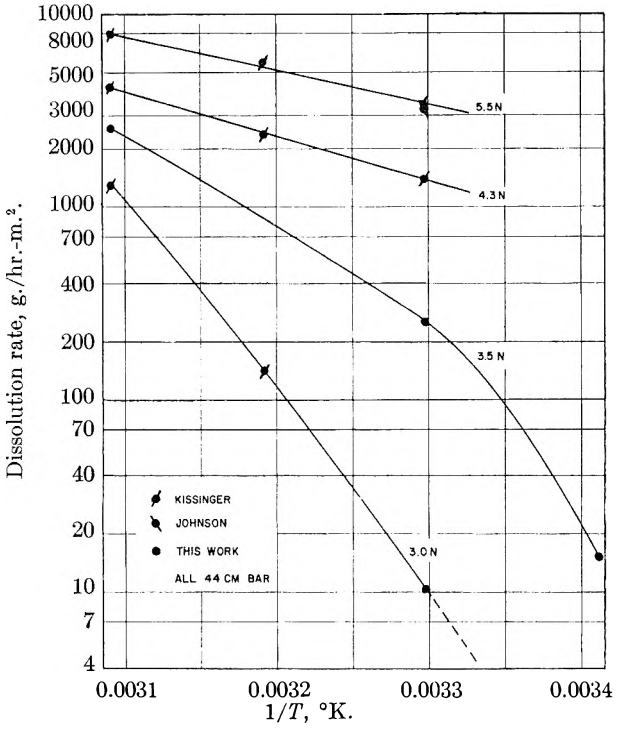

Fig. 2.—Dissolution rate *vs.* $1/T$ °K. with parameters of acid concentration for mass velocity of 6 grams per cm.² sec.

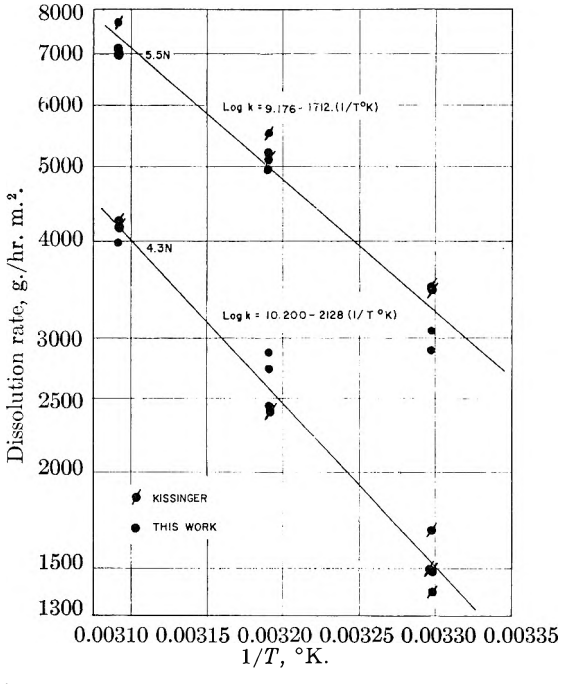

Fig. 3.—Dissolution rate *vs.* $1/T$ °K. with parameters of acid concentration combination of mass velocities of 1, 2, 4 and 6 grams per cm.² sec.

increases, the oxides of nitrogen tend to be removed from the surface of metal more rapidly, reducing the autocatalytic effect.

At low mass velocities the dissolution rate curves become non-linear. The reason for this may be that the heat produced by the reaction cannot be removed rapidly enough; hence, the temperature of the bar increases. The largest temperature rise occurred on run 59 in which the bar length was

TABLE I

DATA AND CALCULATED RESULTS

Bar diameter is 1.800 ±0.125 cm.

Nitric acid, *N*	Mass velocity, g./cm.²-sec.	Dissolution rate g./hr.-m.²
t = 20.0 ± 0.7°; bar length = 43.7 ± 0.2 cm.		
3.02	0.341	28.6
3.02	0.568	17.2
3.02	1.01	15.7
3.02	2.02	8.2
3.02	4.01	2.3
3.02	0.249	35.4
3.02	0.496	25.6
3.50	6.49	15
3.50	3.99	21
3.50	2.04	24
3.50	1.02	36
3.39	0.453	399
3.39	.173	414
3.50	.914	45
4.28	3.84	600
4.28	1.91	725
4.28	1.02	800
t = 30.0 ± 0.03°; bar length = 43.7 ± 0.2 cm.		
3.09	0.250	607
3.09	.494	181
3.09	.981	127.0
3.09	1.99	60.5
3.09	3.97	22.8
3.05	0.445	655
3.05	0.885	377
3.05	1.77	115
3.50	3.84	400
3.50	2.03	595
3.51	0.990	680
3.50	0.462	730
5.49	1.08	3280
Bar length = 21.9 cm.		
3.50	2.15	92
3.50	1.01	400
3.50	0.473	760
3.50	0.236	820
Bar length = 10.9 ± 0.2 cm.		
3.50	1.020	115
3.50	0.488	550
3.50	0.239	760
5.57	2.09	3060
5.49	1.01	2900
t = 40.0 ± 0.1°; bar length = 43.7 ± 0.2 cm.		
4.28	3.95	2730
4.28	1.04	2870
4.28	2.18	2440
Bar length = 11.1 cm.		
5.57	2.05	5250
5.57	1.00	4950
t = 50.0 ± 0.7°; bar length = 43.7 ± 0.2 cm.		
3.45	6.01	2640
3.50	3.65	2850
3.50	2.04	2460
4.14	1.88	4180
5.43 (Run 59)	1.03	9800

5.47	3.94	7180
5.37	2.01	7700
	Bar length = 21.9 cm.	
3.52	3.52	2800
3.45	1.99	2530
3.50	1.02	2560
3.50	0.498	2620
5.28	1.900	6780
5.43	0.960	7600
5.37	3.89	6750
	Bar length = 11.1 ± 0.2 cm.	
3.52	3.62	2990
3.45	1.89	2700
3.50	1.04	2860
3.50	0.488	2750
4.28	6.10	4210
4.28	0.945	4000
5.56	4.00	7030
5.28	0.985	6980
5.43	2.12	7200

44 cm., the acid concentration was 5.4 N, and the mass velocity was 1.03 g./cm.^{2} sec. The temperature of the bar was 65.0° whereas the jacket temperature was 51°. The relatively high temperature of the bar would cause an increase in the reaction rate over that which would be expected at the low flow rate. For majority of the runs the temperatures at the top of the bar were from 2 to 4° greater than the jacket fluid temperature.

Dissolution rates at 30 and 50° as a function of mass velocity and acid concentration also were obtained. As expected, the dissolution rate increases with increasing acid concentration. At 30° and acid concentration of 3 and 3.5 N the rate of dissolution decreases rapidly with increasing mass velocity. For acid concentration of 4.3 and 5.5 N at 30° and for all acid concentrations studied at 50°, the dissolution rate is nearly independent of the mass velocity, see Fig. 1. This can be explained by the fact that at high acid concentration, or temperatures, the dissolution rate is so high that enough nitrous acid is present to make surface reaction controlling. The surface reaction could be that proposed by Hedges[16]

$$CuO + 2HNO_2 = Cu(NO_2)_2 + H_2O \qquad (2a)$$

The effect of bar length and acid mass velocity on the rate of dissolution at 30 and 50° also was studied. In each instance the acid solution was 3.5 N. At the higher temperature, the rate of dissolution is independent of these two variables. This would tend to substantiate the hypothesis that the rate of a surface reaction is controlling.

At 30°, the effect of bar length and mass velocity are evident. Under these conditions the reaction is quite definitely autocatalytically controlled. The feed acid contains relatively small amounts of free oxides of nitrogen; hence the dissolution at the bottom end of the bar is low. As the reaction proceeds, it produces oxides of nitrogen and, in turn, nitrous acid which acts as the catalyst for the reaction. The amount of catalyst present is least at the bottom end of the bar and greatest at the top end. Also, for the long bar the nitric and nitrous acids are in contact with the bar for a greater length of time than for the short bar. Measurements of the bar diameter before and after the run confirm this non-uniform dissolution. This was particularly noticeable at the lower temperatures.

In the interpretation of kinetic data, the Arrhenius equation

$$k = A \exp(-E/RT) \qquad (8)$$

is frequently useful. According to equation 8 a plot of ln k *vs.* $1/T$ would yield a straight line with a slope of $-E/R$ and an intercept of ln A. Arrhenius interpreted the so-called "activation energy," E, as the excess over the average energy that the reactants must possess in order for the reaction to occur.

In Fig. 2 the reaction rates are plotted against $1/T$ for a mass velocity of 6 g./cm.^{2} sec. Similar plots could be made for other values of mass velocity. The parameters are acid concentrations. The experimental curves for the 3.0, 4.3 and 5.5 N acid are approximately straight lines. The 3.5 N curve gives quite large deviation from a straight line.

At the lower temperatures, it is apparent that the rate of dissolution decreases sharply when the acid strength is reduced from 4.3 to 3.5 N. Berg[25] attributed this to the fact that the amount of undissociated acid increased markedly when the concentration increased from 3.5 to 4.3 N at the particular temperature involved. However, the recent dissociation data of Hood and Reilly[30] do not show such an increase in the amount of undissociated acid at the conditions cited. In fact, over the temperature and concentration ranges investigated in this study, there appears to be no direct relationship between dissolution rate and amount of undissociated acid present.

A study of the experimental results, such as those presented in Fig. 2, shows that in certain instances the effect of mass velocity on the dissolution rate is negligible; also, that the effect of bar length is either completely unimportant, or of minor significance. Figure 1 shows more clearly the effect, if any, of these variables. If the data obtained at conditions under which these two variables are unimportant are plotted (log k *vs.* $1/T$), straight lines result when the acid strength is 5.5 or 4.3 N. This plot is included as Fig. 3.

From the data presented in Fig. 3, it is possible to calculate the activation energy, E, of equation 8. The equations of the two curves presented on Fig. 3 were calculated by the method of least squares. From these relations, the activation energies were calculated to be 7.83 kcal./gram atom for 5.5 N acid and 9.73 kcal./gram atom for 4.3 N acid. The standard deviation in the former case was 0.14 kcal. and in the latter case was 0.30 kcal. While activation energies for the other concentrations could not be calculated, it is evident they are a function of concentration and, in some cases, temperature.

Summary

The continuous dissolution of copper by nitric acid has been carried out at 20, 30, 40 and 50° over

a range of acid concentrations from 3 to 5.5 *N*. The effect of bar length and acid mass velocity were studied. In general, an increase in temperature or an increase in acid concentration increased the rate of dissolution. At 30°, the rate of dissolution was influenced by the length of the copper specimen. This was particularly true at the lower acid mass velocities. Contrariwise, at 50° the rate of dissolution was affected to only a minor degree with changes in bar length. This was true for all the acid mass velocities studied.

Examination of the copper bars before and after tests showed that, in the cases where bar length was important, more copper was removed from the upper end of the bar than the lower end. This can be explained by the fact that the nitrous acid which is a product of one of the reactions in the dissolution process acts as an autocatalyst for the reaction.

For a number of runs at temperatures of 30, 40 and 50° and at acid normalities of 4.3 and 5.5, the effects of variations in mass velocity and bar length were shown to be negligible. It was then possible to calculate energies of activation which were at 4.3 *N* acid 9.73 ± 0.30 kcal./gram atom of copper and 7.83 ± 0.14 at 5.5 *N* acid. In general the energy of activation was a function of concentration and temperature.

Acknowledgments.—James H. Weber wishes to acknowledge the financial aid in the form of research grants for this project from the Research Council of the University of Nebraska and the National Science Foundation.

SALT EFFECTS IN THE REACTIONS BETWEEN IODATE AND IODIDE

BY ANTONIO INDELLI

Chemistry Department of the University of Ferrara, Ferrara, Italy

Received June 23, 1960

The effect of twelve different salts on the rate of the reaction between iodate and iodide has been investigated at 25° in a range of ionic strength from 0.00096 to 0.04. Univalent and divalent cations and anions show no specific effects and an extended form of the Brønsted–Debye equation is obeyed through the whole range with an accuracy of about 2.5%. Lanthanum ion gives a retardation slightly greater and thorium ion far greater than uni- or divalent cations at the same ionic strength. The causes of the differences in the salt effects between this reaction and the reaction of bromate with iodide are discussed in terms of the charge of the activated complex. A mixture of thorium nitrate with potassium iodate has an ultraviolet absorption spectrum shifted toward shorter wave lengths with respect to the spectrum calculated for the isolated salts. This could be correlated with the negative salt effect. The results for $Na_3P_3O_9$ suggest that the value reported in the literature for the dissociation constant of $HP_3O_9^{2-}$ is perhaps too low.

In previous papers[1-6] the salt effects in a number of reactions have been investigated, and discrepancies from the Brønsted–Debye equation have been consistently found even at ionic strengths as low as 0.003.[3] As a rule the salt effects were found to be more dependent upon the concentration of some particular ion than upon the ionic strength, in agreement with the findings of Olson and Simonson,[7] specific effects being more important in reactions between ions of the same sign. The charge of the activated complex seems, therefore, to be relevant.[5] In the present paper the reaction between iodate and iodide has been chosen because the main activated complex has a charge of -1,[8,9] and because it involves only univalent ions, although the expected salt effect is as large as that expected for a bimolecular reaction between a uni- and a divalent ion. It has also the additional advantage that, because of its very high velocity, it can be studied at very low ionic strengths. This reaction had been studied previously mainly in buffer solutions, and little attention was given to the salt effects.[9]

(1) A. Indelli, *Ann. Chim. (Rome)*, **46**, 567 (1956).
(2) A. Indelli, *ibid.*, **47**, 586 (1957).
(3) A. Indelli and J. E. Prue, *J. Chem. Soc.*, 107 (1959).
(4) A. Indelli and E. S. Amis, *J. Am. Chem. Soc.*, **82**, 332 (1960).
(5) A. Indelli, G. Nolan and E. S. Amis, *ibid.*, **82**, 3233 (1960).
(6) A. Indelli, G. Nolan and E. S. Amis, *ibid.*, **82**, 3237 (1960).
(7) A. R. Olson and T. R. Simonson, *J. Chem. Phys.*, **17**, 1167 (1949).
(8) S. Dushman, *J. Phys. Chem.*, **8**, 453 (1904).
(9) E. Abel and F. Stadler, *Z. physik. Chem.*, **122**, 49 (1926).

Experimental

Materials.—Most of the salts used were "Carlo Erba" RP products, and were recrystallized from conductivity water. Sodium trimetaphosphate was prepared and purified as described elsewhere.[10] Potassium iodate was used as a primary standard to standardize the $Na_2S_2O_3$ and the KI solutions. Disodium ethylenediaminetetraacetate was used as a primary standard to standardize the $Ca(NO_3)_2$, $Ba(NO_3)_2$, $La(NO_3)_3$ and $Th(NO_3)_4$ solutions. The conductivity water was prepared by passing ordinary distilled water through an ion-exchange column, and had a conductivity less than 10^{-6} ohm^{-1} cm.$^{-1}$.

Kinetic Measurements.—The experimental procedure was similar to that used to study the bromate iodide reaction,[5] and consisted in adding small amounts of $Na_2S_2O_3$ solution to the reacting mixture, and detecting the reappearance of the iodine by the depolarization of a platinum electrode. However, the reaction between iodate and thiosulfate is very fast,[11] and therefore the greatest part of the thiosulfate was added when a substantial amount of iodine was present, and only a very small amount was present in excess before measuring the time. Care was taken to keep the amount of iodine present almost constant throughout the run, as measured by the potential of the electrode, except in the end of each addition when all the iodine was consumed. The volume of the reacting mixture was 400 cm.^{3}, and five points were taken in each run. Due to the very low concentration of the reactants and to the comparatively substantial amounts of $Na_2S_2O_3$ required in each addition, it was necessary to let the reaction proceed for 11% in most cases, so that the measured rate could not be considered the initial rate. It was found, however, that, when the concentrations of iodate and nitric acid were stoichiometrical, a second-order plot of the dimensionless quantity $a/(a - x)$ against time gave a nearly straight line. This

(10) A. Indelli, *Ann. Chim. (Rome)*, **43**, 845 (1953).
(11) R. Rieder, *J. Phys. Chem.*, **34**, 2111 (1930).

should be coincidental, as the order with respect to the hydrogen ion is about 2,[8,9] and on the other hand a continuous enrichment in KI takes place. The product of the slope of the second-order plot times the initial concentration "*a*" has been taken equal to the initial rate of the reaction, and the rate constants have been calculated by dividing the rates by the reactant concentrations raised to the proper orders. Duplicate runs have shown an agreement within about 3%.

A few runs were made to measure the rate of the reaction between iodate and thiosulfate, which, according to Rieder[11] is fifth order too, *i.e.*, second order with respect to the hydrogen and the thiosulfate, and first order with respect to the iodate ion. A solution of $Na_2S_2O_3$ was mixed with a solution of KIO_3 and HNO_3, the concentrations of the three reactants being in stoichiometrical ratios, calculated on the basis of $Na_2S_4O_6$ as a final product.[11,12] At suitable intervals samples were withdrawn and titrated with a solution of I_2 $3 \times 10^{-4}M$, using the polarized electrode as an indicator. When the concentration of the reactants was 2.5×10^{-4} equiv. $l.^{-1}$, a rate constant of 3.4×10^{12} $l.^4$ equiv.$^{-4}$ sec.$^{-1}$ was found. Some runs were also made at a concentration of 5.0×10^{-4} equiv. $l.^{-1}$. The half-life was then too short (about 35 seconds). However, values ranging from 2.5 to 4.5×10^{12} $l.^4$ equiv.$^{-4}$ sec.$^{-1}$ were consistently found.

All the kinetic runs were made in a thermostat at 25 ± 0.02°.

Spectrophotometric Measurements.—The ultraviolet spectra were taken with a Beckman Spectrophotometer Model DU, equipped with a photomultiplier, the cell length being 10 cm.

Results

The reaction between iodate and iodide is reported[9] to be first order with respect to the iodate, and second order with respect to both iodide and hydrogen ions, so that the total order should be five. The order with respect to the iodide at very low concentrations of the latter is reported to become 1,[13] as it is for the reaction between bromate and iodide.[5] Some mechanisms have been suggested to account for these orders.[14-16] More recently, on the basis of measurements on the rate of the exchange reaction between iodate and iodine, the order with respect to the hydrogen ion was found to be 3, and the reaction rate was found to be given by the sum of two terms, one of which is second order with respect to the iodate ion.[17] A third-order dependence upon the hydrogen ion concentration had been found earlier for the iodate–bromide reaction.[18] Throughout this paper the rate constants have been calculated on the assumption that the orders with respect to the hydrogen, the iodide and the iodate ions are, respectively, 2, 2 and 1. The results for the runs with no added salt are reported in Table I, and it can be seen that all the orders appear to be slightly higher than those referred to above. The order with respect to the nitric acid appears to be higher than that relative to the potassium iodide. The causes of these deviations have not been further investigated. The reaction rate law seems to be given by two terms of different total orders, but the fifth order one must be much more important than the other,

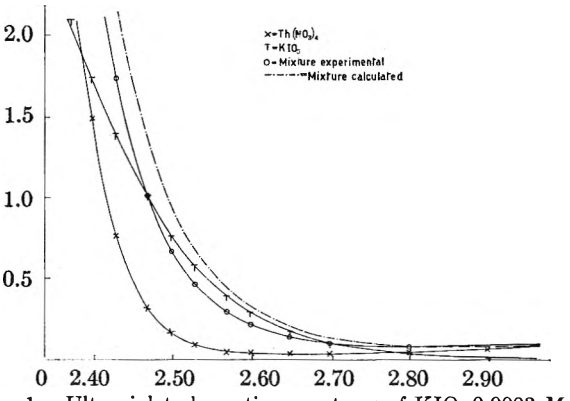

Fig. 1.—Ultraviolet absorption spectrum of KIO_3 0.0003 *M*, $Th(NO_3)_4$ 0.0003 *M* and their mixture.

since the deviations from the over-all fifth order are comparatively small.

TABLE I

FIFTH-ORDER RATE CONSTANTS, 10^{-9} k (L. EQUIV.$^{-4}$ SEC.$^{-1}$) FOR THE REACTION OF IO_3^- WITH I^- AND H^+ AT 25°, AT VARIOUS REACTANT CONCENTRATIONS

N	KI × 10⁴, mole $l.^{-1}$	HNO_3 × 10⁴, mole $l.^{-1}$	KIO_3 × 10⁴, mole $l.^{-1}$	10^{-9} k
1	3.75	5.00	0.833	6.4
2	1.875	5.00	.833	6.0
3	1.875	10.00	.833	6.8
4	7.50	2.50	.833	5.1
5	3.75	5.00	.417	5.6

The rate constants in the presence of different salts are reported in Table II. Apparently the differences among salts of the same valence type are not significant, the only exception being potassium chloride, where probably there is a side reaction of iodate with chloride ion.[5] Sulfates greatly decrease the reaction rate, due to the formation of the HSO_4^- ion, and a similar effect should be expected in the presence of $Na_3P_3O_9$. Table III reports the rate constants corrected for the formation of HSO_4^- and HP_3O_9,[2-5] assuming that the order with respect to the hydrogen ion is 2. It can be seen that the corrected rate constants for the sulfates are very similar to those for calcium and barium nitrates, whereas those for $Na_3P_3O_9$, are higher.

TABLE II

FIFTH-ORDER RATE CONSTANTS, 10^{-9} k (L.^{4} EQUIV.$^{-4}$ SEC.$^{-1}$) FOR THE REACTION OF IO_3^- WITH I^- AND H^+ AT 25° [KIO_3] = 0.833×10^{-4}, [KI] = 3.75×10^{-4}, [HNO_3] = 5.00×10^{-4}, μ = 0.000958 mole $l.^{-1}$, 10^{-9} k = 6.4 $l.^4$ equiv.$^{-4}$ sec.$^{-1}$.

Added salt	Equiv. $l.^{-1}$ → 0.002		0.004		0.01		0.02	
	k	μ	k	μ	k	μ	k	μ
$NaNO_3$	5.7	0.003	5.4	0.005	4.71	0.011	4.21	0.021
KCl	5.7	.003	5.5	.005	5.1	.011	4.74	.021
KNO_3	5.8	.003	5.4	.005	4.81	.011	4.17	.021
$KClO_4$	5.7	.003	5.4	.005	4.77	.011	4.22	.021
Na_2SO_4	4.77	.004	4.08	.007	2.64	.016	1.79	.031
$Na_3P_3O_9$	5.1	.005	4.64	.009	3.70	.021	2.87	.041
K_2SO_4	4.80	.004	3.88	.007	2.62	.016	1.76	.031
$Ca(NO_3)_2$	5.6	.004	5.1	.007	4.30	.016	3.74	.031
$Ba(NO_3)_2$	5.5	.004	5.1	.007	4.32	.016	3.71	.031
$La(NO_3)_3$	5.3	.005	4.82	.009	3.85	.021	2.97	.041
$Th(NO_3)_4$	0.040	.006	..	...	..	...	..	...
$UO_2(NO_3)_2$	2.05	.004	..	...	..	...	..	...

(12) E. Carrière and L. Faysse, *Compt. Rend. Acad. Sci.*, **201**, 1036 (1935).

(13) E. Abel and K. Hilferdings, *Z. physik. Chem.*, **136**, 186 (1928).

(14) W. Bray, *J. Am. Chem. Soc.*, **52**, 3580 (1930).

(15) E. Abel, *Helv. Chim. Acta*, **33**, 785 (1950).

(16) K. J. Morgan, M. G. Peard and C. F. Callis, *J. Chem. Soc.*, 1865 (1951).

(17) O. E. Myers and J. W. Kennedy, *J. Am. Chem. Soc.*, **72**, 897 (1950).

(18) J. Hirade, *Bull. Chem. Soc. Japan*, **10**, 97 (1935); *Chem. Zent.*, **106**, II, 964 (1935).

TABLE III

FIFTH-ORDER RATE CONSTANTS, 10^{-9} k (L.^{4} EQUIV.$^{-4}$ SEC.$^{-1}$) FOR THE REACTION OF IO_3^- WITH I^- AND H^+, IN THE PRESENCE OF SULFATES AND TRIMETAPHOSPHATE, CORRECTED FOR THE FORMATION OF HSO_4^- OR $HP_3O_9^{2-}$ AT 25°

Added salt	Equiv. l.$^{-1}$ → 0.002	0.004	0.01	0.02
Na_2SO_4	5.5	5.15	4.35	3.90
$Na_3P_3O_9$	5.6	5.4	4.89	4.30
K_2SO_4	5.5	4.97	4.31	3.84

The results for some runs on the reaction bromate–iodide in the presence of $Th(NO_3)_4$ are reported in Table IV.

TABLE IV

FOURTH-ORDER RATE CONSTANTS, 10^{-2} k (L.^{3} EQUIV.$^{-3}$ SEC.$^{-1}$) FOR THE REACTION OF BrO_3^- WITH I^- AND H^+ AT 25°, IN THE PRESENCE OF THORIUM NITRATE

N	KI, mole l.$^{-1}$	HNO_3, mole l.$^{-1}$	$KBrO_3$, mole l.$^{-1}$	$Th(NO_3)_4$, mole l.$^{-1}$	10^{-2} k
1	0.0025	0.0025	0.000833	....	7.24 (7.3)
2	.0025	.0025	.000833	0.0005	6.09
3	.0025	.0025	.000833	0.005	6.51

The ultraviolet spectra of KIO_3, $Th(NO_3)_4$ and their mixture were measured at a concentration of 0.0003 M for both reactants. The absorption spectra in the region of 2400 to 2600 Å. for the mixture are shifted by about 30 to 40 Å. toward the higher frequencies with respect to the spectrum calculated from the individual absorptions of the reactants. This effect is shown in Fig. 1.

Discussion

The reaction rate constants should be proportional to the fourth power of the activity coefficient of a univalent ion,[19] that is

$$k = k_0 \frac{f_{IO_3^-} f_{I^-}^2 f_{H^+}^2}{f_\pm} = k_0 \frac{f_1^5}{f_1} \qquad (1)$$

If an extended Debye equation[20] is used to calculate the activity coefficients, equation 1 becomes

$$\log k = \log k_0 - 2.034 \frac{\sqrt{\mu}}{1 + \sqrt{\mu}} + B\mu \qquad (2)$$

where μ is the ionic strength. Equation 2 is followed within 2.5% by all the alkali metal and the earth-alkali metal salts of Table II, the "B" coefficient being about 0. For $La(NO_3)_3$, instead, "B" is about −1.2.

The main differences in the salt effects between this reaction and the similar one of bromate with iodide can be summarized as

Reaction:	$IO_3^- - I^-$	$BrO_3^- - I^-$
Rate law:	$(IO_3^-)(I^-)^2(H^+)^2$	$(BrO_3^-)(I^-)(H^+)^2$
"B" coeff. eq. 2:	*Ca.* 0	1.1
Effect of La^{3+}:	gives a neg. "B" coeff.	same as mono- and bivalent ions
UO_2^{2+}:	gives a small retardation	gives a large acceleration
Th^{4+}	gives an enormous retardation	at most a small effect
SO_4^{2-}	depends on ionic strength	depends on the equiv. concn. of the cation

The iodate–iodide reaction shows a closer conformity to the Brønsted–Debye equation, probably because in this case equation 2 results from the cancellation of a similar factor in equation 1. For the bromate–iodide reaction, instead, it is assumed that the activity coefficient of the activated complex is 1.0. This assumption could be erroneous, particularly if the activated complex has a large dipole moment. The retardation caused by the thorium nitrate can be related to the shift of the absorption spectrum of the mixture of KIO_3 and $Th(NO_3)_4$. A displacement toward shorter wave lengths corresponds to a greater energy requirement for the electron transfer.[4] Day and Stoughton, on the other hand, have shown, from solvent extraction data, that the $ThIO_3^{3+}$ complex is 100 times more stable than $ThBrO_3^{3+}$ at $\mu = 0.5$.[21] It seems likely also that the negative "B" coefficient for $La(NO_3)_3$ is related to the retarding effect of $Th(NO_3)_4$; both these highly charged cations could interact with the anionic activated complex.

The corrected rate constants in the presence of $Na_3P_3O_9$ are greater than expected both in the bromate[5] and in the iodate reaction. In the latter the experimental rate constants before correction are rather similar to those in the presence of $La(NO_3)_3$. It is possible that the dissociation constant of $HP_3O_9^{2-}$ measured by Davies and Monk[22] is too low, because in its determination a somewhat arbitrary value had to be assumed for the ionic mobility of $HP_3O_9^{2-}$. This subject seems to deserve further investigation.

(19) S. Glasstone, K. T. Laidler and H. Eyring, "The Theory of Rate Processes," McGraw-Hill Book Co., New York, N. Y., 1941, p. 404.

(20) E. A. Guggenheim and J. E. Prue, "Physicochemical Calculations," North-Holland Publishing Co., Amsterdam, 1956, p. 466.

(21) R. A. Day, Jr., and R. W. Stoughton, *J. Am. Chem. Soc.*, **72**, 5662 (1950).

(22) C. W. Davies and C. B. Monk, *J. Chem. Soc.*, 413 (1949).

SOLUBILITY OF LEAD SULFATE AS A FUNCTION OF ACIDITY. THE DISSOCIATION OF BISULFATE ION

BY R. W. RAMETTE AND R. F. STEWART

Leighton Hall of Chemistry, Carleton College, Northfield, Minn.

Received June 27, 1960

The solubility of lead sulfate at 25° in 1 molar, varying acidity mixtures of perchloric acid and sodium perchlorate, and of perchloric acid and lithium perchlorate has been determined. The results are interpreted from the viewpoints of specific ionic effects on activity coefficients, and the possibility of ion pairs containing sulfate and bisulfate.

The potentiometric measurements of Eichler and Rabideau[1] indicate that the value of the bisulfate dissociation quotient, $Q = [H_3O^+][SO_4^=]/[HSO_4^-]$, in 1 molar sodium perchlorate is only one-third as large as the value in 1 molar perchloric acid. The calculations of Baes[2] show that a similar difference exists between the values of Q in sodium sulfate and sulfuric acid solutions of unit ionic strength.

It was of interest to determine whether this specific ionic effect would also be found in situations which do not depend upon cell measurements. For this reason the solubility of lead sulfate in 1 molar mixtures of perchloric acid and sodium or lithium perchlorate was determined as a function of acidity.

Experimental

Reagents.—Solid lead sulfate was freshly prepared by the slow addition of a solution of lead nitrate to a hot, stirred solution containing a slight excess of sulfuric acid. The precipitate was digested for an hour with occasional stirring, was collected on a sintered glass filter, and was washed thoroughly with the particular solution with which it was to be equilibrated just before introducing it in excess into that solution.

The mixtures of sodium perchlorate and perchloric acid were prepared by addition of standardized perchloric acid to standardized sodium hydroxide and diluting to known volume. A stock solution of lithium perchlorate (G. F. Smith) was standardized gravimetrically by precipitation as tetraphenylarsonium perchlorate, and also by titration of perchloric acid obtained by ion exchange using Dowex 50X8 resin. Other chemicals were of reagent grade.

Apparatus.—The mixtures were equilibrated by rotation in borosilicate glass-stoppered bottles, lightly sealed with stopcock grease, in a thermostated air-bath at 25.0 ± 0.1°. One week was used for the equilibration. Absorption measurements were made with a Beckman DU spectrophotometer using 1-cm. silica cells.

Analytical Procedure.—Samples of the saturated solutions were obtained by pressure filtration through fine porosity sintered glass, the entire filtration apparatus being immersed in the water-bath, and the first portion of filtrate was discarded. Determination of total dissolved lead was made by two independent methods which gave results checking to within a per cent. The earlier determinations involved the precipitation of lead as chromate from an acetate buffer. The aged precipitate was collected on sintered glass, dissolved in hydrochloric acid, treated with an excess of sodium hydroxide and diluted to known volume. The absorbance of such a solution at 372 mμ is a direct measure of the amount of chromate present, from which the concentration of lead in the original aliquot can be calculated. This method later was superseded by the easier procedure of diluting an aliquot of the saturated solution to a known volume with hydrochloric acid, so that the final molarity of the latter is 2 molar. The absorbance of the resulting solution at 261 mμ is a direct measure of the lead concentration due to the absorptivity of the mixture of chloroplumbates.[3] As long as the final molarity of hydrochloric acid is carefully controlled, the absorbance is very closely proportional to the lead concentration.

Results and Discussion

The values obtained for the solubility of lead sulfate in the various solutions are summarized in Table I.

TABLE I

SOLUBILITY (MOLAR × 10^3) OF LEAD SULFATE IN C M PERCHLORIC ACID, $(1 - C)M$ SODIUM OR LITHIUM PERCHLORATE AT 25.0°

C	Using $NaClO_4$	Using $LiClO_4$
0.050	0.960	0.922
.100	1.120	1.040
.200	1.350	...
.300	1.548	1.411
.400	1.700	1.570
.500	1.844	1.708
.600	1.975	1.835
.700	2.05	1.952
.800	2.12	2.069
.900	2.24	2.175
1.000	2.276	2.276

As a first approximation in the interpretation of these data we may assume that the only chemical effect influencing the increase in solubility with increasing acidity is the formation of the bisulfate ion. Then the system would be represented by an attractively simple equilibrium scheme

$$PbSO_4(s) \rightleftharpoons Pb^{++} + SO_4^=$$
$$+$$
$$H_3O^+ \rightleftharpoons HSO_4^- + H_2O$$

If this scheme shows all of the significant species involving lead and sulfate the total solubility S is given by

$$S = [Pb^{++}] = [SO_4^=] + [HSO_4^-] \quad (1)$$

From the expression for the bisulfate dissociation constant K_2 the molarity of bisulfate ion is

$$[HSO_4^-] = \frac{[H_3O^+][SO_4^=]}{K_2} \times \frac{f_H f_{SO_4}}{f_{HSO_4}} \quad (2)$$

in which f refers to the molar activity coefficient. Likewise, from the expression for the solubility product of lead sulfate K_{sp} we find

$$[SO_4^=] = \frac{K_{sp}}{[Pb^{++}] f_{Pb} f_{SO_4}} \quad (3)$$

Combination of equations 1, 2 and 3 leads to the relationship

$$S^2 = [Pb^{++}]^2 = \frac{K_{sp}}{f_{Pb} f_{SO_4}} + \frac{K_{sp} f_H}{K_2 f_{HSO_4} f_{Pb}} \times [H_3O^+] \quad (4)$$

(1) E. Eichler and S. Rabideau, *J. Am. Chem. Soc.*, **77**, 5501 (1955).
(2) C. F. Baes, *ibid.*, **79**, 5611 (1957).
(3) C. Merritt, H. M. Hershenson and L. B. Rogers, *Anal. Chem.*, **25**, 572 (1953).

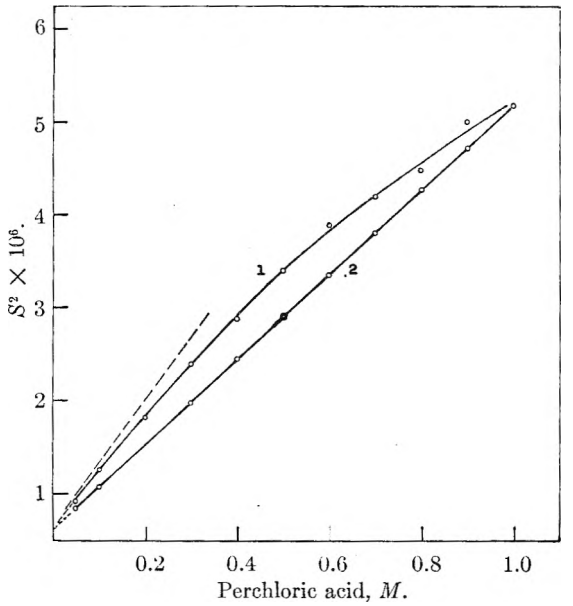

Fig. 1.—Interpretation of solubility of lead sulfate in: curve 1, sodium perchlorate–perchloric acid; curve 2, lithium perchlorate–perchloric acid. The dashed line approximates the limiting slope of curve 1.

This equation predicts that a plot of the square of the total solubility *versus* the controlled and known acidities should be linear except for variations in the activity coefficients. The intercept of the plot at zero acidity would be the value of the classical solubility product of lead sulfate $Q_{sp} = [Pb^{++}][SO_4^{=}]$, and the ratio of intercept to slope would be the value of the bisulfate dissociation constant Q in the series of solutions. However, if the activity coefficients are subject to specific ionic effects as the composition of the solution is varied from 1 molar salt to 1 molar acid, the plot might be curved. The extrapolated intercept would still be the classical value of the solubility product, but with reference only to the 1 molar salt solution. Intercept/slope ratios would have little meaning except at the point of zero acidity, where the limiting slope could be used to calculate the value of Q in the 1 molar salt solution.

The graphical interpretation suggested above is shown in Fig. 1. It is to be expected that the lines should meet at 1 molar acidity since the solutions are identical in each system, with no salt present. The excellent linearity in the lithium system suggests that activity coefficients are indeed invariant in the mixtures used. This is not unexpected, the reason for the use of the lithium salt being the finding as presented in Harned and Owen[4] that the mean activity coefficient of hydrochloric acid is constant in similar 1 molar mixtures when the metal cation is lithium, but not when the metal cation is sodium.

Therefore it is not surprising that the line should be curved for the sodium system, but the virtual coincidence of the two intercepts at zero acidity forces the unwelcome conclusion that the mean activity coefficient of lead sulfate is the same in 1 molar sodium perchlorate as in 1 molar lithium perchlorate.

The intercept values, 6.3×10^{-7}, are thus the values of the product $[Pb^{++}][SO_4^{=}]$ in the 1 molar salt solutions. The slope of the lithium system line is 4.57×10^{-6}, leading to a value of 0.138 for Q in lithium perchlorate–perchloric acid mixtures of unit ionic strength. The limiting slope of the curve for the sodium system, indicated by the dashed line, is estimated to be about 7.1×10^{-6}, yielding a value of 0.092 for Q in 1 molar sodium perchlorate. This is in good agreement with the results of Eichler and Rabideau, who found 0.095 ± 0.002, 0.084 ± 0.012, and 0.30 ± 0.08 in 1 molar sodium perchlorate–perchloric acid solutions containing 0.01, 0.1 and 1.0 molar perchloric acid, respectively. The point of disagreement is between the values of Q in 1 molar perchloric acid, the present lithium system results giving a value about half that obtained by Eichler and Rabideau. No explanation for this difference has been realized, but it has been proposed[5] that the answer may lie in reasonable variations in activity coefficients. For example, assuming these values for the bisulfate dissociation quotient: (Q) (1 M $NaClO_4$) = 0.095, Q(1 M $LiClO_4$) = 0.138, Q(1 M $HClO_4$) = 0.30, can reasonable variations in Q and in the classical solubility product Q_{sp}, with composition account for all the solubility results by the scheme of equilibria shown above? Of course, there are many ways in which Q and Q_{sp} could be varied to fit the results, but it is of considerable interest that if log Q is assumed to vary linearly with composition in the two systems, it is found that log Q_{sp} is also a linear function of composition. Illustrative calculations are summarized in Table II.

TABLE II

POSSIBLE VARIATIONS IN Q AND Q_{sp} CONSISTENT WITH THE SOLUBILITY RESULTS

Parenthetical values are assumed, others are calculated.

	$LiClO_4$			$NaClO_4$		
$[H_3O^+]$	$S^2 \times 10^6$	Q	$Q_{sp} \times 10^6$	$S^2 \times 10^6$	Q	$Q_p \times 10^6$
0.0	0.63	(0.138)	0.63	0.63	(0.095)	0.63
.2	1.54	.160	.69	1.82	.119	.68
.4	2.46	.188	.79	2.89	.149	.79
.6	3.37	.220	.91	3.89	.188	.93
.8	4.29	.258	1.05	4.49	.238	1.03
1.0	5.20	(.300)	1.20	5.20	(.300)	1.20

The values of Q_{sp} were calculated from

$$Q_{sp} = \frac{S^2}{1 + \frac{[H_3O^+]}{Q}}$$

a rearranged form of equation 4 with the activity coefficients incorporated into the equilibrium constants. The intermediate values of Q were read from a plot of log Q *vs.* composition. Thus, if such variations in Q and Q_{sp} are accepted as reasonable, the solubility data may be shown consistent with the results of Eichler and Rabideau. However, the illumination afforded by this view is somewhat dimmed by the comments made in connection with ref. 4 above.

Ion Pair Hypotheses.—Suppose that various

(4) H. S. Harned and B. B. Owen, "The Physical Chemistry of Electrolytic Solutions," third edition, Reinhold Publ. Corp., New York, N. Y., 1958, pp. 597–598.

(5) C. F. Baes, private communication.

cation–anion interactions to form ion pairs are considered as indicated in the following equilibrium scheme

$$\begin{array}{l} \qquad\qquad\qquad\qquad\qquad\qquad M^+ \rightleftharpoons MSO_4^- \\ \qquad\qquad\qquad\qquad\qquad\qquad + \\ PbSO_4(s) \rightleftharpoons PbSO_4(soln.) \\ \qquad\qquad\qquad\qquad \rightleftharpoons Pb^{++} + SO_4^{=} \\ \qquad\qquad\qquad\qquad\qquad\qquad + \\ \qquad\qquad\qquad H_2O^+ HSO_4^- \rightleftharpoons + H_3O + \\ \qquad\qquad\qquad\qquad\qquad + \\ \qquad\qquad MHSO_4\ (soln.) \rightleftharpoons M^+ \end{array}$$

where M represents either sodium or lithium. In other words, suppose that these cations can form ion pairs, even if only slightly stable, with sulfate and bisulfate ion.

As for the existence of $PbSO_4$ ion pairs in solution, van't Riet[6] interprets solubility data[7,8] to show that the concentration of undissociated lead sulfate in the saturated solutions is about 7×10^{-6} molar, which is negligibly small compared to the solubilities of the present work. This is consistent with the general findings[9] that the dissociation constants of 2–2 electrolytes are of the order of 0.005 at low ionic strengths. At $\mu = 1$ as in the present work the dissociation quotient should be about 40 times larger since this is the approximate ratio of Q_{sp} to K_{sp}, giving a value of about 0.2 which indicates virtually complete dissociation in the dilute solutions.

There are reasons to believe that both sodium and lithium ions form ion pairs with sulfate ion,[9] with the dissociation constants of $NaSO_4^-$ and $LiSO_4^-$ being 0.20 and 0.23, respectively, at low ionic strength. The values of these quotients in the 1 molar solutions used in the present work are unknown, but the effect of ionic strength would probably be similar to that shown in the analogous dissociation of the bisulfate ion. Since the latter increases about tenfold from its value at zero ionic strength[10] to that in 1 molar salt solutions, the ion pair dissociation quotients might have values of about 2 at unit ionic strength. This is by no means negligible, for the molarity of lithium or sodium ion approaches unity in the solutions of low acidity, and about a third of the sulfate would be present as the ion pair. If to the right side of equation 1 is added a term for $[MSO_4^-]$, with the realization that $[M^+]$ is very nearly equal to $(1 - [H_3O^+])$, then the introduction of the pertinent equilibrium constants leads to a revised form of equation 4

$$S^2 = K_{sp}(1/f_{Pb}f_{SO_4} + f_M/K_d f_{Pb} f_{MSO_4}) + \frac{K_{sp}}{K_2}(f_H/f_{HSO_4}f_{Pb} - K_2 f_M/K_d f_{Pb} f_{MSO_4})[H_3O^+] \quad (5)$$

where K_d is the dissociation constant of the ion pair MSO_4^-. Equation 5 is simplified by incorporating the activity coefficients with the equilibrium constants to give the classical expressions in terms of molarities rather than activities, and we find

$$S^2 = Q_{sp}(1 + 1/Q_d) + \frac{Q_{sp}}{Q}\left(1 - \frac{Q}{Q_d}\right)[H_3O^+] \quad (6)$$

For tentative simplicity, suppose that the various activity coefficients depend only on the classical ionic strength, and not on the specific ions present, a condition which we might actually expect for the lithium system.

Now, according to equation 6, the existence of the MSO_4^- ion pair does not prevent a plot of S^2 *versus* $[H_3O^+]$ from being linear, but the significance of the intercept and slope is different. The intercept would be higher than Q_{sp} by the factor $(1 + 1/Q_d)$, and if the value of about 2 for Q_d as reasoned earlier is correct, then the actual value of Q_{sp} is $6.3 \times 10^{-7}/1.5 = 4.2 \times 10^{-7}$, in both systems.

Further according to equation 6, the intercept slope ratio is not Q but is

$$Q\frac{1 + Q_d}{Q_d - Q} \approx Q \times 1.5 \text{ if } Q_d \approx 2 \text{ and } Q << Q_d$$

Therefore, for the lithium system the observed value of 0.138 for the ratio of intercept to slope would give $0.138/1.5 \approx 0.092$ for the correct value of Q. Note that this value would hold throughout the lithium series of solutions, including the 1 *M* perchloric acid.

Consideration of the sodium system brings other problems. For one thing, as discussed earlier, it is reasonable to expect activity coefficients to vary as the sodium ion is replaced by hydronium ion so the curvature of the line is not disturbing. Since one would not expect activity coefficients in 1 *M* sodium perchlorate to be nearly identical with those in 1 *M* lithium perchlorate, the coincidence of the two zero-acidity intercepts indicates that the changes in activity coefficients do not show more strikingly because of compensating differences in the MSO_4^- dissociation quotients, and that the values quoted above for $NaSO_4^-$ and $LiSO_4^-$ may be considerably in error. Further, it seems worth mentioning that one might predict the curvature of the sodium line to be concave up, rather than as actually observed. This prediction comes from consideration of the location of the activity coefficients in equation 5, and the knowledge that for hydrochloric acid, at least, the mean activity coefficient is smaller in the presence of sodium ion than when hydronium ion is used.

There is no evidence in the literature pertaining to ion pairs containing the bisulfate ion, but the curvature of the sodium system line may be explained in this way. It does not seem that $LiHSO_4$ ion pair formation can be important, since the plot is quite linear, and such an ion pair would require that the equation for S^2 contain a term involving hydronium ion to the second power. However, if the species $NaHSO_4$ really exists, it would be present to the greatest relative extent in the middle of the acidity range, when the product $[Na^+][H_3O^+]$ is a maximum. Inspection of Fig. 1 shows that the deviation of the sodium system line from the lithium system line is indeed greatest at about the middle.

(6) B. van't Riet, Ph.D. thesis, Univ. of Minnesota, 1957.

(7) I. M. Kolthoff, R. W. Perlich and D. Weiblen, THIS JOURNAL, **46**, 561 (1942).

(8) D. N. Craig and G. W. Vinal, *J. Research Natl. Bur. Standards*, **22**, 55 (1939).

(9) See, for example, C. W. Davies, "The Structure of Electrolytic Solutions," edited by Hamer, John Wiley and Sons, New York, N. Y., 1959, chapter 3.

(10) C. W. Davies, H. W. Jones and C. B. Monk, *Trans. Faraday Soc.*, **48**, 921 (1952).

It is possible to calculate that the dissociation quotient of $NaHSO_4$ should be about 2.3 to account for the curvature quantitatively. That sodium should have more tendency than lithium to form an ion pair with bisulfate might be expected because of the more extensive hydration of the lithium ion.[11] In summary, it seems reasonable to suggest that the solubility of lead sulfate in these solutions is influenced by a combination of ion-pair formation and specific ionic effects on activity coefficients. With a good deal of algebraic manipulation it is possible to show that

$$Q = Q_{ER}\left[\frac{Q_d}{Q_d + [Na^+]}\right]\left[\frac{Q_d' + [Na^+]}{Q_d'}\right] \quad (7)$$

where Q is the true value of the bisulfate dissociation quotient, Q_{ER} is the value calculated by Eichler and Rabideau from their potentiometric data, Q_d is the dissociation quotient for the $NaSO_4^-$ ion pair, Q_d' is the dissociation quotient for the $NaHSO_4$ species, and the sodium ion molarity refers to the solutions actually used in the potentiometric studies. It is seen that the two corrective factors in equation 7 tend to cancel. In any case, Eichler and Rabideau used such small concentrations of sodium ion that each of the factors would be very close to unity, so that their results are not in error as a result of neglecting ion pairs.

In conclusion, there is no wholly satisfactory way to resolve the discrepancy between our value of Q (0.138 or 0.092, depending upon whether ion pairs are invoked) and that of Eichler and Rabideau (0.3) in 1 molar perchloric acid.

Acknowledgment.—We are grateful to the Research Corporation for partial support of this work.

(11) E. Glueckauf, *Trans. Faraday Soc.*, **51**, 1235 (1955).

INTRAMOLECULAR SHIELDING AND THE SOLUTION ENERGY OF *ORTHO* ALKYL BIPHENYLS

BY L. R. SNYDER

Union Oil Company of California, Union Research Center, Brea, California

Received June 27, 1960

A recently postulated relationship between solute conjugation and solution interaction for the alkyl biphenyls has been re-examined in terms of an alternative causative factor. It is shown by application of an additive free energy relationship that anomalous effects in the solution energies of the *ortho*-alkyl biphenyls are largely controlled by intramolecular shielding, and that conjugation in the alkyl biphenyls plays only a small part in determining their energies of solution in the solvent Apiezon M. Gas chromatographic retention volumes for various hydrocarbons, including the alkyl biphenyls, can be quantitatively predicted for Apiezon M as stationary phase by means of a physico-mathematical model which recognizes solute intramolecular shielding.

Beaven, James and Johnson[1] have reported data for the gas chromatographic retention volumes of a number of alkyl biphenyl derivatives, using "Apiezon M" as the stationary phase. The authors provide a qualitative interpretation of their data in terms of the restriction of planarity in the biphenyl ring system, and compare these data with parallel effects in the ultraviolet absorption spectra of the biphenyls. A similar correspondence between solute chromatographic separation factors and ultraviolet absorptivity has been invoked to interpret the relative adsorption of isomeric polyphenyls.[2] While in neither communication[1,2] do the authors state the theoretical basis for an otherwise empirical relationship, the postulated interdependence of solute solvation energy and wave length of the longest ultraviolet absorption band is easy to justify in terms of the energy of the highest ground state π molecular orbital; it is reasonable that electron availability (for solvation bonding) *and* the wave length of the longest ultraviolet absorption should both increase as the energy of this highest lying molecular orbital approaches that of an isolated π-orbital. In both chromatographic systems,[1,2] however, alternate physical effects are theoretically capable of explaining the observed variation of solute separability with structure. The present communication will attempt a relative evaluation of these theoretical factors in the case of the solvation of the alkyl biphenyls[1]; a corresponding analysis of the energies of interaction which determine the relative adsorption of isomeric polyphenyls will be forthcoming.

An Additive Solvation Energy Model: Conjugation Effects.—Pierotti, Redlich, *et al.*,[3-5] have described the relationship (first derived by Martin and James)[6] between gas chromatographic retention volume and solute equilibrium distribution coefficient. These authors have further correlated the dependence of distribution coefficient with structure in terms of a model which assumes additive free energy contributions from the various solute component groups or substituents. The over-all correlation of solute retention volume with molecular structure may be restated and amplified in the formulation of equation 1

$$\log R = a + \sum_{j}^{n} f_j s_j + Q_k \quad (1)$$

R is a gas chromatographic retention volume, cor-

(1) G. A. Beaven, A. T. James and E. A. Johnson, *Nature*, **179**, 490 (1957).

(2) M. Hellman, R. L. Alexander, Jr., and C. F. Coyle, *Anal. Chem.*, **30**, 1206 (1958).

(3) G. J. Pierotti, C. H. Deal, E. L. Derr and P. F. Porter, *J. Am. Chem. Soc.*, **78**, 2980 (1956).

(4) O. Redlich, E. L. Derr and G. J. Pierotti, *ibid.*, **81**, 2283 (1959).

(5) G. J. Pierotti, C. H. Deal and E. L. Derr, *Ind. Eng. Chem.*, **51**, 95 (1959).

(6) A. J. P. Martin and R. L. M. Synge, *Biochem. J.*, **35**, 1358 (1941).

rected for void volume. The parameter a is a constant for a particular chromatographic column at a given temperature. For each structural group j in the solute (*e.g.*, methylene, methyl, aromatic CH, etc.) f_j is a parameter which is proportional to the free energy of interaction of the group j in the stationary phase, relative to the moving phase. s_j is a cross section parameter which represents a restriction of the interaction of group j with its environment as a result of intramolecular shielding. Q_k is a residual term, included here to represent non-additive or specific effects in given cases.

The interpretation by Beaven, *et al.*, can be restated in the language of equation 1. They define for alkyl biphenyls with m alkyl carbons (total carbon number minus 12) an interaction parameter i by means of

$$m \log i = \log (R/R_0)$$

R_0 being the retention volume for biphenyl itself. Equation 1 can now be expressed by the relation

$$\log (R/R_0) = mf_js_j + Q_k$$

in which all differences between alkyl carbons or substituent positions are lumped into Q_k. Thus we have

$$\log i = f_js_j$$

whenever $Q_k = 0$. Beaven, *et al.*, note that i ranges from 0.96 to 1.26 for alkyl biphenyls possessing one or more *ortho* substituents, and from 1.46 to 1.69 for all other alkyl biphenyls. This is in turn interpreted by the authors as meaning that some average constant value of $10f_js_j(1.46–1.69)$ is applicable to both *ortho* and non-*ortho* alkyl carbons, but that destruction of phenyl–phenyl conjugation by *ortho*-substituents introduces a negative value of Q_k (which is mathematically equivalent to a decrease in the average value of i).

Beaven, *et al.*, state that the anomalies in the retention volumes of the alkyl biphenyls parallel the ultraviolet absorption spectra of these solutes. While no detailed discussion is presented in their paper, the correspondence referred to is easy to recognize. Thus, the absorption spectra[7] of the various alkyl biphenyls may be grouped into three classes. First, biphenyl itself and the *m*- and *p*-substituted biphenyls show molar absorptivities in excess of 10^4 at 260 mμ, and less than 10^3 at 300 mμ. Introduction of *o*-methyl groups results in the progressive reduction of the absorptivity at 260 mμ with the number of such groups, presumably as a result of the destruction of ring–ring resonance. Incorporation of both rings of the biphenyl groups into a five- or six-membered non-aromatic ring (as in fluorene or 9,10-dihydrophenanthrene) causes a sharp increase in absorption intensity (above 10^3) at 300 mμ, and it is attractive to interpret this as the result of the two phenyl groups being brought closer to planarity, relative to biphenyl. The values of i for alkyl carbon substituents in the biphenyls may be ordered according to the planarity of the molecule, inferred from its ultraviolet spectrum. Thus, the ranges in i for *ortho*-substituted, non-*ortho*-substituted, and alkyl ring joined biphenyls are 0.96–1.25, 1.46–1.69 and 1.87–2.98, respectively (the latter range in values of i is derived from a combination of data acquired by us and reported by Beaven, *et al.*—see Table I). This parallelism of solute retention volume and ultraviolet absorptivity suggests that the energy of the highest lying π-molecular orbital is determining secondary differences (or value of Q_k) in the retention volumes of the biphenyls.

(7) R. A. Friedel and M. Orchin, "Ultraviolet Spectra of Organic Compounds," John Wiley and Sons, Inc., New York, N. Y.

TABLE I

RETENTION VOLUMES RELATIVE TO BIPHENYL OF VARIOUS SOLUTES USING APIEZON M AS STATIONARY PHASE AT 197°

Solute	Retention volume R Exptl.	Calcd.[c]	Dev., %
Benzene	0.027[a]	0.027	0
Naphthalene	0.45[a]	0.41	− 9
Acenaphthylene	1.57[a]	1.58	1
Phenanthrene	6.6[b]	6.2	− 6
Pyrene	25.5[b]	24.0	− 6
Ethylbenzene	0.074[a]	0.069	− 7
n-Propylbenzene	.114[a]	.112	− 2
n-Butylbenzene	.187[a]	.182	− 3
n-Octylbenzene	1.26[a]	1.22	− 3
m-Diethylbenzene	0.189[a]	0.182	− 4
Biphenyl	(1.00)[a,b]	(1.00)	0
3-Methylbiphenyl	1.55[b]	1.61	4
4-Methylbiphenyl	1.65[b]	1.61	− 2
3,3′-Dimethylbiphenyl	2.40[b]	2.59	8
4,4′-Dimethylbiphenyl	2.95[a]		
	2.69[b]	2.59	− 4
3-Ethylbiphenyl	2.19[b]	2.59	18
4-Ethylbiphenyl	2.45[b]	2.59	6
3,4,3′,4′-Tetramethylbiphenyl	8.10[b]	6.7	−17
3,3′-Diethylbiphenyl	4.55[b]	6.7	47
4,4′-Diethylbiphenyl	5.95[b]	6.7	12
Isopropylbenzene	0.095[a]	0.091	− 4
Isobutylbenzene	.144[a]	.147	2
sec-Butylbenzene	.146[a]	.147	1
t-Butylbenzene	.134[a]	.134	0
p-Di-*i*-propylbenzene	.310[a]	.314	1
2-Methylbiphenyl	.96[b]	.94	− 2
2,2′-Dimethylbiphenyl	1.01[b]	1.02	1
2,6-Dimethylbiphenyl	1.09[b]	1.02	− 7
2-Ethylbiphenyl	1.22[b]	1.23	1
2,6,2′-Trimethylbiphenyl	1.17[b]	1.11	− 5
2-*n*-Propylbiphenyl	1.56[b]	1.57	1
2-Isopropylbiphenyl	1.30[b]	1.31	1
2,4,2′,4′-Tetramethylbiphenyl	2.50[b]	2.55	2
2,6,2′,6′-Tetramethylbiphenyl	1.33[b]	1.20	−10
2,2′-Diethylbiphenyl	1.72[b]	1.73	1
2-Isopropyl-5-methylbiphenyl	1.91[b]	2.12	11
2-*n*-Butylbiphenyl	2.24[b]	2.26	1
2,4,2′,4′,6′-Hexamethylbiphenyl	2.90[b]	3.12	8
2,2′-Di-isopropylbiphenyl	2.20[b]	1.98	−10
2,2′-Di-*t*-butylbiphenyl	5.05[b]	5.05	0
Bibenzyl	1.78[a]	2.24	26
Tetralin	0.38[a]	0.29	−24
Phenylcyclohexane	0.77[a]	0.74	− 4
Acenaphthene	1.87[a]	1.66	−11
Fluorene	2.98[a]	2.63	−12
9,10-Dihydrophenanthrene	5.05[b]	4.2	−17
1,2-Dihydropyrene	18.8[b]	24.5	+30
1,2,6,7-Tetrahydropyrene	11.8[b]	17.8	+51

[a] Data of this study. [b] Data of reference 1. [c] Equation 1 and Table II.

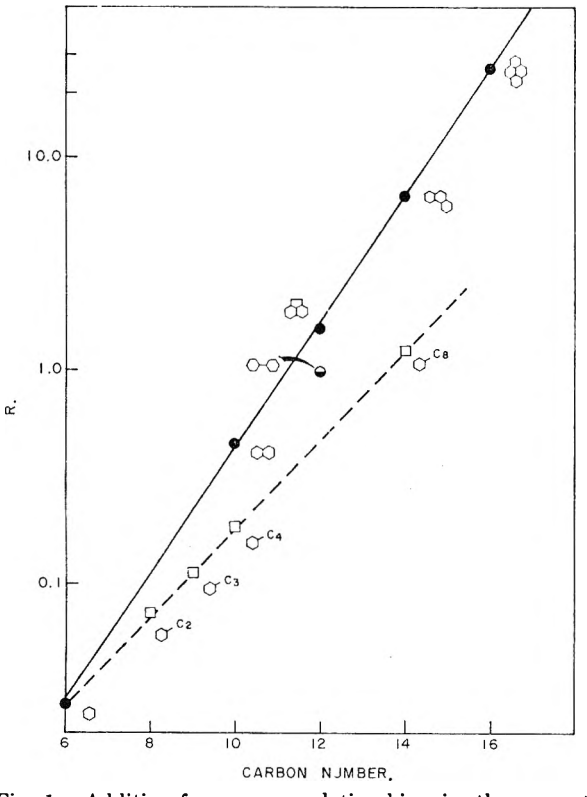

Fig. 1.—Additive free energy relationships in the present chromatographic system.

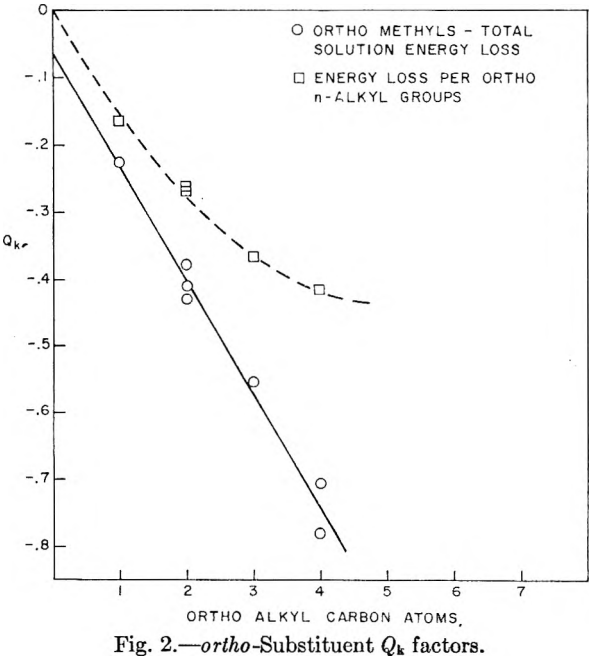

Fig. 2.—*ortho*-Substituent Q_k factors.

Conjugation *vs.* Shielding.—The origin of these anomalous effects in the solution energies of the *ortho*-substituted biphenyls may be sought in a physical agency other than changing resonance between the biphenyl rings. Shielding effects, which are implied by the s_j terms of (1), are different in the *ortho* relative to *meta* and *para*-positions of biphenyl. Thus, an *ortho*-group can partially shield (and be shielded) the aromatic carbons of the opposite ring when the rings are not coplanar (as they are not, after one *ortho*-alkyl substitution). This shielding in turn reduces the interaction with solvent of both the alkyl and opposed aromatic carbons, and leads to decreased retention volumes as observed.

Table I presents gas chromatographic retention volume data for a number of compounds, using "Apiezon M" as stationary liquid at 197°. These data include values previously reported by Beaven, *et al.* (same conditions) as well as supplementary values obtained by us. The application of equation 1 to these data offers a test of the relative importance of shielding *vs.* resonance in determining the solution energies of the *ortho*-alkyl biphenyls. In Fig. 1 the logarithms of the retention volumes of the *n*-alkylbenzenes and of the unsubstituted aromatics are plotted *vs.* total solute carbon number. For the unsubstituted aromatics, all of the data (except for biphenyl) lie on a straight line, as required by (1) with Q_k equal to zero, that is, as required by a model which assumes complete additivity (constants f_j, s_j values) of solution free energy terms for each group (taken as aromatic carbon in this case). From this plot, a value of $f_j s_j$ for the aromatic carbon group is found, equal to +0.293. The small deviation of biphenyl from this curve (equal to a Q_k of −0.235) can reasonably be attributed to small differences in the π-molecular orbital structure of this molecule relative to the remaining more condensed aromatics. The over-all linearity of this latter plot, however, suggests that such effects are relatively unimportant, inasmuch as a wide range in structural types is represented. Similarly, the data for the *n*-alkyl benzenes also fall on a straight line of smaller slope, and a value of $f_j s_j$ for an aliphatic carbon of +0.207 may be inferred from this plot. When these value of $f_j s_j$ and Q_k (for biphenyl), as well as a calculated value of a (−3.33), (totalling four coefficients) are inserted into (1), the retention volumes of the various aromatics and non-*ortho*-alkyl aromatics (21 values) may be calculated with reasonable accuracy (average deviation slightly less than 10%).

If the foregoing values of the parameters of equation 1 are used to calculate log R for the various *ortho*-alkyl biphenyls, subtraction of this value from the experimental one yields a value of Q_k, which is proportional to the loss (or gain) in the energy of solution for the *ortho*-alkyl biphenyls relative to the non-*ortho*-alkyl biphenyls discussed above. One additional factor must first be noted, however, since the *o*-alkyl biphenyls of Table I included some branched alkyl derivatives. These groups, because of the intra-group shielding of the central carbon, make a negative contribution to values of Q_k (or reduced s_j value) equal to −0.091 for a tertiary and −0.134 for a quaternary carbon. The calculated values of the five branched alkyl benzenes of Table I demonstrate the additivity of these terms.

First, it is of interest to note the residual Q_k values for the *ortho*-methyl substituted biphenyls. These are plotted (circles) *vs.* the number (n) of the *ortho*-methyls in Fig. 2. It is seen that all of these points fall on the indicated straight line, with an

accuracy which probably approaches that of the raw experimental data. The extrapolation of the curve to n equal zero gives a small negative contribution (−0.06). It may be concluded that, with the exception of the first *ortho*-methyl group, each additional *ortho*-methyl group results in a constant reduction in the solution energy of the biphenyl solute. It is easy to interpret this observation in terms of intramolecular shielding. If the two biphenyl rings are essentially orthogonal *after* the addition of one or more *ortho*-alkyl groups, the interaction of the various *ortho*-methyls with each other will be negligible, and the loss in solution interaction energy due to shielding of aromatic carbons will be constant for each *ortho* group, since each methyl will lie in an identical configuration above the plane of the opposite ring. The slightly greater effect of the first methyl may be due to the destruction of conjugation between the two rings. This suggests that loss in conjunction is essentially complete upon the addition of the first *ortho*-alkyl group, if conjugation loss is responsible for the greater effect of the first *ortho*-methyl substituent. This interpretation permits the assignment (from the plot of Fig. 2) of a Q_k value of −0.06 to the unconjugated (*ortho*-alkyl substituted) biphenyl system, and a value of −0.172 to Q_k for an *ortho*-methyl group.

While the above interpretation of the *ortho*-methyl Q_k values in terms of shielding effects is physically reasonable and fully borne out by the experimental data, the same cannot be said for hypotheses relying totally upon loss of conjugation. The steric interaction of the *ortho*-methyls would definitely be expected to be energetically non-additive, in that the addition of the third and fourth groups should result in considerably greater deformation of the rings from planarity than the first two groups, providing (as must be assumed in the conjugation explanation) that the rings are *not* already close to orthogonal after two substitutions. As is observed, however, the solvation energy loss ($-Q_k$) is constant for the addition of second, third and fourth methyls.

A further check on these two theories of the solution interaction of the alkyl biphenyls is provided by the different ring–ring configurations assumed in each case for 2-methyl and the more substituted *ortho*-methyl biphenyls. Orthogonality of all of the *ortho*-methyl biphenyls is required by the steric interaction hypothesis, while in the alternative model conjugation (and ring–ring angle θ) must continue to decrease with increasing *ortho*-methyl substitution from 2-methyl- to 2,6,2′,6′-tetramethylbiphenyl. Adrian[8] has calculated the resonance and steric interaction energies of biphenyl as a function of θ. Conjugation between the two rings is essentially insignificant for θ greater than 60°: at that angle, the increase in resonance energy of biphenyl over that of two isolated benzene rings is about 5% of the increase for planar biphenyl. The ring–ring conjugation energy of each of the methylbiphenyls must be very close to the values for biphenyl at various values of θ, and the steric interaction energy for 2-methylbiphenyl can be calculated for various molecular configurations by the procedure of Adrian. Since this energy varies at specified values of θ with the angle of rotation ϕ of the methyl group, the relative probability $P(\theta)$ of the configuration θ must first be calculated from

$$P(\theta) = \int_0^{2\pi} e^{-E(\phi)/RT}\, d\phi$$

with $E(\phi)$ referring to the energy (steric plus conjugation) of the methylbiphenyl system in the configuration (θ, ϕ). Finally, $-RT \log P(\theta)/P(\theta)(90°)$ is equal to the free energy $F(\theta)$ of the configuration θ relative to the orthogonal one. It is calculated that $F(60°)$ is 1.2 kcal. for 2-methylbiphenyl, and in a similar calculation for 2,6-dimethylbiphenyl, $F(60°)$ equals 2.2 kcal. The orthogonal configuration is hence theoretically favored for these two compounds over configurations where appreciable conjugation between the two aromatic rings can occur, thus corroborating the steric interaction model. Since differences in the rotational heat capacity of the methyl groups were ignored in the above calculation, and since the barrier to rotation is about 1 kcal. higher at θ equal 60° relative to the orthogonal position, the stabilization of the orthogonal position in these two compounds must be even larger than indicated.

Another test of the importance of conjugation effects in this instance is presented by contrasting Q_k values for the various *ortho* n- and i-alkyl substituents (reported in Table II, along with other parameter values). As is seen in Fig. 2, (squares; Q_k per *ortho*-n-alkyl group, corrected by +0.06 for loss in ring conjugation) lengthening an n-alkyl substituent results in progressively more negative Q_k values, with the total effect appearing to level out for four or more alkyl carbons. This is expected from the shielding hypothesis, since additional alkyl carbons beyond four must lie largely outside the solvation sphere of the opposite phenyl ring. The Q_k values are also consistent with the conjugation-loss hypothesis, since steric interference should show the same trend. When Q_k values for the branched alkyl substituents are compared with the normal ones, however, it is seen that n-propyl (Q_k equal −0.365) is approximately as effective as is i-propyl (Q_k equal −0.352) in reducing solute interaction energy, while n-butyl (Q_k equal −0.415) is substantially *more* effective than t-butyl (Q_k equal −0.281). These comparative effects are inexplicable in terms of conjugative loss due to steric interaction, but are not unreasonable in terms of a shielding picture. In the case of t-butyl one of the three methyls is always excluded from shielding the opposite ring, while in n-butyl all four carbons are available.

A final comparison of these two theories of the anomalies in the alkyl biphenyl retention volumes will perhaps suffice to establish the relative importance of shielding as a factor. In the case of the solute dibenzyl, the loss in conjugation between the two rings is complete. The conjugation hypothesis would assume that Q_k is as large as any for the alkyl biphenyl solutes. Assuming that conjugation is in fact totally destroyed in the compound

(8) F. J. Adrian, *J. Chem. Phys.*, **28**, 608 (1958).

TABLE II

PARAMETER VALUES FOR EQUATION 1 AND PRESENT CHROMATOGRAPHIC SYSTEM

Group	$f_i s_j$	Q_k
Aromatic carbon	0.293	(0.00)
Aliphatic carbon	0.207	(.00)
Tertiary carbon		− .091
Quaternary carbon		− .134
Biphenyl		− .235
o-Substituted biphenyl		− .295
Biphenyl *ortho*-methyl		− .172
Biphenyl *ortho*-ethyl		− .265
Biphenyl *ortho*-*n*-propyl		− .356
Biphenyl *ortho*-*n*-butyl		− .415
Biphenyl *ortho*-*i*-propyl		− .352
Biphenyl *ortho*-*t*-butyl		− .281
Cycloalkyl ring closure		.21
a equals		−3.33

2,6,2′,6′-tetramethylbiphenyl, a value of Q_k equal to −0.70 can be calculated for complete loss of conjugation. This then permits the calculation of log R for bibenzyl as −0.29. The similar calculation for the shielding theory (using values in Table II) furnishes a value of +0.35 (two alkyl carbons plus loss of conjugation, −0.06, relative to biphenyl). The experimental value in this case is +0.25. The difference between experimental and calculated solution energies is thus over five times as great for the calculation assuming conjugation effects are controlling.

When the retention volumes of the (fifteen) *ortho*-alkyl biphenyls are calculated by means of the parameter values of Table II, the agreement with experimental values is impressive (average deviation of ±4%). As a final commentary on the data of Table I, it is necessary to invoke a Q_k value of +0.21 for cycloalkyl groups in excess of the normal contribution of aliphatic carbons. Since the incorporation of the *ortho*-carbons of the biphenyl system in such a ring prevents orthogonality and hence the shielding of opposite ring carbons (as by *ortho*-alkyl groups,) it is incorrect to assume a negative Q_k value for alkyl groups forming part of such a ring. This combination of effects is responsible for the observed large *i*-values for cycloalkyl biphenyls; it is unnecessary to invoke the greater planarity *and* conjugation of these solutes in this connection. The somewhat poorer correlation of calculated and experimental values for the naphthene aromatics would be substantially improved if the pyrene derivatives were assigned a different value of Q_k for the napthene ring. Since the basis of this naphthene Q_k value is not immediately apparent, although rather general for other vapor–liquid systems, no attempt to classify further this parameter has been attempted.

When all of the data of Tables I and II are compared, it is found that a total of 48 retention volume values have been calculated, using 14 parameters. Moreover, these parameters are not completely independent, inasmuch as their relative values in some cases are required to stand in a certain order; in every such case, the observed order is theoretically reasonable. The average deviation between experimental and calculated values of log R is 0.035, and the maximum deviation is 0.179. The experimental range in log R values is 2.97. The average precision, as well as the extreme deviations, could have been substantially improved by taking cognizance of certain secondary effects such as the retention volume differences in *m*- *vs.* *p*-alkyl biphenyls, vicinal *vs.* non-vicinal substituted aromatics (*e.g.*, 3,3′,4,4′-tetramethylbiphenyl *vs.* *m*-diethylbenzene), and the above pyrene derivative naphthene aromatics. This was not attempted as it was felt that it would detract from the clarity of the central argument of conjugation *vs.* shielding as factors in the solution interaction of the *ortho*-alkyl biphenyls.

Acknowledgment.—The author wishes to thank the Union Oil Company of California for permission to publish the present work, and his associate, Dr. E. P. Parry, for careful editing and criticism of the original manuscript.

THE $V(^1\Sigma^+)$–$N(^1\Sigma^+)$ TRANSITION OF HYDROGEN BROMIDE

BY J. G. STAMPER AND R. F. BARROW

Physical Chemistry Laboratory, Oxford University, Oxford, England

Received July 6, 1960

Observation of part of the $V(^1\Sigma^+)$–$N(^1\Sigma^+)$ system of HBr in emission leads to the estimate $T_0(V) \sim 9.28$ e.v. By analogy with HF and HCl, $\omega_e(V) \sim 790$ cm.$^{-1}$, $r_e(V) \sim 2.7$ Å.

The hydrogen halide molecules HF, DF[1] and HCl[2] give rise to discrete emission spectra in the ultraviolet region, and rotational analyses show that these spectra arise from transitions from low vibrational levels in states $V^1\Sigma^+$ to high vibrational levels in the ground states $N^1\Sigma^+$. The lower electronic states of these molecules have been discussed by Pauling[3] and by Mulliken[4]; their electron configurations may be written

$\sigma^2\pi^4$	N Σ^+
$\sigma^2\pi^3\sigma^*$	Q $^3\Pi$, Π
$\sigma\pi^4\sigma^*$	T $^3\Sigma^+$
$\sigma\pi^4\sigma^*$	V Σ^+

Here, in LCAO terms

σ = a(H 1 sσ) + b(Br 4 $b\sigma$), strongly bonding

σ^* = a'(H 1 sσ) − b'(Br 4 $p\sigma$), strongly anti-bonding

π = Br 4 $p\pi$, atomic, nearly non-bonding; $b > a$, $b' < a'$

(1) J. W. C. Johns and R. F. Barrow, *Proc. Roy. Soc.* (*London*), **A251**, 504 (1959).

(2) J. K. Jacques and R. L. Barrow, *Proc. Phys. Soc.*, **73**, 538 (1959).

(In these—oversimplified—configurations the outstanding omission is probably the contribution of the essentially ionic $\sigma\ \pi^4\ \sigma^*$ configuration to N, and the corresponding contribution of $\sigma^2\pi^4$ to V.)

States N, Q and T correlate with ground state atoms $H(^2S)$ + Hal (^2P): state V in HF and HCl probably gives the ions $H^+ + Hal^-$ on dissociation. In the case, however, of HBr. the combination[5] $H(^2S)$ + Br $(4s^2\ 4p^4, (^1S_0)5s\ ^2S)$ at 75901.9 cm.$^{-1}$ lies lower than the lowest state of $H^+ + Br^-$, and here, therefore, state V is presumably to be correlated with the neutral atoms.

Two points of interest attach to the analysis of the V–N transitions. First, as in HF, this may lead to an unusually complete knowledge of the course of the vibrational and rotational levels of the ground state. Secondly the spectroscopic constants for the V states are valuable for comparison with the results of wave mechanical calculations.

The results which have so far been obtained for HBr are given below. The V–N system for this molecule is both weaker and spectrally less accessible than for HF and HCl, and it has not proved possible to analyze the fragment of the system which has been observed. Nevertheless values for some of the spectroscopic constants for the V state may be derived, partly by analogy with HF and HCl.

Experimental

The V–N system of HF may be excited strongly in hollow cathode sources.[1] However, for HCl, the best source found so far consists of an electrodeless radiofrequency discharge through pure hydrogen chloride or through hydrogen chloride–helium mixtures. The same source was found to excite the V–N system of HBr, but weakly and not very reproducibly and, although a wide range of conditions was examined, no consistently satisfactory source was found. Further, following the trend already shown by HF, for which the long wave length limit of the spectrum is 2650 Å., and HCl, with λ_{max} ~2400 Å. for HBr, the value of λ_{max} was found to be about 2150 Å., so that the system is confined to a rather inaccessible spectral region.

The spectrum was photographed with a Hilger E. 478 large quartz spectrograph on Ilford Q.2 plates. Exposures of up to four hours were given.

Analysis.—The strongest lines lie in the region 45950–48000 cm.$^{-1}$. They all grouped in pairs of equal intensity with separations of 2 to 3 cm.$^{-1}$, and about 100 of these doublets were measured. A few short branches could be picked out, but the analysis of a system of this kind, which consists of branches arising from a large number of overlapping bands whose degradation changes from red to violet as N increases, is not easy, and the attempt was unsuccessful. The doubling no doubt arises from the isotope effect between $H^{79}Br$ and $H^{81}Br$, but the splitting is too small, and varies too little from one line to the next, to help with the analyses.

Constants for the State $V^1\Sigma+$ of HBr.—The long wave length limit, corresponding to the minimum value of ν, of the V–N transitions is given approximately by the position of the band $V(v' = 0) - N(v''_{max})$. Thus $T_0(V) \simeq D_0(N) + \nu_{min}$ (V–N). The relevant figures are given in Table I. $T_0(V)$ is estimated to be 74900 cm.$^{-1}$ or 9.2$_8$ e.v.

Table I

	$D_0(N)$	$\nu_{min.}$	$D_0(N) + \nu_{min.}$	T_0	$D_0(N) + \nu_{min} - T_0$, cm.$^{-1}$
HF	47,270	38,060	85,330	83,275	2055
HCl	35,660	42,105	77,765	76,245	1520
HBr	30,290	45,800	76,090	(74,900)	(1200)

The constants r_e and ω_e may be estimated, less certainly, from the ratios $r_e(V)/r_e(N)$ and $\omega_e(V)/\omega_e(N)$ for HF and HCl. The values are given in Table II.

Table II

	$r_e(N)$, Å.	$r_e(V)$, Å.	$r_e(V)/r_e(N)$	$\omega_e(N)$, cm.$^{-1}$	$\omega_e(V)$, cm.$^{-1}$	$\omega_e(V)/\omega_e(N)$
HF	0.9171	2.092	2.281	4139.0	1158.5	0.280
HCl	1.2746	2.530	1.985	2991.4	877.2	0.293
HBr	1.414	(2.7)	(1.9)	2649.7	(790)	(0.3)

These estimated constants are no substitute for the results of a detailed rotational analysis, but this must await high resolution spectrograms of the shorter wave length end of the system lying in the Schumann region. The long wave length limit of the corresponding system in HI should lie at about 2000 Å.: this system has not yet been observed.

(3) L. Pauling, *J. Am. Chem. Soc.*, **54**, 988 (1932).

(4) R. S. Mulliken, *Phys. Rev.*, **50**, 1017 (1936); **51**, 310 (1937).

(5) C. E. Moore, "Atomic Energy Levels, II." Washington, National Bureau of Standards Circular No. 467, 1952.

THE DIPOLE MOMENTS OF SOME TRIMETHYL-N-ALKYLSILAZANES[1]

BY ROBERT L. COOK AND ALFRED P. MILLS

Department of Chemistry, University of Miami, Coral Gables, Florida

Received July 8, 1960

The dipole moments of $Me_3SiNHEt$, $Me_3SiNHPr$, $Me_3SiNHiPr$ and $Me_3SiNHiBu$ were obtained by solution measurements in benzene and cyclohexane, and by using Onsager's equation and pure liquid measurements. All values fell within the range 0.72 to 0.79 *D*. No significant difference between the benzene and cyclohexane measurements indicates no complex formation between benzene and the silazanes, while no significant difference between the moments obtained from pure liquid and solution measurements indicates the absence of hydrogen bonding. The low dipole moment could not be accounted for on the basis of single bond contributions. It can, however, be accounted for on the basis of p_π–d_π bonding between the silicon and the nitrogen.

Stone and Seyferth[2] summarize and discuss considerable evidence for the utilization of silicon's 3d-orbitals in bonds with such electronegative, electron-pair-containing, elements as F, O, Cl and N.

A number of trimethylamine complexes with fluoro- and chlorosilanes have been prepared.[3–6] Many of these exhibit a coördination number of five. Burg and Kuljian[7] demonstrated that trisilylamine is a far weaker electron-donor than trimethylamine and suggested that this arises through wandering of the lone-pair on nitrogen into the d-orbitals of silicon. Electron diffraction studies by Hedberg and Stosick[8] indicate that trisilylamine is planar, a configuration which could be interpreted as indicating π-bonding between the nitrogen and silicon. Dipole moments have been reported[9] for $(Me_3Si)_2NH$ (0.67 *D*) and $(Me_3Si)_2NMe$ (0.44 *D*).

In this work the dipole moments of trimethyl-N-ethylsilazane, trimethyl-N-propylsilazane, trimethyl - N - isopropylsilazane and trimethyl - N - isobutylsilazane were determined in order to study the possible π-bonding between the silicon and the nitrogen in the silazanes. Measurements were made using both benzene and cyclohexane in order to determine whether or not an intermolecular complex is formed between benzene and the silazanes. Such a complex is possible since the π-electrons of the benzene ring are easily polarizable and could possibly fill the silicon *d*-orbitals forming a $d_\pi p_\pi$ bond.

Experimental

Dielectric Constant.—All measurements were made at 30° using a heterodyne beat apparatus which was constructed,[10] with slight modifications, using the circuitry described in Weissberger.[11] The precision capacitor was obtained from General Radio Company (type 722-ND) and the dielectric cell from J. C. Balsbaugh, Marshfield Hills, Mass. (type 350). This cell was a three-terminal monel-nickel cell having an air capacitance of 35 $\mu\mu$f. It was provided with a Pyrex glass jacket, liquid volume 40–50 ml., dimensions 1.5″ diameter by 5.5″ length. The cell was calibrated with benzene and cyclohexane.

Molar Refractions.—The molar refractions were calculated from densities and refractive indices measured in this Laboratory,[12] and which will be published separately. These molar refractions check quite closely with those predicted using the method of Vogel.[13]

Materials.—Fisher C.P. benzene was purified by obtaining a constant boiling center fraction, refluxing for about 20 hours over P_2O_5, and then distilling from P_2O_5 just before using. Fisher spectrograde cyclohexane was purified by distillation prior to using.

The silazanes were prepared in this Laboratory[12] and purified by reduced pressure fractionation using a column packed with glass helices and having about fifteen theoretical places. The boiling point ranges of the samples measured are listed in Table I.

TABLE I

Compound	B.p. range, °C.	*P*, mm.	R_D 30° Exptl.	R_D 30° Pred.[13]
$Me_3SiNHEt$	40.6–41.0	124	37.74	37.71
$Me_3SiNHPr$	43.2–43.4	70	42.43	42.38
$Me_3SiNHiPr$	40.0–40.3	88	42.40	42.39
$Me_3SiNHiBu$	55.3–55.9	49	47.01	47.03

The solutions for the measurements were made up within the weight fraction range of 0.01–0.05. In making up the solutions, filling the cell, etc., all transfers were made in a dry box under a nitrogen atmosphere in order to minimize hydrolysis of the silazanes.

Experimental Results

The molar polarizations at infinite dilution were calculated from a modified Halverstadt and Kumler equation which was introduced by Estok[14] in 1956. The values of $\alpha = \Delta\epsilon/\Delta\omega_2$ were obtained using the method of least squares. The values of the dipole moments are shown in Table II along with the values for ϵ, ϑ_1, ϑ_2 and α for Estok's equation.

Discussion

Inspection of the moments listed in Table II shows that there is no significant difference between the moments obtained in benzene and those obtained in cyclohexane. This indicates that there is no complex formation between benzene and the silazanes.

The moments obtained by means of the Onsager equation are in fairly good agreement with those calculated from the solution measurements using

(1) (a) This research was supported by a Frederick Gardner Cottrell grant from Research Corporation. (b) Presented at the Meeting-in-Miniature of the Florida Section of the American Chemical Society, Orlando, Florida, May, 1960. Abstracted from the M.S. thesis of Robert L. Cook.

(2) F. G. A. Stone and D. Seyferth, *J. Inorg. & Nuclear Chem.*, **1**, 112 (1955).

(3) H. J. Emeléus and N. Miller, *J. Chem. Soc.*, 819 (1939).

(4) J. H. Simons (Editor), "Fluorine Chemistry," Vol. 1, Academic Press, Inc., New York, N. Y., 1950, p. 108.

(5) C. J. Wilkins and D. K. Grant, *J. Chem. Soc.*, 927 (1953).

(6) A. B. Burg, *J. Am. Chem. Soc.*, **76**, 2674 (1954).

(7) A. B. Burg and E. S. Kuljian, *ibid.*, **72**, 3103 (1950).

(8) K. Hedberg and A. J. Stosick, Abstracts of the XII International Congress of Pure and Applied Chemistry, New York, Sept. 10–13, 1951, p. 543.

(9) T. Moeller (Editor), "Inorganic Syntheses," Vol. V, McGraw-Hill Book Co., Inc., New York, N. Y., 1957, p. 58–59.

(10) Built by Kimball Electronic Laboratory, 2323 N. W. 14th Ave., Miami, Fla.

(11) Weissberger (Editor), "Physical Methods of Organic Chemistry," 2nd Ed., Vol. I, Part II, Interscience Publishers, Inc., New York, N. Y., 1949, p. 1638.

(12) Robert L. Cook, M.S. Thesis, 1960, University of Miami.

(13) A. I. Vogel, W. T. Cresswell and J. Leicester, THIS JOURNAL, **58**, 177 (1954); A. I. Vogel, W. T. Cresswell, G. H. Jeffery and J. Leicester, *J. Chem. Soc.*, 531 (1952).

(14) G. K. Estok, THIS JOURNAL, **60**, 1336 (1956).

TABLE II[a]

Compound	Solv.[b]	ϵ_1	ϑ_1	ϑ_2	α	P_∞	$\mu(D.)$
$Me_3SiNHEt$	B	2.2700	1.1515	1.3654	0.1084	49.18	0.78
	p[c]	2.2751[c]					.72[c]
$Me_3SiNHPr$	B	2.2635	1.1515	1.3410	.1054	54.80	.79
	C	2.0054	1.2893	1.3410	.3009	53.72	.75
$Me_3SiNHiPr$	B	2.2626	1.1515	1.3643	.0442	54.16	.77
	C	2.0029	1.2893	1.3643	.2896	54.06	.76
$Me_3SiNHBu$	B	2.2609	1.1515	1.3339	.0618	59.07	.78
	C	2.0055	1.2893	1.3339	.2572	57.67	.73
	p[c]	2.2523[c]					.72[c]

[a] 30°. [b] B = benzene, C = cyclohexane. [c] Pure liquid, μ calculated using Onsager's equation.

the Debye equation. These results indicate the absence of hydrogen bonding in contrast to dimethylamine, for which the moment calculated by the Onsager equation is considerably higher than the solution moment. This indicates that the electronegativity of the nitrogen atom is reduced in the silazanes; however, steric hindrance may also be a contributing factor and could account for this result.

The moments obtained in solution are nearly the same for all the silazanes measured, the small deviations being well within the expected range of experimental error. The constancy of these moments is what one would expect. Even though more polarizable material is added as the alkyl chain is extended, which could increase the moment due to the inductive effect, such an effect is not detectable beyond the first two carbon atoms of a chain when the moment is of the order of one debye or less.

Undoubtedly the contribution from the atomic polarization would make the moment values in Table II too high. However, it is believed that the contribution from bond bending would be relatively small in the silazanes due to steric hindrance. Regardless, such small uncertainties do not detract from the conclusions since the latter are based on the moments being too low rather than too high.

The moments obtained in solution are nearly the same for all the silazanes measured, the small deviations being well within the expected range of experimental error. The constancy of these moments is what one would expect. Even though more polarizable material is added as the alkyl chain is extended, which could increase the moment due to the inductive effect, such an effect is not detectable beyond the first two carbon atoms of a chain when the moment is of the order of one debye or less.

If one assumes that the silazanes have essentially the same pyramidal type structure as ammonia and that the bond angles are approximately 110°, the three dipoles can be resolved into the following components: $M_x = m_1\cos 20° - m_2\cos 20°\cos 60° - m_3\cos 20°\cos 60°$, $M_y = m_2\cos 20°\sin 60° - m_3\cos 20°\sin 60°$, $M_z = m_1\cos 70° + m_2\cos 70° + m_3\cos 70°$, where m_1 = Me ← Si → N (in the xz-plane), m_2 = R → N, and m_3 = H → N. By using $\mu = (M_x^2 + M_y^2 + M_z^2)^{1/2} = 0.78\ D$, Si → Me = 0.2 D from Altshuller,[15] and R → N = 0.62 D and H → N = 1.3 D from Smyth,[16] the equations when solved yield $m_{Si-N} = (0.82 \pm 0.72i)D$.

If one assumes that the Si–N bond moment is opposite to the previously assumed direction an imaginary result is again obtained. Therefore, some type of process must be lowering the over-all moment of the silazane. Such a lowering could be due to the departure of the bond angles from 110° due to the repulsion of the bonded groups, resulting in an increase in the planarity of the molecule. However, if this were true one would expect the over-all moment to be appreciably affected by changes in the length and branching of the alkyl chain. Since this is not the case, this explanation does not suffice.

Another approach is to account for the lowering as being due to a resonance contribution from the structure $Me_3\overset{-}{Si}=\overset{+}{N}(H)R$. Smyth's values for H → N and R → N could not be used for this structure because these values contained the contribution of the lone pair moment along the N–H and N–R bond lines. Gibbs,[17] using a quantum mechanical treatment, calculated bond moments N → H = 0.85 D and C → N = 0.15 D, which were free from electron pair contributions. The $\overset{-}{Si}=\overset{+}{N}$ moment of 8.02 D was estimated from the product of the electronic charge and an estimated interatomic distance of 1.67 Å.[13] Assuming that the three methyl groups bonded to the silicon atom keep their approximate sp^3 configuration, a moment of 8.07 D is estimated for the above structure.

In order to estimate the moment of the primary structure an Si → N bond value of 1.94 D was estimated by the formula of Wilmshurst.[19] Using this value in the basic equations gave an estimated value of 1.55 D for the primary structure.

A moment of 0.78 D could be obtained if the double-bond structure contributed either 8.0 or 24.2%, this latter value arising from the possibility that the double bond structure might predominate and reverse the direction of the total moment of the molecule. The 8.0% value is indicated by the reported moments[9] of 0.67 D for $(Me_3Si)_2NH$ and 0.44 D for $(MeSi)_2NMe$. The observed lowering of the moment in these cases, where one would expect an increase in double bond character due to an increase in resonance forms, points to the predominance of the primary structure.

The above seems to be the most satisfactory

(15) A. P. Altshuller and L. Rosenblum, *J. Am. Chem. Soc.*, **77**, 272 (1955).

(16) C. P. Smyth, "Dielectric Behavior and Structure," McGraw-Hill Book Co., Inc., New York, N. Y., 1955, p. 311.

(17) J. H. Gibbs, THIS JOURNAL, **59**, 644 (1955).

(18) J. A. A. Ketelaar, "Chemical Constitution," 2nd Ed., Elsevier Pub. Co., Amsterdam, Netherlands, 1958, p. 199.

(19) J. K. Wilmhurst, *ibid.*, **62**, 631 (1958).

explanation at the present time. There is, however, the difficulty that if the hybridization of the nitrogen changes with the back coördination the resulting resonance form would not be very favorable, since the nuclear spatial structure would be different in the two cases. There is, however, considerable evidence for such changes in hybridization, so that possibly such an unfavorable energy requirement is more than compensated for by the formation of the p_π–d_π bond.

ELECTROLYSIS WITH CONSTANT POTENTIAL: REVERSIBLE PROCESSES AT A HANGING MERCURY DROP ELECTRODE[1]

BY IRVING SHAIN AND KENNETH J. MARTIN

Department of Chemistry, University of Wisconsin, Madison, Wisconsin

Received July 5, 1960

The technique of electrolysis with constant potential using a stationary spherical mercury electrode (the hanging mercury drop) was investigated under conditions where the curvature of the electrode surface had to be considered. Current–time curves, covering periods from 1 to 25 seconds after the start of the electrolysis, were compared with theory for several cases. It was found that the results agreed with the classical equations for reactions at potentials where the current was controlled by diffusion alone. In addition, equations for reversible processes taking place at potentials near the equilibrium potential were verified for reactions in which both the reactant and product were soluble in the solution. For systems in which the product of the reaction formed an amalgam, the convergent nature of the diffusion processes within the hanging mercury drop electrode had to be considered. The general suitability of the hanging mercury drop electrode for potentiostatic studies was also investigated, and the effects of shielding of the electrode and convection were characterized.

In recent years, the hanging mercury drop electrode has proved to be useful in a variety of electrochemical applications. Since first reported by Gerischer,[2] the electrode has been used for kinetic studies, including galvanostatic,[3] potentiostatic,[4] and linearly varying potential methods.[5] In addition, it has been applied in a useful series of analytical methods based on voltammetry with linearly varying potential.[6] This stationary spherical electrode is convenient to use, has an exactly reproducible size and shape, and its geometry is such that equations are readily obtainable for processes involving diffusion to the electrode surface. This is particularly true in the case of potentiostatic processes, since application of the Laplace transform frequently leads directly to a useful solution of the boundary value problem involved.

In all of the previous applications of the hanging mercury drop electrode to potentiostatic studies, the curvature of the electrode surface could be ignored, *i.e.*, the experiments were completed in such short times (microsecond to millisecond range) that the corresponding equations for diffusion to a plane electrode could be applied. However, there are many cases in which the accuracy and convenience of more conventional equipment, including pen-and-ink recorders, is required. In such cases, data cannot be obtained at times much shorter than 1 to 2 seconds after the start of electrolysis. Under these conditions, the curvature of the electrode must be considered when using the hanging mercury drop electrode.

Equations describing some of the current–time–potential relations at a spherical electrode for electrolysis with constant potential have been known for many years. However, until recently, a suitable stationary spherical mercury electrode has not been available for rigorous verification of the equations. This paper describes a study of such potentiostatic processes for reactions not complicated by kinetic effects. In addition, the limitations of the hanging mercury drop electrode and the sources of error involved were studied.

Diffusion Controlled Limiting Currents.—If the potentiostatic reduction of substance O to substance R is considered at potentials sufficiently cathodic that the current is controlled entirely by the diffusion of O to a spherical electrode surface, the equation for the current–time curve is[7]

$$i = nFAD_{O}C_{O}^{*}\left[\frac{1}{(\pi D_{O}t)^{1/2}} + \frac{1}{r_{0}}\right] \qquad (1)$$

where i is the current flowing, n is the number of electrons involved in the electrode reaction, F is the faraday, A is the area of the electrode, D_O is the diffusion coefficient of substance O, C^*_O is the bulk concentration of substance O, t is the time after the sudden application of the constant potential, and r_0 is the radius of the electrode. The corresponding equation for diffusion to a plane electrode lacks the term in r_0, and when r_0 is large, or when t is small, the contribution of this term to the total current is small. For the experimental conditions used in this work, however, this contribution was as much as 30% of the total current.

Attempts by Laitinen and Kolthoff[8] to verify

(1) Based, in part, on the Ph.D. thesis of Kenneth J. Martin, University of Wisconsin, 1960.

(2) H. Gerischer, *Z. physik. Chem.*, **202**, 302 (1953).

(3) T. Berzins and P. Delahay, *J. Am. Chem. Soc.*, **77**, 6448 (1955); H. Matsuda, S. Oka and P. Delahay, *ibid.*, **81**, 5077 (1959).

(4) H. Gerischer and W. Vielstich, *Z. physik. Chem., N.F.*, **3**, 16 (1955); W. Vielstich and H. Gerischer, *ibid.*, **4**, 10 (1955); H. Gerischer and K. Staubach, *ibid.*, **6**, 118 (1956).

(5) R. D. DeMars and I. Shain, *J. Am. Chem. Soc.*, **81**, 2654 (1959).

(6) (a) J. W. Ross, R. D. DeMars and I. Shain, *Anal. Chem.*, **28**, 1768 (1956); (b) R. D. DeMars and I. Shain, *ibid.*, **29**, 1825 (1957); (c) K. J. Martin and I. Shain, *ibid.*, **30**, 1808 (1958); (d) W. Kemula and Z. Kublik, *Anal. Chim. Acta*, **18**, 104 (1958); (e) W. Kemula, Z. Kublik and S. Glodowski, *J. Electroanal. Chem.*, **1**, 91 (1959).

(7) P. Delahay, "New Instrumental Methods in Electrochemistry," Interscience Publishers, New York, N. Y., 1954, p. 61.

(8) H. A. Laitinen and I. M. Kolthoff, *J. Am. Chem. Soc.*, **61**, 3344 (1939).

equation 1 at a spherical platinum electrode were unsuccessful because of convection encountered at the relatively long electrolysis times they used. Skobets and Kavetskii[9] used equation 1 to determine diffusion coefficients at a stationary spherical platinum electrode. The current can be plotted as a function of $(1/t)^{1/2}$ and the slope of the resulting straight line can be used to calculate the diffusion coefficient. Equation 1 was used in this work as a standard for evaluation of the characteristics of hanging mercury drop electrodes, as well as for the determination of several diffusion coefficients.

An analysis of the current–time curves obtained for diffusion controlled limiting currents at hanging mercury drop electrodes is shown in Fig. 1 (closed circles). A solution containing 5.19×10^{-4} *M* thallous ion, 1 *M* potassium nitrate and 0.1 *M* acetic acid–sodium acetate buffer was electrolyzed at −0.650 v. (*vs.* S.C.E.), using hanging drop electrodes formed by collecting 1, 2 or 3 drops of mercury from the capillary. Fairly large deviations from the theoretical straight lines were observed. The two major sources of error were found to be convection (currents higher than theory) and shielding of the electrode (currents lower than theory).

Influence of Convection.—In all of the systems studied, interference caused by convection was observed at both very short times, and at relatively long times. The convection at long times was found to be caused by vibration and by density gradients in the cell, and could be noted as abnormally high and unreproducible currents. By carefully isolating the cell from sources of vibration, and by allowing the solution to come to rest for several minutes after performing any manipulations on the cell, it was possible to carry out electrolyses for about 30 seconds without interference from these sources of convection.

Convection at very short times was found to be caused by movement of the hanging mercury drop electrode. On sudden application of the working potential, the surface tension of the mercury changes, resulting in a slight change in the shape of the mercury electrode. Such movement of the electrode is observed easily with a low power microscope.

The effect of this movement of the electrode, and the resulting convection in the solution, is shown in Fig. 1. The high current caused by stirring of the solution is more pronounced with the heavier electrodes, and persists for as long as 4 seconds. No attempts were made to determine when effects of drop movement are first noticeable. However, some recent results obtained by Delahay and Oka[10] indicate that these effects may be present at times as short as 1 millisecond.

In an attempt to minimize the effects of movement of the mercury, an electrode was constructed which supported the mercury drop from below. Such an electrode showed considerably less convection at short times (Fig. 1, open circles). The 3 drop electrode could not be used in this case, however, because the weight of the mercury caused the electrode to flatten out into a distinctly non-spherical shape.

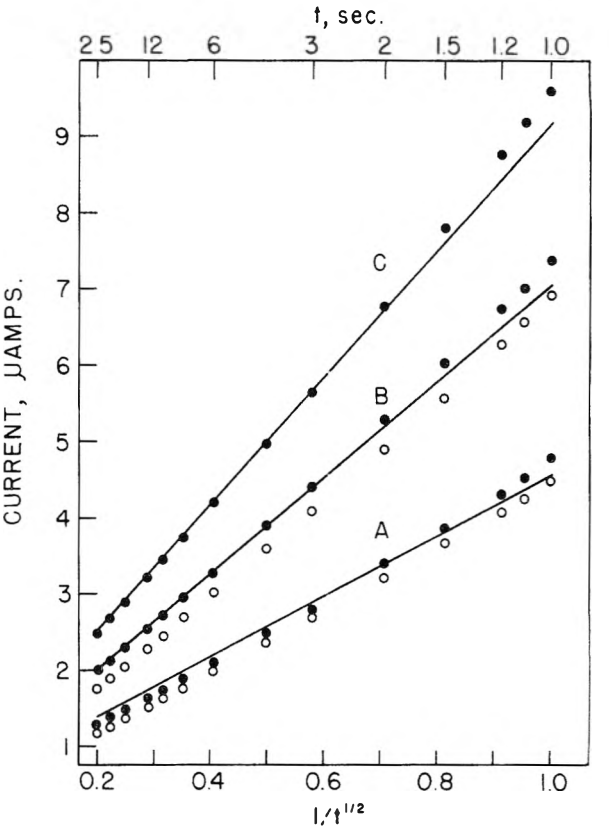

Fig. 1.—Analysis of current–time curves for the reduction of 5.19×10^{-4} *M* thallous ion, at −0.650 v. (*vs.* S.C.E.): A, 1 drop electrode, r_0 = 0.0515 cm.; B, 2 drop electrode, r_0 = 0.0650 cm.; C, 3 drop electrode, r_0 = 0.0744 cm. Lines, theoretical, based on $D_O = 1.79 \times 10^{-5}$ cm.²/sec.; ●, hanging mercury drop electrode; ○, supported mercury drop electrode.

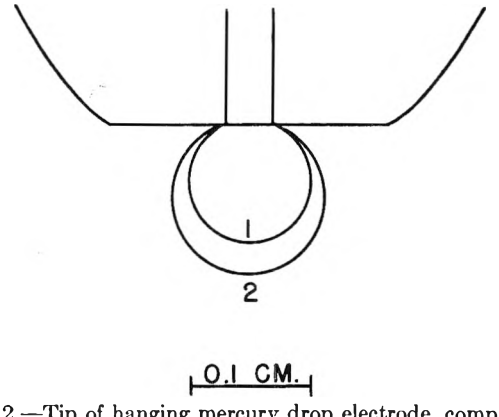

Fig. 2.—Tip of hanging mercury drop electrode, comparing shielding for 1 and 2 drop electrodes.

Influence of Shielding.—The means by which the hanging mercury drop electrode is supported interferes to some extent with the mass transfer process to the electrode surface. The actual point of contact of the mercury with the platinum wire on which the drop is hung is only a very small portion of the total area of the electrode (less than 0.4% in most cases) and the main interference is caused by the distortion of the diffusion layer by the glass. This

(9) E. M. Skobets and N. S. Kavetskii, *Zhur. Fiz. Khim.*, **24**, 1486 (1950).

(10) P. Delahay and S. Oka, *J. Am. Chem. Soc.*, **82**, 329 (1960).

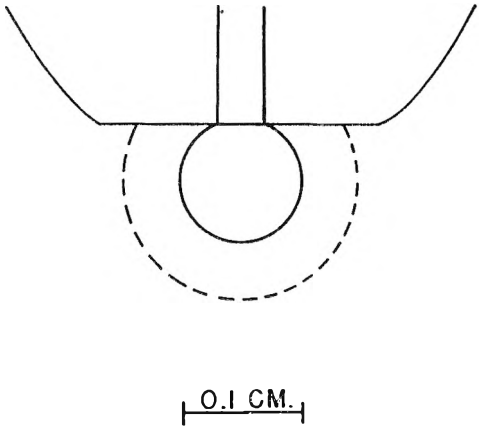

Fig. 3.—Calculated diffusion layer (one per cent. depletion) for a hanging mercury drop electrode: $D_O = 2 \times 10^{-5}$ cm.^{2}/sec., $t = 10$ sec., $r_0 = 0.0515$ cm.

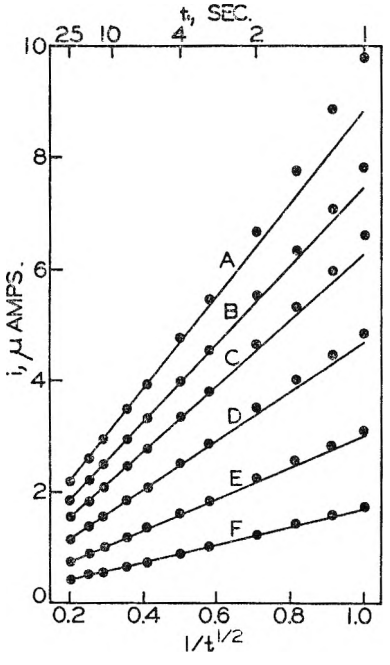

Fig. 4.—Analysis of current–time curves for the reduction of 1.07×10^{-3} M titanium(IV) oxalato complex: points, experimental; lines, theoretical; $r_0 = 0.0678$ cm. The applied potentials were A, −0.450 v.; B, −0.330 v.; C, −0.310 v.; D, −0.290 v.; E, −0.270 v.; F, −0.250 v.; each *vs.* S.C.E.

effect can be minimized by drawing out the glass tip during construction of the electrode. An approximate scale drawing of the tip of the electrode (Fig. 2) indicates that shielding is relatively severe near the top of the mercury drop, but is decreased as larger electrodes are formed by collecting additional drops of mercury from the capillary.

Thus, shielding should result in currents lower than predicted by equation 1, and the effect should decrease as the size of the hanging mercury drop electrode is increased. The results (Fig. 1) are surprising since the deviation in the current is apparently independent of time, at least for times greater than about 4 seconds, when convection due to drop movement ceases. The effect is more severe with a mercury drop electrode supported from below since considerably more glass must be retained in order to have a surface large enough to collect the drops of mercury. However, even with the supported mercury drop electrode, shielding is independent of time for the conditions of these experiments.

Since the radius is the only term in equation 1 which can shift the curve vertically without affecting its slope, the effective radius of the electrode must differ from the geometric radius. That this could occur easily is shown in Fig. 3, since a rapid thickening of the diffusion layer where the mercury approaches the glass could cause the diffusion layer to become hemispherical. The dotted line in Fig. 3 represents the thickness of the diffusion layer (1% depletion) 10 seconds after the start of electrolysis, basing the calculations on equation 1.

As a result of these studies, it is apparent that the use of the hanging mercury drop electrode for potentiostatic investigations involves a compromise between the effects of shielding, and convection caused by drop movement. Interference caused by convection decreases as the size of the electrode decreases, but the effects of shielding are most severe with the small electrodes. The shielding was so severe with supported mercury drop electrodes that they were not considered useful. For this work, hanging mercury drop electrodes formed by collecting 2 drops of mercury from the capillary were used. With these electrodes ($r_0 = 0.06$ cm.) currents measured between about 4 and 25 seconds were not affected by either convection or shielding.

Determination of Diffusion Coefficients.—In the course of this work, it was possible to evaluate the errors involved in the use of equation 1 for determination of diffusion coefficients. Diffusion coefficients obtained from both the slope and the intercept of the i *vs.* $(1/t)^{1/2}$ plots agreed closely. The values are accurate to at least ±2%, indicating that this method should be very useful for the accurate determination of diffusion coefficients.

The diffusion coefficient obtained for thallous ion in 1 M potassium nitrate, 0.1 M acetic acid and 0.1 M sodium acetate was 1.79×10^{-5} cm.^{2}/sec. This agrees exactly with the value in 1 M potassium nitrate reported by Rulfs.[11] The diffusion coefficient of the titanium(IV) oxalato complex in 0.2 M oxalic acid, and 1% sulfuric acid (pH 1.25) was 0.61×10^{-5} cm.^{2}/sec., a value somewhat lower than that calculated from the diffusion current constants given by Pecsok.[12] The diffusion coefficient of iodate ion in 0.1 M potassium nitrate, 0.1 M potassium dihydrogen phosphate, and 0.1 M potassium monohydrogen phosphate (pH 7.2), was 1.01×10^{-5} cm.^{2}/sec., compared with the infinite dilution value of 1.09×10^{-5} cm.^{2}/sec.[13]

Reversible Electrode Reactions: Reactant and Product Soluble in the Solution.—If the applied constant potential is not restricted to very cathodic values as above, the current flowing at the electrode is controlled by potential as well as mass transfer. The equation describing the current–time curves

(11) C. L. Rulfs, *J. Am. Chem. Soc.*, **76**, 2071 (1954).
(12) R. L. Pecsok, *ibid.*, **73**, 1304 (1951).
(13) I. M. Kolthoff and J. J. Lingane, "Polarography," 2nd ed., Interscience Publishers, New York, N. Y., 1952, Vol. I, p. 52.

for the case where substance R is initially absent is

$$i = \frac{nFAD_OC_O^*}{(1 + \gamma\theta)}\left[\frac{1}{(\pi D_O t)^{1/2}} + \frac{1}{r_0}\right] \quad (2)$$

where $\gamma = (D_O/D_R)^{1/2}$, and

$$\theta = \frac{C_O}{C_R} = \exp\left[\frac{nF}{RT}(E - E^0)\right] \quad (\text{at } r = r_0) \quad (3)$$

D_R is the diffusion coefficient of substance R, C_O and C_R are the concentrations of substances O and R, respectively, r is the distance from the center of the electrode, θ defines the ratio C_O/C_R at the electrode surface in terms of the Nernst equation, and the other terms were defined previously. Although equation 2 apparently has not been reported previously, its derivation follows readily from the corresponding case involving a plane electrode.[14] Again, the only difference between the two cases is that the equation for the plane electrode lacks the term in r_0. At very cathodic potentials, $\theta \rightarrow 0$, and equation 2 approaches equation 1.

In order to verify equation 2, the reduction of the titanium(IV) oxalato complex was selected on the basis of its reported reversibility,[12] and because the products of the electrode reaction are soluble in the solution. The current was plotted as a function of $(1/t)^{1/2}$ at various potentials (Fig. 4). By assuming that $\gamma = 1$, an effective E^0 of -0.287 ± 0.001 v. *vs.* S.C.E. was calculated from the slopes of the lines. The agreement between theory and experiment is excellent, except at short times (less than 4 seconds) where convection caused by drop movement was severe.

Reversible Electrode Reactions: Products Soluble in the Mercury.—In attempting to apply equation 2 to the analysis of current-time curves obtained for the reduction of thallous ion, major deviations were observed (Fig. 5). Curve A was recorded at a potential sufficiently cathodic that a diffusion controlled limiting current was obtained; the agreement with equation 1 was satisfactory. At least cathodic potentials, the current was less than that predicted by equation 2, and the deviation was apparently independent of time of electrolysis.

A re-examination of the boundary conditions used in the derivation of equation 2 revealed that the difficulty probably was connected with the convergent nature of the diffusion layer within the mercury drop, and also by the fact that the concentration of substance R builds up within the limited volume of the electrode during the course of the electrolysis. Any attempt to account for both these effects rigorously appeared extremely complex. However, a consideration of the convergent nature of the diffusion layer within the mercury leads to some useful conclusions.

Theory.—The boundary value problem requires solving Fick's second law for spherical diffusion[15]

$$\frac{\partial C_O}{\partial t} = D_O\left[\frac{\partial^2 C_O}{\partial r^2} + \frac{2}{r}\frac{\partial C_O}{\partial r}\right] \quad (4)$$

(14) Ref. 7, p. 52–55.
(15) Ref. 7, p. 60.

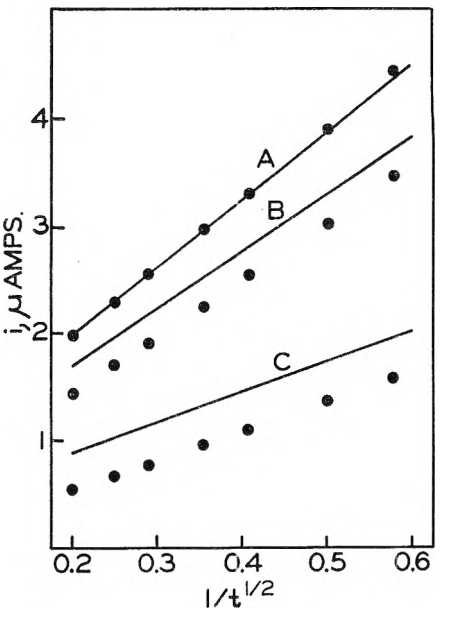

Fig. 5.—Analysis of current-time curves for the reduction of 5.19×10^{-4} *M* thallous ion: points, experimental; lines, calculated from equation 2. The applied potentials were: A, −0.650 v.; B, −0.530 v.; C, −0.480 v.; each *vs.* S.C.E.

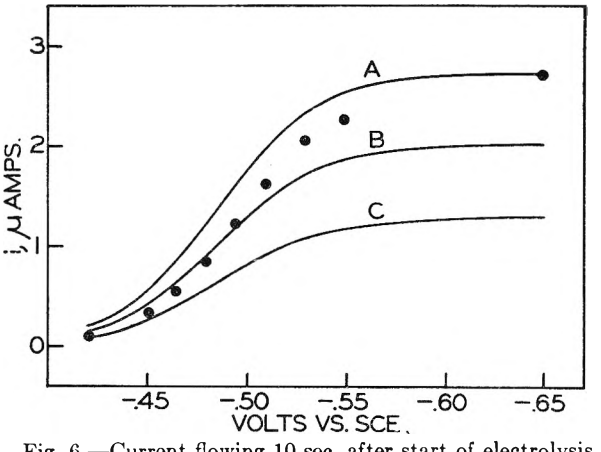

Fig. 6.—Current flowing 10 sec. after start of electrolysis for the reduction of 5.19×10^{-4} *M* thallous ion: points, experimental; lines, theoretical-calculated from: A, equation 2; B, equation for diffusion to a plane electrode; C equation 14.

$$\frac{\partial C_R}{\partial t} = D_R\left[\frac{\partial^2 C_R}{\partial r^2} + \frac{2}{r}\frac{\partial C_R}{\partial r}\right] \quad (5)$$

The initial conditions are

$$C_O = C_O^*\ ;\ C_R = 0, \text{ for } t = 0, \text{ any } r \quad (6)$$

The boundary conditions are

$$C_O \longrightarrow C_O^* \quad \text{as} \quad r \longrightarrow \infty, \text{ any } t \quad (7)$$

$$C_R \longrightarrow 0 \quad \text{as} \quad r \longrightarrow 0, \text{ any } t \quad (8)$$

Equation 8 is valid only until the diffusion layer of substance R reaches the center of the electrode, since the flux of R is zero at $r = 0$. An additional boundary condition reflects the fact that when an amalgam is formed, the flux and direction of diffusion are the same for both reactant and product

$$D_O\left[\frac{\partial C_O}{\partial r}\right] = D_R\left[\frac{\partial C_R}{\partial r}\right] \quad t > 0, r = r_0 \quad (9)$$

Furthermore it is assumed that the Nernst equation holds (equation 3).

Although an exact analytical solution to this problem was not obtained by application of the Laplace transformation because of the complexity of the transform of the solution, an approximate solution was obtained by assuming

$$C_O + C_R = C_O^* \qquad (10)$$

Equation 10 can be derived from geometric considerations involving diffusion to a plane electrode.[16] It is also valid for diffusion to a sphere if the products of the electrode reaction are soluble in the solution, and if it is further assumed that $D_O = D_R$. For the case of amalgam formation, equation 10 is only an approximation which holds best when C_R is low, *i.e.*, when relatively low currents are observed at less cathodic potentials.

Combining equations 10 and 3, an alternate boundary condition is obtained

$$C_R = C_O^*/(1 + \theta) \text{ for } t > 0,\ r = r_0 \qquad (11)$$

A solution to this boundary value problem is[17]

$$C_O = \frac{r_0 C_O^*}{r(1+\theta)} \sum_{n=0}^{\infty} \left[\operatorname{erfc} \frac{(2n+1)r_0 - r}{2(Dt)^{1/2}} - \operatorname{erfc} \frac{(2n+1)r_0 + r}{2(Dt)^{1/2}} \right] \qquad (12)$$

By differentiating equation 12 with respect to r, and evaluating at $r = r_0$, a value of the flux is obtained, which when substituted into Fick's first law yields

$$i = \frac{nFADC_O^*}{(1+\theta)} \left\{ \frac{1}{(\pi Dt)^{1/2}} - \frac{1}{r_0} + \frac{2}{(\pi Dt)^{1/2}} \left[\exp\left(-\frac{r_0^2}{Dt}\right) + \exp\left(-\frac{4r_0^2}{Dt}\right) + \ldots \right] \right\} \qquad (13)$$

For the experimental conditions encountered in this work, the exponential terms can be neglected, and equation 13 reduces to

$$i = \frac{nFADC_O^*}{(1+\theta)} \left[\frac{1}{(\pi Dt)^{1/2}} - \frac{1}{r_0} \right] \qquad (14)$$

This is the same as equation 2 except that the term in r_0 is negative. Thus the convergent nature of diffusion within the electrode apparently affects that contribution to the total current represented in the term in r_0. Equation 14 should be valid at the less cathodic values (large θ), and equation 2 (or 1) should hold at small values of θ.

Results and Discussion

Current-time curves for the reduction of thallous ion were obtained at various potentials in order to test some of the above conclusions. Plots of current *vs.* $(1/t)^{1/2}$ gave straight lines parallel to, but higher than, the theoretical curves predicted by equation 14, except at very anodic potentials where the currents were very low. The effect on the current at various potentials can be seen in Fig. 6 as the controlling diffusion process shifts from the mercury to the solution. The current flowing at $t = 10$ seconds is plotted as a function of potential from equations 2 and 14; and for comparison purposes, the curve obtained from the corresponding equation for a plane electrode is also included. It is interesting to note that the potential at which the current flowing happens to cross the curve for the plane electrode is the calculated effective E^0.

Experimental

Apparatus.—A potentiostat was used in this work. The circuit was arranged so that the potential between the working electrode and a reference electrode was controlled to within 1 millivolt, while the current through the cell passed between the working electrode and a counter electrode. The instrument was based on the operational features of the analog computer amplifiers manufactured by G. A. Philbrick Researches, Inc. (Boston), and used some of the ideas suggested by DeFord.[18] The current–time curves were recorded on a Leeds and Northrup Speedomax recorder, 1 second response, 1 millivolt full scale.

The hanging drop electrode and the electrode assembly were essentially the same as described previously.[6a] The counter electrode was a platinum foil connected to the cell by means of a 2 *M* potassium nitrate salt bridge terminated with a 10 mm. ultrafine sintered glass disc.

The reference electrode was a Beckman calomel electrode, placed in a compartment containing 2 *M* potassium nitrate, and connected to the cell by means of a Luggin capillary salt bridge.

For those experiments in which the mercury drop was supported from below, an electrode was constructed by sealing platinum wire (0.016 inch diameter) into the end of a 6 mm. soft glass tube. The end of the electrode was bent in the shape of a J and then polished slightly concave so that drops of mercury falling from a capillary could be collected.

An effective method of isolating the cell from vibration was devised by mounting the entire cell assembly, water-bath, and a heavy slate block on an inflated inner tube.

All experiments were carried out at 25.0° in a thermostat.

Materials.—Purified $K_2TiO(C_2O_4)_2 \cdot 2H_2O$ was recrystallized once, and analyzed by precipitation with cupferron. The thallium solution was analyzed by precipitation with chromate. All other materials were reagent grade, and were used without further purification. To remove oxygen from the cell, Linde high purity nitrogen was used without further purification.

Acknowledgments.—This work was supported in part by funds received from the United States Atomic Energy Commission, under Contract No. AT(11-1)-64, Project No. 17. Other support was received from the Research Committee of the Graduate School of the University of Wisconsin with funds received from the Wisconsin Alumni Research Foundation. Some of the instruments used in this work were purchased with funds made available by the Standard Oil Foundation, Inc. (Indiana).

(16) Ref. 7, p. 54.

(17) J. Crank, "The Mathematics of Diffusion," Oxford University Press, London, 1956, p. 86; H. S. Carslaw and J. C. Jaeger, "Conduction of Heat in Solids," 2nd ed., Oxford University Press, London, 1959 p. 233.

(18) D. D. DeFord, Division of Analytical Chemistry, 133rd Meeting, A.C.S., San Francisco, California, April, 1958.

ELECTROLYSIS WITH CONSTANT POTENTIAL: IRREVERSIBLE REACTIONS AT A HANGING MERCURY DROP ELECTRODE[1]

BY IRVING SHAIN, KENNETH J. MARTIN AND JAMES W. ROSS[2]

Department of Chemistry, University of Wisconsin, Madison, Wisconsin

Received July 5, 1960

The use of the hanging mercury drop electrode for the potentiostatic study of slow electrode reactions was investigated. Assuming a first-order electron transfer reaction and diffusion as the only means of mass transfer, an equation was derived for the current–time curves which takes into account the spherical nature of the electrode. By comparison of experimental current–time curves with a theoretical family of curves, values of the rate constant for the reaction can be obtained from measurements made at times up to 25 seconds after the start of the electrolysis. The reduction of iodate at *p*H 7.2 was used to test the theory.

The potentiostatic method has been used for the investigation of the rates and mechanisms of electrode reactions which are too fast to study by polarography.[3] The method also has been used for a study of an electrode reaction preceded by a coupled chemical reaction.[4] In all these studies, the hanging mercury drop electrode[5] was used under conditions where the curvature of the electrode surface could be ignored. That is, the time of electrolysis was very short (less than the order of a few milliseconds) and therefore the currents were relatively so high that the contribution to the total current caused by the convergent nature of the diffusion process was negligible.

The potentiostatic method has not been used to study electrode reactions which are slow enough to be studied by polarography. Nevertheless, the method has some distinct advantages over the polarographic method since the interference from charging current is less, and also because it is relatively easy to derive rigorous equations describing the electron transfer and mass transfer processes. These slow electrode processes can be studied conveniently at relatively long times after the start of the electrolysis (up to 25 seconds) making it unnecessary to use oscillographic equipment. A study of the sources of error involved in the use of the hanging mercury drop electrode[6] indicated that accurate data could be obtained in the time interval between 4–25 seconds after the start of electrolysis and that the effects of shielding and convection could be minimized. However, under these conditions, the spherical nature of the electrode results in currents which are up to 30% higher than the currents at a plane electrode of equal area, and the equations which were used in previous investigations are not valid.

Theory

Consider the first-order reduction of a substance O to a substance R, under the conditions that the only way substance O can reach the electrode surface is by means of diffusion, that the electrode is a sphere, that both O and R are soluble in the solution, and that at time zero a constant potential is suddenly applied to the cell such that the reduction of O to R proceeds at a measurable rate. Under these conditions, the current flowing will depend on the flux of substance O at the electrode surface, which, in turn, will be determined by the equations for spherical diffusion[7]

$$\frac{\partial C_O}{\partial t} = D_O\left[\frac{\partial^2 C_O}{\partial r^2} + \frac{2}{r}\frac{\partial C_O}{\partial r}\right] \quad (1)$$

$$\frac{\partial C_R}{\partial t} = D_R\left[\frac{\partial^2 C_R}{\partial r^2} + \frac{2}{r}\frac{\partial C_R}{\partial r}\right] \quad (2)$$

C_O and C_R are the concentrations of substances O and R, D_O and D_R are the diffusion coefficients of substances O and R, t is the time, and r is the distance from the center of the electrode, which is taken as the origin. These equations must be solved for the initial and boundary conditions. The initial conditions are

$$C_O = C_O^* \qquad t = 0, \text{ any } r \quad (3)$$

$$C_R = C_R^* \qquad t = 0, \text{ any } r \quad (4)$$

where C_O^* and C_R^* are the bulk concentrations of O and R.

The first boundary condition assumes that the diffusion processes take place in a semi-infinite medium, and that both O and R are soluble in the solution

$$C_O \longrightarrow C_O^* \qquad t > 0,\ r \longrightarrow \infty \quad (5)$$

$$C_R \longrightarrow C_R^* \qquad t > 0,\ r \longrightarrow \infty \quad (6)$$

The second boundary condition states that the flux of O and R must be equal at the electrode surface

$$D_O\left(\frac{\partial C_O}{\partial r}\right) = -D_R\left(\frac{\partial C_R}{\partial r}\right) \qquad t > 0,\ r = r_0 \quad (7)$$

where r_0 is the radius of the electrode. A final boundary condition is that the current must be proportional to the flux of O at the electrode surface

$$D_O\frac{\partial C_O}{\partial r} = \frac{i}{nFA} = (k_f C_O - k_b C_R) \quad t > 0,\ r = r_0 \quad (8)$$

where i is the current, n is the total number of electrons involved in the electrode reaction, A is the area of the electrode, and k_f and k_b are the heterogeneous rate constants for the forward and back reactions. These rate constants are functions of potential[8] E

(1) Based in part on the Ph.D. theses of James W. Ross, University of Wisconsin, 1957, and Kenneth J. Martin, University of Wisconsin, 1960.

(2) Allied Chemical and Dye Fellow, 1956–1957.

(3) H. Gerischer and W. Vielstich, *Z. physik. Chem., N. F.*, **3**, 16 (1955); W. Vielstich and H. Gerischer, *ibid.*, **4**, 10 (1955); H. Gerischer and K. Staubach, *ibid.*, **6**, 118 (1956).

(4) P. Delahay and S. Oka, *J. Am. Chem. Soc.*, **82**, 329 (1960).

(5) H. Gerischer, *Z. physik. Chem.*, **202**, 302 (1953).

(6) I. Shain and K. J. Martin, *J. Phys. Chem.*, **65**, 254 (1961).

(7) P. Delahay, "New Instrumental Methods in Electrochemistry," Interscience Publishers, Inc., New York, N. Y., 1954, p. 60.

(8) Ref. 7, pp. 34–35.

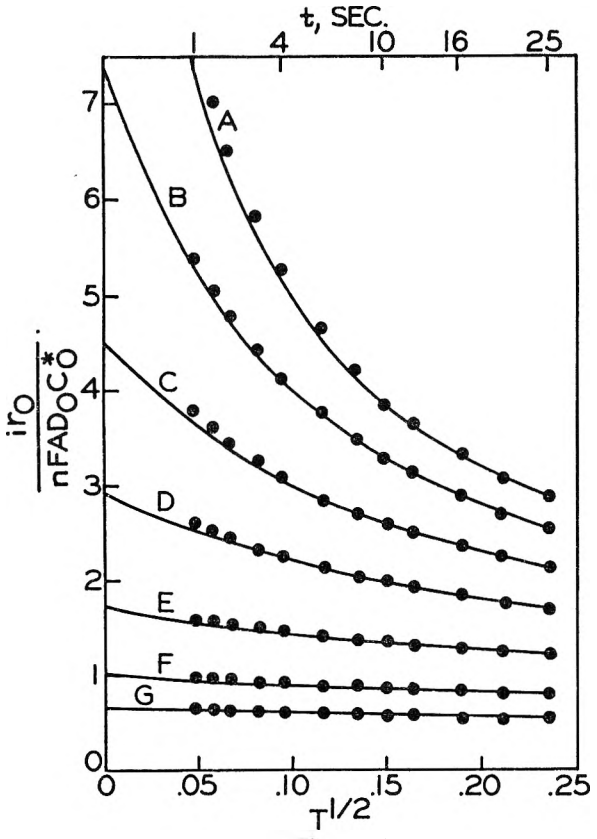

Fig. 1.—Plot of $ir_0/nFAD_0C_0^*$ *vs.* $T^{1/2}$ for 2.53×10^{-4} *M* iodate solution: points, experimental; lines, theoretical (see Table I).

$$k_f = k_s \exp\left[-\frac{\alpha n_a F}{RT}(E - E^0)\right] \quad (9)$$

$$k_b = k_s \exp\left[\frac{(1-\alpha) n_a F}{RT}(E - E^0)\right] \quad (10)$$

where k_s is the standard rate constant at the standard potential, E^0, α is the electron transfer coefficient, n_a is the number of electrons in the rate-determining step, and R, T, F have the usual significance.

The solution to this problem can be obtained by a relatively straight-forward application of the Laplace transformation.[9]

$$i = \frac{nFA(k_f C_O^* - k_b C_R^*)}{1 + \frac{r_0}{D}(k_f + k_b)}\left\{1 + \frac{r_0}{D}(k_f + k_b) \times \exp\left[\left(\frac{1}{r_0} + \frac{k_f + k_b}{D}\right)^2 Dt\right] \operatorname{erfc}\left[\left(\frac{1}{r_0} + \frac{k_f + k_b}{D}\right)(Dt)^{1/2}\right]\right\} \quad (11)$$

The only additional assumption which was made in the derivation was that $D_O = D_R$; the common diffusion coefficient is represented by D.

At large values of r_0, or at very small values of t, equation 11 reduces to the corresponding equation for a plane electrode.[10]

For the totally irreversible reactions which are of interest in this work, equation 11 can be simplified by dropping all terms involving the back reaction, and by substituting the dimensionless parameters

$$\lambda = \frac{k_f r_0}{D_O}$$

$$T = \frac{D_O}{r_0^2} t$$

Thus

$$\frac{ir_0}{nFAD_OC_O^*} = \frac{1 + \lambda \exp[(\lambda+1)^2 T] \operatorname{erfc}[(\lambda+1)T^{1/2}]}{1 + 1/\lambda} \quad (12)$$

When $T = 0$ ($t = 0$) the right side of equation 12 reduces to λ, and equation 12 reduces to the same expression as obtained for a plane electrode at zero time

$$i = nFAC_O^* k_f \quad (13)$$

Expansion of the function $\exp x^2 \operatorname{erfc} x$ as a Maclaurin series

$$1 - \frac{2x}{\pi^{1/2}} + x^2 - \frac{8x^3}{\pi^{1/2} \cdot 3!} + \ldots\ldots$$

indicates that the current should be proportional to $T^{1/2}$ at short times, and that plotting the data in this fashion should serve as a guide for extrapolation of the current to zero time. Thus equation 13 should be useful for determination of the rate constant as in oscillographic studies at constant potential. Unfortunately the straight-line portions of i *vs.* $T^{1/2}$ plots are very short, and are obscured by the convection caused by movement of the hanging mercury drop electrode when the constant potential is applied,[6] except at very low values of λ.

An alternate way of treating the experimental data is to plot $ir_0/nFAD_0C_0^*$ as a function of $T^{1/2}$ for current–time curves obtained at various potentials. These curves then can be compared with a family of curves made up by plotting, on the same scale, the right side of equation 12 *vs.* $T^{1/2}$ for various values of λ. By noting which of the theoretical curves most closely corresponds to the experimental curves, an estimate of λ can be obtained which can be confirmed, if necessary, by calculating additional theoretical curves corresponding to the estimated λ. This method permits the use of data obtained at relatively long times after the start of the electrolysis, and places equal weight on all portions of the current–time curve.

The procedure results in a series of values for λ as a function of potential, which then can be used to calculate rate constants. From equation 9, a plot of log k_f *vs.* the potential furnishes a value for αn_a, and if E^0 is known, a value for k_s can also be obtained.

Results and Discussion

The totally irreversible reduction of iodate at a *p*H of 7.2 was used to test the theory. Current–time curves were obtained at various potentials, including one at a potential (−1.100 v.) so cathodic that a value of the diffusion coefficient could be obtained from the theory of diffusion controlled limiting currents.[6] The value of the diffusion coefficient used was 1.01×10^{-5} cm.²/sec. The data were plotted as described above, and Fig. 1 shows that the agreement between experiment (the points) and the theory (the lines) is excellent, except at times less than 4 seconds, where high currents due to convection are observed. Table I summarizes

(9) R. V. Churchill, "Operational Mathematics," 2nd ed., McGraw-Hill Book Co., New York, N. Y., 1958.

(10) Ref. 7, p. 74.

the values of λ obtained from these curves, and their relation to the potential and k_f.

TABLE I

VALUES OF λ AND k_f AS A FUNCTION OF POTENTIAL FOR THE REDUCTION OF IODATE (FIG. 1)

Curve	Potential (v. vs. S.C.E.)	λ	($k_f \times 10^4$)
A	−0.850	12.5	18.7
B	− .800	7.4	11.1
C	− .750	4.5	6.75
D	− .700	2.9	4.35
E	− .650	1.7	2.55
F	− .600	1.0	1.50
G	− .550	0.65	0.975

The slope of the plot of log k_f *vs.* E gave a value of 0.26 for αn_a, the same as obtained previously using voltammetry with linearly varying potential.[11]

These results indicate that the potentiostatic method should be very useful for characterizing slow electrode reactions using the hanging mercury drop electrode.

(11) R. D. DeMars and I. Shain, *J. Am. Chem. Soc.*, **81**, 2654 (1959).

Experimental

The electrodes, cell assembly and potentiostat were the same as described previously.[6] The hanging mercury drop electrode was formed by collecting two drops from the capillary; the radius of the electrode was 0.0674 cm.

Materials were reagent grade and were used without further purification. Linde high purity nitrogen was used to remove oxygen from the cell. All experiments were carried out in a thermostat maintained at 25.0°.

Acknowledgments.—This work was supported in part by funds received from the United States Atomic Energy Commission, under Contract No. AT(11-1)-64, Project No. 17. Other support was received from the Research Committee of the Graduate School of the University of Wisconsin with funds received from the Wisconsin Alumni Research Foundation. Some of the instruments used in this work were purchased with funds made available by the Standard Oil Foundation, Inc. (Indiana).

THE DIFFERENTIAL THERMAL ANALYSIS OF PERCHLORATES. V. THE SYSTEM $LiClO_4$–$KClO_4$

BY MEYER M. MARKOWITZ, DANIEL A. BORYTA AND ROBERT F. HARRIS

Foote Mineral Company, Research and Development Laboratories, Chemicals Division, P. O. Box 513, West Chester, Pa.

Received July 11, 1960

The system $LiClO_4$–$KClO_4$ was determined to be of the simple eutectic type with the eutectic at 207° and 76.0 mole % $LiClO_4$. Some aspects of the thermal decompositions of the alkali metal perchlorates and of varicus alkali metal perchlorate mixtures were investigated by differential thermal analysis and by thermogravimetric analysis. These results are discussed from the points of view of polarization and of liquid phase formation effects.

Introduction

The previous phase investigations of binary systems involving lithium perchlorate as a component[1,2] have now been extended to include the anhydrous system $LiClO_4$–$KClO_4$. Some insight into the factors influencing the thermal decompositions of perchlorates was gained by differential thermal analyses (DTA) and by thermogravimetric analyses (TGA) carried out at higher temperatures. Thus, DTA and TGA data derived from the pure alkali metal perchlorates and from the salt pairs $LiClO_4$–$KClO_4$, $LiClO_4$–$NaClO_4$, $NaClO_4$–$KClO_4$ and $LiClO_4$–LiCl have been interpreted to indicate two difficultly resolvable effects in the decomposition processes. One effect refers to the polarizing power of the cation atmosphere associated with the perchlorate group; the other effect deals with the relative ease of formation of a perchlorate-containing liquid phase.

Experimental

Equipment and Procedures.—The DTA instrumentation has been described earlier.[1] For the low temperature studies (up to 350°), a vertical crucible furnace-steel heating block arrangement was used.[3] A closed muffle furnace was adopted for all high temperature thermal decomposition investigations (up to 850°) in order to minimize objectionable heat transients during turbulent gas evolution reactions.[4,5]

The recording thermobalance developed for TGA was of the null deflection type with a linear variable differential transformer sensor and an electromagnetic coil restoring assembly[5] ("Recording Balance Accessory," Fisher Scientific Co., 717 Forbes St., Pittsburgh, Penna., catalog no. 13-940-190) attached to an analytical balance. A platinum wire fixed to one end of the balance beam passed into a muffle furnace some distance below the balance case; a circular platinum ring at the bottom of the wire held the sample crucible. The modulated signal from the control unit and a constant fraction of the e.m.f. from a Chromel–Alumel thermocouple placed directly beneath the sample crucible were passed alternately through a stepping switch ("Auto-Step Switch," Fisher Scientific Co., catalog no. 13-940-180) and then to a potentiometric recorder. In this manner, weight change and furnace temperature were recorded on the same time basis.

The numerical values of decomposition temperatures determined by DTA are not necessarily coincident with those obtained by TGA. This is due to the differences in sensitivities between the two techniques and to the fact that in DTA the actual sample temperature is measured whereas in TGA, it is the furnace temperature which is recorded. Nevertheless, trends in temperature-dependent behavior can be followed by consistent use of either technique.

All DTA and TGA runs were carried out at a constant heating rate of 10° per minute. This was achieved by use

(1) M. M. Markowitz, *J. Phys. Chem.*, **62**, 827 (1958).
(2) M. M. Markowitz and R. F. Harris, *ibid.*, **63**, 1519 (1959).
(3) S. Gordon and C. Campbell, *Anal. Chem.*, **27**, 1102 (1955).
(4) M. M. Markowitz and D. A. Boryta, *J. Phys. Chem.*, **64**, 1711 (1960).
(5) M. M. Markowitz and D. A. Boryta, *Anal. Chem.*, **32**, 1588 (1960).

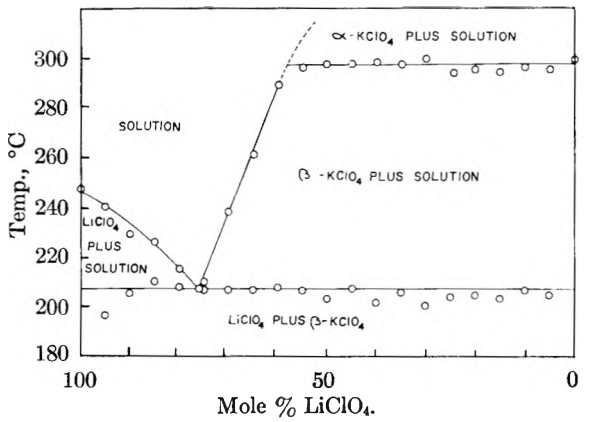

Fig. 1.—The system $LiClO_4$–$KClO_4$.

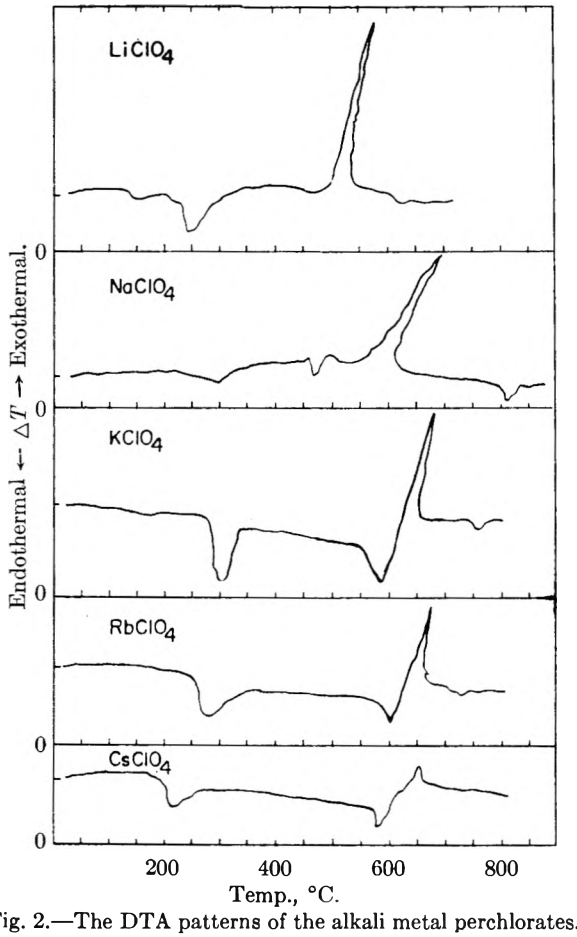

Fig. 2.—The DTA patterns of the alkali metal perchlorates.

of a motorized variable transformer to control the current to the furnace heating elements.[6]

Anhydrous lithium perchlorate, prepared as previously reported,[1] was analyzed by precipitation as nitron perchlorate. Analysis of product: ClO_4^-, 93.8 (calcd., 93.5). Reagent grade potassium and sodium perchlorates, dried under vacuum at 120° for 12 hours, were analyzed in a similar manner. Analyses of products: $KClO_4$:ClO_4^-, 71.7 (calcd., 71.9); $NaClO_4$:ClO_4^-, 81.4 (calcd. 81.2). Rubidium and cesium perchlorates were prepared by reaction of the C.P. carbonate and chloride salts, respectively, with dilute perchloric acid. The precipitated perchlorates, after drying at 120°, were analyzed by conversion to the chlorides through fusion with sodium carbonate in a platinum crucible. Analyses of products: $RbClO_4$:Cl, 18.93 (calcd., 19.18); $CsClO_4$:Cl, 14.87 (calcd., 15.27). Reagent grade lithium chloride was dried under vacuum at 150° for 12 hours. Analysis of product: Cl, 83.2 (calcd., 83.6).

The System $LiClO_4$–$KClO_4$.—Anhydrous lithium perchlorate when heated to about 350° showed but one DTA break, an endotherm corresponding to fusion at 247°. If a small amount of water is present an additional endotherm is introduced at about 150° due to dissociation of the monohydrate[1,7] (Fig. 2, $LiClO_4$). However, cycling of the sample under DTA conditions in a dry atmosphere eliminates this break by driving off the water. Potassium perchlorate evidenced a break at about 300° attributed to a reversible crystallographic transition[8] (Fig. 2, $KClO_4$).

Mixtures of the component salts (5 g.) were prepared and repeatedly subjected to DTA. Each liquidus temperature was determined by visual observation of a sample contained in a test-tube immersed in an oil-bath serviceable to about 275°. Subsequent TGA studies showed that the samples were all thermally stable at the temperatures and time durations encountered in this phase investigation. The persistence of the single eutectic break and of the break for the crystallographic transition of potassium perchlorate (samples containing 40–100 mole % $KClO_4$) indicate no complex interaction between the components. Accordingly, a plot of the data, given as Fig. 1, shows the system to be of the simple eutectic type with the eutectic occurring at 207° and 76.0 mole % $LiClO_4$.

The Thermal Decompositions of Perchlorate Salt Mixtures.—The mixtures (1 g.) of Table I were brought to constant weight during TGA runs carried out to 500–700°. The total weight losses indicated by the thermobalance generally checked to within several milligrams with the weight losses determined by manual weighing of the sample. For each mixture the total weight loss corresponded closely to the conversion of the perchlorate to the respective chloride and oxygen gas.[9] Similar TGA results were found for the decompositions of pure rubidium and cesium perchlorates in the present study.

The temperatures reported in Table I are those corresponding to the occurrence of 10% of decomposition. This criterion avoids misinterpreting slight weight losses due to volatile impurities as decomposition of the salts.

Table I

10% Thermal Decomposition Temperatures of Salt Mixtures

Compn., mole % salt A	Temp., °C. (A)$LiClO_4$–$KClO_4$	(A)$LiClO_4$–$NaClO_4$	(A)$LiClO_4$–LiCl	(A)$NaClO_4$–$KClO_4$
100.0	485	485	485	576
90.0	494	495	454	580
80.0	496	492	446	580
70.0	500	499	433	587
60.0	504	505	434	585
50.0	512	511	433	589
40.0	516	519	435	589
30.0	527	526	438	596
20.0	530	533	438	598
10.0	543	549	435	604
0.0	634	576	..	635

Inspection of Table I shows that a mixture of any two component perchlorates decomposes at a lower temperature than that of the more stable salt, but never at a temperature lower than that of the less stable component. The decomposition temperature of lithium perchlorate is lowered by the presence of lithium chloride but attains a fairly constant value for mixtures containing 20 mole % and more of lithium chloride. For the pure alkali metal perchlorates, the 10% decomposition temperatures are in the order Li—485°, Na—576°, Cs—628°, K—635°, and Rb—640°.

The DTA Patterns of the Alkali Metal Perchlorates.—The thermograms of the alkali metal perchlorates were

Educ., M. M. Markowitz, D. A. Boryta and G. Capriola, *J. Chem.*

(6) in press.

(7) J. P. Simmons and C. D. L. Ropp, *J. Am. Chem. Soc.*, **50**, 1650 (1928).

(8) D. Vorlaender and E. Kaascht, *Ber.*, **56**, 1137 (1923).

(9) G. G. Marvin and L. B. Woolaver, *Ind. Eng. Chem., Anal. Ed.*, **17**, 474 (1945).

redetermined using the closed muffle furnace.[4,5] This was necessitated because of the spurious thermal effects present in earlier studies.[1,3] Recession of the sample from the thermocouple and consequent interaction with the cool, ambient atmosphere gives rise to extraneous endothermal breaks when DTA experiments involving turbulent condensed phase-gas evolution reactions are carried out in the open air. The newly-obtained curves are given in Fig. 2 and the pertinent data are summarized in Table II. Five gram samples were used.

TABLE II

THERMAL BEHAVIOR OF THE ALKALI METAL PERCHLORATES FROM DTA CURVES

Sample	Crystal transition, °C.	Fusion of $MClO_4$, °C., T_f	Onset of rapid decompn., °C., T_d	$T_d - T_f$, °C.	Fusion of MCl, °C.
$LiClO_4$	[a]	247	472	225	613
$NaClO_4$	305	461	561	100	810
$KClO_4$	300	588	588	0	764
$RbClO_4$	278	595	595	0	722
$CsClO_4$	221	571	571	0	646[b]

[a] The small endotherm at about 150° (Fig. 2, $LiClO_4$) corresponds to the dissociation reaction $LiClO_4 \cdot H_2O \rightarrow LiClO_4 + H_2O$. [b] An endotherm for the fusion of cesium chloride does not appear in the DTA curve (Fig. 2, $CsClO_4$) because the decomposition exotherm extends somewhat beyond the melting point of cesium chloride.

Only in the instances of lithium and sodium perchlorates are the fusion and rapid decomposition processes separated by an appreciable temperature interval. Inspection of Fig. 2 shows that for the potassium, rubidium and cesium salts, fusion and decomposition are essentially concomitant processes. For the latter compounds, the exotherms corresponding to rapid decomposition are continuous with the peaks of the fusion endotherms. Slow decomposition of these salts was observed to occur during fusion as evidenced by bubbling of the sample.

Discussion

From the present work the observed order of thermal stability of the alkali metal perchlorates as gauged by the temperatures of rapid decomposition is Li < Na < Cs < K < Rb. This sequence follows the fusion temperatures of the salts rather than the order based solely on consideration of anion distortion by cation polarization effects.[10,11] For the alkali and alkaline earth metals, the polarizing power frequently is equated with the ionic potential, *i.e.*, (cation charge/cation radius) and follows the order Li (r_{M^+} = 0.78 Å.) > Na (0.98 Å.) > K (1.33 Å.) > Rb (1.49 Å.) > Cs (1.65 Å.).[12,13] The importance of a liquid phase in increasing reaction rates has been demonstrated clearly for the thermal decomposition of potassium perchlorate[14–16] and for a number of metathetical reactions.[17] A similar kinetic effect due to liquefaction is believed to be responsible for the determined order of the thermal stabilities of the alkali metal perchlorates.

The decompositions of the mixtures of Table I are influenced by both the polarization and liquefaction effects. The introduction of lithium perchlorate to sodium or potassium perchlorate brings about early formation of a liquid phase during heating and increases the polarizing power of the cation atmosphere surrounding the perchlorate group. The thermal behavior of $NaClO_4$–$KClO_4$ mixtures may be interpreted in the same manner.

Preliminary data for the system $LiClO_4$–$NaClO_4$[18] indicate it to be of the simple eutectic type at liquidus temperatures with the eutectic at about 208° and 72.5 mole % $LiClO_4$. As expected, in this system, sodium perchlorate exhibits a crystallographic transition at about 305°.[8]

The lowering of the decomposition temperature of lithium perchlorate by addition of lithium chloride is believed to be primarily a polarization effect. The components form a simple eutectic at about 235° and 90 mole % $LiClO_4$[19] so that at the decomposition temperatures observed all the perchlorate is in solution. The fact that as the overall $[Li^+]/[ClO_4^-]$ ratio increases, the decomposition temperature reaches a steady value of about 435° might indicate that a maximum coördination and polarization effect of lithium ions about the perchlorate group occurs near the presence of 20 mole % lithium chloride.

There are some phenomena cited in the literature which might be explained on the basis of the previous discussions. Thus, the addition of barium nitrate to potassium perchlorate results in a lowered decomposition temperature for the perchlorate anion.[20,21] The two salts were found to form a eutectic at about 465°,[21] about 125° lower than the fusion temperature of potassium perchlorate as determined by DTA. Furthermore, the polarizing power of the divalent barium ion [$r_{Ba^{++}}$ = 1.43 Å.) can be anticipated to be higher than that of the monovalent potassium ion (r_{K^+} = 1.33 Å.), thereby increasing the net polarizing effect of the cation atmosphere in the melt. Similarly, liquid mixtures of barium nitrate and potassium chloride were found to decompose at higher temperatures than pure barium nitrate but lower than for pure potassium nitrate.[21] Here the presence of the less highly charged potassium ion appears to have resulted in a decrease of the over-all polarizing effects of the cation atmosphere on the nitrate ion over that of pure barium nitrate; the converse is to be expected for the addition of barium chloride to potassium nitrate and this has been reported to be the case.[21]

Acknowledgment.—Portions of these studies were reported under contract AF 33(616)-6057. The permission of the Air Force Flight Test Center, Edwards Air Force Base, California, to publish this work is gratefully acknowledged.

(10) R. K. Osterheld and M. M. Markowitz, *J. Phys. Chem.*, **60**, 863 (1956).

(11) R. T. Sanderson, "Chemical Periodicity," Reinhold Publ. Corp., New York, N. Y., 1960, pp. 162–166.

(12) G. H. Cartledge, *J. Am. Chem. Soc.*, **50**, 2855, 2863 (1928); **52**, 3076 (1930).

(13) Empirical ionic crystal radii taken from V. M. Goldschmidt, "Geochemische Verteilungsgesetze," Vol. VIII, Skrift. d. Norsk Vidensk. Akad. Oslo, Math.-Nat. Kl. I (1926).

(14) L. L. Bircumshaw and T. R. Phillips, *J. Chem. Soc.*, 703 (1953).

(15) A. E. Harvey, Jr., M. T. Edmison, E. D. Jones, R. A. Seybert and K. A. Catto, *J. Am. Chem. Soc.*, **76**, 3270 (1954).

(16) A. E. Harvey, C. J. Wassink, T. A. Rodgers and K. H. Stern, *Ann. N. Y. Acad. Sci.*, **79**, 971 (1960).

(17) H. J. Borchardt and B. A. Thompson, *J. Am. Chem. Soc.*, **81**, 4182 (1959); **82**, 355 (1960).

(18) M. M. Markowitz and R. F. Harris, unpublished results.

(19) M. M. Markowitz and D. A. Boryta, unpublished results.

(20) V. D. Hogan, S. Gordon and C. Campbell, *Anal. Chem.*, **29**, 306 (1957).

(21) V. D. Hogan and S. Gordon *J. Phys. Chem.*, **62**, 1435 (1958); **63**, 93 (1959).

THE FIRST IONIZATION CONSTANT OF HYDROGEN SULFIDE IN WATER

By H. L. Loy and D. M. Himmelblau

Department of Chemical Engineering, The University of Texas, Austin 12, Texas

Received July 14, 1960

Recent developments in radioactive tracing techniques and the availability of radioactive tracers have been exploited together with standard conductance techniques to determine the thermodynamic first ionization constant of hydrogen sulfide: $K_1 = [(m_{H^+})(m_{HS^-})/(m_{H_2S})][(\gamma_{H^+})(\gamma_{HS^-})/(\gamma_{H_2S})]$. The apparent ionization constant of H_2S was determined at successively lower concentrations of H_2S in the range of 1×10^{-3} to 16×10^{-3} molal, and a true thermodynamic constant evaluated by extrapolation to infinite dilution. Water with a conductivity of 0.25×10^{-6} mho at 25° was obtained by distilling deionized water under a hydrogen atmosphere directly into the reaction flask and proceeding with the experiment as soon as the water reached thermal equilibrium with the thermostat. The values obtained for the first ionization constant were $0.271 \times 10^{-7} \pm 4\%$, $0.87 \times 10^{-7} \pm 4\%$, and $1.52 \times 10^{-7} \pm 7\%$ at 0, 25 and 50°, respectively. These values are in general agreement with values obtained by previous investigators, taking into account the high ionic strengths employed by them.

Introduction

In the last 60 years there have been a number of investigators[1-9] employing various techniques who have measured and reported widely varying values for the first ionization constant of hydrogen sulfide. Thermodynamic interpretation and evaluation of the reported values have been uncertain because of the high ionic strengths employed and because of the lack of reliable activity coefficient data when activity corrections were applied.

The purpose of this investigation was to determine the first ionization constant of hydrogen sulfide by exploiting recent developments in radioactive tracer equipment and the availability of radioactive chemicals. With these new techniques it was possible to determine concentrations of hydrogen sulfide as low as 10^{-4} molar within an accuracy of about 3%.

When hydrogen sulfide ionizes in an aqueous solution according to equation (1) (hydration of the proton is assumed but not written down in the analysis given)

$$H_2S(aq) \rightleftarrows H^+ HS^- \qquad (1)$$

the first ionization constant is defined by

$$K_1 = (a_{H^+})(a_{HS^-})/(a_{H_2S}) = (\Gamma)(K_1') \qquad (2)$$

where Γ, the activity coefficient product, is defined as

$$\Gamma = (\gamma_{H^+})(\gamma_{HS^-})/(\gamma_{H_2S})$$

and K', the apparent ionization constant, is defined as

$$K'_1 = (m_{H^+})(m_{HS^-})/(m_{H_2S})$$

K_1' has no thermodynamic significance, but is a convenient value to measure in the evaluation of K_1 since at infinite dilution, where by definition the activity coefficients are equal to unity, $K_1 = K_1'$. By collecting experimental data suitable for the calculation of K_1' at various diminishing molalities, K_1 can be found by plotting K_1' against some function of molality and extrapolating to infinite dilution.

It was not possible to use Ostwald's dilution law[10] in this manner because for weak acids (K_1 *ca.* 10^{-7}) the appropriate extrapolation introduces considerable error into the value of K_1. Instead, equation (3) was employed

$$K_1' = (m_{H_2S}\alpha^2)/(1 - \alpha) = m_{H_2S}\alpha^2 \qquad (3)$$

where the degree of dissociation, $\alpha = \Lambda/\Lambda'$, is the ratio of the equivalent conductance to the equivalent conductance the weak electrolyte would have if it were completely ionized at some definite concentration. In the solutions studied, $m_{H^+} = m_{HS^-} = (\Lambda/\Lambda')m_{H_2S}$. A method of determining Λ' from equivalent conductances of strong electrolytes only was used by MacInnes and Shedlovsky[11] in determining the ionization constants of acetic acid. This method assumes only that Kohlrausch's law of independent ion migration holds at low concentrations and that the strong electrolytes are completely ionized. With these assumptions, Λ' can be obtained from the following relation in which the equivalent conductances of the strong electrolytes are taken not at infinite dilution, but at the concentration at which the degree of dissociation is desired

$$\Lambda'_{H_2S} = \Lambda_{HCl} - \Lambda_{NaCl} + \Lambda_{NaH_3} \qquad (4)$$

Λ values were obtained as a function of temperature and concentration from MacInnes[12] and reference 4.

In the application of conductivity measurements to the study of solutions at very low concentrations, the accuracy and reliability of the conductivity data can be greatly impaired by the solvent effect. For this work, with water of a specific conductance of 0.25×10^{-6} mho, any such effect was of about the same order of magnitude, or less, than the experimental error, and solvent corrections were neglected.

Experimental

Apparatus.—The experimental apparatus consisted of a conductivity bridge, radiocounting apparatus and a constant temperature water-bath. The conductivity apparatus employed an a.c. Wheatstone bridge and an oscilloscope

(1) Th. Paul, *Chem. Z.*, 535 (1899).
(2) J. Walker and W. Comack, *J. Am. Chem. Soc.*, **22**, 5 (1900).
(3) F. Z. Auerbach, *Phys. Chem.*, **49**, 217 (1904).
(4) K. Jellinek and J. Czerweski, *Z. physik. Chem.*, **102**, 438 (1922).
(5) R. H. Wright and O. Maass, *Canadian J. Research*, **6**, 588 (1932).
(6) A. G. Epprecht, *Helv. Chim. Acta*, **21**, 205 (1938).
(7) H. Kubli, *ibid.*, **29**, 1962 (1946).
(8) N. Yiu, *Sci. Rpts. Tohoku Univ., First Series*, **35**, 53 (1951).
(9) T. A. Tumanova and K. P. Mishenko, *Zhur. neoorg. Khim.*, **2**, 1990 (1957).
(10) E. A. Moelwyn-Hughes, "Physical Chemistry," Pergamon Press, New York, N. Y., 1957, p. 825.
(11) D. A. MacInnes and T. Shedlovsky, *J. Am Chem. Soc.*, **54**, 1429 (1932).
(12) D. A. MacInnes, "Principles of Electrochemistry," Reinhold Publ. Co., New York, N. Y., 1939, p. 339.

as a null indicating instrument. A simple dip type conductivity cell was used, which was accurate to within 0.5%.

A vessel used for these measurements was a 1 l., three-neck, round-bottom flask of Pyrex glass or, alternatively, quartz. The center neck accepted the conductivity cell that had been cast into a male ground glass joint with wax. A manifold of three stopcocks with Teflon barrels led to a manometer, a vacuum line, and the H_2 or H_2S supplies. The vessel was leak-tested before each run.

The radioactive tracer-counting system consisted of a standard proportional end window counting tube for use with planchets, and an RIDL SCAMP amplifier and scaler set-up.

Procedure.—The first steps in the experiment were to determine the cell constant of the conductivity cell by the usual standard procedure, and to calibrate the radioactive counting apparatus by counting known concentrations of radioactive sulfur.

The radioactive hydrogen sulfide used was obtained from the Volk Radiochemical Company of Chicago, who prepared it by the method of Bills and Ronzio[13] to have a specific activity of approximately one millicurie per millimole of gas. It was diluted approximately by a factor of ten with 99.9% purified hydrogen sulfide (Matheson Company, Newark, N. J.).

The calibration of the total sulfur concentration in the aqueous solutions (and in effect the H_2S concentrations) was accomplished by neutralizing 100 ml. of 0.1 *N* NaOH with the radioactive H_2S in the presence of H_2. Then 10 *N* NaOH was added, and the sample solution finally was diluted to a volume of 500 ml. Aliquots taken from the 500 ml. of tagged solution were analyzed volumetrically for sulfur following a method recommended by Kolthoff[14]; the solution was found to be 0.0194 molal in sulfur, and was diluted to 0.01422, 0.00916, 0.004467 and 0.002473 molal for use in the counting calibration. The same counting geometry and concentration of NaOH as in the calibration procedure were used in the actual experimental runs. A C-14 plastic disk was employed as a reference standard to ensure that the counting rate always could be referred to the same counter efficiency and geometry. The usual corrections for background and beta decay also were made. When plotted, the calibration curve of counting rate *vs.* sulfur molality was quite linear.

In filling the reaction flask, deionized water with a specific resistance of over four million ohms was distilled directly into the flask under a hydrogen atmosphere. The flask was placed into a water-bath, tested for leaks with hydrogen pressure, a slight vacuum pulled, and the radioactive hydrogen sulfide introduced to about 150 to 200 mm. (gauge) of mercury pressure. After one hour the resistance of the solution was recorded, 1.75 ml. of solution was withdrawn with a hypodermic syringe, 0.25 ml. of 10 *N* NaOH was then pulled into the syringe in order to convert the H_2S to Na_2S, and the sample was counted in a planchet with the proportional counter. A slight vacuum was again pulled and the sequence repeated; this was done four or five times for each run, increasing the concentration of H_2S in the solution each time.

Results and Discussion

The values for K_1' are plotted *vs.* the molality of the H_2S in Fig. 1. A straight line was fitted to the points by the method of least squares. The slopes and intercepts at each of the three temperatures and the intercept confidence limits are shown in Table I. The intercepts represent the true thermodynamic ionization constants.

The confidence limits in Table I are believed to be too low to represent properly the error in the values of K_1, and should be more nearly the order of ±4% at 0 and 25° and 7% at 50°, based on an estimate of the possible experimental error discussed below.

There is no particular theoretical reason for fitting a straight line to the data plotted in Fig. 1;

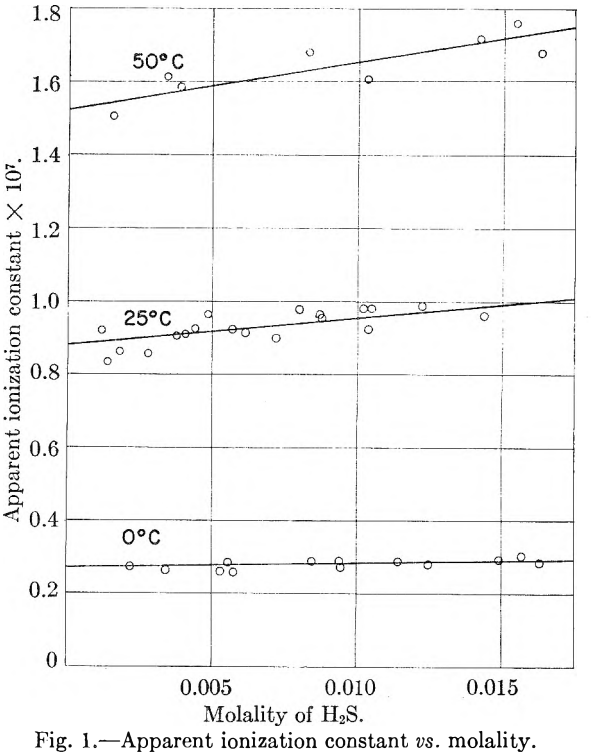

Fig. 1.—Apparent ionization constant *vs.* molality.

TABLE I

VALUES OF SLOPE AND INTERCEPTS OF FIG. 1

Temp., °C.	Slope × 10⁷	Intercept × 10⁷ K_1	95% confidence limits of intercept, %
0	1.00	0.271	±1.9
25	8.77	0.87	±1.7
50	13	1.52	±4.0

in fact, the Debye-Hückel theory would predict a linear relationship for log (K_1'/K_1) as a function of $\sqrt{\mu}$. However, since the range of $\sqrt{\mu}$ was quite small (3 to 6 × 10^{-3}) for this work, it did not appear that a correlation of this nature would be conclusive one way or the other.

From the equilibrium data the free energy of ionization at the standard state of infinite dilution has been calculated by $\Delta F^0 = -RT \ln K$ to yield values of 9440, 9610 and 10,000 cal. per gram mole of H_2S at 0, 25 and 50°, respectively.

The work of previous investigators is plotted in Fig. 2 as a function of temperature. The data of this work were in general agreement with the values reported by the other investigators, taking into account the fact that the ionization constants given by Kubli[7] and Tumanova and Mishenko[9] were for high ionic strengths, and considering the fact that Wright and Maass employed "Ostwald's Constant" at high concentrations of hydrogen sulfide. Latimer,[15] in evaluating the free energies of $H_2S(g)$, $H_2S(aq)$, and HS^- from the available data in 1952, used a value of K_1 of 1.1 × 10^{-7} at 25°. In applying the Van't Hoff equation to determine the heats of reaction, it can be seen from Fig. 2 that the data from this study have the same general trend as do the data of Wright and Maass, and consequently the heats of reaction for either

(13) W. Bills and A. R. Ronzio, *J. Am. Chem. Soc.*, **72**, 5510 (1950).

(14) I. M. Kolthoff and R. Belcher, "Volumetric Analysis," Vol. III, Interscience Publishers, Inc., New York, N. Y., 1957, p. 292.

(15) W. M. Latimer, "Oxidation Potentials," 2d ed., Prentice-Hal Inc., Englewood Cliffs, N. J., 1952.

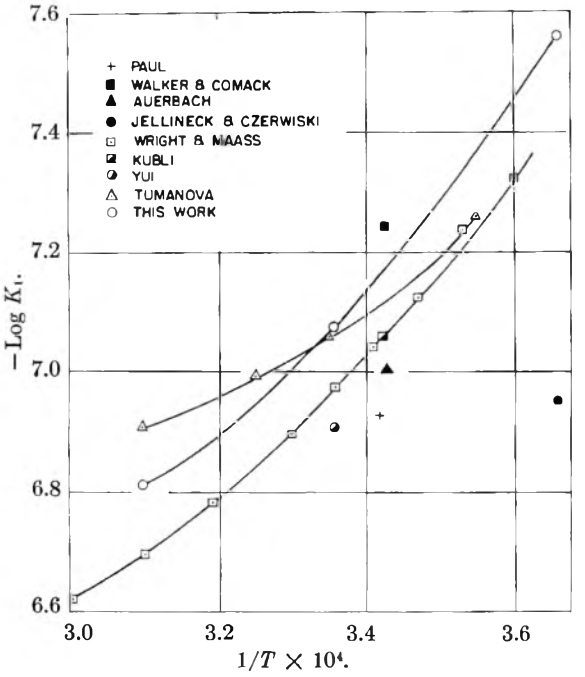

Fig. 2.—$1/T$ *vs.* log K_1 for various investigators.

set of data agree very well. The data of Tumanova and Mishenko have much less slope for the same temperature and consequently their calculated ΔH values would be lower.

In examining Fig. 1, one noticeable feature is the unexpectedly strong dependence of the apparent ionization constant K_1' on the concentration of the H_2S. The activity coefficient product $\Gamma = K_1/K_1'$ can be determined as a function of mean ionic strength as well as the molality of the H_2S as in Table II, and the values of Γ are considerably lower than would be anticipated for the very low ionic strengths existing in this work. Furthermore, for many weak acids such as water and acetic acid, the activity coefficient product is a linear function of the $\sqrt{\mu}$ at low values of $\sqrt{\mu}$, but this was not found true for H_2S in this work.

Table II

Evaluation of the Activity Coefficient Product of H_2S as a Function of Concentration

	0°		25°		50°	
Molality of H_2S	Mean ionic strength $\mu \times 10^5$	Γ	Mean ionic strength $\mu \times 10^5$	Γ	Mean ionic strength $\mu \times 10^5$	Γ
0.001	0.52	0.996	0.93	0.99	1.2	0.99
.005	1.16	.98	2.08	.95	2.8	.96
.010	1.64	.96	2.95	.91	3.9	.92
.020	2.32	.93	4.17	.83	5.5	.85

In the carbon dioxide system, in which the ionization constant has about the same value as this system, Γ for the ionization of CO_2 gas can be determined from the work of Shedlovsky and McInnes,[16] who found no such change as is indicated in Table II even though the concentration range covered for CO_2 gas was about the same as used here for H_2S gas and the ionic strengths were about the same. Wright and Maass, although working with values of H_2S molalities from 10 to 100 times the concentrations used here, did not find K_1 was concentration dependent, nor have other workers who employed relatively high ionic strengths ($\mu \sim 10^{-1}$ to 10^{-2}).

Acknowledging the anomalous results noted above, what explanation can be offered? Certainly one possibility always present with H_2S is that the gas reacted with the vessel containing it and caused the data collected to be erroneous. In this work five hours elapsed between the first admission of hydrogen sulfide and the withdrawal of the last sample of solution. If enough ions were formed (from a source other than the ionization of hydrogen sulfide) to change the conductivity to that of equilibrium conductivity water (10^{-6} mho), then an error of 8% in the conductivity could have resulted. The error would become augmented with time and result in an increase in the slopes shown in Fig. 1 since the samples were taken in increasing order of concentration.

That the slopes increase with increasing temperature would seem to confirm this view, except for the fact that to test this point several runs were made in a quartz reaction vessel, with results not significantly different from those made in the glass one. Certainly by taking data in the most dilute solutions first, and then in the more concentrated ones, any effect of a reaction, if it did exist, was certainly diminished. Fortunately, even if the values of K_1' may possibly have been biased by this effect, the extrapolated value of K_1 is very near the true value since the values in the most dilute solutions would be the least biased.

Assuming that the data are not biased, how can the effect of H_2S on the values of K_1 be interpreted? Γ merely represents the sum of all the non-idealities in the solution. With the concentration of H_2S molecules so low, and with the H^+ and HS^- concentrations being several orders of magnitude less, it is convenient, but not necessarily particularly informative, to ascribe the effects we have noted to solvation of the H_2S molecule (per Wright and Maass), the HS^- ion and/or the proton. Since there are no experimental data available on the primary or secondary solvation of H_2S and HS^-, and since theoretical methods of calculating the solvation number for these components are dubious, this explanation can be only speculative at this time. Certainly the primary solvation effects for H_2S must be different from most other gases which are slightly ionized in water and which can become chemically bound to a molecule of water, as, for example, CO_2 or SO_2.

Another possible explanation is that the undissociated H_2S molecules by themselves, or in conjunction with the water, are partly dimerized or associated in some form. If this were true, the value of m in equation (3) would be in excess of the proper value, and K_1 would not change as drastically with m_{H_2S} as shown in Fig. 1. Dimerization is a phenomenon likely to cause K_1' to change approximately linearly with concentration of un-ionized solute,[17] and has been noted for acetic acid at high concen-

(16) T. Shedlovsky and D. A. McInnes, *J. Am. Chem. Soc.*, **57**, 1705 (1935).

(17) R. A. Robinson and R. H. Stokes, "Electrolytic Solutions," 1st ed., Butterworth's Scientific Publications, London, 1955.

trations. But in the vicinity of one atmosphere, the solubility of H_2S in water follows Henry's law, and this would seem to be incompatible with the concept of dimerization of part of the H_2S. Hence a clearcut explanation of the noted change of the apparent ionization constant with H_2S concentration is not possible at this time.

Acknowledgment.—This work was supported by the National Science Foundation under grant G-5080.

HEATS OF COMBUSTION, ISOMERIZATION, AND FORMATION OF SELECTED C_7, C_8 AND C_{10} MONOÖLEFIN HYDROCARBONS[1]

By John D. Rockenfeller and Frederick D. Rossini[2]

Chemical and Petroleum Research Laboratory, Carnegie Institute of Technology, Pittsburgh 13, Pennsylvania

Received July 14, 1960

Measurements were made of the heats of combustion, in the liquid state at 25°, of 19 selected monoölefin hydrocarbons, including 10 heptenes, 6 octenes and 3 decenes. From these and appropriate other data were calculated values of standard heats of isomerization, formation and hydrogenation, as appropriate, for the liquid state at 25°. For most of the compounds, values are also given for the gaseous state. The relation between energy content and molecular structure for these compounds is discussed.

I. Introduction

Experimental data leading to values of heats of formation have been reported for substantially all of the monoölefin hydrocarbons through the hexenes.[3-5] However, very few data leading to values of heats of formation have been available for monoölefins above the hexenes.[6-9] It has become apparent that new experimental data on selected monoölefins of the C_7 to C_{10} range are needed to provide the basis for testing, within the limits of present-day measurements, any theory relating the energy and molecular structure of the monoölefin hydrocarbons. With a proved theory, one would not only arrive at a better understanding of the relation between energy and structure for these molecules, but one could calculate the heats of formation of an untold number of monoolefin hydrocarbons without recourse to further experimental measurement. Accordingly, the present investigation was carried out to obtain experimental data on 19 selected monoölefin hydrocarbons, including 10 heptenes, 6 octenes and 3 decenes. This report also presents a discussion of the relation between the energy and structure of these molecules.

II. Apparatus and Experimental Procedures

The experimental values of this investigation are based on the absolute joule as the unit of energy. Conversion to the defined thermochemical calorie is made using the relation 1 calorie = 4.184 (exactly) joules. For internal consistency with other investigations from this Laboratory, the molecular weight of carbon dioxide was taken as 44.010 g./mole.

In this investigation, the chemical and calorimetric apparatus and procedures were the same as described by Browne and Rossini.[10] The rise of temperature in each experiment was near 2°, with the final temperature being near 30°, the temperature of the jacket of the calorimeter. The amount of the reaction in each hydrocarbon combustion experiment was determined from the mass of carbon dioxide formed in the combustion, as previously described.[10] The bomb had an initial volume of 380 ml. One ml. of water was placed in the bomb prior to each combustion experiment. The pressure of the oxygen for combustion was made 30 atmospheres (calculated to 25°).

With the exception of the two branched decenes, the compounds measured in the present investigation were API Research hydrocarbons, made available through the API Research Project 44 from materials purified by the API Research Project 6. The API Research samples had the values of purity given in Table I. Description of the purification and determination of purity of these samples has already been given.[11-16] As a result of the methods of

Table I

Purity of the API Research Hydrocarbons Measured

Compound	Purity, mole %
1-Heptene	99.84 ± 0.10
3-Methyl-*cis*-3-hexene	(99.85 ± .10)[a]
3-Methyl-*trans*-3-hexene	(99.85 ± .10)[a]
2,4-Dimethyl-1-pentene	99.88 ± .09
4,4-Dimethyl-1-pentene	99.85 ± .08
2,4-Dimethyl-2-pentene	99.95 ± .04
4,4-Dimethyl-*cis*-2-pentene	99.85 ± .11
4,4-Dimethyl-*trans*-2-pentene	99.81 ± .03
3-Methyl-2-ethyl-1-butene	(99.85 ± .10)[a]
2,3,3-Trimethyl-1-butene	99.95 ± .04
1-Octene	99.77 ± .13
2,2-Dimethyl-*cis*-3-hexene	99.86 ± .12
2,2-Dimethyl-*trans*-3-hexene	(99.85 ± .10)[a]
2-Methyl-3-ethyl-1-pentene	99.81 ± .08
2,4,4-Trimethyl-1-pentene	99.95 ± .03
2,4,4-Trimethyl-2-pentene	99.93 ± .05
1-Decene	99.91 ± .07

[a] Estimated.

(1) This investigation was supported in part by a grant from the National Science Foundation. Submitted in partial fulfillment of the requirements for the degree of Doctor of Philosophy in Chemistry at the Carnegie Institute of Technology.

(2) University of Notre Dame, Notre Dame, Indiana.

(3) F. D. Rossini, K. S. Pitzer, R. L. Arnett, R. M. Braun and G. C. Pimentel, "Selected Values of Physical and Thermodynamic Properties of Hydrocarbons and Related Compounds," API Research Project 44, Carnegie Press, Pittsburgh, Pa., 1953.

(4) E. J. Prosen and F. D. Rossini, *J. Research Natl. Bur. Standards*, **36**, 269 (1946).

(5) H. F. Bartolo and F. D. Rossini, This Journal, **64**, 1685 (1960).

(6) F. M. Fraser and E. J. Prosen, *J. Research Natl. Bur. Standards*, **55**, 329 (1955).

(7) Sister M. Constance Loeffler and F. D. Rossini, This Journal, **64**, 1530 (1960).

(8) M. A. Dolliver, T. L. Gresham, G. B. Kistiakowsky and W. E. Vaughan, *J. Am. Chem. Soc.*, **59**, 831 (1937).

(9) R. B. Turner, D. E. Nettleton, Jr., and M. Perelman, *ibid.*, **80**, 1430 (1958).

(10) C. C. Browne and F. D. Rossini, This Journal, **64**, 927 (1960).

(11) A. J. Streiff, E. T. Murphy J. C. Zimmerman, L. F. Soule, V. A. Sedlak, C. B. Willingham and F. D. Rossini, *J. Research Natl. Bur. Standards*, **39**, 321 (1947).

TABLE II

RESULTS OF THE CALIBRATION EXPERIMENTS WITH BENZOIC ACID

No. of experiments	Range of mass of benzoic acid, g.	Range of k, min.$^{-1}$	Range of K, ohm	Range of U, ohm	Range of ΔR_c, ohm	Range of q_n, j.	Range of q_i, j.	Range of E_i, j./ohm	Mean and stand. dev. of the mean E_i, j./ohm
7	1.54990 to 1.56269	0.001629 to 0.001687	0.000778 to 0.000825	0.000447 to 0.000634	0.199207 to 0.200987	3.7 to 5.0	72.7 to 73.2	205874 to 206038	205966 ± 21

TABLE III

SUMMARY OF THE RESULTS OF THE CALORIMETRIC COMBUSTION EXPERIMENTS ON NINETEEN HYDROCARBONS IN THE LIQUID STATES AT 30°

Compound	No. of experiments	Range of B, ohm/g. CO_2	Mean value of B, ohm/g. CO_2	Stand. dev. of the mean, ohm/g. CO_2
1-Heptene	4	0.0732748 to 0.0732999	0.0732854	±0.0000058
3-Methyl-*cis*-3-hexene	4	.0729775 to .0729969	.0729871	± .0000041
3-Methyl-*trans*-3-hexene	3	.0730325 to .0730441	.0730379	± .0000034
2,4-Dimethyl-1-pentene	4	.0729568 to .0729876	.0729709	± .0000069
4,4-Dimethyl-1-pentene	4	.0730418 to .0730921	.0730720	± .0000119
2,4-Dimethyl-2-pentene	4	.0728695 to .0728840	.0728748	± .0000034
4,4-Dimethyl-*cis*-2-pentene	4	.0731411 to .0731746	.0731551	± .0000078
4,4-Dimethyl-*trans*-2-pentene	4	.0728885 to .0729069	.0728961	± .0000039
3-Methyl-2-ethyl-1-butene	3	.0730020 to .0730326	.0730168	± .0000088
2,3,3-Trimethyl-1-butene	4	.0729437 to .0729806	.0729598	± .0000073
1-Octene	4	.0731292 to .0731405	.0731346	± .0000023
2,2-Dimethyl-*cis*-3-hexene	4	.0730365 to .0731141	.0730706	± .0000164
2,2-Dimethyl-*trans*-3-hexene	4	.0727948 to .0728301	.0728158	± .0000083
2-Methyl-3-ethyl-1-pentene	4	.0729027 to .0729224	.0729130	± .0000045
2,4,4-Trimethyl-1-pentene	4	.0727969 to .0728062	.0728064	± .0000041
2,4,4-Trimethyl-2-pentene	5	.0728166 to .0728997	.0728506	± .0000120
1-Decene	7	.0720709 to .0729167	.0728846	± .0000119
2,2,5,5-Tetramethyl-*cis*-3-hexene	7	.0729890 to .0730317	.0730080	± .0000063
2,2,5,5-Tetramethyl-*trans*-3-hexene	4	.0724894 to .0725390	.0725224	± .0000117

purification, the impurities in these samples are substantially all isomeric, and the amounts are such as to have an insignificant effect on the results.

The samples of 2,2,5,5-tetramethyl-*cis*-3-hexene and 2,2,5,5-tetramethyl-*trans*-3-hexene were supplied by M. S. Newman and W. H. Puterbaugh of Ohio State University, Columbus, Ohio. After purification, the values of the refractive index, n_D, at 20°, were reported to be 1.4266 and 1.4116, respectively, and the values of the boiling point at 760 mm., 144.0 and 125.1°, respectively.[17]

The ampoules for containing the liquid hydrocarbon material were made of soft glass, as previously described, and filled and sealed likewise.[5,10]

The methods of determining absolute and relative heats of combustion and heats of isomerization already have been described.[5,7,10,18]

III. Data of the Present Investigation

The results of the calorimetric combustion experiments with benzoic acid to determine the energy equivalent of the standard calorimeter system are given in Table II. NBS Standard Benzoic Acid, No. 39g, was used, with the value 26,433.8 joules per gram mass for the heat of combustion of this sample under the conditions of the standard bomb process at 25°, with appropriate corrections for the differences between the actual and standard bomb processes. The symbols in Table II are as previously defined.[10]

A summary of the results of the calorimetric combustion experiments on the 19 hydrocarbons is given in Table III. In the 81 experiments referred to in Table III, the following ranges were observed in the several calorimetric quantities: mass of carbon dioxide formed, 2.50195 to 2.91724 g.; k, 0.001502 to 0.001663/mm.; K, 0.000567 to 0.001240 ohm; U, 0.000274 to 0.000917 ohm; ΔR_c, 0.182791 to 0.213082 ohm; Δr_i, 0.000350 to 0.000366 ohm; Δr_n, 0.000009 to 0.000035 ohm. The foregoing symbols, and those in Table III, are as previously defined.[10]

In Table IV are presented values of the standard heat of combustion for 1-heptene, 1-octene and 1-decene, as derived from the present investigation, together with a comparison with the values recommended by Loeffler and Rossini.[7] It is seen that the values from the present investigation are, within the limits of uncertainty, in accord with the recommended values, which constitute part of an extensive assembly of values of thermodynamic properties and should be used. Accordingly, the values for the isomeric monoölefins are presented with reference to the appropriate 1-alkene (normal alkyl monoölefin).

IV. Heats of Isomerization and Differences in the Heats of Hydrogenation

Tables V and VI give for the heptenes and octenes, respectively, the following values: the ratio

(12) A. J. Streiff, J. C. Zimmerman, L. F. Soule, M. T. Butt, V. A. Sedlak, C. B. Willingham and F. D. Rossini, *J. Research Natl. Bur. Standards*, **41**, 323 (1948).

(13) A. J. Streiff, L. F. Soule, C. M. Kennedy, M. E. Janes, V. A. Sedlak, C. B. Willingham and F. D. Rossini, *ibid.*, **45**, 173 (1950).

(14) A. J. Streiff, A. R. Hulme, P. A. Cowie, N. C. Krouskop and F. D. Rossini, *Anal. Chem.*, **27**, 411 (1955).

(15) A. J. Streiff, L. H. Schultz, A. R. Hulme, J. A. Tucker, N. C. Krouskop and F. D. Rossini, *ibid.*, **29**, 361 (1957).

(16) A. J. Streiff, L. H. Schultz, N. C. Krouskop, J. W. Moore and F. D. Rossini, *J. Chem. Eng. Data*, **5**, 193 (1960).

(17) Private communication from Dr. M. S. Newman, Ohio State University, Columbus, Ohio.

(18) D. M. Speros and F. D. Rossini, THIS JOURNAL, **64**, 1723 (1960).

TABLE IV

VALUES[a] OF THE STANDARD HEATS OF COMBUSTION OF 1-HEPTENE, 1-OCTENE AND 1-DECENE, IN THE LIQUID STATE

Compd. (liquid)	$-\Delta E_B$ at 30° ohm/g. CO_2	$-\Delta E_c^0$ at 30° kj./mole	$-\Delta H_c^0$ at 30° kcal./mole	$-\Delta H_c^0$ at 25° kcal./mole	Difference from recommended[b] values of $-\Delta H_c^0$ at 25°, kcal./mole
1-Heptene	4649.65 ± 1.16	4648.17 ± 1.16	1113.05 ± 0.28	1113.37 ± 0.28	0.18 ± 0.35
1-Octene	5303.01 ± 1.14	5301.31 ± 1.14	1269.45 ± 0.27	1269.82 ± 0.27	.37 ± .37
1-Decene	6607.17 ± 1.84	6605.06 ± 1.84	1581.60 ± 0.44	1582.12 ± 0.44	.15 ± .54

[a] The uncertainties in this table are twice the standard deviation. [b] See text. The recommended[15] values, in kcal./mole are: 1-heptene, 1113.19; 1-octene, 1269.45; 1-decene, 1581.97.

TABLE V

HEATS[a] OF ISOMERIZATION, AND THE DIFFERENCE IN THE HEATS OF HYDROGENATION, FOR BOTH THE LIQUID AND THE GASEOUS STATES, AT 25°, FOR CERTAIN HEPTENES

Compound	Ratio of the heats of combustion at 25°	Heat of isomerization for the liquid at 25° kcal./mole	ΔHv^0 (isomer) − ΔHv^0(1-heptene) at 25°, kcal./mole	Heat of isomerization for the gas at 25°, kcal./mole	Standard heat of hydrogenation, ΔHh^0, of 1-heptene less that of the isomer at 25°, kcal./mole: Liquid	Gas
1-Heptene	1.00000	0.00	0.00	0.00	0.00	0.00
3-Methyl-*cis*-3-hexene	0.99593 ± 0.00019	−4.52 ± 0.22	+ .19 ± 0.05	−4.33 ± 0.22	−3.80 ± 0.48	−3.26 ± 0.48
3-Methyl-*trans*-3-hexene	.99662 ± .00018	−3.75 ± .21	+ .04 ± .05	−3.71 ± .21	−3.03 ± .47	−2.64 ± .47
2,4-Dimethyl-1-pentene	.99571 ± .00025	−4.77 ± .40	− .61 ± .05	−5.38 ± .40	−2.23 ± .58	−1.97 ± .58
4,4-Dimethyl-1-pentene	.99709 ± .00036	−3.24 ± .40	−1.07 ± .05	−4.31 ± .40	+0.18 ± .58	+0.09 ± .58
2,4-Dimethyl-2-pentene	.99440 ± .00018	−6.23 ± .20	−0.32 ± .05	−6.55 ± .20	−3.69 ± .47	−3.14 ± .47
4,4-Dimethyl-*cis*-2-pentene	.99822 ± .00026	−1.98 ± .29	− .73 ± .05	−2.71 ± .29	+1.44 ± .52	+1.69 ± .52
4,4-Dimethyl-*trans*-2-pentene	.99469 ± .00018	−5.90 ± .20	− .67 ± .05	−6.57 ± .20	−2.48 ± .47	−2.17 ± .47
3-Methyl-2-ethyl-1-butene	.99634 ± .00029	−4.07 ± .32	− .29 ± .05	−4.36 ± .32	−1.89 ± .53	−1.63 ± .53
2,3,3-Trimethyl-1-butene	.99556 ± .00025	−4.94 ± .28	− .84 ± .05	−5.78 ± .28	−1.94 ± .52	−1.71 ± .52

[a] The uncertainties in this table are twice the standard deviation.

TABLE VI

HEATS[a] OF ISOMERIZATION, AND THE DIFFERENCE IN THE HEATS OF HYDROGENATION, FOR BOTH THE LIQUID AND THE GASEOUS STATES, AT 25°, FOR CERTAIN OCTENES

Compound	Ratio of the heats of combustion at 25°	Heat of isomerization for the liquid at 25°, kcal./mole	ΔHv^0 (isomer) − ΔHv^0 (1-octene) at 25°, kcal./mole	Heat of isomerization for the gas at 25°, kcal./mole	Standard heat of hydrogenation, ΔHh^0, of 1-octene less that of the isomer at 25°, kcal./mole: Liquid	Gas
1-Octene	1.00000	0.00	0.00	0.00	0.00	0.00
2,2-Dimethyl-*cis*-3-hexene	0.99913 ± 0.00045	−1.11 ± 0.57	− .84 ± 0.06	−1.95 ± 0.57	+1.78 ± 0.70	+1.94 ± 0.70
2,2-Dimethyl-*trans*-3-hexene	.99564 ± .00024	−5.53 ± .29	− .81 ± .06	−6.34 ± .29	−2.64 ± .55	−2.45 ± .55
2-Methyl-3-ethyl-1-pentene	.99700 ± .00014	−3.84 ± .18	− .74 ± .06	−4.58 ± .18	−3.89 ± .50	−3.94 ± .50
2,4,4-Trimethyl-1-pentene	.99551 ± .00013	−5.69 ± .16	−1.17 ± .06	−6.86 ± .16	−3.46 ± .63	−3.11 ± .63
2,4,4-Trimethyl-2-pentene	.99612 ± .00033	−4.92 ± .43	−0.76 ± .06	−5.68 ± .43	−2.69 ± .50	−1.93 ± .50

[a] The uncertainties in this table are twice the standard deviation.

of the standard heat of combustion of the given isomer to that of the 1-alkene, for the liquid state at 25°, taken the same as the corresponding ratio for the bomb process at 25°, which is not significantly different from the corresponding ratio for the bomb process at 30°, which was determined experimentally in the present investigation; the standard heat of isomerization of the 1-alkene to the given isomer, for the liquid state at 25°, calculated from the foregoing data, with the values for 1-heptene and 1-octene recommended by Loeffler and Rossini,[7] and taking the difference between ΔH and ΔE to be the same for the several isomers in each group; the standard heat of vaporization of the 1-alkene less that of the given isomer, at 25°, from the data of Camin and Rossini,[19] with the difference between this and the heat of vaporization at saturation pressure being considered not significant; the standard heat of isomerization of the 1-alkene to the given isomer, for the gaseous state at 25°, calculated from the corresponding values for the liquid state and the differences in the heats of vaporization; and the standard heat of hydrogenation of the 1-alkene less that of the given isomer, for both the liquid and gaseous states at 25°, using our standard heats of isomerization for the appropriate paraffin hydrocarbons.

Table VII gives similar information for 1-decene and its two isomers for the liquid state only, as no data are available for the heats of vaporization of the two isomers.

From the values in Tables V, VI, and VII, one can easily calculate the values of the heats of formation of the corresponding substances using the following recommended values of the standard heats of formation at 25°, in kcal./mole[3,7]: 1-heptene (liq), −23.41; 1-heptene (g), −14.89; 1-octene (liq), −29.52; 1-octene (g), −19.82; 1-decene (liq), −41.73.

V. Data of Other Investigations

No data appear to be reported in the literature on the heats of combustion of the compounds measured in the present investigation. However, data on heats of hydrogenation in the gaseous state near 82° have been reported by Doliver, Gresham, Kistiakowsky and Vaughan[18] for the following compounds also measured in the present investigation:

(19) D. L. Camin and F. D. Rossini, *J. Chem. Eng. Data*, **5**, 368 (1960).

TABLE VII

HEATS[a] OF ISOMERIZATION, AND THE DIFFERENCE IN THE HEATS OF HYDROGENATION, FOR THE LIQUID STATE, AT 25°, FOR CERTAIN DECENES

Compound	Ratio of the heats of combustion at 25°	Heat of isomerization for the liquid at 25°, kcal./mole	Standard heat of hydrogenation, ΔHh^0 of 1-decene less that of the isomer, for the liquid at 25°, kcal./mole
1-Decene	1.00000	0.00	0.00
2,2,5,5-Tetramethyl-*cis*-3-hexene	1.00155 ± 0.00026	+2.45 ± 0.41	+9.04 ± 0.76
2,2,5,5-Tetramethyl-*trans*-3-hexene	0.99489 ± 0.00037	−8.06 ± 0.59	−1.47 ± 0.86

[a] The uncertainties in this table are twice the standard deviation.

TABLE VIII

SUMMARY OF THE RESULTS OF TURNER, NETTLETON AND PERELMAN[20] (TNP) AND COMPARISON WITH CORRESPONDING RESULTS FROM THIS LABORATORY[a]

	Compounds	I TNP Heat of hydrogenation in the liquid state in acetic acid soln. at 25°, kcal./mole	II This laboratory Standard heat of hydrogenation of the pure liquid at 25°, kcal./mole	I − II Difference between the heat of hydrogenation in acetic acid soln. and in the pure liquid hydrocarbon at 25°, kcal./mole
A	2,4-Dimethyl-1-pentene	−26.67	−27.99	+1.32
B	2,4-Dimethyl-2-pentene	−25.15	−26.53	+1.38
A − B		(− 1.52)[b]	(− 1.46)[b]	(−0.06 ± 0.65)[c]
A	2,4,4-Trimethyl-1-pentene	−25.52	−26.76	1.24
B	2,4,4-Trimethyl-2-pentene	−26.79	−27.53	0.74
A − B		(1.27)[b]	(0.77)[b]	(0.50 ± 0.65)[c]
A	4-Methyl-*cis*-2-pentene	−27.32	−28.02	0.70
B	4-Methyl-*trans*-2-pentene	−26.38	−26.94	0.56
A − B		(− 0.94)[b]	(− 1.08)[b]	(0.14 ± 0.38)[c]
A	4,4-Dimethyl-*cis*-2-pentene	−30.80	−31.66	0.86
B	4,4-Dimethyl-*trans*-2-pentene	−26.51	−27.74	1.23
A − B		(− 4.29)[b]	(− 3.92)[b]	(−0.37 ± 0.59)[c]
A	2,2,5,5-Tetramethyl-*cis*-3-hexene	−36.24	−39.26	3.02
B	2,2,5,5-Tetramethyl-*trans*-3-hexene	−26.87	−28.75	1.88
A − B		(− 9.37)[b]	(−10.51)[b]	(1.14 ± 0.98)[c]

[a] All the foregoing compounds are reported in this investigation except the *cis* and *trans* isomers of 4-methyl-2-pentene, which were reported by Bartolo and Rossini.[5] [b] Heats of isomerization for the given pair of isomers. [c] Measure of the accord of the values of the heats of isomerization from the two sources.

4,4-dimethyl-1-pentene, 2,4,4-trimethyl-1-pentene and 2,4,4-trimethyl-2-pentene. Also, data on heats of hydrogenation in the liquid phase in solution in acetic acid were reported by Turner, Nettleton and Perelman[9] on the following compounds: 2,4-dimethyl-1-pentene, 2,4-dimethyl-2-pentene, 2,4,4-trimethyl-1-pentene, 2,4,4-trimethyl-2-pentene, 4-methyl-*cis*-2-pentene, 4-methyl-*trans*-2-pentene, 4,4-dimethyl-*cis*-2-pentene, 4,4-dimethyl-*trans*-2-pentene, 2,2,5,5-tetramethyl-*cis*-3-hexene and 2,2,-5,5-tetramethyl-*trans*-3-hexene. The *cis* and *trans* isomers of 4-methyl-2-pentene are included here because they were also measured in our laboratory.[5]

From the data of the present investigation, and the recommended values for the standard heats of formation of the 1-alkenes[3,15] and the corresponding paraffin hydrocarbons[3] which are the products of hydrogenation, one obtains values for the standard heat of hydrogenation for the gaseous state at 25° for the following three monoölefins in kcal./mole: 4,4-dimethyl-1-pentene, −30.09 ± 0.58; 2,4,4-trimethyl-1-pentene, −26.89 ± 0.63; 2,4,4-trimethyl-2-pentene, −28.07 ± 0.50. Conversion to 25° of the experimental data of Dolliver, Gresham, Kistiakowsky and Vaughan[18] on the heat of hydrogenation of these same three monoölefins yields the following values, respectively, in kcal./mole: −29.31 ± 0.20; −27.02 ± 0.20; −28.17 ± 0.20. It is seen that, within the respective limits of uncertainty, the values are in substantial accord.

Table VIII summarizes the results obtained by Turner, Nettleton and Perelman[20] and gives a comparison with corresponding results from this Laboratory, calculated from the recommended heats of formation for the 1-alkenes and the paraffins formed as products in the hydrogenation, together with the measured heats of isomerization of the given olefins. The values in the tables are fully identified. The following points may be noted: (a) The values of the heat of hydrogenation in the liquid state at 25° for the material in solution in acetic acid and for the pure hydrocarbon, excluding the decenes, differ by about 1.0 kcal./mole, on the average, which difference may possibly be accounted for by a difference of this amount in the heat of solution of the olefin and the corresponding paraffin in acetic acid; (b) For the indicated pairs of compounds, the values of the heats of isomerization, marked in parentheses with a footnote "*b*," from the two sets of data are in substantial accord, except for the two decenes, where the difference is somewhat beyond the limits of the

(20) F. D. Rossini, Chapter on "Chemical Thermodynamics of Hydrocarbons" in "The Chemical Background for Engine Research," R. E. Burk and O. Grummit, Editors, Interscience Publishers, New York, N. Y., 1943.

respective uncertainties. In Table VIII, the values marked in parentheses with a footnote "*c*" indicate the measure of accord of the values of heats of isomerization.

VI. Discussion

The data presented in this investigation, and earlier by Turner, Nettleton and Perelman,[9] for the difference in the energy content of the *cis* and *trans* isomers of 2,2,5,5-tetramethyl-3-hexene (symmetrical di-*t*-butylethylene) show how extremely large can be the effect of steric hindrance or molecular constraint in some molecules having bulky radicals adjacent to one another in space. In this case, the *trans* isomer is nearly free of molecular constraint whereas the *cis* isomer has an energy content near 10 kcal./mole greater than that of the *trans* isomer. The *cis* isomer can be put together by nature through synthesis, but the model of the molecule cannot be made intact with the ordinary rigid, solid atomic models scaled to size.

About 20 years ago, one of us (FDR) summarized the status then of our knowledge of the relation of energy content and molecular structure for the aliphatic monoölefin hydrocarbons, somewhat as follows: In the case of the isomers of the aliphatic monoölefins, it appears that, with regard to energy content, increase in the stability of the molecule (toward lower energy content) is produced by (a) having the double bond at the middle of the longest chain of carbon atoms, (b) having the maximum number of alkyl groups attached to each of the doubly bonded carbon atoms, and (c) further increasing the compactness of the molecule by branching on the side chains, up to the point where close proximity in space of hydrogen atoms on different carbon atoms begins to produce steric hindrance or constraint in the molecule and a consequent increase in the energy content. All of the data subsequently reported on the C_6, C_7, C_8 and C_{10} monoölefins are in substantial accord with the foregoing statement.

Careful analysis of the data now available for nearly 50 aliphatic monoölefin hydrocarbons indicates that the value of the heat of hydrogenation of any such given olefin may be estimated within 0.5 kcal./mole by a simple set of rules, which take into account quantitatively the structural factors mentioned above. Since values of the heat of formation are now available for substantially all the paraffin hydrocarbons,[3,21] it thus becomes possible to make a reasonably reliable estimate of the heat of formation of any given aliphatic monoölefin hydrocarbon. The simple rules, pertaining to the heat of hydrogenation, ΔHh^0, at 25°, for the gaseous state, according to the reaction

$$C_nH_{2n}(g) + H_2(g) = C_nH_{2n+2}(g)$$

are as follows.

Extending the correlation presented in the preceding report on the hexenes,[5] one may distinguish seven simple types of olefin hydrocarbons

I, 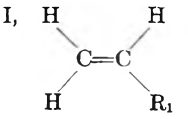

where R_1 is a normal alkyl radical or any alkyl radical with no branching on the carbon atoms once or twice removed from the doubly bonded carbon atom, $\Delta Hh^0 = -30.0$ kcal./mole;

II, 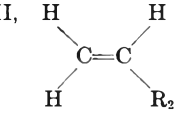

where R_2 is an alkyl radical with branching on one or both of the carbon atoms once or twice removed from the doubly bonded carbon atom, $\Delta Hh^0 = -29.4$ kcal./mole;

III, 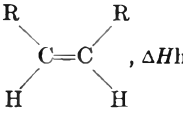 , $\Delta Hh^0 = -28.0$ kcal./mole;

IV, 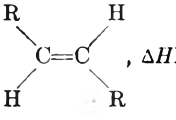 , $\Delta Hh^0 = -27.0$ kcal./mole;

V, 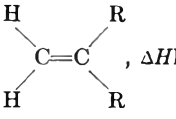 , $\Delta Hh^0 = -27.3$ kcal./mole;

VI, 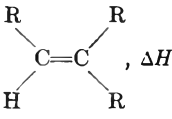 , $\Delta Hh^0 = -26.4$ kcal./mole;

VII, 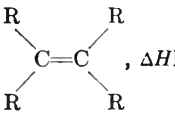 , $\Delta Hh^0 = -25.8$ kcal./mole.

In the foregoing types III, IV, V, VI and VII, R represents any alkyl radical. To the foregoing values of ΔHh^0, selected appropriately according to the structure of the monoölefin, the following structural quantities are to be added algebraically: (a) for each neopentyl group, or equivalent longer group, attached to the doubly bonded carbon atoms, −0.4 kcal./mole; (b) for each *t*-butyl group, or equivalent longer group, attached to the doubly bonded carbon atoms, −0.6 kcal./mole; (c) for a "*cis*" combination of two *t*-butyl groups, −10.0 kcal./mole (in addition to the structural quantity for each *t*-butyl group itself); (d) for a "*cis*" combination of one *t*-butyl group with an effectively smaller alkyl group, of lesser steric hindrance, −3.2 kcal./mole (in addition to the structural quantity for the *t*-butyl group itself).

With the foregoing simple rules, one can reproduce the values of the heats of hydrogenation of the approximately 40 C_6 to C_{10} monoölefin hydrocarbons measured in this Laboratory with an average deviation of ±0.40 kcal./mole, the maximum deviation being 1.2 kcal./mole. It appears then that the above simple rules may be used to calculate reliable values of the heat of hydrogenation of any monoölefin hydrocarbon, with an average uncer-

(21) J. B. Greenshields and F. D. Rossini, THIS JOURNAL, **62**, 271 (1958).

tainty of ±0.5 kcal./mole. With the values for the corresponding paraffin hydrocarbons known or calculable, one can evaluate the heat of formation of any given aliphatic monoölefin hydrocarbon.

THE DIELECTRIC PROPERTIES OF TETRA-*n*-BUTYLAMMONIUM PICRATE, BROMIDE AND TETRAPHENYLBORIDE IN SOME POLAR SOLVENTS AT 25°[1]

BY W. R. GILKERSON AND K. K. SRIVASTAVA

Department of Chemistry, University of South Carolina, Columbia, S. C.

Received July 18, 1960

The dielectric constants of solutions of tetra-*n*-butylammonium picrate in *o*-dichlorobenzene–benzene solvent mixtures (0, 25 and 50 mole %), chlorobenzene and in bromobenzene, of tetra-*n*-butylammonium bromide in chlorobenzene and bromobenzene, and of tetra-*n*-butylammonium tetraphenylboride in chlorobenzene have been determined at 1 Mc. at 25°. Dipole moments for the ion pairs were calculated using Onsager's equation. The observed moment for the picrate showed no increase with increasing solvent polarity. The moments were corrected for shape effect, but still gave distances between charges some 2.5 to 3 Å. less than distances of closest approach determined from conductance measurements. The results have been interpreted in terms of polarization of the ions to yield smaller moments.

The dipole moments of a number of ion pairs have been determined in benzene[2] and recently[3] measurements have been reported on the salts tetra-*n*-butylammonium picrate and bromide in benzene solutions containing small added amounts of nitrobenzene and methanol. In none of these cases have the charge–charge distances calculated from the dipole moments shown any agreement with those determined from the variation in ion pair dissociation constants with dielectric constant of solvent.[4-6] The distances calculated from the dipole moments are from 2 to 3 Å. less than the distances obtained from conductance measurements. Since the conductance measurements are made principally in solvents having a high proportion of polar molecules, the suspicion arises[3,7] that the discrepancy may be due to polar molecules separating the ions in the ion pair in the latter case, while in benzene no such separation takes place. We thought that if the dielectric constants of solutions of several salts could be determined in more polar solvents, an increasing apparent moment of the ion pairs would show this effect.

Tetra-*n*-butylammonium picrate was studied in 0, 25 and 50 mole % *o*-dichlorobenzene (abbreviated DCB hereafter)–benzene solvent mixtures since conductance measurements in this system have been made in this Laboratory.[4] Chlorobenzene and bromobenzene were used as solvents to be certain that the results were not affected by the foregoing mixed solvent system. The bromide had shown evidence of quadruple ion formation in benzene[3] necessitating an extrapolation procedure, so it was examined in chlorobenzene and bromobenzene where such effects should be negligible. The tetraphenylboride salt was studied in chlorobenzene since it has been assumed by Fuoss[8] and co-workers to have ions of almost the same radius and equivalent ionic conductivity.

The experimental method chosen was to measure the capacity of salt solutions (10^{-4} to 10^{-3} *M*) in a dielectric cell at 1 Mc. using a Twin-T impedance bridge modified for conducting solutions.

Experimental

Solvents.—Thiophene-free benzene was passed through a 35 × 2 cm. column packed with Alcoa activated alumina, grade F-20, then recrystallized and distilled from sodium ribbon, a middle cut being taken; b.p. 80.5°. *o*-Dichlorobenzene was passed through a similar alumina column and distilled under reduced pressure, a middle cut being taken. Chlorobenzene (courtesy of Dow Chemical Co.) was passed through alumina and distilled at normal pressure, a middle cut being taken; b.p. 131.0°. Bromobenzene was passed through alumina and distilled, a middle cut being taken; b.p. 156.0°. The physical properties of the pure solvents and the mixtures used are shown in Table I. Values for which other sources are not listed were determined in this Laboratory. All solutions were made up by weight.

Salts.—Tetra-*n*-butylammonium picrate was prepared as previously.[4] Tetra-*n*-butylammonium bromide was prepared from the iodide in ethanol by metathesis with silver bromide. The resulting solution was evaporated to dryness with suction on a water-bath. The residue was recrystallized four times by adding heptane to a benzene solution. The salt was then placed on a vacuum line and heated to 90° for ten hours; m.p. 117.0–118.0°. Tetra-*n*-butylammonium tetraphenylboride was prepared from the sodium salt according to the method of Accascina[9]; m.p. 235.5–236.5°.

TABLE I

DENSITY AND DIELECTRIC CONSTANTS OF SOLVENTS AT 25°

No.	Solvent	Density, g./ml.	Dielectric constant
1	C_6H_6	0.8737[a]	2.275[b]
2	25 mole % DCB–C_6H_6	0.998[c]	4.167
3	50 mole % DCB–C_6H_6	1.111[b]	5.995
4	C_6H_5Cl	1.101[a]	5.621[d]
5	C_6H_5Br	1.490	5.374

[a] J. Timmermans, "Physico-chemical Constants of Pure Organic Compounds," Elsevier, New York, N.Y. 1950. [b] J. Wyman, *Phys. Rev.*, 35, 623 (1930). [c] Ref. 4. [d] A. A. Maryott, National Bureau of Standards, Circular No. 514.

(1) This work has been supported in part by contract with the Office of Ordnance Research, United States Army.

(2) J. A. Geddes and C. A. Kraus, *Trans. Faraday Soc.*, **32**, 585 (1936).

(3) E. A. Richardson and K. H. Stern, *J. Am. Chem. Soc.*, **82**, 1296 (1960).

(4) W. R. Gilkerson and R. E. Stamm, *ibid.*, **82**, 5295 (1960).

(5) H. Sadek and R. M. Fuoss, *ibid.*, **81**, 4511 (1959).

(6) E. Hirsch and R. M. Fuoss, *ibid.*, **82**, 1018 (1960).

(7) H. Sadek and R. M. Fuoss, *ibid.*, **76**, 5905 (1954).

(8) R. M. Fuoss and E. Hirsch, *ibid.*, **82**, 1013 (1960).

Cells.—Two cells were used. Cell I was a nickel concentric cylinder type purchased from Balsbaugh Laboratories. It had an air capacity of 104.70 pf. and a lead capacity of 15.16 pf., determined at 1 Mc. using benzene and chlorobenzene as calibrating liquids. Cell II was a gold-plated cell described previously[4] having an air capacity of 24.64 pf. and a lead capacity of 31.03 pf. Both cells were equipped with guard electrodes, which were connected to the outer ground electrodes for the experiments to be described. The cells were thermostated in a water-bath at 25°.

Bridge.—The measurements were carried out using a General Radio Type 821-A Twin-T impedance measuring circuit. The oscillator was a General Radio Type 1330-A, and the detector was a Hallicrafters model S-53 communications receiver equipped with a shielded connector for the output lead from the bridge. The Twin-T provides both a capacitance and a conductance balance, by means of two capacitors. The conductances of most of the solutions were outside the direct reading range of the bridge. However, there was enough capacitance available in the "initial conductance balance" capacitors to achieve a balance for most of the solutions. Since these latter capacitors were not calibrated, the conductance of the solutions could not be read off. In the case of the tetraphenylboride salt in chlorobenzene, the conductances of the solutions were so great that an external capacitor was connected in parallel with the "conductance balance" capacitors by means of a 22 cm. length of 50 ohm impedance coaxial line terminated in a General Radio Type 722-M air capacitor. A recalculation of the condition for balancing the circuit shows that the insertion of the external capacitor at the point chosen affects only the conductance balance and not the capacitance balance, provided that the coaxial lead has a high enough leakage resistance.

The observed values of the capacity of the solutions in the cells had to be corrected for lead and cell inductance. The observed capacity C_a is related to the actual capacitance C_x by the equation

$$C_a = C_x/(1 - W^2LC_x)$$

where W is 2π times the frequency of the oscillator signal and L is the inductance of cell plus lead. The correction was determined for both cells by measuring the capacity of the cell filled with (benzene I) and *o*-dichlorobenzene (II) at 5 and 10 Mc. The dielectric constant of the latter solvent was taken to be 10.056.[10]

Results

The dielectric increments $\Delta\epsilon$ (defined as the dielectric constant of the solution minus that of the solvent) of the solutions are given in Table II as a function of C_1, the molarity of the salt. Reproducibility was $\pm 2\%$ of $\Delta\epsilon$ upon refilling a cell with solution. A plot of $\Delta\epsilon$ *versus* C_1 was made in each case, resulting in straight lines. The dipole moments were calculated from the slopes, $d\epsilon/dC_1$, of these plots by applying Onsager's equation[11] in a manner similar to that of Gaumann[12] and recently Gilkerson and Srivastava[13] in the form of equation 1

$$\mu_1^2 = F(\mathrm{d}\epsilon/\mathrm{d}C_1)A_1 + [A_2\mu_2^2C_2^0V_1 + A_3\mu_3^2C_3^0V_1 + B_2C_2^0V_1 + B_3C_3^0V_1 - B_1]/A_1 \quad (1)$$

where

$$F = 1 - \sum_i \{4\pi N\mu_i^2(\epsilon_{\infty i} + 2)^2[2\epsilon(2\epsilon_{\infty i} - 1) + \epsilon_{\infty i}]/9000kT(2\epsilon + \epsilon_{\infty i})^3 + B_i\epsilon_{\infty i}/\epsilon(2\epsilon + \epsilon_{\infty i})\}C_i^0$$

$$A_1 = 4\pi N(\epsilon_{\infty i} + 2)^2\epsilon(2\epsilon + 1)/9000kT(2\epsilon + \epsilon_{\infty i})^2, \text{ and}$$

$$B_1 = 3V_i\epsilon(\epsilon_{\infty i} - 1)/(2\epsilon + \epsilon_{\infty i})$$

Table II

DIELECTRIC INCREMENTS AND DIPOLE MOMENTS OF Bu_4NPi, Bu_4NBr AND $Bu_4NB(C_6H_5)_4$ IN SEVERAL SOLVENTS AT 25°

Bu_4NPi					
1[a]		2		3	
10^4C_1	$10^2\Delta\epsilon$	10^4C_1	$10^2\Delta\epsilon$	10^4C_1	$10^2\Delta\epsilon$
10.42	3.59	11.13	4.37	10.46	6.29
7.98	2.76	7.87	2.94	7.45	4.26
4.62	1.66	2.52	0.94	4.81	2.64
				2.86	1.34
μ	15.7		13.8		16.8
d, Å.	3.44		3.05		3.82
4		5			
9.75	4.16	10.42	5.06		
6.42	2.98	6.11	2.88		
3.20	1.55	3.52	1.74		
μ	14.4		14.3		
d, Å.	3.24		3.24		

Bu_4NBr				$Bu_4NB(C_6H_5)_4$	
4		5		4	
16.45	4.64	18.48	6.60	7.05	5.21
10.24	3.32	13.80	4.82	4.52	3.22
6.29	1.76	8.79	2.83	3.07	2.27
3.82	1.09	5.24	2.19		
μ	13.5		11.9		17.3
d, Å.	3.04		2.68		3.90

[a] Solvent number corresponding to that appearing in the first column of Table I.

Subscript 1 refers to solute, while 2 and 3 refer to solvent components. V_i is the molar volume of pure i, C_i^0 is the molar concentration of component i in the pure solvent and $\epsilon_{\infty i}$ is the infinite frequency dielectric constant of pure i. Only the first term on the right in eq. 1 is of importance (within 0.5%) for the highly polar solutes we are dealing with. Also the summation in F need be taken only over the species in pure solvent, and the value of ϵ used to calculate F is that of the pure solvent. The values of $\epsilon_{\infty i}$ for the ion pairs were calculated from the estimated values of the molar refraction. For the picrate, $\epsilon_{\infty i}$, was taken as 3.06.[3] For the bromide, the density of pure salt was calculated from solution data of Stern and Richardson[3] to be 1.2 g./ml. The value of ϵ_∞ calculated for this salt was 2.44. The density of the tetraphenylboride was estimated to be between 1.2 and 1.5 g./ml. This results in an uncertainty of ± 1 debye unit in the calculated moment. But even though the absolute magnitude of the uncertainty is large, it is well within the limit of 10% assigned by Smyth[14] to moments determined from solution data. The values of the moments so calculated, in debyes, are given in Table II at the bottom of each set of data for a given solvent. These moments are uncorrected for shape effect. An examination of Scholte's[15] treatment of the dipole moments of ellipsoidal molecules, based on Onsager's equation[11] shows that

$$(\mu_0/\mu)^2 = 3[\epsilon + A(1 - \epsilon)]/(2\epsilon + 1)$$

where μ_0 is the gas phase moment, corrected for shape, μ is the observed solution moment, and A is a constant determined by the eccentricity of the ellipsoid. For ion pairs we may take the ratio of

(9) F. Accascina, S. Petrucci and R. M. Fuoss, *ibid.*, **81**, 1301 (1959).

(10) P. H. Flaherty and K. H. Stern, *ibid.*, **80**, 1034 (1958).

(11) L. Onsager, *ibid.*, **58**, 1486 (1936).

(12) T. Gaumann, *Helv. Chim. Acta*, **41**, 1956 (1958).

(13) W. R. Gilkerson and K. K. Srivastava, THIS JOURNAL, **64**, 1485 (1960).

(14) C. P. Smyth, "Dielectric Behavior and Structure," McGraw-Hill Book Co., New York, N. Y., 1955, p. 225.

(15) T. G. Scholte, *Rec. trav. chim.*, **70**, 50 (1951).

the long axis (the dipole axis) to the short axis to be 2.0. Then A is 0.174. In benzene, we calculate μ_0/μ to be 1.05 and in solvent 3 to be 1.09. The values of d, the distance between charges in the dipole, shown in Table II have been calculated from μ_0 values.

Discussion

The average value of d for tetra-*n*-butylammonium picrate for all the solvents used is 3.36 ± 0.22 Å. There seems to be no significant trend as the dipole is immersed in more polar solvents. These results show no evidence of an observable concentration of ion pairs separated by one or more solvent molecules. The dielectric increments for the picrate in benzene are in good agreement with those observed by Stern and Richardson. The dipole moments calculated by us differ from those of the latter workers since we used Onsager's equation while they used extrapolation based on Debye's equation. We feel that any discussion should be confined to values calculated using the former equation.

For the picrate, Fuoss[6] reports a distance of closest approach, A, in nitrobenzene–carbon tetrachloride solvent mixtures of 5.91 Å., obtained from a log K *versus* $1/\epsilon$ plot, when K is the dissociation constant for the ion pair determined from conductance measurements. An A value of 6.64 Å. has been found[4] for this salt in DCB–benzene solvent mixtures. The first is 2.57 Å. larger than d, while the latter is 3.30 Å. larger. For the bromide, A is 5.36 Å. in nitrobenzene–carbon tetrachloride,[5] being 2.51 Å. larger than d. The tetraphenylboride salt has an observed A of 7.00 Å. in nitrobenzene-carbon tetrachloride,[8] which is 3.07 Å. larger than the d value.

The low values of d, calculated from the dipole moments, compared to the conductance A values require some explanation. The electrical free energy of formation of an ion pair,[16] $-e^2/\epsilon A$, is certainly only a first approximation to that which actually obtains. The only interaction considered is of the charge–charge type. Further, the dielectric constant is assumed to be the macroscopic value. This last cannot be the case when the two ions approach within one solvent molecular diameter. Qualitatively, both these effects would operate in such a direction that A calculated from the simple $-e^2/\epsilon A$ relation would be a minimum value. This would certainly not increase the agreement between A and d. The dipole moments of alkali halide molecules in the gas phase[17,18] are 20 to 50% less than what one would predict from the product of unit charge and the sum of the crystal radii. Rittner,[19] using the model of two ions of polarizability α_1 and α_2, at a distance r (the sum of the crystal radii), derived the relation for the dipole moment

$$\mu = er - [r^4e(\alpha_1 + \alpha_2) + 4re\alpha_1\alpha_2]/(r^6 - 4\alpha_1\alpha_2) \quad (3)$$

Using equation 2, the calculated moments were within 6% of the observed values. It is possible that the polarizabilities of the ions in the ion pairs would lead to lower moments than one would expect.[20] The principal difficulty in applying equation 2 to the present systems is that of determining the values of α_1 and α_2 to be used. We have already estimated values of the molar refractions for the salts in calculating the dipole moments given in Table II. Until more data is available, we have used the following procedure to obtain the ion polarizabilities. In the case of the tetrabutylammonium ion, the atom refractions were summed and then the result was divided by two,[21] giving 40 cc. for the ion refraction. For the anions, the atom refractions were summed and multiplied by two. The results were 88 cc. for the picrate refraction, 206 cc. for the tetraphenylboride and 12 cc. for the bromide. It is admitted that in the case of the large complex ions this procedure is open to much criticism. It is hoped that such an approach can be eliminated in the future by using experimentally determined values for the refractions. From the foregoing refractions, the ion polarizabilities, α, were calculated using the relation $R = 4\pi N_a\alpha/3$, where R is the ion refraction. We used the observed moments and these values of α to calculate values of r from equation 2. This distance, r, may be interpreted as the separation of charges before polarization takes place. Or if one considered spherical ions, it would be the internuclear distance. For the picrate ion pair, we find r = 5.50 Å.; for the bromide, r = 4.25 Å.; for the tetraphenylboride, r = 6.70 Å. In all cases, these are somewhat less (9–14%) than the hydrodynamic radii of 5.91 Å.,[6] 4.89 Å.,[5] and 7.26 Å.,[8] respectively, found by Fuoss and co-workers. The r values so calculated are also in much better agreement with A values from ion pair dissociation constant data. However, if the dipole moments must be corrected for polarization, then certainly one should correct the ion pair energy of interaction for the same effect. This would lead one down a labyrinth of corrections which at present cannot be made. It probably remains for A values determined from log K *versus* $1/\epsilon$ plots to be the depository of our ignorance of ion–solvent interactions.

(16) J. T. Denison and J. B. Ramsey, *J. Am. Chem. Soc.*, **77**, 2615 (1955).

(17) W. H. Rodebush, L. A. Murray and M. E. Bixler, *J. Chem. Phys.*, **4**, 372 (1936).

(18) J. W. Trischka, *ibid.*, **20**, 1811 (1952).

(19) E. S. Rittner, *ibid.*, **19**, 1030 (1951).

(20) This suggestion was made to us by Dr. William Bennett in a private conversation.

(21) See ref. 14, p. 407. The cation refractions in Smyth's Table 2.1 are approximately one-half those of the isoelectronic noble gas atoms, while the anion refractions are almost double those of the corresponding noble gas atoms.

HEATS OF MIXING OF NON-ELECTROLYTE SOLUTIONS. II. PERFLUORO-*n*-HEPTANE + ISOOCTANE AND PERFLUORO-*n*-HEXANE + *n*-HEXANE[1,2]

BY A. G. WILLIAMSON[3] AND R. L. SCOTT

Department of Chemistry, University of California, Los Angeles, California

Received June 20, 1960

Heats of mixing have been measured for the systems perfluoro-*n*-heptane + isoöctane (2,2,4-trimethylpentane) at 30 and 50° and for the system perfluoro-*n*-hexane + *n*-hexane at 25 and 35°. The results are correlated with the excess Gibbs' free energies of mixing measured by other workers.

Introduction

Almost the only directly measured heats of mixing for fluorocarbon + hydrocarbon systems are three experiments by Mueller and Lewis[4] and two very recent measurements by Dyke, Rowlinson and Thacker.[5] Most of the values quoted in the literature for heats of mixing and for entropies of mixing of these systems are derived from the temperature variation of the Gibbs' free energies of mixing, a notoriously inaccurate method. Since the measured heats of mixing of the system perfluoro-*n*-heptane + isoöctane are not in agreement with the values obtained from the free energy of mixing[6,7] we have begun our study with this system.

Experimental

Apparatus.—The design and testing of the calorimeter and auxiliary apparatus are described in a previous paper.[8]

Materials.—A sample of perfluoro-*n*-heptane purified in this department by Dr. A. P. Watson was used. This had a refractive index ($n^{25}D$ 1.2588) slightly higher than the values previously reported[6] for highly purified perfluoro-*n*-heptane ($n^{25}D$ 1.2582). However, only one peak was obtained from a gas chromatographic analysis at 26° using a 2.5 m. column with $C_{21}F_{44}$ as the stationary phase. The column had been shown to resolve readily mixtures of fully and partially fluorinated compounds. The sample of C_7F_{16} may contain small quantities of branched chain perfluoroheptanes which cannot be resolved by our present gas chromatographic equipment. This should not seriously affect the values of the heats of mixing.

Eastman "spectro"-grade isoöctane (2,2,4-trimethylpentane) was used from a freshly opened bottle.

The perfluoro-*n*-hexane and *n*-hexane were supplied by Professor R. D. Dunlap. Their purification and properties are described elsewhere.[9,10]

Results

The experimental results are shown in Tables I and II. It can be seen from the data that for both systems the variation of the heat of mixing with temperature is very small. The values in Table II with *a* superscript are lower in comparison with the rest; this is probably due to a small amount of phase separation induced by the instantaneous cooling of the mixture at the moment of mixing. The heat of mixing is sufficient to cool the mixture from 25° to below the critical solution temperature (22.65°, $x_{C_6H_{14}} = 0.63$).[9] Unfortunately the stirring in the calorimeter was not sufficiently vigorous to cause rapid mixing of the two layers once they were formed so that it became very difficult to obtain good measurements in this region.

TABLE I

HEATS OF MIXING OF n-C_7H_{16} + i-C_8H_{18}

	$x_{i\text{-}C_8H_{18}}$	$\Delta\bar{H}$/cal. Exper.	Calcd.[a]	Calcd.[b]
T = 30°	0.1515	281	278	279
	.2483	393	397	396
	.3393	466	467	466
	.4327	507	500	502
	.5113	501	504	508
	.5356	498	501	506
	.5865	493	491	496
	.7458	412	412	415
	.8066	357	357	358
T = 50°	0.2447	391	392	393
	.3529	476	475	473
	.5065	512	514	508
	.6235	492	491	484
	.7360	425	425	422

Four coefficients were used in equation 1; h_0, h_1, h_2, h_3: [a] 9 obsn. at 30°, 5 obsn. at 50°. [b] 14 obsn. assumed indep. of temperature.

The experimental results have been represented by equations of the type

$$\Delta\bar{H} = x(1 - x)[h_0 + h_1(1 - 2x) + h_2(1 - 2x)^2 + \ldots] \quad (1)$$

where x is the mole fraction of the hydrocarbon (second component). All the equations were obtained by the method of least squares on the Western Data Processing Center IBM 709 computer using a program devised by Mr. D. B. Myers of this department. The number of constants used (four) is the smallest number for which the deviations between the experimental results and those given by the equation are of about the same magnitude as the estimated experimental uncertainties. The constants for equation 1 are shown in Table III along with values of σ_{h_n} and values of $\sigma_{\Delta H}$ given by the relation

$$\sigma_{\Delta H} = \sqrt{\frac{\Sigma(d_i)^2}{m - n}} \quad (2)$$

(1) This work is supported by the U. S. Atomic Energy Commission under Project 13 of Contract AT(11-1)-34 with the University of California.

(2) Presented at the 135th National Meeting of the American Chemical Society, Boston, Mass., April 9, 1959.

(3) Department of Chemistry, University of Otago, Dunedin, New Zealand.

(4) C. R. Mueller and J. E. Lewis, *J. Chem. Phys.*, **25**, 1166 (1956).

(5) D. E. L. Dyke, J. S. Rowlinson and R. Thacker, *Trans. Faraday Soc.*, **55**, 903 (1959).

(6) C. R. Mueller and J. E. Lewis, *J. Chem. Phys.*, **26**, 278 (1957).

(7) A. G. Williamson, R. L. Scott and R. D. Dunlap, *ibid.*, **30**, 325 (1959).

(8) A. G. Williamson and R. L. Scott, THIS JOURNAL, **64**, 440 (1960).

(9) R. D. Dunlap, C. J. Murphy and R. G. Bedford, *J. Am. Chem. Soc.*, **80**, 83 (1958).

(10) R. G. Bedford and R. D. Dunlap, *ibid.*, **80**, 282 (1958).

TABLE II

HEATS OF MIXING OF n-C_6F_{14} + n-C_6H_{14}

		ΔH/cal.			
	$x_{C_6H_{14}}$	Exper.	Calcd.[b]	Calcd.[c]	Calcd.[d]
T = 25°	0.2897	436	437	441	439
	.4867	519	517	513	516
	.5975[a]	483	489	492	..
	.6680(28°)[a]	462	455	463	..
	.6729[a]	453	452	460	..
	.7129[a]	426	429	437	..
	.7955	367	368	372	377
T = 35°	0.1518	280	282	278	281
	.2149	370	366	365	365
	.2841	430	434	437	434
	.3753	496	490	493	491
	.4856	516	515	513	516
	.5359	508	514	508	514
	.6227	494	494	483	493
	.7538	424	419	408	416
	.8479	317	318	314	315
	.8976	239	241	240	237

[a] Suspected phase separation. Four coefficients used in equation 1; h_0, h_1, h_2, h_3. [b] 7 obsn. at 25°, 10 obsn. at 35°. [c] 17 obsn., assumed indep. of temperature. [d] 13 obsn. (omitting four data where phase separation suspected), assumed indep. of temperature.

where the d_i's are the individual deviations and m and n are the number of experimental measurements and the number of terms in the equation, respectively. Also shown in Table III are the values of $\sigma_{\Delta H}$ for the equation using one less term and one more than the number listed. The apparently very small temperature coefficient of ΔH suggests that we might reasonably regard ΔH as independent of temperature. The third set of constants for each system in Table III was obtained by combining the results for the two temperatures into a single curve. Tables I and II show the values of $\Delta\tilde{H}$ calculated from the individual equations and from the equations for the combined results. The column labelled calcd. (a) was obtained from the equation for the particular temperature and that labelled calcd. (b) was obtained from the equation for the combined results for the two temperatures.

Discussion

Correlation of Heats and Gibbs Free Energies of Mixing.—The simplest test of consistency between the free energy and heat of mixing over a range of temperatures is to compare the measured heat of mixing with the value derived from the temperature coefficient of the free energy of mixing. This widely used approach is, however, not a very good one; an uncertainty of 2 cal. mole^{-1} in the values of $\tilde{G}^E$ over a 20° range would lead to an uncertainty of about 40 cal. mole^{-1} in the estimate of $\Delta\tilde{H}$.

A better method of correlating $\tilde{G}^E$ and $\Delta\tilde{H}$ is *via* the relation

$$\frac{d\tilde{G}^E/T}{dT} = -\frac{\Delta\tilde{H}}{T^2} \qquad (3)$$

which on integration gives

$$\tilde{G}^{E\prime}/T' = \tilde{G}^E/T - \int_T^{T'} \frac{\Delta\tilde{H}}{T^2}\,dT \qquad (4)$$

Thus, if the values of $\Delta\tilde{H}$ are first fitted by an analytical expression such as equation 1 we may use this expression and the values of $\tilde{G}^E/T$ at any temperature T to calculate a set of values of $\tilde{G}^{E\prime}/T'$ at some arbitrary reference temperature T'. If the expression used to represent the values of $\Delta\tilde{H}$ is correct and all the values of $\tilde{G}^E$ and $\Delta\tilde{H}$ are consistent then the values of $\tilde{G}^{E\prime}/T'$ will lie on a single smooth curve.

For the two systems considered here this procedure can be further simplified. If the heat of mixing is independent of temperature, so also is the entropy of mixing. Consequently we can calculate the excess entropy $\tilde{S}^E(T)$ for each of the temperatures from the equation

$$\tilde{S}^E(T) = [\Delta\tilde{H} - \tilde{G}^E(T)]/T \qquad (5)$$

If $\tilde{G}^E$ is expressed as a power series with coefficients g_n analogous to the coefficients h_n in equation 1, we have for each temperature T

$$\tilde{G}^E = x(1-x)[g_0 + g_1(1-2x) + g_2(1-2x)^2 + \ldots.] \qquad (6)$$

Equation 6 can be combined with equation 1 to yield coefficients s_n of the analogous excess entropy series

$$s_n(T) = [h_n - g_n(T)]/T \qquad (7)$$

The coefficients s_n should be independent of temperature if the h_n's are, so we have a test for consistency. If these are reasonably constant we may average them (weighting differently if appropriate) and substitute back into equation 7 to obtain improved values of the g_n's for each temperature.

This treatment has the virtue of representing all the experimental data in a thermodynamically consistent manner.

As a further test of the quality of the data we have used the free energy equation to predict the consolute temperatures for the two systems by solving the equations

$$\frac{\partial^2\Delta\tilde{G}}{\partial x^2} = 0, \quad \frac{\partial^3\Delta\tilde{G}}{\partial x^3} = 0 \qquad (8)$$

and comparing the values of T_c and x_c obtained with the observed results.

n-C_7F_{16} + i-C_8H_{18}.—In analyzing the results for this system we have recalculated the excess Gibbs free energies of mixing from the experimental vapor pressure data of Mueller and Lewis[6] at 30, 50 and 70°. Since these authors give reasons for distrusting the vapor compositions we have used only the total pressure and liquid composition from which equations for the excess Gibbs' free energy are obtained using the method described by Barker.[11] We have also used rather different estimates of the second virial coefficients of the vapors from those used by Mueller and Lewis.[6] The second virial coefficients shown in Table IV were obtained in the following way.

The available data for perfluoro-n-alkanes[12-14] were plotted yielding second virial coefficients as a function of temperature. Assuming that these com-

(11) J. A. Barker, *Austral. J. Chem.*, **6**, 207 (1953).

(12) E. L. Pace and J. G. Aston, *J. Am. Chem. Soc.*, **70**, 566 (1948).

(13) K. E. MacCormack and W. G. Schneider, *J. Chem. Phys.*, **19**, 845 (1951).

(14) C. Booth, this department, unpublished value of −3110 cm.^{3} for n-C_7F_{16} at 5μ°.

TABLE III

$h_n + \sigma h_n$ VALUES FROM LEAST SQUARES FITS

($\Delta\tilde{H}$ in calories)

	System: n-C_7H_{16} + i-C_8H_{18}					
	30° (a)		50° (a)		30° + 50° (b)	
$n = 0$	2019.6	9	2055.4	9	2031.9	8
1	69.3	48	−14.5	48	21.5	42
2	536.9	50	424.3	64	507.1	51
3	−480.8	168	−302.0	236	−368.3	151
$\sigma\Delta\tilde{H}3$		6.7		3.4		6.0
4		4.3		2.9		5.1
5		4.6		..		5.3

	System: n-C_6H_{14} + n-C_6H_{14}							
	25° (c)		35° (c)		25° + 35° (d)		25° + 35°—suspected phase sep. data (e)	
$n = 0$	2063.5	19	2062.9	10	2049.2	14	2065.1	10
1	261.5	79	3.0	46	138.6	54	19.8	49
2	245.1	146	553.1	47	507.3	71	510.5	51
3	−1285.0	401	−410.7	121	−694.6	170	−421.1	139
$\sigma\Delta\tilde{H}3$		9.9		7.5		11.5		7.5
4		5.5		4.8		7.9		5.5
5		6.1		4.6		8.1		5.9

$\sigma\Delta\tilde{H}_4$ = std. dev. of $\Delta\tilde{H}$ using coefficients given here; $\sigma\Delta\tilde{H}_3$ = std. dev. using only three coefficients (h_0, h_1, h_2) in equation 1); $\sigma\Delta\tilde{H}_5$ = std. dev. using h_0, h_1, ..., h_4. In none of these systems is the use of 5 coefficients warranted. Three are probably sufficient in some; the use of four in this paper is based on a preference for consistency.

pounds form a family similar to similar to that observed by McGlashan and Potter for the n-alkanes[15] the curve for perfluoro-n-heptane was estimated and hence values at 30 and 70° were obtained. For isooctane, values of the second virial coefficients were obtained at 25 and 99.24° from the calorimetric latent heat of vaporization and the vapor pressure using the Clapeyron–Clausius equation in the form

$$B = \frac{\Delta\tilde{H}^v}{T\,dP/dT} - \frac{RT}{P} + \tilde{V}^1 \qquad (9)$$

The required data were obtained from the tables of API research project 44.[16] The two values of the second virial coefficient thus obtained were used to calculate values of V_c and T_c in the equation[17]

$$B/\tilde{V}_c = 0.447[3.375 - 2.375 \exp(0.936T_c/T)] \qquad (10)$$

which was then used as an interpolation formula to give the values at the required temperatures. The estimated uncertainty of the values shown in Table IV is about 3–4 × 10^2 cm^3. mole^{-1}.

TABLE IV

SECOND VIRIAL COEFFICIENTS (B) OF n-C_7F_{16} AND i-C_8H_{18}

t, °C.	30	50	70
i-C_8H_{18} B/cm.^{3} mole^{-1}	−3180	−2350	−1470
n-C_7F_{16} B/cm.^{3} mole^{-1}	−3900	−3100	−2500

It was assumed that

$$B_{12} = {}^1/_2(B_{11} + B_{22}) \qquad (11)$$

where B_{12} is the contribution to the second virial coefficient from interactions between unlike molecules. This assumption, while almost certainly incorrect, will not cause an error of more than 2–3 cal. mole^{-1} in the calculation of $\tilde{G}^E$.

(15) M. L. McGlashan and D. J. B. Potter, "Proc. of Conference on Thermodynamic and Transport Properties of Fluids," Institution of Mechanical Engineers and International Union of Pure and Applied Chemistry, London, 1957.

(16) American Petroleum Institute Research Project 44, Selected Values of Physical and Thermodynamic Properties of Hydrocarbons and Related Compounds, Tables 3K and 3M, (Pittsburgh, Carnegie Press, 1953).

(17) E. A. Guggenheim, "Mixtures," Oxford University Press, 1952.

The actual calculations of the g_n's were made on the IBM-709 of the Western Data Processing Center at U.C.L.A. using a program developed by one of us (R.L.S.) as part of the Petroleum Research Fund project (PRF-366A). This program, using essentially the least squares procedure first proposed by Barker[11] but with modifications and generalizations, processes total vapor pressure data and yields sets of g_n (for varying numbers of coefficients) together with standard deviations.

The computer results show clearly that the vapor pressure data are not precise enough to justify more than three coefficients, so in what follows we restrict ourselves to three. (A consideration of column b of Table III shows that the heat of mixing data barely justify four.)

Table V shows the raw coefficients g_n for the three temperature and the entropy coefficients s_n derived from these and the three parameter h_n's (h_0 = 2033 cal., h_1 = −70 cal., h_2 = 492 cal.). The standard deviations for the g_n's are approximately 6, 10 and 20 cal. for g_0, g_1, and g_2, respectively, at all three temperatures.

TABLE V

THERMODYNAMIC COEFFICIENTS FOR THE SYSTEM C_7F_{16} + C_8H_{18}

t, °C.	30	50	70
g_0/cal.	1302 (*1302*)	1250 (*1254*)	1204 (*1206*)
g_1/cal.	−112 (*−115*)	−116 (*−118*)	−123 (*−121*)
g_2/cal.	173 (*171*)	164 (*149*)	111 (*128*)
s_0/cal. deg.$^{-1}$	2.41	2.42	2.41
s_1/cal. deg.$^{-1}$	0.14	0.14	0.15
s_2/cal. deg.$^{-1}$	1.05	1.01	1.11

The entropy coefficients s_n are certainly constant within the experimental uncertainties, so we average these and write for the excess free energy $\tilde{G}^E$

$$\tilde{G}^E/(\text{cal.}) = x(1-x)[(2033 - 2.41T/(\text{deg.})) + (-70 - 0.15T/(\text{deg}))(1-2x) + (492 - 1.06T/(\text{deg.}))(1-2x)^2] \qquad (12)$$

The smoothed values of g_n for the three experi-

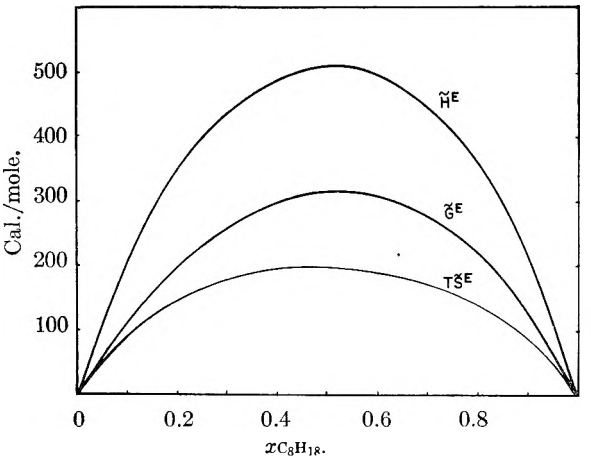

Fig. 1.—Excess functions for C_7F_{16} + C_8H_{18} at 50°.

mental temperatures are shown in Table V (the italicized values in parentheses.) The agreement is excellent for g_0 and g_1 and good even for g_2 considering that the standard deviation of the experimental g_2 is approximately 20 cal. In Fig. 1 are shown the smooth curves for $\tilde{H}^E$, $\tilde{G}^E$ and $T\tilde{S}^E$ at the middle temperature, 50°.

From equation 12 one calculates a critical solution temperature T_c = 304°K. (31°) and a critical composition x_c = 0.67. These are only in fair agreement with the observed values,[18] T_c = 296.9 (23.7°) and x_c = 0.62. It should be noted that equation 12 predicts partial miscibility at 30°, while the experimental fact is that the two liquids are miscible in all proportions.

Better agreement is hardly to be expected for several reasons: the experimental data are subject to considerable uncertainty, and the equations for the critical constants are very sensitive to small uncertainties in the coefficients g_n. Moreover while the correct theoretical form for the thermodynamic functions in the critical region is unknown, the flatness of the coexistence curve and the flatness of the chemical potential μ as a function of x in the vicinity of T_c require a more complex expression than equation 12. Probably a requirement that the excess free energy equation fit the coexistence curve (or at least the point x_c, T_c) would be a valuable addition to a data processing program, and we hope to develop such a program ultimately.

n-C_6F_{14} + n-C_6H_{14}.—The partial vapor pressures of the perfluorohexane + hexane system were measured by Dunlap, *et al.*,[19] at 25, 35 and 45°. From the vapor pressure data and measured vapor compositions, they calculated excess free energies (using the appropriate corrections for gas imperfection) checked consistency with the Gibbs–Duhem relation, and fitted the resulting values to an excess free energy power series by the method of least squares. They concluded that only three parameters were justified, so we have combined their g_n's with our three parameter temperature-independent h_n's (h_0 = 2064 cal., h_1 = −114 cal., h_2 = 551 cal.) to obtain the entropy coefficients shown in Table VI.

TABLE VI

THERMODYNAMIC COEFFICIENTS FOR THE SYSTEM n-C_6F_{14} + n-C_6H_{14}

(g_n's from Dunlap, *et al.*[19])

t, °C.	25	35	45
g_0/cal.	1310 (*1301*)	1271 (*1275*)	1245 (*1250*)
g_1/cal.	−200 (*−197*)	−200 (*−200*)	−199 (*−203*)
g_2/cal.	156 (*143*)	172 (*129*)	50 (*115*)
s_0/cal. deg.$^{-1}$	2.53	2.57	2.57
s_1/cal. deg.$^{-1}$	0.29	0.28	0.27
s_2/cal. deg.$^{-1}$	1.32	1.23	1.57

If, as before we average the s_n's for the three temperatures, we may write for the excess free energy

$$\tilde{G}^E(\text{cal.}) = x(1-x)[(2064 - 2.56T/(\text{deg.})) + (-114 - 0.28T/(\text{deg.}))(1-2x) + (551 - 1.37T/(\text{deg.}))(1-2x)^2] \quad (13)$$

The smoothed free energy coefficients g_n calculated from equation 13 are shown in italics in Table VI; the agreement is good except for the coefficients g_2 and s_2 which vary erratically. It should be noted that the separation of heat and entropy obtained above with the aid of our calorimetric measurements differs markedly from that which Dunlap and his co-workers calculated from the temperature dependence of the vapor pressure. Our coefficients h_n differ from theirs by several times their estimated error.

We have also processed the total vapor pressure data of Dunlap, *et al.*, using our Barker method computer program. In this, the data on vapor composition are not used, but for consistency we used the same reasonable estimates of virial coefficients which Dunlap used. Surprisingly the results of these computations indicate that the total vapor pressure data clearly justify *four* parameters. (The standard deviation of the vapor pressure is reduced from about 3 to 1 mm. in going from three to four parameters; no significant further improvement is obtained by adding a fifth). In Table VII, we show these new coefficients and the entropy coefficients obtained by combining these with the h_n's of Table III, column e.

From Table VII the agreement is significantly better, and as before we obtain an equation for the excess free energy

$$\tilde{G}^E(\text{cal.}) = x(1-x)[(2065 - 2.59T/(\text{deg.})) + (20 - 0.55T/(\text{deg.}))(1-2x) + (511 - 1.12T/(\text{deg.}))(1-2x)^2 + (-4.21 + 1.08T/(\text{deg.}))(1-2x)^3] \quad (14)$$

From equation 14 we estimate a critical solution temperature T_c = 297°K. (24°) in very good agreement with the observed value of 295.8°K. (22.7°). This critical point however is at a critical composition x_c = 0.73 which agrees less well with the observed value of 0.63. If we use equation 13 instead we derive a very unsatisfactory critical solution temperature T_c = 317 (44°) at x_c = 0.67. If we use the free energy equations of Dunlap and coworkers directly (*i.e.*, the unsmoothed g_n's of Table

(18) J. H. Hildebrand, B. B. Fisher and H. A. Benesi, *J. Am. Chem. Soc.*, **72**, 4348 (1950).

(19) R. D. Dunlap, R. G. Bedford, J. C. Woodbrey and S. D. Furrow, *ibid.*, **81**, 2927 (1959).

VI) we find that these predict partial miscibility at all three temperatures, including 45°.

TABLE VII

THERMODYNAMIC COEFFICIENTS FOR THE SYSTEM n-C_6F_{14} + n-C_6H_{14}

(g_n's from Barker analysis of data of Dunlap, *et al.*[19])

t, °C.	25	35	45
g_0/cal.	1298 (*1293*)	1265 (*1267*)	1234 (*1241*)
g_1/cal.	−136 (*−144*)	−151 (*−149*)	−162 (*−155*)
g_2/cal.	162 (*177*)	175 (*166*)	159 (*155*)
g_3/cal.	−125 (*−99*)	−72 (*−88*)	−67 (*−77*)
s_0/cal. deg.$^{-1}$	2.57	2.60	2.61
s_1/cal. deg.$^{-1}$	0.52	0.56	0.57
s_2/cal. deg.$^{-1}$	1.17	1.09	1.11
s_3/cal. deg.$^{-1}$	−0.99	−1.13	−1.11

Direct comparison of the coefficients of equations 13 and 14 is difficult because g_1 and g_3 in equation 14 do the work of g_1 alone in equation 13. The Barker three coefficient treatment yields still another set of g_n's and we have obtained therefrom the following equation for the excess free energy

$$\tilde{G}^E/(\text{cal.}) = x(1-x)[2064 - 2.60T/(\text{deg.}) + (-114 - 0.19T/(\text{deg.}))(1-2x) + (551 - 1.16T/(\text{deg.}))(1-2x)^2] \quad (15)$$

Equation 15 differs from equation 13 principally in the smaller values of s_1 and s_2. Equation 15 is only slightly better than equation 13 for evaluating critical constants, yielding T_c = 309°K. and x_c = 0.71.

Figure 2 shows the excess functions for C_6F_{14} + C_6H_{14} at 35° obtained from equations 13 and 14. It should be noted that neither of these equations gives the minimum in the excess entropy reported by Dunlap, *et al.* Their reported s_2 = 5.3 is much too large (a minimum at x = 1/2 occurs when $s_2 > s_0$).

The better fit of total pressure and critical solution temperature (but not critical composition) for equation 14 suggests that it is preferable, but this is by no means certain. Clearly a careful re-examination of the whole problem of deriving free energies from vapor pressure data is called for, with particular reference to whether the extra effort required to measure vapor compositions is worthwhile. Again, if the equations of Dyke, Rowlinson and Thacker[5] are simplified by assuming that $\tilde{G}^E$ varies linearly with temperature, it is found that the critical solution temperatures predicted from the thermodynamic data are higher than the observed values. For perfluorocyclohexane + cyclohexane the discrepancy is about 8° and for perfluoromethylcyclohexane + methylcyclohexane it is 17° or more depending on the choice of slope for the temperature variation of g_0.

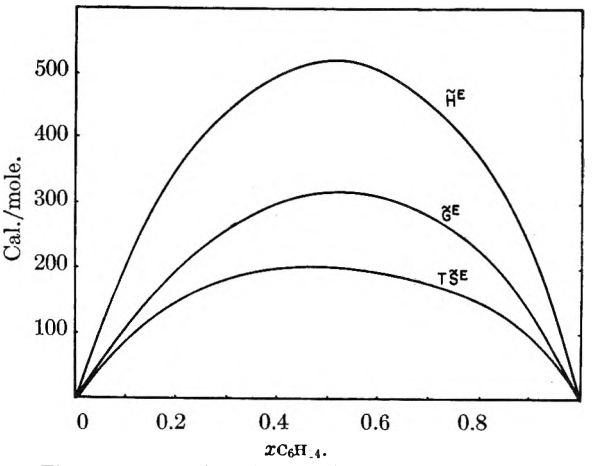

Fig. 2.—Excess functions or C_6F_{14} + C_6H_{14} at 35°.

These discrepancies possibly arise from the inaccuracies in the experimental data as the concave sections of the plots of $\Delta\tilde{G}$ *vs.* x are only 2–3 cal. mole^{-1} "deep." They may also result from the form of the function used to fit the data. In particular, if the experimental data of Dunlap, *et al.*, for n-C_6F_{14} + n-C_6H_{14} at 25° are plotted as $\Delta\tilde{G}$ *vs.* x as well as $\tilde{G}^E$ *vs.* x it can be seen that although the empirical equation does in fact fit the experimental points with σ = ± 2 cal. mole^{-1}, the plot of $\Delta\tilde{G}$ suggests that one measurement around $x_{C_6H_{14}}$ = 0.9 which appears to be less accurate than the other points could be the cause of a spurious concavity in the least squares curve. This apparent discrepancy is not obvious from the plot of $\tilde{G}^E$ *vs.* x. In this case it appears that the false prediction of T_c from the analytical expressions for $\tilde{G}^E$ arises out of the procedure used in fitting these expressions without first taking into consideration all the available data for the system.

Now that computer methods are coming into more common use for fitting analytical expressions to experimental results the danger of errors of this type is increased. We suggest that careful consideration of the criteria for thermodynamic consistency is necessary to ensure that the final representation of the data is as meaningful as possible.

Acknowledgments.—We wish to thank Mr. D. B. Myers of this department for the computer program used in the least squares treatment of the results and Dr. G. N. Malcolm of the University of Otago for helpful discussions.

ABSORPTION OF DEUTERIUM BY PALLADIUM[1]

BY TED B. FLANAGAN

Brookhaven National Laboratory, Upton, New York

Received July 21, 1960

The course of absorption of deuterium by palladium wire specimens has been followed by changes in their electrode potentials and relative resistances in dilute acid solutions. The electrode potential (25°, 1 atm. D_2, W.R.T. Pt/D_2) in the region of coexistence of the α- and β-phases is 31.0 ± 0.5 mv. as compared to 50 mv. for the palladium–hydrogen system. The rate is constant over the majority of the absorption. An absorption isotherm has been constructed from the change of electrode potential with deuterium content of the palladium. The temperature coefficient of the electrode potential has been determined in the two phase region, from which the heat of absorption is calculated as −8795 cal./mole D_2.

Introduction

Although equilibration of hydrogen with palladium wire or foil is usually difficult to obtain in the vicinity of room temperature,[2] absorption directly from hydrogen saturated solutions has been shown to proceed readily following surface activation.[3,4] Measurement of electrode potentials as a function of hydrogen content during absorption has yielded data[5,6] which agrees closely with equilibrium data obtained from measurements using palladium black[7] or thermally-equilibrated palladium foils.[8]

Several investigations of the palladium–deuterium system have been made at elevated temperatures.[9,10] These have shown that the palladium–deuterium system, like the palladium–hydrogen system, exhibits a region of coexistence of two non-stoichiometric phases: low deuterium content, α-phase and the high deuterium content, β-phase. The critical temperature and pressure for palladium–deuterium are 276° and 35 atm.,[10] and the corresponding values for palladium–hydrogen are 310° and 20 atm.[2]

Nace and Aston[7] have recently investigated the equilibration of deuterium and palladium black at room temperature. Sieverts and Danz[9] determined an isobar for the deuterium (740 mm.)–palladium system from 25 to 250°. In both investigations it was found that equilibrium was established at a much slower rate than with hydrogen. It was of interest to see if this slow equilibration would be reflected in absorption studies from solution.

Experimental

Apparatus and Procedure.—The apparatus was similar to that previously described.[3] The deuterium employed was obtained from the Stuart Oxygen Co. and was 99.5% pure; it was passed through a liquid nitrogen trap before bubbling through the solution. The flow rate was measured during a run by a flowmeter. The deuterium content of the "total hydrogen" of the ~0.02 *N* DCl solution employed was approximately 99%. The palladium specimens (~15 cm. long, 0.03211 cm. diam.) were "spec pure" and used as received, in a cold-drawn condition; they were mounted in soft glass, vacuum-tight holders with only palladium exposed to the solution. The platinum leads and the connecting platinum sleeves (which were used to connect the palladium to the leads) were coated with soft glass. The palladium specimen could be transferred to a vacuum system while still attached to its holder to be subsequently degassed *in vacuo* at an elevated temperature (~300°).

Resistances were measured by passing a small, known d.c. current (~6 ma.) along the specimen and determining the *IR* drop. Current was allowed to pass through the specimen only during the actual measurement of resistance and, therefore, current passed along the specimen for only a small fraction of the absorption run. Electrode potentials were measured with respect to a platinized platinum electrode immersed in the same solution. The surface of the palladium specimen was activated prior to an absorption run by preanodic treatment[3] or by electrolytic deposition of a small coating of palladium (palladization). The temperature of the solution was maintained to ±0.2° during a run.

Results and Discussion

Figure 1 shows the electrode potential and relative resistance changes during the absorption of deuterium in a representative run plotted as a function of time (25°, 1 atm. D_2, ~0.02 *N* DCl). The absorption was performed in a dilute DCl solution (~0.02 *N*) so that errors introduced into the resistance measurements by the "drift effect," co-conduction of a part of the measuring current through the solution should be negligible.[4b] This was verified since the resistance immediately registered its maximum value upon initial application of the measuring current.[11,12]

It may be seen in Fig. 1 that the palladium–deuterium system exhibits a region of constant electrode potential (potential plateau) indicative of the coexistence of two non-stoichiometric deuteride phases. The plateau electrode potential is 31 ± 0.5 mv. whereas the corresponding potential of the palladium–hydrogen system is 50 mv.[5,6] The initial electrode potentials, greater than 31 mv., are associated with the solution of deuterium in the α-phase. An electrode potential minimum, which occurred immediately before the establishment of the plateau potential, was observed in most runs (*e.g.*, Fig. 1). An analogous minimum was observed in the palladium–hydrogen system and was associated with supersaturation of α-phase before the surface was converted to the β-phase.[5] The minimum observed in Figs. 1 and 2 was absent in especially "active" specimens, *i.e.*, those which had been subjected to a series of

(1) Work performed under the auspices of the U. S. Atomic Energy Commission.

(2) D. P. Smith, "Hydrogen in Metals," Chicago Univ. Press, 1948.

(3) T. B. Flanagan and F. A. Lewis, *Trans. Faraday Soc.*, **55**, 1400 (1959).

(4) (a) R. J. Fallon and G. W. Castellan, *J. Phys. Chem.*, **64**, 4 (1960). (b) A. W. Carson, T. B. Flanagan and F. A. Lewis, *Trans. Faraday Soc.*, **56**, 371 (1960).

(5) R. J. Ratchford and G. W. Castellan, *J. Phys. Chem.*, **62**, 1123 (1958).

(6) T. B. Flanagan and F. A. Lewis, *Trans. Faraday Soc.*, **55**, 1409 (1959).

(7) D. M. Nace and J. G. Aston, *J. Am. Chem. Soc.*, **79**, 3627 (1957).

(8) L. J. Gillespie and F. P. Hall, *ibid.*, **48**, 1207 (1926).

(9) A. Sieverts and W. Danz, *Z. physik. Chem.*, **B38**, 46 (1937).

(10) L. J. Gillespie and W. R. Downs, *J. Am. Chem. Soc.*, **61**, 2496 (1939).

(11) C. A. Knorr and E. Schwartz, *Z. Elektrochem.*, **39**, 281 (1933).

(12) A. W. Carson, T. B. Flanagan and F. A. Lewis, *Naturwissenschaften*, **46**, 374 (1959).

charging–degassing cycles, indicating that nucleation to the β-phase occurred more readily in these cases.[6]

The attainment of the plateau potential (or the supersaturation minimum) occurs simultaneously with a change of slope of the relative resistance–time curve, in the vicinity of $R/R_0 = 1.06 \pm 0.01$. This change of slope must also reflect the formation of the second phase (β-phase). The region of absorption at small times is shown in more detail in Fig. 2 for two runs under the same experimental conditions. It should be noted that for electrode potentials > 31 mv. the corresponding R/R_0 values (<1.06) represent resistance changes due to absorption in the α-phase. The small time lag, ~5 min., before absorption starts reflects removal of the oxide film arising from the surface pretreatment. After the change of slope near $R/R_0 = 1.06$, R/R_0 increases less sharply with time and finally approaches equilibrium very slowly while simultaneously the electrode potential decays exponentially to zero mv. (Fig. 1). The slow change of R/R_0 and of electrode potential near equilibrium is due to the onset of the reverse reaction; the detailed kinetics for hydrogen absorption in the vicinity of equilibrium have been examined elsewhere[13] and similar considerations would be expected to apply in the present study.

Relationship between Relative Resistance and Deuterium Content.—The relationship between R/R_0 and D–Pd was previously investigated by Sieverts and Danz.[14] Their D–Pd data was determined by electrolytically charging palladium wires with deuterium (in 2 $N D_2SO_4$) and measuring the difference between the deuterium discharged at the surface and that volumetrically collected over the specimen. In addition, two of their final values, which were checked by "degassing" analysis, *i.e.*, measurement of the gas evolved into a known volume from heating the specimen *in vacuo* at ~300°, agreed with their other values.

Recently significant differences have been found between the electrolytically determined hydrogen content–R/R_0 relationships and those determined by "degassing" analysis.[3] It was therefore desirable to reinvestigate the D/Pd–R/R_0 relationship using "degassing" analysis to determine D/Pd. In addition, since the D/Pd–R/R_0 relationship established by Sieverts and Danz[14] did not include data in the α-phase, it was necessary to extend the data to this region.

Deuterium was introduced into the palladium specimens by direct absorption from deuterium-saturated solutions. It has been shown that significant errors can be introduced into the measurement of the electrical resistance of wire specimens (capable of absorbing hydrogen) in acidic solutions (~1 N) due to the occurrence of the "drift effect."[4b] Hence the resistance was again measured in 0.02 N DCl, where co-conduction of the bridge current through the solution is negligible. After the final resistance measurement the specimen was removed, washed with acetone and degassed. As for the hydrogen–palladium system[3] there appeared to be no loss of deuterium during this process.

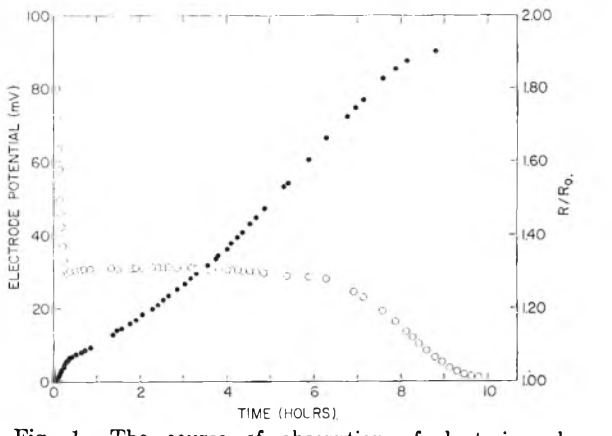

Fig. 1.—The course of absorption of deuterium by palladium from a dilute DCl solution (25°). ○, electrode potential; ●, relative resistance.

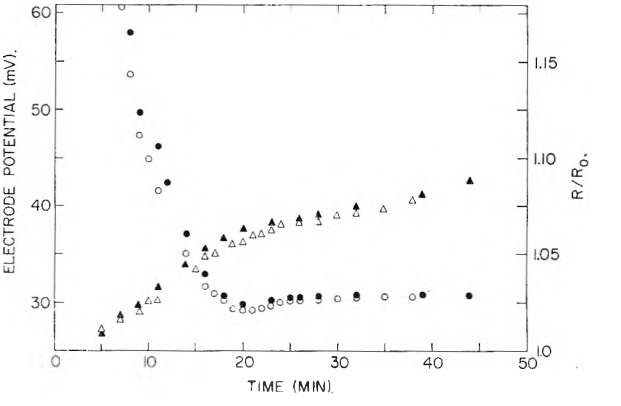

Fig. 2.—Two examples of initial changes of electrode potential and relative resistance during absorption of deuterium from a dilute DCl solution (25°). ●, ○, electrode potential; ▲, △, relative resistance. The open symbols represent one run and the full symbols the other run.

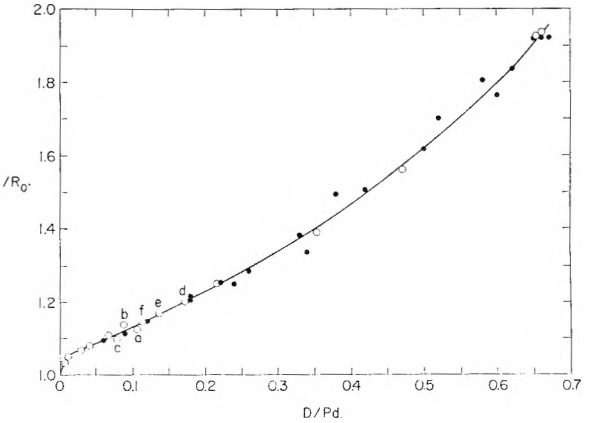

Fig. 3.—Relationship between D/Pd and R/R_0: ●, the data of Sieverts and Danz (ref. 9); ○, data of the present study at 25°; circles labelled a, b, c, d, e and f represent data obtained at 0.5, 10.3, 16.7, 31.3, 38.1 and 48.2°, respectively.

Results are shown in Fig. 3 (see also Table I) together with the data of Sieverts and Danz[14]; it may be noted that the agreement with their data is good. The initial change of slope in the relationship occurs in the vicinity of $R/R_0 = 1.06$

(13) T. B. Flanagan and F. A. Lewis, to be published.
(14) A. Sieverts and W. Danz, *Z. physik. Chem.*, **B38**, 61 (1937).

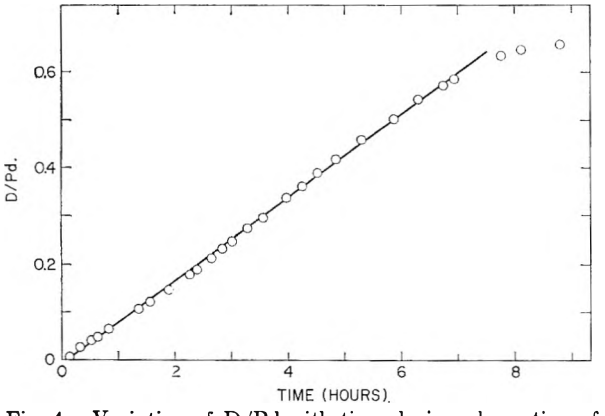

Fig. 4.—Variation of D/Pd with time during absorption of deuterium by palladium (dilute DCl, 25°).

which is in accord with the change of slope observed in the absorption curve (Fig. 1) and represents initial formation of the second, non-stoichiometric hydride phase (β). The content of the specimen at this point, α_{max}, is D/Pd ~0.015 whereas the corresponding hydrogen content is H/Pd ~0.025.[3] In general the relationship has the same shape as the change of R/R_0 with time during an absorption run and also resembles the R/R_0–H/Pd relationships established in the same manner.[3] At equilibrium (25°, 1 atm. D_2), as checked by the final zero mV potential (W.R.T. Pt/D_2), $R/R_0 = 1.92$ and the D/Pd ratio was 0.65 ± 0.01. This value of D/Pd is in excellent agreement with the value of 0.65 (25°, 740 mm.) established by direct equilibration with palladium black[9] and shows that the specimen has absorbed deuterium homogeneously throughout its mass. At equilibrium the corresponding values of the hydrogen–palladium system are: $R/R_0 = 1.78 \pm 0.02$, H/Pd = 0.69 ± 0.01.[3] On an atomic basis absorbed deuterium increases the resistance of palladium more than hydrogen in both the α- and the β-phases.

TABLE I

RELATIONSHIP BETWEEN R/R_0 AND D/Pd (ATOMIC RATIO)

R/R_0	D/Pd	T, °C.
1.035	0.0085	25.0
1.051	.0126	25.0
1.068	.0294	25.0
1.080	.0405	25.0
1.108	.0671	25.0
1.251	.216	25.0
1.389	.354	25.0
1.563	.470	25.0
1.924	.652	25.0
1.936	.661	25.0
1.098	.0787	16.7
1.124	.107	0.5
1.138	.0886	10.3
1.146	.115	48.2
1.169	.137	38.1
1.200	.173	31.3

In the temperature range 0–60° the same relationship between hydrogen content and relative resistance applies reasonably well, especially in the low content region.[13,15] In addition it was recently found for several palladium–platinum alloys the hydrogen content–relative resistance relationship established at 25° is valid from 0–59° (at least to $R/R_0 \sim 1.3$).[16] It would not be unexpected, therefore, if a similar temperature independence would be exhibited by the palladium–deuterium system. This was verified for low relative resistances (~1.2). Several values determined at temperatures in the range 0–48° showed no systematic variation from the data established at 25° (Fig. 3).

Rate of Absorption.—The rate of absorption may be calculated from the measured values of R/R_0 and the D/Pd–R/R_0 relationship (Fig. 3). Results for a typical run are shown in Fig. 4 (25°, 0.02 N DCl, constant flow rate). It may be seen that the rate of absorption is constant (within the experimental limits of the D/Pd–R/R_0 relationship) over almost the entire absorption range, including the α-phase. The final fall-off is, of course, expected as equilibrium is approached.

A constant rate of absorption of hydrogen from solution was also observed for palladium[3,4] and for several platinum–palladium alloys.[4b] Rates of absorption of deuterium were found to be reasonably reproducible provided the same specimen was not repeatedly employed; the use of such a specimen tended to increase the rate. The rate of absorption of deuterium was somewhat dependent upon the flow rate, *i.e.*, stirring rate, except at the higher stirring rates where the stirring efficiency has undoubtedly attained a maximum.

Using the same reaction vessel and specimen holder the absorption of hydrogen was reinvestigated under the same stirring conditions as employed for deuterium absorption. At the high flow rate the velocity of absorption was ~6.8 × 10^{15} molecules H_2 cm.$^{-2}$ sec.$^{-1}$ in good agreement with Fallon and Castellan's value of ~6.9 × 10^{15} molecules H_2 cm.$^{-2}$ sec.$^{-1}$ (also under rapid stirring conditions). Other features of the hydrogen absorption were in agreement with earlier work.[3-6] The average rate for deuterium absorption under rapid stirring conditions was ~5.6 × 10^{15} molecules D_2 cm.$^{-2}$ sec.$^{-1}$. The ratio of the rates of absorption of hydrogen (average of three runs) to the absorption of deuterium (average of five runs) by palladium is ~1.2 under the conditions employed here. This value is close to the ratio of the viscosity of D_2O to that of H_2O (25°)[17] and therefore the Stokes–Einstein law would predict the experimental ratio to be in agreement with diffusion of dissolved hydrogen as the slow step if the solubilities of deuterium in D_2O and hydrogen in H_2O are closely similar (25°). Unfortunately the solubility of deuterium in D_2O does not appear to have been measured in this temperature range and the agreement of the ratio of the rates of absorption with a diffusion-controlled mechanism should be regarded as tentative.

Since the relationship between D/Pd and R/R_0 is approximately invariant over the temperature range 0–50°, at least in the low D/Pd range, rate constants may be evaluated from the time

(15) C. G. Knott, *Trans. Royal Soc. (Edinburgh)*, **33**, 171 (1886).

(16) A. W. Carson, T. B. Flanagan and F. A. Lewis, *Trans. Faraday Soc.*, **56**, 363 (1960).

(17) The writer is grateful to the referee for pointing this out.

dependent behavior of R/R_0 during absorption over this temperature interval. Using this procedure and allowing for the experimental reproducibility, the activation energy is <3.0 kcal./mole. The activation energy for absorption of hydrogen from solution by palladium and several platinum–palladium alloys is <2.0 kcal./mole.[4] Evidence has been presented previously[3,4] which suggests that diffusion within the metal is not the rate-determining step in absorption from solution; some of this evidence also applies here, *e.g.*, an activation energy > 3 kcal./mole would be expected and a linear absorption rate would not be observed. The slow step has been postulated to be transport of hydrogen molecules through the solution up to the metal surface.[4] Fallon and Castellan[4a] have shown that diffusion coefficients for hydrogen gas dissolved in water as calculated from their observed absorption rates agree with those in the literature. In addition, it has been shown that there is no variation in absorption rate between palladized and unpalladized palladium specimens[3] and that alloying the palladium specimens with platinum (up to 8.80% platinum) does not affect the absorption rate.[4b] All of this evidence strongly suggests that transport of hydrogen up to the surface must be the slow step and there appears to be no reason to alter this mechanism for deuterium absorption from dilute DCl solutions.

Electrochemically Derived Absorption Isotherms. —As observed for the palladium–hydrogen system[6] the measured electrode potentials for the palladium–deuterium were reversible and reproducible as a function of D/Pd. The general electrode reactions, which reflect the non-stoichiometric character of the palladium–deuterium system, are

$$x\mathrm{D}{:}y\mathrm{Pd} + \mathrm{D}^+ + \dot{} \longrightarrow (x+1)\mathrm{D}{:}y\mathrm{Pd}\ (\mathrm{Pd\ electrode}) \qquad (a)$$

$$\tfrac{1}{2}\mathrm{D}_2 \longrightarrow \mathrm{D}^+ + \bar{\mathrm{e}}\ (\mathrm{Pt\ electrode}) \qquad (b)$$

where x and y represent actual numbers of atoms and therefore x/y = D/Pd. The sum of reactions (a) and (b) is

$$\tfrac{1}{2}\mathrm{D}_2 + x\mathrm{D}{:}y\mathrm{Pd} \longrightarrow (x+1)\mathrm{D}{:}y\mathrm{Pd} \qquad (1)$$

The over-all cell reaction, (1), indicates that the measured electrode potential reflects the standard partial molar free energy change for the solution of deuterium in the non-stoichiometric palladium deuteride. Absorption isotherms may therefore be constructed from the electrode potential and the corresponding D/Pd value using

$$p = e^{-2FE_0/RT} \qquad (2)$$

(Similar considerations have yielded reasonable agreement between electrochemically determined isotherms and direct gas phase isotherms.[6])

Figure 5 shows an absorption isotherm constructed in this manner (25°, 1 atm. D_2). The supersaturation of α-phase, before the establishment of β-phase on the surface, may be noted. Although isotherms are not available for this system near room temperature to compare with Fig. 5, Nace and Aston[7] have measured equilibrium deuterium pressures over the two-phase region.

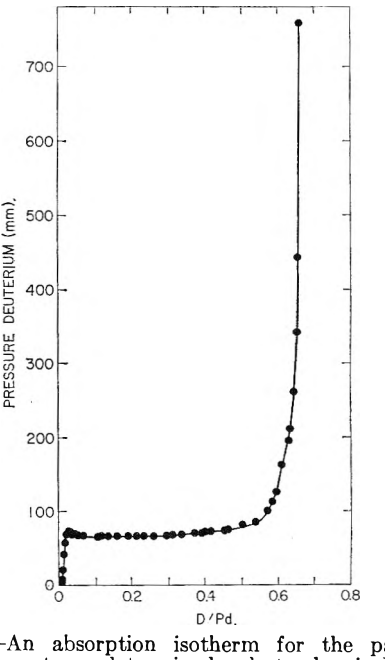

Fig. 5.—An absorption isotherm for the palladium–deuterium system determined electrochemically (25°, unpalladized palladium).

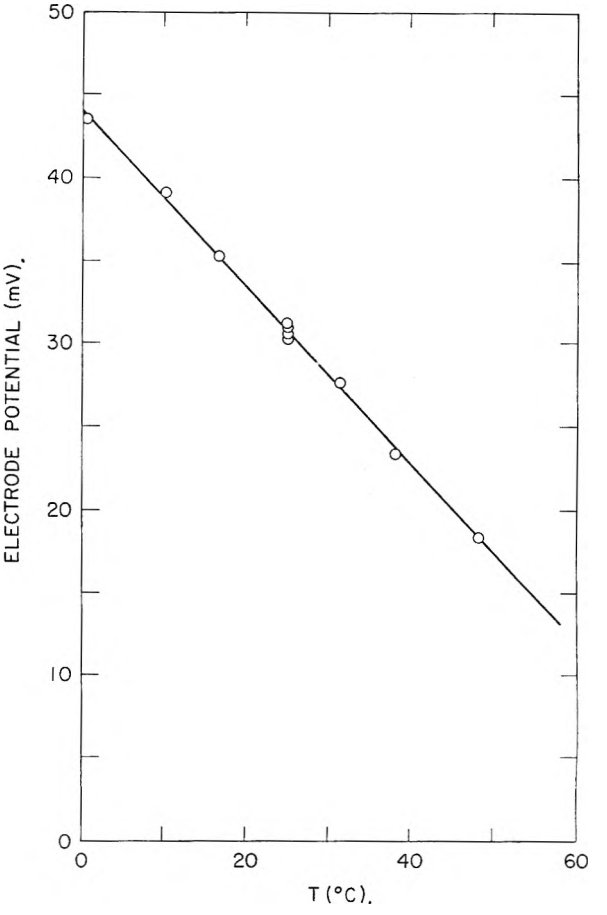

Fig. 6.—The plateau value of the electrode potential as a function of temperature.

After one month's equilibration between deuterium and palladium black, the equilibrium pressure of deuterium was 63 mm.; the corresponding plateau pressure observed here is 65 mm. (25°).

Other absorption experiments at the same flow rate yielded similar system isotherms (25°). Runs with more rapid flow rates yielded higher pressures than those shown in Fig. 5; these pressure increases became most pronounced near the end of the two phase region resulting in the final, large pressure rise coming at a somewhat lower D/Pd value. This behavior is expected because, with rapid flow rates, the concentration of deuterium atoms in the surface and adjacent layers would build up resulting in lower electrode potentials (large deuterium pressures). Palladized palladium specimens exhibited a smaller plateau value of the electrode potential (p = 79 mm.) than for unpalladized specimens. It was observed earlier for the palladium–hydrogen system[6] that the data from unpalladized specimens more closely resembled gas phase absorption isotherms than that from palladized specimens although the rates of absorption were comparable. Rates of absorption of deuterium were also comparable for palladized and unpalladized specimens. The close agreement of the plateau pressure (Fig. 5) with Nace and Aston's value indicates that in the palladium–deuterium system unpalladized specimens also yield more truly equilibrium potentials than palladized palladium.

The reason for the extremely slow equilibration of palladium and deuterium observed in studies made in the absence of solution[7] is not known and has no counterpart in the present study as equilibrium, two-phase electrode potentials are established in $\sim^1/_2$ hour.

Heat of Absorption.—Measurement of the temperature coefficient of the plateau electrode potential has recently been employed to determine the heat of solution of hydrogen in the region of coexistence of the two non-stoichiometric hydride phases.[5,6] This method gave good agreement with heats of solution determined by direct calorimetry or by the variation of the equilibrium, two-phase pressure with temperature (isosteric heats).

The same method has been employed here for determination of the heat of solution of deuterium in the early region of coexistence of the two non-stoichiometric phases. Absorption runs were made at intervals in the temperature range 0–48°. The value of the electrode potential of the two phase region was chosen as the maximum after the supersaturation dip; these potentials all came at approximately the same value of R/R_0. Figure 6 shows the variation of electrode potential with temperature (0.02 N DCl solution, 1 atm. D_2). Employing the Gibbs–Helmholtz equation and the slope of the points in Fig. 6 a heat of solution is obtained, $\Delta H = -8795 \pm 150$ cal./mole D_2. This value is in reasonable agreement with Nace and Aston's isosteric heat of −8635 cal./mole D_2 but both values are somewhat larger than their average calorimetric value of −8379 cal./mole D_2. Using the electrochemically determined free energies and heats of solution for absorption into the β-phase of palladium, we find $\Delta S°_{293} = -23.4$ e.u. (H_2) and −24.7 e.u. (D_2). Thus the smaller free energy of solution for deuterium, as compared to hydrogen, is due to about equal contributions from the increased entropy change and the decreased heat of solution.

THE EFFECT OF DISSOLVED KBr, KOH OR HCl ON THE RAMAN SPECTRUM OF WATER[1]

BY WILLIAM R. BUSING AND

Chemistry Division, Oak Ridge National Laboratory, Oak Ridge, Tennessee

DONALD F. HORNIG

Frick Chemical Laboratory, Princeton University, Princeton, N. J.

Received July 22, 1960

The Raman spectrum of water was studied in the presence of dissolved KBr, KOH and HCl. It shows two main components in the stretching region whose frequencies and polarizations are relatively insensitive to the presence of dissolved ion but whose intensities are consideraby modified. Dissolved KBr has an effect similar to increased temperature; the high frequency peak increases markedly in intensity and the low frequency peak becomes less intense. The intensity of the bending vibration increases sharply. The effect of HCl on the water bands is similar but smaller in magnitude; in addition a broad band ascribed to OH_3^+ appears. KOH causes the intensity of both stretching components to decrease. In addition a sharp peak due to OH^- ions, the protons of which are not hydrogen bonded, appears as well as a broad band ascribed to water molecules hydrogen bonded to OH^- ions. These effects are discussed in terms of the structure of the solutions.

Introduction

It has long been recognized that the O–H stretching region in the vibrational spectra of liquid water is a superposition of two or more peaks, but their origin has been the subject of debate. According to the interpretation of Cross, Burnham and Leighton[2] the band is composed of many individual frequencies, each due to a particular configuration of associated molecules, the high frequencies from the least associated or even unassociated molecules. The fact that the low frequency O–H stretching band of water is observed to decrease in intensity when ionic solutes are added or the temperature is increased, is interpreted, from this point of view, as the result of a decrease in concentration of highly associated molecules.

An alternative interpretation proposed by Ellis

(1) This work was supported by the Office of Naval Research.

(2) P. C. Cross, J. Burnham and P. A. Leighton, *J. Am. Chem. Soc.*, **59**, 1134 (1937).

and Sorge[3] is that the low frequency peak is largely the overtone of the water bending vibration and that the other peaks are the symmetric and antisymmetric vibrations of the molecule. This point of view is supported by the fact that ice, in which all molecules are associated, also shows three peaks in this region.[4] Furthermore, HDO shows single O–D and O–H peaks of the same frequencies in both its infrared[5a] and Raman spectra,[5b] indicating only a single degree of association. In this point of view the intensity variations produced by heating or by ions in solution are produced by variation in the degree of Fermi resonance between 2 ν_2 and ν_1. The resonance is greatest when the hydrogen bonds are strongest since the lower O–H frequency is more nearly that of the overtone.

With the availability of photoelectric Raman apparatus it is now possible to obtain spectra of water and of aqueous solutions which are sufficiently accurate for quantitative studies of band shapes and depolarization ratios. The purpose of this paper is to report such spectra of pure water and solutions of KBr, HCl and KOH of various concentrations. It will be shown that each spectrum can be numerically resolved into several overlapping bands, and that this analysis simplifies the description and interpretation of the effects of adding these solutes.

Experimental

The photoelectric Raman spectrograph which was used for these experiments was designed and constructed in this Laboratory.[6] The monochromator uses as its dispersing elements two large glass prisms, 60 and 30°, respectively, in a Littrow arrangement. Wave length scanning is accomplished by rotating the prism assembly as a unit, and the wave length calibration was obtained by observing the line spectra of Hg and Fe.

Light entering the monochromator was chopped at a frequency of 30 c.p.s., and the emerging beam was focused on an RCA 1P21 photomultiplier tube. The output of this detector was amplified and rectified by means of a commutator attached to the shaft of the chopper. The resulting direct current signal was filtered and recorded on a Leeds and Northrup Speedomax chart recorder.

Exciting light from the Hg 4358 Å. line was provided by two vertical low pressure arc lamps similar to those described by Rank and McCartney.[7] These lamps have water-cooled anodes and were operated at a power of about 500 watts each. Two reflectors in the form of elliptical cylinders focused the exciting light on the sample container, a vertical Pyrex tube 3.5 cm. in diameter and about 15 cm. high. The bottom of this cell consisted of a flat Pyrex window through which the scattered light emerged to be reflected into the spectrograph. A large Pyrex tube surrounded the cell and was sealed to it, forming a jacket through which a filter solution of rhodamine dye (Dupont 5DGN extra) and nitrobenzene in isopropyl alcohol was circulated. A heat exchanger was provided to cool this filter solution and in this way the Raman samples were maintained at room temperature. The length of the sample to be irradiated was defined by baffles and by bands of black paint at the ends of the cell.

Measurements were made using samples of water and solutions of KBr, HCl and KOH of the concentrations included in Table I. These were prepared from reagent grade chemicals and distilled water, and the solutions were usually filtered through a fine sintered glass plate to remove dust particles. The water and KBr solutions were also filtered through decolorizing carbon to remove possible fluorescent

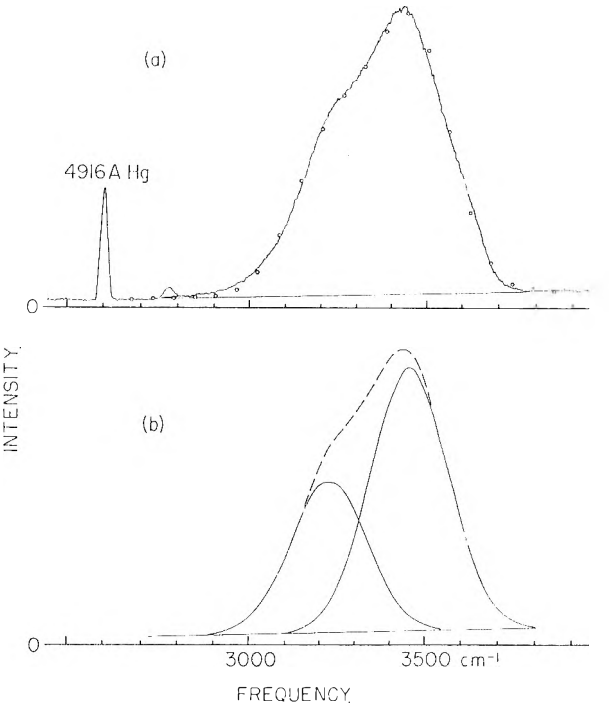

Fig. 1.—The Raman spectrum of water in the OH stretching region. (a) The solid curve is the recorded spectrum while the circles are the calculated values. (b) The component bands (solid) and their sum (dashed).

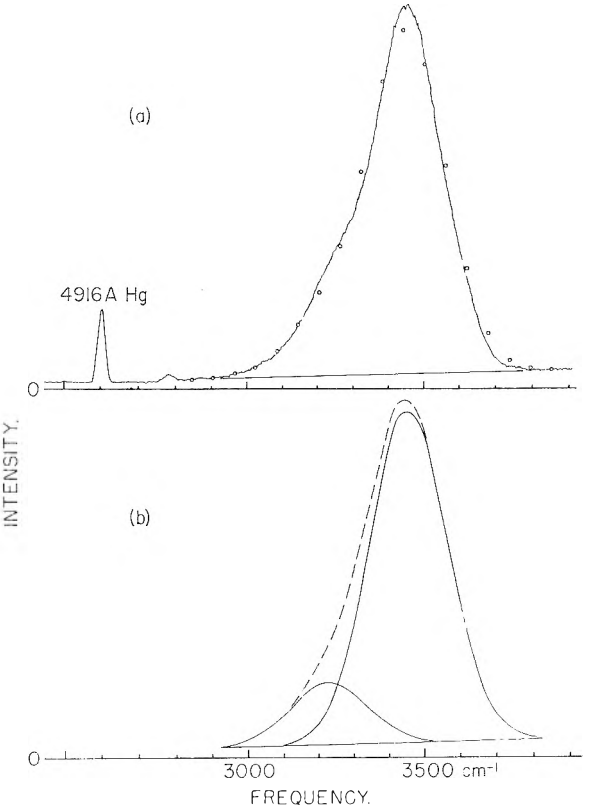

Fig. 2.—The Raman spectrum of 3.5 *M* KBr in the OH stretching region. (a) The solid curve is the recorded spectrum while the circles are in the calculated values. (b) The component bands (solid) and their sum (dashed).

(3) J. W. Ellis and B. W. Sorge, *J. Chem. Phys.*, **2**, 559 (1934).

(4) For a review, see N. Ockman, *Phil. Mag. Supp.*, **7**, 199 (1958).

(5) (a) R. D. Waldron, *J. Chem. Phys.*, **26**, 809 (1957); (b) R. Araujo and D. F. Hornig, unpublished.

(6) W. R. Busing and D. F. Hornig, "Symposium on Molecular Structure and Spectroscopy," Ohio State University, June, 1951.

(7) D. H. Rank and J. S. McCartney, *J. Opt. Soc. Am.*, **38**, 279 (1948).

TABLE I

PARAMETERS OF THE GAUSSIAN CURVES WHICH, WHEN SUMMED, APPROXIMATE THE SPECTRA IN THE OH STRETCHING REGION
The A's and H's Are in cm.$^{-1}$ and the B's Are in Arbitrary Units.

Sample	Band I			Band II			Band III			Band IV			Band V[a]			RMS deviation[b]	No. of points included
	A_I	H_I	B_I	A_{II}	H_{II}	B_{II}	A_{III}	H_{III}	B_{III}	A_{IV}	H_{IV}	B_{IV}	A_V	H_V	B_V		
H_2O	3450	153	114.6	3225	153	66.7										2.0	18
0.5 *M* KBr	3450	153	131.6	3225	153	63.7										1.7	17
1.5 *M* KBr	3450	153	152.8	3225	153	52.5										1.6	19
2.5 *M* KBr	3450	153	180.3	3225	153	41.7										2.1	18
3.5 *M* KBr	3450	153	204.2	3225	153	37.1										2.7	17
3.0 *M* HCl	3450	153	144.8	3225	153	56.2	3025	410	5.8							1.6	28
6.0 *M* HCl	3430	153	179.2	3210	153	45.2	3025	410	13.6							1.0	31
9.0 *M* HCl	3430	153	131.0	3210	153	38.1	3025	410	19.4							1.5	33
11.4 *M* HCl	3410	153	126.0	3190	153	29.7	3025	410	30.3							1.1	36
3.5 *M* KOH	3450	153	106.8	3225	153	53.8				3025	410	12.0	3610	49	12.0	1.2[c]	23[c]
7.0 *M* KOH	3450	153	93.4	3225	153	45.6				3025	410	21.8	3605	49	19.4	1.3[c]	24[c]
10.5 *M* KOH	3450	153	72.7	3225	153	36.3				3025	410	29.1	3595	49	26.2	1.6[c]	24[c]
14.2 *M* KOH	3450	153	56.0	3225	153	28.0				3025	410	38.4	3595	48	34.1	1.7[c]	24[c]

[a] Obtained graphically by subtracting other bands from spectra. [b] Expressed as per cent. of peak height of entire band. [c] Only points with $\nu < 3450$ cm.$^{-1}$ were used.

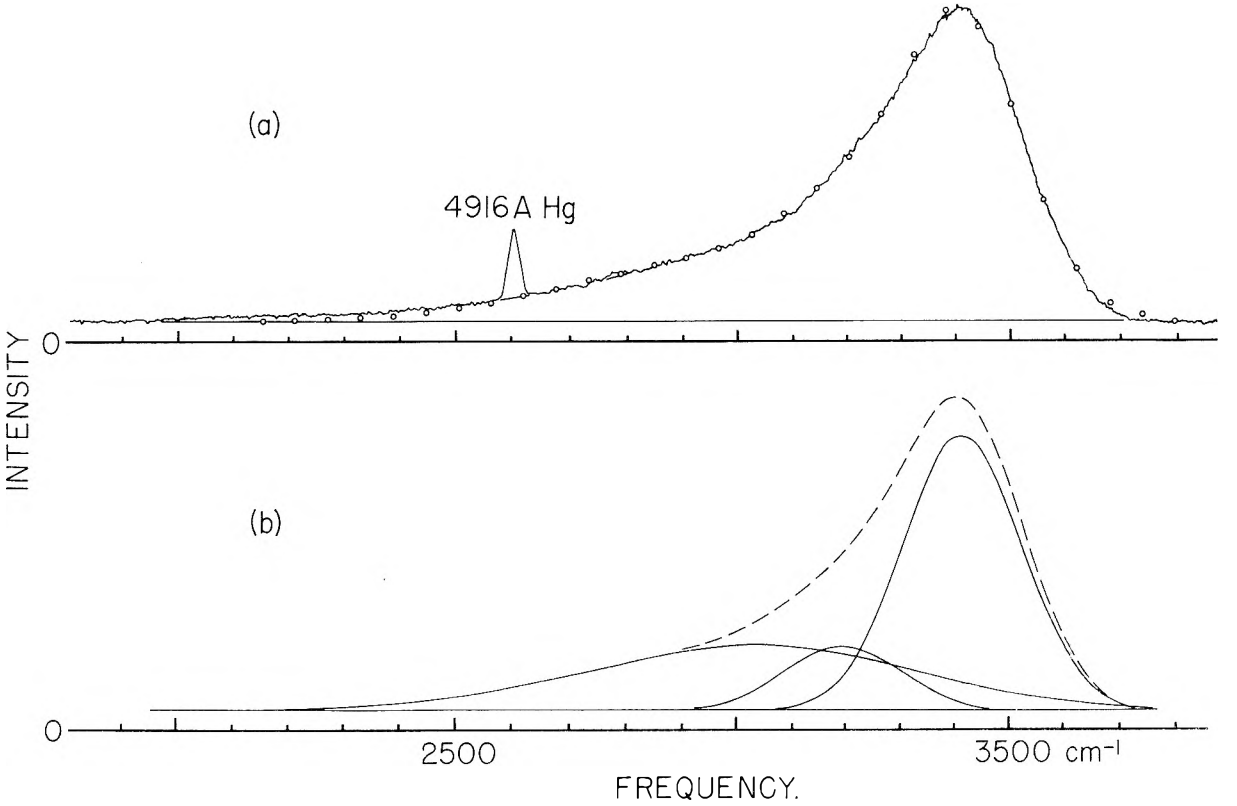

Fig. 3.—The Raman spectrum of 11.4 *M* HCl in the OH stretching region. (a) The solid curve is the recorded spectrum while the circles are the calculated values. (b) The component bands (solid) and their sum (dashed).

impurities, and the clarity of all the solutions was checked by visual observation in the illuminated cell. The concentrations of the nearly saturated solutions were determined by weighing the KBr used and by titration of the HCl and KOH The remaining samples were prepared by accurate dilution.

One unpolarized and two polarized spectra of each sample were observed in the region of the OH stretching fundamental and also in the lower frequency bending and combination region. For the unpolarized and polarized high frequency bands, respectively, spectral slit widths of 16 and 26 cm.$^{-1}$ and time constants of 0.07 and 0.5 min. were used. All the low frequency observations were made with a spectral slit width of 46 cm.$^{-1}$ and a time constant of 0.5 min. A scanning rate of about 46 cm.$^{-1}$/min. was used for all of the spectra reported here.

The polarized spectra were obtained by wrapping polaroid around the sample tube so that the direction of the transmitted electric vector was either parallel or perpendicular to the axis of the sample. No baffles were used to collimate the exciting light, but, instead, the observed depolarization ratios were corrected for convergence by the method of Rank and Kagarise,[8] using CCl_4 as a standard.

Unfortunately the spectra were observed during a period in which a silver plating for the elliptical reflectors in the source was being tested. Although the initial reflectivity of these mirrors was very good they were found to tarnish severely, especially in proximity to the HCl solutions. In order to correct for the resulting intensity changes a standard spectrum of water was obtained five times during the course of the measurements. On the basis of this calibration all the results reported here have been adjusted to the same intensity scale except that the spectra show in Figs. 1–4 were traced directly from the recorder charts and therefore remain uncorrected.

(8) D. H. Rank and R. E. Kagarise, *J. Opt. Soc. Am.*, **40**, 89 (1950).

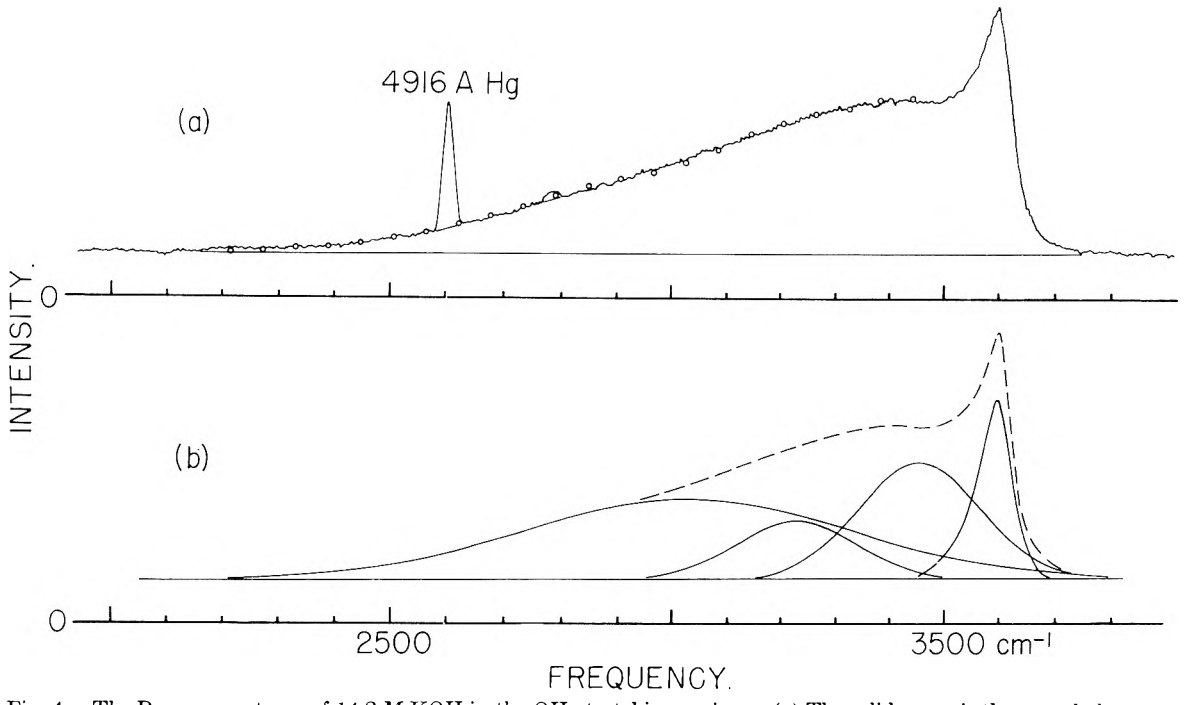

Fig. 4.—The Raman spectrum of 14.2 *M* KOH in the OH stretching region. (a) The solid curve is the recorded spectrum while the circles are the calculated values. (b) The component bands (solid) and their sum (dashed).

Analysis of the Spectra in the OH Stretching Region.—Figures 1a, 2a, 3a and 4a show the broad bands found in the OH stretching region of water, 3.5 *M* KBr, 11.4 *M* HCl and 14.2 *M* KOH, respectively. Because these figures were traced directly from the original charts they show the amount of continuous background and random fluctuations which were present. The relative intensities of the spectra are not correct, however, because of the changes in the source mentioned above. For the analysis which is described below it was assumed that the true spectra could be separated from the background by drawing a straight line across the base of the bands as shown in the figures. The Hg lines at 4916 and 4960 Å. were eliminated in a similar way.

Water and KBr Solutions.—The form of these bands suggest that they can be approximated by the sum of two Gaussian curves, neglecting any contribution from a third (high frequency) peak. The total intensity at each frequency, ν, would then be given by

$$I(\nu) = B_{\mathrm{I}} \exp[(\nu - A_{\mathrm{I}})/H_{\mathrm{I}}]^2 + B_{\mathrm{II}} \exp[(\nu - A_{\mathrm{II}})/H_{\mathrm{II}}]^2$$

The A's are the central frequencies of the bands, the B's are a measure of their intensities, and the H's are proportional to the widths of the bands. The width of each band at half height is $1.66H$.

For water and for each of the four KBr solutions the selection of the best values for the six parameters was made by the method of least squares. The intensity of the band above the assumed background was measured at each of about 18 frequencies across the band and multiplied by a correction factor as described above. Estimated values of the parameters were used for a rough fit and corrections to these were found by solving the six normal equations. While the resulting values of the B's varied widely with changing KBr concentration it was found that the values of the A's and the H's were almost constant for the five spectra and that no trend appeared in the deviations from their average values. This means that the spectra of water and KBr solutions can be approximated by the sum of two Gaussian bands which vary in intensity as the concentration of salt is changed but which do not change in position or band width. The average value of the A's and H's (weighted according to the value of B found in each case) are $A_{\mathrm{I}} = 3450$ cm.$^{-1}$, $A_{\mathrm{II}} = 3225$ cm.$^{-1}$, and $H_{\mathrm{I}} = H_{\mathrm{II}} = 153$ cm.$^{-1}$. Fixing these parameters at their average values, new values of B_{I} and B_{II} were then found for the water spectrum and for each of the four KBr solution spectra by the method of least squares. These results are listed in Table I together with the root mean square deviation of the measured intensity from that calculated, expressed as a per cent. of the peak intensity of the band. The calculated values are shown as circles in Figs 1a and 2a while Figs. 1b and 2b show the form of the Gaussian bands and their sum. The integrated intensities of the two bands (proportional to the products BH) are plotted against concentration in Fig. 5. These results will be discussed below.

HCl Solutions.—It seemed reasonable to suppose that the spectra of HCl solutions would include bands similar to those found in water and salt solutions plus a contribution from OH_3^+ ions. It was clear that the water peaks alone would not be sufficient to describe the long trailing low frequency shoulder, and by graphical trial and error it was found that this shoulder could be approximated by a broad Gaussian curve (band III) with $A_{\mathrm{III}} = 3025$ cm.$^{-1}$ and $H_{\mathrm{III}} = 290$ cm.$^{-1}$. It was also found that the spectrum of 11.4 *M* HCl could not be fitted satisfactorily unless the center of Band I was shifted from 3450 to 3410 cm.$^{-1}$ and that of band II was also lowered to 3190 cm.$^{-1}$. The intensities

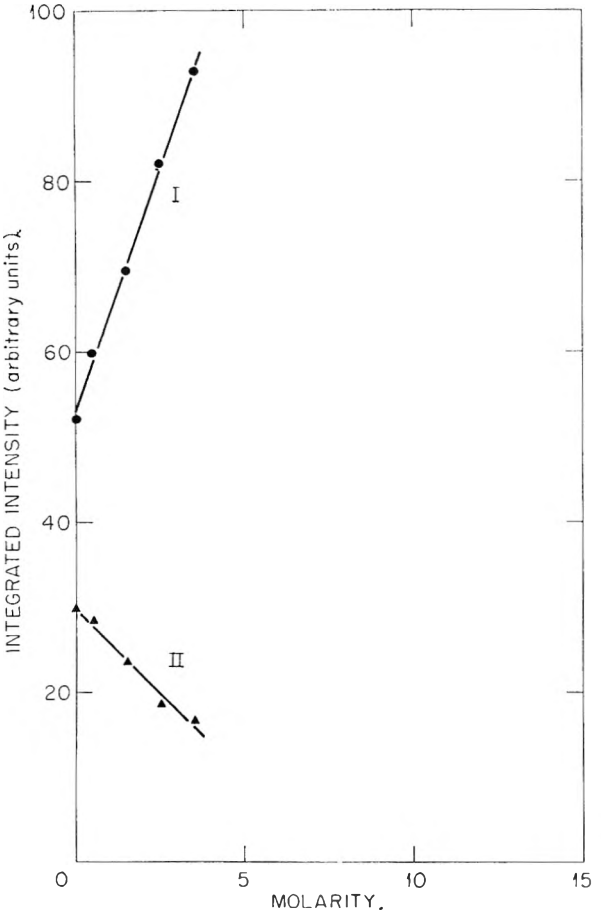

Fig. 5.—Integrated intensities of the components of the OH stretching band as a function of the concentration of KBr. Roman numerals are the band numbers as defined in the text.

(the B's) of the three bands were then determined by the method of least squares. Because of the approximate way in which the A's and H's were found it is not possible to say that they are certainly the best values. The root mean square deviation of the calculated intensities from the measured ones is only about 1% of the peak height, however, and the calculated points plotted in Fig. 3a give an indication of the fit obtained. The band contours are shown in Fig. 3b.

The spectra of the less concentrated HCl solutions were approximated by trying various positions for bands I and II and selecting those which gave the best fit. The parameters are listed in Table I, and the integrated intensities of the three bands are plotted against concentration in Fig. 6. The results will be discussed below.

KOH Solutions.—In addition to bands I and II, the analysis of the KOH solution spectra requires the inclusion of bands designated IV and V. The former describes the low frequency trailing shoulder, and because of the similarity of this feature for KOH and HCl it appeared reasonable to assume that $A_{IV} = A_{III}$ and $H_{IV} = H_{III}$. The fit obtained in this way seems to justify this somewhat arbitrary procedure.

Band V is a relatively sharp peak near 3600 cm.$^{-1}$ and undoubtedly represents the OH^- stretching

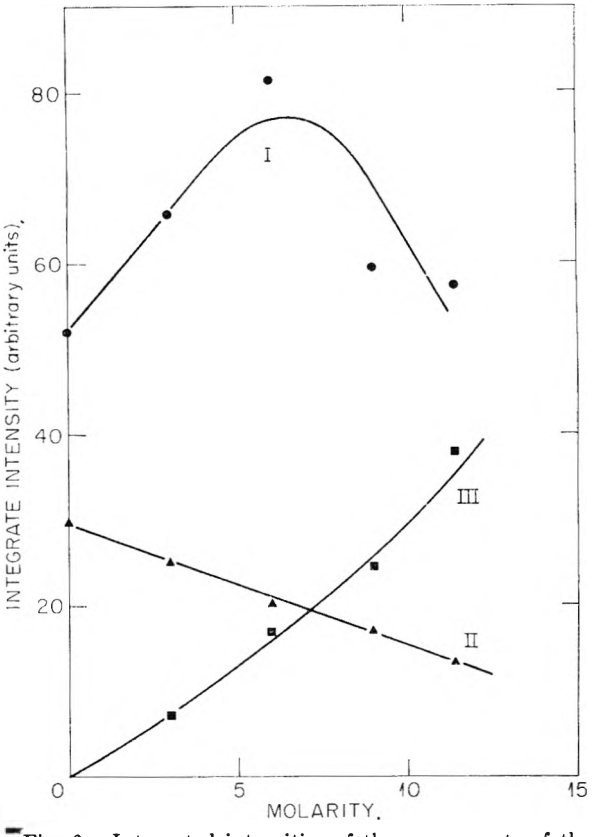

Fig. 6.—Integrated intensities of the components of the OH stretching band as a function of the concentration of HCl. Roman numerals are the band numbers as defined in the text.

vibration.[9] The least squares calculation to determine the B's was made using only points of frequency less than 3450 cm.$^{-1}$ and including only bands I, II and IV. The complications which would have been introduced by considering band V were thus avoided. The form of the latter was then determined by difference and A_V, H_V and B_V were found by measuring the plots of band V. Figures 4a and 4b show the calculated points and the forms of the component bands for 14.2 M KOH. The parameters are listed in Table I and Fig. 7 shows the integrated intensity of the bands as a function of concentration.

Depolarization Ratios.—Using the A's and H's found above, the B's for the parallel and perpendicular spectra were found by the method of least squares. The depolarization factor, ρ, for each band was then computed as the ratio of the parallel and perpendicular intensities, $\rho_I = B_I(\parallel)/B_I(\perp)$. These results were then corrected for the convergence of the exciting light by the method of Rank and Kagarise.[4] For each of the KOH spectra band V was again determined by difference, and its depolarization factor was taken as the ratio of the planimetered areas of the parallel and perpendicular bands.

The results for the various solutions are listed in Table II together with an average for each band which was computed by weighting each measurement according to the value of $B(\perp)$ from which it

(9) In LiOH·H_2O, for example, this band is found at 3574 cm.$^{-1}$. See L. H. Jones, *J. Chem. Phys.*, **22**, 217 (1954).

TABLE II

THE DEPOLARIZATION RATIOS OF THE BANDS IN THE OH STRETCHING REGION.
These values have been corrected for convergence by the method of Rank and Kagarise[2]

Sample	ρ_I	ρ_{II}	ρ_{III}	ρ_{IV}	ρ_V
H_2O	0.450	0.145			
0.5 *M* KBr	.452	.146			
1.5 *M* KBr	.460	.121			
2.5 *M* KBr	.464	.087			
3.5 *M* KBr	.467	.035			
3.0 *M* HCl	.440	.261	0.20		
6.0 *M* HCl	.459	.387	.30		
9.0 *M* HCl	.462	.579	.50		
11.4 *M* HCl	.435	.566	.588		
3.5 *M* KOH	.410	.218		0.52	0.63
10.5 *M* KOH	.339	.356		.51	.33
14.2 *M* KOH	.394	.243		.595	.34
Weighted av.	0.449 ± 0.013	0.20 ± 0.09	0.46 ± 0.10	0.56 ± 0.03	0.38 ± 0.07

was obtained. It will be seen that the results for band I are remarkably consistent. The factors for the other bands are reasonably constant with the larger deviations from the average occurring for samples in which the particular bands made only a small contribution, *e.g.*, band I in the concentrated KBr and HCl solutions, band III in the dilute HCl solutions, and bands IV and V in 3.5 *N* KOH.

Treatment of the Low Frequency Bands.—The study of the bands at 2115 and at 1640 cm.$^{-1}$ was complicated by their low intensity as compared with the background. Moreover, the 1640 cm.$^{-1}$ band is coincident with the OH stretching band which is excited by the 4047 Å. Hg line in spite of the filter solution. It was again assumed that the background could be approximated by a straight line and the intensity above this line was measured at regular intervals. The shape of the OH stretching band was known in each case from the previous measurements and a constant fraction of this band was subtracted from the measured intensity. The differences were then plotted and the solid curves in Figs. 8 and 9 (water and 3.5 *M* KBr, respectively) are typical of the results. The dashed curves show the size and shape of the OH stretching bands which were subtracted. The baseline of the 1640 cm.$^{-1}$ band was taken as a straight line drawn between the two minima while the x-axis was taken as the baseline for the 2115 cm.$^{-1}$ band. The integrated intensities were obtained by planimetering the bands and correcting for variations in the source intensity as described above. The band widths at half height were measured and the central frequencies were found by bisecting the bands at half height. These results are listed in Table III together with the average frequencies and band widths. In Fig. 10 the intensities of the 1640 cm.$^{-1}$ band are plotted against concentration for water and the three kinds of solutions.

The polarized spectra were treated in the same way and the depolarization factors were taken as the ratios of the measured areas. The values, corrected for convergence, are given in Table IV. The fact that most of these ratios are greater than the theoretical maximum of 6/7 probably means that we have overcorrected for the OH stretching band. Subtracting too much of a polarized band will tend to increase the observed depolarization factor of the remaining band.

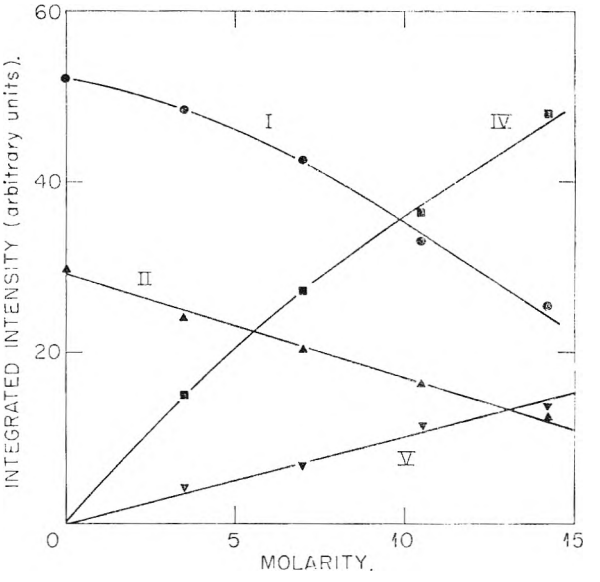

Fig. 7.—Integrated intensities of the components of the stretching band as a function of the concentration of KOH. Roman numerals are the band numbers as defined in the text.

Discussion

The most striking feature of these Raman spectra is the width of the O–H stretching band which is several times greater than that usually associated with fundamental vibrations. Cross, Burnham and Leighton[2] have assumed that the band is a composite of many individual frequencies, each due to a particular configuration of water molecules. While our results do not contradict this assumption we have shown that a simpler postulate, that of two broad Gaussian bands, will approximate the spectra of water and KBr solutions. The widths of these component bands, about 250 cm.$^{-1}$ at half height, are about the same as those of the O–H stretching band in the Raman spectrum of HOD (in D_2O)[5] but are considerably broader than the 80 cm.$^{-1}$ found for the infrared bands of hydrogen bonded crystals such as H_3BO_3[10] and H_2O_2.[11]

TABLE III

FREQUENCIES (CM.$^{-1}$), BAND WIDTHS AT HALF HEIGHT (CM.$^{-1}$), AND INTEGRATED INTENSITIES (ARBITRARY UNITS) OF LOW FREQUENCY BANDS

Sample	Bending vibration			Combination band		
	Frequency	Width	Intensity	Frequency	Width	Intensity
H_2O	1633	110	6.7	2130	260	4.3
0.5 *M* KBr	1640	120	9.3	2155	230	3.6
1.5 *M* KBr	1640	120	13.4	2130	260	4.1
2.5 *M* KBr	1640	120	16.8	2100	250	6.1
3.5 *M* KBr	1630	115	20.8	2075	225	8.2
3.0 *M* HCl	1625	140	12.2	2120	230	4.0
6.0 *M* HCl	1625	110	15.8	2100	210	4.0
9.0 *M* HCl	1620	120	15.1	2110	235	3.6
11.4 *M* HCl	1620	125	21.1	2110	210	5.1
3.5 *M* KOH	1643	145	8.6	[a]		
7.0 *M* KOH	1650	130	7.8			
10.5 *M* KOH	1656	130	6.3			
14.2 *M* KOH	1667	140	7.0			
Av.	1638 ± 10	125 ± 8		2115 ± 15	235 ± 13	

[a] Not observed because of a high background and noise level from KOH solutions.

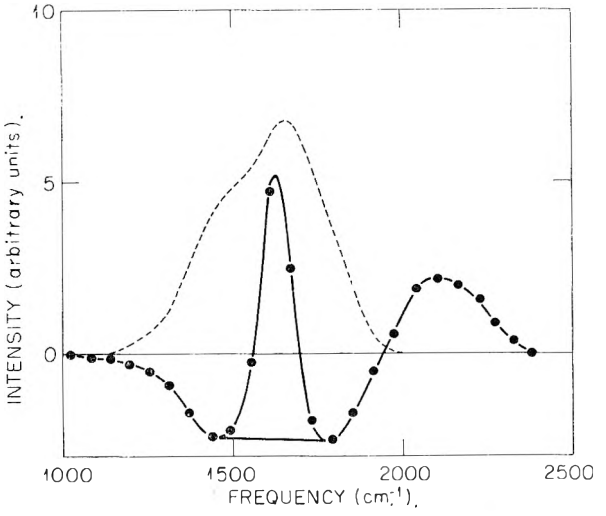

Fig. 8.—The low frequency bands in water. The solid curve shows the spectrum after correcting for background and for the OH stretching band excited by the 4047 Å. Hg line. The dashed curve shows the assumed shape and size of the latter.

TABLE IV

THE DEPOLARIZATION RATIOS OF THE LOW FREQUENCY BANDS

Sample	ρ for 1640 cm.$^{-1}$	ρ for 2115 cm.$^{-1}$
H_2O	1.0	0.8
3.5 *M* KBr	1.3	[a]
11.4 *M* HCl	0.9	1.0
14.2 *M* KOH	[a]	[a]

[a] These values could not be observed because of an excessive noise level.

On the basis of our polarization measurements we may say, in agreement with Cross, Burnham and Leighton[2] and contrary to earlier conclusions,[12-14] that the antisymmetric stretching vibration of water makes no significant contribution to these Raman spectra. That vibration should have a depolarization factor of 6/7.

The Effect of Salts on the Structure of Water.—It has long been known that dissolved salts affect the Raman spectrum of water in a way which is similar to the effect of increased temperature and it has generally been assumed that both these effects are the result of the breakdown of the associated water structure.[14-19] That increasing temperature does have such an effect on the structure of water is well known.[20]

Evidence for the effect of dissolved salts on the structure of water has been summarized by Frank and Evans[21] who considered such properties as the partial molar entropy of water in solutions, the viscosity of solutions, and the partial molar heat capacities of solutes in water. They concluded that many ions tend to alter the crystallinity of water and that in the case of the alkali and halide ions the structure breaking effect increases with increasing ionic radius. Cesium and iodide ions decrease the crystallinity greatly while lithium or fluoride ions have little effect on the long range order in water.

Lyons[22] has examined the Raman spectra of equimolar solutions of alkali halides in both H_2O and D_2O, determining for each solution the intensity ratio of bands corresponding to our Bands I and II. He found that the ions studied (Li^+, K^+, Cs^+, Cl^-, Br^- and I^-) fell into the proper order if the intensity ratio (Band I/Band II) was considered to be a measure of the breakdown of the solvent structure.

Suhrmann and Breyer[23] have found that the effect of salts on the near infrared spectrum of water is similar to that of increased temperature[24] and

(10) D. F. Hornig and R. C. Plumb, *J. Chem. Phys.*, **26**, 637 (1957).
(11) R. L. Miller and D. F. Hornig, *ibid.* (in press).
(12) R. Ananthakrishnan, *Proc. Ind. Acad. Sci.*, **3A**, 201 (1936).
(13) J. H. Hibben, *J. Chem. Phys.*, **5**, 166 (1937).
(14) J. H. Hibben, "The Raman Effect and its Chemical Applications," Reinhold Publ. Corp., New York, N. Y., 1939, Chapter 22.
(15) I. R. Rao, *Proc. Roy. Soc.* (*London*), **130A**, 489 (1931).
(16) Z. Ollano, *Z. Physik.*, **77**, 818 (1932).
(17) I. R. Rao, *Phil. Mag.*, **17**, 1113 (1934).
(18) Cabannes and J. Riols, *Compt. rend.*, **198**, 30 (1934).
(19) J. Burnham and P. A. Leighton, *J. Am. Chem. Soc.*, **59**, 424 (1937).
(20) J. D. Bernal and R. H. Fowler, *J. Chem. Phys.*, **1**, 515 (1933).
(21) H. S. Frank and N. W. Evans, *ibid.*, **13**, 507 (1945); see in particular pp. 521-528.
(22) P. A. Lyons, private communication.
(23) R. Suhrmann and Breyer, *Z. physik. Chem.*, **B20**, 17 (1933).

they too have interpreted this as a result of breakdown in the structure. They also found that the structure breaking properties of the alkali halides generally increased with increasing ionic radius.

Brady and Krause[25,26] have studied the X-ray scattering from concentrated KCl, KOH and LiCl solutions and concluded that K^+ goes into the water structure without distortion whereas Li^+ and Cl^- both produce distortion. Although OH^- seems to distort the water structure very little, Brady concludes that OH^- is six coördinated.

Many workers[14] have reported that the O–H band of water has a component centered at 3600 cm.$^{-1}$, but we have not attempted to include this band in our analysis. Careful examination of Fig. 1a reveals a small hump in this region of the water spectrum, and at high temperatures the maximum is known to shift to this frequency.[1] It is clear that our bands I and II would not be sufficient to approximate the high temperature spectrum and it is possible that the poorer fit in the case of 3.5 *M* KBr can be partly attributed to our failure to consider a third component.

Figure 10 shows that the band at 1640 cm.$^{-1}$, the bending vibration of the water molecule,[14] shows a marked increase in intensity with the addition of KBr. If the intensity of this band is accepted as another criterion of the structure breaking effect of a solute then, referring again to Fig. 10, we may say that HCl has less effect than the same concentration of KBr while KOH has practically no effect on the structure. This conclusion regarding hydroxides is in contradiction to that reached by Hibben from his studies of the lattice vibrations in water, but it is in harmony with viscosity studies[27] which indicate that the hydroxide ion has only a small structure breaking effect, as does the isoelectronic fluoride ion.

The Spectra of HCl and KOH Solutions.—The relatively sharp peak found at 3600 cm.$^{-1}$ in the spectra of KOH solutions is undoubtedly the stretching frequency of the hydroxide ion.[14] Vibrations in this region are found in the infrared and Raman spectra of solid alkali hydroxides.[28] The band is polarized as is to be expected.

The most interesting feature of the HCl and KOH solution spectra is the existence of a low frequency trailing shoulder in the two cases. The origin for band III in the HCl solutions is almost certainly associated with the OH_3^+ ion or some more highly polymerized species of protonated water. Its central frequency is not far from the upper OH_3^+ stretching frequency found in crystalline hydronium halides, OH_3NO_3[29] or OH_3ClO_4,[30] and the entire band is similar to that ascribed by Falk and Giguere[31] to the OH_3^+ ion in the infrared spectrum of HCl solutions.

Referring to Fig. 6 we note that with the addition of HCl to water bands I and II at first increase and

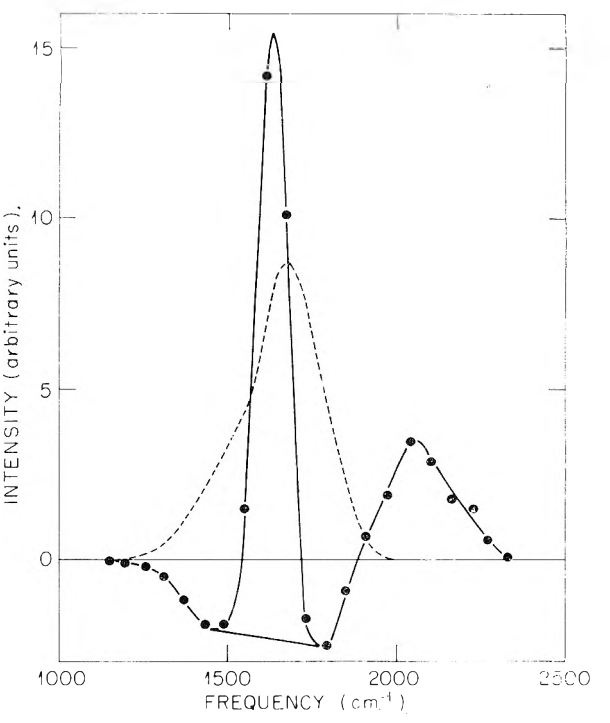

Fig. 9.—The low frequency bands in 3.5 *M* KBr. The solid curve shows the spectrum after correcting for background and for the OH stretching band excited by the 4047 Å. Hg line. The dashed curve shows the assumed shape and size of the latter.

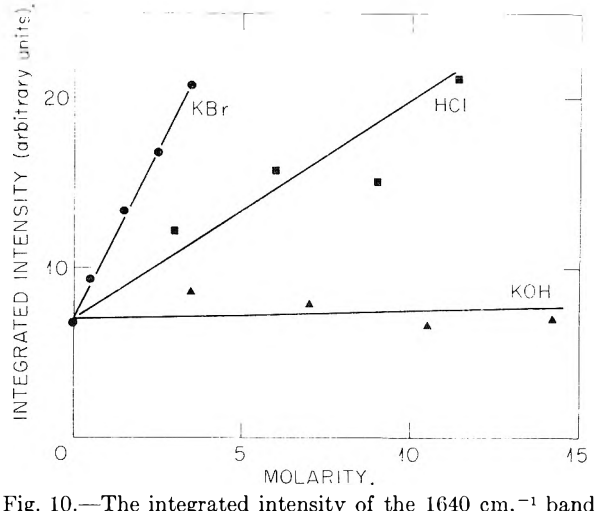

Fig. 10.—The integrated intensity of the 1640 cm.$^{-1}$ band as a function of solute concentration.

decrease, respectively, but less markedly than in KBr solutions of the same concentration. This is to be expected because the structure breaking effect of Cl^- is less than that of Br^-. At still higher concentrations the intensity of band I begins to fall off sharply. If our previous conclusion as to the origin of band III is accepted then we can interpret this decrease as due to the decrease in concentration of un-ionized water molecules so that an appreciable fraction of the intensity has been transferred from band I to band III, that of the OH_3^+ ions.

The origin of the broad low frequency band IV, in the KOH solutions is not absolutely certain. The sharpness of band V, the OH^- stretching vibration,

(24) J. R. Collins, *Phys. Rev.*, **26**, 771 (1925).
(25) G. W. Brady and J. T. Krause, *J. Chem. Phys.*, **27**, 304 (1957).
(26) G. W. Brady, *ibid.*, **28**, 464 (1958).
(27) E. C. Bingham, *J. Phys. Chem.*, **45**, 885 (1941).
(28) For a summary see B. A. Phillips and W. R. Busing, *ibid.*, **61**, 502 (1957).
(29) D. E. Bethell and N. Sheppard, *J. Chem. Phys.*, **21**, 1421 (1953).
(30) J. T. Mullhaput and D. F. Hornig, *ibid.*, **24**, 169 (1956).
(31) M. Falk and P. A. Giguere, *Can. J. Chem.*, **35**, 1195 (1957).

is evidence that the OH^- hydrogens are not strongly hydrogen bonded. This is also the case in the crystals of the anhydrous alkali hydroxides.[32] In the crystalline hydrates of alkali hydroxides, too, the OH^- ions apparently do not enter into hydrogen bonds *via* their hydrogens[9] since the OH^- line is fairly sharp. On the other hand, the stretching region of the water molecules does include frequencies as low as those of band IV. X-Ray structure studies[33] show that the shortest hydrogen bonds in $LiOH \cdot H_2O$, 2.69 Å., are those between a water oxygen and one from OH^-. Therefore it seems likely that the lowest frequencies are those of H–O–H. . . OH^- bonds. A parallel interpretation of the present spectra seems reasonable, that each OH^- ion involves at least one water molecule in a strong hydrogen bond. The similarity between bands III and IV in HCl and KOH, respectively, is intriguing, but no common origin is apparent at present.

Figure 7 shows that the addition of KOH to water brings about a steady decrease in the intensity of band I. We would not expect to find an initial enhancement of intensity because, as we have already seen, KOH does not have much tendency to break down the water structure. The steady decrease in band I may then be attributed to the hydrogen bonding of H_2O molecules to OH^- which we have postulated to explain the increase of band IV. No obvious explanation of the effect of KOH on the intensity of band II suggests itself. We can only point out that in these concentrated solutions band II forms only a small fraction of the total spectrum and therefore our figures for its intensity may be in error. Band V, the hydroxide ion stretch, increases with concentration as is to be expected.

In summary, the solution of either KBr or HCl in water produces a considerable increase in the total Raman scattering intensity of the water in the region of the O–H stretching frequencies. In both cases the low frequency component at 3250 $cm.^{-1}$ decreases in intensity while the intensity of the high frequency component at 3450 $cm.^{-1}$ increases strikingly. The effect on both bands is more marked with KBr and this fits well the notion that the structure breaking effect of the large ion, Br^-, is greater than that of Cl^-.

HCl solutions also show a broad low frequency band which is attributed to OH_3^+ and as the concentration of HCl is increased its intensity grows at the expense of both of the water bands.

KOH solutions show only a steady decrease in the intensity of the water bands as the concentration is increased. At the same time the intensity of the OH^- stretching band as well as that of the broad low frequency band attributed to H_2O molecules coördinated to OH^- grows steadily.

Finally, it should be remarked that these striking changes in the intensity of the water bands in the presence of dissolved salts makes them quite unsuitable as intensity standards for any quantitative Raman studies in aqueous solution.

(32) W. R. Busing, *J. Chem. Phys.*, **23**, 933 (1955).
(33) R. Pepinsky, *Z. Kryst.*, **A102**, 119 (1940).

SPECTROSCOPIC STUDIES ON THE COLOR REACTION OF ACID CLAY WITH AMINES

By Hajime Hasegawa

Department of Applied Chemistry, Faculty of Science and Engineering, Waseda University, Tokyo, Japan

Received July 25, 1960

In order to study the mechanism of the color reaction of acid clay with benzidine and tetramethylbenzidine in benzene, the absorption spectra of colored acid clay and their changes with *p*H were measured between 350 and 1000 mμ, by a new spectrophotometric technique for translucent materials. For identifying the colored products, the absorption spectra of meriquinoid compound of tetramethylbenzidine were also measured, changing the *p*H of the solutions, and the results were compared with the spectra of colored acid clay. The analysis of the results thus obtained revealed that the quinoidal and meriquinoidal forms of benzidine or tetramethylbenzidine are responsible for the color reactions with acid clays.

Introduction

It has been known that the addition of a solution of benzidine to acid clay develops a blue color in water and a green color in benzene. The color reaction in water was attributed to the formation of benzidine ion on the lattice of acid clay minerals.[1–3] However, these studies were limited to the color reaction in water, and no spectroscopic study has been made on the color reactions in benzene, so that the structure of the green pigment formed by the color reaction has not been clarified yet. In the present study, the mechanism of the color reaction in benzene was studied spectroscopically, using benzidine and tetramethylbenzidine as the reagent. The absorption spectra of the colored acid clay suspensions were measured by a new technique of using an opal glass,[4] which was recently developed for obtaining sharp absorption bands of translucent materials. In order to interpret the spectra obtained and to look into the mechanism of the color reaction, the oxidation of tetramethylbenzidine without acid clay were studied separately, and two oxidized forms of tetramethylbenzidine were identified spectroscopically. It was found that these oxidized forms play an

(1) P. Meunier, *Compt. rend.*, **217**, 449 (1943).
(2) N. E. Vedeneeva, *Akad. sci. U.S.S.R., Kolloid Zhur.*, **12**, 17 (1950); *Doklady Akad. Nauk S.S.S.R.*, **98**, 585 (1954); **105**, 1248 (1955).
(3) E. I. Kotov, *Optika i Spektroskopiya*, **1**, 500 (1959).
(4) K. Shibata, "Spectrophotometry of Translucent Biological Materials—Opal Glass Transmission Method," in "Methods of Biochemical Analysis," D. Glick, ed., Vol. VII, Interscience Publishers, Inc., New York, N. Y., 1959.

important role in the color reaction of acid clay with tetramethylbenzidine. The results on the color reaction of acid clay with benzidine were discussed in its relation to the color reaction with tetramethylbenzidine.

Experimental

Apparatus.—Absorption spectra were observed with a Shimadzu Spectrophotometer Model QB-50, using cell of 1 mm., thick for the observation of the strongly colored suspensions; 0.3 ml. of a benzene solution of benzidine or tetramethylbenzidine (concentration, 0.001 g./ml.). The absorption spectrum of the colored suspension was measured by the opal glass transmission method,[4] using the same clay suspension without amine as the reference. The observations of solutions were carried out by a common method, using a 1 cm. cell.

Reagents.—Benzidine and tetramethylbenzidine used for the color reaction were purified, recrystallizing them from the benzene solution. The dark green meriquinoid compound (1:1 complex of the base and the quinoidal form) of tetramethylbenzidine was prepared from the HCl salt of tetramethylbenzidine, using $FeCl_3$ as the oxidizing agent.

Acid Clay.—Three different clays were used; one is a natural Itoigawa Clay of montmorillonite group and the others are the clays prepared by treating the natural clay with acid or alkali under the following condition. (i) Acid-treated clay: The natural clay was boiled in 3 *N* solution of hydrochloric acid for 3 hours. The boiling mixture consisted of 1 part acid clay and 5 parts of the HCl solution. After the treatment, the clay was washed with water and dried. (ii) Alkali-treated clay: the natural clay was boiled in 1 or 3 *N* solution of sodium hydroxide for 3 hours. The treated clay was washed and dried.

Results and Discussion

(I) The Coloration with Benzidine.—When the suspensions of natural and acid-treated clays are mixed with a benzidine solution, a greenish yellow color appeared. The absorption spectra of these colored suspensions are shown by curves A and B in Fig. 1 which indicate that the color reaction with the acid-treated clay is the same as that with the natural clay. The absorption maxima of the observed peaks were located at 440, 780 and 880 mμ, and the peak at 440 mμ was higher than the other bands.

The absorption spectrum of the bright green suspension of alkali-treated clay colored with benzidine is shown by curve C in Fig. 1. As seen from the figure, curve C is different from the spectra (curves A and B) of the colored natural and acid-treated clay. Namely, new absorption bands appeared at 380 and 640 mμ on curve C, and the band at 440 mμ on curves A and B was lowered on curve C of the alkali-treated clay. Furthermore, the bands at 780 and 880 mμ on curve C are higher than the corresponding bands in the spectra of the natural and acid-treated clay.

The clay treated already with acid was boiled in 1 or 2 *N* sodium hydroxide solution. The color reaction of this clay with benzidine was similar to that of the alkali-treated clay. The acid-treated clay was boiled in 5 *N* NaCl or KCl solution, and the color reaction with benzidine was measured spectroscopically. The spectrum of the colored clay showed that the treatment with the NaCl or KCl solution has no effect on the color reaction of the acid-treated clay. In other words, the replacement of proton on the acid clay by sodium or potassium ion is not essential for the difference between the color reactions exhibited by acid- and alkali-treated clays.

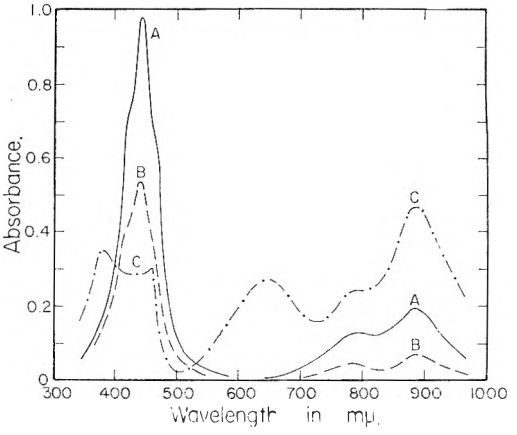

Fig. 1.—Absorption spectra of acid clays colored with benzidine: curve A, natural clay; curve B, acid-treated clay (3 *N* hydrochloric acid); curve C, alkali-treated clay (1 *N* sodium hydroxide).

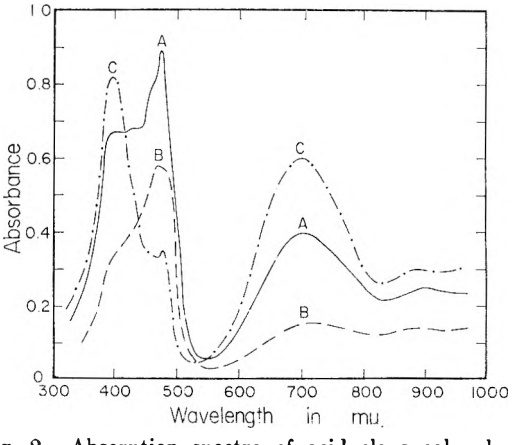

Fig. 2.—Absorption spectra of acid clays colored with tetramethylbenzidine: curve A, natural clay; curve B, acid-treated clay (3 *N* hydrochloric acid); curve C, alkali-treated clay (3 *N* sodium hydroxide).

Apart from the mechanism of the color reaction thus observed, the color reaction with benzidine in benzene may be classified into two; one is the reaction with the natural or acid-treated clay and the other is the reaction with the alkali-treated clay.

(II) The Coloration with Tetramethylbenzidine.—The absorption spectra of natural, acid-treated and alkali-treated clays colored with tetramethylbenzidine are shown by curves A, B and C in Fig. 2, respectively. The color reaction with tetramethylbenzidine may be grouped also into two different reactions. In the Soret region, the spectra (curves A and B) show a high band near 470 mμ and relatively lower bands at 400 and 430 mμ, whereas the band at 400 mμ on curve C is much higher than the other bands and practically no band was observed at 430 mμ in the spectrum. Another characteristic of the spectrum for the alkali-treated clay is that the bands near 700 and 880 mμ are higher than those for the natural and acid-treated clays.

Let us next compare those bands observed for the clays colored with tetramethylbenzidine with those observed with benzidine. Since the acid-treated clay colored with benzidine has characteristic band at 440 mμ, the band observed near 470 mμ with tetra-

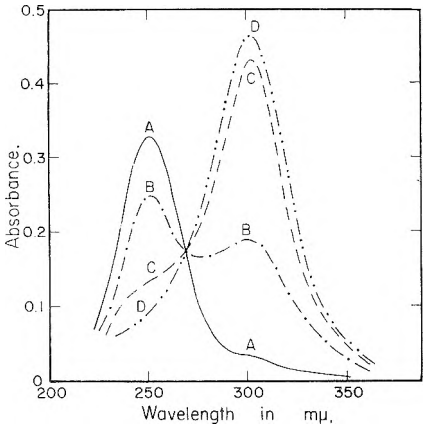

Fig. 3.—Effect of *p*H change on the absorption spectra of tetramethylbenzidine (concentration, 1.67×10^{-9} mole/liter) in 30% ethanol solution: curves A, B, C and D represent the solutions of *p*H values, 2.02, 3.00, 4.12 and 5.60, respectively.

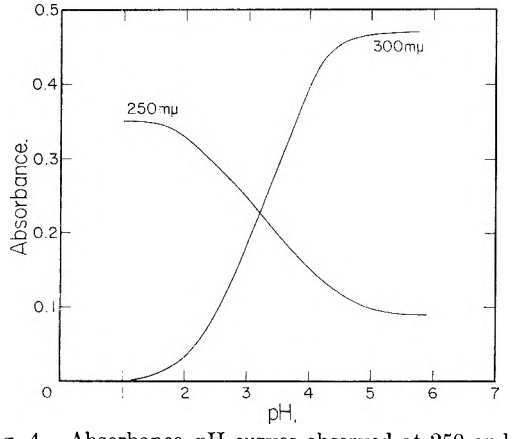

Fig. 4.—Absorbance–*p*H curves observed at 250 and 300 mμ of the solution of tetramethylbenzidine (concentration, 1.67×10^{-9} mole/liter).

methylbenzidine may correspond to the band at 440 mμ. This correspondency may be supported by the following calculation. The shift of the band from 440 to 470 mμ amounts to 0.14×10^4 cm.$^{-1}$ in wave number. If we allow the same amount of shift on the basis of wave number also for the other bands at 380, 640, 780 and 880 mμ, which are observed for the colored alkali-treated clay with benzidine, the hypothetical wave lengths of the maxima for the bands with tetramethylbenzidine become 402, 704, 877 and 1000 mμ, in which the first three values agree well with the observed values, 400, 700 and 880 mμ. The presence of the band corresponding to the calculated maximum of 1000 mμ was not confirmed because of the low sensitivity of the measurement, but was clearly observed in the spectrum of meriquinoidal form of tetramethylbenzidine as demonstrated later.

(III) The Absorption Spectra of Tetramethylbenzidine.—The spectra of tetramethylbenzidine were measured at 18°, changing *p*H of the solution. For the measurement, tetramethylbenzidine was first dissolved in 1 part of ethanol and was diluted with 2 parts of water. A small amount of a hydrochloric acid or sodium hydroxide solution was added successively to the solution, and the progressive change of the spectrum and the *p*H of the solution were measured. The total amount of acid or alkali added was negligible to the total amount of the solution. The concentration of tetramethyl benzidine in the solution was 1.67×10^{-9} mole/liter. Example of the spectra obtained by the observation are shown in Fig. 3, which indicates that the acid solution has a band at 250 mμ and the alkaline solution has a peak at 300 mμ. The presence of the clear isosbestic point revealed that the transformation effected by the change of *p*H is a simple process from one form to the other. This transformation process was studied more precisely by following the change of the absorbance at 250 and 300 mμ, which are shown by sigmoid curves in Fig. 4. These curves show that the *p*H range for the transformation is approximately 2.0, which suggest that one mole of hydrogen ion is involved in the transformation of one mole of tetramethylbenzidine. Since the alcoholic solution of tetramethylbenzidine has the band at 300 mμ, the band observed at 300 mμ for the alkaline solution must be due to the absorption by the non-ionized form of tetramethylbenzidine. We shall designate this form of tetramethylbenzidine as T for the convenience of the further description. Since one hydrogen ion is involved in the transformation into the acid form, the form in the acid solution may be represented as TH^+. Probably, hydrogen ion may be attached on one of two dimethylamino radicals of the molecule. Assuming equation 1 for the transformation, we obtain equations 2 and 3 under the equilibrium condition, where K_1 and C stand for the equilibrium constant and the sum of the concentrations, T and TH^+, respectively.

$$T + H^+ \rightleftarrows TH^+ \tag{1}$$

$$K_1 = \frac{[T]\,[H^+]}{[TH^+]} \tag{2}$$

$$pK = pH + \log \frac{C - [T]}{[T]} \tag{3}$$

The pK value estimated from the curves in Fig 4 was 3.23, so that K_1 is 5.88×10^{-4}.

(IV) The Absorption Spectra of Meriquinoid Compound of Tetramethylbenzidine.—The spectrum of meriquinoid compound of tetramethylbenzidine was measured in 30% ethanol solution, changing the *p*H of the solution at 18°. The total amount of meriquinoid compound was 1.67×10^{-9} mole/liter. The result shown in Fig. 5 indicates that the acid solution has two bands at 250 and 470 mμ. When the *p*H of the solution is raised, five bands appeared at 300, 400, 700, 880 and 990 mμ. In addition to T and TH^+, the following compounds may exist in the solution of meriquinoid compound; *i.e.*, the quinoidal form, Q of tetramethylbenzidine, the meriquinoid compound, TQ. One may, therefore, assume the following equations for the solution in addition to equations 1, 2 and 3.

$$T + Q \rightleftarrows TQ \tag{4}$$

$$K_2 = \frac{[T]\,[Q]}{[TQ]} \tag{5}$$

In order to study the transformation in the solution of meriquinoid compound, the changes of the heights of the representative bands of TH^+, T, Q

and TQ at 250, 300, 470 and 880 mμ, respectively, were scrutinized, changing the *p*H of the solution, and the result is shown in Fig. 6. The absorbance change at 400, 700 and 990 mμ with *p*H are similar to that of the band at 880 mμ. Therefore, it may be assumed that these bands are due to the absorption by the same compound, TQ. Then the band at 880 mμ was selected from among these bands as representative band of TQ. In Fig. 6, the absorbance change at 250 mμ represents the change of TH^+. The increase of absorbance at 300 mμ between *p*H 1.5 and 4.5 may, therefore, indicate the formation of T from TH^+. By a separate experiment, the spectrum of the ethanol solution of the quinoidal form, Q was observed, and the band was located at 470 mμ. The decrease of absorbance at 470 mμ in Fig. 6 proves that the concentration of Q decreases with the increase of *p*H, being in parallel with the increase of absorbance at 880 mμ. This fact suggests that T formed by the dissociation of TH^+ combines with Q, resulting the formation of TQ.

The presence of three marked isosbestic points at 275, 410 and 525 mμ in Fig. 5 is an indication that the whole transformation process may be represented by equations 1 and 4, and no other side reaction occurred below *p*H 4.5. If the total amount of the meriquinoid compound dissolved in unit volume is designated as C, we obtain the relation

$$C = [TH^+] + [T] + [TQ] = [Q] + [TQ] \quad (6)$$

From equations 2, 5 and 6, we have

$$K_2 = \frac{[T]}{\frac{K_1 C}{[T]\,(K_1 + [H^+])} - 1} \quad (7)$$

we may calculate the value of K_2 from the absorbance change at 300 mμ with below *p*H 4.5 in Fig. 6, and the calculated value was 3.58×10^{-5}.

If the solution is more than *p*H 4.5, another complication arises. Namely, the absorbance at 300 mμ increased and the absorbance values at 470 and 880 mμ decreased with the further increase of *p*H. In order to see the mechanism of reaction in this *p*H range, pure quinoidal form of tetramethylbenzidine was dissolved in 30% ethanol solution and the change of the spectrum of the solution with *p*H was observed. With the increase of *p*H, the band at 470 mμ of the acid solution of Q decreased and a new band appeared near 300 mμ. This process was found to be irreversible, and formaldehyde was identified as a product of this reaction with alkali. The release of formaldehyde from Q suggests the decomposition of Q in the process. The same decomposition process may be considered for the alkaline solution of TQ, so that the increase of absorbance at 300 mμ more than *p*H 4.5 may be attributed to the absorption of the decomposition product and the decrease at 470 mμ may indicate the decomposition of Q, which will naturally cause the lowering of the band of TQ at 880 mμ.

(V) **Discussion.**—As seen from section 1 and 2, the color reactions of acid clay with benzidine or tetramethylbenzidine in benzene may be classified into two; one is the reaction of the natural or

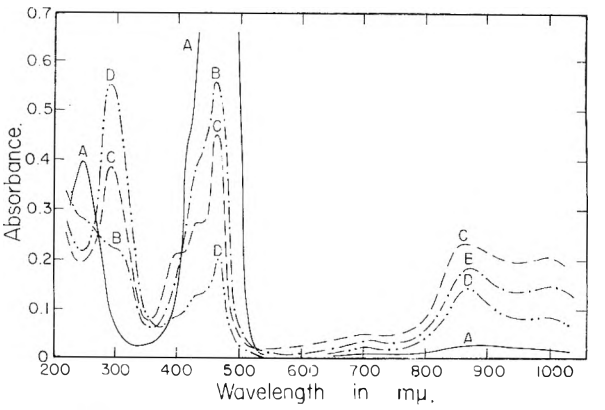

Fig. 5.—Effect of *p*H change on the absorption spectra of meriquinoid compound of tetramethylbenzidine (concentration, 1.67×10^{-9} mole/liter) in 30% ethanol solution: curves A, B, C and D represent the solutions of *p*H values, 2.02, 3.42, 4.80 and 6.16, respectively.

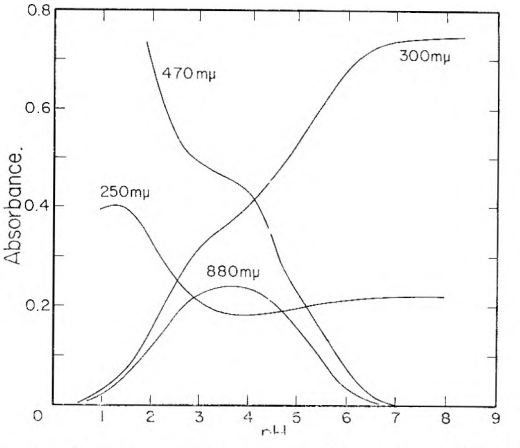

Fig. 6.—Absorbance–*p*H curves observed at 250, 300, 470 and 880 mμ of the solution of meriquinoid compound of tetramethylbenzidine (concentration, 1.67×10^{-9} mole/liter).

acid-treated clay and the other is the reaction of the alkali-treated clay. The positions of the characteristic bands of natural and acid-treated clay colored with tetramethylbenzidine agree with the band positions of quinoidal form of tetramethylbenzidine. The band positions of alkali-treated clay with tetramethylbenzidine agree with those of its meriquinoidal form. It may be, therefore, concluded that the quinoidal form or a compound with electronic structure similar to that of the quinoidal form is responsible for the color developed with natural and acid-treated clay, and the meriquinoidal form for the alkali-treated clay. The band positions of clays colored with benzidine are shifted toward shorter wave lengths from those observed for the derivatives of tetramethylbenzidine. However, the differences between their corresponding bands were found to be the same in terms of wave number, which bears evidence that the colors developed with benzidine are due to the formation of quinoidal or meriquinoidal form of benzidine, or the formation of compounds having the electronic structures similar to the benzidine derivatives. The further investigation is awaited to correlate the mechanism of the color reactions in

benzene found in the present study to that of the color reaction in water studied by various workers.

Acknowledgment.—The author wishes to express his hearty thanks to Prof. K. Yamamoto and Prof. K. Shibata for their kind guidance and valuable suggestions throughout this investigation.

METAL COMPLEXING BY PHOSPHORUS COMPOUNDS. III. THE COMPLEXING OF CALCIUM BY IMIDODI- AND DIIMIDOTRIPHOSPHATE

BY R. R. IRANI AND C. F. CALLIS

Monsanto Chemical Company, Research Department, Inorganic Chemicals Division, St. Louis 66, Mo.

Received July 27, 1960

The stabilities of the complexes of imidodiphosphate, diimidotriphosphate and their monohydrogen forms with calcium have been evaluated from nephelometric titrations in the presence of oxalate, as a function of *p*H, temperature and ionic strength. The free-energy changes at 25°, taking unit mole fraction standard states, for the formation of the complexes $CaP_2O_6(NH)^{-2}$, $CaHP_2O_6(NH)^{-1}$, $CaP_3O_8(NH)_2^{-3}$ and $CaHP_3O_8(NH)_2^{-2}$ from the corresponding ions were found to be −5.6, −2.2, −7.4 and −3.9 kcal./mole, respectively. For the complexing of calcium by $P_2O_6(NH)^{-4}$ and $P_3O_8(NH)_2^{-5}$, the enthalpies were evaluated to be −5.7 and −9.1 kcal./mole, respectively, with the corresponding entropy changes being about zero.

Introduction

In a previous paper[1] of this series, the thermodynamics of association of linear polyphosphates with calcium was reported. In order to investigate the effect on complexing of the groups connecting the phosphorus atoms in the linear chain, the complexing of calcium by imidophosphates is reported in this paper.

Experimental

Chemicals.—The hexahydrate sodium salts of imidodi- and diimidotriphosphate were used as the source for the imidophosphate anions. These sodium salts were kindly supplied by Dr. M. L. Nielsen of Monsanto's Research and Engineering Division. Infrared spectra[2] as well as nuclear magnetic resonance and wet chemical analyses[3] established that the imidodi- and diimidotriphosphate were better than 98 and 96% pure, respectively.

The imidophosphates were converted to the tetramethylammonium salts using ion exchange, as previously described. However, due to their relatively low hydrolytic stability, the stock solutions were maintained at room temperature and a *p*H of 13, and were used within a few days, during which time no significant hydrolysis is expected.[4]

The tetramethylammonium bromide and hydroxide were Eastman Kodak reagent grade. All other chemicals were C.P. grade.

Procedure.—The nephelometric procedure, previously described,[1] was utilized as a measure of the competition for the calcium ions between the oxalate and imidophosphate anions. However, the temperature of the solutions was controlled to better than ±0.1° using a highly sensitive heat-sensing element.[5] The concentrations of calcium and oxalate were taken into account in calculating the total ionic strength which was made up to the desired value using tetramethylammonium bromide.

No P_2O_5 was detected in the precipitates formed upon addition of a slight excess of Ca^{++} to a solution containing oxalate and imidophosphate at the end-point. X-Ray as well as wet-chemical analyses also established the precipitates to be $CaC_2O_4 \cdot H_2O$.

Results and Discussion

Table I gives the cc. of 8.86×10^{-2} *M* $Ca(NO_3)_2$ that must be added to solutions containing tetramethylammonium oxalate and imidophosphate to reach the point of incipient precipitation of CaC_2O_4. Using previously described procedures,[1] it was found that the experimental data are best fit by assigning only one complexing site per calcium, as shown in Table II. Obviously, a negative number of phosphorus atoms per site is meaningless. Therefore, the general equation for the association reaction is as follows, omitting charges on the ions

TABLE I

SUMMARY OF DATA FOR THE Ca^{++}–H^+–$C_2O_4^{=}$–IMIDOPHOSPHATE SYSTEM[a]

Temp., °C.	*p*H	Imidophosphate (C_1) × 10^{-3}, *M*	Oxalate (C_2) × 10^{-2}, *M*	Cc. (*y*) of 8.86×10^{-2} *M* Ca soln. to nephelometric end-point at ionic strengths of 0.1	0.3	1.0
		Imidodiphosphate				
25	12.0	2.33	0.745	2.42	..	1.65
			1.49	1.73	1.62	1.26
			2.23	1.44	0.95	0.90
	9.5	2.33	0.372	0.71	..	1.21
			.745	0.35	..	0.67
37	12.0	2.33	.745	..	..	1.08
			1.49	1.85	..	0.88
			2.23	1.30	..	..
50	12.0	2.33	0.745	..	..	1.24
			1.49	1.76	..	0.74
			2.23	1.53	..	..
		Diimidotriphosphate				
25	12.0	1.71	0.745	4.24	..	3.77
			1.49	4.05	3.47	3.67
			2.23	3.88	2.80	3.12
	9.0	1.71	0.372	3.46	..	..
			0.745	2.68	..	1.55
			1.49	..	..	1.00
37	12.0	1.71	0.745	..	..	3.24
			1.49	3.40	..	2.84
			2.23	3.26	..	..
50	12.0	1.71	0.745	..	..	3.22
			1.49	3.55	..	3.02
			2.23	3.32	..	..

[a] The total volume of the solution was 250 ml. in all cases.

(1) R. R. Irani and C. F. Callis, *J. Phys. Chem.*, **64**, 1398 (1960).

(2) J. V. Pustinger, W. T. Cave and M. L. Nielsen, *Spectrochim. Acta*, **11**, 909 (1959).

(3) M. L. Nielsen, private communication.

(4) O. T. Quimby, A. Narath and F. H. Lohman, *J. Am. Chem. Soc.*, **82**, 1099 (1960).

(5) For details, *cf.* R. R. Irani and C. F. Callis, *J. Phys. Chem.*, **64**, 1741 (1960).

$$Ca\cdot(H_2O)_a + S(\theta)\cdot(H_2O)_b = CaS(\theta)\cdot(H_2O)_c + (a + b - c)H_2O \quad (1)$$

where a, b and c are hydration numbers, and θ is the number of phosphorus atoms per calcium-complexing site, S. As shown in Table II, the value of θ was found to be two and three for imidodiphosphate and diimidotriphosphate, respectively, immaterial of whether the imidophosphate had a hydrogen bound to it or not. Therefore, the simple mass action expression for combination of ligand with metal ion applies here.

TABLE II

SITES OCCUPIED BY ONE CALCIUM

Complexing anion	No. of sites per calcium	Calcd. no. of phosphorus atoms per site (θ) Range	Average
Imidodiphosphate	1	1.8 to 2.3	2.0
	2	−4 to 0.3	..
	3	−10 to −3	..
Diimidotriphosphate	1	2.5 to 3.6	3.3
	2	1.0 to 3.0	2.1
	3	−0.5 to 2.6	..

At the point of incipient precipitation of CaC_2O_4, it can be shown[1] that

$$\frac{C_2}{\left(\frac{C_1A}{yz} - 1\right)} = K_{sp}\left\{\frac{1}{\beta_{CaS(\theta)}[1 + [H^+]/\beta_{HS(\theta)}]} + \frac{1}{\beta_{CaHS(\theta)}[1 + \beta_{HS(\theta)}/[H^+]]}\right\} \quad (2)$$

where C_1 and C_2 are the molar concentrations of imidophosphate and oxalate, respectively, A the total volume of solution in ml., and y is the ml. of a z molar Ca^{++} solution that must be added to reach the point of incipient precipitation of CaC_2O_4. K_{sp} is the solubility product of CaC_2O_4 at the appropriate ionic strength and temperature, and $\beta_{CaS(\theta)}$ and $\beta_{HS(\theta)}$ are the apparent dissociation constants of the calcium and hydrogen imidophosphates, respectively

$$\beta_{CaS(\theta)} = \frac{[Ca^{++}][S(\theta)]}{[CaS(\theta)]} \quad (3)$$

$$\beta_{HS(\theta)} = \frac{[H^+][S(\theta)]}{[HS(\theta)]} \quad (4)$$

$$[Ca^{++}] = K_{sp}/[C_2] \quad (5)$$

At a pH of 12, only the non-hydrogen phosphate species exist,[6] namely

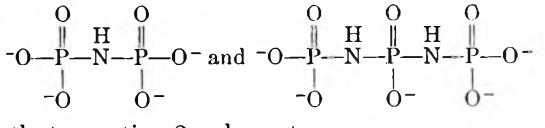

so that equation 2 reduces to

$$\frac{C_2}{\left(\frac{C_1A}{yz} - 1\right)} = \frac{K_{sp}}{\beta_{CaS(\theta)}} \quad (6)$$

because $\beta_{CaHS(\theta)}$ is much larger than $\beta_{CaS(\theta)}$ and the ratio $[H^+]/\beta_{HS(\theta)}$ is much smaller than 1. The data at a pH of 12 in Table I were interpreted with equation 6 to obtain the apparent dissociation constants of the calcium imidodiphosphate and calcium diimidotriphosphate at several combinations of temperatures and ionic strengths. The results are given in Table III; the errors shown as ± are the statistical 95% confidence limits.

The data in Table I at 25° and lower pH values were then utilized to evaluate the dissociation constants of the calcium monohydrogen imidophosphate species using equation 2 and the already evaluated dissociation constants of the calcium imidophosphates and the previously determined acid dissociation constants[4] at the same temperature and ionic strength. The results are also given in Table III.

Attempts to evaluate the stability of the possible complex between calcium and the first homolog the imidophosphate family, namely, the anion of phosphoramidic acid were unsuccessful with the procedure employed in this work, due to unfavorable competition with the oxalate ion. Within the sensitivity of the procedure, the presence of up to 0.5 M phosphorimidate did not change the point of precipitation of calcium oxalate, so that the possible calcium phosphorimidate complex must have a dissociation constant greater than 10^{-3}.

The thermodynamic dissociation constants at 25, 37 and 50° are shown in Table IV and were evaluated by extrapolating the apparent dissociation constants to infinite dilution.[1,7] Since the extrapolation covers a wide concentration range, larger errors consistent with previous extrapolations (1) are assigned to these constants. Table IV is also a compilation of the changes at 25° in free energy, $\Delta F°$, enthalpy, $\Delta H°$, and entropy, $\Delta S°$, accompanying the association reaction typified by equation 1. These thermodynamic quantities were computed from the constants in Table III as previously described.[1] However, they were corrected to the absolute scale of a hypothetical unit mole fraction standard state by adding 2.4 kcal. and subtracting 7.9 e.u. from the $\Delta F°$ and $\Delta S°$ obtained for the hypothetical one molal standard state.[8]

In contrast with the complexing of calcium by pyrophosphate and tripolyphosphate, the enthalpies for the association reactions of calcium with imidophosphates are significantly more exothermic and the entropies of association are much lower. These differences reflect having an –NH– rather than an –O– linking the phosphorus atoms. In the case of the calcium pyrophosphate and calcium tripolyphosphate complexes, the large entropy changes accompanying association contributed significantly toward the free-energy term and were attributed to release of waters of hydration.

For the complexing of calcium by imidodiphosphate and diimidotriphosphate, one of two possibilities may be valid. The first possibility is to assume that neither waters of hydration were released nor any significant structural changes were involved, and assume that the stability of the calcium imidophosphates is solely due to some type of direct bonding. However, calculation of Bjerrum radii[9,10] for the distance of closest approach between calcium and imidodiphosphate or diimidotriphos-

(6) R. R. Irani and C. F. Callis, *ibid.*, **65**, in press (1961).

(7) A. E. Martell and M. Calvin, "Chemistry of the Metal Chelate Compounds," Prentice-Hall, Inc., New York, N. Y., 1952, p. 133.

(8) A. W. Adamson, *J. Am. Chem. Soc.*, **76**, 1578 (1954).

(9) N. Bjerrum, *Kgl. Danske Selskab.*, **7**, No. 9 (1936).

(10) R. M. Fuoss and C. A. Kraus, *J. Am. Chem. Soc.*, **55**, 1019 (1933).

TABLE III

THE APPARENT DISSOCIATION CONSTANTS OF CALCIUM IMIDOPHOSPHATES

Calcium complex of	Temp., °C.	Negative log of dissociation constant at ionic strengths of— 0.1	0.3	1.0
Imidodiphosphate	25	5.59 ± 0.07	5.20 ± 0.05	4.59 ± 0.09
	37	5.37 ± .02	.....	4.14 ± .09
	50	5.14 ± .04	.....	3.86 ± .04
Monohydrogen imidodiphosphate	25	3.33 ± .10	.....	3.15 ± .10
Diimidotriphosphate	25	6.74 ± .12	6.11 ± 0.06	5.66 ± .12
	37	6.21 ± .05	.....	5.12 ± .10
	50	6.01 ± .08	.....	4.86 ± .10
Monohydrogen diimidotriphosphate	25	4.44 ± .10	.....	4.16 ± .10

TABLE IV

CHANGES IN THERMODYNAMIC QUANTITIES FOR CALCIUM COMPLEXING BY IMIDOPHOSPHATES

Calcium complex of	Temp., °C.	Negative log of thermodynamic molal dissociation constant	$[\Delta F^0]$,[a,b] kcal.	ΔH^0, kcal.	$[\Delta S^0]$,[a,b] e.u.
Imidodiphosphate	25	6.07 ± 0.1	−5.6 ± 0.1	−5.7 + 0.9	0 ± 3
	37	5.89 ± .1	−6.1 ± .1		
	50	5.76 ± .1	−6.1 ± .1		
Monohydrogen imidodiphosphate	25	3.4 ± .2	−2.2 ± .2	.....	.....
Diimidotriphosphate	25	7.10 ± .2	−7.4 ± .2	−9.1 ± 2	−6 ± 7
	37	6.90 ± .2	−7.4 ± .2		
	50	6.60 ± .2	−7.4 ± .2		
Monohydrogen diimidotriphosphate	25	4.6 ± .2	−3.9 ± .2	.....	.....

[a] Taking the standard state as a hypothetical unity mole fraction. [b] The influence of temperature was taken into account in applying the corrections to obtain the unit mole fraction standard state.

phate yields values of 3.1 and 3.5 Å., respectively, so that bonding by this criterion is ionic rather than covalent.

The second possibility is to assume that waters of hydration were released, together with the formation of a more ordered structure, with both entropy change contributions cancelling one another.

Acknowledgment.—The authors thank Mr. W. W. Morgenthaler for making some of the measurements.

OXIDATION OF AMMONIA IN FLAMES

BY C. P. FENIMORE AND G. W. JONES

General Electric Research Laboratory, Schenectady, N. Y.

Received July 28, 1960

The rate of the reaction of nitric oxide with ammonia has been measured in low pressure flat flames at 1700 to 1900°K. by probe sampling, and simultaneous estimates of [H] obtained. The data support the view that the equilibrium $K[NH_2][H_2] = [NH_3][H]$ is satisfied for small ratios of $[NO]/[H_2]$, and that nitric oxide decays *via* reaction 1, $NO + NH_2 \xrightarrow{k_1} \ldots \rightarrow$ eventually $N_2 + \ldots$, with $k_1/K = 6 \times 10^{10}$ l. mole^{-1} sec.$^{-1}$. Reaction 1 is important in other, superficially different, decompositions of ammonia also. Much nitric oxide is generated in the reaction zone of H_2–NH_3–O_2 flames, probably by attack of O atoms on ammonia, and nitrogen is formed chiefly by reaction 1. Furthermore, residual ammonia survives into the post-flame gas of rich enough ammonia flames and decomposes there, in the absence of appreciable oxygen or nitric oxide, much more slowly than in the reaction zone; and this too may be due to a slow formation of transient nitric oxide followed by rapid 1.

Introduction

Adams, Parker and Wolfhard[1] showed that nitric oxide decays faster in ammonia than in hydrogen flames, and since nitric oxide rapidly scavenges NH_2 radicals according to

$$NO + NH_2 \xrightarrow{k_1} \ldots \longrightarrow \text{eventually } N_2 + \ldots \quad (1)$$

even at room temperature,[2,3] they suggested that the same process occurs in flames. In this paper we show that the decomposition of ammonia in many flames involves reaction 1. If nitric oxide is not supplied as a reactant, it is generated by oxidation of part of the ammonia and then consumed *via* reaction 1.

Adams and co-workers considered that a reaction, NH + NO → N_2 + OH, might be important as well. But under the conditions we used, it was unnecessary to assume an important role for NH radicals.

Experimental

A water-cooled, porous, flat flame burner,[4] mounted in a bell jar with movable quartz probe and quartz coated thermocouple, was fed with reactants metered through

(1) G. K. Adams, W. G. Parker and H. G. Wolfhard, *Disc. Faraday Soc.*, **14**, 97 (1953).

(2) C. H. Bamford, *ibid.*, **35**, 568 (1939).

(3) A. Serewicz and W. Albert Noyes, Jr., *J. Phys. Chem.*, **63**, 843 (1959).

(4) W. E. Kaskan, "6th Symposium on Combustion," Reinhold Publ. Corp., New York, N. Y., 1957, p. 134.

critical flow orifices. Commercial nitric oxide from cylinders contains a trace of nitrogen dioxide and, when mixed with ammonia, forms a solid which tends to plug the porous burner, but this difficulty was overcome by passing the nitric oxide at pressures of several atmospheres through an aluminum coil, 1 m. long by 3 cm. i.d., immersed in a Dry Ice trap.

Gas samples, taken through the fine quartz probe into a sample bottle maintained at 1 mm. pressure or less, were analyzed on a mass spectrometer.

Estimating [H] in the Reaction Zone.—Reaction 1 was studied by adding small amounts of ammonia and nitric oxide to low pressure, fuel-rich N_2O–H_2 flames. In these flames, nitrous oxide decomposes mostly by reaction with H atoms at a known rate[5]

$$-d[N_2O]/dt = 4 \times 10^{11} e^{-16.3/RT} [H][N_2O] \text{ mole l.}^{-1} \text{ sec.}^{-1}$$

and therefore [H] can be estimated in the reaction zone. Figure 1 shows some profiles through a typical flame, without added ammonia or nitric oxide, and illustrates the measurement of [H].

Using the diffusion coefficient plotted, we recast the nitrous oxide profile as the curve for $-d[N_2O]/dt$ at the bottom of the figure,[5] and derive [H] values which approximately double through the reaction zone. The increase may be greater than we have found in other low pressure flames; [H] determined in the same way in mixed H_2–air–N_2O flames appeared more constant.[4]

The constant for the nitrous oxide reaction is based on measurements of [H] *via* the exchange reaction $H + D_2O = HD + OD$; and although such measurements parallel results obtained in other ways, for example from Kaskan's optical measurement of [OH] in the same laboratory,[6] they are smaller in absolute value by about a factor of two. A systematic error, if one exists, could not affect relative [H], however, nor a derived rate constant relative to the constants for the $H + N_2O$ or $H + O_2$ reactions as given in this paper.

Checks of [H] by exchange reactions with D_2 or D_2O[5] in about half the runs showed that the value of the rate constant given above for $H + N_2O \rightarrow N_2 + OH$ remained unchanged.

Since the reaction of added nitric oxide was studied in flames like that plotted in Fig. 1, we should state that a little nitric oxide was formed in this flame. The generated nitric oxide, however, was less than 1/10 of the nitric oxide decomposed in the studies to be described in the next section.

Rate of $NH_2 + NO \rightarrow \ldots \rightarrow N_2 + \ldots$—Figure 2 shows some profiles through the same flame as Fig. 1 except that the pressure was raised to 12 cm. and additions were made to the reactants. For the dotted curves, 0.15 mole of nitric oxide was added per mole of nitrous oxide fed; for the solid curves, the same nitric oxide and also 0.12 mole of ammonia was added. The nitric oxide survived when ammonia was absent, but largely reacted when ammonia was present. At 0.6 cm. from the burner surface, 74% of the added nitric oxide and almost all the added ammonia had disappeared; so the reaction proportions were approximately equimolar.

(5) C. P. Fenimore and G. W. Jones, *J. Phys. Chem.*, **63**, 1154 (1959).

(6) W. E. Kaskan, *Combustion & Flame*, **2**, 286, 229 (1958).

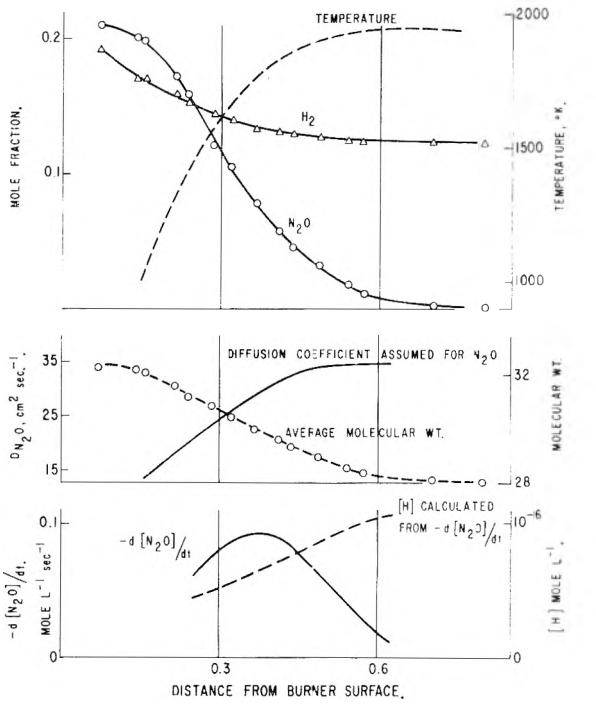

Fig. 1.—Profiles through a flame of $N_2O + 1.6\ H_2 + 2.32$ A burnt at 6 cm. P with a mass flow of 3.56×10^{-3} g. cm.$^{-2}$ sec.$^{-1}$.

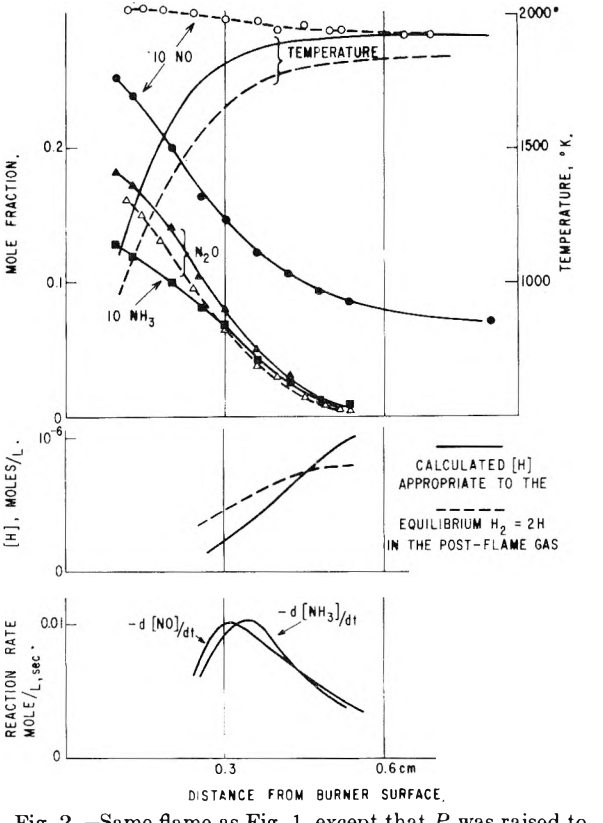

Fig. 2.—Same flame as Fig. 1. except that P was raised to 12 cm. and additives included in the reactants. For dotted curves, 0.15 mole of NO added per mole of N_2O. For solid curves, 0.15 mole of NO and 0.12 mole of NH_3 added per mole of N_2O.

The reaction rates of nitric oxide and ammonia are plotted at the bottom of the figure. They were

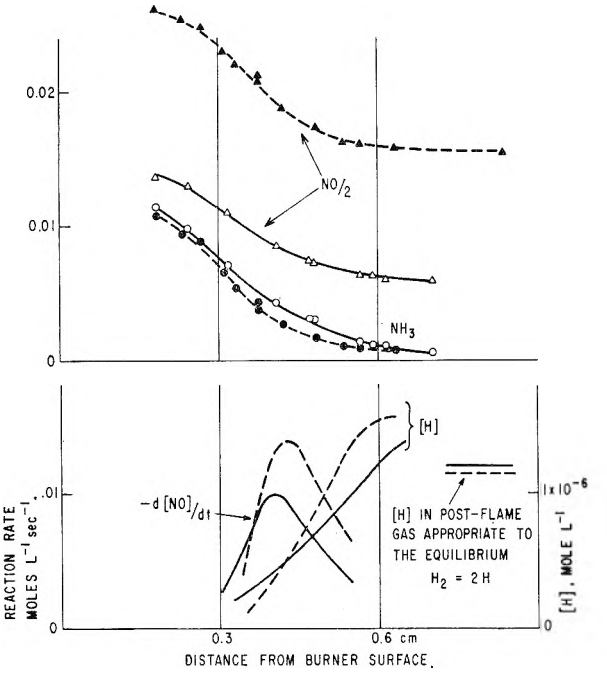

Fig. 3.—Same flame as Fig. 1, burnt at 6 cm. P and additives included. For solid curves, 0.13 NO + 0.06 NH_3 added per mole N_2O. For dotted curves, 0.35 NO + 0.084 NH_3 added per mole N_2O.

obtained by assuming that the diffusion coefficient of Fig. 1 varied inversely at any temperature, both with pressure and with the square root of molecular weight of the species considered. The curve for $-d[NO]/dt$ is the more reliable because the diffusion corrections were smaller.

[H] as obtained from $-d[N_2O]dt$ is also plotted through the reaction zone.

If nitric oxide reacted with ammonia directly, the quantity $-d[NO]/[NH_3][NO]dt$ should be expressible as $Ae^{-E/RT}$ over the distance 0.275 to 0.55 cm. But this is not possible, rather a parallel trend of [H] and of $-d[NO]/[NH_3][NO]dt$ suggests the importance of radical processes.

The possibility that nitric oxide reacts with NH_2 radicals (perhaps *via* $NH_2 + NO \rightarrow NH_2NO \rightarrow NH{=}NOH \rightarrow N_2 + H_2O$) suggests other expressions to test. Either of two functions is essentially constant over the $-d[NO]/dt$ curve in Fig. 2: $-d[NO]/[H][NH_3]dt$ is $5 \pm 1 \times 10^9$ l. mole^{-1} sec.$^{-1}$, with no systematic variation, $-[H_2]d[NO]/[H][NH_3][NO]dt$ is $6 \pm 1 \times 10^{10}$. By varying $[NO]/[H_2]$, one can show that the second function is generally constant but the first is not.

Figure 3 shows two runs in which $[NO]/[H_2]$ was varied. Considerably more nitric oxide and a little more ammonia was fed to the flame represented by the dotted curve, but the traverses for temperature, hydrogen, and nitrous oxide were similar. [H] and $[H_2]$ were nearly the same at the maximum values of $-d[NO]/dt$. In the flame containing 2.2 times more [NO] and 0.6 times as much $[NH_3]$ at the maximum $[d[NO]/dt$, one would expect the maximum to be $2.2 \times 0.6 = 1.3$ times larger if $-[H_2]d[NO]/[H][NH_3][NO]dt$ remains generally constant, and we observe it to be 1.4 times larger. But if $-d[NO]/dt$ were proportional only to $[H][NH_3]$, the solid curve should have had 1.7 times the larger maximum $-d[NO]/dt$, and it does not.

The results from six flames, including the three of Figs. 2 and 3, are recorded in Table I. In every case, the average through the reaction zone of quantities containing $-d[NO]/dt$ extends 0.03 to 0.06 cm. upstream of the maximum value of $-d[NO]/dt$ and 0.15 cm. or more downstream of it. We have not attempted to carry the calculations all the way upstream to $-d[NO]/dt$ approaching zero because this would put a heavy burden on the diffusion corrections.

Table I suggests that reaction 2 is equilibrated in the reaction zone

$$NH_2 + H_2 = NH_3 + H,\ K_2[NH_2] = [NH_3][H]/[H_2] \quad (2)$$

and

$$-d[NO]/dt = k_1[NO][NH_2]$$

so that

$$-[H_2]d[NO]/[H][NH_3][NO]dt = k_1/K_2$$

k_1/K_2 is insensitive to temperature over the range 1700 to 1900°K., and has the approximate value 6×10^{10} l. mole^{-1} sec.$^{-1}$. The insensitivity to temperature is expected; k_1 cannot have a large activation energy if reaction 1 occurs readily in the neighborhood of room temperature,[2,3] and the temperature dependence of equilibrium 2 must be small.

The last entry in Table I gives a smaller k_1/K_2. An obvious explanation is that when [NO], and hence the rate of (1), is increased enough, NH_2 radicals are consumed too quickly for equilibrium 2 to be maintained. An alternate possibility, that sufficiently great [NO] might catalyze the decomposition of nitrous oxide and so lead to an erroneously large [H] and too small a k_1/K_2, can be excluded. Using the [H] and [NO] of the last entry in Table I, and the known rate constant for $NO + N_2O \rightarrow NO_2 + N_2$,[7] one finds that at 1930° this process is a negligibly 160 times smaller than the rate of $H + N_2O \rightarrow N_2 + OH$.

We do not know how NH_2 is maintained in equilibrium with ammonia. Farkas' measurements of the exchange of D_2 with ammonia at 1000°K.[8] suggest that $NH_2 + H_2 \rightarrow NH_3 + H$ would not be fast enough even at 1800°K. But it is possible that the equilibrium $H + H_2O = OH + H_2$ could be fairly well maintained and that $OH + NH_3 \rightarrow NH_2 + H_2O$ and its reverse could also be rapid; and if so, equilibrium 2 would be maintained even if $NH_2 + H_2 \rightarrow NH_3 + H$ and its reverse did not occur at all.

Decay of NH_3 with Little or No Added Nitric Oxide.—It was shown above that no decay of nitric oxide occurred under our conditions except in the presence of added ammonia. If ammonia is added to H_2–O_2 or H_2–N_2O flames, however, much or all of it is destroyed even without added nitric oxide, and at least a transient occurrence of generated nitric oxide is always observed. The observation suggests a possible objection to the interpretation

(7) F. Kaufman and J. R. Kelso, *J. Chem. Phys.*, **23**, 602 (1955).
(8) A. Farkas, *J. Chem. Soc.*, 26 (1936).

TABLE I

SUMMARY OF MEASUREMENTS OF $-d[NO]/dt$ IN PRESENCE OF AMMONIA

Flame P cm.	$[NO]/[NH_3]$ fed in reactants	Values at max. $-d[NO]/dt$ Mole fraction $\times 10^3$ NO	NH_3	H	T, °K.	Av. through the reaction zone $\frac{-d[NO]}{[H][NH_3]dt} \times 10^{-9}$	$\frac{-[H_2]d[NO]}{[H][NH_3][NO]dt} \times 10^{-10}$
12	1.3	14	6.0	0.27	1830	5 ± 1	6 ± 1
10	1.3	12	5.0	.26	1880	7 ± 2	5 ± 1
6	1.4	17	4.0	.85	1720	7 ± 2	7 ± 2
6	2.1	38	2.4	.96	1740	16 ± 2	6 ± 1
6	3.5	67	3.4	0.41	1780	21 ± 1	4.5 ± 0.5
6	4.5	98	1.3	1.5	1930	25 ± 3	3.3 ± 0.4

in the last section: That the observed $-d[NO]/dt$ might not have represented the whole decomposition of nitric oxide; but that part of the ammonia might also have formed nitric oxide which partially decayed, and that our estimate of k_1/K_2 was therefore too small.

We forced this situation, to see what errors it might introduce, by repeating the run of Fig. 2 with added nitric oxide and ammonia, but with the ammonia increased to 1.35 mole per mole of nitric oxide fed. The final temperature was now 130° higher than when less ammonia was fed. The greater addition of ammonia disappeared entirely in the flame, and the nitric oxide surviving was 16% of that fed. On the assumption that part of the ammonia formed nitric oxide and the remainder reacted *via* (1) as NH_2 radicals, the gross $-d[NO]/dt$ would be the average of $-d[NO]/dt$ observed and $-d[NH_3]/dt$ observed. This average was 30% greater than the observed $-d[NO]/dt$ at the point of greatest difference. In the flames discussed in the last section, to which more nitric oxide than ammonia was fed, the greatest difference would be far less than 30%, as indeed it is in Fig. 2. Any error from this cause should be less than the uncertainty indicated by $k_1/K_2 = 6 \pm 1 \times 10^{10}$.

We now want to consider the formation of nitric oxide in ammonia flames not containing added nitric oxide. This can be observed in N_2O–NH_3 or O_2–NH_3 flames, or in either with added hydrogen. It is better to work with oxygen flames, however, since then no question arises about the source of the N atom in the nitric oxide.

Figure 4 shows some profiles through an oxygen flame. Most of the nitrogen must be formed *via* (1), for $d[N_2]/dt$ is a maximum when [NO] is a maximum and these quantities decrease toward zero together even though undecomposed ammonia lives on into the post-flame gas. The peak concentration of nitric oxide is small because of the speed of reaction 1 in the presence of excess NH_2 radicals, but it will be shown below that enough nitric oxide is generated to account for the whole formation of nitrogen *via* reaction 1.

Since nitric oxide is formed rapidly only when oxygen molecules are disappearing rapidly, and almost not at all by the OH or water in the post-flame gas, it is probably formed either from O atoms or O_2 molecules. On the hypothesis that all the nitrogen is formed *via* reaction 1, it can be shown that nitric oxide could not be formed from molecular oxygen, but could arise from attack of O atoms on ammonia molecules. This conclusion is consistent with the literature, for O atoms are known to react with ammonia to give nitrogen oxides, etc., even at room temperature.[9]

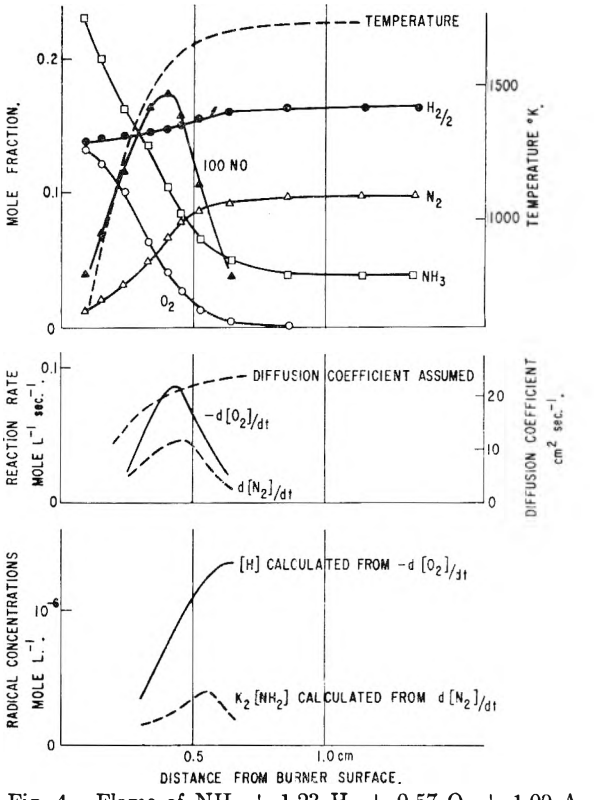

Fig. 4.—Flame of NH_3 + 1.23 H_2 + 0.57 O_2 + 1.09 A burnt at 14 cm. P with a mass flow of 3.85×10^{-3} g. $cm.^{-2}$ $sec.^{-1}$.

The demonstration follows: On the hypothesis that nitrogen is formed *via* reaction 1, half of the ammonia which decomposed did so by forming intermediate nitric oxide. The ammonia fed was 82% consumed. Therefore if nitric oxide derived its oxygen from molecular oxygen, 0.41 mole of molecular oxygen would have had to react per mole of ammonia fed to form nitric oxide; and since only 0.57 mole of molecular oxygen was fed per mole of ammonia, 72% of the molecular oxygen would have had to form nitric oxide and not more than 28% of the oxygen molecules could have reacted by the known reaction, H + O_2 → OH + O, which consumes all the oxygen molecules in pure H_2–O_2 flames and most of it even in many hydrocarbon flames.[10]

(9) P. Harteck and U. Kopsch, *Z. physik. Chem.*, **B12**, 327 (1931). Also, G. E. Moore, K. E. Shuler, S. Silverman and R. Herman, *J. Phys. Chem.*, **60**, 813 (1956).

(10) C. P. Fenimore and G. W. Jones, *ibid.*, **63**, 1834 (1959).

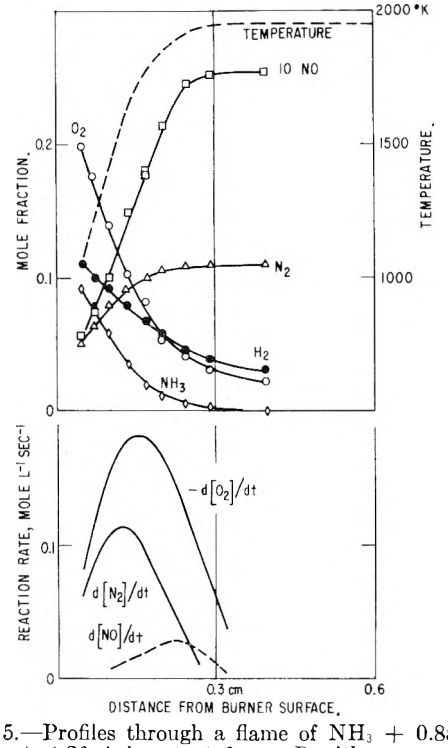

Fig. 5.—Profiles through a flame of NH_3 + 0.85 H_2 + 1.23 O_2 + 1.26 A burnt at 6 cm. P with a mass flow of 4.43×10^{-3} g. cm.$^{-2}$ sec.$^{-1}$.

In the reaction zone of Fig. 4, [H] can be determined in two ways. On our hypothesis that nitrogen is formed by reaction 1 and that equilibrium 2 is maintained for small ratios of [NO]/[H_2], we can write

$$\frac{d[N_2]}{6 \times 10^{10}\,[NO]dt} = K_2[NH_2] = [H][NH_3]/[H_2]$$

The values of $K_2[NH_2]$ obtained from $d[N_2]/dt$ are plotted at the bottom of Fig. 4 and [H] can also be obtained by multiplying these by the observed ratio of [H_2]/[NH_3] at any point.

If all oxygen molecules are destroyed by reaction with H atoms, [H] can also be obtained from the rate of reaction H + O_2 → OH + O. The rate constant is $6 \times 10^{11}\ e^{-18/RT}$ l. mole^{-1} sec.$^{-1}$, a value determined under the same conditions as our constant for H + N_2O → N_2 + OH[5] and also in good agreement with other recent estimates.[11] But if only 28% of the oxygen molecules reacted with H atoms, the upper limit, if nitric oxide derives its oxygen from molecular oxygen, then [H] calculated on the assumption that all oxygen molecules reacted with H atoms should be on the average at least 3.6 times larger than [H] calculated from $d[N_2]/dt$.

Over the region in Fig. 4 where most of the reaction occurs, 0.3 to 0.65 cm. from the burner, [H] from $-d[O_2]/dt$ is 95 ± 10% of the [H] calculated from $d[N_2]/dt$. Therefore, not merely 28% but approximately all of the oxygen molecules must have reacted with hydrogen atoms and nitric oxide could not have been formed by a direct reaction with oxygen molecules, but was probably formed from O atoms.

(11) G. L. Schott and J. L. Kinsey, *J. Chem. Phys.*, **29**, 1177 (1958)

A possible error in this comparison of [H] values should be considered. Flames often contain large excess concentrations of O and OH radicals relative to the thermodynamic equilibrium concentrations, and in such cases an estimate of [H] from $-d[O_2]/dt$ may not be accurate unless the reverse process of oxygen consumption is allowed for, O + OH → H + O_2. This is not a serious objection for the flame of Fig. 4 because the over-all decomposition of ammonia does not form large excess concentrations of radicals when ammonia is in excess. The post-flame gas, for example, from flames with excess ammonia contains only the thermodynamic equilibrium [H], [OH] and [O]. Even in pure O_2–H_2 flames where the reverse process is important, it does not become so until the oxygen is half or more reacted; so if necessary, one could restrict the argument to the first half of the consumption of oxygen and reach the same conclusion, that nitric oxide derives its oxygen from free O atoms.

In the reaction forming nitric oxide, the reaction partner for the O atom must have been present in comparatively large concentration; for of the 0.57 mole of O formed, 0.41 reacted to give nitric oxide despite the fairly rapid competing reaction

$$O + H_2 \xrightarrow{k_3} OH + H \qquad (3)$$

This consideration eliminates NH_2 and NH radicals as reaction partners, and suggests that nitric oxide was formed *via*

$$O + NH_3 \xrightarrow{k_4} \ldots \longrightarrow \text{eventually NO} + \ldots \qquad (4)$$

If so, k_4 must be larger than k_3.

On the assumption that $d[NO]/dt = k_4[O][NH_3] - d[N_2]/dt$; and that [O], which is mostly consumed *via* reaction 4, can be approximated by the steady state $-d[O_2]/dt = [O](k_3[H_2] + k_4[NH_3])$; one can solve Fig. 4 at the point where $d[NO]/dt$ = zero and obtain $k_4/k_3 = 4.2$.

If the ratio of oxygen fed to ammonia is increased enough, too little ammonia remains to destroy all the nitric oxide formed and [NO] rises smoothly through the reaction zone into the post-flame gas. Figure 5 shows one such flame and assuming the same steady state [O] again, though this is more dubious when most O atoms are no longer destroyed by irreversible reaction 4, one can solve

$$d[NO]/dt = -d[N_2]/dt - \frac{k_4[NH_3]\ d[O_2]}{(k_3[H_2] + k_4[NH_3])dt}$$

for k_4/k_3 through the flame. The ratio is found to be 5 ± 1 over the distance 0.125 to 0.275 cm. from the burner, the same as found from Fig. 4.

Table II gives the results of probing three other flames; and shows that for great enough $[O_2]$/[NH_3] fed, at least 40% of the ammonia fed can be recovered as nitric oxide in the products. The large yield of nitric oxide from fuel-lean flames, and its transient existence in flames with excess ammonia, is good evidence that the formation of nitrogen occurs chiefly *via* reaction 1.

The flames summarized in Table II also contained transient nitrous oxide which attained its peak mole fraction at the point where ammonia

TABLE II

NITROGEN OXIDES FORMED FROM REACTANT COMPOSITION $H_2 + 0.45\ NH_3 + 6.26\ (O_2 + A)$, BURNT WITH POST-FLAME TEMPERATURES OF APPROXIMATELY 1500°K.

O_2 used	P, cm.	Moles NO in products per mole NH_3 fed	Peak moles of N_2O[a] in reaction zone per NH_3 fed
2.27	6	0.40	0.048
1.16	8	.24	.039
0.70	12	.08	.027

[a] Obtained by dividing the peak $[N_2O]/[A]$ in the reaction zone by $[NH_3]/[A]$ fed in the reactants.

fell to zero in the reaction zone. This must not be formed in the main path of reaction 1, for the transient nitrous oxide was largest in the flame which gave the greatest recovery of nitric oxide and in which, therefore, reaction 1 took place least. It has been shown by reactants marked isotopically in the nitrogen atoms that the reaction $NH_2 + NO \rightarrow N_2O + \ldots$ does not occur in the scavenging of NH_2 radicals by nitric oxide at room temperature.[12] But a little nitrous oxide might arise from side reactions of HNO either with itself[3,12] or with nitric oxide, and it would not be surprising if reaction 4 involved the intermediate HNO.

Decay of NH_3 in the Post-flame Gas.—The post-flame gas from fuel-rich flames contains residual ammonia if enough is added in the reactants. This should be expected; for if all oxygen is consumed by $H + O_2 \rightarrow OH + O$ and if ammonia in the flame decomposes *via* reaction 4 and 1, each oxygen molecule can destroy only two ammonia molecules, or less than two if reaction 3 also consumes some of the O atoms.

The residual ammonia decays at high enough temperature and pressure, even after $[O_2]$ and transient [NO] have become inappreciable, but much more slowly than it does in the reaction zone. We have not been able to reach a very firm conclusion about the mode of decomposition of ammonia in the post flame gas. Therefore, we will discuss it only briefly.

A study of 16 fuel-rich NH_3–H_2–O_2–A flames at atmospheric pressure and at five temperatures, 1760 to 2037°K., showed that in post-flame gas of always about the same composition, the ammonia suffered an approximately first-order decomposition

$$-\mathrm{d}[NH_3]/[NH_3]\mathrm{d}t = 10^{13}\, e^{-97\pm5\ \mathrm{kcal.}/RT}\ \mathrm{sec.}^{-1}$$

In the post-flame gas from four flames at 1910°K. but at variable pressure, the first-order decay constant for ammonia decreased with decreasing total pressure. Within the large experimental error, the variation could be expressed either as a dependence of the constant on total pressure or on the equilibrium [OH] which varied as $[H_2O]^{1/2}/[H_2]$.

[H] was estimated *via* added D_2O[5] in these post-flame gases and found present in concentrations appropriate to the equilibrium $H_2 = 2H$. Therefore, OH and O are also present only in thermodynamic equilibrium.[13] Our interpretation of the reaction zone allows the conclusion that $NH_3 = NH_2 + 1/2H_2$ is also equilibrated in the post-flame gas.

The slow decay of ammonia is consistent with the formation of nitric oxide in a slow rate-determining step, followed by fast reaction 1. We cannot observe nitric oxide in the post-flame gas with certainty, but should not hope to if its rate of formation is very slow compared to reaction 1.

Nitric oxide could not be formed in the post-flame gas in the reaction $O + NH_3 \rightarrow \ldots \rightarrow NO + \ldots$ as it is in the reaction zone itself; for in the reaction zone, O atoms are continuously generated by $H + O_2 \rightarrow OH + O$; but this process is equilibrated in the post-flame gas, and [O] is only $\approx 10^4 e^{-118/RT}[H_2O]/[H_2]$ and would require a larger temperature dependence than is observed. Also the pressure dependence of the first-order constant would remain unexplained.

If nitric oxide is formed by reaction of one of the following N containing species which are considered equilibrated among themselves, $NH_3 = NH_2 + {}^1/_2\ H_2 = NH + H_2$, with one of the O containing species which are also equilibrated among themselves, $H_2O = OH + {}^1/_2\ H_2 = O + H_2 = {}^1/_2\ O_2 + H_2$; the only products of reaction partners which could give a pressure dependence of the right sign to the observed first-order decay constants are $[NH_3][H_2O]$ and the two equivalent products $[NH_3][OH]$ and $[NH_2][H_2O]$. $[NH_3][H_2O]$ is implausible on several grounds, and only $[NH_3][OH]$ or the equivalent $[NH_2][H_2O]$ seems probable.

Substituting the equilibrium [OH] for the post-flame gas into the observed decay constant, and this is not a real test of dependence on this species because [OH] changed little at a fixed pressure and temperature, one can rewrite the experimental results as

$$-\mathrm{d}[NH_3]/\mathrm{d}t = 2 \times 10^{12} e^{-(38\pm5)/RT}[NH_3][OH]\ \mathrm{mole\ l.}^{-1}\ \mathrm{sec.}^{-1}$$

The rate-determining formation of nitric oxide would be ${}^1/_2$ of this, for nitric oxide disappears *via* reaction 1 as fast as formed. Our inability to observe nitric oxide in the post-flame gas can be put in the form that any steady level of $[NO]/[H_2O] < 4 \times 10^{-4}$; and this upper limit applied to the equality, $-\mathrm{d}[NH_3]/2\mathrm{d}t$ = rate of reaction 1 at 1900°K., implies a lower limit for $k_1/K_2 > 10^{10}$. Of course, we have already found that $k_1/K_2 = 6 \times 10^{10}$ so we should not expect to observe nitric oxide in the post-flame gas. But because we cannot hope to verify the postulated existence of [NO] in this region, our interpretation of the ammonia decomposition in the post-flame gas is more speculative than it is in the main reaction zone.

(12) R. Srinivasan, *J. Phys. Chem.*, **64**, 579 (1960).

(13) E. M. Bulewicz, C. G. James and T. M. Sugden, *Proc. Roy. Soc. (London)*, **A235**, 89 (1956).

THE HOMOGENEOUS BASE-CATALYZED DECOMPOSITION OF HYDROGEN PEROXIDE[1]

BY FREDERICK R. DUKE AND TRICE W. HAAS

Institute for Atomic Research and Department of Chemistry, Iowa State University, Ames, Iowa

Received August 1, 1960

The decomposition of hydrogen peroxide in alkaline aqueous solution was found to be homogeneous in polyethylene vessels when the reactants were sufficiently pure. The rate equation found is rate = k_1 $[H_2O_2][HO_2^-]$ over a wide range of concentrations of reactants.

Introduction

The study of the base-catalyzed decomposition of hydrogen peroxide has been the subject of many investigations.[2] Erdey and Inczedy[3] have established the kinetics for this decomposition in glass vessels where the reaction is found to be heterogeneous. The kinetics for the homogeneous base-catalyzed decomposition of hydrogen peroxide, however, appear not to have been successfully completed for two reasons. First the vessels used must be shown to have inactive surfaces and second there must be assurance that foreign ions are not catalyzing the decomposition. It is felt that both of these difficulties are overcome in this work.

Experimental

Adequate purification of the KOH used in this work was a major problem. Various methods were tried and finally a method using as adsorbing agents $Fe(OH)_3$ and $Mg(OH)_2$ was adopted. Last traces of iron were removed by complexing with phenyl-2-pyridyl ketoxime and extraction into isoamyl alcohol according to the method of Trusell and Diehl.[4]

The KNO_3 and Na_2SO_4 used to adjust the ionic strength were reagent grade materials recrystallized two times from redistilled water. Water and hydrogen peroxide used in this work were redistilled at least once. All other chemicals used were reagent grade materials.

Analyses for peroxide were carried out by titration with standard Ce(IV) solution. Analyses for traces of heavy metal impurities in the reagents used were carried out by various spectrophotometric methods.

Sixteen oz. polyethylene bottles were used for the reaction vessels. These were submerged in a constant temperature bath held to $\pm 0.05°$.

Samples of the decomposing solutions were withdrawn periodically with 10-ml. pipets and quenched in dilute H_2SO_4. Samples were then ready for titration. This quenching technique was found to be effective.

The polyethylene bottles used as reaction vessels were tested for surface activity in the following manner. One of the bottles of the kind actually used was "frozen" in Dry Ice and ground into fine particles using an ordinary wood file. The polyethylene was then cleaned to remove dirt, etc. This was added to a solution and the change in the rate studied. It is estimated that the surface area was increased by a factor of at least 50. No effect due to the added polyethylene was ever found. This experiment was carried out under various conditions such as various hydroxyl and initial hydrogen peroxide concentrations and at several temperatures. It was concluded that polyethylene vessels have inert surfaces for this decomposition.

Some experiments were done using glass and paraffin lined glass vessels. It appeared as though the paraffin surface was also inert, but in the glass vessels the reaction was definitely surface catalyzed. This is in agreement with other reports.

Results

Evidence that harmful impurities were absent was inferred from two things. First in early work on this project disodium dihydrogen ethylenediaminetetraacetate (EDTA) was added as an inhibitor. This results in the complexing of all heavy metal ions present which are catalysts for this reaction; the EDTA greatly diminished their activity, although it was found that they were still slightly active. The rate was independent of the amount of EDTA present above a small minimum. When EDTA was added to the purified reagents in the final work no detectable effect was noted.

Secondly, many of the runs were made using commercial H_2O_2 and purified KOH, KNO_3 and water. It was known that a small amount of iron and possibly copper was added from the peroxide. Redistillation of the peroxide removed the last traces of these ions (analyses were sensitive to 1 part per billion; they were below this level). This last lowering of the impurity concentrations had no effect on the rate, hence the level of impurity concentrations from the peroxide must have already been low enough so as not to be harmful. Some catalytic decomposition due to other impurities must have occurred, but it is felt that this term in the rate equation was small compared with the uncatalyzed rate (see Fig. 1).

Most of the work was done at an ionic strength of 2.0. In the majority of cases this was adjusted by adding the proper amount of a KNO_3 solution. It was felt necessary to show that the NO_3^- ion was not entering into the reaction. To this end a series of solutions were made using Na_2SO_4 instead of KNO_3 to adjust the ionic strength. No difference was found, hence it was concluded that nitrate ions were not entering into the reaction. Since Na_2SO_4 instead of K_2SO_4 was used, and since ionization is essentially complete for these two electrolytes, it was also concluded that NaOH would give the same result as KOH, that is the K^+ or the Na^+ ions do not directly enter into the reaction.

Varying the initial $[H_2O_2]$ showed that the rate at a particular $[H_2O_2]$ and $[OH^-]$ was independent of the initial $[H_2O_2]$. This indicates that the initial $[H_2O_2]$ does not appear in the final rate equation.

More interesting results were obtained when the hydroxide concentration was varied. In this case the rate for a particular $[H_2O_2]$ was found to go through a maximum. This maximum was found, for example, when the $[H_2O_2]$ = 1.0 and the $[OH^-]$ = 0.5. This was explained by assuming a rate equation of the form

(1) Contribution No. 910. Work was performed in the Ames Laboratory of the U. S. Atomic Energy Commission.

(2) W. C. Schumb, C. N. Satterfield and R. L. Wentworth, "Hydrogen Peroxide," Reinhold Publ. Corp., New York, N. Y., 1955, Ch. 8 and 9.

(3) L. Erdey and I. Inczedy, *Acta Chim. Hung.*, **7**, 93 (1955).

(4) F. Trusell and H. Diehl, *Anal. Chem.*, **31**, 1978 (1959).

TABLE I

VALUES OF $(H_2O_2)(HO_2^-)$ AND $-\frac{d(H_2O_2)_T}{dt}$ FOR VARIOUS VALUES $(OH^-)_T$ AND $(H_2O_2)_T$ AT 35°

	$(OH^-)_T = 0.1\ m$		$(OH^-)_T = 0.5\ m$		$(OH^-)_T = 1.0\ m$	
$(H_2O_2)_T$	$(HO_2^-)(H_2O_2)$	$-\frac{d(H_2O_2)_T}{dt}$	$(H_2O_2)(HO_2^-)$	$-\frac{d(H_2O_2)_T}{dt}$	$(HO_2^-)(H_2O_2)$	$-\frac{d(H_2O_2)_T}{dt}$
1.1	0.1000	0.290	0.2999	0.600	0.1141	0.260
1.0	.0900	.235	.2500	.490	.0412	.218
0.9	.0800	.232	.2002	.400	.0141	.0120
.8	.0700	.201	.1506	.280	.00551	.0090
.7	.0600	.175	.1035	.250	.....	.0075
.6	.0500	.161	.0576	.190	.....	.0045
.5	.0400	.125	.0145	.110	.....	.0035
.4	.0300	.077	.00314	.050	.....	.0030
.3	.0197	.056	.000596	.030	.....	....
.2	.0100	.034	.000199	.015	.....	....
.1	.0011	.012	.....	.001	.....	....

$$\frac{-d[H_2O_2]_T}{dt} = k[H_2O_2][HO_2^-] \qquad (1)$$

where

$[H_2O_2]_T$ is the total hydrogen peroxide concn.
k is the specific rate constant
$[HO_2^-]$ is the concn. of the singly ionized hydrogen peroxide
$[H_2O_2]$ is the concn. of the un-ionized hydrogen peroxide
t is the time

The mechanism proposed is

$$H_2O_2 + OH^- \rightleftharpoons HO_2^- + H_2O \qquad (I)$$

$$H_2O_2 + HO_2^- \longrightarrow \left[\begin{array}{c} H \quad H \\ O \quad O \\ \\ O \quad O \\ H \end{array}\right] \longrightarrow HOH + O_2 + OH^- \qquad (II)$$

It is clear that the rate will go through a maximum when the peroxide is 50% ionized, that is $[H_2O_2] = [HO_2^-]$. If one works out the rate equation in terms of the $[H_2O_2]_T$, the total hydroxide ion concentration, $[OH^-]_T$, and K, the equilibrium constant for the reaction I above, one obtains

$$\frac{-d[H_2O_2]_T}{dt} = k\left(\frac{X - \sqrt{X^2 - 4[OH^-]_T[H_2O_2]_T}}{2}\right)\left([H_2O_2]_T = \frac{X - \sqrt{X^2 - 4[OH^-]_T[H_2O_2]_T}}{2}\right) \qquad (2)$$

where $X = [H_2O_2]_T + [OH^-]_T + 1/K$

Using the method of calculus and inserting the proper values into this equation, it is found that a maximum in rate is predicted for 35° at about $[OH^-]_T = 0.5$ and $[H_2O_2]_T = 1.0$, in agreement with experimental results. The values of K used were obtained by extrapolating the data of Evans and Uri[5] to 35°.

Integration of equation 2 would be very difficult, hence the best way to determine the specific rate constant appeared to be graphical differentiation of the concentration *vs.* time curve, followed by plotting $-d[H_2O_2]_T/dt$ *vs.* $[H_2O_2][HO_2^-]$. The graphical differentiation was accomplished using a tangentimeter similar to the one suggested by Latshaw.[6] Typical data are listed in Tables I and II.

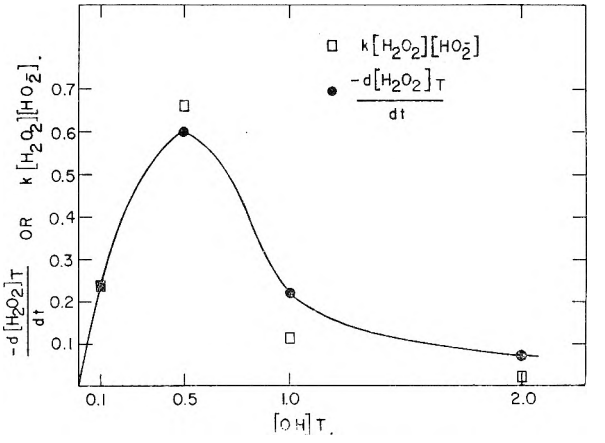

Fig. 1.—A comparison of theoretical and experimental values of the rate according to eq. 1.

Figure 1 shows $-d[H_2O_2]_T/dt$ varies with the $[OH^-]_T$ for a given $[H_2O_2]_T$. Also shown is how calculated values of k $[H_2O_2][HO_2^-]$ vary with $[OH^-]_T$ at the same $[H_2O_2]_T$, k being taken from low $[OH^-]$. The deviations are ascribed to impurities added with the base. The rate constants for this reaction are estimated at 2.65 ± 0.40 l. mole^{-1} hour^{-1} at 35° and 0.95 ± 0.01 l. mole^{-1} hour^{-1} at 15°. From these data the activation energy is 9 ± 1 kcal./mole.

TABLE II

VALUES OF $(HO_2^-)(H_2O_2)$ AND $-\frac{d(H_2O_2)_T}{dt}$ FOR VARIOUS VALUES OF THE $(OH^-)_T$ AND THE $(H_2O_2)_T$ AT 15°

$(H_2O_2)_T$	$\frac{(HO_2^-)}{(H_2O_2)}$	$-\frac{d(H_2O_2)_T}{dt}$	$(HO_2^-)(H_2O_2)$	$-\frac{d(H_2O_2)_T}{dt}$
0.9	0.0793	0.085	0.2007	0.240
.8	.0694	.075	.1521	.200
.7	.0595	.072	.1045	.140
.6	.0496	.068	.0594	.115
.5	.0397	.061	.0245	.070
.4	.0296	.045	.00832	.040
.3	.0197	.037	.00262	.015
.2	.0100	.025	.00008	.005
.1	.00148	.010	.00005	...

It is concluded from this work that this decom-

(5) M. G. Evans and N. Uri, *Trans. Faraday Soc.*, **45**, 224 (1949).

(6) M. Latshaw, *J. Am. Chem. Soc.*, **47**, 792 (1925).

position does not proceed by a free radical mechanism; it is not affected by light; the initial peroxide concentration does not appear in the rate equation; the reaction is relatively slow; it is not affected by the surface area; and there was no period of induction.

As predicted by the rate equation, solutions with initial $[H_2O_2]_T = 1.0$ and the $[OH^-]_T$ greater than 1.0 should decompose quite slowly. This was found to be the case. A solution with $[OH^-]_T = 2.0$ and $[H_2O_2]_T = 1.0$ takes about 40 days to decompose. This allows studies of catalytic decompositions in basic solutions to be carried out without need to account for the uncatalyzed decomposition. Several such studies were made. Arsenic (added as potassium arsenite), zirconium (added as $ZrOCl_2$) and lead (redissolved as a plumbite ion) were studied. The ZrO_2 redissolved when the H_2O_2 was added, hence all of these potential catalysts were made to behave homogeneously. The catalysis by these ions under these conditions was found in all cases to be negligible. Lead oxide acts as a very active heterogeneous catalyst but has virtually no activity when made homogeneous. The arsenite is initially oxidized to arsenate, but beyond this does not appear to enter into the reaction.

When EDTA was added to a basic solution containing a small amount of $Fe(OH)_3$, nothing perceptible appeared to happen to the iron precipitate. When H_2O_2 was added, however, the iron redissolved with the formation of a purple complex ion. The composition of this ion was not determined; however, this ion was much less active in promoting the decomposition than the $Fe(OH)_3$.

In all the cases of heavy metal ion catalysis it was found that when a heterogeneous catalyst was made to behave homogeneously it either lost its catalytic activity entirely or was greatly reduced in activity. Thus, adsorption activation is very important in catalyzed peroxide decomposition.

ACTIVITY COEFFICIENTS OF BIPOLAR ELECTROLYTES. SILVER SUCCINATE AND SEBACATE IN AQUEOUS SODIUM NITRATE[1]

BY F. R. MEEKS AND R. A. MARCUS

Department of Chemistry, Polytechnic Institute of Brooklyn, Brooklyn 1, N. Y.

Received August 4, 1960

Activity coefficients of silver succinate and sebacate in aqueous sodium nitrate were determined by a solubility method. The silver ion concentration was measured potentiometrically in solutions of various ionic strengths using an empirical calibration equation. A simple, approximate theoretical model for these "bipolar" ions is observed to be in good agreement with results inferred from the electrostatic contribution to the activity coefficients. It treats a bipolar ion as two point charges separated by a fixed distance in the solvent. Its applicability to zwitterions is also considered. These studies are used to discuss the interaction of certain activated complexes of chemical reactions with their ionic atmospheres. Studies of bipolar ions also provide information about nearest neighbor interaction in polyelectrolytes.

Introduction

The electrostatic interaction between two charges attached to the same molecule in various ionic media enters into several problems. These include the nearest neighbor repulsion of ionized groups in polyelectrolytes[2] and the activity coefficients of certain activated complexes in chemical reactions. In the latter case, for example, it is usually assumed[3] that the activated complex interacts with the ionic medium in the same way as a single localized charge, even when it may consist of essentially two charges separated by a fixed distance.

Interest in these problems prompted the present investigation of the activity coefficients of salts containing dicarboxylate ions. The simplest such system theoretically is one which is dilute in dicarboxylate ions and in which the latter interact primarily with those of a 1–1 electrolyte. In this study the activity coefficients of slightly soluble silver succinate and sebacate in aqueous sodium nitrate were measured by a solubility method. The comparison of the activity coefficients of two salts differing in their hydrocarbon chain length permits the approximate cancellation of certain non-electrostatic factors in the interpretation of the results.

It seems appropriate to term molecules containing two separate charges "bipolar ions." Examples of this class include dipolar ions (amino acids in the zwitterion form) and "bolaform" electrolytes.[4]

Experimental

Procedure.—The solubility of the silver salts in aqueous sodium nitrate at 24.8° was determined by a potentiometric measurement of the silver ion concentration. An empirical calibration equation was first obtained using solutions containing known concentrations of silver and sodium nitrate. The electrochemical cell employed in the calibration and in the solubility determination contained a saturated sodium nitrate–agar salt bridge and is represented by the expression

$$Hg,Hg_2Cl_2\,(s)\,\|KCl\ (satd.)\,\|NaNO_3\ (aq.\ satd.)\ \begin{vmatrix}\text{exptl.}\\ \text{soln.}\end{vmatrix}\ AgCl(s),Ag$$

A Leeds and Northrup Type K-2 potentiometer was employed, and the cell was thermostated at 24.80°. E.m.f. readings were made on the calibration solutions which varied from 1.2×10^{-4} to 1.5×10^{-3} *m* $AgNO_3$ and from 0.05 to 2.5 *m* $NaNO_3$. E.m.f. readings were then made on filtered solutions previously saturated with a silver dicarboxylate at 24.8° and containing known concentrations of sodium

(1) Abstracted in part from a dissertation submitted by Frank R. Meeks in partial fulfillment for the degree of Doctor of Philosophy, Polytechnic Institute of Brooklyn, June 1956.

(2) R. A. Marcus, THIS JOURNAL, **58**, 621 (1954); S. Lifson, *J. Chem. Phys.*, **26**, 727 (1957); **29**, 89 (1958) and references cited therein.

(3) *Cf.* S. Glasstone, K. J. Laidler and H. Eyring, "The Theory of Rate Processes," McGraw-Hill Book Co., New York, N. Y., 1941.

(4) R. M. Fuoss and D. Edelson, *J. Am. Chem. Soc.*, **73**, 269 (1951)

nitrate. The empirical equation was then used to calculate the silver ion concentration.

Reagents.—Sebacic and succinic acids (Eastman Kodak) were purified by conversion to the disodium salts in concentrated aqueous solution and treatment with decolorizing carbon while boiling, followed by suction filtration and treatment with mineral acid to regenerate the organic acid. This was followed by four recrystallizations from hot distilled water, vacuum drying and a melting point check. The silver salts were generated by titration of the sodium salt of the acid with Mallinckrodt Analytical Reagent silver nitrate. The salts were filtered, washed with a little water, dried in a vacuum desiccator and stored over phosphorus pentoxide.

Sodium nitrate (Mallinckrodt A.R.) was recrystallized four times from hot water. Unrecrystallized sodium nitrate became slightly milky in the presence of 0.001 m $AgNO_3$ if the sodium nitrate exceeded 0.5 m. However, even after one recrystallization no milkiness occurred. A colorimetric test[5] for chloride on recrystallized sodium nitrate also proved negative. Sodium nitrate was selected as a suitable 1–1 electrolyte both because of its solubility and because of its relative freedom from contamination with halide ions. Care was taken to ensure low CO_2 content to minimize possible hydrolysis of the dicarboxylate salts. Direct titration of these solutions of sodium nitrate in water using phenolphthalein then showed that hydrolysis could be ignored (being of the order of 1%).

Results

The mean molal ion activity coefficient of the silver dicarboxylate, $\nu_\pm$, in a solution in equilibrium with the solid can be expressed in terms of the measured silver ion molality, m_{Ag^+}, and in terms of the latter's value at zero ionic strength, $m^0_{Ag^+}$, according to the thermodynamic expression

$$-\log \gamma_\pm = \log (m_{Ag^+}/m^0_{Ag^+}) \qquad (1)$$

Values of m_{Ag^+} were inferred from the e.m.f. using the empirical calibration formula

$$\text{e.m.f.} = 0.55074 + 0.05910 \log m_{Ag^+} - 0.01254\sqrt{\mu}$$

where μ is the ionic strength.

Since $m^0_{Ag^+}$ was not determined, only relative values of $\gamma_\pm$ (relative to $\gamma_\pm$ at 0.05 m $NaNO_3$) are reported in Table I.

TABLE I

RELATIVE ACTIVITY COEFFICIENTS OF SILVER SUCCINATE AND SEBACATE

	Silver succinate		Silver sebacate	
$\sqrt{\mu}$	E.m.f. (v.)	$-\log \gamma_{\pm}/\gamma_{\pm}^{(0.05)}$	E.m.f. (v.)	$-\log \gamma_{\pm}/\gamma_{\pm}^{(0.05)}$
0.224	0.35440	0.000	0.32850	0.000
.316	.35905	.099	.33310	.098
.447	.36320	.196	.33520	.161
.548	.36387	.229	.33638	.202
.707	.36612	.301	.33670	.241
.837	.36685	.341	.33615	.259
1.000	.36780	.391	.33625	.296
1.225	.36732	.431	.33473	.318
1.414	.36638	.455	.33430	.351
1.581	.36647	.492	.33360	.374

The ionic strength in Table I is actually only the sodium nitrate contribution. The additional contribution due to the silver salts was estimated in the following way to be small. In a dilute solution of 0.05 m $NaNO_3$ the value of $\gamma_\pm$ for a 2–1 electrolyte can be found approximately from the Guntelberg expression[6] to be 0.65. Introducing this and the corresponding m_{Ag^+} into eq. 1, $m^0_{Ag^+}$ is estimated to be about $3.4 \cdot 10^{-4}$ and $1.3 \cdot 10^{-4}$ m for silver succinate and sebacate, respectively. The corresponding contributions to $\sqrt{\mu}$ when μ is 0.05 m are only 1 and 0.5% and may be ignored for the present purposes.

The use of the calibrated potentiometric method for measurement of the silver ion concentration tacitly assumed that electrochemically the dilute silver dicarboxylate and nitrate in aqueous sodium nitrate behave similarly. This assumption is valid when the silver salt makes only a small contribution to $\sqrt{\mu}$, a condition which was just seen to be adequately satisfied for the data of Table I. A few calibration points obtained at $\sqrt{\mu}$'s less than 0.2 showed appreciable deviation from the calibration equation. For the reasons cited a different type of measurement will be necessary to determine the solubility of the silver salts at low μ's and the absolute value of the $\gamma_\pm$'s in Table I.

To test the possibility of experimentally significant ion pair formation between silver ions and the dicarboxylate anions, a small amount of a sodium dicarboxylate (to make 10^{-5} M) was added to a solution of 2×10^{-5} M $AgNO_3$ in a solution containing excess sodium nitrate. No detectable e.m.f. change (0.1 mv. detection limit) was found indicating negligible change in activity coefficient of the silver salt (*i.e.*, less than 1%).

Discussion

Two of the major factors influencing activity coefficients are electrostatic and hydration effects.[6b] The latter becomes increasingly important with increasing electrolyte concentration: the ions bind some solvent so that the solution is effectively more concentrated than the molality itself implies. In the present system the silver salts are so dilute that they will bind only a negligible fraction of the solvent. The extent of bound solvent will therefore be the same in silver succinate and sebacate solutions containing a given sodium nitrate concentration. Accordingly, the difference in chemical potential of the two silver salts in these two solutions will be independent of this hydration effect.[7] The same remarks apply to the ratio of mean ion activity coefficients of these salts. Relative values of this ratio are computed from the data of Table I and are plotted in Fig. 1, together with a theoretical curve which will now be discussed.

Because of their dilution the ions of the silver salts will interact primarily with those of sodium nitrate rather than with themselves. Accordingly the chemical potential of the silver ions will be the same in both solutions and attention can be focused on that of the dicarboxylate ions. Denoting by γ the single ion activity coefficient of a dicarboxylate ion, by γ^{el} its electrostatic factor, and by the subscripts A and B the succinate and sebacate, respectively, eq. 2 obtains in the present system.

$$\log \gamma_{\pm,A}/\gamma_{\pm,B} = \frac{1}{3} \log \gamma_A/\gamma_B = \frac{1}{3} \log \gamma_A^{el}/\gamma_B^{el} \qquad (2)$$

(5) I. Iwasaki, *Bull. Chem. Soc. Japan*, **25**, 226 (1952).

(6) (a) E. Güntelberg, *Z. physik. Chem.*, **123**, 199 (1926); (b) *cf.* R. A. Robinson and R. H. Stokes, "Electrolyte Solutions," Butterworths Scientific Publications, London, 1955.

(7) This tacitly assumes a model in which the number of bound solvent molecules is the same for all important ionic configurations occurring at a given ionic concentration. This model is the one generally employed.

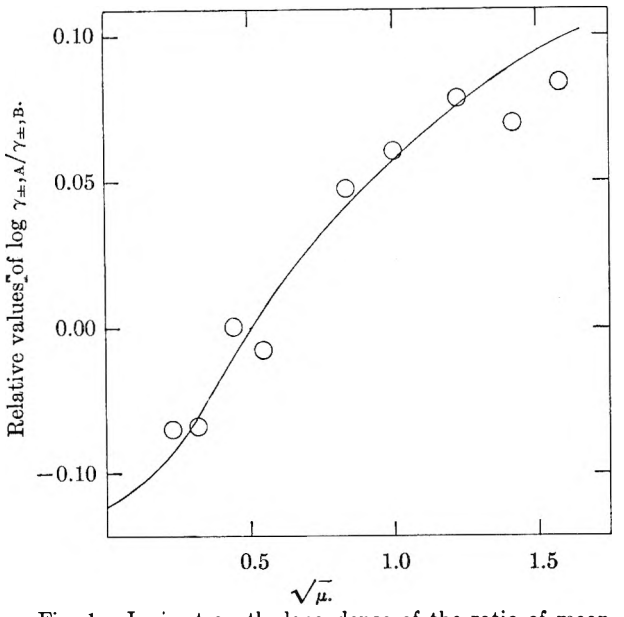

Fig. 1.—Ionic strength dependence of the ratio of mean ion activity coefficients of silver sebacate ($\gamma_{\pm,B}$) and succinate ($\gamma_{\pm,A}$). The value of log $\gamma_{\pm,B}/\gamma_{\pm,A}$ relative to its value at $\sqrt{\mu} = 0.5$ is plotted: experimental, O; theoretical, —.

For simplicity, the model to be used for the computation of γ^{el} will be the same as that employed by Bjerrum[8] for his treatment of the successive ionization constants of dicarboxylic acids. He treated the two ionized groups of the dicarboxylate ion as two point charges separated by a distance r in the solvent and he related the ratio of the ionization constants to the Coulombic repulsion. From his expression, the values of r estimated for succinate[9] and for sebacate[10] ions are 3.65 and 13 A., respectively. Considering the approximation, these r's are moderately close to the actual values. However, for very short chain length dicarboxylic acids this equation is less valid and a more elaborate model[11] is needed.

In the approximation to be employed here molal and rational activity coefficients may be taken to be the same. The two charges 1 and 2 will be denoted by Z_1e and Z_2e, respectively. A charging process will be considered such that at any stage each charge of the bipolar ion has a fraction λ of its final value, Z_ie. The distances of the field point from these two point charges will be denoted by r_1 and r_2. It may then be shown by standard methods that at any stage of the charging process the solution of the linearized Poisson–Boltzmann equation for the electrostatic potential ψ satisfying the boundary conditions of the model ($\psi \to 0$ as r_1 and $r_2 \to \infty$; $\psi \to \lambda Z_ie/Dr_i +$ constant as $r_i \to 0$, where $i = 1,2$) is given by

$$\psi(r_1, r_2) = \frac{\lambda Z_1 e}{Dr_1} e^{-\kappa r_1} + \frac{\lambda Z_2 e}{Dr_2} e^{-\kappa r_2}$$

where κ^2 has its usual value,[5b] $8\pi e^2\mu/DkT$.

Subtracting from this expression the self-potential of ion i ($i = 1,2$) the remaining contribution to ψ at $r_i = 0$ will be designated by ψ_i^0. The work required to charge up the bipolar ion at a given ionic strength is

$$\sum_{i=1}^{2} \int_{\lambda=0}^{1} \psi_i^0 d(\lambda Z_i e)$$

Subtracting from this the work required to charge up this ion when $K = 0$, the electrostatic contribution to the chemical potential of the bipolar ion is found to be

$$kT \ln \gamma^{el} = -\frac{(Z_1^2 + Z_2^2)e^2\kappa}{2D} + \frac{Z_1Z_2e^2\kappa}{D} \frac{e^{-\kappa r} - 1}{\kappa r} \quad (3)$$

Alternatively, when $Z_1 = \pm Z_2$ this equation may be deduced as a special case of a more elaborate model due to Scatchard and Kirkwood.[12] These authors treated the two charges as spheres of radii a separated by a fixed distance r. They solved the differential equation for ψ inside and outside the spheres in an approximate way which becomes increasingly exact as a approaches zero. Their equation becomes identical with eq. 3 when a is set equal to zero there and Z_1 is set equal to $\pm Z_2$ in eq. 3.

Equation 3 may also be compared with that obtained[13] for an ellipsoidal model of a dipolar ion in solutions of very low ionic strength. The two charges were assumed to lie at the foci of the ellipsoid. When the eccentricity of the ellipsoid approaches unity, the latter degenerates into a straight line and the model becomes in fact one of two point charges. The resulting equation should therefore be identical with eq. 3 when one sets $Z_1 = Z_2 = -1$ there and expands eq. 3 in a power series in κr, retaining only the first term

$$kT \ln \gamma^{el} = -e^2\kappa^2 r/2D \quad (4)$$

This is indeed the case.[14]

Equation 3 approaches the simple Debye–Hückel expression for a single localized charge $(Z_1 + Z_2)e$ when the ionic atmosphere is sufficiently far removed. This occurs when Kr is small. It approaches that for two isolated localized charges (plus a now-shielded Coulombic repulsion term $Z_1 Z_2 e^2/Dr$) when the atmosphere is drawn in close about each charge (large κr). The transition region occurs at $\kappa r \sim 1$ when $Z_1 \sim Z_2$.

Introducing into eq. 3 the r-values obtained earlier for sebacate and succinate ions, the curve of Fig. 1 was computed. The agreement with the data is surprisingly close. From eq. 3 it may be inferred that the transition discussed in the preceding paragraph occurs at low ionic strengths for sebacate ion and an ionic strength of the order of 0.7 m for the succinate ion ($\kappa \sim 1/r$ where $r = 3.65$ Å.).

Similar remarks concerning a transition region apply to activated complexes of chemical reactions consisting of two separated charge centers. When

(8) N. Bjerrum, *Z. physik. Chem.*, **106**, 219 (1923).

(9) This estimate is based on the ionization constants of G. D. Pinching and R. G. Bates, *J. Research Natl. Bur. Standards*, **45**, 322 (1950).

(10) *Cf.* F. H. Westheimer and M. W. Shookhoff, *J. Am. Chem. Soc.*, **61**, 555 (1939). These authors summarize the r-values obtained by application of the simple Bjerrum expression to all dicarboxylate ions up to sebacate. The r-value for sebacate can then be obtained by a straightforward extrapolation.

(11) J. G. Kirkwood and F. H. Westheimer, *J. Chem. Phys.*, **6**, 506 (1938).

(12) G. Scatchard and J. G. Kirkwood, *Phys. Z.*, **33**, 297 (1932).

(13) J. G. Kirkwood in "Proteins, Amino Acids and Peptides," edited by E. J. Cohn and J. J. Edsall, Reinhold Publ. Corp., New York, N. Y., 1939, Chap. 12.

(14) A typographical error of a factor of two in eq. 17 of ref. 12 disappears in eq. 18 there.

Z_1 and Z_2 are about equal the usual assumption that this complex behaves as a single charge in its interaction with its atmosphere is a reasonable one according to eq. 3 if $\kappa << r^{-1}$. In the case of many isotopic exchange reactions it is expected that r is of the order of 7 Å. and therefore that this behavior would be exhibited at μ's appreciably below $0.2m$. Because of the highly specific interactions which occur between multiply charged ions of opposite sign these remarks apply primarily to an "inert" salt medium consisting of a 1–1 electrolyte.

The linear dependence of the activity coefficient of a zwitterion on the ionic strength in dilute solution, embodied in eq. 4, has been abundantly confirmed experimentally. We have found that application of eq. 4 to the experimental data of Cohn and others[15] yields r-values for amino acids which are in fair agreement with those inferred from pH data using the simple Bjerrum (Coulombic) expression. When the amino acids are small these r's are somewhat less than those estimated on the basis of free rotation about the bonds in these molecules.

Acknowledgment.—The authors wish to express their appreciation to the Research Corporation for the support of this research by a grant-in-aid.

(15) *Cf.* Reference 12 and Chap. 11 in that monograph.

PREFLAME REACTIONS IN THE AUTODECOMPOSITION OF ACETYLENIC COMPOUNDS[1]

BY U. V. HENDERSON, JR.

Combustion Laboratory, Experiment Incorporated, Richmond, Va.

Received August 4, 1960

The autodecomposition reactions of compounds such as dipropargyl ether and 1,6-heptadiyne have been studied by examination of the high-pressure autodecomposition flame and by analysis of the products of the low-pressure pyrolysis of these and related compounds. The gaseous products of pyrolysis at 900° indicate the splitting of the long-chain molecules into two smaller molecules by a homogeneous gas-phase reaction proceeding by way of a cyclic intermediate and involving an internal proton shift and displacement. At this pyrolysis temperature polymerization also occurs to a considerable extent (about 50%) and homolytic cleavages to a slight extent (about 1–2%). Evidence was also found that the unimolecular cleavage either precedes or occurs concurrently with the high-pressure autodecomposition reaction.

The thermal reactions of gaseous acetylene, and particularly the mechanism of energy release in its autodecomposition, have evolved considerable interest during recent years.[2] Because of the general interest in energy-producing reactions, in our laboratory we have been studying the decomposition reactions of higher-molecular-weight acetylenics such as dipropargyl ether, 1,6-heptadiyne and 1,7-octadiyne which are capable of sustaining an autodecomposition flame under the proper conditions. Although Egloff, *et al.*,[3] have reviewed rather comprehensively the earlier work on the polymerization and decomposition of acetylene hydrocarbons, including some of the long-chain species such as heptyne, octyne and 2,4-hexadiyne, none of the work reported was related specifically to the flame reactions, nor were the analytical data sufficiently detailed to be useful for correlating with decomposition mechanisms. The work reported in this paper has been directed primarily toward determining probable preflame reactions since the ultimate energy-releasing reactions of the carbon–carbon triple bond are in all likelihood quite similar, if not identical, to those which have been proposed for the parent compound.

(1) This work has been supported by the Office of Naval Research under contract Nonr-2487(00). Reproduction of the article in whole or in part is permitted for any purpose of the United States Government.

(2) (a) E. W. R. Steacie, "Atomic and Free Radical Reactions," 2nd Ed., Reinhold Publ. Corp., New York, N. Y., 1954, p. 173 ff.; (b) W. E. Prout and R. C. Anderson, *Fuel*, **33**, 125 (1954); (c) E. A. Westbrook, K. Hellwig and R. C. Anderson, "Fifth Symposium (International) on Combustion," Reinhold Publ. Corp., New York, N. Y., 1955, p. 631; (d) F. C. Stehling, F. H. Coats and R. C. Anderson, Abstracts of Papers, 132nd Meeting of A. C. S., New York, N. Y., 1957, p. 23-S; (e) C. G. Silcocks, *Proc. Roy. Soc.* (*London*), **A242**, 411 (1957); (f) C. M. Drew and A. S. Gordon, Paper presented at 134th Meeting of A. C. S., Chicago, Ill., 1958; (g) W. W. Robertson, E. M. Magee and F. A. Matsen, *J. Appl. Chem.*, **8**, 401 (1958); (h) E. F. Greene, R. L. Taylor and W. L. Patterson, Jr., THIS JOURNAL, **62**, 238 (1958); (i) G. J. Minkoff, *Can. J. Chem.*, **36**, 131 (1958).

(3) G. Egloff, C. D. Lowry, Jr., and R. E. Schaad, THIS JOURNAL, **36**, 1457 (1932).

Experimental

Reagents.—Dipropargyl ether was prepared by General Aniline and Film Corporation and was found to have only trace impurities by gas-chromatographic analysis (b.p. [corr.] 121.3° at 762 mm.).

1,6-Heptadiyne was prepared by Air Reduction Co. and contained as the principal impurities about 5% of a nonconjugated allenic isomer and a trace of alkyl chloride which were not readily removable by distillation. For one of the pyrolysis runs a small sample of the heptadiyne was purified by gas-chromatographic fractionation. There was no observable difference in the results obtained from this extremely pure sample and from those obtained when the material was used as received.

The following materials were used as obtained from their suppliers: 1,7-octadiyne from Air Reduction Co., 1-hexyne from Farchan Research Laboratories, monovinylacetylene from Elastomers Chemicals Dept., E. I. du Pont de Nemours and Co., propyne (methylacetylene) from Matheson Co., Inc., allene (propadiene) from Columbia Organic Chemicals Co., Inc., and diallyl ether from Dow Chemical Co.

Analyses.—The majority of the analyses of the decomposition products of the substances under investigation have been made by a Perkin–Elmer Model 13 infrared spectrometer and a gas chromatograph using helium as a carrier gas and a Gow-Mac Model TE-3 thermal conductivity cell operated at 300 ma. The 30-ft. chromatographic column packed with dimethylsulfolane on fire brick was calibrated with Phillips Hydrocarbon Mixture No. 40 and individual hydrocarbons of that mixture.[4] In the analysis of pyrolysis products, ambiguities were resolved and cross checks ob-

(4) *Cf.* F. T. Eggertsen and F. M. Nelsen, *Anal. Chem.*, **30**, 1040 (1958).

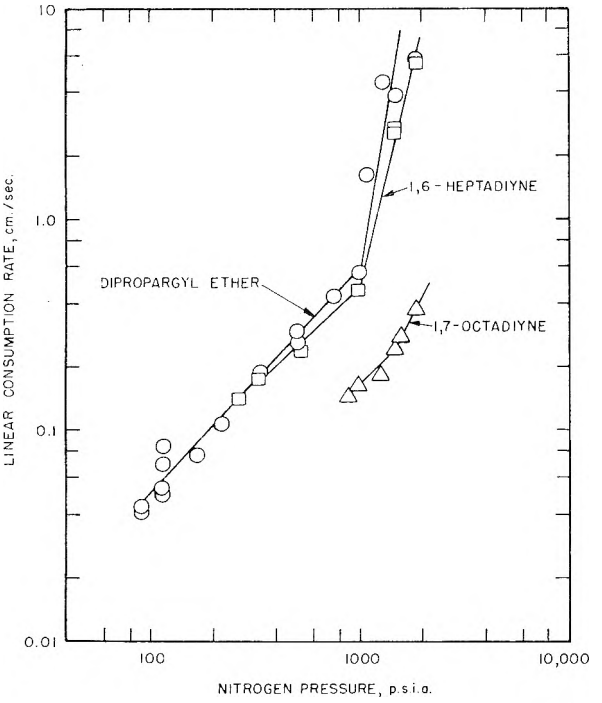

Fig. 1.—Decomposition rates of acetylenic compounds.

tained when necessary by trapping the chromatographic eluent at the appropriate intervals and transferring to a small-volume infrared gas cell for positive identification. Analyses of the polymeric material formed were not made. Quantitative data given are in mole per cent. and were estimated by combining information obtained from infrared spectra and gas chromatography with data obtained from a mass-spectrographic analysis.

Decomposition Experiments.—Decompositions were achieved in three ways. The first procedure was to cause the liquid to decompose by an autodecomposition flame in 8-mm. Pyrex tubes at varying pressures maintained by an inert pressurizing gas surrounding the decomposition tube. Measurements made on photographs of a decomposition flame showed that the actual reaction zone (an extremely bright luminous area) was only about 0.1 mm. thick. The thinness of the reaction zone and the fact that any probe was immediately chocked with carbon made it impossible to remove reaction intermediates and products from the reaction zone for analysis. By the interruption of an electrical circuit as the flame passed over carefully spaced, thin, fusible wires, it was possible to measure the variation in linear consumption rate with pressure.[5] The results of such measurements are shown in Fig. 1. The break in the pressure–rate curve at about 1000 p.s.i.a. is attributable to the onset of turbulent burning as shown in a typical case in Fig. 2. This phenomenon has been observed in other systems and has been discussed by Whittaker.[6]

The second procedure was used in an attempt to spread out the decomposition reaction zone in time and space so that it might be sampled at various positions. Resort was taken to a laminar diffusion flame established by blowing a stream of nitrogen through the warmed liquid and allowing the nitrogen–fuel mixture to burn in air under a chimney. The nitrogen flow rate was regulated to give a laminar flame of an appropriate size and shape. The assumption was made that as the fuel vapor approached the hot combustion zone, it would undergo similar thermal processes to those in the actual decomposition flame, but would occur over a larger space interval. The flame was then probed with a 0.5-mm. i. d. quartz capillary on the side of the unburned gas to remove the intermediate products. Analyses of the products obtained in this manner showed the presence of CO and CO_2 even in the very center of the flame, which indicated the very rapid diffusion of oxygen through the flame. In view of the observation of Smith and Gordon[7] that the small amount of oxygen that diffuses into the center of a diffusion flame cone plays a vital role in the mechanism of pyrolysis, *e.g.*, readily converting methane to methyl radicals under temperature conditions where methane is normally inert, it was considered necessary to study the autodecomposition chemistry under oxygen-free conditions.

In the third procedure pyrolyses under oxygen-free conditions were carried out in the apparatus shown in Figs. 3 and 4. In operation, a measured amount of the material to be pyrolyzed (0.1 to 1.0 ml. of liquid) was frozen with liquid nitrogen in a tube on the vacuum manifold. The system was then pumped down to a pressure of less than 10^{-4} mm., the sample allowed to melt, and its vapor caused to pass through the 7-mm. i.d. Vycor pyrolyzer tube at a rate such that the temperature was not caused to vary over a very large range. The vapor pressure of the material in the pyrolyzer tube was no greater than 1 mm. In a typical experiment the mass flow rate was of the order of 0.1 g./min. The condensable products were immediately condensed on the cold walls of the liquid-nitrogen-cooled outer jacket. The non-condensable gas passed into the activated charcoal trap, also cooled with liquid nitrogen, where hydrogen, methane and carbon monoxide, if evolved, were trapped. Both fractions of the volatile pyrolyzate could then be handled as necessary for analysis by proper manipulation of the vacuum manifold. The temperature of the pyrolysis and the length of wall heated were controlled by activating one or both of the two 3-in. long coils of Nichrome wire (Rockbestos, 4.251 ohm/in.) wrapped around the inner tube. The temperature was measured by an iron–constantan thermocouple placed inside the tube approximately 1 in. from the bottom of the tube against the wall.

Results

Dipropargyl Ether.—The low-pressure pyrolysis of dipropargyl ether at indicated temperatures of up to 900° results, aside from polymerization, primarily in the formation of propargyl aldehyde and allene. In a typical experiment at 900° at least 46% of the total reaction resulted in these products. Separate experiments showed that under the pyrolysis conditions used in these experiments, allene and propargyl aldehyde were not appreciably changed at temperatures up to 900°. At the highest temperature obtainable in the apparatus, approximately 1000°, dipropargyl ether pyrolyzates included significant amounts of hydrogen, carbon monoxide, acetylene and ethylene, thus indicating the onset of more complete degradation. The products obtained from the low-pressure pyrolysis of dipropargyl ether at an indicated temperature of 900° through a 3-in. section of Vycor tubing were as follows: allene, 46%; propargyl aldehyde, 46%; ethylene, 2%; acetylene, 2%; propyne, 1%; 1,3-butadiene, 0.5%; propylene, 0.5%; 1-butene, 0.5%; propane, 0.2%; butane, 0.1%; and several unidentified higher-molecular-weight species.

A sample of dipropargyl ether was "burned" in an autodecomposition flame in a bomb under an atmosphere of 150 p.s.i.g. of helium. The resulting gaseous products were trapped according to the procedure of Eggertsen and Nelsen[4] in order to concentrate the trace components (under these conditions, the principal components are hydrogen, carbon, carbon monoxide and methane). Gas-chromatographic analyses of the trapped material showed the same products and approximately the

(5) The linear consumption (or burning) rate is the rate of progress of the decomposition reaction along a sample of material burning cigarette fashion. The linear consumption rate times cross-sectional area times density is the mass burning rate.

(6) A. G. Whittaker, T. M. Donovan and H. Williams, THIS JOURNAL, **62**, 908 (1958).

(7) S. R. Smith and A. S. Gordon, paper presented before the A. C. S. Division of Gas and Fuel Chemistry, Urbana, Ill., 1958.

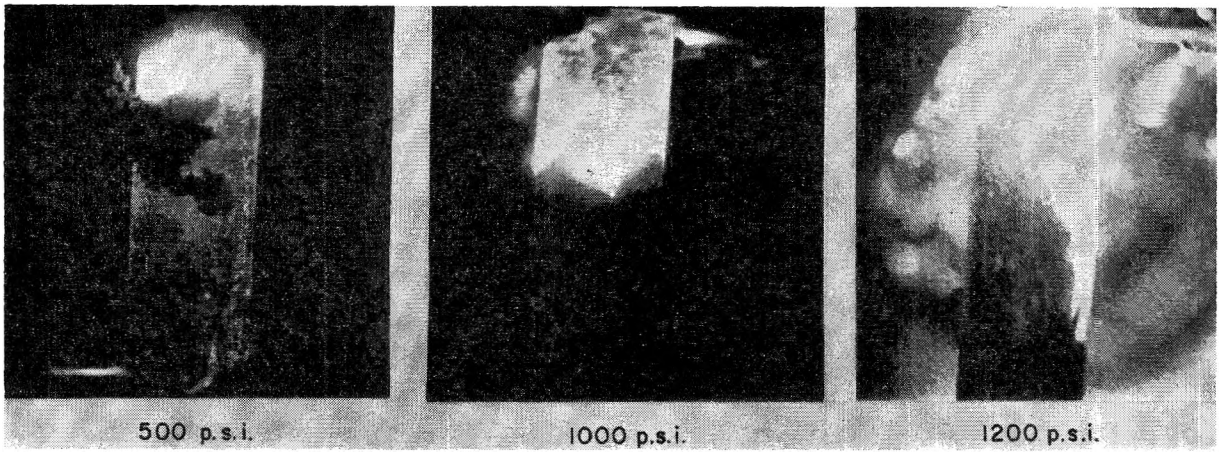

Fig. 2.—Effect of pressure on mode of burning.

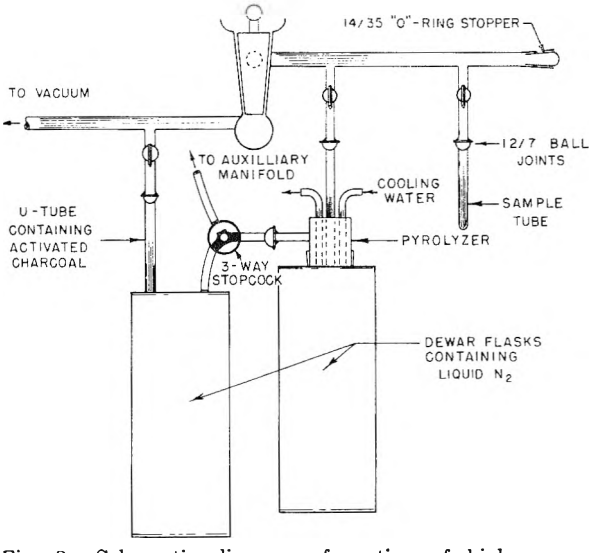

Fig. 3.—Schematic diagram of section of high-vacuum manifold used in pyrolysis experiments.

same relative composition as indicated in the previous paragraph (the less stable materials were reduced some in relative concentration).

1,6-Heptadiyne.—When subjected to low-pressure pyrolysis through a 3-in. section of Vycor tubing heated to an indicated temperature of 900°, 1,6-heptadiyne was found to react completely, giving as the principal volatile products monovinylacetylene and allene. The complete analysis of the volatile products formed under these conditions was as follows: allene, 45%; monovinylacetylene, 45%; ethylene, 3%; acetylene, 1.5%; 1-pentene-5-yne, 1%; butadiene, 1%; propyne, 0.2%; propylene, 0.2%; 1-butene, 0.2%; butane, 0.1%; diacetylene, 0.1%; and several unidentified species. One experiment indicated that under these conditions only about 31% of the reaction went to give these products, the remainder being polymerized. At higher temperatures more complete degradation ensued with hydrogen being formed. Separate experiments have shown that even at an indicated wall temperature of 900° over a 6-in. length of tubing, monovinylacetylene, allene and propyne, are essentially unchanged in the stay times involved in these experiments.

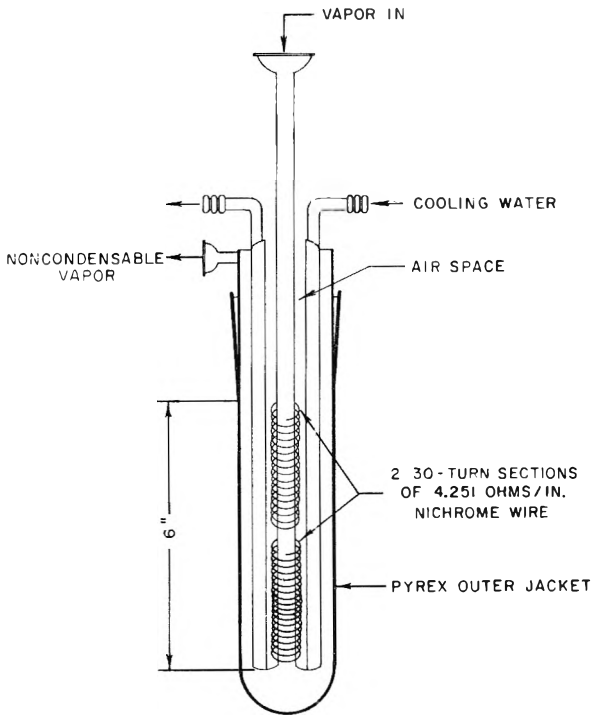

Fig. 4.—Schematic diagram of Vycor pyrolysis tube.

Again, as in the case with dipropargyl ether, when the products of an autodecomposition flame under helium at 500 p.s.i.g. were trapped and analyzed, besides the major autodecomposition products of carbon, hydrogen and methane, the volatile pyrolysis products were also observed.

1-Hexyne.—Although 1-hexyne will not support an autodecomposition flame in the manner of dipropargyl ether or 1,6-heptadiyne, it was of interest to compare its behavior with these compounds under the conditions of the low-pressure pyrolysis. At an indicated wall temperature of 900°, through a 6-in. section of Vycor tubing it was found to pyrolyze to give the following products: allene, 15%; propylene, 25%; ethylene, 20%; 1,3-butadiene, 15%; monovinylacetylene, 10%; ethane, 1%; 1-butene, 4%; 1-butyne, 2%; acetylene, 2%; butane, 0.5%; propane, 0.8%; propyne, 0.5%; pentene, 0.5%; diacetylene, 0.4%; and several unidentified species. Traces of meth-

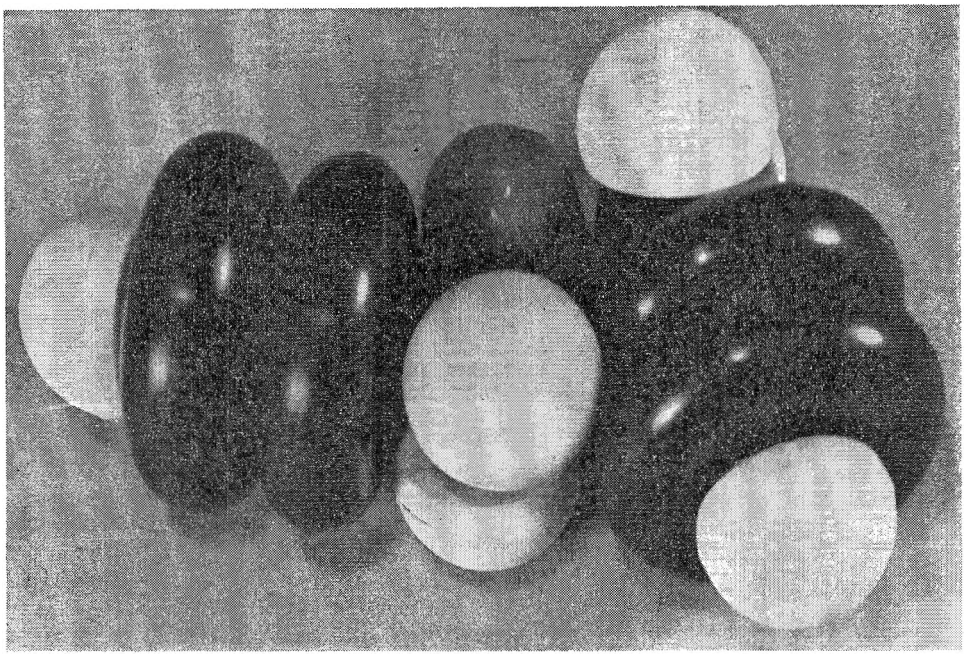

Fig. 5.—Dipropargyl ether orientation showing methylene hydrogen approaching acetylenic carbon atom.

ane were also detected. An experiment showed that about 25% of the hexyne reacted decomposed to give gaseous products, the remainder polymerizing.

Diallyl Ether.—Diallyl ether will not support an autodecomposition flame but was subjected to the low-pressure pyrolysis because of its similarity to dipropargyl ether as an olefinic analog. At an indicated wall temperature of 900° through a 6-in. section of Vycor tubing it was found to give acrolein[8] and propylene in approximately equal amounts with traces (1% or less) of ethylene, acetylene and allene. The formation of acrolein and propylene accounted for 53% of the total reaction in one experiment.

Discussion

From the observed products of the pyrolysis experiments described, there appear to be at least three different processes taking place. The first and most prevalent in most cases is the polymerization reaction. The experimental difficulties involved in removing and analyzing the resinous material formed has precluded any theoretical discussion of this process for the time being.

A second process, which is the one of primary interest in this discussion, is the splitting of the long-chain molecule into two smaller molecules. Although a heterogeneous wall reaction cannot positively be excluded without kinetic experiments, it seems probable that the process is a homogeneous, gas-phase, unimolecular reaction proceeding by way of a cyclic intermediate and involving an internal proton shift and displacement. Such a reaction is thermodynamically and stereochemically feasible in each case and is mechanically quite similar to the gas-phase pyrolysis of esters and related compounds.[9]

There is also obviously occurring a small amount of homolytic cleavage producing free-radical intermediates and resulting in the diversity of trace products observed and probably at least part of the polymeric material. However, this process cannot account satisfactorily for the formation of the predominant gaseous products. The most probable radicals formed by homolysis would result in a different product distribution from that observed.

It must not be overlooked that the long-chain molecules undergo the second process under conditions which do not affect the thermodynamically unstable monovinylacetylene, allene and propyne. It should be stressed that the 900° temperature which is indicated by the thermocouple in the pyrolysis tube is not the minimum temperature for the reaction. It is a wall temperature at which the rearrangement reaction is sufficiently fast to convert a sizable fraction of the molecules, yet which is not so high that further degradation obscures its occurrence.

An additional factor which mitigates against homolysis as the initiating step is the almost exclusive occurrence of allene as a product rather than an equilibrium mixture of allene and propyne. If, in the case of 1-hexyne, the first step were the breaking of the weakest bond,[10] an activation energy

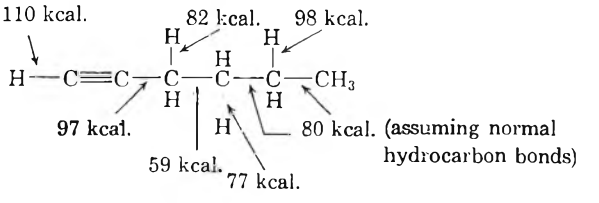

of at least 59 kcal. would be required, and the resulting fragments would be a propynyl radical and

(8) The pyrolysis of diallyl ether has been used industrially for the preparation of acrolein; *cf.* F. G. Watson, *Chem. Eng.*, **54**, 106 (1947).

(9) W. J. Bailey, *J. Org. Chem.*, **23**, 996 (1958); A. Maccoll, *J. Chem. Soc.*, 3398 (1958).

(10) The bond energies in the 1-hexyne molecule can be approximated from the data of Coats and Andersen [*J. Am. Chem. Soc.*, **79**, 1340 (1957)], which are derived from appearance potential measurements.

an *n*-propyl radical. Propynyl radicals that reacted by hydrogen-atom capture would be expected to give about 80% propyne and 20% allene.[11] The formation of the other major products, *e.g.*, monovinylacetylene and ethylene, would require even higher activation energies.

The most feasible course would then seem to be a concerted cyclic mechanism in which a proton is transferred from a methylene group to the π-electrons of a double or triple bond with a concurrent shifting of electrons to give the observed products. Such cyclic concerted reactions and prototropic shifts are well known in organic chemistry[12] and are appealing in that only small activation energies are required inasmuch as a bond is being formed simultaneously with a bond breakage.

The stereochemistry of dipropargyl ether (Fig. 5) and 1,6-heptadiyne permits an easy orientation of these molecules into a suitable transition state which can decompose to give the observed products, *i.e.*

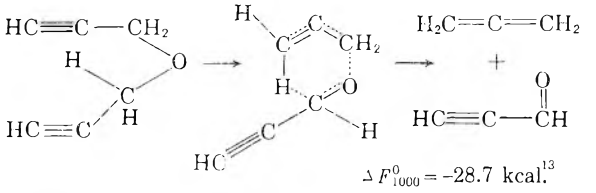

$\Delta F^0_{1000} = -28.7$ kcal.[13]

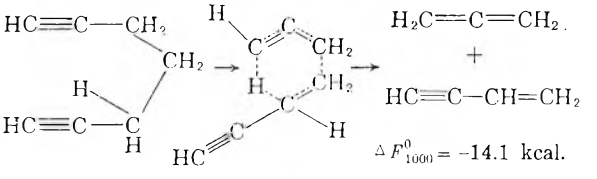

$\Delta F^0_{1000} = -14.1$ kcal.

For 1-hexyne, the products indicate three almost equally feasible courses for the reaction

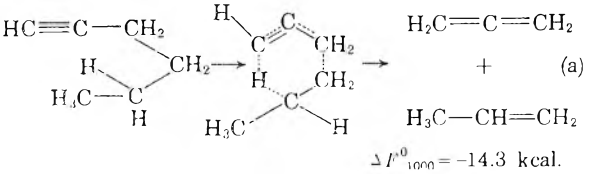

(a)

$\Delta F^0_{1000} = -14.3$ kcal.

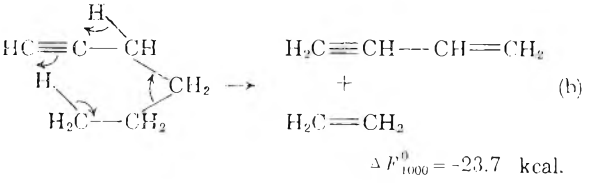

(b)

$\Delta F^0_{1000} = -23.7$ kcal.

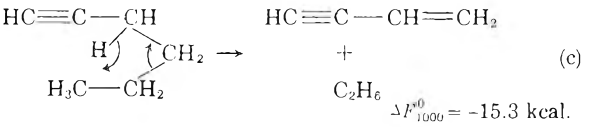

(c)

$\Delta F^0_{1000} = -15.3$ kcal.

Reaction (c) is obviously exceptional in that it does not involve the π-electrons directly. It is also open to question because the requisite amount of ethane was not observed in the pyrolysis products. Undoubtedly the picture is somewhat clouded in the case of 1-hexyne because of the occurrence of homolytic cleavage to a greater extent than in the other cases.

On the basis of experiments with hexyne, dipropargyl ether and 1,6-heptadiyne, it was predicted that the reaction was not dependent on a triple bond, and that the π-electrons of a double bond could also accept a proton from another part of the molecule, as

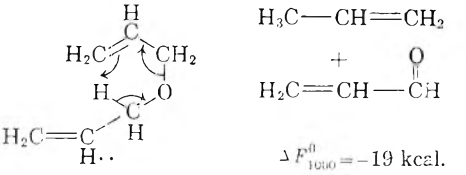

$\Delta F^0_{1000} = -19$ kcal.

As previously noted, the predicted products were obtained in a comparatively clean reaction.

The fact that traces of the rearrangement products were observed in the products of the autodecomposition reaction of dipropargyl ether and 1,6-heptadiyne and the high speed of the rearrangement reaction indicate that it is at least proceeding concurrently with the autodecomposition, if not actually preceding it.

Acknowledgment.—The author wishes to express his appreciation to the Office of Naval Research for the support of this work, to the Texaco Research Center, Beacon, N. Y., for mass-spectrographic analyses, and to the many persons who have contributed so much in the way of conduct of experiments, discussion of results, and preparation of this paper.

(11) J. F. Cordes and H. Günzler, *Chem. Ber.*, **92**, 1055 (1959).

(12) *Cf.* C. K. Ingold, "Structure and Mechanism in Organic Chemistry," University Press, Ithaca, N. Y., 1953, pp. 553, 598–599.

(13) Free-energy changes at 1000°K. were estimated by Franklin's method of group contributions, J. L. Franklin, *Ind. Eng. Chem.*, **41**, 1070 (1949).

THERMODYNAMIC STUDIES OF THE SYSTEM: ACETONE–CHLOROFORM. II. THE RELATION OF EXCESS MIXING FUNCTIONS TO ASSOCIATION COMPLEXES[1]

BY EDWARD R. KEARNS

Sterling Chemistry Laboratory, Yale University, New Haven, Connecticut

Received August 8, 1960

The assumption of 1:1 and 1:2 association complexes in the acetone–chloroform system is sufficient for close reproduction of previously reported excess free energy of mixing data and Hirobe's calorimetric heat of mixing data throughout the experimental range of composition and from 25–50°. Equilibrium constants are obtained from a linear plot of the type used by McGlashan and Rastogi. The heat of association for the 1:1 complex is in agreement with previous estimates for the energy of the C–H.....O=C hydrogen bond.

Introduction

In a previous paper,[2] herein denoted (I), excess free energies of mixing, G_X^E, were reported for the acetone–chloroform system at 25, 35 and 50°. These data were fitted to a function of mole fraction similar to those used by Wohl,[3] and from the temperature-dependence of parameters, it proved possible to calculate the heats of mixing[4] with fair precision, by fitting an equation to selected data points. Röck and Schröder[5a,b] have recently raised questions about the precision of the reported data, which led to a re-examination of the acetone–chloroform system to see how closely one could predict heat of mixing data from activity measurements. It was found that the treatment of McGlashan and Rastogi[6] could be applied to the acetone–chloroform system. Calculated values of H_X^E agreed with the experimental values of Hirobe,[4] almost to the precision of the original data. This evidence that the G_X^E data is consistent with H_X^E measurements serves to refute contentions[7,8] of unreliability of measurements made with the same equilibrium still.

Association Complexes.—McGlashan and Rastogi[6] have given a theoretical treatment for the case where two components, A and B, form complexes AB and AB_2. In this paper, every mention of a numbered equation refers to that given in the paper of McGlashan and Rastogi.[6,9] Acetone and chloroform are designated as A and B, respectively. K_1 and K_2, the equilibrium constants for the formation of complexes AB and AB_2, respectively, were obtained by least squares fitting of the data to the relation of equation 12. Standard deviations for the equilibrium constants at each temperature were of the order of 0.016 to 0.027. Clearly, for the calculation of H_X^E, knowledge of the variation of the equilibrium constants with temperature is required. Since K's are known at only three temperatures, it is impossible to draw accurate slopes in a plot of ln K against $1/T$, unless the data seems to lie on a straight line. However, estimates of slopes were made, and h_1 and h_2 were calculated. From equation 17, values of H_X^E were calculated. Both h_1 and h_2 were then multiplied by a factor sufficient to cause equation 17 to fit the experimental data closely. The resulting values of h_1 and h_2 are given in Table I. Temperature derivatives of ln K_1 and ln K_2, calculated from h_1 and h_2, were well within the graphically estimated uncertainty.

TABLE I

EQUILIBRIUM CONSTANTS AND HEATS OF ASSOCIATION

t, °C.	K_1	K_2	$-h_1$, kcal./mole	$-h_2$, kcal./mole
25	0.967	1.117	2.42	3.29
35	.844	0.924	2.44	3.73
50	.698	0.668	2.46	4.32

Using specific heats for the acetone–chloroform system,[10] heats of mixing at 25° were corrected to 35 and 50°. As before, equation 17 was fitted closely to the data by adjustment of the factor used to multiply both h_1 and h_2. Standard deviations, σ, of calculated values of H_X^E from the interpolated experimental values were: 7.8, 11.3 and 10.5 cal./mole, at 25, 35 and 50°, respectively. Changing the value of δ_{AB} by a factor sufficient to double β_{AB} made no significant difference in the closeness of fit or the value of h_1 at 25°.

In an attempt to eliminate the error resulting from interpolation of Hirobe's measurements, calculations of H_X^E were made at the experimental concentrations used by Hirobe.[4] For this purpose, a_B was determined at these values of X_B by an iteration procedure, using equation 11. After adjusting h_1 and h_2 to give closest fit of equation 17 to the calorimetric data ($h_1 = -2.48$ kcal./mole and $h_2 = -3.37$ kcal./mole), the deviation from experiment was estimated to be: σ, 7.7 cal./mole. Activities calculated by the iteration procedure referred to are considerably different from the experimental values given in Table II–IV; the difference is of the order of 2–3%. From the form of the equation for X_B, it is clear that it should be much more sensitive to uncertainties in a_B than equations 15 and 17. This discrepancy is not particularly important to the main thesis of this paper, since mixing quanti-

(1) Based in part on the MS Thesis of Edward R. Kearns, Purdue University, August 2, 1957.

(2) C. R. Mueller and E. R. Kearns, *J. Phys. Chem.*, **62**, 1441 (1958).

(3) K. Wohl, *Trans. Am. Inst. Chem. Engrs.*, **42**, 215 (1946).

(4) H. Hirobe, *J. Fac. Sci., Imp. Univ. Tokyo, Sect. I*, **1**, Part 4, 155 (1926).

(5a) H. Röck and W. Schröder, *Z. physik. Chem. (Frankfurt)*, **11**, 41 (1957).

(5b) H. Röck and W. Schröder, *ibid.*, **20**, 103 (1959).

(6) M. L. McGlashan and R. P. Rastogi, *Trans. Faraday Soc.*, **54**, 496 (1958).

(7) A. G. Williamson, R. L. Scott and R. D. Dunlap, *J. Chem. Phys.*, **30**, 325 (1959).

(8) C. R. Mueller, *ibid.*, **30**, 326 (1959).

(9) In equation 17 an a_B has been erroneously omitted.

(10) L. A. K. Staveley, W. I. Tupman and K. R. Hart, *Trans. Faraday Soc.*, **51**, 323 (1955).

ties are much more important for correlating the properties of liquid mixtures than are activities. One might attribute the discrepancy, however, to a number of things: slight errors in the values of the equilibrium constants affect the calculated mole fractions disproportionately; the experimental activities might be wrong, due to a poor choice of δ_{AB}[11]; or finally, and perhaps most reasonably, the assumption of non-interaction of the species A, B, AB and AB_2 is incorrect in this case.[6,12]

TABLE II

MIXING FUNCTIONS FOR ACETONE–CHLOROFORM, 25°

X_B	a_A	a_B	$-G_X^E$, cal./mole	$-H_X^E$, cal./mole
0.0377	0.9739	0.0178	9.9	40
.2206	.7622	.1268	80.3	243
.3969	.5415	.2708	128.4	405
.4810	.4336	.3571	140.1	455
.6588	.2197	.5758	143.2	454
.7362	.1467	.6826	124.7	400

TABLE III

MIXING FUNCTIONS FOR ACETONE–CHLOROFORM, 35°

X_B	a_A	a_B	$-G_X^E$, cal./mole	$-H_X^E$, cal./mole
0.1226	0.8799	0.0677	43.1	128
.2718	.7031	.1739	90.0	286
.3904	.5549	.2742	119.5	386
.5477	.3591	.4403	137.1	459
.6631	.2303	.5846	129.6	443
.7963	.1107	.7600	98.8	333

TABLE IV

MIXING FUNCTIONS FOR ACETONE–CHLOROFORM, 50°

X_B	a_A	a_B	$-G_X^E$, cal./mole	$-H_X^E$, cal./mole
0.1323	0.8634	0.0838	41.6	134
.2466	.7303	.1696	74.4	248
.3916	.5581	.2936	106.1	363
.5479	.3671	.4586	123.1	431
.6660	.2397	.6006	115.4	417
.8059	.1137	.7806	83.2	308

Using the iteration procedure to calculate a_B, computations of G_X^E were made at intervals of 0.1 in mole fraction, and comparisons were made with values obtained from graphical smoothing of experimental data (with plots of ln γ against X_B) at 25°. Agreement was good, with a standard deviation, σ, of 1.87 cal./mole. The uncertainty of the graphical smoothing was estimated to be ±0.59 cal./mole. A smooth curve may be drawn through a plot of the smoothed values of G_X^E against mole fraction, the shape of which is quite similar to a plot of H_X^E against X_B. Each of these curves might be useful for estimation of mixing functions for the acetone–chloroform system at compositions outside the experimental range.

It would be of little value to attempt a closer fit of calculated heat of mixing data to experiment, by adjusting both h_1 and h_2 independently, in the method used by McGlashan and Rastogi,[6] because of uncertainty in the calorimetric data. There is evidence[13] that the 25° data of Hirobe[4] is slightly less exothermic than it would be in the absence of a vapor space; an error of about 3 cal./mole at an equimolar composition is indicated. To this error we must add the suspected error due to the C_P^E values,[10] in estimating heats of mixing at 35 and 50°; the values given in Tables III-IV agree more closely with the experimental values of U. Onken[5a,14] at 40° than with values calculated using the C_P^E values of Staveley, *et al.*[10]. The latter data is difficult to use, in any case since one has only four widely spaced data points for use in interpolation.

(11) Calculations showed about the same discrepancy in activity when δ_{AB} was assumed to have a value consistent with doubling β_{AB}, and K_1 and K_2 were recalculated from a fit of activities to equation 12.

(12) I. Prigogine and R. Defay, "Chemical Thermodynamics," Longmans Green and Co., New York, 1954, p. 417.

Discussion

For the 1:1 complex, the following structure, proposed by a number of investigators, seems quite reasonable: $(CH_3)_2C{=}O\ldots\ldots H{-}CCl_3$. The value of the heat of association, given in Table I, is nearly constant at −2.4 kcal./mole. Alexander and Lambert[15] estimated the energy of the C–H . . . . . .O hydrogen bond in acetaldehyde at 2.6 kcal./mole, in close agreement with the finding of this paper.

The AB_2 complex might be represented as an association of the following type

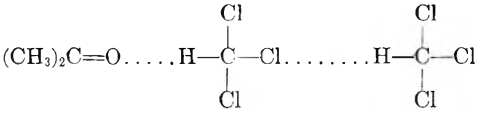

where the dipoles are considered to be aligned along the dotted lines. Extreme polarization of the central chloroform molecule would enable it to interact with a second chloroform molecule. Evidence for the association of chloroform molecules in the pure liquid has been reviewed by Nikuradse and Ulbrich[16]; one can add to this the recent proton resonance evidence of Reeves and Schneider.[17]

Freezing-point diagrams for the acetone–chloroform system[18] indicate the presence in the solid phase of only a 1:1 complex. Aside from the question whether an association might be present in the solid phase but not indicate its presence in the freezing-point diagram, it is clear that freezing-point diagrams can only indicate the *possibility* of an association in the liquid phase. Evidence that a 1:2 complex is possible for the liquid phase of the acetone–chloroform system comes from the freezing-point diagram for the ether–chloroform system, which indicates the existence of a 1:2 complex in the solid phase. It is submitted that a 1:2 complex for the latter system is inherently less likely than the presumably similar complex in the former system, because of the less exposed dipole of the ether molecule.

Using the values of $-h_2$ given in Table I, and assuming that the energy of formation of the first

(13) I. Brown and W. Foch, *Australian J. Chem.*, **8**, 361 (1955).

(14) W. Schröder, personal communication, November 14, 1957.

(15) E. A. Alexander and J. D. Lambert, *Trans. Faraday Soc.*, **37**, 421 (1941).

(16) A. Nikuradse and R. Ulbrich, *Z. physik. Chem. (Frankfurt)*, **2**, 9 (1954).

(17) L. W. Reeves and W. G. Schneider, *Can. J. Chem.*, **35**, 251 (1957).

(18) G. J. Korinek and W. G. Schneider, *Can. J. Chem.*, **35**, 1157 (1957).

bond is little affected by the formation of the second, the energy of the second bond is 0.9–1.9 kcal./mole in the temperature range considered. This value corresponds closely with the value of 1.6 kcal./mole, obtained by McGlashan and Rastogi[6] for the energy of the second bond in the dioxane–chloroform system.

The advantage of the McGlashan–Rastogi analysis in terms of a 1:1 and a 1:2 complex is that only two parameters, obtainable from experimental data, are required to reproduce the *form* of G_X^E and H_X^E. There is reason to believe that if the data were available over a wide temperature range, H_X^E could be calculated precisely, directly from G_X^E data. More complicated equilibria, involving complexes of the type A_2B, A_2B_2, A_2, B_2, etc., have been considered and rejected, because in each case it appears that more than three parameters would be required to fit the data, and apparently with less precision than the analysis of this paper.

It would be interesting to see whether other data on the acetone–chloroform system can be interpreted better from the standpoint of the formation of two complexes. Equally interesting would be an attempt to apply the analysis of McGlashan and Rastogi[6] to other systems, such as ether–chloroform or benzyl acetate–chloroform.[19]

Appendix

Treatment of Data.—The calculations of gas imperfections affect the calculated values of G_X^E somewhat, and the values of a_A and a_B considerably, so the exact treatment of this paper will be given. In (I), it was assumed, in accordance with the suggestion of Barker and Smith,[20] that δ_{AB} ($\equiv 2\beta_{AB} - \beta_{AA} - \beta_{BB}$) had the same value for the acetone–chloroform system at each temperature as the known values for the ether–chloroform system.[21] In this paper, β_{AB} is assumed to be the same at each temperature for the two systems. The resulting values of $-\beta_{AB}$ are only slightly higher than those given for the methyl acetate–chloroform system.[22]

The equations used for extrapolation of the second virial coefficients for the pure components[23] to 25–50° were of the form used by Cox and Andon.[24]

$$\log(-\beta_{AA}) = 11.8239 - 3.442 \log T,\ \sigma = 38.45 \text{ ml./mole}$$
$$\log(-\beta_{BB}) = 9.91467 - 2.7548 \log T,\ \sigma = 6.73 \text{ ml./mole}$$
$$\log(-\beta_{AB}) = 18.2151 - 5.9744 \log T,\ \sigma = 38.09 \text{ ml./mole}$$

The resulting values of the second virial coefficients are given in Table V. The equation given here for $(-\beta_{AA})$ fits the experimental data slightly better than the equation of Pennington and Kobe[25] for acetone.

TABLE V

SECOND VIRIAL COEFFICIENTS, ACETONE–CHLOROFORM

t, °C.	$-\beta_{AA}$, ml./mole	$-\beta_{BB}$, ml./mole	$-\beta_{AB}$, ml./mole	$-\delta_{AB}$, ml./mole
25	2001	1253	2702	2151
35	1786	1144	2219	1507
50	1516	1004	1670	820

Thermodynamic Consistency.—It has not been found possible to distinguish between the data of Röck and Schröder[5a,b] and that of this paper, *on a basis of tests for thermodynamic consistency*. One can not compare directly values of J_T, because of the uncertainty of extrapolation to the composition extremes in the Herington–Redlich–Kister[26a,b] plot. Röck and Schröder neglected the correction for vapor interactions, δ_{AB}, in estimating J_T. J_T will itself depend on δ_{AB}, and hence *should not* equal zero unless a reasonable value of δ_{AB} is chosen. It appears, from comparison of plots of $RT \ln(\gamma_A/\gamma_B)$ against X_B drawn for different values of δ_{AB}, that non-zero values of δ_{AB} give smaller relative areas, *i.e.*, smaller values of J_T. Further, there appears to be little difference between plots for the data of this paper and that given by Röck and Schröder, assuming $\delta_{AB} = 0$ in each case: the curves are approximately superimposable.

(19) W. R. Moore and G. E. Styan, *Trans. Faraday Soc.*, **52**, 1156 (1956).

(20) J. A. Barker and F. Smith, *J. Chem. Phys.*, **22**, 375 (1954).

(21) J. H. P. Fox and J. D. Lambert, *Proc. Roy. Soc.* (*London*), **A210**, 557 (1952).

(22) J. D. Lambert, J. S. Clarke, J. F. Duke, C. L. Hicks, S. D. Lawrence, D. M. Morris and M. G. T. Shone, *ibid.*, **A249**, 414 (1959).

(23) J. D. Lambert, G. A. H. Roberts, J. S. Rowlinson and V. J. Wilkinson, *ibid.*, **A196**, 113 (1949).

(24) J. D. Cox and R. J. L. Andon, *Trans. Faraday Soc.*, **54**, 1622 (1958).

(25) R. E. Pennington and K. A. Kobe, *J. Am. Chem. Soc.*, **79**, 300 (1957).

(26a) E. F. G. Herington, *Nature*, **160**, 610 (1947).

(26b) O. Redlich and A. T. Kister, *Ind. Eng. Chem.*, **40**, 345 (1948)

THE EXCHANGE REACTION BETWEEN Cl_2 AND CCl_4

BY FRANCIS J. JOHNSTON AND JOHN E. WILLARD

Department of Chemistry of the University of Wisconsin, Madison, Wisconsin

Received August 8, 1960

The thermal exchange of chlorine between Cl_2 and liquid CCl_4 is readily measurable at temperatures in the range of 180° and above. The photochemical exchange occurs with a quantum yield of the order of unity in the liquid phase at 65° using light absorbed only by the Cl_2. In the gas phase, with 10^{-3} mole/liter of Cl_2 and 10^{-2} mole/liter of CCl_4, quantum yields of the order of 10^{-2} have been observed at 85°. Despite extensive attempts to obtain highly pure reagents, serious difficulty was experienced in obtaining reproducible rates of reaction. It appears possible to set a lower limit of about 14 kcal./mole for the activation energy of the abstraction of a chlorine atom from a carbon tetrachloride molecule by a chlorine atom to form CCl_3 radical. The rate of the gas phase exchange reaction appears to be proportional to the first power of the absorbed light intensity indicating that the radical intermediates are removed at the walls or by reaction with an impurity rather than by bimolecular radical combination reactions.

Introduction

Because of the simplicity of the molecules, isotopic exchange reactions between elemental halogens and the corresponding carbon tetrahalides would appear to offer particularly fruitful possibilities for obtaining unambiguous basic kinetic data. It would appear that it should be possible to determine unique mechanisms for the thermal and photochemical reactions in both the liquid and gas phases and to determine values for activation energies of some of the intermediate reactions of atoms and free radicals, as well as information on the heat of dissociation of the carbon–halogen bond. The reaction of chlorine with carbon tetrachloride seemed particularly suited for such studies. It should be possible to prepare very pure chlorine by oxidation of inorganic chlorides on a vacuum system followed by multiple distillation of the liquid. It should be possible to free carbon tetrachloride of any interfering substances by the usual purification methods followed by prechlorination prior to addition of radioactive chlorine. Furthermore, the exchange would not be expected to be sensitive to trace amounts of impurities because it would not be apt to be a chain reaction since the activation energy for abstraction of chlorine by a chlorine atom would be expected to be too high; also it would be expected that Cl_2 would compete very effectively with any impurities as a scavenger for CCl_3 radicals. Contrary to these expectations we have found it impossible to obtain the degree of reproducibility one would wish, even with extensive efforts to prepare especially pure reagents. We are reporting these investigations here briefly because of their relevancy to problems of the study of apparently simple exchange reactions of chlorine and because the results furnish some information on the activation energy for abstraction of chlorine atoms from carbon tetrachloride.

Experimental[1]

Reagents.—Matheson highest purity tank chlorine was passed through a tube of resublimed P_2O_5 into an evacuated Pyrex system where it was condensed with liquid air. It was then distilled at least three times from a trap at −78° to a liquid air trap with only a small middle fraction being retained in each distillation. The purified product was stored at −78° in a tube equipped with a break seal.

Of several methods employed for tagging chlorine with radiochlorine, the exchange of inactive chlorine with tagged aluminum chloride at room temperature was found to be the most satisfactory. To prepare the latter, silver chloride was precipitated from a solution containing HCl^{36} obtained from the Oak Ridge National Laboratory. The silver chloride was fused under vacuum in the presence of aluminum chips with the resultant product of $AlCl_3$ which was sublimed into a flask on the vacuum line. Previously purified chlorine was subsequently admitted and the exchange was allowed to take place. The radiochlorine was stored at −78° in a tube equipped with a break seal.

Liter quantities of Mallinckrodt, low sulfur, reagent grade carbon tetrachloride were saturated with Cl_2 and ClO_2[2] and illuminated for about 50 hours with a 1000 watt tungsten lamp at a distance of a few inches. The mixture was then extracted with alkali and with water following which the carbon tetrachloride was distilled on a Vigreux column, a 25% center cut being retained which was then degassed under vacuum in the presence of P_2O_5. Purified inactive chlorine was then added from one of the tubes described above and the mixture frozen out and sealed off in a flask equipped with a break seal. This chlorine–carbon tetrachloride solution was illuminated for a day following which the flask was resealed onto a vacuum system and the excess chlorine distilled off. The required amount of carbon tetrachloride was distilled into a series of reaction cells on a manifold on a vacuum line. The desired amounts of inactive chlorine and radioactive chlorine were likewise condensed in these cells on the vacuum line following which they were frozen down and the manifold as a whole was sealed off. The contents of the manifold for liquid phase experiments were then mixed by shaking, redistributed to the reaction tubes, frozen down, and each tube was then sealed off. The reactants for the gas phase experiments were first frozen out in a side-arm attached to the manifold and then allowed to distil slowly into the manifold of pre-cooled reaction cells before sealing off. This method in general solved the problem of obtaining fairly equal concentrations of reactants in each of the six cells from a set.

Reaction Conditions and Analysis.—The samples for liquid phase thermal reaction studies were prepared in Pyrex capillary tubing 2.5 mm. i.d. and about 15 cm. long. In a few experiments the tubes were made from standard 6 mm. i.d. Pyrex tubing of 1 mm. wall thickness. Both types of tube withstood the pressure of approximately 20 atmospheres exerted by the carbon tetrachloride at 220°. The photochemical reaction cells consisted of 10 mm. i.d. Pyrex tubing, 5.5 cm. long, diffraction effects being minimized by the fact that the light passed through only liquid–glass interfaces and not gas–glass interfaces. These cells were used rather than square Pyrex tubing because of the tendency of the latter to shatter when thawing frozen carbon tetrachloride. The round cells were reproducibly positioned in the light beam which entered the thermostated mineral oil-bath through a window. Two types of light source were used, a thousand watt projection lamp and an AH6 high pressure mercury arc. The light was filtered by the soft glass window of the thermostat thus ensuring that only light absorbed by the chlorine and not by the carbon tetrachloride could enter the reaction cell. Relative incident light intensities were measured with a thermopile potentiometer system. Changes of intensity on the cell were achieved by use of a

(1) Further details of these investigations are given in the Ph.D. thesis of Francis J. Johnston, filed with the University of Wisconsin Library in 1952.

(2) R. G. Dickinson and C. E. P. Jeffreys, *J. Am. Chem. Soc.*, **52**, 4288 (1930).

wire screen and by varying the distance of the light source from the cell.

Following reaction the cells were scratched with a file and opened under a 20% aqueous sodium iodide solution. Carrier CCl_4 was added and the aqueous and organic phases were separated (cells containing gaseous reactants were immersed in liquid air before opening under sodium iodide). After titration of the liberated I_2 with $S_2O_3^{--}$, aliquots of the aqueous and of the organic phase were counted in a solution-type Geiger tube. In the liquid phase runs the amount of carbon tetrachloride in each reaction tube was determined by weighing the tube before opening and weighing the fragments after emptying. The fraction of exchange was determined as the ratio of the counts/minute observed in the carbon tetrachloride to the counts/minute calculated for the carbon tetrachloride fractions for equilibrium distribution of the activity between the chlorine and carbon tetrachloride, empirically determined correction being made for the difference in counting efficiency of Cl^{36} in H_2O and CCl_4.

Results

The Thermal Reaction.—In studying the liquid phase thermal reaction, some 70 tubes from 12 different manifold fillings were prepared and analyzed. Experiments were done at 180, 200, 210, 220°. Following observation of the fact that the reaction rates of supposedly identical reaction mixtures prepared on the same filling manifold and exposed under identical conditions often differed by several hundred per cent., a systematic series of experiments was undertaken to see whether the difficulty could be ascribed to the method of preparing the chlorine, to the effects of oxygen or moisture or to the effect of surface to volume ratio in the reaction tubes. In addition to the method described in the section above, chlorine and radiochlorine were prepared by the electrolysis of a Pb-Cl_2–AgCl eutectic on the vacuum line, and by exchange of Cl_2 with molten AgCl. Calcium hydride was substituted for P_2O_5 as a drying agent for carbon tetrachloride. No correlation between these variables and the irreproducibility of the results was found.

The reaction rates observed at 200° ranged from 2×10^{-3} of the chlorine exchanged per hour to 0.7 exchanged per hour. In most cases the chlorine concentration was about 5×10^{-3} mole/liter. Sets of reaction tubes containing 0.2 of an atmosphere of added oxygen in one case and added moisture in another, both gave reaction rates in the range of 0.1 to 0.4 of the chlorine exchanged per hour. No detectable reaction was found at room temperature for reaction mixtures allowed to stand up to 5 hours.

The Liquid Phase Photochemical Reaction.—The liquid phase photochemical exchange between chlorine and carbon tetrachloride was more reproducible than the thermal exchange, although still erratic. The improvement was most noticeable in the greater consistency among reaction cells prepared as a group on the same manifold. Rather large differences were still found between reaction cells from different manifold fillings. Some 80 reaction tubes from 13 manifold fillings were illuminated in the temperature range from 40 to 85° in a further endeavor to determine the cause of the irreproducibility and to obtain information on the activation energy and the effect of light intensity. In all cases there was readily measurable exchange after as little as one hour of illumination. By comparing reaction cells sealed from the same manifold temperature dependency corresponding to activation energies ranging from 11 to 18 kcal./mole was observed while dependence on the first power of the light intensity seemed to be indicated in most cases.

It was possible to make estimates of the quantum yield by observing the extent of reduction of a uranyl oxalate actinometer solution illuminated for a known time in a typical reaction cell and making appropriate conversions based on the differences in the absorption spectra of uranyl oxalate and of chlorine, and considering the spectral distribution of the light source. These estimates indicated that the quantum yield for the exchange of chlorine with liquid carbon tetrachloride at 35° is of the order of magnitude of unity.

When typical reaction cells to which 0.3 of an atmosphere of oxygen had been added were illuminated, chlorine and phosgene were produced. Exchange was also observed in these cells, which had chlorine present at 1 to 5×10^{-2} mole/liter.

The Photochemical Exchange in the Gas Phase.—Although there was some variation in results which must be attributed either to trace impurities or to variation in wall effects, the photochemical exchange in the gas phase was sufficiently reproducible so that it seemed meaningful to compare the reaction rates in different series of reaction tubes for the purpose of obtaining information on the effect of chlorine concentration and of carbon tetrachloride concentration on the reaction rate. Data on such comparisons together with data on the effect of light intensity are given in Table I.

In series I the relative light intensity was varied by varying the distance of the lamp from the reaction cell over the range from 14.7 to 29.2 cm. The last column shows the rate of exchange that would have been observed at a relative intensity of 4 (14.7 cm. distance) calculated on the assumptions that the incident light intensity is inversely proportional to the square of the distance of the lamp from the cell and that the rate is directly proportional to the incident light intensity. Direct proportionality of the rate to the incident intensity has also been assumed in obtaining the value in the last column for the fourth sample of series II where the light intensity was reduced by use of a screen. When calculated on this basis the rates at fixed concentrations are equal within experimental error indicating a first power dependence on the light intensity.[3]

Series I, II, III and IV contained approximately the same carbon tetrachloride concentration. For these series the ratios of the rates at both temperatures after correction for light intensity differences were within experimental error equal to the ratios of the chlorine concentration. Since the concentrations of chlorine were sufficiently low so that the amount of light absorbed was nearly proportional to the concentration, this result indicates zero-order dependence on the chlorine concentration if there is

(3) The assumption that the incident light intensity was inversely proportional to the square of the distance between the lamp and the cell is not rigorous for this system because of the difference in refractive indices of the mineral oil-bath and air, because of possible reflectance effects at the circular interfaces of the cell and because the lamp was not a point source. The first-order dependence shown when the intensity was varied by the screen used in Series II of Table I is not subject to these uncertainties.

TABLE I

EFFECT OF TEMPERATURE, LIGHT INTENSITY AND CONCENTRATION ON THE GAS PHASE PHOTOCHEMICAL EXCHANGE OF Cl BETWEEN Cl_2 AND CCl_4[a]

T, °C.	Relative light intensity[b]	t, hr.	F	Rate of exchange[c] cor. for light intensity[d] × 10^4
Series I: $[Cl_2]$ = 4.86 × 10^{-3} mole/l.; $[CCl_4]$ ~10 × 10^{-3} mole/l.				
83.5	1	6.00	0.164	8.89
	1.36	8.50	.320	10.2
	2.6	5.00	.363	10.8
	2.6	5.00	.338	9.76
	4	5.10	.462	10.8
68	4	5.00	.208	4.23
Series II: $[Cl_2]$ = 0.96 × 10^{-3} mole/l.; $[CCl_4]$ = 10.8 × 10^{-3} mole/l.				
83.5	4	4.00	0.362	2.06
		4.63	.412	2.11
		6.00	.478	1.99
	1.8	5.08	.216	1.98
68	4	5.00	.198	0.810
		10.00	.363	0.829
Series III; $[Cl_2]$ = 0.96 × 10^{-3} mole/l.; $[CCl_4]$ ~10 × 10^{-3} mole/l.				
83.5	4	2.00	0.170	1.71
		4.00	.364	2.06
		6.00	.485	2.02
68		6.00	.235	0.816
		7.30	.232	.665
		11.00	.333	.674
Series IV: $[Cl_2]$ = 2.10 × 10^{-3} mole/l.; $[CCl_4]$ = 9.1 × 10^{-3} mole/l.				
83.5	4	2.00	0.197	4.11
		5.00	.360	3.38
		10.00	.648	3.96
68		4.00	.167	1.72
		8.00	.261	1.43
		12.00	.357	1.39
Series V: $[Cl_2]$ = 2.20 × 10^{-3} mole/l.; $[CCl_4]$ = 24.3 × 10^{-3} mole/l.				
83.5	4	2.00	0.237	5.71
		4.00	.427	5.85
		6.00	.559	5.75
68		6.00	.296	2.69
		11.50	.490	2.69

[a] All runs with A-H6 lamp. [b] Light intensities varied by varying lamp-cell distance 14.7 to 29.2 cm. except for intensity of 1.8 in Series II for which distance was 14.7 cm. and intensity was reduced by screen. [c] $R = -\frac{\ln(1-E)}{t} \frac{4[Cl_2][CCl_4]}{[Cl_2]+2[CCl_4]}$ g. atoms $l.^{-1}$ $hr.^{-1}$. [d] Rate at lamp distance of 14.7 cm. calculated from observed rate assuming the rate to be proportional to the first power of the light intensity.

first-order dependence on the absorbed light intensity.

Comparison of the rates observed in Series IV and V where the chlorine concentration was nearly the same and the carbon tetrachloride concentration was varied by a factor of 2.7 indicates that the rate is approximately proportional to the square root of the carbon tetrachloride concentration.

The estimated quantum yield for the gas phase reaction at 83° is 6 × 10^{-3}, *i.e.*, about 1% of the quantum yield estimated for the liquid phase. For each series of cells prepared from a single manifold measurements were made at both 83.5 and 68°. The individually calculated activation energies for nine such series ranged from 13.1 to 14.9 kcal./mole with an average of 14.0 kcal./mole.

Discussion

Previous Work.—Rollefson and Libby[4] have reported a single experiment in which chlorine tagged with Cl^{38} (37 min.) was illuminated in CCl_4 at room temperature long enough to allow four photons to be absorbed per Cl_2 molecule. Within their experimental accuracy no exchange occurred and they set an upper limit of (0.007) on the quantum yield. The absence of exchange as compared to the results obtained in the present work may have been due to the lower temperature, the presence of dissolved air, or other impurities, or a combination of these variables.

The only other tests of the exchange recorded in the literature of which we are aware are three experiments of Schulte[5] using about 1 × 10^{-3} mole/l. of Cl_2 tagged with Cl^{36} in liquid CCl_4. He reports exchange rates at about 20° of 0.16 × 10^{-5}, 0.92 × 10^{-5} and 1.41 × 10^{-5} g. atoms of Cl per liter-hr., respectively, in the dark, in "sunlight," and in an illumination at 12 inches from a GE VA-2 250 watt ultraviolet lamp. The quartz sample bulbs allowed CCl_4 to absorb an appreciable fraction of the light energy from the ultraviolet lamp. From the data presented it appears that the "exchange" observed in the dark may have been due to reaction with hydrogen-containing impurities.

The thermal exchange between gaseous CCl_4 and Cl_2 has been tested in our laboratory[6] using varying concentrations of the reactants in the range of 10^{-3} mole/l. and temperatures from 300–330°. Under these conditions the transfer of radioactivity followed the first order exchange law with half times of the order of a few hours.

Other exchange reactions between halogens and carbon tetrahalides which have been reported include the thermal exchange of bromine with gaseous carbon tetrabromide[7] which was found to obey the rate law: Rate = $k(Br_2)^{1/2}(CBr_4)$ in both the gaseous and liquid states; the photochemical exchange of bromine with carbon tetrabromide in CCl_4 solution,[8] which is very sensitive to impurities and gives quantum yields in the range of tens to hundred at room temperature; and the thermal exchange of bromine with liquid[9a] and gaseous CCl_3Br.[9] The CCl_3Br reaction has given reproducible results with agreement between two laboratories for the vapor phase exchange, and the interesting result that the rate constants and activation energies are the same in the vapor, liquid and solution phases.

(4) G. K. Rollefson and W. F. Libby, *J. Chem. Phys.*, **5**, 569 (1937).
(5) J. W. Schulte, *J. Am. Chem. Soc*, **79**, 4643 (1957).
(6) Paul Ehrlich, M.S. report, 1948.
(7) J. H. Hodges and A. S. Micelli, *J. Chem. Phys.*, **9**, 725 (1941).
(8) (a) L. B. Seely, Jr., and J. E. Willard, *J. Am. Chem. Soc.*, **69**, 2061 (1947); (b) L. B. Seely, Jr., Ph.D. Thesis, University of Wisconsin, 1942.
(9) (a) A. A. Miller and J. E. Willard, *J. Chem. Phys.*, **17**, 168 (1949); (b) N. Davidson and J. H. Sullivan, *ibid.*, **17**, 176 (1949).

Mechanism of Cl_2–CCl_4 Exchange.—The fact that the Cl_2–CCl_4 exchange is greatly accelerated by light absorbed by the Cl_2 indicates the Cl atom is an important reaction intermediate. The present results are unable to distinguish with certainty between a mechanism involving the steps $CCl_4 + Cl \rightarrow CCl_3 + Cl_2$ followed by $CCl_3 + Cl_2^* \rightarrow CCl_4^* + Cl$ and a displacement reaction of the type $Cl^* + CCl_4 \rightarrow CCl_4^* + Cl$. It has been shown[9b] that the CCl_3Br reaction occurs by the abstraction mechanism and it is known from the present work and many other observations that when Cl_2 is illuminated in the presence of CCl_4 containing oxygen $COCl_2$ is formed. These facts argue in favor of the abstraction mechanism. For conditions of low quantum yield[10] the rate by either mechanism would be dependent on the steady-state concentration of Cl atoms and would be equal to $k(Cl)(CCl_4)$.

The fact that the observed photochemical reaction in the gas phase is proportional to the first power of the absorbed light intensity[11] indicates the reactive intermediates responsible for exchange (presumably Cl and CCl_3) cannot be removed by reaction with each other in reactions such as $2Cl + M \rightarrow Cl_2 + M$. The alternative possibilities are that they are removed by the walls or by trace impurities. It may be estimated that under the conditions used in these experiments a chlorine atom averaged about 10^5 collisions sec.$^{-1}$ with the walls. If no removal of chlorine atoms occurred at the walls and they all formed Cl_2 at a rate equal to $k[Cl]^2[CCl_4]$, with a value of k similar to that for bromine atom recombinations in the presence of bromine as a "third body,"[12] the steady-state concentration of Cl atoms would have been about 10^{13} atoms cc.$^{-1}$ and the rate of recombination about 10^{14} atoms cc.$^{-1}$. sec.$^{-1}$. Since 10^{13} atoms would undergo about 10^{18} collisions sec.$^{-1}$ with the walls the rate of removal by the walls would compete significantly with the homogeneous recombination if the "sticking coefficient" for the walls were 10^{-5} or higher. Sticking coefficients for chlorine atoms on glass walls have been variously estimated as 10^{-3} to $10^{-4.8}$.[13] According to these considerations it is therefore plausible that recombination may occur predominantly by a wall catalyzed reaction rather than as a homogeneous reaction.

At 68° a reaction with an activation energy of 14 kcal./mole requires an average of about 10^9 collisions between reaction partners if the frequency factor is unity. Since it may be estimated that in the present experiments a Cl atom averaged about 2×10^9 collisions sec.$^{-1}$ with CCl_4 molecules and 10^5 collisions sec.$^{-1}$ with the walls it is not surprising that the quantum yield was much less than unity if chlorine atoms are removed by the walls.

Perhaps more surprising than the first power dependence on the light intensity is the apparent 0.5 power dependence on the CCl_4 concentration indicated by the single test of this in the comparison of Series IV and Series V Table I. In this connection it may be noted that the rate of the reaction might be expressed by the relation

$$R = \frac{k_{Cl_2-CCl_4} I_{ab} \phi [CCl_4]}{k_{Imp}[Imp] + k_w}$$

where ϕ is the quantum yield for primary dissociation of the halogen (unity in the gas), k_{Imp} is the rate constant for reaction with impurity, [Imp] is the concentration of impurity and k_w is the rate of reaction with the walls. If the impurity concentration were proportional to the CCl_4 concentration such an expression would give a $[CCl_4]$ dependence between zero and unity depending on the relative magnitude of k_{Imp} [Imp] and k_w.

Aside from the limited evidence for a dependence on less than the first power of the CCl_4 concentration the results favor removal of Cl atoms by the walls in the gas phase photochemical reaction. In further support of this conclusion is the following experiment. The CCl_4 from six sample tubes in which the photochemical exchange between radiochlorine and CCl_4 had occurred was combined and diluted to 250 cc. following which it was fractionally distilled, using a Vigreux column, to give four 50-cc. fractions and a pot residue. Equal aliquots of the five fractions gave the following relative counting rates: 88 ± 3, 86 ± 3, 88 ± 3, 87 ± 3 and 90 ± 3 indicating that essentially all of the organic activity was in the form of CCl_4. The only impurity which could lead to the activity entering organic combination as CCl_4 is $CHCl_3$ and it seems highly improbable that this could have been introduced into the system following the type of preillumination with inactive chlorine on the vacuum line which was used in the purification.

If the process of removal of Cl atoms by impurities or (in the gas phase) walls, has an activation energy the observed apparent activation energy of exchange would be lower than the true activation energy of exchange. Therefore the value of 14 kcal./mole obtained from the photochemical gas phase studies may be considered a minimum value for the activation energy of the $Cl + CCl_4 \rightarrow CCl_3 + Cl_2$ reaction.

The fact that the rate of the thermal exchange of bromine with CCl_3Br in the region of 180–200° is proportional to the square root of the bromine concentration and is quite reproducible[9] must mean either that this compound is easier to purify than CCl_4 or that Br atoms react with the impurities less readily than Cl atoms or that the lower energy of

(10) It is interesting to consider a limiting case in which every Cl atom formed by $Cl_2 \xrightarrow{h\nu} 2Cl$ would undergo the displacement reaction $Cl^* + CCl_4 \rightarrow CCl_4^* + Cl$. The quantum yield (Cl atoms exchanged/photon absorbed) would then be 2 and would be independent of light intensity (*i.e.*, the rate would be proportional to the light intensity) since any further exchange with CCl_4 by the non-radioactive Cl displaced would not lead to further transfer of radioactivity. New radioactive chlorine atoms might be generated by a $Cl + Cl_2^* \rightarrow Cl_2 + Cl^*$ exchange, however.

(11) Such dependence has been observed in a number of gas phase reactions involving chlorine. (a) T. D. Stewart and B. Weidenbaum, *J. Am. Chem. Soc.*, **57**, 2036 (1935); 1702 (1935); (b) R. G. Dickinson and J. L. Carrico, *ibid.*, **56**, 1473 (1934); (c) L. T. Jones and J. R. Bates, *ibid.*, **56**, 2282 (1934); (d) H. J. Schumacher and D. Sundhoff, *Z. physik. Chem.*, **34B**, 300 (1936); (e) M. Bodenstein, S. Lenher and C. Wagner, *ibid.*, **3B**, 459 (1929); (f) W. J. Kramers and L. A. Moignard, *Trans. Faraday Soc.*, **45**, 903 (1949).

(12) W. G. Givens, Jr., and J. E. Willard, *J. Am. Chem. Soc.*, **81**, 4773 (1959).

(13) R. M. Noyes and L. Fowler, *ibid.*, **73**, 3043 (1951).

dissociation of the bromine molecules results in a sufficiently higher steady-state concentration so that the atom recombination reaction can compete effectively with the reaction with impurities. One might predict that the atom recombination reaction in the photochemical exchange of Cl_2 with CCl_4 might be made to complete effectively with wall reactions and impurity reactions by using much increased light intensities.

Acknowledgment.—This work has been supported in part by the United States Atomic Energy Commission and in part by the University Research Committee with funds made available by the Wisconsin Alumni Research Foundation.

X-RAY POWDER DATA AND STRUCTURES OF SOME BIS-(ACETYLACETONO)-METAL(II) COMPOUNDS AND THEIR DIHYDRATES

By R. H. Holm and F. A. Cotton

Department of Chemistry, Massachusetts Institute of Technology, Cambridge, Mass.

Received August 8, 1960

X-Ray powder diffraction patterns have been recorded for the following compounds (A = $C_5H_7O_2$, acetylacetono): MnA_2, $MnA_2 \cdot 2H_2O$, CoA_2, $CoA_2 \cdot 2H_2O$, NiA_2, $NiA_2 \cdot 2H_2O$, CuA_2, ZnA_2, PdA_2. From the data it appears probable that CuA_2 and PdA_2 are isomorphous, completely certain that $CoA_2 \cdot 2H_2O$, $NiA_2 \cdot 2H_2O$ and $MnA_2 \cdot 2H_2O$ are isomorphous, but doubtful if there are any other isomorphisms, contrary to a previous report of Shibata. It also appears that Shibata's data on NiA_2 are at least in part incorrect.

Introduction

Very little is known of the structures of bis-(acetylacetono)-metal(II) compounds (hereafter abbreviated MA_2). The only compounds which have been studied closely are CuA_2[1,2] and $CoA_2 \cdot 2H_2O$.[3] The former has a planar structure with D_{2h} symmetry, within the limits of experimental error. The latter contains an essentially planar CoA_2 unit with Co–O distances of 2.05 Å. and the two water molecules are coördinated to the Co atom in *trans* positions above and below this plane with the Co–OH_2 distances equal to 2.23 Å. Bullen has also reported[4] collecting three-dimensional data for single crystals of NiA_2 but was unable to deduce the structure in detail. He did, however, show definitely that in some manner trimers are formed in the crystal since the nickel atoms were found in linear groups of three with Ni–Ni distances of 2.80 ± 0.10 Å. Despite this unusual structural feature, Shibata[5] claims that NiA_2 and ZnA_2 are isomorphous but that both are anisomorphous with CuA_2. He also states without recourse to supporting data, that NiA_2 and CoA_2 are isomorphous.

We have examined the X-ray powder diffraction patterns of the compounds MnA_2, CoA_2, NiA_2, CuA_2, ZnA_2, PdA_2, $MnA_2 \cdot 2H_2O$, $CoA_2 \cdot 2H_2O$ and $NiA_2 \cdot 2H_2O$. Our data do not, for the most part, support Shibata's conclusions. The last three compounds are shown to be isomorphous.

Experimental

All powder diffraction patterns were obtained photographically utilizing a General Electric XRD3 X-ray diffraction unit operated at 45 Kv. and 15 ma. All samples were enclosed in 0.3 mm. diameter sealed Pyrex capillary tubes and irradiated with Cu Kα or Cr Kα radiation in a North American Phillips standard powder camera of 57.3 mm. radius. Ni and V filters were used with Cu and Cr radiation, respectively. Powder photos were indexed in the standard way[6] and a correction for effective camera radius as obtained from a NaCl calibration was applied to each arc length measured. In the calculations of the interplanar spacings the intensity-weighted averages of the Cu Kα and Cr Kα radiations were used, *viz.*, $K\alpha = 1/3\,(K\alpha_2 + 2K\alpha_1) =$ 1.5418 and 2.2909 Å., respectively.[7] The authors are grateful to Ronald Chandross for his coöperation and assistance.

Preparation of Compounds.—Bis-(acetylacetono)-manganese(II) was prepared by refluxing 5 g. of Mn powder with 100 ml. of acetylacetone (Eastman white label grade, redistilled (b.p. 138–140°) once) for 3 hours or until nearly all metal had disappeared. The dark solution containing MnA_3 was cooled and filtered quickly in air to yield a light brown powder which was washed well with ligroin. About 50 ml. of ethanol was brought to a boil in a 125-ml. flask and 5 g. of the crude product added with stirring. The dark solution was immediately filtered into a flask immersed in an ice-salt bath. Water was added slowly to the filtrate until crystallization started, and the solution cooled for 6 hr. Yellow crystals of the dihydrate were filtered off and air dried.

Anal. Calcd. for $C_{10}H_{18}MnO_6$: C, 41.53; H, 6.27; Mn, 19.00. Found: C, 41.86; H, 6.49; Mn, 18.7.

The dihydrate readily lost water and by heating at 60° for 4 hours it was converted to the light brown anhydrous compound.

Anal. Calcd. for $C_{10}H_{14}MnO_4$: C, 47.45; H, 5.57; Mn, 21.70. Found: C, 47.28; H, 5.56; Mn, 21.6.

Bis-(acetylacetono)-Co(II) was prepared by the method of Charles and Pawlikowski,[8] which yielded first the dehydrate.

Anal. Calcd. for $C_{10}H_{18}CoO_6$: C, 40.98; H, 6.18; Co, 20.11. Found: C, 41.24; H, 6.39; Co, 19.9. The dihydrate on heating 6 hr. at 58° *in vacuo* yielded the purple, crystalline anhydrous material.

Anal. Calcd. for $C_{10}H_{14}CoO_4$: C, 46.71; H, 5.48; Co. 22.94. Found: C, 46.89; H, 5.56; Co, 22.8.

Bis-(acetylacetono)-Ni(II) was prepared by the method of ref. 8, which yielded first the aqua colored dihydrate.

Anal. Calcd. for $C_{14}H_{18}NiO_6$: C, 41.00; H, 6.18; Ni, 20.04. Found: C, 39.76; H, 6.31; Ni, 19.1.

(1) E. A. Shugam *Doklady Akad. Nauk, S.S.S.R.*, **81**, 853 (1951); *C.A.* **46**, 3894*d* (1952).

(2) H. Koyama, Y. Saito and H. Kuroya, *J. Inst. Polytech., Osaka City Univ.*, **C4**, 43 (1953); *C.A.* **48**, 3097a (1954).

(3) G. J. Bullen, *Acta Cryst.*, **12**, 703 (1959).

(4) G. J. Bullen, *Nature*, **177**, 537 (1956).

(5) S. Shibata, *Bull. Chem. Soc. Japan*, **30**, 842 (1957).

(6) L. V. Azeroff and M. J. Buerger, "The Powder Method," McGraw-Hill Book Co., New York, N. Y., 1958, Chap. 7.

(7) Ref. 6, p. 34.

(8) R. G. Charles and M. A. Pawlikowski, *J. Phys. Chem.*, **62**, 440 (1958).

Table I

Comparison of Interplanar Spacings for Bis-(acetylacetonates)[a]

ZnA_2	NiA_2	CoA_2	MnA_2	CuA_2	PdA_2
11.1s	9.44vs	11.7vs	9.51vs	8.43m	
9.84s	7.73s	(10.4)m	8.91vs	7.68vs	7.56s
8.63s	6.66w	8.51vs	7.36vs	6.20vw	7.08s
7.56m	6.44m	7.47vw	6.25m	5.68s	5.38m
7.01s	6.00w	6.83m	5.66s	5.16s	5.00m
6.85s	(5.87)vw	6.35w	(4.86)m	3.75vw	4.59w
6.47vw	(5.41)vvw	(5.86)s	4.24w	3.58s	4.16vvw
5.86m	(4.46)vvw	(5.40)s	4.01vvw	3.38s	3.81vw
4.97vvw	(3.81)m	5.10vw	(3.84)w	3.26s	3.53vw
4.72vvw	3.69w	(4.81)s	3.60vw	2.94vw	3.44vs
4.35vw	3.60w	3.54m	3.38s	2.83m	3.36vw
4.20ms		3.16vw	3.00w	2.52vw	3.14vvw
4.08vw			2.79w	2.45vw	2.94vw
3.96w			2.60w	2.32w	2.45vw
3.76m				2.22m	
3.61m				2.02m	
3.50s				1.92w	
3.42m				1.89w	
				1.79m	

[a] Intensities estimated visually; distances in Å.; distances in parentheses indicate coincidence with lines of corresponding dihydrate; Cr Kα radiation.

Table II

Comparison of Interplanar Spacings for Bis-(acetylacetonate) Dihydrates[a]

$NiA_2 \cdot 2H_2O$[b]	$CoA_2 \cdot 2H_2O$[b]	$MnA_2 \cdot 2H_2O$[c]
11.5m	11.4m	
10.3s	10.5vs	10.7vs
	8.70w	8.90m
5.92w	5.87m	
5.38vs	5.40vs	5.46s
5.02vw	5.04vw	
4.77vs	4.80s	4.85s
4.55vs	4.58s	4.62m
4.29w	4.28vw	
4.15m	4.19m	4.19m
3.79s	3.79vs	3.82m
3.46m	3.48m	3.55vw
3.41s	3.42s	3.43s
3.34w	3.35w	
3.05s	3.06s	3.08vw
2.97s	2.98s	3.01w
2.87vw	2.86vw	
2.79w	2.80w	
2.65m	2.67m	2.72w
2.58mw	2.58m	
2.48mw	2.49mw	2.48vvw
2.42vw	2.43vvw	
2.39ms	2.40ms	
2.35m	2.36m	

[a] Intensities estimated visually; distances in A. [b] Cr Kα radiation; more lines were observed in high angle scattering region but are omitted from this comparison. [c] Cu Kα radiation.

The deep green anhydrous NiA_2 was obtained on heating the dihydrate at 80° *in vacuo* overnight.

Anal. Calcd. for $C_{10}H_{14}NiO_4$: C, 46.75; H, 5.49; Ni, 22.84. Found: C, 46.38; H, 5.46; Ni, 22.5.

CuA_2 and ZnA_2 were also prepared by the method of ref. 8 and purified by sublimation. They gave good analyses for C, H and metal. PdA_2 was prepared by the method of West and Riley[9] and also gave good C and H analyses.

(9) R. West and R. Riley, *J. Inorg. Nucl. Chem.*, **5**, 295 (1958).

Discussion

The interplanar spacings together with the visually estimated relative intensities of the corresponding lines are listed in Tables I and II. Not all of the weaker lines observed in the high angle (>20° for Cr Kα) diffraction region are listed since they are not useful for comparison. In most cases, back reflections were not observed and when they were, they were too diffuse to permit accurate indexing.

The patterns of the five bis-(acetylacetonates) can be divided into two groups on the basis of superficial similarities. CuA_2 and PdA_2 produce patterns which are totally unlike the other four patterns and are rather similar to each other. This result is not unexpected because Pd(II), like Cu(II), always forms planar complexes in the absence of steric strain. Comparison of the d_{hkl} values of Table I shows a reasonable correspondence between the two compounds which indicates isomorphism. In fact, dilute mixed crystals of CuA_2 in PdA_2 have been grown.[10]

The diffraction patterns of ZnA_2, CoA_2, NiA_2 and MnA_2, while completely dissimilar to those of CuA_2 and PdA_2, are not very similar to each other. Examination of the data of Table I reveals that there are a number of coincidences in spacings and approximate intensities, but that these coincidences and intensities are hardly convincing enough to warrant a postulation of isomorphism. Previously, Shibata,[5] has reported that ZnA_2 and NiA_2 are isomorphous, and the data he reports do certainly support this contention. However, while our results for CuA_2 and ZnA_2 agree moderately well with Shibata's, the comparison of data for NiA_2, Table III, reveals only one coincidence of his data with our own and that is in the high angle region.

On the other hand, as also indicated in Table III, our powder data are in much better agreement with line positions calculated from Bullen's unit cell

(10) A. H. Maki and B. R. McGarvey, *J. Chem. Phys.*, **29**, 31 (1958).

Table III

Comparison of Interplanar Spacings Observed with Those Calculated from Data of Bullen[a] for Ni(II) Acetylacetonate

d_{hkl} (Å.) This work[c]	Shibata[b]	Extinctions (Å.)	d_{hkl} calcd. from Bullen (Å.)
9.44vs			9.33 (120), 9.64 (001)
	8.66vs		8.91 (011)
7.73s		7.74 (030)	7.73 (111), 7.83 (200)
	7.41vw	7.42 (210)	7.42 (021)
	6.82mw		
6.66w			6.70 (121)
6.44m			6.49 (220)
6.00w			6.04 (031), 6.08 (201)
(5.87)vw			5.88 (211), 5.81 (040)
	5.67mw		5.63 (131)
(5.41)vvw			5.38 (221), 5.45 (140)
	(4.80)mw		4.67 (320), 4.78 (231), 4.82 (002)
(4.46)vvw		4.45 (150)	4.45 (022), 4.50 (311), 4.52 (112)
	(4.18)vw		4.19 (051)
(3.81)m	(3.78)m	3.86 (410)	3.76 (160), 3.87 (060, 222)
3.69w			3.71 (042, 420)
3.60w			3.58 (411), 3.59 (061), 3.60 (341), 3.63 (232, 401)
	(3.39)mw	3.32 (070)	3.35 (242), 3.39 (322)
	(3.07)w	3.10 (510), 3.13 (500)	3.04 (123, 402), 308 (1.71, 252, 441)
			3.10 (043), 3.11 (360), 3.12 (113)
	(2.83)w	2.80 (370)	2.81 (034), 2.82 (262, 352), 2.83 (432), 2.86 (180, 451)
	(2.61)w	2.58 (090), 2.59 (610)	2.58 (272, 333), 2.61 (362, 600)
		2.60 (550), 2.63 (502)	2.64 (053)
	(2.38)w		2.36 (353, 034, 263, 561)
			2.37 (114, 282, 433)
			2.38 (640), 2.39 (542),
			2.40 (014), 2.14 (004)

[a] Reference 3. [b] Reference 5. [c] Cr Kα radiation. [d] Values in parentheses indicate coincidence with lines of $NiA_2 \cdot 2H_2O$ (Table II).

parameters (a = 15.65 ± 0.02 Å., b = 23.23 ± 0.04 A., c = 9.64 ± 0.02 Å.) and observing the expected absences ($h0l$ when h is odd and $hk0$ when k is odd) for space groups Pmab or $P2_1ab$. For every spacing of NiA_2 observed in our work there is at least one non-extinct calculated spacing, whereas agreement of this sort is poorer for Shibata's data, particularly for his 8.66 *vs.* and 6.82 mw lines. Coincidences in the region below 3.39 are probably of doubtful significance because of the very large numbers of lines (150 from 2.00 to 3.40 Å.) arising because of the elongated unit cell. While it cannot be unequivocally concluded that our data are consistent with Bullen's, it appears that Shibata's, on which he rests his assertion of the isomorphism of NiA_2 and ZnA_2, are definitely inconsistent. We note that all of Shibata's spacings below 5.67 Å. are compatible with the presence of $NiA_2 \cdot 2H_2O$ in his sample. We found that even on twelve hour exposure rigorously dry NiA_2 gave no lines strong enough to index below 3.60 Å. whereas $NiA_2 \cdot 2H_2O$ gives quite intense lines in this region.

The data in Table II provide conclusive evidence that dihydrates of MnA_2, CoA_2 and NiA_2 are isomorphous. On the basis of the reported structure of $CoA_2 \cdot 2H_2O$[3] the observed isomorphism and nearly identical scale factors for $NiA_2 \cdot 2H_2O$ and $MnA_2 \cdot 2H_2O$ permit us to conclude that these molecules are isostructural and nearly isometric with $CoA_2 \cdot 2H_2O$.

Acknowledgments.—We thank the U. S. Atomic Energy Commission for financial support under Contract AT (30–1)-1965. We are also grateful to the General Electric Company for a Charles A. Coffin Fellowship to R. H. H. in 1958–59.

HYDROGEN ATOM REACTIONS WITH PROPENE AT 77°K. DISPROPORTIONATION AND RECOMBINATION

BY RALPH KLEIN[1] AND MILTON D. SCHEER

National Bureau of Standards, Washington, D. C.

Received August 15, 1960

The investigation of the reaction products of deuterium atoms with ordinary propene helps to establish the relative importance of the atom addition to the propyl radical with respect to disproportionation of two propyl radicals. The distribution of the isotope species among the propenes and propanes is caculated. It is concluded that the D atom addition to the propyl radical accounts for little, if any, of the propane formed, and the radical disproportionation reaction is the predominant one.

The reaction of hydrogen atoms with solid olefins such as propene at 77°K. gives as products the corresponding alkanes and the alkyl radical dimer.[2] Deuterium atoms, generated from molecular deuterium on a hot tungsten ribbon in the gas phase, impinge on a layer of condensed propene at 77° to diffuse into and react with it. So-called "cracking" products, resulting from C–C bond ruptures of excited species, are never observed. This contrasts with the corresponding gas phase reactions. Another striking difference is that the ratio of the alkane to the radical recombination products is found to be an order of magnitude higher in the solid at 77°K. than in the gas at 300°K. It has been observed that even with a hundred-fold dilution of propene with an inert diluent such as butane or dichlorodifluoromethane, the alkane/dimer ratio remains unaffected. This would indicate that isopropyl radicals diffuse rather readily in the solid. The reaction products of the hydrogen atom addition to solid propene at 77°K are propane and 2,3-dimethylbutane. The possible reactions that may occur include

$$C_3H_6 + H \longrightarrow C_3H_7 \text{ (isopropyl)} \quad (1)$$

$$2C_3H_7 \longrightarrow C_3H_6 + C_3H_8 \quad (2)$$

$$2C_3H_7 \longrightarrow C_6H_{14} \quad (3)$$

$$C_3H_7 + H \longrightarrow C_3H_8 \quad (4)$$

$$C_3H_7 + H \longrightarrow C_3H_6 + H_2 \quad (5)$$

The ratio propane/2,3-dimethylbutane was found to be 9 over a wide range of conditions such as propene dilution and hydrogen atom concentration. The ratio of 9 contrasts with the gas phase value of 0.5.[3] It may be speculated that (4) occurs more readily in the solid than in the gas (especially in view of the easy paths for energy transfer out of the molecule of the exothermic heat of the C–H bond formation). The occurrence of (4), however, would not be in accord with the constancy of the propane/2,3-dimethylbutane ratio since (4) would be expected to increase with dilution relative to (3) and hence increase the ratio. The occurrence of (5) would be shown by the formation of HD, but this was absent. Insofar as the isotope distribution among the products is concerned, it must lie within the limits imposed by (a) the formation of propane by (4) exclusively, and (b) the absence of reaction (4). Case (a) would be evidenced by the complete absence of deuteration of the residual propene. Mass spectrometric analysis showed that the propene was deuterated, Table I, so that at least (4) is accompanied by (2), the only mechanism by which propene deuteration could be effected. (Exchange reactions have too high an activation energy.)

The calculation of the isotope distribution among the products requires some care. It is possible in principle, by using the steady-state hypothesis for isopropyl radical concentration directly, to arrive at a distribution, but the complexities inherent in the variety of the isotopically labelled species makes the method ineffectual. It is only necessary to consider the stable species. Since it has been shown that propane formation is first order with respect to propene,[4] the individual isotope species must also be represented by first-order processes. In detail, a propene species a_i gives the radical r_{i+1} upon D atom addition. The index refers to the number of deuterium atoms in the molecule. The radical r_{i+1} disproportionates with any other radical r_j. In the process, r_{i+1} may lose an H or a D to become a_{i+1} or a_i, or it may gain an H or a D to become propane A_{i+1} or A_{i+2}. This can be expressed as

$$\frac{da_i}{dt} = \frac{6-i}{6} k a_{i-1} - \frac{5-i}{6} k a_i - k' a_i \quad (A)$$

$$(i = 0, 1, \ldots, 5 \text{ and } a_{-1} = 0)$$

The first term on the right refers to the D atom addition to a_{i-1} to form r_i, the r_i then disproportionating with loss of H to give a_i. The numerical coefficient $(6 - i)/6$ accounts for the $6 - i$ abstractable H's in r_i.[5] The second term describes D atom addition to a_i to give r_{i+1} followed by H atom abstraction to give a_{i+1}. The third term accounts for loss of a_i by way of propane formation, and if (4) did not occur, k' would equal k.

There is derived from (A)

$$a_0 = a_0^0 e^{-(5/6\,k + k')t}$$

$$a_1 = 5a_0^0 [e^{-(4/6\,k + k')t} - e^{-(5/6\,k + k')t}]$$

$$a_2 = 10a_0^0 [e^{-(5/6\,k + k')t} - 2e^{-(4/6\,k + k')t} + e^{-(3/6\,k + k')t}] \quad (B)$$

etc.

The analogy to a sequence of radioactive decay processes is obvious.

$$\sum_{i=0}^{5} a_i = a_0^0 e^{-k't} \quad (C)$$

(1) Now at Melpar, Inc., Falls Church, Va.

(2) R. Klein and M. D. Scheer, THIS JOURNAL, **62**, 1011 (1958).

(3) P. J. Boddy and J. C. Robb, *Proc. Roy. Soc.* (*London*), **249**, 518 (1959).

(4) R. Klein, M. D. Scheer and J. Waller, THIS JOURNAL, **64**, 1247 (1960).

(5) The hydrogen on the carbon containing the free spin is not considered abstractable.

The isotope distribution among the propanes A_i can be derived from the set

$$\frac{dA_i}{dt} = (1 - B)k''a_{i-2} + Bk''a_{i-1} + k'''a_{i-2} \quad (D)$$

B is the fraction of the potentially abstractable hydrogen in the radical which is of the H variety. The first term on the right of (D) arises from the D atom addition to a_{i-2} with its subsequent participation in a disproportionation reaction in which it abstracts a deuterium from an isopropyl radical. The second term refers to the D atom addition to a_{i-1} followed by its abstracting hydrogen from another radical. The third term is associated with reaction (4). The derivation of B from set (B) is simply

$$B = \frac{\sum_{i=0}^{5} (5 - i)a_i}{\sum_{i=0}^{5} 6a_i} = 5/6e^{-k/6t} \quad (E)$$

Calculation of the A's gives

$$A_1 = 5/6a_0^0 \frac{k''}{k + k'} [1 - e^{-(k + k')t}] \quad (F)$$

$$A_2 = \frac{(31k'' + 6k''')a_0^0}{5k + 6k'} [1 - e^{-(5/6\,k + k')t}] - \frac{31}{6} \frac{k''}{k + k'} a_0^0 [1 - e^{-(k + k')t}]$$

etc.

$$\sum_{i=1}^{7} A_i = a_0^0[1 - e^{-(k'' + k''')t}]$$

This gives $k'' + k''' = k'$ since, neglecting (3) which is small,

$$\sum_{i=0}^{5} a_i + \sum_{i=1}^{7} A_i = a_0^0$$

If (4) does not occur, then $k''' = 0$ and $k = k' = k''$.

Propene with butane as a diluent reacted at 77° K. with deuterium atoms. The propene was diluted so that a condition of constant atom concentration through the film could be maintained.[4] After reaction, the propene and propane were separated by gas phase chromatography and each fraction analyzed by mass spectrometry. k' was determined from equation (C) with the analytical data for diminution of total propene with time. With the assumption that $k = k' = k''$, the isotopic propene fractions were calculated from the set (B). Although the fractions could not be determined unambiguously from the data of Table I because of lack of reference spectra, the results are in moderately good agreement with the calculated values.[6] This is confirmatory evidence that (4) occurs, if at all, only to a small fraction of (2) under the experimental conditions used in this work.

TABLE I

MASS SPECTRA OF PROPENES FROM THE D + PROPENE REACTION[a]

	Reaction time, minutes			
m/e	0	10	30	100
36	1.0	1.0	1.0	1.0
37	4.8	4.3	3.8	4.0
38	6.5	6.0	6.0	6.0
39	28.0	24.8	23.6	19.3
40	10.8	11.8	12.4	13.3
41	41.7	36.3	33.0	27.3
42	25.9	26.1	27.2	25.3
43	1.0	4.5	8.4	13.3
44		0.9	3.3	7.7
45		0.1	0.3	1.7
46			0.1	0.3

[a] Relative to the 36 peak.

(6) Data for the propane fractions were also obtained but again lack of reference spectra for the more highly deuterated species precluded a rigidly critical comparison between calculated and observed values.

SOLVENT EXTRACTION STUDIES OF INTERHALOGEN COMPOUNDS OF ASTATINE[1]

BY EVAN H. APPELMAN[2]

The Department of Chemistry and the Lawrence Radiation Laboratory of the University of California, Berkeley, California

Received August 22, 1960

The distribution of astatine between aqueous solutions and CCl_4 has been used to study the reactions of this synthetic element with I_2, I^-, IBr, Br^- and Cl^-. The species AtI, AtBr, AtI_2^-, $AtIBr^-$, $AtICl^-$, $AtBr_2^-$ and $AtCl_2^-$ have been characterized, and the equilibrium constants interrelating them have been evaluated. These constants have been shown to correlate well with the analogous constants involving the lighter halogens. In the course of this investigation the equilibrium constant for the distribution of IBr between water and CCl_4, and the formation constant of IBr_2^- have been redetermined, and the results are in substantial agreement with previous work.

Introduction

The investigations of the solvent extraction behavior of astatine that have been carried out heretofore have been qualitative in nature.[3-5] The principal obstacle to quantitative studies has been the necessity of working with this highly radioactive element only at exceedingly low concentrations. At such concentrations it is difficult to prevent the astatine from reacting with impurities in the experimental system.

(1) Based on work performed under the auspices of the U. S. Atomic Energy Commission.

(2) (a) Argonne National Laboratory, Argonne, Illinois. (b) Abstracted from the Ph.D. thesis of the author, University of California (Berkeley), June, 1960 (UCRL-9025).

(3) G. Johnson, R. Leininger and E. Segrè, *J. Chem. Phys.*, **17**, 1 (1949).

(4) H. M. Neumann, *J. Inorg. Nucl. Chem.*, **4**, 349 (1957).

(5) E. H. Appelman, *J. Am. Chem. Soc.*, **82**, 000 (1960).

TABLE I

EQUILIBRIUM CONSTANTS USED IN ASTATINE COMPUTATIONS (21°)

Quotient	K^0	Salt effect[a]	Ref.
$(I_2)_{CCl_4}/(I_2)_{aq}$	86	$0.13(NaClO_4)^b + 0.1[(NaCl) + (NaBr)]^c + 0.05(NaI)^c + 0.03(HClO_4)^b$	9–11
$(Br_2)_{CCl_4}/(Br_2)_{aq}$	27.1	[d]	9
$(IBr)_{CCl_4}/(IBr)_{aq}$	4.31	$.12(NaClO_4) + 0.096(NaBr) + 0.03(HClO_4)$	This work
$(I_3^-)/(I_2)(I^-)$	800	$.02(NaX) + 0.05(HClO_4)$	11
$(I_2Br^-)/(I_2)(Br^-)$	14.3	[d]	12
$(I_2Cl^-)/(I_2)(Cl^-)$	~3	[d]	12
$(Br_3^-)/(Br_2)(Br^-)$	17	[d]	13
$(IBr_2^-)/(IBr)(Br^-)$	444	$.02(NaX) + 0.053(HClO_4)$	This work
$[(IBr)^2/(I_2)(Br_2)]_{CCl_4}$	384[e]	[f]	14, 15
$(I^-)(IBr)/(Br^-)(I_2)$	2.20×10^{-6}	[f]	9, 14, 15

[a] Expressed as "A" in the expression $\log K = \log K^0 + A$. Stoichiometric salt concentrations are used. Thus, for example, IBr_2^- is assumed to have the same effect as Br^-. "NaX" is sodium perchlorate or any sodium halide. [b] Assumed equal to the effect on the solubility of I_2 in water.[11] [c] Estimated from the general salting behavior of these ions.[10] [d] Assumed to be the same as for the analogous I_2 and I_3^- equilibria. [e] Calculated from the value at 25°[16] with the heat of dissociation of IBr in CCl_4 assumed equal to the vapor phase value of 1.36 kcal.[15] [f] Assumed to be independent of salt.

We might hope to minimize such troubles by studying the astatine in systems containing macro quantities of lighter halogens, which then ought to react preferentially with impurities that would otherwise react with the astatine. Under such conditions the astatine should usually be present in the form of interhalogen species. Comparison of the characteristics of these species with those of the homologous compounds formed among the lighter members of the halogen family ought to provide considerable insight into the periodic variation of chemical properties.

Experimental

Unless otherwise indicated, all reagents were prepared from commercial products of "Analytical Reagent" grade. Distilled water was redistilled from alkaline permanganate for use in these experiments, and Mallinckrodt "low-sulfur" carbon tetrachloride was used as the non-aqueous solvent for all extractions.

Sodium perchlorate solutions were prepared by dissolving sodium hydroxide in a stoichiometric amount of perchloric acid, and the solutions were analyzed by conversion to the sulfate.[6]

Sodium halide solutions were analyzed by the Fajans method, using gravimetrically standardized silver nitrate solutions.[7] Sodium chloride and bromide solutions were tested for iodide by oxidation to iodate, followed by boiling to remove excess oxidant, reduction with iodide, and detection of any I_3^- with starch.[8] Bromine was the oxidant used on the chloride solutions, while the bromide solutions were oxidized with excess chlorine in 0.2 M acid. Lower limits of 2×10^6 and 1×10^6 were found, respectively, for Cl^-/I^- in the NaCl solutions and Br^-/I^- in the NaBr solutions.

Fisher Scientific Co. "Purified" IBr was dissolved in CCl_4, and the solution was tested for an excess of either parent halogen by extracting away the IBr with several portions of 1 M NaBr and examining the residual CCl_4. Sufficient iodine was added to react with the slight excess of bromine that was found.

Halogen solutions were analyzed by addition to excess aqueous iodide, followed by titration with a sodium thiosulfate solution that had been standardized against potassium iodate.[8]

The procedures used for the preparation and analysis of the astatine have been described previously.[5] The astatine analyses had standard deviations of about 3%, due principally to statistical counting uncertainties.

Solvent extractions were carried out in Teflon-stoppered glass vessels at 21 ± 0.5°. Mixtures were agitated continuously until the extraction coefficients became invariant. This condition was usually reached within a minute, but the agitation was generally continued for five to ten minutes. The phases were separated by centrifugation. Sodium and hydrogen were the only cations present in solvent extraction mixtures. Mixtures at pH 5 and 7 were buffered with acetate and phosphate, respectively. Otherwise, perchlorate was the only non-reacting anion.

Solvent extractions involving astatine were carried out in black-taped vessels. Most of the mixtures were unaffected by light, but some were found to be so photosensitive that the extraction coefficient was altered when the vessel was opened for analysis. These mixtures were worked with in a darkroom illuminated with a Wratten Series 1 Red Safelite (Eastman Kodak Co.).

Astatine concentrations ranged from 10^{-15} to 10^{-12} M, and variation of the astatine concentration never had any effect on the extraction. Re-extraction of either phase of an astatine extraction mixture with a fresh portion of the other phase generally did not alter the distribution coefficient.

Calculations

The equilibria used in calculations are listed in Table I. The astatine extraction results are expressed in terms of the distribution coefficient

$$D = (\text{total At})_{CCl_4}/(\text{total At})_{\text{aqueous}} \qquad (1)$$

Unless otherwise specified, all concentrations are in moles per liter, and all species are understood to be in the aqueous phase.

Results

The IBr–Br^- System.—The equilibrium constants and salt dependences of the reactions

$$IBr(aq.) = IBr(CCl_4) \qquad (2)$$

$$IBr + Br^- = IBr_2^- \qquad (3)$$

at 21° were needed for the interpretation of astatine experiments. This information was obtained from the experiments reported in Table II. The result-

(6) W. Hillebrand, G. Lundell, H. Bright and J. Hoffman, "Applied Inorganic Analyses," John Wiley and Sons, Inc., New York, N. Y., 1953, p. 651.

(7) I. Kolthoff and V. Stenger, "Volumetric Analysis," Interscience Publ., New York, N. Y., 1947, Vol. II, Chapt. VIII.

(8) I. Kolthoff and R. Belcher, 1957, ref. 7, Vol. III, Chapt. VI–VII.

(9) A. Seidell, "Solubilities of Inorganic and Metal Organic Compounds," D. Van Nostrand Co., New York, N. Y., 1958, Vol. I.

(10) H. S. Harned and B. B. Owen, "The Physical Chemistry of Electrolytic Solutions," Reinhold Publ. Corp., New York, N. Y., 1950, p. 565–566.

(11) L. I. Katzin and E. Gebert, *J. Am. Chem. Soc.*, **77**, 5814 (1955).

(12) "Gmelins Handbuch der Anorganischen Chemie," Verlag Chemie, Berlin, 1933, System No. 8, p. 427.

(13) Ref. 12, System No. 7, p. 283–284.

(14) D. Yost, T. Anderson and F. Skoog, *J. Am. Chem. Soc.*, **55**, 552 (1933).

(15) Wendell M. Latimer, "The Oxidation States of the Elements," Prentice-Hall, Inc., New York, N. Y., 1952.

(16) J. H. Faull, Jr., *J. Am. Chem. Soc.*, **56**, 522 (1934).

ing constants, from which the "D_{calcd}" were computed, are

$$\log K_2 = \log 4.31 + 0.12(NaClO_4) + 0.096(NaBr) + 0.03(HClO_4) \quad (4)$$

$$\log K_3 = \log 444 + 0.02(NaX) + 0.053(HClO_4) \quad (5)$$

where "NaX" is $NaClO_4$ or NaBr.

Due to the limited data, the salt dependences are not unique, but were assigned by analogy with the corresponding dependences shown by the I_2 and I_3^- equilibria. Their subsequent use in this paper cannot introduce any great error.

TABLE II

DISTRIBUTION OF IBr BETWEEN CCl_4 AND AQUEOUS BROMIDE SOLUTIONS[a]

R	$HClO_4$ $\times 10^2$	$\Sigma NaBr$ $\times 10^3$	Titer (as IBr) Aqueous $\times 10^3$	CCl_4 $\times 10^3$	Free Br^- $\times 10^3$	D Exptl. $\times 10^2$	D Calcd. $\times 10^2$
1.136[b]	100	1.438	15.91	1.822	0.905	318	318
2.028[c]	99	12.18	3.348	1.930	10.58	73.7	73.4
4.50	89	110.0	1.579	14.84	95.5	9.66	9.68
4.48	6.0	109.4	1.622	14.49	95.2	10.16	10.14
4.52[d]	6.0	110.3	1.694	14.39	96.2	10.70	10.71
4.48[e]	6.0	109.4	1.829	13.74	96.0	12.08	12.05
47.3	6.5	960	2.051	134.4	826	1.385	1.384

[a] R = organic volume/aqueous volume. $D = (IBr)_{CCl_4}/[(IBr)_{aq} + (IBr_2^-)]$. In the calculation of the D's, correction has been made for the generation of I_2 and Br_2 in each phase by dissociation of IBr, and for the formation of I_2Br^- and Br_3^-. $\Sigma NaBr$ is the stoichiometric concentration added to the mixtures. Free $Br^- = \Sigma NaBr - IBr_2^-$. Unless otherwise indicated, the stoichiometric concentrations of IBr and I_2, expressed as if all the halogen remained in the CCl_4, are $(\Sigma I_2)_{CCl_4} = 1 \times 10^{-6}$ and $(\Sigma IBr)_{CCl_4} = 4.88 \times 10^{-3}$. High acid and excess I_2 are present in the experiments at low bromide concentrations to repress the hydrolysis of the IBr. [b] $(\Sigma I_2)_{CCl_4} = 0.01058$ and $(\Sigma IBr)_{CCl_4} = 6.94 \times 10^{-3}$. [c] $(\Sigma I_2)_{CCl_4} = 1.953 \times 10^{-3}$ and $(\Sigma IBr)_{CCl_4} = 2.40 \times 10^{-3}$. [d] The aqueous phase was 0.28 M in $NaClO_4$. [e] The aqueous phase was 0.785 M in $NaClO_4$.

Astatine in the I_2–I^- System.—In this system the distribution of astatine is independent of the iodine concentration between 10^{-1} and 2×10^{-5} M $(I_2)_{CCl_4}$. The distribution coefficient is independent of acidity between pH 1 and 5, but drops about 25% at pH 7, when the iodide concentration is 10^{-4} M.

The iodide dependence of the distribution is illustrated in Fig. 1. The smooth curve has been calculated from the equation

$$D = K_7/[1 + K_8(I^-)] \quad (6)$$

with the assumption of the equilibria

$$K_7 = (AtI)_{CCl_4}/(AtI)_{aq} = 5.5 \quad (7)$$

$$K_8 = (AtI_2^-)/(AtI)(I^-) = 2000 \quad (8)$$

The dependence of the distribution on inert salt may be represented approximately as

$$\log D = \log D^0 + 0.1(NaClO_4) \quad (9)$$

The sodium iodide itself would be expected to have a much smaller effect.[10]

From the lack of pH dependence we may set an upper limit of 10^{-11} to the equilibrium constant for the hydrolysis reaction

$$H_2O + AtI = HOAt + H^+ + I^- \quad (10)$$

The lack of I_2 dependence rules out any oxidation–reduction reaction, and also excludes the reaction of AtI with iodine to give AtI_3.

In a series of early experiments with this system, the initial values of D were sometimes as much as

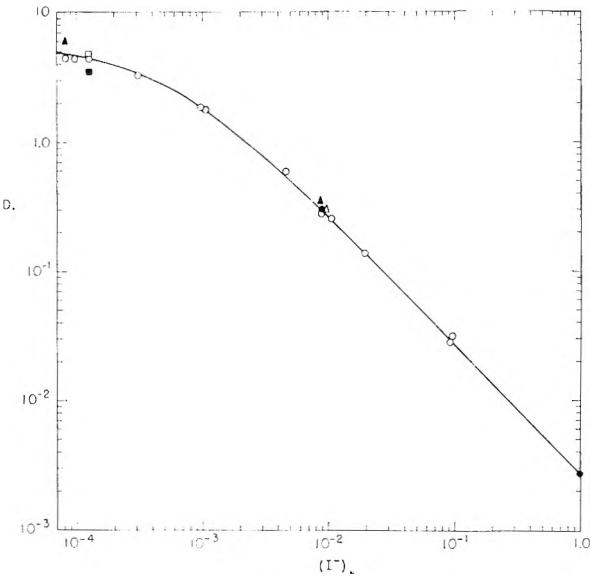

Fig. 1.—Distribution of astatine between aqueous iodide solutions and iodine-containing CCl_4: ○, 5–10 $\times$ 10^{-4} M $(I_2)_{CCl_4}$, pH 3.0 (other experiments deviate from these conditions only as indicated); ▲, 0.8–1.0 M $NaClO_4$; □, pH 1.1 and pH 4.6 (identical results from two experiments); ■, pH 6.9; △, 0.08 M $(I_2)_{CCl_4}$; ●, 2–3 $\times$ 10^{-5} M $(I_2)_{CCl_4}$.

50% above the calculated curve of Fig. 1, and usually decreased slowly over several hours. The cause of this behavior was never determined, but the difficulty was eliminated by preparing new reagent solutions, suggesting that an unknown impurity was at fault.

In mixtures with high iodide concentrations, D sometimes dropped as much as 15% when the aqueous phase was re-extracted with a fresh organic phase. Further re-extraction did not alter D. This drop may be due to the extraction of small quantities of compounds of astatine with impurities. Assuming this to be the case, we have taken the final value of D to be the correct one.

Astatine in the I_2–IBr–Br^- System.—These results appear in Table III. The distribution of the astatine is seen for the most part to be a function of only the Br^- concentration and the ratio IBr/I_2. At a given Br^- concentration, D decreases with increasing IBr/I_2, leveling off at high values of the ratio. Increasing Br^- decreases D at any value of IBr/I_2. This suggests the reactions

$$AtI + IBr = AtBr + I_2 \quad (11)$$

$$AtI + Br^- = AtIBr^- \quad (12)$$

$$AtBr + Br^- = AtBr_2^- \quad (13)$$

The calculated D values of Table III have therefore been computed from the expression

$$D = \frac{K_7 + K_{11}K_{15}(IBr/I_2)}{1 + K_{12}(Br^-) + K_{11}(IBr/I_2)[1 + K_{13}(Br^-)]} \quad (14)$$

in which the aqueous IBr/I_2 ratios are twenty times the tabulated CCl_4 values. K_{11}, K_{12} and K_{13} have been set at 190, 120 and 320, respectively, and

$$K_{15} = (AtBr)_{CCl_4}/(AtBr)_{aq} = 0.040 \quad (15)$$

Since most of the mixtures have high salt concentrations, the effect of the medium on these equilibrium must be considered. The most important effect is probably that of sodium salts on

TABLE III

DISTRIBUTION OF ASTATINE IN THE I_2–IBr–Br^- SYSTEM[a]

	Aqueous		CCl_4			D	
R	ΣNaBr $\times 10^3$	Br^- $\times 10^3$	ΣI_2 $\times 10^4$	ΣIBr $\times 10^4$	IBr/I_2 $\times 10^2$	Exptl. $\times 10^2$	Calcd. $\times 10^2$
			$Br^- \sim 9 \times 10^{-4}$ M				
1.89	0.94	0.93	960	0.374	0.034	240	220
1.89	.94	.91	960	3.74	0.34	33	37
2.07	.94	.92	87	1.71	1.73	9.7	10
1.96	1.08	.93	930	18.2	1.71	11	10
1.89	0.94	.93	9.5	0.374	3.4	5.6	6.6
1.86	1.64	.91	980	96	8.5	4.9	4.5
1.86[b,c]	1.64	.86	980	96	8.4	4.9	4.5
0.91	0.94	.91	8.0	3.90	37	2–4[d]	3.4
0.94	0.94	.93	0.73	1.50	160	3.6	3.2
1.93	1.08	.93	9.5	18.5	170	3.5	3.2
2.02	1.63	.97	1.09	88	1700	2.7	3.1
2.02[b,c]	1.63	.92	1.09	88	1700	2.5	3.1
			$Br^- \sim 9 \times 10^{-3}$ M				
0.91	9.1	9.0	1000	0.364	0.021	110	120
.90	9.0	8.8	1000	1.38	.065	60	53
.91	9.1	9.1	100	0.426	.20	18	20
.91	9.1	8.8	1000	4.30	.20	17	20
.93[c]	9.3	9.0	980	3.72	.171	17	21
.94[b,c]	9.0	8.7	960	4.68	.22	15	17
.97[e]	9.2	8.9	930	4.56	.24	16	17
.88	8.9	8.3	990	12.7	.61	7–9[d]	8.0
.93	9.1	9.1	9.7	0.460	2.2	2.9	2.8
.93	10.8	9.1	860	38.2	2.1	3.1	2.9
.90	16.7	9.0	700	195	13	1.6	1.3
.91	10.8	9.2	81	38.8	22	1.3	1.2
.93	9.1	9.1	0.81	0.460	27	0.95	1.2
.93	9.2	9.0	7.6	4.74	29	1.2	1.2
.91[c]	9.4	9.3	0.54	1.26	100	1.0	1.0
.92	9.4	9.4	0.30	1.46	220	0.79	1.0
.91	23.4	8.6	105	390	180	1.2	1.1
.93	10.1	9.3	0.402	19.0	1300	1.0	1.0
.91	23.4	8.7	4.29	393	1600	0.39	1.1
			$Br^- \sim 0.09$ M				
1.86	94	93	980	0.356	0.0168	16	19
1.86	94	92	980	3.72	.069	5.5	6.7
1.86	94	94	9.6	0.356	.65	0.74	0.90
1.84	101	94	990	48.5	.84	.63	.73
1.86	94	93	8.1	3.72	7.9	.24	.20
2.00[f]	160	89	910	446	9.4	.31	.19
0.96[f]	119	118	3.16	12.7	33	.13	.12
0.92[f]	121	121	0.243	1.54	49	.11	.11
0.90[f]	102	102	0.585	4.86	73	.20	.13
1.84	103	96	10.0	48.5	81	.22	.13
0.91[f]	101	93	1.21	96	670	.19	.13
2.00[f]	184	110	9.3	446	680	.14	.11
			$Br^- \sim 0.9$ M[c]				
1.86	940	930	980	3.80	0.0206	1.8	2.0
1.86	940	920	960	38.2	.099	0.57	0.57
1.87	940	940	9.7	0.356	.173	.34	.34
1.87	940	940	7.9	3.80	1.17	.16	.064
1.95	1000	900	910	446	1.28	.11–0.16[d]	.063
1.82	930	920	10.0	48.5	11.5	.13	.019
1.94	900	870	1.27	172	340	.026[g]	.015
2.04	960	920	0.99	172	460	.11	.014
2.04[h]	960	920	0.99	172	460	.10	.014

[a] The D's are defined by equation 1. The other symbols are those defined in note (*a*) to Table II. To obtain (IBr/I_2)$_{CCl_4}$ from the raw data it was necessary to correct for the distribution of the halogens between the phases, for the formation of I_2Br^- and IBr_2^-, for the dissociation of IBr, and for reaction 16. Unless otherwise specified, $HClO_4$ = 0.063 M and $NaClO_4$ = 0.40 − ΣNaBr. [b] $HClO_4$ = 1.02 M. [c] No $NaClO_4$ was present. [d] The results of duplicate experiments scattered over this range. [e] $HClO_4$ = 0.03 M. [f] $NaClO_4$ = 0.48 − ΣNaBr. [g] Re-extraction of the aqueous phase with two successive portions of pure CCl_4 gave successive D's of 1.8 and 1.3 × 10^{-4}. [h] $HClO_4$ = 0.0063 M.

K_7, which is reflected in equation 9. Accordingly, in the use of equation 14, K_7 has been corrected for salt concentration by means of equation 9, in which D and D^0 are replaced by K_7 and $K_7°$. We have further assumed all sodium salts to have the same effect. Other salt effects should be considerably less important, and this is the only correction that has been made. This procedure appears justified by the observed effect of acid and inert salt on the astatine distribution in these systems. We may note that the distribution is independent of acid concentration between 0.006 and 1 M.

Most of the mixtures with high IBr/I_2 ratios were found to be photosensitive, exposure to light causing a several-fold increase in D.

We see that the astatine becomes less extractable than predicted at very high IBr and low I_2 concentrations. This may indicate oxidation of the AtBr to the higher positive state to which bromine is known to oxidize astatine.[3,5] On the other hand, at high bromide concentrations, when "D_{calcd}" is less than 10^{-4}, the observed D is generally several-fold greater. This may result from the extraction of impurity compounds suggested in the preceding section, an effect which would now become much more prominent due to the very low values of the "true" distribution coefficients. In this case a drop in D might be expected upon successive re-extraction of an aqueous phase with fresh organic phases, and such drops were sometimes observed.

Astatine in the I_2–I^-–Br^- System.—This system links the two preceding ones, and the results obtained in it appear in Table IV. Although no IBr has been added to these mixtures, the interhalogen is generated by the reaction

$$I_2 + Br^- = IBr + I^- \qquad (16)$$

Although equilibrium in this reaction lies to the left ($K = 2.2 \times 10^{-6}$), the ratio IBr/I_2 can reach significant values at low iodide and high bromide concentrations.

Values of "D_{calcd}" have therefore been computed from equation 14 as in the previous section, with the addition of the term "$K_8(I^-)$" in the denominator to account for formation of AtI_2^-. We note that when the iodide concentration is varied at constant bromide concentration, a maximum in D is predicted, since D is reduced at low iodide by the formation of AtBr and at high iodide by the formation of AtI_2^-.

These experiments showed about the same salt effects as those of the preceding section, and the distribution was independent of acid concentration between 10^{-3} and 6×10^{-2} M.

Although the data in Table IV generally follow the trend of the calculated D's, the observed D's decrease much too sharply at high IBr/I_2, suggesting that some further unknown reaction is coming into play. Also disturbing is the fact that in some of the systems D drops markedly upon re-extraction of the aqueous phase.

Astatine in the I_2–I^-–Cl^- System.—Table V gives the results in this system, which is the chloride analog of the I_2–I^-–Br^- one. In this case, however, instead of introducing the ICl-producing reaction analogous to equation 16, we shall write the astatine reactions

TABLE IV

DISTRIBUTION OF ASTATINE IN THE I_2–I^-–Br^- SYSTEM[a]

Aqueous		CCl_4		D	
I^- × 10^4	Br^- × 10^2	ΣI_2 × 10^4	IBr/I_2 × 10^5	Exptl. × 10^2	Calcd. × 10^2
		$Br^- \sim 0.01$ M			
42.0	1.01	10.0	0.26	48	52
10.5	1.01	10.0	1.06	130	130
1.92[b,c]	0.89	19.6	5.1	250	240
0.387	1.02	10.0	29	200	200
.114[b,c,d]	0.88	1000	85	180	180
(.0470)					
.130	1.03	10.0	87	110	150
		$Br^- \sim 0.1$ M			
102	9.8	10.0	1.06	19	17
10.5	10.1	10.0	10.5	38	34
2.23[b]	9.0	9.8	44	31	36
2.32[c]	9.3	9.8	44	27	32
1.27	10.1	10.0	87	16	23
0.138	10.3	0.81	820	2.6	4.8
(.130)					
.116[c,e,f]	9.3	10.0	880	3.1	5.3
(.0243)					
.116[e,f]	9.3	10.0	880	3.1	5.3
(.0243)					
		$Br^- \sim 1$ M			
109	87	9.1	8.8	6.8	4.9
9.6	90	9.4	103	4.4[g]	3.0
6.7[c]	92	1000	152	2.2	2.4
(0.0245)					
2.80[c]	91	19.6	360	1.3	1.3
(2.36)					
0.91[c]	93	10.1	1110	0.42[h]	0.51
(.097)					
.91	93	10.1	1110	0.40[i]	0.51
(.097)[i]					

[a] The symbols are explained in note (a) to Table III. The bromide concentration has been corrected for the small amount tied up as I_2Br^-. The iodide concentration has been corrected for I_3^- formation and for the iodide produced by reaction 16. When the correction exceeds 2%, the stoichiometric concentration of added sodium iodide is indicated in parentheses in the I^- column. The IBr is produced by reaction 16 and has been calculated accordingly. Unless otherwise indicated, the reaction mixtures are at pH 3.0 with no added salt. The ratio R ranged between 0.9 and 1.8. The exact value of the ratio is only indicated for those experiments in which it significantly affected the computations. [b] $NaClO_4 = 0.40$ M. [c] $HClO_4 = 0.063$ M. [d] $R = 0.90$. [e] $NaClO_4 = 0.29$ M. [f] $R = 1.80$. [g] Re-extraction of the aqueous phase with fresh CCl_4 of the original I_2 content gave a D of 0.024, which was unaltered by another re-extraction. A duplicate experiment yielded identical results. [h] Treatment as described in note (g) reduced D to 0.0033. [i] $HClO_4 = 0.0063$ M. Treatment as described in note (g) did not alter D.

$$AtI + Cl^- = AtICl^- \qquad (17)$$

$$AtICl^- + Cl^- = AtCl_2^- + I^- \qquad (18)$$

We may expect reaction 18, like reaction 16, to proceed largely to the left unless the ratio of chloride to iodide is very great. For the distribution coefficient we have

$$D = \frac{K_7}{1 + K_8(I^-) + K_{17}(Cl^-)[1 + K_{18}(Cl^-)/(I^-)]} \qquad (19)$$

and again we predict a maximum in D as the iodide is varied at constant chloride. The "D_{calcd}" values of Table V have been computed with $K_{17} = 9$ and $K_{18} = 2.0 \times 10^{-4}$. K_7 has been corrected for

salt concentration in the manner previously described, and the observed salt dependence again appears to justify the correction. As in the preceding section, no acidity dependence was observed between 10^{-3} and 6×10^{-2} M acid.

TABLE V

DISTRIBUTION OF ASTATINE IN THE I_4–I^-–Cl^- SYSTEM[a]

$(I_2)_{CCl_4} \times 10^4$	$I^- \times 10^5$	$Cl^- \times 10^2$	D Expt'l.	D Calcd.
19[b]	19.0	0.95	3.9	4.1
2.1[c]	22.4	10.6	2.6	2.8
19[b]	19.2	9.6	2.4	2.6
2.2[c]	0.84	10.6	1.5	1.6
2.1	530	100	0.35	0.33
9.5[d]	95	94	.53	.52
19	23.0	96	.37	.40
9.5[d]	5.8	95	.18	.18
2.2	5.4	102	.16	.15

[a] Unless otherwise indicated the $HClO_4$ concentration was 0.063 M and no inert salt was added. The $(I_2)_{CCl_4}$ has been corrected by 1–2% for the amount extracted into the aqueous phase and for the formation of I_2Cl^-. A small correction for I_3^- formation has been applied to the iodide concentration. [b] $NaClO_4 = 0.40\ M$. [c] $NaClO_4 = 0.97\ M$. [d] $HClO_4 = 0.001\ M$.

Discussion

The values of K_2 and K_3 obtained in the IBr–Br^- system are compatible with Faull's 25° values of 3.9 and 370, respectively.[16] In a more recent paper Pungor, *et al.*, claim on the basis of potentiometric measurements that the complex formed between IBr and Br^- has the formula IBr_4^{-3}.[17] However, their interpretation is fundamentally in error, and correct evaluation of their data gives results consistent with Faull's work.[18]

The assignment of the species involved in the astatine reaction hinges on the assumption that we start with AtI. Although this assumption is a plausible one that leads to reasonable conclusions, we must remember that from a different starting compound an entirely different set of species would be derived to fit the data.

The scatter of the astatine data is greater than might be desired, but may be inevitable in a system of this nature. Because of this scatter the constants can easily be in error by as much as 10%, and some minor reactions may have gone undetected. However, the wide range covered by the experiments makes it appear fairly certain that the principal reactions are those indicated.

Table VI compares the extraction behavior of the various halogens and interhalogens. The astatine species fit in fairly well with the trend of decreasing extractability with increasing polarity. The agreement between AtI and IBr is particularly significant as support for the identity of the former. However, the extractability of AtBr is lower than we might have expected.

It is of interest to note that when other halogens are absent the distribution of "zero-state" astatine between water and CCl_4 has been found to vary erratically from one experiment to another, with D's generally very much greater than those found in the present study.[3] This indicates that the interhalogen astatine compounds with which we have been dealing here are considerably more polar than the "At(0)" species formed in the absence of other halogens. The nature of the latter species has been discussed in a previous paper, in which it has been suggested that they are organoastatine compounds formed with impurities.[5]

TABLE VI

DISTRIBUTION CONSTANTS OF HALOGENS AND INTERHALOGENS (21°)

$K = (XY)_{CCl_4}/(XY)_{aq}$

XY	K	Ref.
AtBr	0.040	[a]
ICl	0.34[b]	16
IBr	4.3	[a]
AtI	5.5	[a]
Br_2	27	9
I_2	86	9

[a] This work. [b] 25°.

In Table VII the stability constants of the known XYZ^- polyhalide ions are intercompared. The complexes tend to become progressively more stable as the atoms involved become heavier and more polarizable, and symmetrical complexes are more stable than asymmetrical ones. The astatine complexes appear in quite satisfactory agreement with the others.

TABLE VII

EQUILIBRIUM CONSTANTS FOR THE REACTIONS

$XY(aq.) + Z^- = XYZ^-$

(21–25°)

XYZ^-	K	Ref.
Cl_3^-	0.12	19
Br_2Cl^-	1.4	13
I_2Cl^-	3	12
$AtICl^-$	9	[a]
I_2Br^-	14	12
Br_3^-	17	13
$IBrCl^-$	43	16
$AtIBr^-$	120	[a]
ICl_2^-	170	16
$AtBr_2^-$	320	[a]
IBr_2^-	440	[a]
I_3^-	800	11
AtI_2^-	2000	[a]

[a] This work.

The IBr analog of equation 10 has an equilibrium constant of 1.5×10^{-7}.[16] Hence IBr is much more extensively hydrolyzed than AtI. This accords with the rapid decrease in the extent of hydrolysis of the simple halogens as they grow heavier.

We may rewrite equation 11

$$AtI + {}^1/_2Br_2 = AtBr + {}^1/_2I_2 \qquad (20)$$

and compare it with

$$IBr + {}^1/_2Cl_2 = ICl + {}^1/_2Br_2 \qquad (21)$$

In the aqueous phase, these reactions have respective equilibrium constants of 4.2×10^4 (21°) and 270 (25°).[16] The difference is surprisingly great.

We may similarly compare the reactions

(17) E. Pungor, K. Berger and E. Schulek, *J. Inorg. Nucl. Chem.*, **11**, 56 (1959).

(18) E. H. Appelman, *ibid.*, **14**, 308 (1960).

(19) M. S. Sherrill and E. F. Izard, *J. Am. Chem. Soc.*, **50**, 1665 (1928).

$$AtICl^- + Cl^- = AtCl_2^- + I^- \quad (18)$$
$$AtIBr^- + Br^- = AtBr_2^- + I^- \quad (22)$$
$$IBrCl^- + Cl^- = ICl_2^- + Br^- \quad (23)$$

which have equilibrium constants of 2×10^{-4}, 1.1×10^{-3} and 6×10^{-3}, respectively, the last at 25°.[15,16]

The photosensitivity of the astatine distribution in the presence of IBr should come as no great surprise after the striking photochemical reactions reported previously,[5] and we see once again that the influence of light on tracer-level reactions cannot be safely disregarded.

Acknowledgment.—I wish to express my gratitude to Professor I. Perlman for his direction of this research and to Professor Robert E. Connick for a great deal of helpful discussion.

SOLUBILITY AND ENTROPY OF SOLUTION OF He, N_2, A, O_2, CH_4, C_2H_6, CO_2 AND SF_6 IN VARIOUS SOLVENTS; REGULARITY OF GAS SOLUBILITIES

BY Y. KOBATAKE AND J. H. HILDEBRAND

Department of Chemistry, University of California, Berkeley, California

Received August 22, 1960

Careful measurements of gas solubility in selected solvents have been made in the range 5–30°. The apparatus and procedure are described in some detail. The gas, solvent, mole fraction $\times 10^4$ at 1 atmosphere and 25°, and the entropy of solution, cal. mole^{-1}dg.$^{-1}$, respectively, are: N_2/CS_2 2.215, −1.77; CH_4/CS_2 12.69, −1.77, CO_2/CS_2 32.80, −4.83; SF_6/CS_2 9.245, −0.30; CO_2/C_7F_{16} 208.8, −7.53; CH_4/C_7F_{16} 82.62, −3.40; He/C_7F_{16} 8.90, 5.30; SF_6/C_7F_{16} 224.3 −8.00; $N_2/(C_4F_9)_3N$ 34.90, −0.54; $A/(C_4F_9)_3N$ 50.03, −1.71; $O_2/(C_4F_9)_3N$ 52.0, −1.90; $CO_2/(C_4F_9)_3N$ 200, −7.30; $C_2H_6/(C_4F_9)_3N$ 332.7, −8.60; $O_2/i\text{-}C_8H_{18}$ 28.14, −1.32; $C_2H_6/i\text{-}C_8H_{18}$ 293.8, −10.15; $SF_6/i\text{-}C_8H_{18}$ 153.5, −7.45. These and many other figures are plotted as (a) entropy of solution *vs.* $-R \ln x_2$; (b) $\log x_2$ *vs.* solubility parameters of solvents; (c) $\log x_2$ *vs.* force constants of gases. They show extensive regularities with high predictive value and theoretical significance.

The work here reported is a continuation of systematic studies of gas solubility in the light of regular solution theory extending over many years and recently greatly intensified.[1–5] Careful determinations by Reeves[4] of the solubility of argon in five non-polar solvents over a range of temperature yielded important information about the different temperature coefficients of gas solubility. Jolley and Hildebrand[5] published values for partial molal volumes and gave quantitative relations between

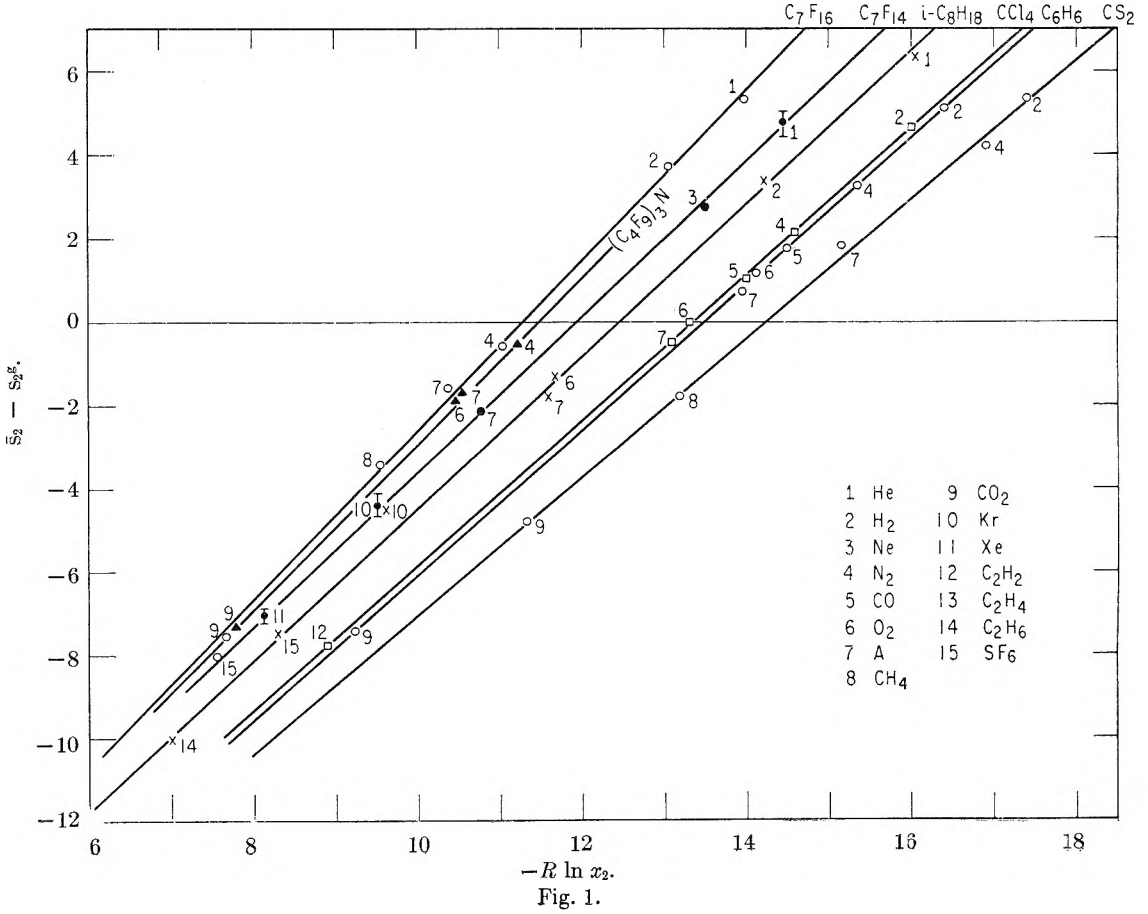

Fig. 1.

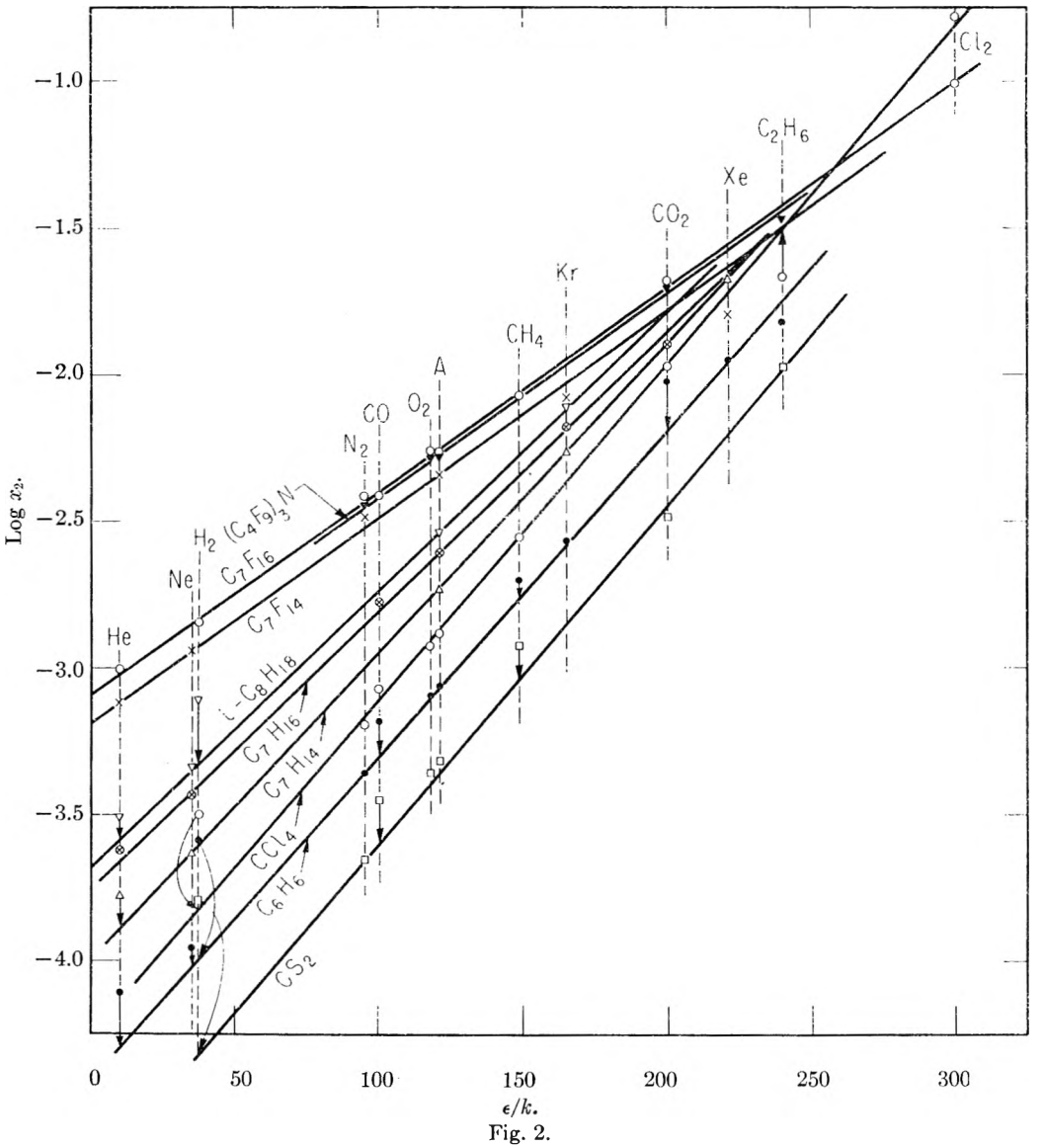

Fig. 2.

mole fraction, entropy of solution, solubility parameters of solvents and force constants of gases. We present now solubility and entropy of solution of 8 gases in various solvents that serve to extend the relations revealed by Jolley and Hildebrand over a wide area of gas and liquid parameters.

Measurements.—The apparatus consists of a gas-measuring buret, an absorption pipet, and reservoir for solvent with suitable connections. The buret is thermostated at 25°, the pipet at any temperature from 5 to 30°. The pipet contains a glass-enclosed piece of iron to provide gentle, continuous magnetic stirring.

Pure solvent is degassed by freezing with liquid nitrogen, evacuating, then boiling with a heat lamp. This process is repeated three times. The solvent is then allowed to flow into the pipet, where it is again boiled under low pressure for final degassing. Incomplete degassing is one of the most serious sources of error in measuring gas solubilities.

Our manipulation is such that the solvent never comes in contact with stopcock grease. The liquid in the pipet is sealed off by mercury. Its volume is the difference between the capacity of the pipet and the volume of mercury which confines it.

Gas is then admitted to the pipet. Its exact amount is determined by P–V measurements in the buret before and after introduction of gas into the pipet. The stirrer is then set in motion. While gas is being absorbed, the stopcock in the long capillary tube connecting buret and pipet is kept closed in order to prevent solvent vapor from entering the buret, but it is opened at intervals to allow gas, always near 1 atmosphere, to replace gas dissolving in the solvent. Equilibrium is usually attained within 24 hours.

Measurements at other temperatures are made by resetting the thermostat at a higher or lower temperature, depending upon the temperature coefficient of the particular solution.

It is hardly necessary to explain to readers of THIS JOURNAL how to calculate from data thus obtained the mole fraction of gas dissolved at each temperature and pressure. Henry's law may safely be used for gases of low solubility, and departures from it readily measured for highly soluble gases.

Materials. CS_2: "Analytical Reagent" purchased from Mallinckrodt Chemical Works was shaken with Hg and then with mercuric chloride. After separation and filtration CS_2 was distilled under reduced pressure. The distillate was kept over Hg more than 5 days before using.

(1) N. W. Taylor and J. H. Hildebrand, *J. Am. Chem. Soc.*, **45**, 682 (1923).

(2) J. C. Gjaldbaek and J. H. Hildebrand, *ibid.*, **71**, 3147 (1949); **72**, 609 (1950).

(3) J. K. Hildebrand, *J. Phys. Chem.*, **58**, 671 (1954).

(4) L. W. Reeves and J. H. Hildebrand, *J. Am. Chem. Soc.*, **79**, 1313 (1957).

(5) J. E. Jolley and J. H. Hildebrand, *ibid.*, **80**, 1050 (1958).

TABLE I

MOLE FRACTION OF GAS, x_2, AT EQUILIBRIUM AT $t°$ AND 1 ATMOSPHERE AND ENTROPY OF SOLUTION, CAL. MOLE^{-1} DEG.$^{-1}$

								$\bar{S}_2$-S_2 at 25°, 1 atmos.
N_2/CS_2	t, °C.	6.22	15.41	25.00	31.20			4.02
	10^4x_2	1.941	2.072	2.215	2.307			
CH_4/CS_2	t, °C.	15.01	25.00	34.80				−1.77
	10^4x_2	13.51	13.12	12.69				
CO_2/CS_2	t, °C.	8.50	16.55	25.00	33.21			−4.83
	10^4x_2	37.85	35.38	32.80	30.20			
CO_2/C_7F_{16}	t, °C.	19.00	22.01	25.00	26.02	30.00		−7.53
	10^4x_2	223.1	216.85	(208.8)	205.9	195.9		
CH_4/C_7F_{16}	t, °C.	17.92	21.75	25.00	25.68	30.01		−3.40
	10^4x_2	86.10	84.14	(82.62)	82.22	80.26		
He/C_7F_{16}	t, °C.	18.25	22.32	25.00	26.09	30.08		5.30
	10^4x_2	8.314	8.58	(8.90)	8.991	9.294		
SF_6/C_7F_{16}	t, °C.	4.52	10.00	15.01	25.00	26.12	30.22	−8.00
	10^4x_2	296.6	272.5	251.2	224.3	219.9	207.9	
$N_2/(C_4F_9)_3N$	t, °C.	10.68	14.03	20.41	25.00	26.00	30.45	−0.54
	10^4x_2	35.37	35.24	35.02	(34.90)	34.88	34.74	
$A/(C_4F_9)_3N$	t, °C.	4.50	11.63	19.43	25.00	25.59	31.83	−1.71
	10^4x_2	53.22	52.05	50.83	(50.03)	49.92	49.06	
$O_2/(C_4F_9)_3N$	t, °C.	5.65	14.35	24.01	25.00	31.50		−1.90
	10^4x_2	55.42	53.95	52.18	52.0	50.96		
CO_2 in	t, °C.	4.01	9.52	17.98	24.87	25.00	31.15	−7.30
$(C_4F_9)_3N$	10^4x_2	260.6	236.3	217.9	200.0	(200.0)	185.0	
C_2H_6 in	t, °C.	13.55	20.60	25.00	25.61	30.89		−8.60
$(C_4F_9)_3N$	10^4x_2	394.0	354.1	(332.7)	330.0	306.3		
O_2/i-C_8H_{18}	t, °C.	9.72	18.85	25.00	30.21			−1.32
	10^4x_2	29.12	28.53	28.14	27.83			
C_2H_6/i-C_8H_{18}	t, °C.	14.01	20.50	25.00	31.80			−10.15
	10^4x_2	353.27	319.34	(293.8)	260.34			
SF_6/i-C_8H_{18}	t, °C.	9.69	18.51	24.51	25.00	30.12		−7.45
	10^4x_2	185.2	167.8	154.35	(153.5)	142.8		
SF_6/CS_2	t, °C.	15.14	20.12	25.00	25.45	30.13	30.50	−0.30
	10^4x_2	9.23	9.20	(9.245)	9.237	9.18	9.222	

C_7F_{16} was purified by the method described by Glew and Reeves.[6]

$(CH_3)_8Si_4O_4$: kindly donated by General Electric Company, was distilled under reduced pressure.[7] The distillate was dried over calcium hydride and distilled again. The distillate was then further purified by partially freezing and discarding the liquid phase several times.

$(C_4F_9)_3N$ kindly presented by the Minnesota Mining and Manufacturing Company was dried with silica gel and fractionated through a 15-plate column at a reflux ratio of 20:1. A middle fraction was used, with a boiling range of 178.5 ~ 179.0°.

i-C_8H_{18} a Phillips "pure" product was dried with anhydrous magnesium perchlorate and fractionated through a 15-plate column at a reflux ratio of 20:1, the b.p. was 99.1° compared with the reference value 99.2°.[8]

CO_2. "Standard Grade" of California Dry Ice Company was dried by passing through, first, a trap cooled in a solid CO_2–acetone bath, then a tube containing $CaCl_2$, and finally over P_2O_5. The gas was condensed in a bulb cooled in liquid N_2 and evacuated for 30 minutes. The solid was then allowed to evaporate slowly, while chilled in a Dry Ice–acetone bath, and recondensed in a second bulb cooled in liquid N_2. The evacuation and distillation procedure was repeated several times.[9]

SF_6.—The gas was purchased from the Matheson Company with a specified minimum purity of 99%. It was further purified by a multiple trap sublimation at Dry Ice–alcohol temperature, the same procedures as those of MacCormack and Schneider.[10]

CH_4 and C_2H_6: "Research Grade" gases of the Matheson Company products were 99.90% pure. The gases were dried by passing through a P_2O_5 bulb, and further purified by multiple trap vaporization and evacuation at liquid N_2 temperature.[11]

N_2, O_2 and He were Linde Oxygen Company "Standard Grade." They were reported to be 99.9, 99.7 and 99.9% pure, respectively.

Argon[4] was "Standard Grade" argon from a cylinder of Linde Company which was 99.9% pure.

The vapor pressures of the solvents at the temperatures used were taken from literature: CS_2,[13] C_7F_{16},[6] $(CH_3)_8Si_4O_4$,[7] $(C_4F_9)_3N$,[12] i-C_8H_{18}.[8]

Results

Table I gives our results expressed as mole fraction of gas, x_2, at 1 atmosphere and the given temperature. We estimate our maximum error at ±0.3%. The last column on the right gives the

(6) D. N. Glew and L. W. Reeves, *J. Phys. Chem.*, **60**, 615 (1956).

(7) R. C. Osthoff and W. T. Grubb, *J. Am. Chem. Soc.*, **75**, 2227 (1953).

(8) American Petroleum Inst. Research Project 44, Natl. Bur. Standards.

(9) K. E. MacCormack and W. G. Schneider, *J. Chem. Phys.*, **18**, 269 (1950).

(10) K. E. MacCormack and W. G. Schneider, *ibid.*, **19**, 845 (1951).

(11) J. Horiuchi, *Sci. Papers, Inst. Phys. Chem. Research, Tokyo*, **17**, 125 (1931).

(12) G. J. Rotariu, R. J. Hanrahan and R. E. Fruin, *J. Am. Chem. Soc.*, **76**, 3752 (1954).

(13) "International Critical Tables," Vol. 3, McGraw-Hill Book Co., New York, N. Y.

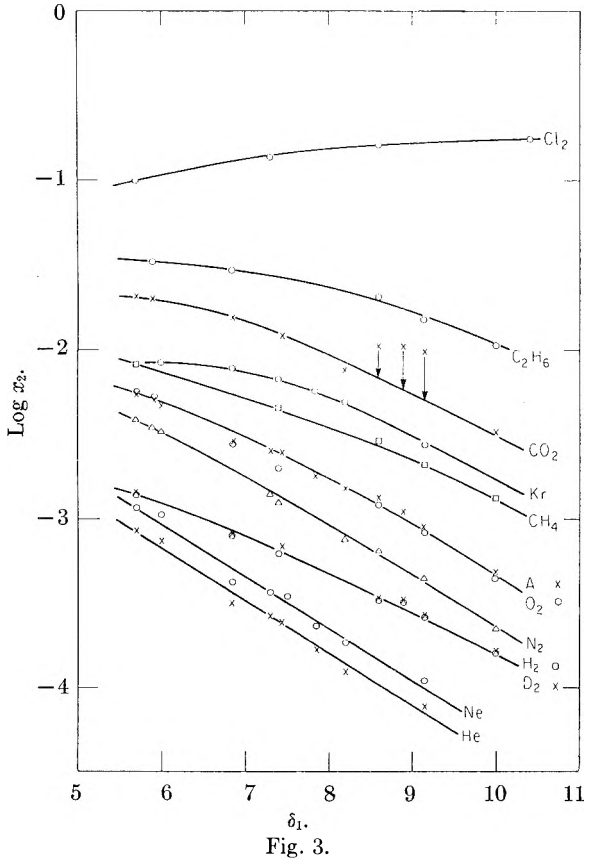

Fig. 3.

entropy of solution at 25° from the gas at 1 atmosphere into its saturated solution, $\bar{s}_2 - s_2^g$ (1 atm.). The relation between log x_2 and log T is almost exactly linear in every case, and the slope multiplied by the gas constant, R, gives the value of $\bar{s}_2 - s_2^g$. The linearity of the relation affords a valuable check on the accuracy of solubility data. We find data which give 3 points not on a straight line. One more point, at least, would have served to reveal one of the four as suspect.

In Figs. 1, 2 and 3, we show correlations between solubility, entropy of solution, force constants of gases, and solubility parameters of solvents in the manner of Figs. 1–3 in the paper by Jolley and Hildebrand, adding to the data there used those of this paper, data by Gjaldbaek,[14] and figures for solubility of the rare gases published by Clever, Battino, Saylor and Gross.[15] These last measured solubility at only three temperatures, except in the case of Xe, and some of their data unfortunately do not meet the test of linearity.

Figure 1 shows the relation between $\bar{s}_2 - \bar{s}_2^g$ and $-R \ln x_2$. We see that the points for different gases in any one solvent fall upon a straight line within the errors of measurement except in certain cases. From this it would be possible to predict with confidence the temperature coefficient of solubility from a value at a single temperature not too far from 25°. Qualitatively, all cases above the line for $\bar{s}_2 - s_2^g = 0$ have negative, all below have positive temperature coefficients of solubility.

(14) J. Chr. Gjaldbaek. *Acta Chem. Scand.*, **12**, 611 (1958).

(15) H. L. Clever, R. Battino, J. H. Saylor and P. M. Gross, *J. Phys. Chem.*, **61**, 1078, 1082 (1957); **62**, 89, 375 (1958).

Second, the slopes of these lines are all much greater than unity, varying from 1.67 for CS_2 to 2.03 for C_7F_{16}. The intercepts at $-R \ln x_2 = 0$ correspond to the entropy of solution of a vapor at 1 atmosphere whose molecular attractive forces are identical with those of the solvent, *e.g.*, for the vapor of the solvent itself at a hypothetical pressure of 1 atmosphere. The values of the intercepts plus the entropy of expansion of vapor from 1 atmosphere to the vapor pressure of the solvent agree remarkably well, in view of the long extrapolation, with the measured entropy of vaporization at 25°, as illustrated by the figures for four solvents.

	C_7F_{16}	i-C_8H_{18}	CCl_4	CS_2
Δs^{vap} from intercept	27.4	27.8	27.1	23.8
Δs^{vap} measured	27.2	28.2	26.3	22.5

The slopes of these lines would be unity if the increase in entropy were the result only of increasing dilution in going from the more to the less soluble gases. We interpret the excess, as in the cases of iodine[16] and stannic iodide,[17] as the result of the progressive weakening of the attraction for solvent molecules, with expansion and increased freedom of thermal motion, as was explained by Jolley and Hildebrand.[5]

In Fig. 2 log x_2 is plotted against force constants of gases, ϵ/k. Values of the latter are taken from Hirschfelder, Curtis and Bird.[18] This plot may serve to predict the solubility of a gas not included in the plot. The following features are noteworthy: 1. The spacing of the lines in the left-hand region is closely proportional to the solubility parameters of the solvents. 2. The point for CO_2 in C_6H_6 falls above its line, doubtless the result of acid–base interaction. 3. CO shows somewhat enhanced solubilities, related probably to its chemical reactivity. 4. Points for H_2, and, to a lesser extent those of He and Ne, fall increasingly above the lines in going from C_7F_{16} to CS_2. The most plausible explanation appears to be one based upon the uncertainty principle.

In Fig. 3, log x_2 is plotted against solubility parameters of solvents, δ_1. This "map" can be used to predict the solubility of any of these gases in another solvent from its solubility parameter. The slopes of the lines decrease in going to the more soluble gases, until the case of Cl_2, which forms a practically ideal solution with CCl_4, but is much less soluble in C_7F_{16}.

The different slope of the line for H_2 is remarkable and awaits a really satisfactory explanation.

We defer a discussion of the theoretical significance of this material pending the results of additional measurements now under way. Meanwhile, the extensive maps of relationships presented in Figs. 1–3 can serve to reveal doubtful data, and chemical interactions, and to predict solubilities and their temperature coefficients.

(16) J. H. Hildebrand, *ibid.*, **64**, 370 (1960).

(17) E. B. Smith and J. Walkley, *Trans. Faraday Soc.*, **56**, 1276 (1960).

(18) J. O. Hirschfelder, C. F. Curtis and R. B. Bird, "Molecular Theory of Gases and Liquids," John Wiley and Sons, New York, N. Y., 1954.

We wish to thank Drs. E. Brian Smith, John Walkley and Berni J. Alder for many helpful discussions in the course of the work, and the Atomic Energy Commission for its generous support.

APPLICATION OF QUASI-LATTICE THEORY TO HEATS OF MIXING IN SOME ALCOHOL–HYDROCARBON SYSTEMS

BY J. R. GOATES, R. L. SNOW AND M. R. JAMES

Department of Chemistry, Brigham Young University, Provo, Utah

Received August 25, 1960

Heats of mixing of the systems cyclohexane–ethanol, benzene–methanol and benzene–ethanol were measured calorimetrically at 25° and varying compositions. Maxima in the heats of mixing were found at mole fractions of the alcohols of 0.40(157 cal./mole) for cyclohexane–ethanol, 0.30(175 cal./mole) for benzene–methanol, and 0.30(216 cal./mole) for benzene–ethanol. The temperature coefficients of the heat of mixing at the composition of the maximum were calculated to be 0.31 cal. mole^{-1} deg.$^{-1}$ for benzene–methanol and 0.35 cal. mole^{-1} deg.$^{-1}$ for benzene–ethanol in the range 20–45°. The experimental data were satisfactorily interpreted by a generalized quasi-lattice theory in which each molecule was assigned a definite number of sites in the lattice, and three different types of contact points were assigned to the alcohol molecules.

The general theoretical method for evaluating thermodynamic properties of solutions described by Barker[1,2] appears to have value in interpreting thermodynamic data of solutions of associated liquids. The theory is based on the usual quasi-lattice model, but has been generalized by recognizing different types of contact points on the same molecule. Barker and associates[3,4] have successfully applied such a model to several systems involving associated liquids. The objective of the study reported here was to determine whether or not a reasonable and consistent set of interaction energies could be found that would apply to both methanol and ethanol solutions. The systems chosen for study were benzene–methanol, benzene–ethanol and cyclohexane–ethanol. The latter system, from the point of view of the theory, is less complex than the benzene systems. Investigating the cyclohexane system allowed us to establish the value of an energy parameter needed in the benzene systems.

Many of the tests of quasi-lattice theory have been made with free energy of mixing data. Since, however, heat of mixing–composition curves are generally more asymmetric than free energy of mixing curves, it was felt that heat of mixing data would provide a more exacting test of the theory.

Experimental

Reagent grade chemicals were further purified by both fractional distillation and crystallization, and stored under an atmosphere of dry nitrogen. Indices of refraction agreed with those in the Dow Chemical tables[5] to within one unit in the fourth decimal place. The amount of liquid soluble–solid insoluble impurities in benzene and cyclohexane was estimated by freezing points to be 0.02%.

The calorimeter was the same as has been used in previously reported work.[6,7] It consisted of two metal compartments separated by an aluminum foil disc. The disc was punctured by a pointed plunger when the calorimeter was inverted. Stirring was accomplished by the motion of the plunger as the calorimeter was continuously tipped end for end. The change in temperature was followed by a single junction copper–constantan thermocouple connected to a sensitive (0.2 μv./mm.) galvanometer.

The galvanometer deflection obtained during the mixing process was later approximately matched by adding energy to the calorimeter by means of an electrical heating coil. The heat leakage was calculated by integration of the area under the mixing and heating curves. Since the heat leakage during mixing and heating were opposite in sign and about the same in magnitude, the net heat leakage correction required was usually less than 1% of the total heat of mixing.

The uncertainty of most of the measurements has been calculated to be 1% or 1 calorie (whichever is larger). Where heats of dilution of a solution rather than direct heats of mixing of the pure components were necessary, the uncertainty is approximately 1.5%. This is true of the region $x_2 < 0.35$ and $x_2 > 0.9$ in the benzene–methanol system, and $x_2 < 0.15$ and $x_2 > 0.9$ in the other two systems.

Experimental Results

The heats of mixing per mole of solutions, ΔH_x^M, for the three systems at 25° are given in Table I. These data were plotted, and the points connected by a smooth line, which for the most part passed directly through the points. Those points not on the line were on the average within one calorie of the line. The smoothed values at 0.1 mole fraction intervals are recorded in Table II. The third column of this table gives the deviation of the smoothed value from the value calculated from the power series equation

$$\Delta H_x^M = x_1 x_2 [A_0 + A_1(x_1 - x_2) + A_2(x_1 - x_2)^2 + \ldots\ldots] \quad (1)$$

in which x_1 and x_2 are the mole fractions of the hydrocarbon and alcohol, respectively. The coefficients of equation 1, which are given in Table III, were calculated by the method of least squares from 19 points read from the smooth curve at mole fraction intervals of 0.05. As can be seen in Table II, the fit of the data by the analytical equation is within the experimental error over a wide range of composition in the middle of the table, but deviates at the extreme ends. A better fit at the ends could have been obtained by using weighting factors, but since the uncertainty is higher at the ends, and since we did not want to sacrifice the fit over the rest of the curve, we chose not to do this.

The experimental values of ΔH_x^M are shown as circles in Figs. 1-3. The broken line in these fig-

(1) J. A. Barker, *J. Chem. Phys.*, **20**, 1526 (1952).

(2) J. A. Barker, *ibid.*, **21**, 1391 (1953).

(3) J. A. Barker, I. Brown and F. Smith, *Disc. Faraday Soc.*, **15**, 142 (1953).

(4) J. A. Barker and F. Smith, *J. Chem. Phys.*, **22**, 375 (1954).

(5) R. R. Dreisbach, "Physical Properties of Chemical Substances," Dow Chemical Co., Midland, Michigan, 1952.

(6) J. R. Goates and R. J. Sullivan, *J. Phys. Chem.*, **62**, 188 (1958).

(7) J. R. Goates, R. J. Sullivan and J. B. Ott, *ibid.*, **63**, 589 (1959).

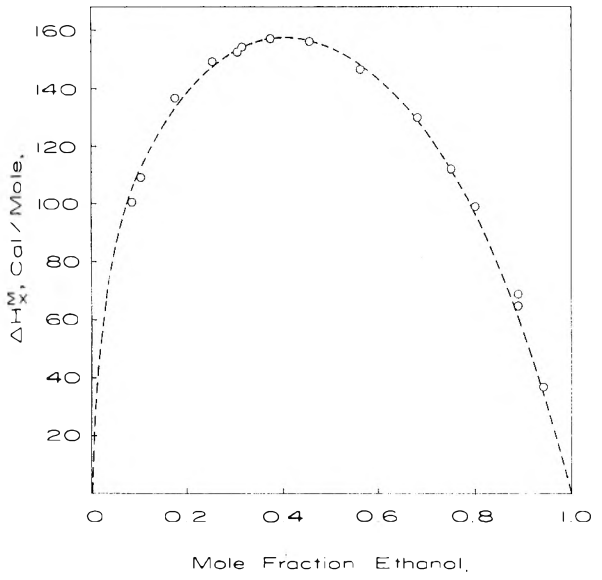

Fig. 1.—Heats of mixing of cyclohexane–ethanol at 25°. (The circles are experimental values; the line was calculated from quasi-lattice theory.)

Table I

Experimental Heat of Mixing Values at 25°

Mole fraction alcohol	ΔH_x^M, cal./mole	Mole fraction alcohol	ΔH_x^M, cal./mole
	Cyclohexane–Ethanol		
0.0870	100.6	0.5611	146.4
.1056	109.3	.6812	129.8
.1756	136.5	.7506	112.2
.2536	149.3	.8029	99.5
.3061	152.2	.8891	69.1
.3122	153.6	.8916	64.9
.3758	156.5	.9431	36.8
.4551	155.9		
	Benzene–Methanol		
0.1276	152.8	0.5770	138.4
.1531	159.4	.5978	130.7
.2118	169.5	.6499	116.2
.2356	172.4	.6755	107.3
.2361	172.6	.7068	96.5
.2388	171.7	.7453	84.3
.2734	175.2	.7706	75.3
.3429	175.4	.8078	63.3
.3470	173.3	.8862	39.1
.4022	170.5	.9025	32.1
.5030	155.8	.9245	24.9
.5199	152.9		
	Benzene–Ethanol		
0.0983	165.6	0.5668	165.6
.1723	204.0	.5797	161.8
.2089	210.7	.6515	136.4
.2572	213.9	.6693	130.8
.3397	215.8	.7227	107.6
.3618	215.1	.7542	97.1
.4207	207.5	.8751	50.3
.4677	196.4	.9069	37.7
.5580	170.6	.9687	11.4

ures is a theoretical curve that will be discussed below. The two benzene systems, plotted as they are on a scale that brings the maximum value of both sets of data to the same height, are strikingly similar in shape. The maximum ΔH_x^M value of the ethanol system (216 cal./mole), however, is considerably higher than that of the methanol system (175 cal./mole). The composition of the maximum in both benzene systems is at 0.30 mole fraction alcohol. The cyclohexane–ethanol system has its maximum value (157 cal./mole) at 0.40 mole fraction ethanol.

Table II

Smoothed Heat of Mixing Values, 25°

Mole fraction alcohol	ΔH_x^M, cal./mole	Dev. from eq. 1, cal./mole
	Cyclohexane–Ethanol	
0.1	108.0	1.0
.2	141.5	−0.4
.3	153.2	.8
.4	156.7	− .2
.5	153.3	− .4
.6	142.5	− .3
.7	125.1	1.1
.8	99.8	0.7
.9	61.2	−3.5
	Benzene–Methanol	
0.1	139.6	2.5
.2	168.4	−2.3
.3	175.1	1.0
.4	170.8	1.1
.5	156.5	−0.6
.6	131.8	− .8
.7	99.0	.4
.8	66.0	1.6
.9	33.1	−3.3
	Benzene–Ethanol	
0.1	165.7	9.7
.2	208.5	−1.0
.3	216.2	−2.7
.4	210.6	1.7
.5	187.3	0.1
.6	155.7	−0.3
.7	118.3	.2
.8	79.0	.3
.9	39.8	−1.6

Table III

Least Square Coefficients for Equation 1

	A_0	A_1	A_2	A_3	A_4
Cyclohexane–ethanol	615.0	132.4	195.9	251.5	521.7
Benzene–methanol	628.4	365.7	0.0	521.9	819.8
Benzene–ethanol	748.8	534.1	265.7	408.7	434.1

Williamson and Scott[8] have very recently published ΔH_x^M data on the benzene–methanol system at 25°. Our data are slightly higher than theirs; at the maximum value the two sets of data differ by 2.3%. The general shape of the ΔH_x^M–composition curves are in good agreement.

Comparing Scatchard's, *et al.*,[9] value for benzene–methanol at 20° with our data at 25° gives a value for $(\partial \Delta H_x^M/\partial T)_{x_2 = 0.3}$ of 3.2 cal. mole^{-1} deg.$^{-1}$; comparing the 20° data with Williamson and Scott's[8] 45° data gives 3.1 cal. mole^{-1} deg.$^{-1}$; and compar-

(8) A. G. Williamson and R. L. Scott, *J. Phys. Chem.*, **64**, 440 (1960).

(9) G. Scatchard, L. B. Ticknor, J. R. Goates and E. R. McCartney, *J. Am. Chem. Soc.*, **74**, 3721 (1952).

ing our 25° data with the 45° data gives 3.1 cal. mole^{-1} deg.$^{-1}$. The constancy of these three temperature coefficients of ΔH_x^M indicates consistency among the three sets of data, since the temperature range over which the measurements were made is small and ΔH_x^M might therefore be expected to be very nearly linear with temperature.

Using Williamson and Scott's[8] 45° data with our 25° data on the benzene–ethanol system gives $(\partial \Delta H_x^M/\partial T)_{x_2 = 0.3} = 3.5$ cal. mole^{-1} deg.$^{-1}$. Thus, both benzene–alcohol systems have rather high, positive temperature coefficients.

Quasi-lattice Theory.—The generalized quasi-lattice theory requires a knowledge of the number and type of contact points on each molecule, and the interaction energies for all possible combinations of contact points. The number and type of contact points were fixed at the start by considering the geometry and chemistry of the molecules involved. Each carbon or oxygen atom was assumed to occupy one site in the lattice; and each site was assigned four contact points, some of which are satisfied within the molecule. The remainder, those available for making contact with another molecule, were designated by the letter Q with the superscript of A for alcohol and S for the hydrocarbon solvent. The subscripts H, O, and I are used to refer to the three chemically different types of contact points of an alcohol molecule—the hydroxyl hydrogen, the oxygen, and the hydrocarbon part of the molecule, respectively. Table IV lists the values used in this study.

TABLE IV

PARAMETERS OF THE QUASI-LATTICE THEORY

	Q_H^A	Q_O^A	Q_I^A	Q^A	Q^S
CH_3OH	1	2	3	6	..
C_2H_5OH	1	2	5	8	..
C_6H_6	..	..	..	..	12
C_6H_{12}	..	..	..	..	12

In addition to these parameters, it is necessary to fix values for the energies of interaction for each of the ten possible combinations of I, H, O and S contact points. Four of these energies ($U_{S\text{-}S}$, $U_{I\text{-}I}$, $U_{O\text{-}O}$ and $U_{H\text{-}H}$) are zero by definition, since $U_{i\text{-}j}$ is defined as the energy change of the quasi-chemical process $^1/_2$(i-i) + $^1/_2$(j-j) = i-j, with i and j representing any of the four types of contact points.

Of the remaining six interactions, two (O–H and I–S) were singled out as the most significant in the cyclohexane–ethanol system, O–H because its energy is relatively high and I–S because there are more such contacts than any other type. The values of $U_{O\text{-}H}$ and $U_{I\text{-}S}$ that came the closest to giving the position and height of the maximum ΔH_x^M value were then determined.

The benzene systems were handled in a similar manner. The aromatic hydrocarbon, however, complicated these systems, since four interactions (O–H, I–S, O–S and H–S) were considered to have major importance, O–H and I–S for the same reasons given above, O–S and H–S because they would be expected to be fairly strong dipole-induced dipole attractions. The value of $U_{O\text{-}H}$ was already fixed from the cyclohexane system. The I–S interaction in the benzene systems is an aliphatic–aromatic hydrocarbon contact, which would be expected to be different from that in the cyclohexane system. Since the difference in the ΔH_x^M of methanol–benzene and ethanol–benzene is determined principally by the number of I–S contacts in the two systems, $U_{I\text{-}S}$ was fixed at a value that gave the correct difference in ΔH_x^M(maximum) between the two systems. The values of $U_{O\text{-}S}$ and $U_{H\text{-}S}$ were then arbitrarily varied until the best fit at the maximum ΔH_x^M value was obtained. The values of the energy parameters are listed in Table V. The empirically determined values appear to be of correct sign and reasonable magnitude for the physical significance assigned to them in the theory.

The heats of mixing for the cyclohexane system were calculated from the equation

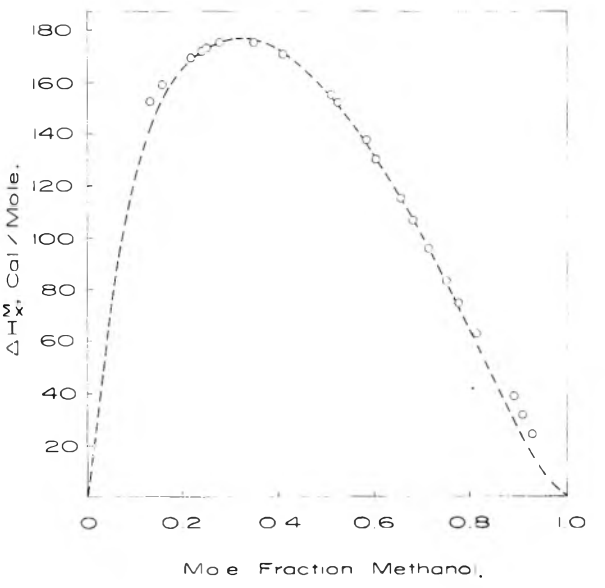

Fig. 2.—Heats of mixing of benzene–methanol at 25°. (The circles are experimental values; the line was calculated from quasi-lattice theory.)

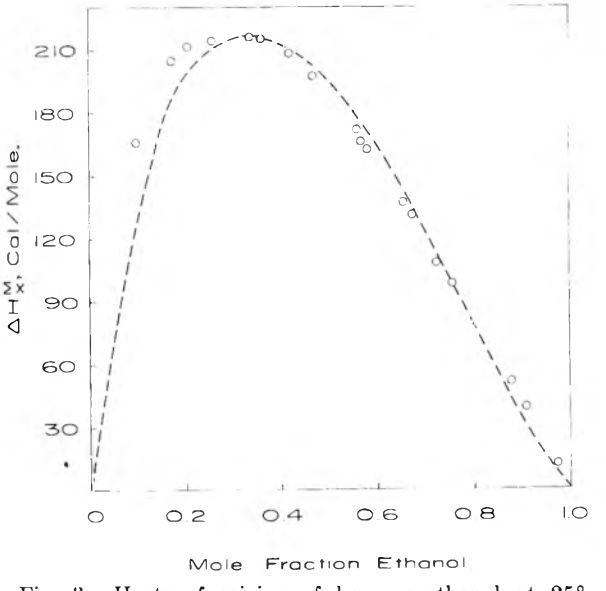

Fig. 3.—Heats of mixing of benzene–ethanol at 25°. (The circles are experimental values; the line was calculated from quasi-lattice theory.)

$$\Delta H_x^M = -2RT[(X_O X_H - x_A X_O' X_H')\eta_{O-H} \ln \eta_{O-H} + X_I X_S \eta_{I-S} \ln \eta_{I-S}] \quad (2)$$

with the X parameters defined as solutions of the equations

$$\left.\begin{aligned} X_H[X_H + X_I + X_O\eta_{O-H} - X_S] &= x_A/2 \\ X_I[X_H + X_I + X_O + X_S\eta_{I-S}] &= 5x_A/2 \\ X_O[X_H\eta_{O-H} + X_I + X_O - X_S] &= x_A/2 \\ X_S[X_H + X_I\eta_{I-S} + X_O + X_S] &= 6x_S \end{aligned}\right\} \quad (3)$$

in which x_A and x_S are the mole fractions of alcohol and hydrocarbon, respectively; and $\eta_{i-j} = e^{-U_{i-j}/RT}$. The X' terms in equation 2 are found by solving equation 3 for the special case $x_A = 1$.

The analogous equation for the benzene systems are

$$\Delta H_x^M = -2RT[(X_O X_H - x_A X_O' X_H')\eta_{O-H} \ln \eta_{O-H} + X_I X_S \eta_{I-S} \ln \eta_{I-S} + X_H X_S \eta_{H-S} \ln \eta_{H-S} + X_O X_S \eta_{O-S} \ln \eta_{O-S}] \quad (4)$$

$$\left.\begin{aligned} X_H[X_H + X_I + X_O\eta_{O-H} + X_S\eta_{H-S}] &= Q_H x_A/2 \\ X_I[X_H + X_I + X_O + X_S\eta_{I-S}] &= Q_I x_A/2 \\ X_O[X_H\eta_{O-H} + X_I + X_O + X_S\eta_{O-S}] &= Q_O x_A/2 \\ X_S[X_H\eta_{H-S} + X_I\eta_{I-S} + X_O\eta_{O-S} - X_S] &= Q_S x_S/2 \end{aligned}\right\} \quad (5)$$

Equations 2–5 are special cases of the general equations derived by Barker.[1] The computations were made with an IBM 650 computer.

The extent of agreement between experiment and theory can be seen in Figs. 1–3. The theoretical curve in Fig. 1 involved two energy parameters. The curves in Figs. 2 and 3 involved four energy parameters, one of which was fixed by the cyclohexane–ethanol system and one by the difference in ΔH_x^M(maximum) of the two benzene systems; the remaining two were arbitrarily adjusted to give the best fit of the experimental data. If the interaction energies in the benzene–methanol system are used to calculate the heat of mixing of the ethanol–benzene system, so that no arbitrarily determined energy values are used, the agreement between theory and experiment is still fairly good. The maximum value is the same, and it occurs at the same composition. The fit along the sides of the curve is not quite as good as that in Fig. 3. Because of the greater positive inductive effect of an ethyl over a methyl radical, one would expect, however, that U_{H-S}, U_{O-S} and also U_{O-H} would be somewhat different for ethanol than for methanol. Everything considered, the theory appears to do rather well in describing the experimental data.

TABLE V

INTERACTION ENERGIES OBTAINED FROM THE QUASI-LATTICE THEORY

	U_{O-H}	U_{I-S}	U_{H-S}	U_{O-S}
Cyclohexane–ethanol	−3200	49	...	...
Benzene–methanol	−3200	87	−410	−210
Benzene–ethanol	−3200	87	−545	−300

Success in fitting the experimental data is very much dependent on the right choice of those interactions to be regarded as the significant ones. For example, in the cylohexane–ethanol system, we first tried the set U_{O-H}, $U_{I-H} = U_{H-S}$, and $U_{O-I} = U_{O-S}$, with $U_{I-S} = 0$. Even with the three arbitrary parameters we could not get a satisfactory fit of the experimental curve, and when the U_{O-H} value determined from the best fit that we could get from this set of interactions was used in the benzene systems, the calculated ΔH_x^M in the ethanol system actually turned out to be lower than that of the methanol.

Acknowledgment.—The authors gratefully acknowledge the support given this project by the National Science Foundation.

THERMODYNAMICS OF THE MONOHYDROGEN DIFLUORIDES. I. DECOMPOSITION REACTION, FUSION, PHASE TRANSITION AND ELECTRICAL CONDUCTIVITY OF β-POTASSIUM MONOHYDROGEN DIFLUORIDE[1]

BY MERTON L. DAVIS AND EDGAR F. WESTRUM, JR.

Department of Chemistry, University of Michigan, Ann Arbor, Michigan

Received August 29, 1960

The thermophysical properties of β-KHF_2, including the enthalpy of the α-β transition (2682 ± 10 cal./mole at 196.7°), the enthalpy of fusion (1582 ± 3 cal./mole at 238.8°), and the enthalpy of the decomposition reaction, $KHF_2 = KF + HF$ (18.52 ± 0.05 kcal./mole at 226.8°). were determined by a direct adiabatic calorimetric approach. These values serve as an independent test of previously reported values determined by other techniques and confirm important terms in the thermodynamic evaluation of the decomposition reaction leading to the assignment of a single minimum potential well for the proton in the $(FHF)^-$ ion. The electrical conductivity of α-, β- and liquid KHF_2 was also determined.

Introduction

The problem of the structure of the difluoride ion has stimulated considerable investigation, both theoretical and experimental, of this ion in the KHF_2 crystal. Bernal and Megaw[2] distinguished two possibilities in a symmetrical hydrogen bond of this type: either the proton occupies a symmetrical position between the nuclei of the two bound particles, or it can be considered more closely attached to either of them, the "actual state" being one "in

(1) The work described herein was included in a thesis submitted by Merton L. Davis in partial fulfillment of the requirements for the Doctor of Philosophy degree in chemistry at the University of Michigan.

(2) J. D. Bernal and H. D. Megaw, *Proc. Roy. Soc.* (*London*), **A151**, 384 (1935).

which the hydrogen oscillates between the two positions."

The determination that the proton in the $(F-H-F)^-$ ion is located in a single potential minimum midway between the two fluoride ions, rather than unsymmetrically placed as in the O–H–O case in ice, was established by Westrum and Pitzer[3,4] by a thermodynamic cycle which included measurements of the heat capacities of crystalline KF and KHF_2 from 14 to 500°K. These data, together with the third law of thermodynamics and a statistically calculated entropy of HF(g), yielded an entropy increment for the reaction

$$KHF_2(c,\beta) \longrightarrow KF(c) + HF(g) \qquad (1)$$

The agreement of this value with the entropy increment obtained from enthalpy of reaction and equilibrium measurements led to the conclusion that KHF_2 must have a perfectly ordered structure at low temperatures, and hence that the $(F-H-F)^-$ ion is symmetrical over the temperature range investigated.

Subsequently, Couture and Mathieu[5] presented their analysis of the Raman spectrum of KHF_2. They found two intense lines at 595 and 604 cm.$^{-1}$, almost exactly at the point at which Ketelaar[6] expected the symmetrical valence frequency. Couture and Mathieu at first considered the possibility that the observed splitting of the symmetrical valence frequency was due to a resonance between the two configurations of a double minimum model of the $(F-H-F)^-$ ion. After a tensor analysis of the relative intensities of the two lines, they later attributed the splitting to a coupling between the $(F-H-F)^-$ ionic units in the crystal.[7] Their final conclusion is thus in harmony with the postulate of a single minimum potential well. An alternative interpretation of the KHF_2 spectrum has been offered by Halverson.[8] He assigned the doublet at 1300 cm.$^{-1}$ to the $(FHF)^-$ deformation frequency and attributed its splitting to a lattice perturbation giving rise to preferred directions of vibration in the crystal. This interpretation was disputed by Mathieu and Couture–Mathieu.[7]

Westrum and Pitzer[3] measured the enthalpy increment of the α–β transition at 196° by the method of mixtures and reported only an approximate value for the enthalpy of fusion of the β-phase. They evaluated the enthalpy change for reaction 1 by employing the Clausius–Clapeyron equation on β-KHF_2 decomposition pressure data. However, the small magnitude of the decomposition pressures and the corrosiveness of the hydrogen fluoride gave rise to considerable uncertainty in their calculated enthalpy of decomposition. Therefore, it was considered desirable to confirm this enthalpy of decomposition by a direct calorimetric measurement if possible and to test the consistency of the reported decomposition pressure data.

A second motive for undertaking this study was interest in investigating the curious β-phase of KHF_2. The α-phase crystallizes in the tetragonal system of D^{18}_{4h} (I 4/mcm).[9] At 196.0° the α-phase undergoes a transition into the soft wax-like, solid β-phase with an entropy increment more than twice that of fusion at 238.7°. The volume increment at the α-β transition is also large compared to that of fusion.[10] A study of the crystal structure of the isotropic β-phase by X-ray diffractional analysis by Kruh, *et al.*,[11] was interpreted on the basis that the four difluoride ions are arranged at random in the crystal along the four body diagonals of the cubes formed by the potassium ions. The large volume and entropy increment accompanying the transition to the β-phase may arise from the random occupation by each difluoride ion of only one out of four possible positions. Free rotation of the ions is excluded because of an unreasonably close approach between fluorine and potassium. The β-phase satisfies the phenomenological criteria of a "plastic crystal" as defined by Timmermans[12] despite the strong deviation from "globularity" of the difluoride ion. Rubidium and cesium monohydrogen difluorides exist in cubic modifications at high temperatures[11] and in tetragonal phases at low temperatures.

The decomposition pressure in the β-region was found to be sufficiently high and the decomposition rapid enough to make the direct measurement of the enthalpy of the reaction practicable. The enthalpy of decomposition, the enthalpy of transition and the enthalpy of fusion of KHF_2 were determined by direct adiabatic calorimetry. The values found were in essential accord with those reported by Westrum and Pitzer[3] and thus confirm the thermodynamical evaluation of the single minimum in the potential energy diagram of KHF_2.

Neutron diffraction measurements[13] on α-KHF_2 single crystals have also provided strong support for the central position of the proton within the linear ion.

No other unambiguous examples of a single minimum hydrogen bond like that in $(FHF)^-$ have been reported. However, the possibility that a single minimum in the $(Cl-H-Cl)^-$ bond in the tetramethylammonium monohydrogen dichloride has been suggested by Waddington[14] on the basis of the similarities of the infrared spectrum of this ion to that of the difluoride ion. This possibility is currently being studied with a thermodynamic cycle in this Laboratory.

Experimental

Preparation and Purity of KHF_2.—The KHF_2 used in the transition and fusion measurements was prepared by adding reagent KF slowly to hot, reagent grade 48% aqueous HF solution until the HF was present to 10% in excess of stoich-

(3) E. F. Westrum, Jr., and K. S. Pitzer, *J. Am. Chem. Soc.*, **71**, 1940 (1949).

(4) K. S. Pitzer and E. F. Westrum, Jr., *J. Chem. Phys.*, **15**, 526 (1947).

(5) L. Couture and J. P. Mathieu, *Compt. rend.*, **228**, 555 (1949).

(6) J. A. A. Ketelaar, *Rec. trav. chim.*, **60**, 523 (1941).

(7) J. P. Mathieu and L. Couture-Mathieu, *Compt. rend.*, **230**, 1054 (1950).

(8) F. Halverson, *Rev. Modern Phys.*, **19**, 87 (1947).

(9) R. W. G. Wyckoff, "Crystal Structures," Interscience Publishers, Inc., New York, N. Y., 1948, Chapter VI, p. 1.

(10) R. W. Fink and E. F. Westrum, Jr., THIS JOURNAL, **60**, 800 (1956).

(11) R. Kruh, K. Fuwa and T. E. McEver, *J. Am. Chem. Soc.*, **78**, 4526 (1956).

(12) J. Timmermans, *Bull. soc. chim. belg.*, **44**, 17 (1935); *Ind. chim. belg*, **16**, 178 (1951).

(13) S. W. Peterson and H. A. Levy, *J. Chem. Phys.*, **20**, 704 (1952).

(14) T. C. Waddington, *J. Chem. Soc.*, 1708 (1958).

iometric proportions. The solution was then cooled with constant stirring while the salt crystallized. The crystals were separated on a Büchner-type polyethylene funnel, washed once with cold water, twice with 10% aqueous ethyl alcohol, and were then dried several days in a vacuum desiccator until an acidimetric titration indicated the HF content to be 100.1 ± 0.1% of theoretical and further pumping produced no change.

Adiabatic Calorimetric Apparatus.—Several of the experiments required the maintenance of adiabatic conditions for several hours at temperatures above 200° with a calorimetric substance of poor compactness and poor thermal conductivity. These requirements led to some adaptation and modification of several designs[15] of adiabatic calorimeters. One required modification was the provision of a tube for the removal of the HF gas evolved in the decomposition process. No suitably well-characterized standard with an accurately known enthalpy increment in the region of interest was available for calibration.

Thermostat and Submarine.—Adiabaticity of the submarine relative to the enclosed calorimeter was maintained by a vigorously stirred and circulated bath of heavy mineral oil contained within a cylindrical 30-l. vessel with a hemispherical bottom and a steel cover plate supporting the apparatus within the bath. Nichrome grid heaters were mounted over the entire external surface of the bath. Thick Sil-o-Cel insulation surrounded the bath and thick blankets of glass wool provided thermal insulation over the cover plate. In addition to the grids, two immersion heaters plus a coiled, copper-sheathed, manually-adjusted control heater were located within the stirring well. Stirring was provided by a 7.2 cm. dia. tetradentate propellor rotated at 800 r.p.m. near the bottom of a cylindrical stirring well. A survey thermocouple detected temperature differentials of less than 0.1° at various positions in the bath at operating temperatures. A copper–constantan thermocouple on the submarine wall was used to control the bath temperature to within ± 0.02°.

The submarine was of 0.6 cm. wall brass tube 10 cm. in dia. and 20 cm. long. A removable flanged cover plate was sealed vacuum tight with a metal to metal V-groove. All interior surfaces of the submarine were goldplated. It was supported from the cover plate by two tubes. One was an evacuation tube leading to a diffusion pump for the insulating vacuum in the submarine. This tube also conducted electrical leads out through a high vacuum-tight seal. The other tube, which permitted the removal of HF from the calorimeter, terminated in an 8 mm. dia. by 0.02 mm. wall Monel tube between the calorimeter and the submarine; the upper end extended from the bath with a 16 mm. dia. Monel tube to a Teflon stopcock.

HF Collection System.—The Teflon stopcock in a Monel seat permitted the control of the flow of HF and its diversion into either of two identical 2.0 cm. dia. by 0.02 mm. wall Monel tubes 28 cm. long. These removable tubes had Monel bottom plates and were internally Teflon-coated to provide protection from attack by aqueous HF. The coatings withstood repeated immersion in liquid nitrogen. The tops of these tubes were readily sealed to the Monel line with an adaptor and exterior vacuum closure of Apiezon-W. Leading from the traps and concentric with them were two 1.0 cm. dia. Monel tubes to a high vacuum line. It was possible to shut off either or both traps from the vacuum line and to add anhydrous nitrogen.

Energy Circuitry.—Energy was supplied to the calorimeter heater by a bank of lead storage cells and sit magnitude was determined with calibrated standard cells, standard resistors, and an autocalibrated White double potentiometer. The energy current was exercised through a ballast resistor; switching the current to or from the calorimeter automatically activated an electrical timer.

Thermometry.—The single junction absolute thermocouple in the calorimeter thermocouple well, with the reference junction in an ice-bath, was constructed of No. 32 B. and S. gauge copper and No. 27 B. and S. gauge constantan wire. It was calibrated at the freezing point (231.9°) of a standard freezing point sample of tin. A calibration curve was constructed by assuming a linear deviation from the points representing the e.m.f. of a copper–constantan thermocouple.[16] The reference points were zero deviation at 0° and −0.5° deviation at 231.9°. This calibration was sufficiently accurate for the data presented here because an error of ±0.2° in temperature has a negligible effect on the probable error of the enthalpies of decomposition, while the enthalpies of transition and fusion were determined in a manner independent of thermocouple calibration. That the error in temperature measurements did not greatly exceed ±0.2° was furthermore substantiated by the close agreement of the peaks of the apparent heat capacity curves for transition and fusion shown in Fig. 1 with the previously determined transition point,[3] 196.0°, and the melting point,[3] 238.7°.

In addition to the absolute thermocouple with its hot junction in the entrant well, a four junction thermel, constructed from No. 32 B. and S. gauge copper–constantan Fiberglas insulated wire, indicated the temperature differential between calorimeter and submarine. Moreover, single junction differential couples made from the same spool of duplex wire were placed about the calorimeter surface in such positions as to enable the temperature differential between the top and middle portion of the calorimeter, and between the middle and bottom, to be read. The junctions of the thermel and the differential couples were insulated from each other and from the walls of the calorimeter and submarine by inserting the soldered beads on the junction tips into minute mica spacers, sheathed in copper and clamped to the calorimeter (or submarine) wall.

For the enthalpy of transition and enthalpy of fusion measurements, the leads from the four junction differential couple were placed directly across the terminals of a galvanometer system with a working sensitivity, in terms of temperature, of 0.0004°/mm. This galvanometer arrangement was found to be inadequate for the decomposition measurements. Instead, the e.m.f. from the differential couple was applied through shielded leads to the input of a Perkin–Elmer Breaker Type D.C. Amplifier and the output recorded on a micromax recorder. A millivolt potentiometer was employed to provide a bucking potential to center the recorder at the truly adiabatic point.

Axial Heater Calorimeter.—This copper calorimeter with bright chromium-plated exterior was used for most of the determinations. It was 4 cm. in diameter and 8 cm. in length with 0.7 mm. wall thickness and was provided with a 4.8 mm. i.d. entrant axial heater well and six radial conduction fins machined from a solid copper block. A 15 mm. length of well was reduced to 0.4 mm. wall where it was silver alloy brazed to the shell. Approximately 400 ohms of No. 36 B. and S. gauge Fiberglas insulated Advance wire with No. 34 copper leads were formed into a cylindrical insert and baked into thermal contact with Formvar enamel. Potential leads were joined to the heater midway between calorimeter and submarine. The leads were brought to thermal contact with the shell by being baked to a copper spool at the bottom of the calorimeter. A goldplated brass foil was enameled over the bottom of the heater well. An entrant Monel thermocouple well with a silver tip was provided from the top of the calorimeter and an 8 mm. dia. axial HF exit tube was also provided as previously described.

Helical-heater Calorimeter.—This calorimeter, used for some of the decomposition measurements, had dimensions similar to those of the axial-heater calorimeter, but differed in that the axial heater was replaced with two coaxial helical coils (1.6 and 3.2 cm. dia.) The coils contained a total of 2.4 meters (79 ohms) of No. 32 Fiberglas insulated wire with a seamless copper sheath drawn down tightly on the wire (over-all dia. = 0.6 mm.). They were held rigidly in place by four slotted radial vanes of 0.2 mm. copper sheet. The ends of the coils were silver soldered to the bottom of the calorimeter.

Technique for Fusion and Transition Runs.—The axial-heater calorimeter was filled with about 0.8 mole of KHF_2. It was then evacuated and anhydrous nitrogen added and the exit tube sealed off by means of a plug and a copper pinch-off. After assembling the calorimeter and submarine and subsequently evacuating the latter, the bath temperature was adjusted, adiabaticity was maintained, and the nearly zero foredrift was measured. A predetermined energy was then added with manual balancing of power to the

(15) W. P. White, THIS JOURNAL, **34**, 1121 (1930); H. Moser, *Physik. Z.*, **37**, 737 (1936); N. S. Osborne and D. C. Ginnings, *J. Research Natl. Bur. Standards*, **39**, 453 (1947); L. D. Armstrong, *Can. J. Research*, **28A**, 44 (1950).

(16) "International Critical Tables," Vol. I, McGraw-Hill Book Co., Inc., New York, N. Y., 1926, p. 58.

bath to maintain adiabatic conditions. The zero afterdrift was established within approximately 7 minutes of the end of the energy input except within the transition region when the steady state was not reached until 30 to 50 minutes after the power was turned off. The difference thermocouples on the surface indicated a maximum temperature inhomogeneity of 0.03 to 0.10 degree depending on the power input level.

Enthalpy of Decomposition.—The above calorimetric apparatus and the HF collection system were used for these measurements. The procedure for the enthalpy of decomposition determination (adopted after 24 preliminary runs to ascertain the optimum conditions) was to heat bath and calorimeter to the desired temperature, to hold the bath constant to ascertain the thermocouple setting (on micromax recorder) required for adiabatic conditions and to observe the absolute temperature of the calorimeter. The Teflon stopcock was opened and the power switched to the calorimeter. This automatically started the timer and permitted the collection of HF in one of the Monel traps.

During the course of the run periodic adjustments had to be made in the calorimeter power to maintain the adiabatic condition (± 0.01°) as observed by the chart record of the differential couple. This was always done by varying the power to the calorimeter in predetermined and reproducible steps. At the end of the run the power to the calorimeter was diverted to the ballast heater and the Teflon stopcock closed. About twenty minutes was then allowed for equilibrium conditions to be reestablished and if necessary the absolute temperature was adjusted slightly. Finally the HF was distilled to the bottom of the trap by lowering the liquid nitrogen level. Then the level was raised again and nitrogen gas admitted to the trap. The seal was broken, and the Monel trap removed while still immersed in liquid nitrogen. At the same time the inner Monel tube was washed down. While gradually removing the Monel trap from the liquid nitrogen, it was flushed and 80% filled with distilled water. The dilute solution and washing were quantitatively transferred to a polyethylene beaker and the HF content was determined by titrating with NaOH standardized against analytical grade potassium acid phthalate using phenolphthalein and thymol blue as indicators.

In order to avoid undesirable sudden changes in temperature at the beginning and end of the determinations, the bore through the Teflon stopcock was reduced to restrict the flow rate. The temperature of the gas leaving the calorimeter was ascertained to be at that of the calorimeter by a thermocouple; corrections for quasi-adiabatic conditions were made from the differential thermocouple record and the thermal leakiness modulus obtained for each run.

Electrical Conductivity Measurements.—The electrical conductivity of KHF_2 was determined in a cell 1.0 cm. in dia. and 11 cm. in length machined from Teflon rigidly confined in a massive copper cylinder, the temperature of which was controlled automatically. Platinum electrodes (7 mm. dia.) supported by 0.8 mm. dia. platinum wires were used. Temperatures were determined with a calibrated thermocouple.

Resistance measurements were made on a Type U_1 Solar AC bridge with a capacitance balance arm which provided direct reading of resistances from 20 to 250,000 ohms. Calibration of the bridge against standard resistors, over the entire range, indicated that the resistances observed were reliable to better than 1%.

The cell was loaded by fusing the salt in the Teflon liner. Then the electrode in the Teflon cap was inserted into the melt. After the conductivity measurements were made on the original sample the cell constant was determined using 0.02 demal KCl with the electrodes in place and found to be 22.5 ± 0.2 $cm.^{-1}$. Then another set of measurements was made for the very low conductivity region (below 200°) with the electrodes approximately 1/4 inch apart. The cell constant for the latter arrangement was found to be 1.364 ± 0.008 $cm.^{-1}$. The conductivities reported are those observed after an equilibrium reading was obtained. This sometimes required several hours.

Results and Discussion

Enthalpy of α-β Transition.—A typical series of inputs (Series 2) through the transition region is presented in Table I. The mean temperature of the input, the temperature increment, the energy added and the apparent heat capacity of KHF_2 together with a typical calculation of the enthalpy of transition are shown. Because the enthalpy increment rather than the heat capacities was the desideratum of this study the heat capacity of the calorimeter was not measured. It was almost entirely of copper and its total heat capacity calculated as 12.3 cal./(deg. mole) over the transition region. This value was applied to give the figures in the last column of Table I and Fig. 1. The correction for normal heat capacity of calorimeter and sample in Table I represents, however, an integration of the extrapolation of the normal heat capacities of the α and β phases (plus calorimeter) to the transition temperature to obtain the "extra" enthalpy of transition. A typical plot of heat capacity *versus* temperature (for Series 2) is shown in Fig. 1. It indicates rather clearly the essentially first-order nature of the peak involved and that 93% of the energy required was adsorbed

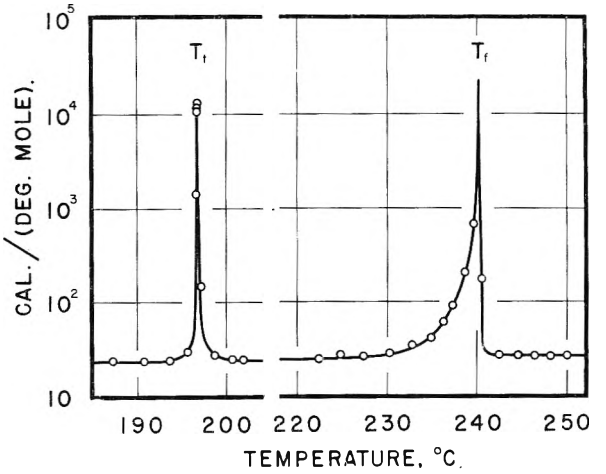

Fig. 1.—The heat capacity of α-, β- and liquid KHF_2 with transition and fusion values.

TABLE I

A TYPICAL ENTHALPY OF TRANSITION SERIES

(Series 2 - 12 Energy Inputs)

Mean T, °C.	ΔT, °C.	Power, watts	Energy, j.	Apparent heat capacity, KHF_2 (j./mv.)
187.2	3.34	0.48	430.4	2417
190.7	3.34	.48	430.5	2409
193.6	2.21	.48	286.9	2431
195.6	1.77	.48	286.8	3032
196.6	0.27	1.27	2288.1	1.58×10^5
196.7	.03	1.27	2287.2	1.35×10^6
196.7	.03	1.27	2289.6	1.27×10^6
196.8	.02	1.27	1527.0	1.53×10^6
197.1	.82	0.48	680.5	1.56×10^4
198.6	1.92	.48	287.1	2792
200.6	2.14	.48	287.0	2511
-201.8	2.18	.48	286.9	2456

Total energy increment (185.45 to 202.88°)	=	2305 cal.
Corr. for deviations from adiabaticity (253 min.)	=	12.9 cal.
Corr. for normal heat capacity of calorimeter and samples	=	151 cal.
Net enthalpy of transition for 0.7983 mole KHF_2	=	2141 cal.
(Molal) enthalpy of transition	=	2683 cal./mole

within a range of less than 0.3°. A summary of the 13 series made over the region 185 to 205° (± 5°) is presented in Table II. Some of these (*e.g.*,

TABLE II

ENTHALPY OF α-β TRANSITION OF KHF_2

Series designations	No. of energy inputs	Av. power input (watts) Heat capacity region	Transition region	ΔH of transition (cal./mole)
		(0.7983 mole of KHF_2)		
1	14	0.56	1.27	2675
2	12	.48	1.27	2683
3	6	.48	1.27	2672
4	6	.48	1.27	2670
5	9	.48	1.29	2683
		(1.2647 mole of KHF_2)		
6	11	0.71	1.43	2676
7	9	.71	1.44	2696
8	4	.71	1.44	2692
9	3	.71	1.45	2684
10	3	.71	1.45	2678
11	6	.71	1.45	2693
12	4	.71	4.04	2687
13	5	.68	3.29	2674
			Av. value	2682 ± 10

Series 2) had relatively small temperature increments and yielded heat capacity type data; others (especially Series 9, 10, 12 and 13) spanned the entire transition region and thereby eliminated entirely the long thermal equilibrium times and minimized the effect of deviation from adiabaticity in yielding enthalpy-type data. The amount of sample and the level of power input were varied. In addition, rigorous tests were made of the adiabaticity, the thermal leakiness modulus, and the adequacy of thermal equilibrium between the energy leads and the surface of the calorimeter. The average value of the enthalpy increment of the α–β transition is 2682 ± 12 cal./mole at 196.7° (269.8° K.). This is to be compared with the value 2659 ± 10 cal./mole previously determined by Westrum and Pitzer[3] using the method of mixtures. The values fall just outside the estimated probable errors. Since both values are of nearly equal reliability, best values of 2671 ± 10 cal./mole for the enthalpy of transition and corresponding entropy of transition of 5.69 ± 0.02 cal./(deg. mole) are selected.

Enthalpy of Fusion.—The four series of runs made over the range 220 to 245° are summarized in Table III and a typical series (Series 1) is shown in Fig. 1. The increase in slope begins about 232° and reaches a sharp maximum at 238.8°. The low decomposition pressure and small free volume in the calorimeter ensured no deviation from stoichiometric composition of the condensed phases. The fusion enthalpy increment, which was calculated in the same manner as that already described for the enthalpy of the α–β transition, was 1582 ± 3 cal./mole at 238.7° (511.8°K.). This was well within the uncertainties with the rough value of 1575 ± 25 cal./mole determined by Westrum and Pitzer[3] using the method of mixtures. The value from the present research is adopted with the corresponding entropy of fusion of 3.09 ± 0.01 cal./(deg. mole).

TABLE III

ENTHALPY OF FUSION OF KHF_2

Run designation	No. of inputs	Av. power input (watts) Heat capacity region	Fusion region	ΔH of fusion (cal./mole)
		(0.7983 mole of KHF_2)		
1	16	0.45	0.92	1582
2	13	.45	1.01	1581
		(1.2647 mole of KHF_2)		
3	8	0.59	1.20	1587
4	5	.61	1.94	1577
			Av. value	1582 ± 3

Enthalpy of Decomposition.—The isothermal enthalpy increment in reaction 1 is designated as the enthalpy of decomposition. Summaries of the 29 final decomposition runs are listed in Table IV. Experimental periods generally varied from 30 to 45 minutes; run 8, however, was done over 80 minutes. Most determinations were made at 0.60 ± 0.10 watts; those numbered 15 through 19 were made at twice this power, 26 and 27 at 0.4 as much. From 15 to 39 mmoles of HF were collected from each run. Approximately one mole of salt was present in each calorimeter. Runs 1 through 8 were made in the axial-heater-type calorimeter, those from 9 through 19 in a second calorimeter of similar design, and those numbered 20–29 in the helical-heater-type calorimeter. This calorimeter proved superior in this type of experiment in that no detectable temperature difference existed

TABLE IV

SUMMARY OF ENTHALPY OF DECOMPOSITION OF KHF_2

Run no.	Temp., °K.	ΔHd obsd., kcal./mole	Deviation from smooth curve, kcal./mole
26	484.4	18.58	+0.06
27	486.2	18.56	− .05
9	489.1	18.60	0
10	489.1	18.60	0
11	489.1	18.53	−0.07
13	490.0	18.76	+ .16
14	490.0	18.68	+ .08
12	490.1	18.73	+ .13
20	491.2	18.62	+ .02
21	491.5	18.46	− .13
1	493.2	18.52	− .06
2	494.8	18.58	0
22	496.1	18.47	−0.10
23	496.2	18.56	− .01
24	496.3	18.65	+ .07
25	496.3	18.61	+ .03
3	496.6	18.59	+ .02
4	496.7	18.62	+ .05
28	497.8	18.52	− .05
5	498.4	18.61	+ .04
7	499.1	18.52	− .05
29	499.1	18.43	− .13
15	499.5	18.38	− .19
16	499.5	18.47	− .10
18	499.8	18.58	+ .02
17	499.9	18.37	− .19
6	500.2	18.51	− .05
19	500.2	18.45	− .11
8	500.6	18.43	− .13

on its surface. The data from the two types of calorimeters are distinguished in Fig. 2.

Using an average value of $\Delta C_p d = -4.1 \pm 0.3$ cal./(deg. mole) based upon heat capacity data[3] for the decomposition reaction, the $\Delta H d$ was represented by

$$\Delta H d = 20.57 - 0.0041T \text{ kcal./mole}$$

using the method of averages. This relationship is shown by a solid line in Fig. 2. The probable error of a single determination was found to be ± 0.08 kcal./mole. At 500° K. the assumption of a probable error of 0.2° in T yielded a probable error for a point on the curve of 0.02 kcal./mole. After taking into account also the probable errors in the circuitry and in the titration, a total probable error of 0.05 kcal./mole in the enthalpy of decomposition was assigned.

This value of the enthalpy of decomposition at 500°K. equals 18.52 ± 0.05 kcal./mole and is nearly within the combined precision indexes of the values 18.30 ± 0.15 kcal./mole obtained from decomposition pressure measurements by Westrum and Pitzer.[3]

Electrical Conductivity Measurements.—The data of Table V were observed in the cell with a constant of 22.5 cm.$^{-1}$. This series of measurements included both the β-phase and the fused salt region. The data were reproducible with both increasing and decreasing temperatures provided sufficient time were allowed for the attainment of thermal equilibrium. The data of Table VI were observed for the cell with a constant of 1.364 cm.$^{-1}$ and includes the α- and β-phase regions. The data are not entirely reproducible in the α-phase region because of supercooling of the β-phase and possibly other irreversible effects. The supercooling is illustrated by the dashed curve in Fig. 3. It was often necessary to cool to 182° before transition to the α-phase occurred. Marked changes in the trend of the conductivity are noted at transition and fusion temperatures.

TABLE V

ELECTRICAL CONDUCTIVITY OF KHF_2

Cell constant 22.5 cm.$^{-1}$

Temp., °C.	Phase	Resistance, ohms	Conductivity, ohm^{-1} cm.$^{-1}$ × 10^5
194.9	α	224,000	1.55
198.8	β	207,000	2.38
201.9	β	198,000	2.87
205.1	β	190,000	3.35
210.0	β	177,500	4.20
216.2	β	161,000	5.48
220.3	β	148,800	6.65
223.9	β	133,800	8.31
224.2	β	123,000	9.80
226.4	β	101,500	13.7
229.1	β	26,400	85.1
231.8	β	8,670	259
236.8	β	793	2830
239.2	Liq.	277	8110
241.3	Liq.	237	9480
246.8	Liq.	158	14200

In Fig. 3 the logarithm of the conductivity is plotted against $1/T$ in the β-phase region and the slope and the intercept of this line show that the conductivity in this region can be expressed by the equation[17]

$$\text{Conductivity} = A \exp(E/kT) = 1.15 \times 10^5 \exp(-1.05 \times 10^4/T)$$

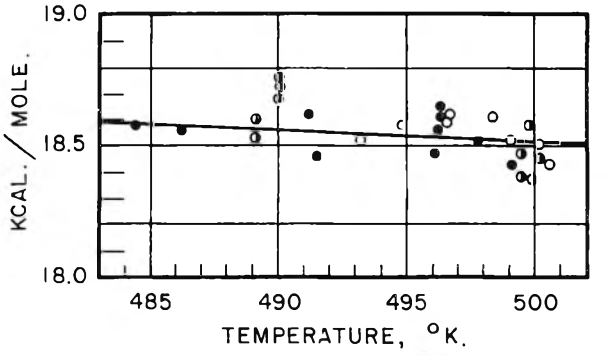

Fig. 2.—Enthalpy of decomposition of KHF_2. The points represented ○ were made in the axial-heater-type calorimeter; ◑ in a modified calorimeter of the same type; and ● in a helical-heater-type calorimeter.

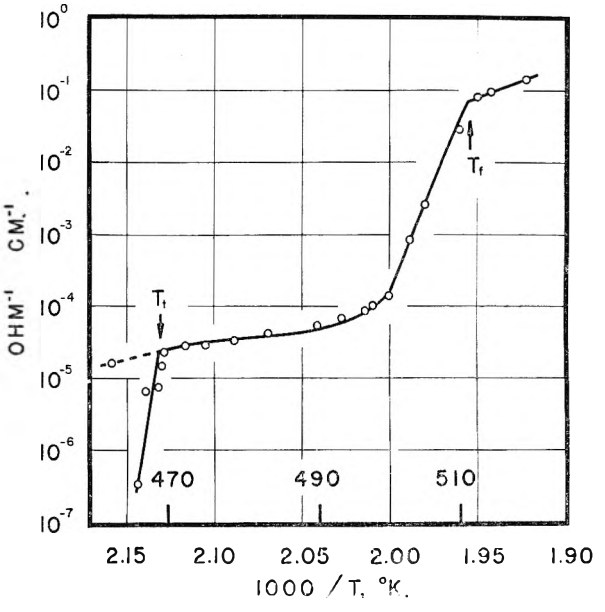

Fig. 3.—Electrical conductivity of KHF_2.

TABLE VI

ELECTRICAL CONDUCTIVITY OF KHF_2

Cell constant 1.364 cm.$^{-1}$

Temp., °C.	Conductivity, ohm^{-1} cm.$^{-1}$ × 10^5	Temp., °C.	Conductivity, ohm^{-1} cm.$^{-1}$ × 10^5
226.3	48.80	189.8	1.68
223.0	8.32	...	...
217.3	5.52	193.1	0.034
211.7	4.26	193.8	0.657
209.0	4.20	194.3	0.673
205.5	3.34	195.8	0.757
203.1	2.46	196.2	1.49
200.8	2.23	196.4	2.29
199.3	2.56	196.6	2.50
199.1	2.02	197.3	2.62
197.9	1.95	197.8	2.73
195.8	1.79	199.2	2.82
193.1	1.64		

(17) *Cf.* N. F. Mott and R. W. Gurney, "Electronic Processes in Ionic Crystals," The Clarendon Press, Oxford, England, 1940.

This equation assumes a single type of equilibrium lattice defect and a single ion contributing to the conductivity. It gives a value of 2.09×10^4 cal. per mole for the activation energy or 0.91 e.v. per ion pair. Comparison of these values, as well as the value for A and the conductivities in this temperature region, with values observed in the literature[18] for crystalline salts near their melting points show them to be of the same order of magnitude.

The maximum deviation of the reported data, taken both during ascending or descending temperatures, equals 3%. It is quite apparent that there is a discontinuity in the electrical conductivity at 196°, the transition point, since the temperature range over which the measurements were taken in this region was so small. But in the temperature region just preceding fusion, no definite conclusions can be drawn since there is some doubt as to the homogeneity of the sample above 226°. This temperature is close to that representing the KF–HF eutectic and a possible pre-melting would lead to a decreased resistance. If, however, this curve actually represents the conductivity of β-KHF_2 in the temperature range before melting, then a possible explanation is that another ion becomes conducting at this temperature. No estimate has been made of the contributions to the conductivity of irreversible effects, such as the possible presence of microscopic fissures or separation of grain boundaries, which would tend to increase the apparent conductivity. No evidence of gross fissures was observed.

Conclusion.—On the basis of thermodynamic, dielectric, neutron diffraction and some spectroscopic evidence, the potential curve of the $(FHF)^-$ ion has a single minimum between the fluorine nuclei. There can be no question that if a potential hill does exist it is very small, but more confirmatory evidence is needed to interpret correctly the infrared spectra of KHF_2. As suggested,[7] a reflection spectrum, obtained with infrared light polarized in a plane parallel to the c-axis, should allow one to decide whether the reflection at 1222 cm.$^{-1}$ can be attributed to ν_2 according to the hypothesis of Westrum and Pitzer or to a splitting of ν_3 as interpreted by Ketelaar.

(18) W. Seith, *Z. Elektrochem.*, **42**, 635 (1936).

THERMODYNAMICS OF THE MONOHYDROGEN DIFLUORIDES. II. HEAT CAPACITIES OF LITHIUM AND SODIUM MONOHYDROGEN DIFLUORIDES FROM 6 TO 305°K.[1]

BY EDGAR F. WESTRUM, JR., AND GLENN A. BURNEY

Department of Chemistry, University of Michigan, Ann Arbor, Michigan

Received August 8, 1960

The meager quantitative thermodynamic data on the hydrofluorides is augmented by low temperature thermal measurements made by an adiabatic calorimetric technique. Apparent anomalies over the range 202 to 227°K. in $NaHF_2$ involving only 11 cal./mole are caused by the presence of traces of higher hydrogen fluorides. The heat capacity (C_p), entropy (S^0), free energy function ($[F^0 - H_0^0]/T$), and enthalpy increment ($H^0 - H_0^0$) at 298.15°K. are: 16.77 and 17.93 cal./(deg. mole), 16.97 and 21.73 cal./(deg. mole), −7.49 and −10.54 cal./(deg. mole), and 2826 and 3334 cal./mole, for $LiHF_2$ and $NaHF_2$, respectively. The dissociation pressure of $LiHF_2$ was determined from 25 to 115°, and yielded a heat of decomposition of 13.7 kcal./mole and a standard free energy of formation of −208.1 kcal./mole at 298.15°K.

Introduction

Few physico-chemical studies have been made on lithium and sodium monohydrogen difluorides ($LiHF_2$ and $NaHF_2$) apart from heat of solution measurements by de Forcrand[2] and crystal structure determinations on $NaHF_2$.[3] However, the existence of the symmetrical hydrogen bond definitely established by Westrum and Pitzer[4,5] in KHF_2 and the existence of a higher temperature "plastic crystal"[6] phase in this substance[5] suggested the desirability of extending thermal measurements to other alkali monohydrogen difluorides. The sodium compound was an obvious choice with its sandwich-type structure and parallel $(F–H\cdots F)^-$ groups, and although the stability and the structure of $LiHF_2$ was unknown when this work was begun, it too was considered potentially interesting.

Experimental

Preparation and Purity of $LiHF_2$.—Both difluorides were prepared by the addition of the corresponding metal carbonate to boiling reagent aqueous 48% HF solution in a platinum evaporating dish. The reagent lithium fluoride contained (in p.p.m. by weight): <200 other alkali metals, <400 Ca, <200 Mg, <50 Fe and <20 Pb. The $LiHF_2$ crystals obtained by controlled cooling of the hot solution were separated with a büchner-type funnel and subsequently dried with air passed through a drying train. The crystals were of tabular habit, transparent, and typically 1 to 3 mm. in width. The decomposition pressure of HF is equal to 2 mm. above the system LiF–$LiHF_2$ at 25°. Because of the loss of HF on drying $LiHF_2$ in air, the salt was transferred to a polyethylene desiccator containing $CaSO_4$ in which a pressure of 10 to 20 mm. of HF was maintained until the small percentage of LiF present was reconverted to the monohydrogen difluoride. The product was stored in a sealed polyethylene desiccator and loaded into the calorimeter in a refrigerated room at −10°. It is suspected that Li_2SiF_6

(1) This work was submitted in partial completion of the requirements for the degree of Doctor of Philosophy at the University of Michigan and was supported in part by the Division of Research of the U. S. Atomic Energy Commission.

(2) M. de Forcrand, *Compt. rend.*, **152**, 1556 (1911).

(3) C. C. Anderson and O. Hassel, *Z. physik. Chem.*, **123**, 151 (1926).

(4) E. F. Westrum, Jr., and K. S. Pitzer, *J. Am. Chem. Soc.*, **71**, 1940 (1949).

(5) K. S. Pitzer and E. F. Westrum, Jr., *J. Chem. Phys.*, **15**, 526 (1947).

(6) J. Timmermans, *Ind. chim. belge*, **16**, 178 (1951).

was a significant contaminant in the $LiHF_2$ prepared by some previous workers who reported quite high decomposition temperatures. The initial samples of $LiHF_2$ prepared for this work acquired a high silica content after storage in a polyethylene boat within a glass desiccator with a protective coating. However, subsequent storage of $LiHF_2$ in a polyethylene desiccator yielded a product free from silica which was used for decomposition pressure and calorimetric measurements.

After heat capacity measurements were completed, analysis of the salt was made by: (1) titration of the hydrogen ion with NaOH standardized against reagent grade potassium acid phthalate using phenolphthalein as the indicator,[7] and (2) gravimetric analysis for fluoride by the lead chlorofluoride method.[8] All quantitative determinations were performed in polyethylene beakers. The precision indices used herein are probable errors based on the reproducibility of the determinations. Volumetric determination of hydrogen ion yielded 99.83 ± 0.07% of the theoretical amount. Gravimetric analysis for fluoride showed 99.78 ± 0.015% of the theoretical. On the basis of this analysis the sample was found to be 99.48% $LiHF_2$ plus 0.52% LiF. The heat capacity data were corrected for this amount of lithium fluoride using the heat capacity measurements on lithium fluoride reported by Clusius.[9] The correction varies from 0.1% of the heat capacity at 15°K. to 0.5% above 200°K. In order to make buoyancy corrections and to correct for the heat capacity of helium gas present in the calorimeter, an approximate value of the density of $LiHF_2$, 2.05 ± 0.1 g./cc., was determined pycnometrically using benzene dried over sodium.

Preparation and Purity of $NaHF_2$.—The $NaHF_2$ obtained from reagent Na_2CO_3 (spectrochemical analysis in p.p.m.: <150 Ca plus Mg, <200 K, <50 SiO_2, <10 Fe, <5 other heavy metals) was dried under vacuum in a Fluorothene container. The salt was then heated in a platinum dish within a Monel container evacuated through a protecting liquid nitrogen trap for 24 hours. The crystals were of a platy habit, leaf-shaped with a serrated edge, of an average width of one millimeter and a length of two millimeters. Volumetric acidimetric determination of hydrogen ion by the previously described method yielded 100.03 ± 0.07% of the theoretical amount. Gravimetric analysis for fluoride showed 100.56 ± 0.26% of theoretical. The quantitative fluoride analysis was slightly high, but at the time this work was being performed sodium was erroneously thought to form only a monohydrogen difluoride.[10,11] Therefore, the high fluoride analysis was considered to be within the accuracy of the quantitative method employed.

Calorimetric Technique.—The Mark I calorimetric cryostat is similar to one already described by Westrum, Hatcher and Osborne[12] and used liquid helium as the lowest temperature refrigerant. The adiabatic method of operation was also similar. Calibrated resistors, standard cells, and an autocalibrated White potentiometer were employed. Duration of the energy input was determined with a vacuum jacketed tuning fork calibrated against signals from the National Bureau of Standards Station WWV. The platinum resistance thermometer (laboratory designation A-3) was also calibrated by the NBS over the range 10 to 717°K. and a provisional temperature scale was used at lower temperatures.

Calorimeters.—The calorimeter used for $NaHF_2$ (laboratory designation W-5) was of gold-plated copper, 3.8 cm. in diameter and 7.7 cm. long with a shell thickness of 0.4 mm. It contained 8 vanes of 0.1 mm. copper foil to aid in establishing thermal equilibrium. An entrant well contained the platinum capsule-type thermometer within a cylindrical gold-plated copper heater sleeve carrying 170 ohms of B. and S. No. 40 gauge Advance double-Fiberglas-insulated wire wound bifilarly in conforming grooves and cemented in place with Formvar enamel. The glass head of the thermometer was entirely within the enlarged portion of the well. The lead wires to both thermometer and heater were brought to temperature equilibrium by means of a small gold-plated copper spool around which the leads were wound and cemented with Formvar enamel. The spool was held in place with brass, hexagonal head, 00–90 screws. A small tube was soldered to the calorimeter as a well for the differential thermocouple junction. Weighed amounts of Lubriseal grease were used to establish thermal contact between calorimeter, heater, thermometer, spool and thermocouple.

After the sample was weighed into the calorimeter and the cover soldered on with Cerroseal solder (50% Sn + 50% In by weight), one atmosphere of helium (to provide thermal conduction) was added to the calorimeter sample space through a small hole drilled in the top of a thin walled Monel stud and soldered shut. Corrections were applied for minute differences in the amount of solder and helium employed.

Another calorimeter (laboratory designation W-6) was used for heat capacity measurements on lithium monohydrogen difluoride, which has an appreciable dissociation pressure at 300°K. This calorimeter was constructed with a short Monel neck soldered to the copper calorimeter. The cover of the calorimeter was a snug fit in the Monel neck and was soldered in place with Cerroseal solder after the calorimeter was filled with the compound. The poor thermal conductivity of Monel kept the calorimeter and the compound from heating appreciably during the soldering operation. Moreover, the evacuation of the calorimeter was done at −70°, one atmosphere of helium was added, the system was warmed to 25°, and the small hole soldered shut. Consequently, it was possible to load $LiHF_2$ without appreciable decomposition occurring.

The mass of each calorimeter (including the heater and thermometer) was approximately 86 g. Calorimetric samples (*in vacuo*) of 42.8260 g. of $LiHF_2$ and 57.0424 g. of $NaHF_2$ were employed. The fraction of the total observed heat capacity contributed by the calorimeter–thermometer–heater assembly gradually decreased from 60% at 10°K. to 34% at 300°K. for $LiHF_2$, and from 39 to 32% over the same range for $NaHF_2$. The mole weights used were 45.948 and 61.999 g., respectively.

Decomposition Pressure Measurements.—Approximate decomposition pressures were taken on the system $LiHF_2$–LiF over the temperature range 36 to 115° in a Monel vessel within a thermostated bath, with a Monel HF reservoir and a Fluorothene manometer. Because the translucent nature of the Fluorothene precluded accurate readings of the mercury menisci with a cathetometer, probable errors of 0.5 mm. are assigned to the observed pressures.

Results and Discussion

Decomposition Pressure of $LiHF_2$–LiF System.—Pressure measurements were made on compositions of 15, 40, 55, 60 and 93 mole % $LiHF_2$, approaching equilibrium pressures both from higher and lower temperatures. These are presented in Table I and Fig. 1. The enthalpy of decomposition (ΔH_d) equal to 13.7 ± 0.3 kcal./mole was calculated by the Clausius–Clapeyron relation. Using extrapolated heat capacity values based upon the $LiHF_2$ measurements from this work, LiF data of Clusius,[9] and calculated values for HF in the ideal gas state,[13] values of ΔC_p for the reaction

$$LiHF_2(c) = LiF(c) + HF(g, ideal) \qquad (1)$$

ranging from −0.35 cal./(deg. mole) at 300°K. to −1.47 cal./(deg. mole) at 375°K. were calculated. The small contributions made by these values of ΔC_p affect ΔH_d by less than 0.15 kcal./mole over this temperature interval. Therefore, within the limit of experimental uncertainty, the enthalpy of dissociation of lithium monohydrogen difluoride can be considered to be constant and equal to 13.7 ± 0.3 kcal./mole over the range 300 to 375°K.

(7) H. H. Willard and N. H. Furman, "Elementary Quantitative Analysis," D. Van Nostrand Co., New York, N. Y., 1942.

(8) W. W. Scott, "Standard Methods of Chemical Analysis," Vol. I, D. Van Nostrand Co., New York, N. Y., 1939, p. 405.

(9) K. Clusius, *Z. Naturforsch.*, **1**, 79 (1946).

(10) J. H. Simons, "Fluorine Chemistry," Vol. I, Academic Press, Inc., New York, N. Y., 1950, p. 27.

(11) R. V. Winsor and G. H. Cady, *J. Am. Chem. Soc.*, **70**, 1500 (1948).

(12) E. F. Westrum, Jr., J. B. Hatcher and D. W. Osborne, *J. Chem. Phys.*, **21**, 419 (1953).

(13) G. M. Murphy and J. E. Vance, *J. Chem. Phys.*, **7**, 806 (1939).

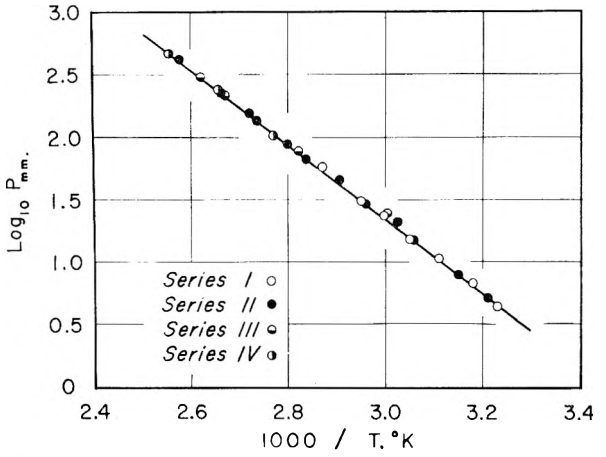

Fig. 1.—Decomposition pressure of system $LiHF_2(c) = LiF(c) + HF(g)$.

TABLE I

DECOMPOSITION PRESSURE OF $LiHF_2$

Mole % $LiHF_2$ ±2%	T, °C. ±0.2°	P, mm. ±0.5	Mole % $LiHF_2$ ±2%	T, °C. ±0.2°	P, mm. ±0.5
	Series I		55	44.2	7.9
			55	57.4	20.1
93	36.3	4.5	55	70.9	46.0
93	49.1	10.6	15	93.9	153.8
93	62.1	24.3	15	102.3	224.0
93	75.2	57.2			
93	65.7	31.0		Series III	
93	53.9	15.3			
93	41.3	6.7	40	61.3	24.3
			40	81.4	78.9
	Series II		40	101.5	218.2
			40	108.5	307.6
92	37.9	5.1			
92	52.9	14.7		Series IV	
92	64.5	29.0			
92	79.3	66.9	60	87.9	107.7
92	84.4	90.3	60	103.0	237.7
92	92.4	135.6	60	117.8	470.8
92	114.9	422.5			

The standard free energy increment of reaction 1 was found to be 3.50 ± 0.1 kcal./mole at 298.15°K. from the relationship $\Delta F^0 = -RT \ln K$ using a decomposition pressure (2.0 mm.) extrapolated from measurements made at slightly higher temperatures.

Troost[14] reported that the decomposition of $LiHF_2$ yielded LiF and HF at red heat. Wartenburg

TABLE II

HEAT CAPACITIES OF MONOHYDROGEN DIFLUORIDES [IN CAL./(DEG. MOLE)]

T, °K.	C_p	T, °K.	C_p	T, °K.	C_p
Lithium monohydrogen difluoride ($LiHF_2$, mole weight = 45.948 g.)					
Series I		262.45	15.71	22.01	0.213
		271.53	15.99	24.13	.274
109.21	7.948	281.10	16.28	26.54	.359
118.45	8.721	291.07	16.58	29.08	.465
126.20	9.312	301.36	16.88	31.86	.607
134.89	9.939			34.99	.791
143.98	10.54	Series II		38.60	1.044
152.89	11.10			42.58	1.355
161.77	11.61	6.57	0.008	46.81	1.725
170.86	12.09	7.84	.013	51.47	2.167
180.33	12.56	9.01	.020	53.04	2.323
189.93	13.01	10.11	.029	57.98	2.826
199.35	13.51	11.19	.037	63.82	3.452
208.59	13.83	12.39	.045	69.90	4.101
217.69	14.20	13.71	.062	76.55	4.802
226.72	14.57	15.10	.079	84.12	5.601
235.72	14.84	16.53	.101	92.36	6.427
244.63	15.13	18.18	.126	101.02	7.234
253.55	15.42	20.07	.166	109.74	7.998
Sodium monohydrogen difluoride ($NaHF_2$, mole weight = 61.999 g.)					
Series I		305.09	18.14	227.51	16.04
				228.32	16.00
5.73	0.013	Series II			
8.15	.031			Series V	
9.67	.061	172.99	14.12		
10.84	.083	184.69	14.48	199.54	15.16
12.07	.108	196.04	15.10	208.17	15.44
13.32	.146	202.24	18.90	216.65	15.73
14.61	.190	204.99	15.48	225.00	15.96
16.02	.248	212.28	15.77	233.24	16.18
17.53	.318	222.90	16.22		
18.92	.392	233.39	16.16	Series VI	
20.43	.482				
22.63	.634	Series III		196.40	15.00
25.17	.833			198.57	15.11
27.71	1.060	186.08	14.61	199.60	15.21
30.64	1.344	193.96	14.91	200.56	15.32
34.06	1.737	196.78	15.03	201.27	15.58
37.82	2.201	197.90	15.09	201.72	16.07
41.98	2.736	199.02	15.16	202.06	16.30
46.44	3.344	200.13	15.26	202.28	16.40
51.28	4.030	200.96	15.39	202.49	17.29
56.56	4.779	201.51	15.69	202.68	23.40
57.23	4.870	202.06	16.04	202.84	35.43
63.14	5.702	202.54	22.42	203.02	15.63
69.40	6.532	203.00	19.60	203.68	15.41
75.58	7.308	203.79	15.38	204.76	15.44
83.07	8.175	204.88	15.47	209.90	15.69
90.92	9.024	209.67	15.66	217.63	15.97
98.57	9.733	214.95	15.92	222.64	16.23
106.90	10.44	217.03	15.95	224.14	16.37
115.85	11.12	218.60	16.01	224.90	16.35
124.79	11.73	220.16	16.10	225.40	16.39
134.42	12.33	222.22	16.25	225.90	16.50
144.75	12.87	224.20	16.30	226.40	16.24
154.92	13.39	226.24	16.30	226.90	16.05
164.96	13.82	228.29	16.02	227.66	16.03
174.96	14.13	233.41	16.16		
184.93	14.59	241.54	16.41	Series VII	
194.91	14.95				
204.83	16.00	Series IV		183.22	14.53
215.04	15.88			191.83	14.83
225.59	16.19	200.04	15.89	198.12	15.05
236.03	16.21	208.81	15.63	201.86	16.22
246.38	16.50	218.03	16.02	206.11	15.41
256.62	16.76	223.34	16.32	211.05	15.61
266.70	17.06	224.61	16.42	216.22	15.78
276.65	17.30	225.39	16.45	222.92	15.98
286.45	17.58	225.91	16.40	231.16	16.08
296.11	17.86	226.44	16.14	239.49	16.31
		226.96	16.11		

(14) M. L. Troost, *Ann. chim. et phys.*, **51**, 103 (1857).

and Bosse[15] reported the "decomposition temperature" as under 200°, while Hopkins[16] claimed it to be 105°. This work yielded an extrapolated decomposition pressure of hydrogen fluoride of one atmosphere at 129.5°.

The standard enthalpy of formation of $LiHF_2$ at 298.15°K. was found to be equal to −224.2 kcal./mole from the enthalpy of formation of LiF(c) and HF(g)[17] and the above enthalpy of decomposition.

Heat Capacity Data on $LiHF_2$.—The experimental values of the heat capacities of $LiHF_2$ and $NaHF_2$ are shown in Table II in chronological sequence in terms of the defined thermochemical calorie equal to 4.1840 abs. j. and an ice point of 273.15°K. The data have been corrected for curvature (*i.e.*, for the difference between

$$\left(\frac{Q}{\Delta T}\right)_p \text{ and } \lim_{\Delta T \to 0}\left(\frac{Q}{\Delta T}\right)_p$$

in which Q is the energy input producing the increment in temperature (ΔT) under essentially constant pressure conditions). The actual temperature increments employed can usually be estimated from the differences in adjacent mean temperatures in Table II. The values of the heat capacity are considered to have a probable error of about 5% at 5°K. decreasing to 1% at 10°K. and to less than 0.2% above 25°K. No anomalies appear over the range studied. No correction has been made for the energy involved in the slight reversible decomposition of $LiHF_2$ above the ice point. At 270°K. the correction is less than 0.01% and increases to 0.03% at 300°K. Corrections for lithium fluoride present in the sample have been made as noted.

Heat Capacity Data on $NaHF_2$.—These data are also presented in Table II and have likewise been subjected to curvature correction. Anomalies were found in the form of a sharp peak at 202.8°K. and a hump extending over the temperature range 203 to 227°K. (*cf.* Fig. 2) and involve a total of 11 cal./mole or 0.05 e.u. It was possible, upon cooling to temperatures only several degrees below the transition, to measure heat capacities over the transition region (of an apparently metastable state) which were in accord with values interpolated from adjacent values outside the transition region. The effect was confirmed only on warming in a series of thermal analyses of six compositions between limits corresponding to NaF·HF and NaF·4HF. Solubility measurements of NaF in anhydrous liquid HF[18] indicated the existence of the compound NaF·4HF. Phase studies on the ternary system NaF–HF–H_2O by Tananaev[19] indicated the existence of $NaF \cdot xHF$ with x = 1, 2, 3 and 4. These findings have been recently confirmed by Morrison and Jache[20] in an examination of the ternary system by Schreinemakers' method of wet residues. Unpublished thermal analysis data from this Laboratory[21] on the system NaF–HF indicate that

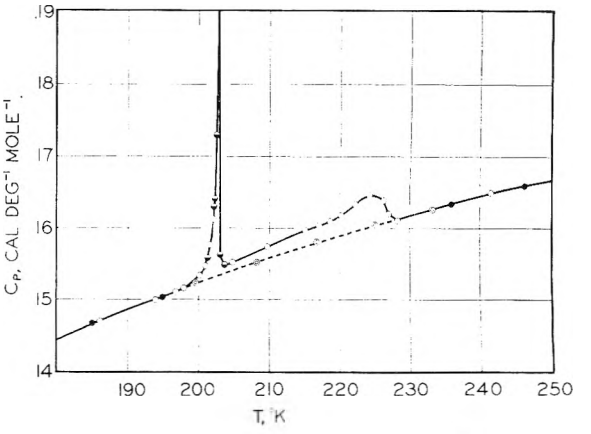

Fig. 2.—Anomaly in heat capacity of $NaHF_2$. Separate series of measurements are indicated by different symbols.

the transition is probably due to an unidentified effect in NaF·2HF present in the sample as a contaminant (*cf.* analytic data indicating excess HF). The phase study of Adamczak, Mattern and Tieckelmann[22] does not show the phenomenon.

If the anomalous effect was due to the presence of a higher sodium hydrofluoride, it might be precluded by eliminating the apparent local excesses of hydrogen fluoride. An attempt to prepare such a sample was made by heating the original sample to 135°, at which temperature the pressure of hydrogen fluoride above the compound was several millimeters, and some hydrogen fluoride was pumped off. Analysis showed the resulting salt to correspond to 3% NaF and 97% $NaHF_2$. Heat capacity measurements on this sample showed the anomalous effects over the same temperature range; however, the total extra energy involved in the transition region was only two-thirds that of the original sample. It is considered that the method of decomposition may have allowed for reformation of some of the higher hydrofluoride compound and that the gaseous HF in equilibrium with the sample should have been evacuated continuously while cooling to room temperature.

Thermodynamic Functions for $LiHF_2$ and $NaHF_2$.—The molal values of the heat capacity and the derived thermodynamic functions are presented in Table III at selected temperatures. The heat capacities have been read from large scale plots and the functions obtained by numerical quadrature. The entire mathematical operation has been confirmed by a least squares curve fitting and integration program on a digital computer. The thermodynamic functions of both compounds are considered to have a probable error of ±0.2% because of the correction for LiF present in the $LiHF_2$ and for a higher hydrofluoride contaminant in the $NaHF_2$.

The entropy of $LiHF_2$ together with those of Li, H_2 and F_2,[17] and the enthalpy of formation from this work yield the standard free energy of formation of $LiHF_2$ at 298.15°K. of −208.1 kcal./mole.

Since the anomaly in $NaHF_2$ has been attributed to a higher hydrofluoride contaminant, the heat

(15) H. v. Wartenburg and O. Bosse, *Z. Elektrochem.*, **28**, 384 (1922).

(16) B. S. Hopkins, "Chapters in the Chemistry of Less Familiar Elements," Stipes Publishing Co., Champaign, Ill., 1940, p. 7.

(17) "Selected Values of Chemical Thermodynamic Properties," Circular 500, National Bureau of Standards, Washington, D. C., 1952.

(18) A. W. Jache and G. H. Cady, THIS JOURNAL, **56**, 1106 (1952).

(19) I. V. Tananaev, *J. Gen. Chem.* (*U.S.S.R.*), **11**, 267 (1941).

(20) J. S. Morrison and A. W. Jache, *J. Am. Chem. Soc.*, **81**, 1821 (1959).

(21) R. Euler, unpublished data.

(22) R. L. Adamczak, J. A. Mattern and H. Tieckelmann, THIS JOURNAL, **63**, 2063 (1959).

TABLE III

THERMODYNAMIC FUNCTIONS OF MONOHYDROGEN DIFLUORIDES

T, °K.	C_p, cal./(deg. mole)	S^0, cal./(deg. mole)	$H^0 - H_0^0$, cal./mole	$-(F^0 - H_0^0)/T$, cal./(deg. mole)
	Lithium monohydrogen difluoride ($LiHF_2$, mole weight = 45.948 g.)			
10	0.027	0.009	0.065	0.002
15	.077	.028	.313	.007
20	.164	.061	.896	.016
25	.303	.111	2.039	.030
30	.510	.184	4.040	.049
35	.792	.283	7.265	.075
40	1.148	.411	12.085	.109
45	1.563	.569	18.837	.151
50	2.025	.758	27.791	.202
60	3.040	1.215	53.05	.331
70	4.109	1.764	88.78	.496
80	5.170	2.382	135.21	.692
90	6.190	3.051	192.09	.917
100	7.141	3.753	258.82	1.165
110	8.018	4.476	334.69	1.433
120	8.838	5.209	419.02	1.717
130	9.592	5.947	511.2	2.014
140	10.29	6.683	610.7	2.321
150	10.92	7.415	716.8	2.637
160	11.50	8.139	828.9	2.958
170	12.04	8.853	946.7	3.284
180	12.55	9.556	1069.7	3.613
190	13.03	10.247	1197.7	3.944
200	13.48	10.928	1330.3	4.276
210	13.90	11.596	1467.4	4.609
220	14.30	12.252	1608.5	4.941
230	14.66	12.896	1753.3	5.273
240	14.99	13.527	1901.5	5.604
250	15.31	14.145	2053.0	5.933
260	15.63	14.752	2207.7	6.261
270	15.94	15.348	2365.5	6.586
280	16.25	15.933	2526.5	6.910
290	16.55	16.508	2690.5	7.231
300	16.82	17.074	2857.3	7.550
273.15	16.04	15.53	2416	6.69
298.15	16.77	16.97	2826	7.49
	Sodium monohydrogen difluoride ($NaHF_2$, mole weight = 61.999 g.)			
10	0.064	0.021	0.159	0.005
15	.205	.071	0.792	.018
20	.454	.161	2.396	.041
25	.819	.300	5.536	.078
30	1.284	.489	10.752	.130
35	1.848	.727	18.525	.198
40	2.480	1.015	29.330	.282
45	3.144	1.345	43.365	.381
50	3.847	1.712	60.83	.495
60	5.270	2.539	106.41	.766
70	6.612	3.454	165.91	1.084
80	7.837	4.418	238.25	1.440
90	8.930	5.406	322.24	1.825
100	9.865	6.396	416.33	2.233
110	10.69	7.376	519.2	2.656
120	11.42	8.338	629.8	3.090
130	12.07	9.278	747.2	3.530
140	12.64	10.193	870.8	3.973
150	13.16	11.083	999.8	4.417
160	13.62	11.947	1133.7	4.861
170	14.03	12.785	1272.0	5.303
180	14.42	13.598	1414.2	5.741
190	14.78	14.387	1560.2	6.175
200	15.11	15.154	1709.7	6.606
210	15.43	15.899	1862.4	7.030
220	15.74	16.624	2018.2	7.450
230	16.03	17.330	2177.1	7.865
240	16.32	18.018	2338.8	8.273
250	16.60	18.690	2503.4	8.676
260	16.87	19.346	2670.8	9.074
270	17.14	19.988	2840.8	9.466
280	17.41	20.617	3013.6	9.854
290	17.69	21.233	3189.1	10.236
300	17.98	21.837	3367.5	10.612
273.15	17.21	20.21	2902	9.59
298.15	17.93	21.73	3334	10.54

capacities used across the transition interval are those interpolated across this region by a probable curve in good accord with the data on the supercooled sample. Hence the anomaly has been omitted in the smoothed heat capacities and the thermodynamic functions. Inclusion of the anomaly would increase the entropy at 298.15°K. by 0.2%.

Decomposition pressure measurements made on the system $NaHF_2$–NaF by Froning and Richards[23] from 100 to 250° (to determine optimum conditions for the removal of hydrogen fluoride from the gases evolved in the production of fluorine by electrolysis) yield a value of the enthalpy of the reaction

$$NaHF_2(c) = NaF(c) + HF(g, ideal) \qquad (2)$$

equal to 14.8 ± 0.5 kcal./mole. The scattering of the points observed on plotting the data reported by these workers was so great that a constant ΔH was necessarily assumed over the entire temperature range. This value of the enthalpy of decomposition is considerably lower than the value of 16.4 kcal./mole calculated from tabulated enthalpy of formation data[17] for NaF(c), $NaHF_2$(c) and HF (g, ideal). The enthalpy of formation of $NaHF_2$(c) equal to −216.6 kcal./mole is based on the measurements of de Forcrand.[2] Utilizing the ΔHf tabulated[17] and data on the entropy of NaF and HF from the same source yields a free energy of formation of $NaHF_2$ equal to −193.0 kcal./mole.

Acknowledgment.—The coöperation of Dr. D. W. Osborne and the Chemistry Division of the Argonne National Laboratory in making liquid helium available for this study prior to the receipt of our cryostat, the digital computer checking of the smoothing and integration of the data by Bruce H. Justice, and the financial support of the Division of Research of the U. S. Atomic Energy Commission are gratefully acknowledged.

(23) J. F. Froning, M. K. Richards, T. W. Stricklin and S. G. Turnbull, *Ind. Eng. Chem.*, **39**, 275 (1947).

THERMODYNAMICS OF THE MONOHYDROGEN DIFLUORIDES. III. HEAT CAPACITIES OF CESIUM, RUBIDIUM AND THALLIUM MONOHYDROGEN DIFLUORIDES FROM 7 TO 305°K.[1]

BY GLENN A. BURNEY AND EDGAR F. WESTRUM, JR.

Department of Chemistry, University of Michigan, Ann Arbor, Michigan

Received August 29, 1960

Low temperature heat capacities of $CsHF_2$, $RbHF_2$ and $TlHF_2$ were measured by adiabatic calorimetry and the thermodynamic functions were calculated from these data. No thermal anomalies were observed over the range studied. The standard entropies of $CsHF_2$, $RbHF_2$ and $TlHF_2$ at 298.15°K. are 32.31, 28.70, and 34.92 cal./(deg. mole), respectively. The corresponding standard free energy functions $[-(F^0 - H_0^0)/T]$ are 18.22, 15.51 and 20.47 cal./(deg. mole), respectively. The entropies of these compounds are correlated with those of other known monohydrogen difluorides.

Introduction

Aside from the system $KHF_2 = KF + HF$ investigated by Westrum and Pitzer[2,3] and more recently by Davis and Westrum[4] and others, the known monohydrogen difluorides have been little studied except for X-ray diffractional structure determinations on $NaHF_2$,[5] KHF_2[6,7] and NH_4HF_2[8,9]; temperature–composition studies on KF–HF,[10] on RbF–HF,[11] on CsF–HF[12]; heat of solution measurements,[13] and lattice energies of KHF_2, $RbHF_2$ and $CsHF_2$.[14]

The monohydrogen difluorides have already stimulated considerable theoretical interest from the single minimum $(F–H\ldots F)^-$ hydrogen bond[2] which they possess to a degree not presently revealed by other substances. The nature and occurrence of the transitions transforming (in the case of KHF_2) the relatively hard tetragonal α-phase at 196° to a waxy, plastic[15] crystal with a heat of transformation considerably greater than that of fusion is worthy of further study. The phase investigations on CsF–HF[12] indicated a transition in $CsHF_2$ at 40–50°. $TlHF_2$, moreover, was reported[16] to be of cubic structure and thus to have much higher symmetry than that of other hydrofluorides. It was considered, therefore, that this substance might undergo transition below 25°. However, after heat capacity measurements were made on $TlHF_2$, a subsequent report[17] was found indicating that further chemical analysis had shown that the previously reported studies[16] were actually done on $TlF{\cdot}2HF{\cdot}{}^1/_2H_2O$ despite the fact that an exact analysis for $TlHF_2$ was given in the original article. As a preliminary to higher temperature measurements, the low temperature heat capacities of three monohydrogen difluorides were examined and reported here.

Experimental

Preparation and Purity of the Calorimetric Sample.—Reagent grade Rb_2CO_3, containing <200 p.p.m. Ca, Mg, Na and Si by spectrochemical analysis, was used for the preparation. The mixture of hydrofluorides obtained upon treatment of Rb_2CO_3 with hot aqueous HF was heated at 100° in a platinum vessel within an evacuated, liquid nitrogen trapped, Fluorothene container until the hydrofluorides richer in HF than $RbHF_2$ decomposed. The sample, fused during the initial stages of decomposition, was broken into pieces with an average dimension of 1 mm. after decomposition to $RbHF_2$ was complete. Volumetric acidimetric determination of hydrogen ion with standard sodium hydroxide indicated 100.01 ± 0.07% of theoretical. Gravimetric analysis for fluoride by precipitation of lead chlorofluoride[18] showed 99.97 ± 0.15% of theoretical. Due to the slightly hygroscopic nature of the compound, handling the sample and loading the calorimeter was done in a dry box.

Cesium carbonate of stated purity in excess of 99.5% and estimated by semi-quantitative spectrochemical analysis to contain less than 0.1% of Ca, Mg and Na was used as reactant for the preparation of $CsHF_2$. The mixture of hydrofluorides, obtained by treatment of Cs_2CO_3 with hot aqueous HF, was very soluble and hygroscopic. This material, contained in a platinum boat, was heated under vacuum to 300° in a nickel furnace for 24 hours. Anhydrous hydrogen fluoride at room temperature was then passed over the anhydrous CsF to form hydrofluorides. Decomposition to $CsHF_2$ was effected by heating to 135° and by evacuating through a protective liquid nitrogen trap. The material fused during decomposition due to the low eutectic temperature (35°) for the CsF·HF–CsF·2HF system. The fused material was broken into pieces with an average dimension of 0.2 to 1 mm. for the heat capacity measurements. Volumetric acidimetric determination of hydrogen ion with standard sodium hydroxide indicated 99.95 ± 0.07% of theoretical. Gravimetric analysis for fluoride by precipitation of lead chlorofluoride showed 99.92 ± 0.16% of theoretical. Handling and loading were done in a dry box because the salt was highly hygroscopic.

Thallium monohydrogen difluoride was obtained by dissolution of thallium metal of 99.99% purity in hot, 48% aqueous HF and subsequent precipitation upon cooling the solution. The acid salt was repeatedly recrystallized under carefully controlled temperatures. It was extremely soluble, and considerable difficulty was encountered in obtaining well-formed acicular crystals with an average diameter of 0.5 mm. and length of 1 mm. These were dried in a polyethylene desiccator over $CaSO_4$ and were held at −10°

(1) This work was submitted in partial completion of the requirements for the degree of Doctor of Philosophy at the University of Michigan and was supported in part by the Division of Research of the U. S. Atomic Energy Commission.

(2) E. F. Westrum, Jr., and K. S. Pitzer, *J. Am. Chem. Soc.*, **71**, 1940 (1949).

(3) K. S. Pitzer and E. F. Westrum, Jr., *J. Chem. Phys.*, **15**, 526 (1947).

(4) M. L. Davis and E. F. Westrum, Jr., THIS JOURNAL, **65**, 338 (1961).

(5) C. C. Anderson and O. Hassel, *Z. physik. Chem.*, **123**, 151 (1926).

(6) R. M. Bozorth, *J. Am. Chem. Soc.*, **45**, 2128 (1923).

(7) R. Kruh, K. Fuwa and T. E. McEver, *ibid.*, **78**, 4256 (1956).

(8) L. Pauling, *Z. Krist.*, **85**, 380 (1933).

(9) T. R. R. McDonald, *Acta Cryst.*, **13**, 113 (1960).

(10) G. H. Cady, *J. Am. Chem. Soc.*, **56**, 1431 (1934).

(11) E. B. R. Prideaux and K. R. Webb, *J. Chem. Soc.*, 1 (1937); K. R. Webb and E. B. R. Prideaux, *ibid.*, 111 (1939).

(12) R. V. Winsor and G. H. Cady, *J. Am. Chem. Soc.*, **70**, 1500 (1948).

(13) M. de Forcrand, *Compt. rend.*, **152**, 1556 (1911).

(14) T. C. Waddington, *Trans. Faraday Soc.*, **54**, 25 (1958).

(15) J. Timmermans, *Bull. soc. chim. belg.*, **44**, 17 (1935); *Ind. chim. belge*, **16**, 178 (1951).

(16) O. Hassel and H. Kringstad, *Z. anorg. allgem. Chem.*, **191**, 36 (1930).

(17) O. Hassel and H. Kringstad, *ibid.*, **208**, 382 (1932).

(18) W. W. Scott, "Standard Methods of Chemical Analysis," Vol. I, D. Van Nostrand Co., New York, N. Y., 1939, p. 405.

in a refrigerated room until loaded into the calorimeter. The decomposition pressure of HF over the salt was small so that no further hydrofluorination was necessary after drying. However, slight decomposition could be detected if the salt was allowed to stand at 25° for periods of several weeks. Volumetric acidimetric determination of hydrogen ion with standard sodium hydroxide yielded 100.02 ± 0.07% of theoretical. Gravimetric analysis for thallium by precipitation of thallium iodide showed 100.03 ± 0.05% of theoretical.

Cryostat, Calorimeter and Technique.—The measurements described in this paper on $RbHF_2$ and $CsHF_2$ were made in calorimeter W-5 described in an earlier paper in this series[19]; those on $TlHF_2$ were made in calorimeter W-6.[20] Helium cryostat Mark I (similar in most essential details to one previously described[21]) was used. An adiabatic technique of operation was employed. Circuitry of this unit included calibrated standard cells, standard resistors and an autocalibrated White potentiometer. Duration of the energy input was determined with a calibrated tuning fork checked against signals from station WWV. The platinum resistance thermometer (laboratory designation A-3) was calibrated above 10°K. by the National Bureau of Standards. Below this temperature a provisional scale was adopted. The sample masses used (*in vacuo*) were 128.3223, 216.9169 and 153.1626 g., for $RbHF_2$, $CsHF_2$ and for $TlHF_2$, respectively. The contribution of the calorimeter–heater–thermometer assembly was less than 25% of the total heat capacity below 80°K. and between 30 and 40% at higher temperatures for each of the compounds. Buoyancy corrections were made on the basis of densities determined pycnometrically in benzene. Values of 3.1 ± 0.2, 3.7 ± 0.2 and 6.3 ± 0.3 g./cc. were used for $RbHF_2$, $CsHF_2$ and $TlHF_2$, respectively. The heat capacity of a standard sample of benzoic acid (prepared for calorimetric purposes by NBS[22]) was determined to test the accuracy of the calorimetry.

Results and Discussion

Heat Capacity Values.—The experimental molal values of the heat capacities of these three substances are presented in Table I in chronological order to permit estimation of the temperature increments employed in the measurements. These data are presented in terms of the defined thermochemical calorie equal to 4.180 abs. j., an ice point of 273.15°K., and mole weights of 124.49, 171.92 and 243.40 g. for $RbHF_2$, $CsHF_2$ and $TlHF_2$, respectively. These values have been corrected for curvature to yield true differential heat capacities. The slight decomposition pressure of $TlHF_2$ makes no sensible contribution to the heat capacity below 300°K. The probable error of these values approximates 5% at 5°K., decreasing to 1% at 10°K. and to less than 0.1% above 25°K.

TABLE I

HEAT CAPACITIES OF MONOHYDROGEN DIFLUORIDES [IN CAL./(DEG. MOLE)]

T, °K.	C_p	T, °K.	C_p	T, °K.	C_p
Cesium monohydrogen difluoride ($CsHF_2$, mole weight = 171.92 g.)					
Series I		201.06	17.21	7.10	0.138
		210.18	17.46	8.32	0.264
58.01	10.22	218.96	17.69	9.36	0.409
57.93	10.21	198.58	17.14	10.45	0.578
63.79	10.99	207.46	17.38	11.62	0.754
69.83	11.64	216.36	17.62	12.91	0.989
76.46	12.27	225.29	17.88	14.31	1.266
83.91	12.89	234.28	18.15	15.82	1.580
92.31	13.46	243.30	18.48	17.48	1.934
101.20	13.94	252.31	18.74	19.33	2.342
110.08	14.36	261.25	19.06	21.39	2.816
119.07	14.74	270.05	19.41	23.69	3.349
118.34	14.71	278.70	19.79	26.33	3.979
127.28	15.06	287.00	20.20	29.35	4.693
136.21	15.37	294.94	20.65	32.61	5.464
145.54	15.68	302.74	21.17	36.04	6.243
155.09	15.97			39.65	7.033
164.38	16.22	Series II		43.51	7.806
173.53	16.48			47.84	8.618
182.71	16.72	4.76	0.048	52.78	9.446
191.83	16.96	5.65	0.072	58.01	10.22
Rubidium monohydrogen difluoride ($RbHF_2$, mole weight = 124.49 g.)					
Series I		204.02	16.73	10.50	0.200
		213.02	16.95	11.67	0.279
53.29	7.998	222.14	17.16	12.76	0.374
58.62	8.867	231.24	17.37	13.76	0.473
65.29	9.822	240.21	17.60	14.87	0.610
71.70	10.59	249.12	17.83	15.99	0.755
78.39	11.31	258.04	18.00	17.22	0.929
85.99	12.02	267.02	18.21	18.43	1.110
94.42	12.65	276.08	18.43	19.86	1.349
103.38	13.22	285.14	18.64	21.64	1.661
112.37	13.70	294.21	18.87	23.70	2.050
121.54	14.15	303.24	19.10	25.95	2.496
130.93	14.56			28.44	3.009
140.40	14.92	Series II		31.29	3.621
149.82	15.25			34.64	4.349
159.10	15.54	5.34	0.020	38.41	5.161
168.20	15.81	6.34	0.033	42.34	5.968
177.15	16.05	7.31	0.046	46.61	6.811
186.07	16.28	8.34	0.081	51.37	7.688
195.05	16.51	9.41	0.133	56.40	8.529
Thallium monohydrogen difluoride ($TlHF_2$, mole weight = 243.40 g.)					
Series I		300.97	21.43	36.29	7.566
				39.74	8.233
158.10	16.17	Series II		43.43	8.883
167.53	16.44			47.65	9.571
177.00	16.69	7.08	0.391	52.50	10.28
186.48	16.95	7.36	0.472	57.63	10.94
195.73	17.20	8.34	0.702	52.78	10.30
204.83	17.45	9.84	1.132	58.52	11.03
213.85	17.70	11.14	1.444	64.35	11.68
222.89	17.96	12.28	1.706	70.59	12.24
231.86	18.23	13.45	2.039	77.45	12.79
220.22	17.86	14.69	2.380	85.06	13.34
229.13	18.14	16.09	2.751	93.50	13.81
238.03	18.42	17.82	3.197	102.15	14.21
246.94	18.73	19.92	3.754	110.95	14.59
255.88	19.05	22.28	4.354	120.01	14.94
264.91	19.41	24.72	4.962	129.01	15.26
273.98	19.81	27.24	5.566	138.04	15.56
283.05	20.25	29.98	6.203	147.11	15.84
292.07	20.78	33.02	6.880	156.26	16.11

Thermodynamic Properties.—Molal values of the thermodynamic properties were obtained by numerical quadrature of the smooth curve drawn through a large scale plot of the heat capacity and independently checked by a curve fitting, smooth-

(19) E. F. Westrum, Jr., and G. A. Burney, THIS JOURNAL, **65**, 344 (1961).

(20) E. Benjamins and E. F. Westrum, Jr., *J. Am. Chem. Soc.*, **79**, 287 (1957).

(21) E. F. Westrum, Jr., J. B. Hatcher and D. W. Osborne, *J. Chem. Phys.*, **21**, 419 (1953).

(22) D. C. Ginnings and G. T. Furukawa, *J. Am. Chem. Soc.*, **75**, 522 (1953).

TABLE II

THERMODYNAMIC FUNCTIONS OF MONOHYDROGEN DIFLUORIDES

T, °K.	C_p, cal./(deg. mole)	S^0, cal./(deg. mole)	$H^0 - H_0^0$, cal./mole	$-(F^0 - H_0^0)/T$, cal./(deg. mole)
	Cesium monohydrogen difluoride ($CsHF_2$, mole weight = 171.92 g.)			
10	0.493	0.164	1.23	0.041
15	1.466	0.527	5.86	0.136
20	2.492	1.078	15.57	0.299
25	3.666	1.760	30.97	0.521
30	4.849	2.533	52.25	0.791
35	6.014	3.369	79.44	1.099
40	7.106	4.244	112.28	1.437
45	8.093	5.139	150.31	1.798
50	8.994	6.039	193.07	2.178
60	10.50	7.816	290.78	2.970
70	11.66	9.527	401.89	3.786
80	12.58	11.146	523.2	4.606
90	13.31	12.671	652.8	5.417
100	13.88	14.104	788.9	6.215
110	14.36	15.450	930.1	6.995
120	14.78	16.717	1075.8	7.752
130	15.16	17.915	1225.5	8.488
140	15.50	19.052	1378.8	9.204
150	15.81	20.132	1535.4	9.896
160	16.10	21.162	1695.0	10.568
170	16.38	22.146	1857.4	11.220
180	16.65	23.090	2022.6	11.854
190	16.91	23.997	2190.4	12.469
200	17.18	24.872	2360.8	13.068
210	17.44	25.716	2533.9	13.650
220	17.72	26.534	2709.7	14.217
230	18.02	27.328	2888.4	14.770
240	18.33	28.101	3070.1	15.309
250	18.66	28.856	3255.0	15.836
260	19.02	29.595	3443.4	16.351
270	19.31	30.320	3635.5	16.855
280	19.85	31.034	3831.8	17.349
290	20.37	31.739	4032.8	17.833
300	20.98	32.440	4239.5	18.308
273.15	19.54	30.54	3697	17.01
298.15	20.86	32.31	4201	18.22
	Rubidium monohydrogen difluoride ($RbHF_2$, mole weight = 124.49 g.)			
10	0.165	0.055	0.41	0.014
15	0.622	0.197	2.25	0.048
20	1.370	0.473	7.13	0.117
25	2.306	0.877	16.26	0.226
30	3.344	1.388	30.37	0.376
35	4.427	1.985	49.80	0.562
40	5.489	2.646	74.59	0.781
45	6.497	3.351	104.58	1.027
50	7.437	4.085	139.44	1.296
60	9.080	5.591	222.28	1.886
70	10.41	7.093	319.94	2.523
80	11.47	8.555	429.52	3.186
90	12.32	9.957	548.6	3.861
100	13.02	11.292	675.4	4.538
110	13.59	12.561	808.6	5.210
120	14.08	13.765	947.0	5.873
130	14.51	14.909	1090.0	6.525
140	14.90	16.000	1237.1	7.163
150	15.25	17.040	1387.9	7.787
160	15.57	18.034	1542.1	8.397
170	15.86	18.987	1699.2	8.992
180	16.13	19.902	1859.2	9.573
190	16.38	20.781	2021.8	10.140
200	16.63	21.627	2186.8	10.693
210	16.87	22.444	2354.3	11.233
220	17.11	23.234	2524.2	11.761
230	17.36	24.001	2696.6	12.276
240	17.59	24.744	2871.3	12.780
250	17.83	25.467	3048.4	13.273
260	18.06	26.171	3227.9	13.756
270	18.28	26.857	3409.6	14.229
280	18.52	27.526	3593.6	14.692
290	18.76	28.180	3779.9	15.146
300	19.02	28.820	3968.8	15.591
273.15	18.36	27.07	3467	14.38
298.15	18.97	28.70	3934	15.51
	Thallium monohydrogen difluoride ($TlHF_2$, mole weight = 243.40 g.)			
10	1.140	0.380	2.85	0.095
15	2.454	1.092	11.86	0.302
20	3.772	1.980	27.45	0.608
25	5.029	2.959	49.50	0.979
30	6.205	3.981	77.62	1.394
35	7.297	5.021	111.42	1.838
40	8.281	6.061	150.40	2.301
45	9.150	7.088	194.04	2.776
50	9.925	8.093	241.78	3.257
60	11.20	10.020	347.67	4.225
70	12.20	11.825	464.88	5.184
80	12.99	13.508	591.0	6.120
90	13.62	15.075	724.2	7.029
100	14.12	16.537	862.9	7.908
110	14.55	17.903	1006.3	8.755
120	14.94	19.186	1153.8	9.571
130	15.29	20.396	1305.0	10.358
140	15.62	21.542	1459.6	11.116
150	15.93	22.630	1617.3	11.848
160	16.22	23.667	1778.1	12.554
170	16.50	24.659	1941.7	13.237
180	16.77	25.610	2108.1	13.899
190	17.04	26.525	2277.2	14.539
200	17.32	27.406	2449.0	15.161
210	17.59	28.257	2623.6	15.764
220	17.87	29.082	2800.9	16.351
230	18.17	29.883	2981.0	16.922
240	18.49	30.663	3164.3	17.478
250	18.84	31.424	3350.9	18.021
260	19.21	32.170	3541.1	18.551
270	19.63	32.903	3735.2	19.069
280	20.10	33.625	3933.8	19.576
290	20.64	34.339	4137.4	20.073
300	21.38	35.052	4347.6	20.560
273.15	19.77	33.13	3797	19.23
298.15	21.25	34.92	4308	20.47

ing, and integrating program on a high speed digital computer. The probable error of the functions thus obtained and presented in Table II is less than 0.1% above 100°K. No contribution for isotope mixing or for nuclear spin effects has been

TABLE III

THERMODYNAMIC PROPERTIES OF MONOHYDROGEN DIFLUORIDES AT 298.15°K.

	$LiHF_2$	$NaHF_2$	KHF_2	$RbHF_2$	$CsHF_2$	$TlHF_2$	NH_4HF_2	$AgHF_2$
C_p, cal./(deg. mole)	16.77[a]	17.93[a]	18.37[c]	18.97	20.86	21.25	25.50[d]	...
S^0, cal./(deg. mole)	16.97[a]	21.73[a]	24.92[c]	28.70	32.31	34.92	.....	30.5[f]
$-(F^0 - H_0^0)/T$, cal./(deg. mole)	7.49[a]	10.54[a]	12.66[c]	15.51	18.22	20.47	.....	...
$H^0 - H_0^0$, kcal./mole	2.826[a]	3.334[a]	3.655[c]	3.933	4.201	4.308	4.243[d]	...
ΔHd (dec.), kcal./mole	13.7[a]	16.4[b]	21.3[c]	21.8[b]	25.0[b]	....	.....	...
$-\Delta Hf$ (formation), kcal./mole	224.2[a]	216.6[b]	220.0[b]	217.3[b]	216.1[b]	....	191.4[e]	...

[a] Westrum and Burney.[19] [b] "Selected Values . . ."[24] [c] Westrum and Pitzer.[2] [d] Burney.[25] [e] Higgins.[26] [f] Interpolated, Fig. 1.

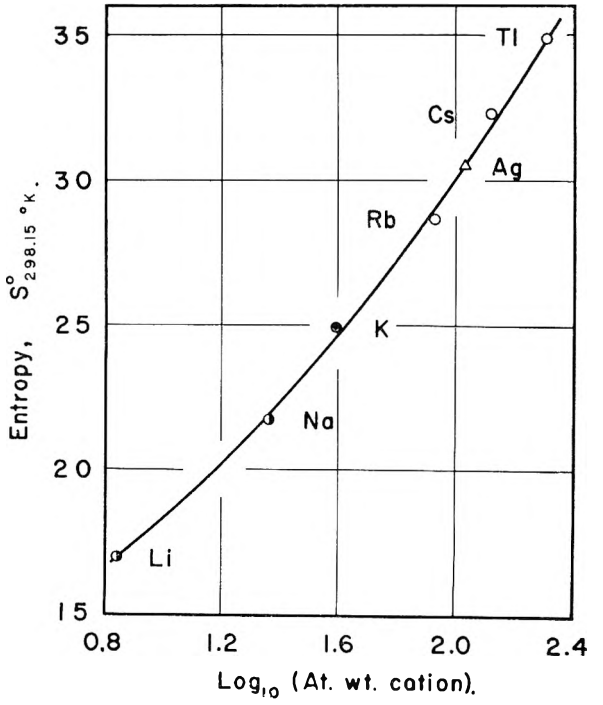

Fig. 1.—Correlating of standard molal entropies of monohydrogen difluorides: O, this research; ◑, Westrum and Burney[19]; ●, Westrum and Pitzer[2]; △, interpolated value for $AgHF_2$.

included. and the values given are thus suitable for use in chemical thermodynamic calculations.

An empirical attempt to correlate the entropies of these compounds with those of other monohydrogen difluorides[19] is presented in Fig. 1 by a plot of the entropy at 298.15°K. *versus* the decadic logarithm of the atomic weight of the cation.[23] Interpolation of the smooth curve drawn through the experimental values yields an $S^\circ_{298.15\,^\circ K.}$ equal to 30.5 e.u. for $AgHF_2$, the only other known monohydrogen difluoride for which low temperature heat capacity data are not available. This value is subject to the usual limitations of predictive attempts. In spite of the structural dissimilarity between KHF_2 and $NaHF_2$ and among other members of this series, the trend with temperature in the values of heat capacities, entropies and the Debye characteristic temperatures, shows a marked regularity. NH_4HF_2 does not fit the pattern of the other monohydrogen difluorides exactly, but the dissimilarity can be partially explained on the basis of the contribution of the added nitrogen–hydrogen frequencies.

A further summary of the known thermodynamic properties is presented in Table III. Heats of decomposition

$$MHF_2(c) \longrightarrow MF(c) + HF(g, ideal)$$

were usually taken from differences in the heats of formation of the substances involved.[24]

Further elucidation of the interesting properties of these compounds will be provided by calorimetric studies at higher temperatures.

Acknowledgment.—The coöperation of Dr. D. W. Osborne and the Chemistry Division of the Argonne National Laboratory in making liquid helium available for this study prior to the receipt of our cryostat, the digital computer checking of the smoothing and integration of the data by Bruce H. Justice, and the financial support of the Division of Research of the U. S. Atomic Energy Commission are gratefully acknowledged.

(23) W. M. Latimer, *J. Am. Chem. Soc.*, **73**, 1480 (1951).

(24) "Selected Values of Chemical Thermodynamic Properties," Circular 500, National Bureau of Standards, Washington, D. C., 1952.

(25) G. A. Burney, Doctoral Dissertation, University of Michigan, 1953.

(26) T. L. Higgins, Doctoral Dissertation, University of Michigan, 1955.

HEAT CAPACITIES AND CHEMICAL THERMODYNAMICS OF CERIUM(III) FLUORIDE AND OF CERIUM(IV) OXIDE FROM 5 TO 300°K.[1]

BY EDGAR F. WESTRUM, JR., AND ALVIN F. BEALE, JR.

Department of Chemistry, University of Michigan, Ann Arbor, Michigan

Received August 29, 1960

The heat capacities of CeF_3 and CeO_2 have been determined from 5 to 300°K. by adiabatic calorimetry. Both substances reveal normal sigmoid-shaped thermal behavior over this range. The entropy (S^0), enthalpy increment ($H^0 - H_0^0$), and free energy function ($[F^0 - H_0^0]/T$) at 298.15°K. are 27.54 cal./(deg. mole), 4237 cal./mole, and −13.33 cal./(deg. mole) for CeF_3 and 14.89 cal./(deg. mole), 2478 cal./mole, and −6.58 cal./(deg. mole) for CeO_2, respectively.

Introduction

Thermophysical data for magnetically concentrated lanthanide compounds are still relatively scarce. Since cerium(III) fluoride and cerium(IV) oxide are both important intermediate compounds in the production of cerium metal, their chemical thermodynamics are of some interest. Moreover, these compounds were intermediates in our preparation of cerium(IV) fluoride, a compound of special relevance in our attempt to develop a corresponding states theory for isostructural crystalline solids, and were studied because of their availability from the preparation of that compound.

Experimental

Preparation of Samples.—Both samples were prepared from reference standard ceric ammonium nitrate of certified 99.98% purity obtained from the G. Frederick Smith Chemical Company. Spectrochemical analysis of this material indicated slight traces of aluminum, iron and vanadium and the absences of chromium, cobalt, magnesium, nickel and osmium.

The hydroxide was precipitated from an aqueous solution of the nitrate using gaseous ammonia and was ignited in air to the dioxide at 1000° for 72 hours. The final product was very slightly yellowish in color.

The hydrated fluoride was prepared by the addition of excess aqueous HF (48%) to a solution of ceric ammonium nitrate. The precipitate was washed by decantation, filtered using a polyethylene Büchner funnel, dried at 110°, ignited in a platinum dish over a Meker burner, and finally heated at 500° in the presence of high purity hydrogen fluoride gas within a Monel reactor. Chemical analysis on the resulting trifluoride indicated 71.12% of cerium and 28.88% of fluorine (theoretical: 71.09 and 28.91%, respectively). Both materials were in the form of granular solids.

Cryostat and Calorimeter.—The Mark I calorimetric cryostat utilized in this work is similar to one already described by Westrum, Hatcher and Osborne[2] and uses liquid helium as the low temperature refrigerant. The adiabatic method of operation was employed. Calibrated resistors and standard cells and an autocalibrated White potentiometer were employed. Duration of the energy input was determined with a vacuum-jacketed tuning fork calibrated against signals from the National Bureau of Standards station WWV. The platinum resistance thermometer (laboratory designation A-3) was calibrated by the National Bureau of Standards over the range 10 to 705°K. A provisional temperature scale was employed at temperatures from 4 to 10°K. The goldplated calorimeter (laboratory designation W-5) was constructed of copper as described previously.[3] After the samples were weighed into the calorimeter and the cover sealed with Cerroseal solder (50% Sn + 50% In by weight), one atmosphere of purified helium (to provide thermal conduction) was added to the sample space through a small hole drilled in the top of a thin wall Monel stud. The hole was then soldered shut. Corrections were applied for the minute differences in the amount of helium employed with the samples and with the empty calorimeter as run to determine the heat capacity of the calorimeter–heater–thermometer assembly.

The masses of the calorimetric samples (*in vacuo*) were 163.2574 g. for CeF_3 and 244.2719 g. for CeO_2. The fraction of the total heat capacity contributed by the calorimeter–heater–thermometer assembly was 30 ± 5% for CeF_3. It represented 65% of the total heat capacity with CeO_2 at 10°, 40% at 50°, and decreased gradually to 28% at 300°K. A few milligrams (in weighed amount) of Lubriseal stopcock grease were used to provide thermal contact between heater, thermometer and calorimeter. Buoyancy corrections were made on the basis of crystallographic densities.

Results and Discussion

The experimental values of the heat capacity are listed in chronological sequence in Table I so that the approximate temperature increments employed in the measurements may be determined from the tabulated adjacent mean temperatures. These results are expressed in terms of the defined thermochemical calorie equal to 4.1840 abs. j. The ice point was taken as 273.15°K. Mole weights of 197.13 and 172.13 g. were used for CeF_3 and CeO_2, respectively. Neither substance behaves anomalously, but the heat capacities are of a normal sigmoid shape in line with expectation for crystalline salts. There is no evidence of magnetic or electronic contributions. Corrections have been applied to the heat capacity values in Table I for curvature (*i.e.*, for the finite temperature increments used for the measurements). The probable errors of the heat capacity values are considered to be less than 0.1% above 25°K., increasing gradually to 1% at 10°K. and to 5% below this temperature.

The entropy and enthalpy were computed by appropriate numerical quadrature of the heat capacity curve plotted against log T. Values for these functions below 5°K. were obtained by a Debye T^3 extrapolation and the assumption that S°_0 was zero. These functions, the free energy function obtained by difference, and smoothed heat capacities are represented in Table II. The evaluation of the heat capacities and integration of these functions were done independently with an IBM 704 digital computer program which provided a smooth curve through the experimental points. The thermodynamic functions are considered to have a probable error of less than 0.1% at temperatures above 100°K. The entropy and free energy functions have not been adjusted for nuclear spin and isotope mixing contributions and are hence practical values for use in chemical thermodynamic purposes. An additional digit beyond that warranted by the precision index of the data is retained

(1) This work was supported in part by the Michigan Memorial Phoenix Project of the University of Michigan and by the Division of Research of the U. S. Atomic Energy Commission.

(2) E. F. Westrum, Jr., J. B. Hatcher and D. W. Osborne, *J. Chem. Phys.* **21**, 419 (1953).

(3) E. F. Westrum, Jr., and G. A. Burney, THIS JOURNAL, **65**, 344 (1961).

TABLE I

HEAT CAPACITIES OF TWO CERIUM COMPOUNDS

T, °K.	C_p	T, °K.	C_p	T, °K.	C_p
Cerium trifluoride					
[CeF_3, mole weight = 197.13 g.; in cal./(deg. mole)]					
Series I		212.41	20.10	10.30	0.112
		221.99	20.40	11.40	.148
62.96	6.782	231.60	20.72	12.60	.205
67.81	7.550	241.08	21.02	13.82	.282
74.47	8.556	250.55	21.25	15.17	.381
82.00	9.687	260.06	21.50	16.70	.502
89.77	10.78	269.45	21.72	18.50	.648
97.82	11.81	278.95	21.94	20.52	.832
105.97	12.79	288.55	22.13	22.65	1.009
114.18	13.72	296.88	22.31	24.95	1.223
122.67	14.56	303.99	22.43	27.44	1.501
131.47	15.41			30.22	1.829
139.38	16.07	Series II		33.46	2.247
148.33	16.75			36.89	2.726
157.19	17.36	4.65	0.031	40.07	3.183
166.02	17.94	5.60	.022	44.19	3.802
174.91	18.45	6.75	.025	48.65	4 505
184.09	18.88	7.74	.036	53.65	5.296
193.54	19.34	8.56	.055	59.46	6.226
202.97	19.74	9.39	.078		
Cerium dioxide					
[CeO_2, mole weight = 172.13 g.; in cal./(deg. mole)]					
Series I		38.85	1.106	129.59	8.135
		42.85	1.395	138.75	8.731
4.81	0.009	47.02	1.717	147.95	9.302
6.14	.008	51.65	2.083	157.15	9.840
7.97	.011	56.66	2.485	166.34	10.34
9.40	.019	55.32	2.376	175.63	10.81
9.94	.023	60.96	2.849	185.01	11.25
10.70	.026	66.86	3.335	194.26	11.66
11.74	.032	73.12	3.847	203.32	12.03
13.15	.041	80.15	4.429	212.20	12.37
14.38	.053	88.36	5.100	220.94	12.68
15.66	.066	96.76	5.758	229.62	12.97
17.16	.088	121.27	7.569	238.51	13.26
19.00	.119			247.55	13.52
21.10	.171	Series II		256.58	13.77
23.26	.238			265.54	14.00
25.49	.323	84.27	4.767	274.58	14.23
27.84	.429	92.55	5.431	283.63	14.43
30.37	.561	101.64	6.130	292.64	14.63
32.82	.703	110.92	6.821	301.69	14.80
35.37	.865	120.31	7.497		

TABLE II

THERMODYNAMIC PROPERTIES OF TWO CERIUM COMPOUNDS

T, °K.	C_p, cal./(deg. mole)	S^0, cal./(deg. mole)	$H^0 - H^0_0$, cal./mole	$-(F^0 - H^0_0)/T$, cal./(deg. mole)
Cerium trifluoride (CeF_3, mole weight = 197.13 g.)				
10	0.094	0.032	0.236	0.008
15	0.362	0.113	1.289	0.027
20	0.782	0.272	4.103	0.067
25	1.128	0.490	9.055	0.131
30	1.805	0.768	16.635	0.213
35	2.455	1.094	27.252	0.315
40	3.172	1.468	41.297	0.435
45	3.933	1.885	59.05	0.573
50	4.720	2.340	80.67	0.727
60	6.315	3.342	135.84	1.078
70	7.886	4.434	206.88	1.478
80	9.391	5.586	293.33	1.919
90	10.80	6.774	394.37	2.392
100	12.09	7.980	508.9	2.891
110	13.26	9.188	635.8	3.408
120	14.31	10.388	773.7	3.940
130	15.26	11.572	921.7	4.482
140	16.11	12.734	1078.6	5.030
150	16.88	13.873	1243.7	5.581
160	17.56	14.984	1415.9	6.135
170	18.17	16.067	1594.6	6.687
180	18.70	17.121	1779.0	7.238
190	19.18	18.145	1968.5	7.785
200	19.61	19.140	2162.4	8.328
210	20.00	20.106	2360.5	8.866
220	20.36	21.05	2562.3	9.398
230	20.68	21.96	2767.5	9.925
240	20.97	22.84	2975.8	10.444
250	21.24	23.71	3186.8	10.958
260	21.50	24.54	3400.3	11.464
270	21.74	25.36	3616.8	11.964
280	21.96	26.15	3835.3	12.456
290	22.16	26.93	4055.8	12.942
300	22.37	27.68	4278.5	13.421
273.15	21.81	25.61	3685	12.12
298.15	22.34	27.54	4237	13.33
Cerium dioxide (CeO_2, mole weight = 172.13 g.)				
10	0.022	0.007	0.05	0.002
15	0.059	0.022	0.24	0.006
20	0.142	0.049	0.72	0.013
25	0.303	0.096	1.80	0.024
30	0.541	0.172	3.88	0.042
35	0.842	0.277	7.32	0.068
40	1.186	0.411	12.38	0.102
45	1.559	0.572	19.23	0.145
50	1.951	0.757	28.00	0.197
60	2.765	1.184	51.56	0.325
70	3.593	1.672	83.34	0.482
80	4.419	2.206	123.42	0.664
90	5.228	2.774	171.67	0.866
100	6.004	3.365	227.88	1.086
110	6.750	3.973	291.74	1.321
120	7.475	4.592	362.94	1.568
130	8.162	5.218	441.16	1.825
140	8.812	5.847	526.1	2.089
150	9.426	6.476	617.3	2.361
160	9.999	7.103	714.5	2.638
170	10.53	7.725	817.1	2.919
180	11.02	8.341	924.9	3.203
190	11.47	8.949	1037.4	3.489
200	11.90	9.549	1154.3	3.777
210	12.29	10.139	1275.2	4.066
220	12.65	10.719	1399.9	4.356
230	12.99	11.289	1528.1	4.645
240	13.30	11.848	1659.6	4.933
250	13.59	12.397	1794.1	5.221
260	13.86	12.936	1931.4	5.507

270	14.11	13.464	2071.3	5.792
280	14.35	13.981	2213.6	6.075
290	14.57	14.489	2358.3	6.357
300	14.77	14.986	2505.0	6.636
273.15	14.19	13.63	2116	5.88
298.15	14.73	14.89	2478	6.59

in some portions of the table for internal consistency and to permit interpolation.

Since these data were measured, the heat capacity of CeF_3 from 51 to 298°K. was reported by King and Christensen.[4] Their measurements deviate systematically by several tenths of a per cent. from the values of the present investigation above 150°K. Very nearly parallel deviations are noted also in $ZnFe_2O_4$ (for which see deviation plot)[5] and La_2O_3[6] with data from the Bureau of Mines Laboratory at Berkeley.[7] These differences between laboratories have not yet been resolved. In defense of the reliability of our data it is to be noted that they are in excellent agreement over this range with the heat capacity of the standard samples of benzoic acid prepared by the National Bureau of Standards for the Calorimetry Conference.[8] However, the entropy reported by King and Christensen[4] as 27.6 ± 0.2 e.u. at 298.15°K. is in good accord with the more precise value reported in this investigation.

Like ThO_2 and the actinide dioxides, CeO_2 has the cubic fluorite structure.[9] Despite the large change in gram atomic mass from cerium dioxide to diagmagnetic thorium dioxide (140.1 to 232.1 g.) and an increase in cell dimension (from 5.41 to 5.59 A.) the 298.15°K. entropies of these substances differ by only 0.7 e.u. (CeO_2 = 14.88 e.u. and ThO_2 = 15.59 e.u.).

Acknowledgment.—The authors thank Doris H. Terwilliger and Donald H. Payne for extensive participation in the measurements and Bruce H. Justice for digital computer evaluation of the thermodynamic functions. The partial support of the U. S. Atomic Energy Commission and of the Michigan Memorial Phoenix Project are gratefully acknowledged.

(4) E. G. King and A. U. Christensen, Bureau of Mines Report of Investigations 5510, U. S. Department of the Interior, Washington, D. C., 1959.

(5) E. F. Westrum, Jr., and D. M. Grimes, *Phys. and Chem. Solids*, **3**, 44 (1957).

(6) B. H. Justice and E. F. Westrum, Jr., unpublished data.

(7) For $ZnFe_2O_4$—E. G. King, THIS JOURNAL, **60**, 410 (1956); for La_2O_3—K. K. Kelley, personal communication.

(8) G. T. Furukawa, R. E. McCoskey and G. J. King, *J. Research Natl. Bur. Standards*, **47**, 256 (1951).

(9) W. H. Zachariasen, *Acta Cryst.*, **2**, 388 (1949).

IDEAL TWO-DIMENSIONAL SOLUTIONS. I. DETERGENT-PENETRATED MONOLAYERS

BY FREDERICK M. FOWKES

Shell Development Company, Emeryville, California and Martinez Research Laboratory, Shell Oil Company, Martinez, California

Received September 9, 1960

Insoluble monolayers on the surface of aqueous solutions act as solvents to dissolve penetrating detergent molecules. Often these are such ideal solutions that the Gibbs free energy of the detergent molecules in the mixed film decreases with dilution as $dG_2 = RT\ d\ln x_2\Phi_2$, where x_2 is the mole fraction and Φ_2, the activity coefficient, is near unity. The decrease in free energy results in an increase in the amount of penetration and in the magnitude of the film pressure (π) over the pressure π_2^0 observed in undiluted films of detergent. At equilibrium $\pi = \pi_2^0 - (kT/\sigma_2)\ln x_2\Phi_2$, where σ_2 is the partial molecular area of a detergent molecule. This equation is shown to predict equilibrium pressures and compositions of a wide variety of penetrated monolayers; all appear to form ideal solutions rather than stoichiometric complexes.

One of the most interesting types of film balance experiments is the penetration of water-soluble surface-active agents into an insoluble monolayer spread on an aqueous substrate.[1-4] The resulting film pressures are sometimes so large that many investigators have been led to postulate specific interactions between the penetrating and the insoluble components. However, we can now explain these results quantitatively by considering the penetrated monolayer to be an ideal two-dimensional solution in which the activity of the water-soluble species has been reduced by dilution with the insoluble species. The consequence is an increased tendency for the water-soluble species to enter the monolayer which then expands at constant pressure. If the area of the insoluble film is kept constant the system behaves like an osometer, for the pressure increases to an equilibrium value which can be calculated from the composition.

In a number of investigations the insoluble monolayer has been a protein or other polymeric material. These systems are not discussed in this paper since the free energy change on dilution of polymers is not conveniently expressed by the equations for ideal solutions. A later publication will deal with this subject.

The general approach is to assume that the surface monolayer is a separate phase with a composition different from that of the bulk phase and subjected to the two-dimensional film pressure, while the water-soluble surface active species in the monolayer is in equilibrium with the substrate. This approach has been used successfully for binary solutions by a number of investigators[5-23] but has

(1) E. D. Goddard and J. H. Schulman, *J. Colloid Sci.*, **8**, 309 (1953).

(2) W. D. Harkins, "Physical Chemistry of Surface Films," Reinhold Publ. Corp., New York, N. Y., 1952.

(3) B. A. Pethica, *Trans. Faraday Soc.*, **51**, 1402 (1955).

(4) D. G. Dervichian, in "Surface Phenomena in Biology and Chemistry," by J. F. Danielli, K. G. A. Pankhurst and A. C. Riddiford, Pergamon Press, New York, N. Y., 1958.

never been extended to explain penetration experiments. A step in this direction was made by Crisp[24] who related film pressures and compositions of mixed insoluble films, and by Lisbeth Ter. Minassian-Saraga and Prigogine[25] who calculated demixing conditions for two-phase monolayers as a function of film pressure. The author has previously demonstrated that the film pressures and compositions of monolayers formed on solutions of two water-soluble surface-active agents can be calculated in the manner described.[26] A second paper[27] describes the use of this method to calculate the area per molecule and film pressure of gaseous monolayers of insoluble surface-active agents and of monolayers of charged surface-active agents in which the water molecules of the surface film play a major role.

Theory and Notation.—Consider the molecules of water-soluble component 2 which have penetrated into the insoluble monolayer of component 1. The Gibbs free energy of these is a function of the mole fraction in the monolayer (x_2), and the film pressure (π).

$$dG_2 = \left(\frac{\partial G_2}{\partial x_2}\right)_\pi dx_2 + \left(\frac{\partial G_2}{\partial \pi}\right)_{x_2} d\pi \qquad (1)$$

where

$$\left(\frac{\partial G_2}{\partial x_2}\right)_\pi dx_2 = RT\, d \ln x_2\Phi_2 \qquad (2)$$

where Φ_2 is the film-pressure-independent activity coefficient in the monolayer, and

$$\left(\frac{\partial G_2}{\partial \pi}\right)_{x_2} d\pi = N\sigma_2\, d\pi \qquad (3)$$

where σ_2 is the partial molecular area of component 2 in the monolayer. If component 2 is also in equilibrium with the bulk phase

$$dG_2 \text{ (monolayer)} = dG_2 \text{ (substrate)}, \text{ or}$$
$$\sigma_2 d\pi + kT\, d \ln x_2\Phi_2 = kT\, d \ln c_2 f_2 \qquad (4)$$

where c_2 is the concentration and f_2 the activity coefficient in the substrate. Since dilute solutions of detergents are generally used, f_2 is considered constant, and since it is very often found that monolayer solutions are ideal[7] Φ_2 is considered to be unity unless the two components of the monolayer are very different in structure. This assumption is proved acceptable by agreement with experimental data as shown later. Consequently, for most systems considered we may use

$$\sigma_2 d\pi = -kT\, d \ln x_2/c_2 \qquad (5)$$

In order to use this equation, we must define standard states

$$(\pi_2^0,\ \sigma_2^0,\ x_2^0\ c_2^0)$$

and integrate

$$\int_{\pi_2^0}^{\pi} \sigma_2 d\pi = -kT \ln x_2/x_2^0 + kT \ln c_2/c_2^0 \qquad (6)$$

We may use also an average σ_2 where

$$\bar{\sigma}_2 = \frac{\int_{\pi_2^0}^{\pi} \sigma_2\, d\pi}{\pi - \pi_2^0}$$

so that

$$\pi - \pi_2^0 = \frac{-kT \ln x_2/x_2^0}{\bar{\sigma}_2} - \frac{kT \ln c_2/c_2^0}{\bar{\sigma}_2} \qquad (7)$$

"Water-continuous" *vs.* "Surfactant Continuous" Monolayers.—As has been discussed by Ter Minassian-Saraga and Prigogine,[25] monolayers may act as solutions in water at low pressures and upon reaching saturation a second phase appears in which the hydrocarbon chains are in contact and in which very little water is soluble. We may differentiate between the two types of monolayers with the terms "water-continuous" and "surfactant continuous." In penetration experiments the insoluble monolayers are nearly always surfactant-continuous; in these the free energy depends on the mole fraction of the tail groups of penetrant 2 in the hydrocarbon layer of the monolayer. On the other hand, the penetrants are usually ionic and consequently (in reference films of pure component 2) have hydrocarbon contact only at higher film pressures (over 10 or 15 dynes/cm., for example). At low pressures reference films of pure ionic penetrants are "water-continuous" and the free energy is a function of the mole fraction of the penetrant "heads" to the total number of molecules in the "heads" layer. This involves the water molecules in the surface layer which dilute the head groups. The mole fraction of water molecules (component ω) in the head layer is given by[27]

$$kT \ln x_\omega = kT \ln (1 - x_2) = -\pi\sigma_\omega \qquad (8)$$

where σ_ω is 10 Å.^{2}. Thus at 10 dynes/cm., x_ω = 0.78 and x_2 (in the "heads" layer) = 0.22. As will be demonstrated, x_2 in the heads layer determines the pressure only in "water-continuous" films and x_2 for the hydrocarbon layer determines the pressure in "surfactant-continuous" films. Only soluble surfactants reduce the activity of water in the "water-continuous" films. Soluble films under high pressures have pressure–area relations calculable by either procedure.

(5) J. A. V. Butler, *Proc. Roy. Soc.* (*London*), **A135**, 348 (1932).
(6) J. E. Verschaffelt, *Bull. Classe Sci. Acad. Roy. Belg.*, **22**, 373, 390, 402 (1936).
(7) A. Schuchowitzky, *Acta Physicochim. U.S.S.R.*, **19**, 176, 508 (1944).
(8) J. W. Belton and M. G. Evans, *Trans. Faraday Soc.*, **41**, 1 (1945).
(9) E. A. Guggenheim, *ibid.*, **41**, 150 (1945).
(10) E. A. Guggenheim, "Surface Chemistry," Interscience Publishers, Inc., New York, N. Y., 1949, p. 11.
(11) R. Defay and I. Prigogine *Bull. Classe Sci. Acad. Roy. Belg.*, **32**, 36, 176, 335, 400 (1946).
(12) R. Defay and I. Prigogine, *J. chim. phys.*, **43**, 217 (1946).
(13) I. Prigogine and R. Defay, *ibid.*, **46**, 367 (1949).
(14) R. Defay, *ibid.*, **46**, 375 (1949).
(15) I. Prigogine and R. Defay, *Bull. soc. chim. Belg.*, **59**, 255 (1950).
(16) I. Prigogine, *J. chim. phys.*, **47**, 33 (1950).
(17) I. Prigogine and L. Sarolea, *ibid.*, **47**, 807 (1950).
(18) J. Marechal, *Trans. Faraday Soc.*, **48**, 601 (1952).
(19) I. Prigogine and J. Marechal, *J. Colloid Sci.*, **7**, 122 (1952).
(20) S. Ono, *Memoirs Faculty Eng. Kyushu Univ.*, **10**, 195 (1947).
(21) S. Ono, *ibid.*, **12**, 1 (1950).
(22) T. Murakami, S. Ono, M. Tamura and M. Kurata, *J. Phys. Soc.* (*Japan*), **6**, 309 (1951).
(23) J. H. Hildebrand and R. L. Scott, "The Solubility of Nonelectrolytes," 3rd ed., Reinhold Publ. Corp., New York, N. Y., 1950, pp. 406–415.
(24) D. J. Crisp, "Surface Chemistry," Interscience Publishers, Inc., New York, N. Y., 1949, pp. 17–22, 23–25.
(25) Lisbeth Ter Minassian-Saraga and I. Prigogine, *Mem des services chim. de l'etat*, **38**, 109 (1953).
(26) W. M. Sawyer and F. M. Fowkes, THIS JOURNAL, **62**, 159 (1958).
(27) F. M. Fowkes, to be published.

Requirements for Penetration Experiments.— It has been an aim of this paper to find out whether the two-dimensional solutions of penetrated monolayers are ideal monolayers; that is, whether activity coefficients Φ_2 differ appreciably from unity. The necessary conditions for testing these equations are not met in many of the penetration experiments in the literature since the phenomenon was not understood.

The mole fraction of penetrant x_2 in a mixed monolayer can be determined from experimental data in several ways. Experiments are generally conducted so that the surface concentration of insoluble component 1 is known, so a measure of component 2 is needed. This can be done directly by radiotracer methods,[28] by surface potential measurements where there is reason to believe the two potentials are additive,[24] or by knowledge of the pressure–area isotherms of both components and their mixtures. If penetration experiments are made over a range of concentrations of component (2), σ_2 in the monolayer may be determined by Gibbs' absorption equation

$$\sigma_2 = kT \left(\frac{\partial \ln c_2}{\partial \pi}\right)_{x_2} \qquad (9)$$

If A_1 is the total area of surface per molecule of component 1, and σ_1 and σ_2 are the partial molecular areas, x_2 has been calculated by

$$x_2 = \frac{(A_1 - \sigma_1)}{(A_1 - \sigma_1 + \sigma_2)} \qquad (10)$$

If the insoluble monolayer has a low compressibility and is under pressure π_1^0 of several dynes/cm.,[1,3] the area available to component 2 at higher pressures may be a small difference between large numbers and be difficult to estimate accurately. Furthermore the value of x_2 then is very sensitive to pressure so that equation 9 is not applicable. In fact, as A-σ_1 is made smaller, $d\pi/d \ln c_2$ decreases rapidly.[3] Consequently, it is better to start penetration experiments at larger values of A_1.

In order that equations 5, 6 or 9 may be used accurately, ionic strengths should be constant so that the activity coefficient in the bulk phase (f_2) is constant. Furthermore, since this paper is concerned only with equilibrium measurements, only those experiments in which there was sufficient time for equilibration can be used.

While experiments made at constant pressure are of interest in regard to the kinetics of penetration, thermodynamic data can only be determined by measurements at constant area of the insoluble film.

The following sections describe certain penetration experiments in the literature which conform to the above requirements.

Penetration of Cetyl Sulfate into Cetyl Alcohol.—This combination of penetrant and film has been studied by several investigators. The experimental data of Harkins, Gordon and Copeland[2] are chosen for analysis because of the wide range in values of both the area per insoluble molecule (A_1) and the concentration of the detergent solution (c_2), despite the lack of salt to provide constant ionic strengths. In this system σ_1 is 20 Å.^{2} and σ_2^0 (in pure detergent films) is 39 Å.^{2} over a wide range of pressures. Using these values in equations 7 and 10, the π–A_1 relationships for ideal surface solutions have been calculated and are shown as solid lines in Fig. 1. Excellent agreement with the experimental results are obtained for values of A_1 greater than 40 Å.^{2}, showing that in this region the mixed monolayer is an ideal solution of the "surfactant-continuous" type. At values of A_1 between 20 and 40 Å.^{2} where the surface solution is concentrated in cetyl alcohol, film pressures rise above the values calculated for σ_2 = 39 Å.^{2} and indicate that in this region the cetyl sulfate chains are compressed to 25 Å.^{2} at all values of A_1 less than 35 Å.^{2}. This is a well known phenomenon which has been illustrated by a variety of experimental techniques[2,4] and amounts to a condensation of an expanded monolayer by adding an excess of a condensed monolayer. It should be noted that, as indicated by the dashed lines of Fig. 1, the surface solutions remain ideal solutions with the cetyl sulfates condensed to a molecular area of 25 Å.^{2}. This agrees very well with the conclusions of Dervichian[4] for the nature of the "interaction" of trimyristic and myristic acid which is a purely physical change of state despite the fact that this change of state starts at some stoichiometric ratio.

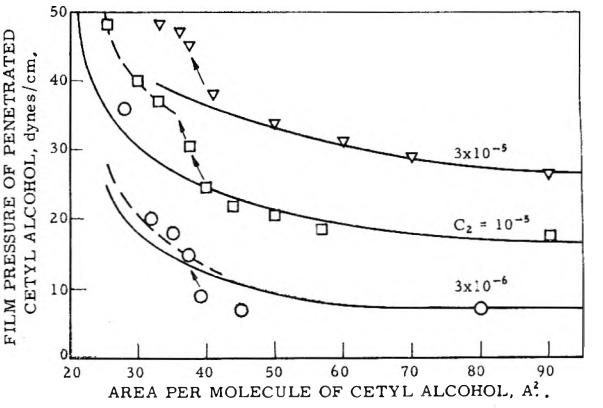

Fig. 1.—Penetration of cetyl alcohol monolayers at 25° by sodium cetyl sulfate. Data of Harkins, Gordon and Copeland. Arrows = pressure rise resulting from decrease of σ_2 from 39 to 25 Å.^{2}; solid lines = predicted film pressures for ideal surface solutions with σ_1 = 20 Å.^{2}, σ_2 = 39 Å.^{2}; dashed lines = σ_2 = 25 Å.^{2}

In Fig. 1 the curve for $c_2 = 10^{-5}$ mole liter was calculated with a π_1^0 of 12.5 dynes/cm. and the other two curves were calculated from the same value by using equation 7 and assuming no change in the activity coefficient f_2.

Penetration of Lauryl Sulfate into Cholesterol.— Cholesterol forms a condensed monolayer of low compressibility even at low film pressures.[3] At 20° the film pressure is 24 dynes/cm. at σ_1 = 37 Å.^{2} and is nearly zero at σ_1 = 38 Å.^{2}. Consequently, unusually large pressure changes occur when a cholesterol film at 38 Å.^{2} per molecule is penetrated by detergents and for this reason cholesterol films are favorite subjects for penetration experiments.[1,3,4] The studies of Pethica[3] with sodium lauryl sulfate are chosen for analysis because he used salt to provide constant ionic strength over a range of concentrations and because he has some data where A_1 is

(28) A. Wilson, M. B. Epstein and J. Ross, *J. Colloid Sci.*, **12**, 345 (1957).

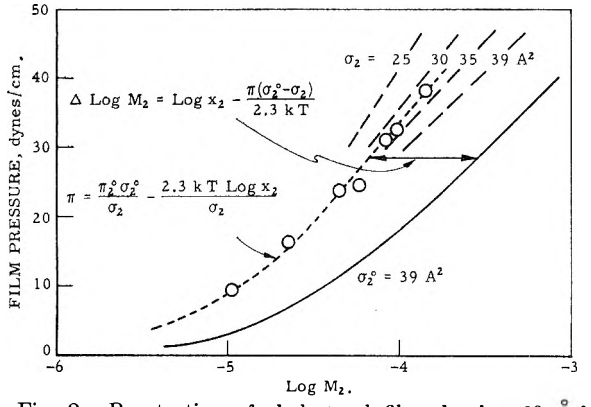

Fig. 2.—Penetration of cholesterol films having 60 Å.² molecule substrate of 0.145 *M* NaCl (OH 7.0) at 20° by sodium dodecyl sulfate of various concentrations (M_2). Solid line = film pressure of detergent without cholesterol monolayer.

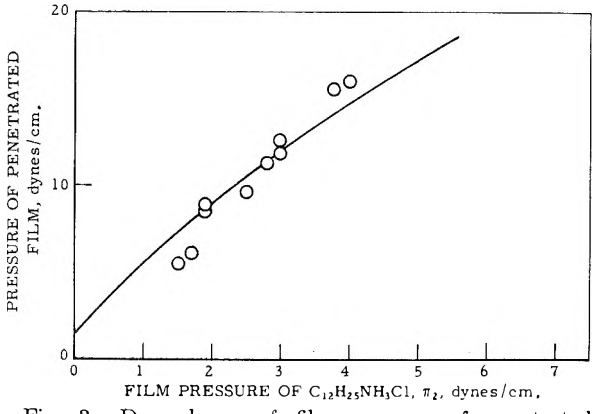

Fig. 3.—Dependency of film pressure of penetrated myristic acid on film pressure π_2 of dodecylamine solutions. Substrate is 0.01 *N* HCl at 20°. Solid lines = pressures to be expected for ideal solutions as calculated by equation 12; circles = Pethica's experimental points.

much larger than σ_1 so that $A_1-\sigma_1$ may be accurately estimated. Moreover, he has provided good data for determining $(\partial\pi/\partial \ln c_2)_{x_2}$.

All mixed films with cholesterol are "surfactant-continuous" and at pressures over 20 dynes/cm. homogeneous films of sodium lauryl sulfate may be so treated; consequently, the film pressures should be a function of the mole fraction of detergent "tails" among the cholesterol "tails."

Figure 2 shows some of Pethica's data on penetration of lauryl sulfate ions into cholesterol films where A_1 = 60 Å.²/ molecule of cholesterol. The π *vs.* log c_2 relations were calculated with equation 6 using the assumption that the surface films are ideal solutions (Φ_2 = 1) and that the activity coefficient in the bulk solution (f_2) is constant. Here the integral

$$\int_{\pi_2^0}^{\pi} \sigma_2\, d\pi = \pi\sigma_2 - \pi_2^0\sigma_2^0$$

(where σ_2 is pressure-independent in the region integrated)

Since we know from previous work on such systems that cholesterol tends to condense expanded films at high ratios of cholesterol to detergent,[4] the calculations show the π *vs.* log c_2 relations to be expected for σ_2 = 39, 35, 30 and 25 A.². Since the condensation is generally a function of mole fraction[4] and in these experiments the mole fraction is essentially constant when A_1 is constant, we would expect that σ_2 would be constant over an appreciable range of film pressures. The experimental results are seen to show that the lauryl sulfate ion has a molecular area (σ_2) of 33 A.² in the mixed films, and a mole fraction (x_2) of 0.4 at A_1 = 60 A.². But more important is the finding that these mixed films act as ideal solutions. This shows that the much discussed "stoichiometric complexes" of detergents with cholesterol[4] are not really combinations that act osmotically as one molecule but physical mixtures in which the more condensed substance reduces the molecular area of the more expanded substance. This condensing effect often appears negligible at mole ratios of condensed phase (x_1) less than 0.5, and increases as x_1 becomes larger. The fact that the condensing effect often starts at x_1 = 0.5 (a mole ratio of 1:1) appears indisputable, but we see this is not evidence of formation of an osmotically significant complex.

Penetration of Dodecylammonium Chloride into Myristic Acid Monolayers.—The previously mentioned publication of Pethica[3] includes penetration experiments of dodecylammonium chloride into myristic acid monolayers with rather dilute solutions of this detergent. It is interesting to analyze this system because of two differences from the usual experiments: the insoluble monolayer is in an expanded state of high compressibility and the detergent is at such concentrations that the absorbed film in the absence of the myristic acid is an entirely "water-continuous" monolayer. For these reasons π-π^0 is not just a function of the mole fraction x_2 of detergent in the film.

In this problem the penetrating dodecylammonium ion has a hydrocarbon group so like the myristic acid (n-$C_{12}H_{25}$- *vs.* n-$C_{13}H_{27}$-) that in dilute films of the detergent these molecules may be considered to have the same molecular area ($\sigma_2 = \sigma_1$). These are compressible films in which the area per molecule can be expressed by an analytical function given by Langmuir[29]

$$\sigma_1 = 16.5 \times kT(\pi + 11.2)$$

As the detergent molecules penetrate into the myristic acid film (with A_1 = 48 Å.², π_1^0 = 1.5 dynes/cm.) and the pressure rises a certain amount of work is done to compress them to the film pressure π. This work is an increase in free energy of component 2 given by

$$\int_0^{\pi} \sigma_2\, d\pi = 16.5\pi + kT \ln\left(\frac{\pi + 11.2}{11.2}\right)$$

This equation may be used with equation 6 to calculate the pressure rise in the penetrated films. However, it is desired to relate the final pressure (π) to the initial pressure (π_2) at each concentration. This is done with the adsorption equation of Gibbs which may be integrated as

$$kT \ln c_2/c_2^0 = \int_{\pi_2^0}^{\pi_2} A_2\, d\pi_2 \qquad (11)$$

for detergent films on dilute aqueous solutions. The result is

(29) I. Langmuir, *J. Chem. Phys.*, **1**, 756 (1933).

$$\int_{\pi_2^0}^{\pi} A_2 \, d\pi_2 = \int_0^{\pi} a_2 \, d\pi + kT \ln x_2/x_2^0 \quad (12)$$

The definition of π_2^0 in this system is not obvious because the reference film is water-continuous." It has been done here by equating π_2^0 to the π_2 for the concentration c_2^0 which causes the right side of equation 12 to be zero. For as π increases the first term increases from zero to a positive value and the second increases from negative infinity toward zero, and for the case in point these are equal at $\pi = 12$ dynes/cm. The value of π_2 leading to $\pi = 12$ is then π_2. Since at this point (and this point only) in the penetrated films the free energy of the detergent tails are unchanged due to the presence of the myristic acid, π_2 must be the pressure in a pure detergent film of equal area per detergent molecule (A_2). In this problem $A_2 = 164$ Å.^{2}, and $\pi_2^0 = 3.0$ dynes/cm. With π_2^0 established, equation 12 was then used to calculate the solid line of Fig. 3, which is shown to fit the experimental data quite well.

This shows that dodecylammonium chloride forms ideal surface solutions in myristic acid monolayers (on 0.02 *N* HCl substrates) without any tendency to form complexes.

THE HYDROTHERMAL CRYSTALLIZATION OF YTTRIUM IRON GARNET AND YTTRIUM GALLIUM GARNET AND A PART OF THE CRYSTALLIZATION DIAGRAM Y_2O_3–Fe_2O_3–H_2O–Na_2CO_3

BY R. A. LAUDISE, J. H. CROCKET AND A. A. BALLMAN

Bell Telephone Laboratories, Incorporated, Murray Hill, New Jersey

Received October 15, 1960

Yttrium iron garnet, $Y_3Fe_2(FeO_4)_3$, and yttrium gallium garnet, $Y_3Ga_2(GaO_4)_3$, have been crystallized under hydrothermal conditions. Yttrium gallium garnet was observed to transport in a temperature gradient and crystallized on a seed in 1 *M* Na_2CO_3 at 1500 atm. and 360°, when the starting materials were Ga_2O_3 and Y_2O_3. The system Fe_2O_3–Y_2O_3–H_2O–Na_2CO_3 was investigated and yttrium iron garnet was found to form in optimum yields in from one to six days between 685 and 765° at 1330 atm. in approximately 3 *M* Na_2CO_3. Slow decompositions of both garnet and Fe_2O_3 to Fe_3O_4 were observed to decrease the yields at longer times and a mechanism for this effect is proposed. Yttrium iron garnet was found to be congruently saturating and parts of the crystallization diagram were determined. Garnets as large as 2 mm. were prepared.

Introduction

A series of magnetic compounds with a garnet structure has recently been discovered[1,2] and a method for the growth of single crystals of $R_3Fe_2(FeO_4)_3$ where R is Y, Sm, Er or Gd has been published.[3] These crystals were grown from molten PbO and from PbO–PbF_2 mixtures where yttrium iron garnet (Y.I.G.) is incongruently saturating. Parts of the Fe_2O_3–$YFeO_3$ phase diagram where yttrium iron garnet has been found to be incongruently melting and the PbO–Y_2O_3–Fe_2O_3 phase diagram were determined.[3] Since crystals free of molten salt inclusions and of Fe^{++} grown at low temperature might present some advantages, hydrothermal crystallization suggested itself as a new means of preparation for these magnetic garnets.

Experimental

Attempts to form yttrium gallium garnet, $Y_3Ga_2(GaO_4)_3$ (Y.G.G.), according to the reaction

$$3Y_2O_3 + 5Ga_2O_3 = 2Y_3Ga_2(GaO_4)_3 \quad (1)$$

from reagent purity Y_2O_3 and Ga_2O_3 were made directly in steel vessels of the sort described by Walker and Buehler.[4] Identification of phases was made by means of microscopic examination and X-ray powder pictures. Chromium radiation was used with a camera in which the sample holder was a wedge. This arrangement was found better capable of detecting small quantities of one phase in the presence of another than the conventional capillary or filamentary sample holder.

Preliminary experiments showed a need for the careful determination of parts of several hydrothermal systems in which yttrium iron garnet could be formed by the reaction

$$3Y_2O_3 + 5Fe_2O_3 = 2Y_3Fe_2(FeO_4)_3 \quad (2)$$

in a hydrothermal vessel which did not present metallic iron or any other reducing agents to the solution. Weighed quantities of the component oxides, ground and mixed as nearly as possible to a uniform particle size in an agate mortar, were placed in gold capsules one end of which had been previously welded on a microarc welder. The capsule dimensions were 2.50 inch length × 0.160 inch inside diameter × 0.005 inch wall thickness. The capsule was filled by means of a microburet to a predetermined fraction of its free volume with the appropriate solvent. The per cent. of fill was calculated from Kennedy's[5] *p–v–t* data for pure water since the pressures in a hydrothermal solution of the sort studied in this work would not be expected to be greatly different. The capsules were placed in individual 0.25 inch internal diameter × 10 inch internal length cold-seat-cone-closure vessels.[6] The vessels were connected to Bourdon gauges and an air driven intensifier,[7] heated by kanthal wound tube furnaces and so arranged that they could be individually brought to any predetermined temperature from 100 to 800° and any pressure up to pressures in excess of 2000 atm. The pressure transmitting fluid outside the capsules was water. Provision was made for rapid quenching by means of an air blast at the conclusion of a run. Reliability in the pressures reported is probably no better than ±2%, and in the temperature no better than ±3°.

Parts of the system Ga_2O_3–Y_2O_3–H_2O–Na_2CO_3 were investigated in an effort to form the gallium garnet, Y_3Ga_2-

(1) F. Bertaut and F. Forrat, *Compt. rend. Acad. Sci. (Paris)*, **242**, 382 (1956).

(2) S. Geller and M. A. Gilleo, *Acta Cryst.*, **10**, 239 (1957).

(3) J. W. Nielsen and E. F. Dearborn, *J. Phys. Chem. Solids*, **5**, [3] 202 (1958).

(4) A. C. Walker and E. Buehler, *Sci. Monthly*, **69**, 148 (1949).

(5) G. C. Kennedy, *Am. J. Sci.*, **248** 540 (1950).

(6) Obtained from Tempress, Inc., State College, Pa.

(7) Manufactured by Sprague Engineering Corp., P. O. Box 121, Gardena, Calif.

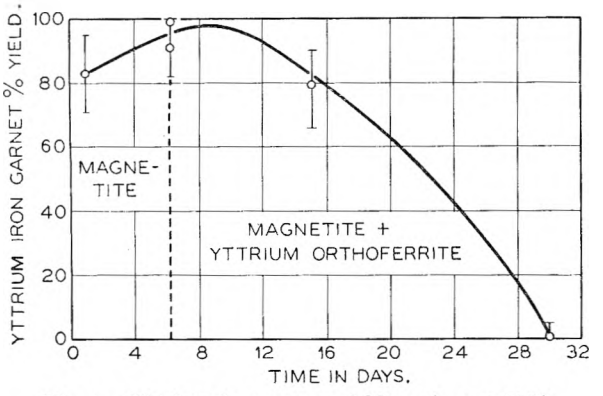

Fig. 1.—Yttrium iron garnet yield *vs.* time at 725°.

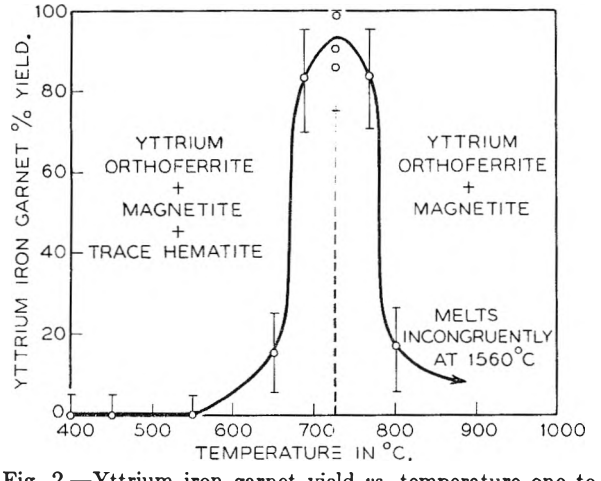

Fig. 2.—Yttrium iron garnet yield *vs.* temperature one to six days.

$(GaO_4)_3$. In all cases the ratio Ga_2O_3/Y_2O_3 was 5/3 (the stoichiometry of the garnet). Temperatures from 360 to 500° were investigated; sodium carbonate concentrations varied between 1.0 and 5.0 *M* and pressure between 1000 and 3000 atm. In all cases the gallium garnet was the principal phase formed. Time of runs varied between one day and several weeks. The only contaminating phase formed, which was present in very small quantities in a few runs, was gallium oxyhydroxide, GaOOH.

The gallium garnet was observed to transport in a temperature gradient and deposit on a seed as evidenced by the formation of growth steps on a smoothly polished seed easily visible under 50× magnification. Conditions where growth was observed were: crystallization temperature 360°, temperature difference (Δt) between dissolving and growth zone 40°, nutrient Ga_2O_3/Y_2O_3 ratio 5/3, pressure about 1500 atm. and solvent 1 *M* Na_2CO_3.

In gold capsules, parts of the system Fe_2O_3–Y_2O_3–H_2O–Na_2CO_3 were investigated. More than one hundred runs were made so that only data finally shown to be pertinent to the observed transitions will be mentioned here. Figure 1 summarizes certain runs important to the deduction of equilibrium time at a temperature of 725°. The mole ratio Fe_2O_3/Y_2O_3 was 5/3. Unless otherwise mentioned, the weight fraction of Na_2CO_3 was held constant at 0.228 which in most cases corresponded to a solution about 3.1 *M* in Na_2CO_3.

The height of the bars on the points of Figs. 1 and 2 gives some indication of the precision in the estimation of the abundance of phases. Phase abundances were estimated visually from the intensity of the X-ray powder diagrams. Standards of varying percentages of magnetite and yttrium iron garnet were used for comparison where appropriate. It was found that as little as 5% magnetite could be detected in the presence of garnet. The runs were made in gold tubes at a pressure of 1330 atm. As can be seen six days or a time slightly greater is sufficient for the complete conversion to garnet and the garnet yield varies little between one and six days. The only phase detected in addition to garnet up to six days was magnetite. At 30 and 15 days the products were magnetite and yttrium orthoferrite, $YFeO_3$. Crystalline flux grown garnet decomposed similarly in 30 days. A precession picture of a representative single crystal of the magnetite confirmed that it was not γ-Fe_2O_3 whose X-ray powder pattern is nearly identical to that of magnetite.

Figure 2 shows the dependence of garnet yield on temperature for reaction times of one to six days. The conditions of the runs of Fig. 2 were generally similar to those of Fig. 1. As can be seen the optimum yield of garnet occurred near 725°. The phases in addition to the garnet which were found below 725° were magnetite, yttrium orthoferrite and hematite. Above 725° magnetite and yttrium orthoferrite were found to be the coexisting phases. In general, the yield of magnetite increased with increasing temperature.

The effect of variation in the Fe_2O_3/Y_2O_3 ratio was studied under the following conditions: temperature, 725°; pressure, 1330 atm.; $N_{Na_2CO_3}$ 0.228; time of run, one to six days, and $N_{Fe_2O_3} + N_{Y_2O_3}$ = constant = 0.128. Under these conditions small quantities of magnetite were observed to form at all Fe_2O_3/Y_2O_3 ratios. The garnet stability region was extremely narrow, when the Fe_2O_3/Y_2O_3 ratio was 5/3 garnet and magnetite formed; however, when the ratio was increased by two mole per cent. hematite, garnet and magnetite formed and when the ratio was decreased by two mole per cent. yttrium orthoferrite, garnet and magnetite formed.

Yttrium iron garnet crystals as large as 1 to 2.5 mm. have been prepared when the ratio was 5/3. The habit is similar to that sometimes observed of molten PbO grown crystals[3] and in natural garnets, that is dodecahedral showing (110) faces. Lattice constants agreed with those measured on PbO grown and ceramic garnets. The crystals were ordinarily black but became green when ground to a fine powder and were magnetic with a Curie temperature in the neighborhood of 272° in agreement with the properties of PbO grown crystals. No inclusions of other phases were visible upon microscopic examination of ground spheres. Because of their color $YFeO_3$ and Fe_2O_3 would be especially easy to detect in such an examination but magnetite might escape notice.

Discussion

Yttrium gallium garnet was found to be congruently saturating under all conditions investigated. The small amounts of GaOOH found in several runs probably formed when the vessels were cooled since Hill, Roy and Osborn[8] have shown that in the system Ga_2O_3–H_2O GaOOH is stable only below about 300° from 1 to 2000 atm. The pressure–temperature dependence of a similar equilibrium Al_2O_3–AlOOH in the system Al_2O_3–H_2O has been shown to be little influenced by the presence of low concentrations of Na_2CO_3.[9] Yttrium gallium garnet has been shown to dissolve, transport and recrystallize on a seed crystal under conditions where it is congruently saturating.

At 1560°, Y.I.G. melts incongruently into orthoferrite and an Fe_2O_3 rich liquid.[3] Eugster[10] has discussed the magnetite–hematite equilibrium and shown that in the absence of water hematite will be stable at ambient pressure over the temperature range of this work. However, in the presence of water under hydrothermal conditions the dissocia-

$$H_2O \rightleftharpoons H_2 + 1/2O_2 \qquad (3)$$

(8) V. G. Hill, R. Roy and E. F. Osborn, *J. Am. Ceram. Soc.*, **35**, [6] 136 (1952).

(9) R. A. Laudise and A. A. Ballman, *J. Am. Chem. Soc.*, **80**, 2655 (1958).

(10) H. P. Eugster. "Researches in Geochemistry," edited by P. H. Abelson, John Wiley and Sons, New York, N. Y., 1959, p. 397.

tion must be considered. Wagman, *et al.*[11] have tabulated K_p for reaction 3 at a total pressure of one atmosphere for several temperatures, Eugster[10] has interpolated values from these results, and Baker[12] has calculated the pressure dependence of the dissociation. These data show that in contact with an excess of pure water at the pressure of our experiments hematite would be the stable solid phase at temperature below 1050°.

Yet, as Fig. 1 shows in the system Y_2O_3–Fe_2O_3–H_2O–Na_2CO_3, slow decomposition of both garnet and hematite to magnetite does occur. The data of Fig. 1 were obtained in gold tubes, since the diffusivity of hydrogen in platinum could result in the gradual loss of hydrogen formed in the capsule or the gradual incursion of hydrogen into the capsule from corrosion reactions with the wall of the vessel. The weight fraction of solids was low, so that the system was probably not buffered with respect to solid. Four runs were made at 30 days to decrease the possibility that improper welds in the gold could have allowed hydrogen to enter. Identical results were obtained in all these runs and it was shown that flux grown crystalline garnet decomposed in the same way. Preliminary runs were made in gold tubes in the systems Fe_2O_3–Fe_3O_4–H_2O, Fe_2O_3–Fe_3O_4–H_2O–Na_2CO_3 and Fe_2O_3–Fe_3O_4–H_2O–NaOH at 400° and 1330 atm. The duration of the runs was 30 days and 3 *M* carbonate and hydroxide solutions were used. In all three systems when the starting material was either Fe_2O_3 or Fe_3O_4, the products were mixtures of Fe_2O_3 and Fe_3O_4. The yield of hematite was somewhat higher when hematite was the starting material and was perhaps higher in the absence of base.

The preliminary data on the magnetite–hematite equilibrium discussed in the preceding paragraph suggest that both the magnetite–hematite equilibrium and equation 3 may be *p*H dependent or that there may be a measurable diffusivity of H_2 through gold at the conditions of these experiments. It should be pointed out that the equilibrium oxygen pressure over garnet might be markedly different from that over hematite.

On first sight the extremely long times necessary to achieve equilibrium are surprising. However, in the system Mn–O–H_2O at high water pressures, it has been noted that P_{O_2} near a solid phase whose oxidation state is undergoing change may be quite different from P_{O_2} in the remainder of the system.[13] The mean free path of the oxygen molecules is so reduced that mixing times in such a system may be quite long.[13] Consequently, one might expect that the decomposition of garnet might proceed slowly and an equilibrium time of the order of 30 days is not inordinately long.

Thus we can see that the ratio Fe^{++}/Fe^{+++} will be important in effecting the formation of garnet and that the time for optimum garnet formation is probably of the order of a few days. Certainly, exact replication of optimum time for a heterogeneous reaction of this sort will be hard to achieve since it will depend on particle size, tube geometry, slight temperature and pressure changes and other variables which are hard to control. However, in view of the size of the heterogeneously nucleated Y.I.G., true recrystallization and not sintering was responsible for garnet growth.

The formation of $YFeO_3$, magnetite and hematite at temperatures below 725° as shown in Fig. 2 can be explained on the assumption that garnet formation proceeds through orthoferrite and that unreacted hematite decomposes to magnetite.

The formation of magnetite at times below six days as shown in Fig. 1 can be explained by the reduction of unreacted Fe_2O_3 and the fact that the unreacted Y_2O_3 may have a high enough solubility to remain in solution. The formation of magnetite and orthoferrite at temperatures above 725° as shown in Fig. 2 and the formation of magnetite and orthoferrite at 30 days as shown in Fig. 1 is not surprising in view of the fact that garnet melts incongruently into orthoferrite and an Fe_2O_3 rich liquid at 1560°, if we assume that water may lower the liquidus temperature substantially.

Small quantities of white phases found at the higher temperatures and occasionally under other conditions gave powder pictures which were identifiable as YOOH or were phases which could not be indexed. Both the YOOH and the unidentified phases were shown by spectrochemical analysis to contain principally yttrium. YOOH has been recently identified by Shafer and Roy[14] in the system Y_2O_3–H_2O. YOOH was shown by Shafer and Roy to be stable only below 650° at 1330 atm. and may have formed in the system described here during the cooling of the vessels, especially since Shafer and Roy report that YOOH is best formed from the high temperature side in the system. The unidentified phases are probably also oxyhydroxides or basic carbonates of yttrium which formed during cooling. It is interesting to note that in the system Y_2O_3–H_2O yttrium oxide was found to be stable only above 650° at 1330 atm. As Fig. 2 shows, no garnet was formed below 650° although in preliminary longer term runs in the presence of metallic iron, garnet was formed at temperatures as low as 400°. Perhaps a change in the yttrium containing species at 650° greatly increases the velocity of garnet formation.

The effect of the variation of the Fe_2O_3/Y_2O_3 ratio is as would be expected even for a slightly soluble but congruently saturating substance where decomposition to magnetite can take place.

Acknowledgments.—The authors would like to thank G. T. Kohman for advice and encouragement throughout the work. Mrs. M. H. Read is especially to be thanked for identification of phases by X-ray diffraction as is J. W. Nielsen for many interesting discussions of the problems of garnet synthesis. S. Geller is especially to be thanked for advice in the precession camera work.

(11) D. D. Wagman, J. E. Kilpatrick, W. J. Taylor, K. S. Spitzer and F. D. Rossini, *J. Res. Natl. Bur. Standards*, **34**, 143 (1945).

(12) D. R. Baker, private communication.

(13) C. Klingsberg and R. Roy, *Am. Mineral.*, **44**, 819 (1959).

(14) M. W. Shafer and R. Roy, *J. Am. Ceram. Soc.*, **42**, 563 (1959).

THE VAPOR PRESSURE, HEAT OF VAPORIZATION AND HEAT CAPACITY OF METHANE FROM THE BOILING POINT TO THE CRITICAL TEMPERATURE

BY P. HESTERMANS AND DAVID WHITE

Cryogenic Laboratory, Department of Chemistry, The Ohio State University, Columbus 10, Ohio

Received November 11, 1960

The vapor pressures, heats of vaporization and heat capacities of methane from the boiling point to the critical temperature have been measured. The vapor pressure data have been represented in the form $\log P_{atm} = 3.984667 - 444.6667/T - \delta(T)$, where $\delta(T)$ is tabulated at equal intervals of temperature. The normal boiling point of methane is 111.42°K. Critical constants have been calculated from the vapor pressure data. It is shown that the measured heats of vaporization are in good agreement with those calculated from the above vapor pressure equation and the known liquid and gaseous densities. The heat capacity data, when combined with the measured heats of vaporization, yield entropies for the gas along the saturation curve in excellent agreement with those from statistical calculations.

Introduction

The entropy of liquid methane, from the boiling point to the critical temperature, has been determined by Wiebe and Brevoort[1] from heat capacity measurements along the saturation curve. From these results, the entropies of gaseous methane along the saturation curve were calculated using the vapor pressures and saturated vapor and liquid densities of Keyes, Taylor and Smith.[2] If these gaseous entropies are compared with those calculated from spectroscopic data[3] (corrected for nonideality[3] and pressure) it is found that the agreement is generally poor. The entropies calculated from the calorimetric and vapor pressure data are consistently larger than those calculated from the spectroscopic data. The deviations are approximately 0.1 e.u. at the boiling point and increase to approximately 1.0 e.u. at 180°K.

This discrepancy cannot be ascribed to any known anomalous behavior of either the saturated liquid or vapor. The heat capacity of the saturated liquid between the boiling point and critical temperature appears normal. There is no evidence of association, or any similar phenomena, occurring in the vapor phase in this temperature range. The reason for the discrepancy probably lies in the uncertainty of the derived heats of vaporization from vapor pressure data. Some considerable improvement in the agreement between calorimetric and spectroscopic entropies can be obtained, if the more recent vapor pressure and saturated liquid and vapor density data of Bloomer and Parent[4] are used. The improvement is pronounced from the boiling point to approximately 150°K. Above this temperature, however, the calorimetric values are now lower than the spectroscopic ones.

In order to unambiguously resolve this discrepancy, the heat capacity of the saturated liquid from the boiling point to the critical temperature have been redetermined and the heat of vaporization, in this same temperature range, has been measured calorimetrically. In addition the vapor pressures, of the same sample used in the above experiments, were measured in order that a comparison between calorimetric heats of vaporization and those derived from vapor pressures could be made. The results are reported below.

(1) R. Wiebe and M. J. Brevoort, *J. Am. Chem. Soc.*, **52**, 623 (1930).

(2) F. G. Keyes, R. S. Taylor and L. B. Smith, *J. Math. Phys.*, **1**, 211 (1922).

(3) F. D. Rossini, *Am. Pet. Inst.*, R. P. 44 April 30 (1957).

(4) O. T. Bloomer and J. D. Parent, *Res. Bull. Inst. Gas Techn.*, No. 17 (1952).

Apparatus

The calorimeter used in all of the experiments was a modified version of that described by Rifkin, Kerr and Johnston.[5] The thermodynamic temperature scale, upon which the results are based, is that of Rubin, Johnston and Altman.[6] A standard copper–constantan thermocouple, which had been calibrated by means of a helium thermometer,[6] was used for the temperature measurement. In the vapor pressure determinations, pressures from 1.0 to 2.5 atmospheres were measured with an open-end mercury manometer. The manometer was read with a cathatometer which was calibrated to 0.02 mm. For pressures greater than 2.5 atmospheres, a calibrated modified M.I.T. type dead weight gauge was used.[7] At the lowest pressures the dead weight gauge has a precision of one part in ten thousand, whereas at higher pressures it is precise to one part in thirty thousand.

The experimental procedures for the heat capacity and heat of vaporizations measurements in this research were identical to those already reported in the hydrogen investigations.[5,8] The vapor pressure measurements were made in a manner previously described by White, Friedman and Johnston.[9]

Purity of Methane.—The methane used in this research was part of a sample prepared by the late Dr. Eisman of the National Bureau of Standards. The source, purification procedure and method of analysis is given by Eisman and Potter.[10] The purity of the original sample obtained from NBS was 99.93 mole % the major impurity being nitrogen. Additional purification by distillation brought the sample purity to 99.96 mole %.

Results and Discussion

(a) Vapor Pressure.—The vapor pressure data are given in the first three columns of Table I. T and P are the temperatures and pressures, respectively. An attempt was made to represent the data by means of some of the common three term polynomial equations.[4,9] It was found that such equations, although adequately reproducing the observed pressures, do not yield unique values of the first derivatives, (dP/dT). These are important in calculations of the heats of vaporization. This difficulty can be avoided by the use of higher order

(5) E. B. Rifkin, E. C. Kerr and H. L. Johnston, *J. Am. Chem. Soc.*, **75**, 785 (1963).

(6) T. Rubin, H. L. Johnston and H. Altman, *ibid.*, **73**, 3401 (1951).

(7) F. G. Keyes, *Ind. Eng. Chem.*, **23**, 1375 (1931).

(8) D. White, J. H. Hu and H. L. Johnston, *J. Phys. Chem.*, **63**, 1181 (1959).

(9) D. White, A. S. Friedman and H. L. Johnston, *J. Am. Chem. Soc.*, **72**, 3927 (1950).

(10) J. H. Eisman and E. A. Potter, *J. Research Natl. Bur. Standards*, **58**, 253 (1957).

polynomial equations or, as was done in this case, the generation of a smooth diagonal difference table at equal temperature intervals and calculation of the derivatives by numerical methods. To simplify the smoothing of the data the following equation was used to represent the data.

TABLE I

VAPOR PRESSURE OF METHANE

T, °K.	P, atm., obsd.	P, atm., calcd.	$P_{obsd.} - P_{calcd.}$
109.38	0.8470	0.8469	+0.0001
114.34	1.2574	1.2572	+ .0002
117.26	1.5596	1.5630	− .0034
119.98	1.8941	1.8970	− .0029
126.50	2.9217	2.9208	+ .0009
135.57	4.9851	4.9779	+ .0072
141.93	6.9641	6.9575	+ .0066
146.54	8.7147	8.7156	− .0009
151.61	11.006	11.003	+ .003
155.12	12.823	12.826	− .003
161.05	16.369	16.373	− .004
167.51	20.995	20.991	+ .004
172.39	25.043	25.044	− .001
176.44	28.801	28.805	− .004
180.02	32.461	32.464	− .003
183.76	36.642	36.642	.000
187.24	40.922	40.915	+ .007
189.52	43.953	43.955	− .002

$$\log P_{atm} = 3.984667 - \frac{444.6667}{T} - \delta(T) \quad (1)$$

where $\delta(T)$ is in essence a deviation function. The constants of equation 1 were arbitrarily chosen so as to minimize the magnitude of $\delta(T)$. The function $\delta(T)$ was then tabulated at equal intervals of temperature and the fourth difference smoothed. A comparison of the pressure calculated from eq. 1 and the smoothed $\delta(T)$ table, with the experimental values, is shown in the last two columns of Table I. The smoothed vapor pressure data and the derivatives (dP/dT) as a function of temperature are given in Table II.

TABLE II

VAPOR PRESSURES OF METHANE. SMOOTHED DATA

T, °K.	P, atm.	log P	$\delta(T) \times 10^{-3}$	dP/dT, atm. deg.$^{-1}$
110	0.8914	−0.04992	−0.784	0.07328
115	1.3220	+ .12124	− .324	.09994
120	1.9001	+ .27887	+ .034	.1323
125	2.6551	.42408	+ .325	.1709
130	3.6187	.55855	.560	.2158
135	4.8237	.68338	.746	.2674
140	6.3043	.79964	.884	.3260
145	8.0958	.90826	.974	.3918
150	10.234	1.01006	1.016	.4648
155	12.757	1.10575	1.010	.5456
160	15.700	1.19590	0.960	.6332
165	19.100	1.28103	.869	.7281
170	22.995	1.36164	.734	.8314
175	27.427	1.43819	.552	.9432
180	32.442	1.51111	.319	1.0651
185	38.116	1.58111	− .005	1.2098
190	44.626	1.64959	− .527	1.4034

A comparison of the vapor pressures of this research with those most recently published[4] is shown in Fig. 1. In this figure $\delta(T)$'s calculated from equation 1 are plotted as a function of temperature. It can readily be seen from this plot that the precision of the present results are considerably greater than that of Bloomer and Parent.[4] Excepting in the vicinity of the critical temperature (above 170°K.), the magnitude of the vapor pressure at a given temperature in both investigations, are in good agreement.

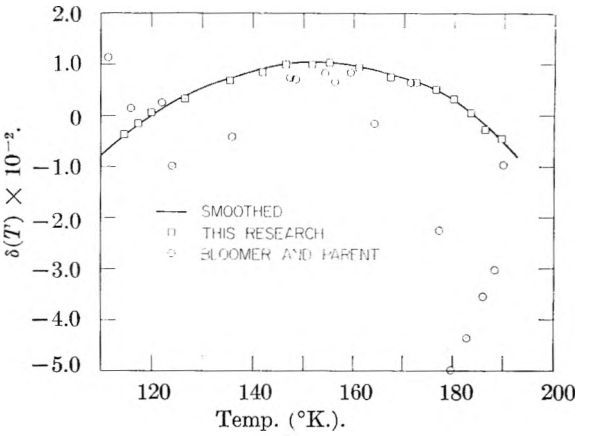

Fig. 1.—Comparison of $\delta(T)$'s calculated from observed (present and recent) vapor pressures and eq. 1 with the smoothed values (Table II).

The normal boiling point and critical constants for methane calculated from the vapor pressure data are shown in Table III and compared with those previously reported. In this comparison the results of Armstrong, Brickwedde and Scott,[11] obtained from a critical review of the literature, are included.

TABLE III

NORMAL BOILING POINT AND CRITICAL CONSTANTS OF METHANE

	This research	Keyes,[2] *et al.*	Bloomer,[3] *et al.*	Armstrong,[11] *et al.*
Normal boiling point, °K.	111.42	111.51	111.71	...
Critical pressure (atm.)	45.41[a]	46.0	45.47	45.6
Critical temp., °K.	(190.55)	191.0	190.55	190.6

[a] This value was computed using the critical temperature of Bloomer, *et al.*[4]

(b) Heat Capacities and Heats of Vaporization.—The heat capacities of the saturated liquid C_{sl} are shown in Table IV below. They were calculated from the data using the thermodynamic relation

$$C_{sl} = \frac{Q}{n\Delta T} + \frac{(N_g \Delta H_v)_{av}}{(T)_{av}} - \frac{N_g^f \Delta H_v^f - N_g^i \Delta H_v^i}{\Delta T} \quad (2)$$

where Q is the energy input to the calorimeter for a temperature rise ΔT, n the total number of moles in the calorimeter, N_g, the mole fraction of gas in the calorimeter and ΔH_v, the molar heat of vaporization. The superscripts i, f, refer to the initial and final temperature of the run. In the second term on the right-hand side of equation 2 with the subscript av., the substituted quantities are those at the average temperature of the run. The heats

(11) G. T. Armstrong, F. G. Brickwedde and R. B. Scott, *ibid.*, **55**, 39 (1955).

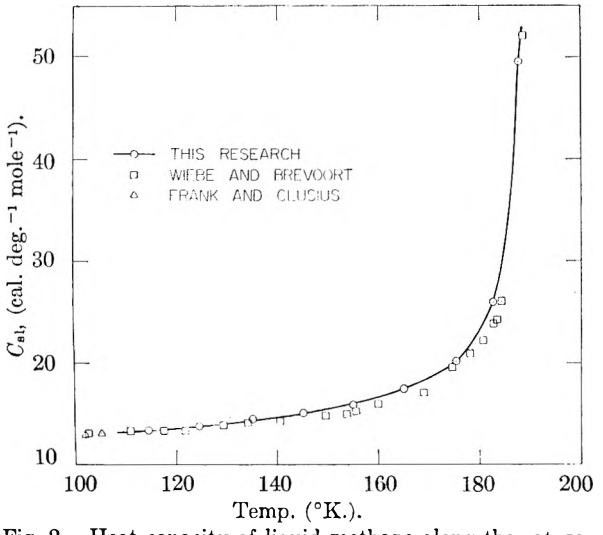

Fig. 2.—Heat capacity of liquid methane along the saturation curve.

of vaporizations used in the calculation were obtained from the measurements given in Table V. The liquid and gaseous densities necessary to calculate the mole fraction of gas in the calorimeter were obtained by smoothing the data of Bloomer and Parent[4] and Matthews and Hurd.[12] The smoothing was done with the aid of the rectilinear diameter relation.

A comparison of the liquid heat capacities reported here with those of previous investigations is shown in Fig. 2. The results of Wiebe and Brevoort[1] are somewhat lower than those of the present research, however, both sets of data tie in well with the liquid heat capacities at lower temperatures of Frank and Clusius.[13]

TABLE IV

HEAT CAPACITY OF LIQUID METHANE

Run no.	Temp., °K.	C_{sl}, cal. deg.$^{-1}$ mole^{-1}
1	114.50	13.11
2	125.49	13.83
3	134.92	14.50
4	145.12	15.05
5	155.02	15.93
6	164.97	17.49
7	174.99	20.17
8	182.57	26.00
9	187.48	49.46

The heats of vaporization of methane, ΔH_v, from the boiling point to the critical temperature were calculated from the data in the same way as previously reported for hydrogen.[8] These results are shown in Table V. Since the calculated heats of vaporization depend on a prior knowledge of liquid and gaseous densities, specifically the ratio $d_l/d_l - d_g$), (where d_l and d_g are the liquid and gaseous densities, respectively, the values of this ratio used in the calculation[4,12] are included in the table.

In order to compare the calorimetrically determined heats of vaporization (Table V) with those calculated from vapor pressure data, the data of Table V were numerically smoothed and interpolated to the same temperature as those of Table II. These results together with a comparison of heats of vaporization calculated from vapor pressure data are shown in Table VI. In the last column the $V_g - V_l$, the difference in the gaseous and liquid molar volumes, used in the calculation of the data from Table II are shown. These are the smoothed values[4,12] previously referred to.

TABLE V

HEAT OF VAPORIZATION OF METHANE

T, °K.	Moles collected	$\frac{d_l}{d_l - d_g}$	Total moles vaporized	ΔH_v, cal./mole
111.88	0.1594	1.005	0.1601	1951
111.85	.1595	1.005	.1602	1946
119.96	.1810	1.008	.1824	1891
129.99	.1474	1.015	.1496	1796
140.07	.1411	1.028	.1450	1690
150.00	.1662	1.048	.1742	1582
160.05	.1740	1.081	.1881	1421
170.00	.1945	1.143	.2209	1243
180.15	.2354	1.282	.2994	962
184.71	.2208	1.442	.3184	759

TABLE VI

HEATS OF VAPORIZATION OF METHANE[a]

	ΔH_v, cal. mole^{-1}			
T, °K.	Interpolated from Table V	Calcd. Table II	Wiebe and Brevoort[4]	$V_g - V_l$, cc. mole^{-1}
100	2030	..	2048	....
105	1997	..	2015	....
110	1963	1974	1983	622.7
115	1927	1928	1950	430.5
120	1888	1883	1917	305.3
125	1846	1840	1883	221.7
130	1800	1793	1847	164.4
135	1751	1740	1808	124.1
140	1698	1690	1767	95.21
145	1640	1631	1721	73.92
150	1577	1572	1670	57.99
155	1507	1503	1612	45.76
160	1431	1425	1546	36.20
165	1343	1332	1470	28.55
170	1242	1227	1382	22.36
175	1123	1107	1276	17.26
180	961	947	1141	12.72
185	743	743	939	8.54
190	171	187	..	1.80

[a] ΔH_v at 99.54°K. of Frank and Clusius.[13] 2036 ± 2 cal. mole^{-1}.

It is obvious from the data in Table VI that there is very good agreement between the calorimetrically determined heats of vaporization and those derived from the vapor pressure data of this research. The values of Wiebe and Brevoort[4] obtained from the data of Keyes, *et al.*,[2] are substantially larger than those of this research practically over the entire temperature range from the boiling point to the critical temperature.

(c) **Entropy of Saturated Liquid and Vapor Methane from 100–190°K. Comparison with Statistical Entropy.**—The entropy of the saturated liquid, S_l, was calculated from the value of the

(12) C. S. Matthews and C. O. Hurd, *Trans. Am. Inst. Chem. Engrs.*, **42**, 55 (1946).

(13) A. Frank and K. Clusius, *Z. physik. Chem.*, **B3**, 41 (1929); **B36**, 291 (1937); **B42**, 395 (1949).

entropy at 100°K. given by Frank and Clusius[13] and the data in Table IV from the relation

$$S_l = S_l(100°K.) + \int_{100}^{T} \frac{C_{sl}}{T}\,dT \qquad (3)$$

The entropy of the saturated vapor S_g was calculated from the saturated liquid and the heat of vaporization data obtained both calorimetrically and from vapor pressure data (Table VI).

$$S_g = S_l + \frac{\Delta H_v}{T} \qquad (4)$$

The results are summarized in Table VII. Two values for S_g are given. The super script "c" refers to the entropy calculated from equation 4 using the calorimetric heats of vaporization (Table VI, column 2). The super script "vp" refers to the entropy calculated from heats of vaporization derived from the vapor pressure data (Table VI column 3).

In order to check the self-consistancy and accuracy of the various experiments, the entropy of methane in the ideal gas state S^0 has been calculated and compared with those obtained from statistical calculations. The ideal gas entropy has been calculated from the expression

$$S^0 = S_g + R \ln p - (S_r - S_i) \qquad (5)$$

The term $R \ln p$ was computed from the data in Table II and the last term, the difference between real and ideal gas entropy, from A. P. I. tables.[3] The results are shown in columns 6 and 7 of Table VII. S^0(cal.) and S^0(v. p.) were calculated from $S_g{}^c$ and $S_g{}^{v.p.}$, respectively. In the last column of Table VII the statistical entropy of methane is given. It can be seen that these entropies are in excellent agreement with those calculated from the experimental data except for the last point (190° K.). This is probably due to the large uncertainty in the extrapolation of the heat of vaporization from 185°K. to the critical temperature.

TABLE VII

T, °K.	S_l, e.u.	$S_g{}^c$, e.u.	$S_g{}^{v.p.}$, e.u.	$-(S_r - S_i)$, e.u.	S^0 (cal.), e.u.	S^0 (v.p.), e.u.	S^0 (Stat), e.u.
100	17.43[a]	37.73	...	0.09	35.71	...	35.72
105	18.07	37.09	...	.12	36.07	...	36.10
110	18.68	36.53	36.62	.17	36.48	36.57	36.48
111.42	18.79	36.35	36.39	.19	36.54	36.58	36.59
115	19.27	36.03	36.04	.22	36.80	36.81	36.83
120	19.85	35.58	35.54	.28	37.14	37.10	37.17
125	20.42	35.19	35.14	.34	37.47	37.42	37.49
130	20.97	34.82	34.76	.40	37.77	37.71	37.80
135	21.51	34.48	34.40	.49	38.10	38.02	38.10
140	22.04	34.17	34.11	.59	38.42	38.36	38.39
145	22.56	33.87	33.81	.68	38.71	38.65	38.67
150	23.08	33.59	33.56	.78	38.99	38.96	38.94
155	23.59	33.31	33.29	.93	39.30	39.28	39.20
160	24.11	33.05	33.02	1.08	39.60	39.57	39.46
165	24.62	32.76	32.69	1.24	39.86	39.79	39.71
170	25.16	32.46	32.38	1.42	40.11	40.03	39.95
175	25.71	32.13	32.04	1.68	40.39	40.30	40.18
180	26.32	31.66	31.58	1.89	40.46	40.38	40.40
185	27.07	31.09	31.08	2.30	40.63	40.62	40.62
190	28.42	29.32	29.40	2.92	39.79	39.87	40.83

[a] Entropy of liquid methane at 100°K. = 17.43 cal. deg.$^{-1}$ mole^{-1} from Frank and Clusius.[13]

Acknowledgement.—One of the authors (P.H.) is indebted to the "Institut pour L'Encouragement de la Researche Scientifique dans l'Industrie et l'Agriculture" for a grant which permitted his visit to the Cryogenic Laboratory, to the du Pont Chemical Co. which in part supported the research and to Dr. L. Deffet, Director of the "Institut Belge des Hautes Pressions" for the arrangements which made the visit possible.

We would also like to thank Dr. P. N. Walsh and Mr. A. Brooke for their help and advice during the experimental investigations.

NOTES

IONIC STRENGTH EFFECT IN THE THIOSULFATE–α-CHLOROTOLUENES REACTION

BY RICHARD FUCHS AND ALEX NISBET

Department of Chemistry, The University of Texas, Austin 12, Texas

Received July 1, 1960

Changes in solvent composition and dielectric constant (D) affect unequally the rates of reaction of α-chloro-*p*-nitro-, α-*p*-dichloro-, α-chloro- and α-chloro-*p*-isopropyltoluene with sodium thiosulfate. The relative rates (or Hammett ρ constant) are in most solvent mixtures a logarithmic function of $1/D$.[1] The solvent must not, therefore, be acting *solely* by affecting the activity coefficient of the attacking species, thiosulfate ion, for this would lead to uniform rate changes for all the α-chlorotoluenes as the solvent was varied. One might more reasonably consider for the several α-chlorotoluenes differences in the localization of charge in the (somewhat different) transition states,[1] with resultant differences in the degree of solvation. Another viewpoint would consider differences in the degree of thiosulfate–carbon bond formation in the transition states for the various α-chlorotoluenes, with concomitant variations in the amount of deformation of the thiosulfate solvation shell required to attain these configurations.

It is usually stated[2] that ion–neutral molecule reactions proceed relatively rapidly in solvents of low dielectric constant. This is not confirmed by work with the α-chlorotoluene–thiosulfate system in 40% water–60% organic solvent mixtures,[1] and is definitely contradicted by work involving butyrolactone–water mixtures of varying composition.[3]

(1) R. Fuchs and A. Nisbet, *J. Am. Chem. Soc.*, **81**, 2371 (1959).

(2) K. J. Laidler and H. Eyring, *Ann. N. Y. Acad. Sci.*, **39**, 303 (1940); subsequent citations are numerous.

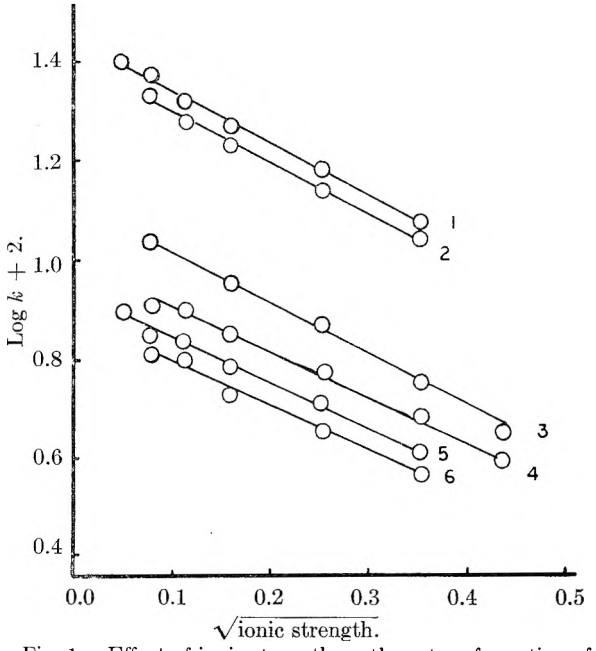

Fig. 1.—Effect of ionic strength on the rates of reaction of α-chlorotoluenes with thiosulfate: (1) p-NO_2 in acetone; (2) p-NO_2 in dioxane; (3) p-isopropyl in acetone; (4) p-H in acetone; (5) p-isopropyl in dioxane; (6) p-H in dioxane.

It is, therefore, of interest to determine for the same reacting systems whether an "anomalous" ionic strength (μ) effect accompanies the unexpected solvent effect. Agreement on an "expected" ionic strength effect is not complete. Qualitatively, an increase in μ might be expected, as would an increase in solvent dielectric constant, to inhibit slightly the rate of a bimolecular ion–neutral molecule reaction. Other considerations afforded predictions of no ionic strength effect, or a dependence of rate on the first power of the μ.[4]

The present work contradicts these predictions; the rate constants are logarithmically dependent on $\sqrt{\mu}$. Thus the rate constants are directly proportional to the activity coefficient of sodium thiosulfate as calculated from the Debye–Hückel limiting law. The satisfactory experimental agreement (Fig. 1 and Table I) up to ionic strengths greater than 0.1 is particularly surprising, for the solvents used (60% dioxane–40% water, D = 25, and 60% acetone–40% water, D = 45.5) should encourage deviations from the Debye–Hückel equation at even lower ionic strengths than does water. It has been suggested[4] previously that rates are dependent on the product of the charges of the reacting species and $\sqrt{\mu}$, which, for an uncharged reactant, predicts k independent of μ. Two causes of failure of this relationship are deviations from the Debye–Hückel equation, and the influence of μ on the activity coefficients of neutral molecules (see below).

The presence of inert salts in the reacting systems produced a variety of effects on the rates. The additions of various amounts of sodium perchlorate not only depressed rates of reaction, but did so below that of solutions of the same ionic strength made up only of sodium thiosulfate (Table II). The addition of assorted inert salts (to μ = 0.1) increased the rate slightly (tetramethylammonium chloride), decreased the rate slightly (sodium perchlorate and nitrate, lithium perchlorate), or decreased the rate strongly (calcium perchlorate and chloride, magnesium perchlorate) (Table II). No quantitative rationalization of this behavior is offered, but qualitatively it is to be expected that the highly charged Mg^{++} and Ca^{++} ions enhance ion-pair formation (compared with Na^+) with thiosulfate ion (and depress the activity coefficient of thiosulfate ion), and that the large, diffusely charged tetramethylammonium ion should have the opposite effect.[5]

Slight differences in slope (Fig. 1) which appear for the several α-chlorotoluenes show no systematic trends. Even if these be attributed to variations in the influence of μ on the different transition states, this must be a minor consideration compared with other factors, perhaps, the influence on the activity coefficients of thiosulfate. Figure 1 also reveals that the slope is virtually independent of the solvent dielectric constant, whereas the Debye-

TABLE I

RATES[a] OF REACTION OF α-CHLOROTOLUENES WITH THIOSULFATE AT VARIOUS IONIC STRENGTHS

$(S_2O_3^=)$[b]	(p-H)	(p-i-Pr)	(p-NO_2)
	In 60% acetone		
0.06	3.85	4.43	..
.04	4.71	5.58	11.9
.02	5.90	7.28	15.1
.008	6.76	8.85	18.7
.004	7.89	9.74	20.7
.002	8.01	10.8	23.3
.0008	..	..	25.2
	In 60% dioxane		
0.04	3.63	4.03	10.9
.02	4.42	5.08	13.7
.008	5.22	6.03	16.8
.004	6.25	6.75	18.8
.002	6.30	6.89	21.3
.0008	..	7.82	..

[a] Second-order rate constants at 30°; $k \times 10^{-3}$ l. mole^{-1} sec.$^{-1}$. All values are averages of two or more determinations. [b] Contains added potassium acetate as a buffer; total ionic strength 0.192, 0.128, 0.640, 0.0256, 0.128, 0.00640 and 0.00256, respectively. (RCl) approximately 60% of $(S_2O_3^=)$. For a description of the method of measurement and the purification of reagents, see ref. 1.

(3) Unpublished studies in this Laboratory.

(4) For references, see A. A. Frost and R. G. Pearson, "Kinetics and Mechanism," John Wiley and Sons, Inc., New York, N. Y., 1953, Ch. 7.

(5) (a) Similar rate accelerations have been reported. See, for example, S. Winstein, L. G. Savedoff and S. Smith, *Tetrahedron Letters*, No. 9, 24 (1960), for an acceleration of chloride ion displacement by added tetrabutylammonium perchlorate; J. D. Reinheimer, W. F. Kieffer, S. W. Frey, J. C. Cochran and E. W. Barr, *J. Am. Chem. Soc.*, **80**, 164 (1958), for an acceleration of the reaction of methoxide ion with 2,4-dinitrochlorobenzene by added potassium salts. (b) Evidence for ion-pair formation in sodium thiosulfate has been reported: J. R. Bevan and C. B. Monk, *J. Chem. Soc.*, 1392, 1396 (1956), and earlier publications. These authors found that the rate of reaction of sodium thiosulfate with 1-bromopropane is directly proportional to the fraction of sodium thiosulfate dissociated (assuming ion-pairs unreactive), and not otherwise dependent on the ionic strength and the nature of the cation present (except as these factors affect the degree of dissociation). (c) Highly specific salt effects have previously been reported. See, for example, ref. 5a, and F. A. Long, W. F. McDevit and F. B. Dunkle, *J. Phys. Colloid Chem.*, **55**, 813, 829 (1951).

Hückel theory predicts a considerable difference for $D = 25$ *vs.* $D = 45.5$. The lack of correlation with theory is hardly unexpected in the light of previous work[1] in which absolutely no relationship was found to exist between the rate of the α-chlorotoluene–thiosulfate reaction and dielectric constant of the solvent. The rates in 60% dioxane and in 60% acetone (Table I) differ only by about 10%, which certainly does not reflect the "predicted" variation with D. Both solvent mixtures contain 40% water, and it may well be that the bulk dielectric constants are not reflected in large differences in the degree of ion solvation, in solvated-ion radii, and in distance of closest approach, because of a tendency of water to be present in the solvation shell at a higher concentration than in the bulk solution.

Another route by which μ may affect the reaction rates is through an influence on the activity coefficient of the neutral molecule.[4,6] In the acid hydrolysis of butyrolactone the effect of added salts on the rate parallels the effect on the independently determined activity coefficient of butyrolactone.[5c] This relationship is between the logarithm of the activity coefficient and μ,[7] rather than $\mu^{1/2}$ as was observed in the present work.

TABLE II

EFFECT OF ADDED SALTS ON THE RATE OF REACTION OF α-CHLOROTOLUENE WITH THIOSULFATE IN 60% ACETONE[a,b]

Salt	Molar concn.	$k \times 10^3$, l. mole^{-1} sec.$^{-1}$
$NaClO_4$	0.010	6.21
	.025	5.55
	.10	4.05
	.20	3.08
	1.0	1.80
$Ca(ClO_4)_2$	0.033	3.03
$Mg(ClO_4)_2$	.033	2.98
$CaCl_2$	.033	2.73
$LiClO_4$	.10	4.63
$NaNO_3$	.10	4.27
$(CH_3)_4NCl$	.10	7.74

[a] Initial $(S_2O_3^=) = 0.008$ *M*, $(RCl) = 0.005$ *M*. [b] Second-order rate constants at 30°; $k \times 10^3$ l. mole^{-1} sec.$^{-1}$. All values are average of two more determinations.

Acknowledgment.—This work was supported by National Science Foundation Grant NSF-G10033, and by The University of Texas Research Institute Grant 934-Srf.

(6) We are indebted to Dr. F. A. Long for suggesting this possibility.

(7) For an expression in which the logarithm of the activity coefficient of a molecule or of the rate constant is a linear function of μ see ref. 4, p. 140.

THE INTERACTION OF H_2, D_2, CH_4 AND CD_4 WITH GRAPHITIZED CARBON BLACK[1]

BY G. CONSTABARIS, J. R. SAMS, JR., AND G. D. HALSEY, JR.

Department of Chemistry, University of Washington, Seattle 5, Washington

Received July 5, 1960

The adsorption of the isotopic pairs H_2–D_2 and CH_4–CD_4 on the graphitized carbon black P33 (2700°) has been investigated in the very dilute range (coverages of less than about 10% of the monolayer). The precision apparatus employed in this study is described elsewhere.[2] The experiments consist of measurements of the apparent volume of the sample bulb containing the solid.

$$V_a = n_b RT/P \qquad (1)$$

where n_b is the number of moles of gas inside the bulb, R is the gas constant, T the Kelvin temperature and P the pressure. Values for the apparent volume extrapolated to zero pressure are presented in Table I.

TABLE I

APPARENT VOLUME AT ZERO PRESSURE

Temp., °K.	$V_a(H_2)$, ml./g.	$V_a(D_2)$, ml./g.
	H_2–D_2	
90.057	1.9388	1.9523
97.122	1.7999	1.8073
104.156	1.7164	1.7242
109.903	1.6737	1.6742
117.049	1.6339	1.6362
124.128	1.6088	1.6098
131.069	1.5906	1.5917
138.128	1.5774	1.5783
Temp., °K.	V_a (CH_4), ml./g.	V_a (CD_4), ml./g.
	CH_4–CD_4	
224.118	1.9425	1.9277
230.203	1.8829	1.8737
234.982	1.8441	1.8330
242.278	1.7976	1.7886
250.486	1.7532	1.7471
263.276	1.7052	1.6998
277.219	1.6643	1.6622
287.283	1.6458	1.6441
297.153	1.6276	

The gases employed in this investigation were as follows: assayed reagent grade hydrogen obtained from Air Reduction Sales Company; cylinder deuterium from Stuart Oxygen Company; cylinder methane from the Phillips Petroleum Company; flask tetradeuteriomethane from Merck and Company, Ltd. The CD_4 (minimum isotopic purity 99%) and H_2 were used without further purification. The D_2, which was reported to be better than 99.5% pure, was passed through a charcoal-filled trap at liquid nitrogen temperature prior to use. This procedure may cause a shift of the ortho–para equilibrium; but at least, no uncertainty in the interaction energy due to such a shift appears in the experimental results. The CH_4 was distilled several times, with intermittent pumping, between nitrogen and oxygen temperatures. The CH_4 was analyzed mass spectrometrically in this Laboratory and was found to contain traces of nitrogen (0.03%) and oxygen (0.005%). The CD_4 was tested for the presence of light gases (*e.g.*, H_2 or D_2) by condensing the gas at nitrogen temperature and measuring the vapor pressure on a McLeod gauge, then pumping off the gas phase and remeasuring the vapor pressure. No difference in pressure could be detected.

The data have been analyzed in terms of a virial coefficients treatment.[3,4] The apparent volume extrapolated to zero pressure is related to the molecular configuration integral for gas–surface interaction, B_{AS}, through the equation

(1) This research was supported in part by the United States Air Force through the Air Force Office of Scientific Research of the Air Research and Development Command.

(2) G. Constabaris, J. H. Singleton and G. D. Halsey, Jr., *J. Phys. Chem.*, **63**, 1350 (1959).

(3) W. A. Steele and G. D. Halsey, Jr., *J. Chem. Phys.*, **22**, 979 (1954).

(4) W. A. Steele and G. D. Halsey, Jr., *J. Phys. Chem.*, **59**, 57 (1955).

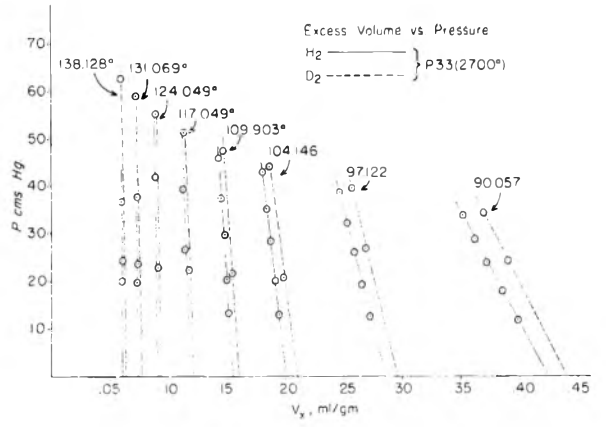

Fig. 1.—Experimental values of the excess volume as a function of pressure: H_2 and D_2 on P33 (2700°).

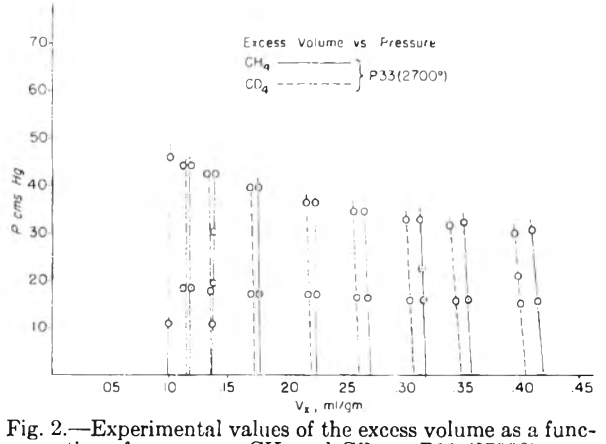

Fig. 2.—Experimental values of the excess volume as a function of pressure: CH_4 and CD_4 on P33 (2700°).

$$V_0 - V_{geo} = V_x = B_{AS} \qquad (2)$$

V_{geo} is found from the helium dead space volume at the ice point and B_{AS}, which is equal to the experimental excess volume V_x, is defined as

$$B_{AS} = \int V_{geo} [\exp(-\epsilon_{is}/kT) - 1] \, dV \qquad (3)$$

where ϵ_{is} is the interaction energy of a single gas system with the surface, in a given volume element dV. No quantum mechanical correction to the classical configuration integral has been made for a reason explained below. We have investigated four models for the interaction potential ϵ_{is}: an inverse cube attraction coupled with a hard-sphere repulsion $(3 - \infty)$, and three Lennard-Jones type functions (3-9, 3-12 and 4-10).[5] These four models all yield equations of the form

$$B_{AS}/As_0 = f(\epsilon_{is}^*/kT) \qquad (4)$$

where A is the area of the solid adsorbent, s_0 is the apparent distance between the gas system and the surface at zero net interaction energy, and ϵ_{is}^* is the maximum energy of gas-surface interaction.

In Figs. 1 and 2 the pressure is plotted against experimental values of V_x for the H_2-D_2 and CH_4-CD_4 pairs, respectively. These volume data, extrapolated to zero pressure, were fitted to the curves generated by each of the four equations of the type (4) to determine the best-fit values of the two parameters As_0 and ϵ_{is}^* for each potential model. The details of the calculations and a discussion of the limits of error to be expected in the values of the parameters obtained are given in ref. 5.

The gas-surface attractive potential may be identified with the London forces attraction of two isolated systems.[3,4] Then, from the experimental ϵ_{is}^* and any one of several formulas which have been proposed for the constant of proportionality in the London expression,[5] a value for s_0 can be calculated, and an apparent area of the adsorbent emerges. Areas determined through the use of two such formulas, those of Kirkwood and Müller[6,7] and of London[8] are reported here (as A_{KM} and A_L). These represent the lower and upper limits, respectively, of areas found by the five formulas discussed in a previous publication.[5]

In the case of the H_2-D_2 pair, D_2 shows the anticipated higher interaction energy and lower area (Table II). Freeman[9] found for this same isotopic pair adsorbed on the low ash sugar charcoal SU-60 these values of interaction energies when the data were analyzed in terms of the classical configuration integral using a 3-9 potential law: H_2, 1866 cal./mole; D_2, 1914 cal./mole. The percentage difference found by Freeman is slightly higher than the present results indicate.

The V_a data can be converted into the usual terms of volume adsorbed at STP (ref. 5, eq. 8), and conventional adsorption isotherms then can be plotted. The isosteric heats of adsorption at zero coverage obtained in this manner are 1293 and 1337 cal./mole for H_2 and D_2, respectively. Pace and Siebert[10] have obtained low temperature calorimetric heats of adsorption of parahydrogen and orthodeuterium on Graphon. The difference in their values at low coverage ($\theta \cong 0.2$) compares favorably with that found in our isosteric heat values.

The CH_4-CD_4 results are surprising in that CH_4 is found to yield a higher energy of interaction with the surface than does CD_4 (Table II). The isotherms of both gases were found to be quite reproducible on outgassing the system overnight and introducing a fresh charge of gas. Illustrative of this are the following pairs of values for the apparent volumes at zero pressure in ml./g. of adsorbent for CH_4 and CD_4 at 235°K., each value representing a different gas dose: CH_4, 1.8444 and 1.8437; CD_4, 1.8333 and 1.8327.

The isosteric heats of adsorption at zero coverage are found to be 3032 cal./mole for CH_4 and 3005 cal./mole for CD_4.

The rather large inversion in interaction energies with the methane pair is reflected in sizable differences in areas computed from the data. As can be seen from Table II, these differences amount to more than 1 m.^{2}/g. in some cases, or almost 10%. The area differences in the case of the hydrogen pair are commensurate with the small differences in interaction energies.

It is clear from Figs. 1 and 2 that there is no possibility to explain this effect with the methanes

(5) For a discussion of these potential functions see: J. R. Sams, Jr., G. Constabaris and G. D. Halsey, Jr., *J. Phys. Chem.*, **64**, 1689 (1960).

(6) J. G. Kirkwood, *Z. Physik*, **33**, 57 (1932).

(7) A. Müller, *Proc. Roy. Soc. (London)*, **A154**, 624 (1936).

(8) H. Margenau, *Rev. Modern Phys.*, **11**, 1 (1939).

(9) M. P. Freeman, *J. Phys. Chem.*, **64**, 32 (1960).

(10) E. L. Pace and A. R. Siebert, *ibid.*, **63**, 1398 (1959).

TABLE II

INTERACTION ENERGIES AND AREAS FOR VARIOUS POTENTIAL MODELS

Model	ϵ_{12}*, cal./mole	A_{KM}, m.²/g.	A_L, m.²/g.
	H_2		
3-9	1141	13.50	17.45
3-12	1145	14.52	18.86
3-∞	1298	19.69	25.54
4-10	1097	13.12	15.93
	D_2		
3-9	1151	13.20	17.12
3-12	1155	14.34	18.54
3-∞	1306	19.45	25.22
4-10	1109	12.81	15.53
	CH_4		
3-9	2947	7.57	12.96
3-12	2955	8.19	13.99
3-∞	3297	11.99	20.50
4-10	2846	7.85	11.74
	CD_4		
3-9	2881	8.24	14.13
3-12	2889	8.91	15.20
3-∞	3227	12.97	22.15
4-10	2846	8.59	12.87

in terms of the mass effect on the vibrational energy levels. It also appears that even though the H_2–D_2 experiments could be fitted to such a theory there is the strong probability that there is a second effect here, too. We surmise that the effect is a rotational one; for the same factor of change in the moment of inertia, the relative mass change on going from CH_4 to CD_4 is much smaller than for the pair H_2–D_2. The results of Armstrong, Brickwedde and Scott[11] for the vapor pressures of the pure methanes should be mentioned here. Between the melting point and the critical point, the heavier species is found to have the higher vapor pressure.

We intend to extend this work to other isotopic and spin-isomer species and other surfaces in the future.

(11) G. T. Armstrong, F. G. Brickwedde and R. B. Scott, *J. Research Natl. Bur. Standards*, **55**, 39 (1955).

LIGHT SCATTERING BY AQUEOUS SUCROSE SOLUTIONS

BY W. PRINS

Cellulose Research Institute, State University College of Forestry, Syracuse, New York

Received July 18, 1960

In recent years the light scattering of aqueous sucrose solutions has received considerable attention, due to the fact that these solutions form convenient primary standards for the calibration of light scattering photometers. Maron and Lou[1] have measured the Rayleigh ratios, R_{90}, due to solute scattering for concentrations up to $c = 0.6$ g./ml. and found correspondence within a few per cent. with the measured osmotic pressures according to the well known formula

$$R_{90} = \frac{KcRT}{\partial P/\partial c}\,\frac{6 + 6\rho}{6 - 7\rho} \qquad (1)$$

$K = 2\pi^2\nu^2(\partial\nu/\partial c)^2/\lambda_0^4 N_A$; ν is the refractive index of the solution, λ_0 the wave length *in vacuo* of the light used, N_A Avogadro's number, P the osmotic pressure, ρ the depolarization ratio, *i.e.*, the ratio of the horizontally polarized to the vertically polarized light at 90° with unpolarized incident light.

Hill[2] and Stigter[3,4] have pointed out recently that eq. 1 is not quite correct. The calculated deviations are for sucrose solutions, however, within the accuracy obtainable with light scattering instruments. We will therefore use eq. 1 in this Note.

The following remarks can be made in connection with these data.

1. Maron and Lou as well as Stigter deduce from measurements at 90° that the total turbidity of the solute is

$$\tau' = (16\pi/3)R_{90}$$

This τ' differs, however, slightly from the real turbidity τ as shown by Cabannes[5] and restated by several authors.[6] This is due to the fact that the form of the depolarization factor $(6 + 6\rho)/(6 - 7\rho)$ changes with the angle of observation and can therefore not be considered constant during the integration over all angles as is necessary to obtain τ from R_{90}. The real turbidity τ is

$$\tau = (16\pi/3)R_{90}\,\frac{1 + \rho/2}{1 + \rho}$$

The numerical differences between τ and τ' are usually small for solutions, but can be appreciable for liquids. It seems advisable to keep this difference in mind and to report light scattering measurements in terms of R_{90} rather than τ', although both, of course, yield exactly the same $\partial P/\partial c$ (or osmotic coefficient in Hill's formulation).

2. Various authors[7] have introduced orientation correlation in gases, liquids and solutions. Benoit and Stockmayer have theoretically deduced that this type of ordering would be impossible to detect in gases and probably obscured by internal field difficulties in liquids. However, considering the case of non-interacting rigid rod-like molecules in solution, these authors estimate that orientation correlation may amount to 12% of the second virial, which in this model is due solely to the finite size of the molecules. Since Stigter[4] has shown that in the case of sucrose there is a definite attractive potential between sucrose molecules, the orientation correlation may well be appreciably enhanced above the amount estimated by Benoit and Stockmayer. It seems interesting, therefore, to calculate this effect from Maron and Lou's data. Using the notation developed by Prins and Prins,[7] we have

(1) S. H. Maron and R. L. H. Lou, *J. Phys. Chem.*, **59**, 231 (1955).

(2) T. L. Hill, *J. Chem. Phys.*, **30**, 93 (1959).

(3) D. Stigter, *J. Phys. Chem.*, **64**, 114 (1960).

(4) D. Stigter, *ibid.*, **64**, 118 (1960).

(5) J. Cabannes, "La Diffusion Moleculaire de la Lumière," Paris, 1929, p. 33.

(6) W. H. Stockmayer quoted in W. B. Dandliker and J. Kraut, *J. Chem. Phys.*, **23**, 1544 (1955); J. A. Prins and W. Prins, *Physica*, **22**, 576 (1956).

(7) M. Goldstein and E. R. Michalik, *J. Appl. Phys.*, **26**, 1450 (1955); H. Benoit and W. H. Stockmayer, *J. Phys. Rad.*, **17**, 17 (1956); J. A. Prins and W. Prins, *Physica*, **23**, 253 (1957).

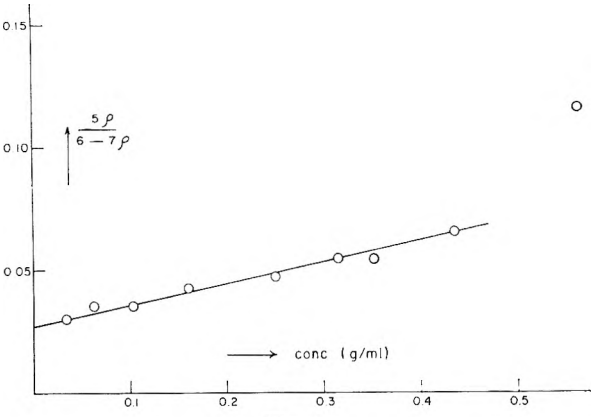

Fig. 1.

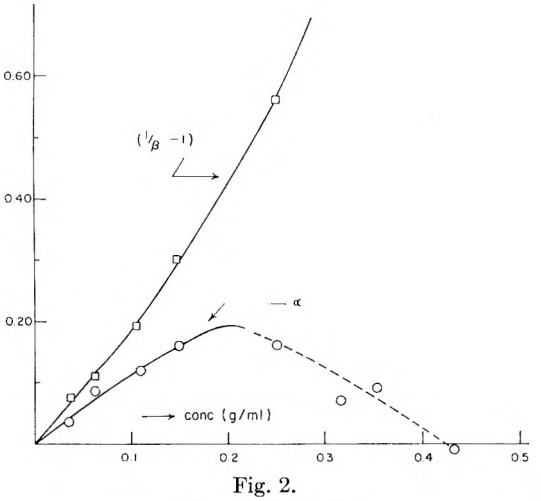

Fig. 2.

$$\frac{5\rho}{6-7\rho} = \frac{1+\alpha}{\beta}\delta^2 \qquad (2)$$

In this equation, the "compressibility ratio" β is defined by

$$\beta - 1 = \int g(\vec{r})\mathrm{d}\vec{r}$$

and can be related to the osmotic pressure by

$$\beta = \frac{\beta_{\text{real}}}{\beta_{\text{ideal}}} = \frac{-(1/V(\partial V/\partial P)}{1/nRT} = \frac{RT}{\partial P/\partial n} = \frac{RT}{M\partial P/\partial c} \qquad (3)$$

where n is the number of molecs/ml., α is an integral over the orientation correlation function $h(r,\psi)$ and the radial distribution function $g(r)$ of the solute is

$$\alpha = \int 2\pi r^2 \mathrm{d}r \sin\psi \mathrm{d}\psi\, g(r)\, \mathrm{h}(r,\psi)$$

δ^2 is the molecular anisotropy $(a-b)^2/(a+2b)^2$, a and b being the principal polarizabilities of the sucrose molecule. δ^2 can be obtained by extrapolating $5\rho/(6-7\rho)$ to infinite dilution where $\alpha = 0$ and $\beta = 1$.

In Fig. 1 Maron and Lou's depolarization data are plotted. The straight line obtained then is used to calculate α from eq. 1, 2 and 3. The results are given in Fig. 2. Restricting ourselves to concentrations below 0.20 g./ml. α is found to be positive and increasing, which means that there is an increasing tendency for the sucrose molecules to orient themselves parallel to each other (paratropic case). The value of α is seen to constitute at least 50% of $(1/\beta - 1)$. The latter quantity is the second virial at the lower concentrations ($c < 0.1$ g./ml.). Thus the orientation effect is much larger than the 12% calculated on the basis of non-interacting rigid rod-like molecules. This is in line with the strong attractive forces operative between sucrose molecules as calculated by Stigter. Interpretation of depolarization data in conjunction with the total scattered intensity as measured by R_{90} therefore can furnish additional, useful information regarding the structure of solutions.

Above a concentration of about 0.2 g./ml. α starts to fall and even seems to become negative, which would correspond to a tendency for perpendicular arrangement of the molecules (diatropic case). It is very doubtful, however, whether the calculation of α is meaningful in this range. Maron and Lou's data have not been corrected for secondary scattering.[8] Moreover, it is possible that at these high concentrations the internal field uncertainty invalidates eq. 2.

In the above the optical activity of the sucrose molecules has not been taken into account. In natural light, however, any effect due to the asymmetry of the polarizability tensor should be negligible. Although at present no data exist, measurable differences in the light scattering envelope can perhaps be found if right and left circularly polarized incident light is used. Such studies are planned by Professor Heller at Wayne State University.

(8) J. Kraut and W. Dandliker, *J. Polymer Sci.*, **18**, 571 (1955); E. P. Geiduschek, *ibid.*, **13**, 408 (1954).

TWO URANYL PEROXIDES

BY LOUIS SILVERMAN AND ROBERT A. SALLACH

Atomics International, A Division of North American Aviation, Inc. P.O. Box 309, Canoga Park, California

Received July 15, 1960

In a recent investigation of the precipitation of uranium peroxide from concentrated uranyl sulfate solutions (such as used in the Atomics International "water boiler reactors"), and in certain analytical separations of uranium as peroxide, it was found that two different crystalline forms of uranium peroxide could be precipitated readily.

The first is obtained by precipitation from hot solutions (1 to 2 M UO_2SO_4, pH 2, 80°). Chemical analysis showed that it is a di-hydrate, $UO_4 \cdot 2H_2O$ (theoretical analysis 70.4% uranium, 9.46% peroxide oxygen; found 70.2% uranium, 9.6% peroxide oxygen).

The second is obtained when precipitation is made at room temperature (1 to 2 M UO_2SO_4, pH 2). By chemical analysis it is a tetra-hydrate, $UO_4 \cdot 4H_2O$ (theoretical analysis: 63.6% uranium, 8.55% peroxide oxygen; found 62.3% uranium, 8.7% peroxide oxygen).

The tetra-hydrate can be converted easily to the di-hydrate by digestion in acidified water (pH 2) at 80° for 4 hours. (50% conversion in 45 minutes.)

The procedure for preparing these compounds is as follows: To a solution of UO_2SO_4 (1 to 2 M with sufficient sulfuric acid to lower the pH to 2) at the *selected* temperature, an excess of 30% H_2O_2 is added, causing essentially all the uranium to precipitate. The thick precipitate is immediately

filtered and generously washed with water, followed by several washings of methanol. The compound now is air dried at room temperature.

X-Ray Diffraction Pattern Discussion.—Based on the analytical chemical results (analysis for U, analysis for H_2O_2 and conversion to U_3O_8), there are two hydrates, of which the tetrahydrate easily can be converted to the dihydrate by boiling in *p*H 2 water at 80°. The comparisons of the X-ray diffraction patterns for these materials show: (1) that Watt's[1] dihydrate X-ray patterns are essentially correct, (2) that Zachariasen's[2] early "tetrahydrate" material is really the dihydrate, and (3) that Dunn's[3] "dihydrate" material is really the tetrahydrate.

(1) G. W. Watt, S. L. Achorn and J. L. Marley, *J. Am. Chem. Soc.*, **72**, 3341 (1950).
(2) W. H. Zachariasen, General Physics Research Report, Part I, CP-1249, January 28, 1944, p. 14.
(3) H. W. Dunn, "X-Ray Diffraction Data for Some Uranium Compounds," ORNL-2092, August 15, 1956, p. 41.

THE APPLICATION OF HIGH-SPEED COMPUTERS TO THE LEAST SQUARES DETERMINATION OF THE FORMATION CONSTANTS OF THE CHLORO-COMPLEXES OF TIN(II)[1]

BY S. W. RABIDEAU AND R. H. MOORE

University of California, Los Alamos Scientific Laboratory, Los Alamos, New Mexico

Received July 18, 1960

Bjerrum[2] has emphasized the need not only to investigate new systems in the study of the stability of complex ions, but also has appealed for increased accuracy of measurement and for the determination of the temperature coefficients of the complexing reactions. Equally important to progress in this field, perhaps, is the selection of the best method with which to carry out the analysis of the data. We would like to suggest that the significance of measurements of even the highest quality often may be improved by the application of the least squares criterion to the data. Rydberg, *et al.*,[3,4] have shown how digital computers may be used in the least squares analysis of data for the case in which the coefficients of the function defining the formation constants of the successive complex ions appear in a linear form. However, with developments in programming and the availability of high-speed computers, it is not necessary to restrict the application of the method to the linear cases and, in fact, there are often advantages in the use of the non-linear form of the defining function. If the function in question is non-linear in the coefficients, the usual methods of solving the normal equations do not apply. In this case, as Moore and Zeigler[5] have demonstrated, the iterative method due to Gauss and Seidel can be applied to obtain the least squares solutions.

In an ideal method for the calculation of the successive formation constants (a) full use is made of all the data, (b) the subjectivity of the computational method is removed, (c) the maximum amount of information is obtained from the data, including the determination of uncertainty estimates, and (d) appropriate weights can be conveniently applied if necessary. The usual graphical methods, such as the Leden[6] method, have difficulty in meeting any of these requirements; however, it is believed that all these specifications are admirably met by the suitably programmed high-speed computer.

As a first example of the use of the non-linear least squares solution of equations pertaining to the chloro-complexes of Sn(II), the work of Duke and Courtney[7] was considered. With tin amalgam electrodes, these authors determined the effect of added chloride ion on the potential of a concentration cell. Perchlorates were added to one compartment and chlorides to the other under the conditions of constant acidity (2.00 M) and ionic strength (2.03 M). The expression which they obtained and used for the graphical and determinant method of evaluating the formation constants can be written as

$$\exp(-nFE/RT) = 1 + \beta_1[Cl^-] + \ldots + \beta_n[Cl^-]^n \quad (1)$$

The amount of chloride ion in the tin chloro-complexes was neglected since the total Sn(II) concentration was 5×10^{-3} M and became smaller as a result of dilution. If the natural logarithm of equation 1 is taken it follows that

$$-E = (RT/nF)\ln(1 + \beta_1[Cl^-] + \ldots + \beta_n[Cl^-]^n) \quad (2)$$

By this transformation we have obtained an expression which is non-linear in the coefficients; however, we have also obtained the equation in a form which permits us to minimize the sums of the squares of the differences between the directly measured quantity, E, and the function on the right side of equation 2. That is, Q is minimized and takes the form

$$Q = \frac{\sum_{i=1}^{21} w_i[E_i - F(Cl^-)]}{(21 - n)} \quad (3)$$

where w_i is the weight factor, $F(Cl^-)$ represents the quantity on the right side of equation 2 and the number 21 refers to the fact that there were 21 data points in Duke and Courtney's data.[7] Inasmuch as the electromotive force measurements were made with equal precision, it can be shown that whatever constant weight w_i is applied, it will cancel in the subsequent treatment of the equations; accordingly it is convenient to assign a unit weight to all the data points. However, this is *not* the

(1) (a) This work was done under the auspices of the U. S. Atomic Energy Commission. (b) Presented in part at the Northwest Regional Meeting of the American Chemical Society, Richland, Washington, June 17, 1960.
(2) J. Bjerrum, *Chem. Revs.*, **46**, 381 (1950).
(3) J. Rydberg, J. C. Sullivan and W. F. Miller, *Acta Chem. Scand.*, **13**, No. 10, 2023 (1959).
(4) J. Rydberg and J. C. Sullivan, *ibid.*, **13**, No. 10, 2057 (1959).
(5) R. H. Moore and R. K. Zeigler, Los Alamos Scientific Laboratory report, LA-2367, October 15, 1959. Available from the Office of Technical Services, U. S. Dept. of Commerce, Washington 25, D. C., $2.25. This reference contains a useful bibliography to the literature of least squares methods and discusses functions in which the parameters appear both linearly and non-linearly.
(6) I. Leden, *Z. physik. Chem.*, **A188**, 160 (1941).
(7) F. R. Duke and W. G. Courtney, *Iowa State College J. Sci.*, **24**, 397 (1950).

case if equation 1, the linear form, were used in setting up the normal equations.

In the application of the non-linear program as prepared for the IBM-704 to the data, there are two fixed parameters: namely, unity, the first term in the polynomial, and the constant, RT/nF. In addition, there are n parameters corresponding to the successive formation constants for the Sn(II) chloro-complexes to be evaluated. With minor programmatic alterations, it is possible to allow n to assume increasing integral values. It has been considered that a given parameter was not significant if twice the standard deviation of the parameter encompassed zero. It has been found that the number of significant parameters as judged by this criterion with Duke and Courtney's data is equal to three. In Table I are given the results of the computations.

TABLE I

LEAST SQUARES VALUES OF FORMATION CONSTANTS OF Sn(II) CHLORO-COMPLEXES AT 25° AT AN IONIC STRENGTH OF 2.03

	σ^a Standard deviation
$\beta_1 = 11.4$	0.26
$\beta_2 = 52.3$	1.8
$\beta_3 = 31.4$	2.3

A comparison with the values obtained by the authors[7] is not possible since they assumed a total of four significant formation constants to be defined by their data. It is to be recognized that the standard deviations given in Table I are a measure of the precision with which the data are represented by equation 2, it is only by repeated experiments that it is possible to demonstrate whether these uncertainty estimates are realistic.

Vanderzee and Rhodes[8] also have made electromotive force measurements with a concentration cell method to evaluate the formation constants of the Sn(II) chloro-complexes. In addition to the equilibria

$$Sn^{++} + nCl^- \rightleftharpoons SnCl_n^{+2-n} \qquad (4)$$

the equilibrium constants for which we have assigned the designation β_n, there is also the hydrolysis reaction of Sn^{++} which may be important in solutions of sufficiently low acidity, *i.e.*

$$Sn^{++} + H_2O \rightleftharpoons SnOH^+ + H^+ \qquad (5)$$

Following the notation of Vanderzee and Rhodes, the equilibrium quotient for this reaction is defined as h. There is also the possibility of the formation of mixed complexes of the form

$$SnOH + nCl^- \rightleftharpoons SnOH(Cl^-)_n^{+1-n} \qquad (6)$$

the equilibrium quotient expression for which is given the notation δ_n. It can be shown that the total tin(II) concentration, $[Sn^{II}]$, is related to the uncomplexed bivalent tin, $[Sn^{++}]$, by the relation

$$[Sn^{II}] = [Sn^{++}]\,\Sigma_n(\beta_n + \delta_n h/[H^+])[Cl^-]^n \qquad (7)$$

Since the total stannous ion concentration is the same in the two cell compartments, the relationship between the cell e.m.f. and the uncomplexed chloride ion concentration can be written

$$f^0 = \exp(-nFE/RT) = 1 + A_1[Cl^-] + \ldots + A_n[Cl^-]^n \qquad (8)$$

or

$$-E = (RT/nF)\ln(1 + A_1[Cl^-] + \ldots + A_n[Cl^-]^n) \qquad (9)$$

where

$$A_n = \frac{\beta_n + \delta_n h/[H^+]}{1 + h/[H^+]} \qquad (10)$$

If we represent by ν the average number of chloride ions per tin atom in the complexes, then the uncomplexed chloride ion $[Cl^-]$ can be shown to be related to the total chloride ion $[Cl^-]_t$ by

$$[Cl^-] = [Cl^-]_t - \nu[Sn^{II}](f^0 - 1)/f^0 \qquad (11)$$

Also, the average number of chlorine atoms per tin atom is

$$\nu = \mathrm{d}\ln(f^0 - 1)/\mathrm{d}\ln[Cl^-] = \frac{A_1[Cl^-] + \ldots + kA_k[Cl^-]^k}{1 + A_1[Cl^-] + \ldots + A_k[Cl^-]^k} \qquad (12)$$

With the substitution of the expression for ν in equation 12 into equation 11 and simplifying, a k + 1th polynomial is obtained

$$A_k[Cl^-]^{k+1} + \{A_{k-1} - A_k([Cl^-]_t - k[Sn^{II}]\}[Cl^-]^k + \{A_{k-2} - A_{k-1}([Cl^-]_t - (k-1)[Sn^{II}])\}[Cl^-]^{k-1} + \ldots + \{1 - A_1([Cl^-]_t - [Sn^{II}])\}[Cl^-] - [Cl^-]_t = 0 \qquad (13)$$

Preliminary values of the A_k coefficients were obtained with the least squares solution of equation 9 with the assumption that $[Cl^-] = [Cl^-]_t$. These quantities are not equal in the work of Vanderzee and Rhodes (whereas they were considered to be equal in the experiments of Duke and Courtney) because Sn^{II} concentrations of about 0.01 M were used and were maintained constant at the various chloride ion concentrations, hence, a small but significant quantity of chloride ion is present in the tin complexes. The A_k-coefficients then were inserted in equation 13. The roots of equation 13 were obtained with an iterative numerical program developed at Los Alamos Scientific Laboratory by Mr. J. K. Everton. It is called the "floating point polynomial solver." No ambiguity was involved in trying to decide which root to select since in each instance the number of positive real roots turned out to be one. After obtaining the first approximation to the uncomplexed chloride ion concentration by solving equation 13, these concentrations were resubstituted into equation 9 to get a second approximation to the A-coefficients. This process was repeated by the computer until convergence within 1 part in 10^6 was obtained.

In Table II are given the results of the least squares calculations of the A-coefficients with Vanderzee and Rhodes' data. It was found that three A-coefficients were sufficient to describe the system, even at 45°. However, at 45°, it appears that from the similarity of the A_2-coefficients at 0.500 M acid at 35 and 45°, additional data at concentrations of chloride ion above 0.6 M would have been desirable. In a comparison of the least squares values of the A-coefficients with those determined by Vanderzee and Rhodes, it is noted that there is fairly good greement in the A_1 results, less satisfactory agreement in the A_2 values and poor agreement in the A_3 terms.

(8) C. E. Vanderzee and D. E. Rhodes, *J. Am. Chem. Soc.*, **74**, 3552 (1952).

TABLE II

LEAST SQUARES VALUES OF A-COEFFICIENTS AS FUNCTIONS OF TEMPERATURE AT $\mu = 3.0$

Temp., °C.	H^+, M	A_1	σ_1[a]	A_2	σ_2[a]	A_3	σ_3[a]
0°	0.500	9.03	0.1	32.1	1.0	21.8	1.6
	.100	9.27	.2	25.6	1.9	26.8	3.2
25	.500	13.70	.08	49.7	0.8	45.6	1.4
	.100	12.97	.09	44.7	0.9	32.4	1.6
35	.500	15.92	.09	64.4	1.0	57.5	1.8
	.100	13.74	.07	55.9	0.8	37.9	1.4
45	.500	18.3	.4	64.1	4.1	109.9	8
	.100	15.8	.2	70.7	1.6	52.5	3

[a] The authors regard these numbers only as approximate standard deviations because the procedure used in this particular problem involved more than the usual least squares methods. Because of the modification of the chloride ion concentration together with the A-coefficients, straight-forward least squares error analysis does not apply.

With the values of A_2 and A_3 as a function of acidity, Vanderzee and Rhodes calculated the hydrolysis constant, h, as a function of temperature. However, with the results shown in Table II, inconsistent values of the hydrolysis constant were obtained. Accordingly, it was decided to calculate the heats for the A-coefficients since an accurate value of the hydrolysis constant of Sn(II) does not appear to be available. Values of 2800, 3100 and 4770 cal./mole were obtained from the temperature dependence of A_1, A_2 and A_3 at the 0.500 M acidity level. These values are in essential agreement with those reported[7] for the corresponding β-coefficients.

THE HIGH PRESSURE LIMIT OF UNIMOLECULAR REACTIONS

BY M. C. FLOWERS AND H. M. FREY

Chemistry Department, The University, Southampton, England

Received July 25, 1960

Of the large number of homogeneous decompositions that have been studied kinetically in the gas phase, few are simple, most involve complex steps. In addition there is often a heterogeneous component of the decomposition as well as the simultaneous occurrence of side reactions. As a result few experimental data are available to test the predictions of the various detailed theories of unimolecular reactions. The data that are available for such cases as N_2O_5,[1] cyclopropane[2] and cyclobutane[3] support the prediction of the theories that at sufficiently low pressures a decrease in the apparent first-order rate constants of unimolecular processes will occur.

Until now no unimolecular reaction has been studied over a pressure range extending from the region where the "fall off" of the rate constant begins to pressures very many times greater than this. This region is of added interest since it has been suggested[4] recently that (subject to a hypothetical restriction on the reactivity of molecules just after the instant of energization) the rate constant may pass through a maximum, and then diminish, with increasing pressure. We wish to report a study in this pressure range on the thermal isomerization of 1,1-dimethylcyclopropane. This has been shown to be a unimolecular reaction[5] whose apparent first-order rate constant begins to decrease below 10 mm. The apparatus and analytical technique have been described elsewhere.[6] Runs were carried out at 460.4° in the pressure range 16 to nearly 1600 mm. The rate constants obtained are shown below.

Pressure, mm.	16	39	54	55	104	217
$10^4 k$, sec.$^{-1}$	2.44	2.43	2.43	2.47	2.44	2.43
Pressure, mm.	253	283	294	567	774	
$10^4 k$, sec.$^{-1}$	2.46	2.42	2.44	2.40	2.41	
Pressure, mm.	1008	1057	1240	1447	1596	
$10^4 k$, sec.$^{-1}$	2.41	2.43	2.41	2.44	2.44	

Increasing the pressure one hundred and fifty-fold from the point where the high pressure limit is first reached has no effect on the rate constant. It must be concluded that the high pressure rate constant of this unimolecular reaction does not go through a maximum.

The authors thank the Esso Petroleum Company for the award of a research studentship to M.C.F.

(1) R. L. Mills and H. S. Johnston, *J. Am. Chem. Soc.*, **73**, 938 (1951).

(2) H. O. Pritchard, R. G. Sowden and A. F. Trotman-Dickenson, *Proc. Roy. Soc.* (*London*), **218A**, 416 (1953).

(3) C. T. Genaux, F. Kern and W. D. Walters, *J. Am. Chem. Soc.*, **75**, 6196 (1953).

(4) D. J. Wilson, *J. Phys. Chem.*, **64**, 323 (1960).

(5) M. C. Flowers and H. M. Frey, *J. Chem. Soc.*, 3953 (1959).

(6) M. C. Flowers and H. M. Frey, *Proc. Roy. Soc.* (*London*), **257A**, 122 (1960).

A STUDY OF EQUILIBRIA IN THE SYSTEM IODINE CYANIDE–POTASSIUM IODIDE–WATER–HEPTANE

BY G. LAPIDUS[1] AND G. M. HARRIS

Department of Chemistry, University of Buffalo, Buffalo 14, N. Y.

Received July 25, 1960

In some earlier work in this Laboratory,[2] the almost instantaneous exchange of iodine between ICN and KI in aqueous solution was explained in terms of a rapid establishment of the equilibrium

$$ICN + H^+ + I^- \rightleftharpoons I_2 + HCN \qquad (1)$$

along with the well-known iodide/iodine equilibration

$$I_2 + I^- \rightleftharpoons I_3^- \qquad (2)$$

A search of the literature showed there to be considerable disagreement in regard to the magnitude of K_1. Kovach[3] and Gaugin[4] in independent determinations based on electrode potentials arrived at the values 1.37 and 1.99, respectively, for the constant at 25°. These studies took no account of the intermediate complexes I_2CN^- and $I(CN)_2^-$ which have been identified by Yost.[5] The latter author corrected Kovach's result by allowing for the complexes, obtaining a value of $K_1 = 1.50$.

(1) Work done by G. Lapidus as part of the M.A. requirement of the University of Buffalo, 1958.

(2) F. E. Jenkins and G. M. Harris, *J. Phys. Chem.*, **61**, 249 (1957).

(3) L. Kovach, *Z. physik. Chem.*, **80**, 107 (1912).

(4) R. Gaugin, *Bull. soc. chim.* (*France*), **15**, 1052 (1948).

(5) D. M. Yost and W. E. Stone, *J. Am. Chem. Soc.*, **55**, 1889 (1933).

None of these investigators made reference to possible anomalous I^+-containing species which have been suggested in recent work on low-concentration aqueous iodine-containing systems.[6] The purpose of the present study was to re-establish the magnitude of K_1, taking into account as many of the complications as possible. Incidental results of the work have been exact determinations of the distribution coefficients between heptane and water of ICN and I_2, and reconfirmation of the value of K_2.

Experimental

A. Materials.—ICN was prepared by standard technique,[7] purified by vacuum sublimation, and stored in a refrigerated desiccator. I_2 was the commercial resublimed product, subjected to an additional sublimation. The phosphate buffer was prepared from recrystallized reagent grade KH_2PO_4. "Spectral grade" heptane was obtained by the following treatment of Eastman C.P. *n*-heptane: The hydrocarbon, after a preliminary pass through a silica gel column, is shaken with 1:1 H_2SO_4/H_2O, and washed several times with water. I_2 is then dissolved in the heptane, and at the end of 12 hours standing is reduced by shaking the mixture with dilute aqueous thiosulfate. After further washing with water, the heptane is dried over $CaCl_2$, followed by a double pass through a four foot column of 200 mesh silica gel. Heptane treated in this manner is completely transparent down to a wave length of 232 mμ.

B. Distribution Coefficient Measurements.—Freshly prepared solutions of ICN in conductivity water were shaken with approximately equal volumes of spectral grade heptane at 25°. The ICN concentration in each phase was determined by decomposition of the ICN with an aqueous HCl/KI solution and titration of the resulting I_2 with thiosulfate. For the I_2 distribution experiments, solutions of varying concentrations of the halogen in spectral grade heptane were shaken with suitable volumes of water or dilute aqueous $HClO_4$[8] at 25°. The iodine concentration in the heptane phase was measured spectrophotometrically[9] and in the water phase by titration with thiosulfate. The HCN distribution was studied by shaking portions of 0.03 to 0.05 *M* KCN acidified with acetic acid to *p*H 5 with equal volumes of heptane at 25°. Aqueous HCN was determined directly by the method of Liebig[10]; the HCN in the heptane was first extracted with dilute aqueous ammonia and the cyanide determination was made on the extract.

C. Equilibrium Constant Measurements.—Equimolar solutions of ICN and KI in conductivity water each containing phosphate buffer to maintain a *p*H of about 5 were mixed in 1-liter volumetric flasks and brought to the mark at 25°. Pairs of determinations were made by pipetting 200-ml. portions of the aqueous solution into separate 500-ml. flasks, adding 200 ml. of heptane, and shaking for 10 to 20 minutes at 25°. After 2 hours standing in the thermostat to allow complete phase separation, the various required concentration determinations were made as follows: I_2 in the heptane phase by spectrophotometry usually in a 10 cm. quartz cell; the sum of ICN and I_2 in the heptane phase by decomposition of the former on shaking with dilute aqueous HCl/KI and titration of the total I_2 with thiosulfate; I_3^- in the water phase by spectrophotometry[11] in a 1 cm. or 1 mm. quartz cell; H^+ in the water phase with a Beckman Model G *p*H Meter, fitted with semi-micro electrodes.

Results and Discussion

A. Distribution Coefficients.—The data obtained for ICN and I_2 are given in Tables I and II; in each case the distribution coefficient *D* is defined as the ratio of the concentration of the species in the heptane phase (h) to that in the water phase (w). It turned out that the solubility of HCN in heptane is too low to enable accurate determination of D_{HCN}. The average value of D_{HCN} obtained from several determinations was approximately 0.005, a value so low that (HCN) in the heptane phase can be neglected in the equilibrium constant calculation (see below).

TABLE I

DISTRIBUTION OF IODINE CYANIDE BETWEEN HEPTANE AND WATER AT 25°

Total (ICN), *M*	(KNO_3), *M*, in water phase	Values obtained for *D*: A. Using fresh stock soln. i. Detn. made 1 hr. after shaking	A. Using fresh stock soln. ii. Detn. made 20 hr. after shaking	B. Using stock soln. aged for one day i. Detn. made 1 hr. after shaking	B. Using stock soln. aged for one day ii. Detn. made 20 hr. after shaking
0.01	....	0.0612	0.0582	0.0582	0.0583
.01	0.0016	.0599	.0581	.0583	.0582
.01	.01	.0589	.0580	.0580	.0582
.03	....	.0597	.0585	.0574[a]	.0577[a]
.03	.005	.0596	.0580	.0586	.0585
.03	.03	.0593	.0587	.0586	.0585
.05	....	.0596	.0586	.0574[a]	.0579[a]
.05	.0083	.0598	.0583	.0589	.0584
.05	.05	.0595	.0585	.0589	.0589

[a] Stock solutions aged 3 days before use.

It is apparent from Table I that, except for the very "new" solutions (col. 3) and the "old" solutions (superscript "a"), D_{ICN} is independent of time of standing, or of concentrations of ICN or of added neutral salt up to 0.05 *M*. The mean and standard deviation of all values exclusive of those obtained from the "new" and "old" solutions is 0.0584 ± 0.0003. The consistently higher values in the "new" solutions probably result from incomplete equilibration between ICN and its hydrolysis products in the aqueous phase. In the "old" solutions, D_{ICN} must fall off as a result of very slow irreversible processes for which the analytical technique fails to allow.

TABLE II

DISTRIBUTION OF IODINE BETWEEN HEPTANE AND WATER AT 25°

Total (I_2), *M*	0.0007	0.001	0.002	0.003	0.004	0.005
D_{I_2} (no acid)[a]	34.10	34.99	35.40	35.26	35.78	35.59
D_{I_2} (acidified)[b]	35.34	35.13	35.22	35.01	35.16	35.01
D_{I_2} (acidified)[c]	35.22	35.25	35.19	35.42	35.38	35.24

[a] Mean of two series. [b] Minimum acidity as defined in footnote 8. [c] Double the minimum acidity.

Table II shows that inconsistent data are obtained only at low (I_2) and in absence of acid. These are the conditions under which I_2 hydrolysis and perhaps other processes[6] in the aqueous phase will interfere most strongly. The presence of sufficient acid in the aqueous phase suppresses such processes and removes the difficulty. This leads to an acidity-independent value for D_{I_2} with a

(6) M. L. Good and R. R. Edwards, *J. Inorg. Nuclear Chem.*, **2**, 196 (1956); R. G. Wille and M. L. Good, *J. Am. Chem. Soc.*, **79**, 1040 (1957).

(7) R. F. Arnold, *Org. Syntheses*, **32**, 29 (1952).

(8) The minimum amount of acid to be added was determined from the equilibrium constant expression for the reaction $I_2 + H_2O \rightleftarrows H^+ + I^- + HOI$ for which $K = 5.4 \times 10^{-13}$ at 25° (T. L. Allen and R. M. Keefer, *J. Am. Chem. Soc.*, **77**, 2957 (1955)). The acidity was set such that (HOI) $\leq 0.1\%$ of (I_2).

(9) The molar extinction coefficient of I_2 in heptane at 25° was determined in this work to be 898 ± 2 at λ 521 mμ over the concentration range 10^{-4} to 10^{-3} *M* (*i.e.*, Beer's Law held exactly in this range).

(10) H. Willard, N. Furman and C. Bricker, "Elements of Quantitative Analysis," 4th ed., D. Van Nostrand Co., New York, N. Y., 1956, p. 133.

(11) Molar extinction coefficient of I_3^- in water at 25° was taken as 26,400 at 353 mμ, as given in reference 16.

mean and standard deviation of 35.21 ± 0.13 at 25°. D_{I_2} is also independent of total (I_2), as expected on comparison with the carbon tetrachloride/water distribution of iodine.[5]

Table III summarizes the data on the equilibrium constants K_1 and K_2. The method of calculation makes use of the distribution coefficients reported above, the known equilibrium constants[5] $K_3 = 1.17$ and $K_4 = 2.5$ at 25° for the aqueous reactions

$$ICN + I^- \rightleftharpoons I_2CN^- \quad (3)$$

$$ICN + CN^- \rightleftharpoons I(CN)_2^- \quad (4)$$

and the dissociation constant[12] of HCN, $K_5 = 6.1 \times 10^{-10}$ at 25°.

From stoichiometry, it follows that[13]

$$(I^-) = (KI)_0 - [(I_2)_h + (I_2)_w + 2(I_3^-) + (I_2CN^-)]$$

and

$$(I(CN)_2^-) + (CN^-) + (HCN)_h + (HCN)_w = (I_2)_h + (I_2)_w + (I_3^-)$$

whence it is seen that

$$(I^-) = \frac{\left\{(KI)_0 - \left[(I_2)_h\left(\frac{D_{I_2}+1}{D_{I_2}}\right) + 2(I_3^-)\right]\right\}}{[1 + K_3(ICN)_h/D_{ICN}]}$$

and

$$(HCN)_w = \frac{\left[(I_2)_h\left(\frac{D_{I_2}+1}{D_{I_2}}\right) + (I_3^-)\right]}{[1 + D_{HCN} + K_4K_5(ICN)/(H^+) + K_5(H^+)]}$$

In practice, the denominator of the expression for (HCN) reduces to unity, since all the other terms are negligible under the experimental conditions.[14]

TABLE III

EQUILIBRIA IN AQUEOUS ICN + KI AT 25°

Run no.	Initial (ICN) = (KI), M	pH	Total ionic strength[a]	γ_{I^-}[b]	K_1[c]	$K_2 \times 10^{-3}$
1	0.003	5.79	0.042	0.85	0.85	0.64
2	.003	4.96	.012	.90	.89	.70
3	.003	4.98	.010	.91	.93	.71
4	.003	5.03	.010	.91	.93	.69
5	.006	5.94	.045	.85	.96	.67
6	.006	5.06	.015	.89	.87	.73
7	.006	5.13	.013	.90	.93	.79
8	.006	5.18	.013	.90	.99	.71
9	.009	5.96	.045	.85	1.00	.72
10	.009	5.25	.017	.89	0.98	.73
11	.009	5.36	.016	.89	1.00	.68
12	.03	5.53	.037	.86	1.08	.79
13	.06	5.62	.067	.83	1.73	.95

[a] Includes ionic reactants and phosphate buffer. [b] Interpolated from data of Latimer.[15] [c] Corrected for activity of I^-.

(12) K. P. Ang, *J. Chem. Soc.*, 3822 (1959).

(13) It is assumed that the concentration of ionic species in heptane is negligible.

(14) In a typical run (No. 3), 2.63 ml. of 0.00783 N thiosulfate was needed to titrate 50 ml. of heptane phase; absorbancy of I_2 in heptane phase was 0.4235 and of I_3^- in water phase was 0.743; a_{H^+} was 1.05×10^{-5}. Whence, $[(I_2) + (ICN)]_n = 2.06 \times 10^{-4}$ M, $(I_2)_h = 4.75 \times 10^{-5}$ M, and $(I_3^-) = 2.81 \times 10^{-5}$ M, leading to $K_{exp} = 0.845$ and $K_1 = 0.93$.

(15) W. M. Latimer, "The Oxidation States of the Elements and Their Potentials in Aqueous Solutions," 2nd Ed., Prentice-Hall, Inc., New York, N. Y., 1952, p. 355.

It is noted that for initial ICN and KI concentrations less than 0.01 M, K_1 is essentially independent of reactant concentration, indicating that the assumption that $pH = -\log a_{H^+}$ and application of the I^- activity corrections are justified in these circumstances. The average value and standard deviation for K_1 in runs 1–11 is 0.94 ± 0.05. There is a slight upward trend in the separate averages of the groups of runs at different reactant concentration in this range but the experimental error is such that the trend is not significant. The acceptable constancy of K_1 by our method of calculation at low concentrations of reactants would appear to rule out any significant contribution to the equilibrium by the so-called "anomalous I^+ containing species" mentioned earlier. The large disparity between Kovach's corrected value[5] for K_1 and the present one is not cause for concern, since Kovach's conductivity method[3] was undoubtedly subject to considerable error. The values for K_2 have been calculated on the assumption that $\gamma_{I^-} \sim \gamma_{I_3^-}$, and they are seen to be subject only to random error in the low-concentration runs. The mean and standard deviation of K_2 for runs 1–11 is $(0.71 \pm 0.04) \times 10^3$, in excellent agreement with other determinations of this constant.[16,17] The limited data at ICN and KI concentrations in excess of 0.01 M suggest that both K_1 and K_2 become greater but more experiments would be necessary to determine the exact nature of this effect.

Financial support of this work through Contract No. AT(30-1)-1578 between the U. S. Atomic Energy Commission and the University of Buffalo is gratefully acknowledged.

(16) A. D. Awtrey and R. E. Connick, *J. Am. Chem. Soc.*, **73**, 1842 (1951).

(17) L. I. Katzin and E. Gilbert, *ibid.*, **77**, 5814 (1955).

THE ACTIVATION ENERGY FOR HYDROGEN ATOM ADDITION TO PROPYLENE

BY MILTON D. SCHEER AND RALPH KLEIN

National Bureau of Standards, Washington, D. C.

Received July 25, 1960

The kinetics of the addition of hydrogen atoms to propylene to form isopropyl has been studied in both the gas[1–5] and condensed phases.[6,7] Melville and Robb[2] measured a gaseous H atom concentration by the molybdenum oxide technique and determined the rate constant to be 1.3×10^{11} cc./mole sec. at 291°K. They calculated an activation energy of 2.6 kcal., assuming a steric factor of 10^{-2}. Callear and Robb[4] measured H atom concentration with a sensitive platinum resistance thermometer and found a value of 4.8×10^{11} for the room temperature rate constant. Back[5] measured the com-

(1) B. S. Rabinovitch, S. G. Davis and C. A. Winkler, *Can. J. Res.*, **B21**, 251 (1943).

(2) H. W. Melville and J. C. Robb, *Proc. Roy. Soc.* (*London*), **A196**, 494 (1949); **A202**, 181 (1951).

(3) B. deB. Darwent and R. Roberts, *Disc. Faraday Soc.*, **14**, 55 (1953).

(4) A. Callear and J. C. Robb, *Trans. Faraday Soc.*, **51**, 638 (1955).

(5) R. A. Back, *Can. J. Chem.*, **37**, 1834 (1959).

(6) R. Klein and M. D. Scheer, THIS JOURNAL, **62**, 1011 (1958).

(7) M. D. Scheer and R. Klein, *ibid.*, **63**, 1517 (1959).

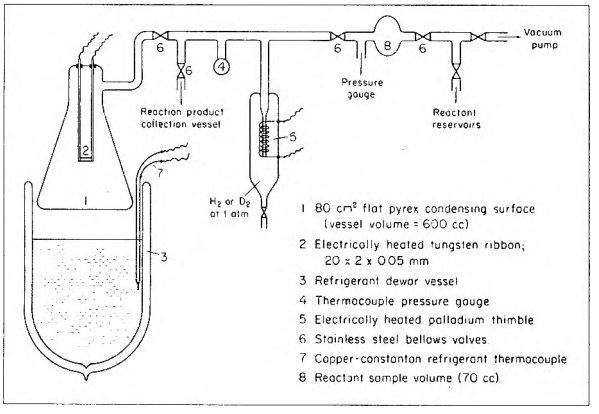

Fig. 1.—Schematic diagram of apparatus.

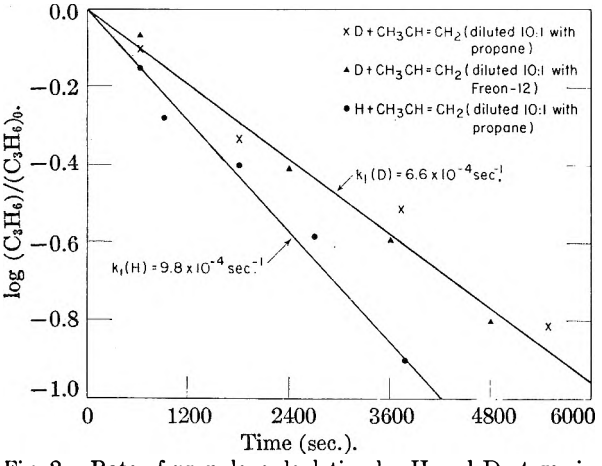

Fig. 2.—Rate of propylene depletion by H and D atoms in thin, dilute films at 77.3°K.

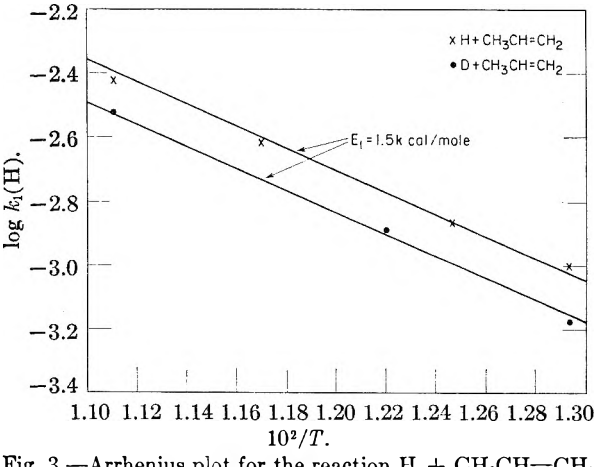

Fig. 3.—Arrhenius plot for the reaction H + $CH_3CH=CH_2$ → $CH_3\dot{C}HCH_3$.

petition for H atoms by propylene and propane at ambient temperatures, and found a value near 10^{11} for the addition reaction. Darwent and Roberts[3] measured the rate of H_2 production from the photolysis of H_2S in the presence and absence of propylene at 298 and 478°K. They postulated a mechanism for this process and derived an activation energy of 5.0 kcal./mole with a steric factor of 0.5 for the addition reaction. Their rate constant was 1.6×10^{11} at 300°K., in agreement with the values obtained by other investigators. We have measured the rate of this reaction as a function of temperature in dilute propylene films below 100°K. and find a considerably lower activation energy.

Experimental

A schematic diagram of the apparatus used is shown in Fig. 1. Dilute (10:1) mixtures of propylene (in either propane or Freon-12) were made from gases containing less than 0.1 mole % impurity. The flat surface (1) is initially immersed in refrigerant and valve (6) quickly opened to the reactant sample volume (8) containing 8 micromoles of propylene and 80 micromoles of diluent. In this way a film about 10^{-4} cm. thick is condensed on the cold surface. The entire reaction vessel is then immersed in the refrigerant. Twenty micromoles of hydrogen is admitted through a heated palladium thimble. The tungsten ribbon is heated electrically to a temperature of 1800°K. and maintained constant. After an arbitrary time, the hydrogen is pumped away, the products warmed up, collected and analyzed for residual propylene by gas phase chromatography. Different mixtures of liquid oxygen and nitrogen were used as refrigerant baths. Temperatures were measured with a calibrated copper–constantan thermocouple.

Results and Discussion

Unlike butene-1, 3-methylbutene-1 or isobutene, propylene does not produce HD with D atoms.[7,8] The reactions which occur below 90°K. in propylene films are[9]

$$H + CH_3CH=CH_2 \xrightarrow{k_1} CH_3\dot{C}HCH_3$$

$$2CH_3\dot{C}HCH_3 \xrightarrow{k_2} CH_3CH_2CH_3 + CH_3CH=CH_2$$

$$2CH_3\dot{C}HCH_3 \xrightarrow{k_3} \begin{matrix} CH_3CHCH_3 \\ | \\ CH_3CHCH_3 \end{matrix}$$

The ratio k_2/k_3 is about 9, independent of temperature from 77 to 90°K. and concentration up to one hundred-fold dilution of the propylene.[9] Assuming a steady-state concentration for R, the following expression for the propylene concentration as a function of time (t) results

$$\log \frac{(C_3H_6)}{(C_3H_6)_0} = -0.24k_1\,(H)t \qquad (1)$$

where $(C_3H_6)_0$ is the propylene concentration at t = 0 and (H) is the hydrogen atom concentration in the solid film. It has been demonstrated[6] previously that the reaction rate in the film is proportional to the gaseous H atom concentration generated by the dissociation of H_2 on a hot tungsten surface. Further if the films are sufficiently thin, and dilute in olefin, the hydrogen atoms diffuse with sufficient rapidity so that their concentration is essentially constant through the film.[9]

Figure 2 shows how equation 1 is followed at 77.3°K. when films of propylene, diluted with either propane or Freon-12, react with either D or H atoms. The 30% difference in rate between the H and D atom reactions, seen in Fig. 2, can probably be ascribed to a difference between (D) and (H) in the film. Similar measurements were made at different film temperatures up to the boiling point of liquid oxygen. In all cases, the reaction rate was proportional to the propylene concentration up to 90% conversion. This strict first-order behavior demonstrates that the H atom concentra-

(8) A. N. Ponomorov and V. L. Talrose, *Doklady Acad. Sci. U.S.S.R.*, **130**, 120 (1960).

(9) R. Klein, M. D. Scheer and J. G. Waller, THIS JOURNAL, **64**, 1247 (1960).

tion remains unchanged even after the reaction rate has dropped to 1/10 of its initial value. Therefore under the conditions of these experiments the rate of supply of H atoms from the gas is considerably greater than their rate of depletion due to reaction with the propylene in the film.

The results plotted in Fig. 3 in the Arrhenius form yield an activation energy of 1500 cal./mole showing no appreciable isotope effect when D instead of H is the reactant. The data in Fig. 2 show that a change of diluent from propane to Freon-12 has no effect upon the reaction rate. It is unlikely that strong interactions between diluent and reactant exist and the activation energy obtained approximates that for free molecules in the gas. Darwent and Robert's value of 5 kcal./mole was determined from measurements at only two temperatures and depended upon their postulated mechanism for the H_2S photolysis.[3] Their result is well outside of any reasonable limits of error in our determination provided the H atom concentration in the film does not change significantly in the 77 to 90°K. temperature range of these experiments. From our measured E_1, the 300°K. rate constant, and a 5.5 Å. collision diameter for H + C_3H_6, a steric factor of 3×10^{-3} is computed. Evans and Szwarc[10] give a value of 10^{-2} for propylene addition reactions on theoretical grounds. The value of 0.5 given by Darwent and Roberts appears to be too large.

The results in Fig. 3 show that $k_1(H) = 18 \exp(-1500/RT)$ sec.$^{-1}$. The maximum gas phase concentration of H atoms, calculated from the hydrogen pressure and temperature of the tungsten surface, is 4×10^{-10} moles/cc. It is of interest to note that if (H) in the film is about a factor of 10 lower than this maximum gas phase value, $k_1 = 10^{12} \exp(-1500/RT)$ and 10^{11} is obtained for the rate constant at 300°K.

(10) M. G. Evans and M. Szwarc, *Trans. Faraday Soc.*, **45**, 940 (1949).

REACTIONS BETWEEN DRY INORGANIC SALTS. XI. A STUDY OF THE Fm3m → Pm3m TRANSITION IN CESIUM CHLORIDE–RUBIDIUM CHLORIDE MIXTURES

BY LYMAN J. WOOD WITH GERVASIO J. RICONALLA AND JOSEPH D. LAPOSA

Department of Chemistry, Saint Louis University, Saint Louis, Missouri

Received July 29, 1960

In the course of a recent study of solid solutions of rubidium chloride and high temperature cesium chloride[1] a curious phenomenon was observed when working with crystals which were formed by freezing low rubidium chloride (under 35 mole %) melts. When these crystals, which were translucent, were cooled to some 300 to 400° below the freezing point, they changed quite suddenly to a white opaque mass and the change was accompanied by an evolution of heat and an audible click. The opaque white mass was quite brittle and easily reduced to a fine powder by slight grinding. By contrast crystals of pure cesium chloride, which readily undergo the Fm3m–Pm3m transition upon cooling, do not exhibit the click phenomenon and at room temperature these crystals are somewhat rubber-like and quite difficult to grind. However cesium chloride containing as little as one mole per cent. of rubidium distinctly shows the click phenomenon!

(1) L. J. Wood, Chas. Sweeney, S.J. and Sr. M. Therese Derbes, *J. Am. Chem. Soc.*, **81**, 6148 (1959).

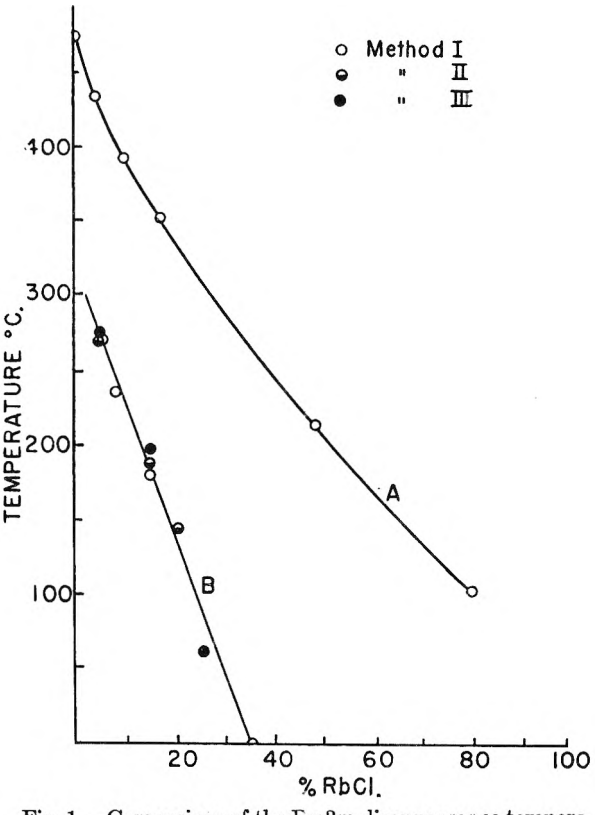

Fig. 1.—Comparison of the Fm3m disappearance temperature (curve A) with the click temperature (curve B). Three different cooling procedures were used in the determination of curve B.

It has been shown[1] recently that a complete series of solid solutions of rubidium chloride and high temperature (Fm3m) cesium chloride is stable over certain temperature ranges. In the high rubidium chloride end of the series, the solid solutions are stable at room temperature but at lower rubidium chloride percentages a partial unmixing of the solid solution occurs as the temperature is lowered.

In the previous paper[1] it was shown that the solid solution of rubidium chloride and high temperature cesium chloride, which has Fm3m symmetry, is stable in the region above curve A of Fig. 1. Upon cooling from above curve A to room temperature it was found that some of the high temperature cesium chloride undergoes the Fm3m → Pm3m transition and separates out of the solid solution as pure low temperature cesium chloride. The work reported in this note shows that the unmixing of solid solutions in the 5 to 35 mole % rubidium chloride range does not begin at curve A but rather that there is a long delay before unmixing can be detected. When the solid solution crystals are prepared directly from the melt, the delayed unmixing temperatures (click temperatures) are represented by curve B.

TABLE I

X-RAY (HIGH TEMPERATURE CAMERA) RESULTS FOR VARIOUS HEAT TREATMENTS OF THE 90:10 CsCl–RbCl MIXTURE[a]

Film no.	Pre-heat,[b] °C	Subsequent treatment	X-Ray lines after 4 hr. Exposure to Mo rays Pm3m	Fm3m	Remarks
La-31	398	Exposed to X-rays at once[c]	None	Strong	Above completion temp. of Pm3m–Fm3m previously found at 395°[1]
La-40	392	Exposed to X-rays at once[c]	Weak	Strong	Below completion temp. of Pm3m–Fm3m
La-41	392	Cooled to 178°—exposed to X-rays at once[c,d]	Medium	Strong	With Pm3m initially present, the amt. of this phase became greater upon cooling
La-30	423	Cooled to 68°—exposed to X-rays at once	Strong	Medium strong	Strong Pm3m lines—low reappearance temp.—delayed unmixing of Fm3m solid soln. indicated

[a] This mixture was melted, cooled to room temperature and reduced to a fine powder by grinding. The fine powder was screened through a 200 mesh sieve and placed in a fine capillary tube for X-ray analysis. After each X-ray exposure, the sample was allowed to cool to room temperature (this was necessary for the removal of the film from the camera). [b] This temperature was approached from below and maintained constant (±0.75°) by careful hand control for 30 minutes before X-ray exposure. [c] Temperature maintained constant (±0.75°) during X-ray exposure by means of thyratron control. [d] This temperature was approached from above and care was taken not to drop below this selected temperature at any time.

Rapid cooling of melts containing one to five mole per cent. of rubidium chloride exhibited the click phenomenon but slow cooling (cooling over a period of from three to five hours) of these mixtures brought about gradual unmixing of the solid solution and no sudden evolution of heat corresponding to the click phenomenon was observed.[2]

The high temperature solid solutions were readily formed again by reheating from below the click temperature (curve B). Upon cooling these reformed solid solutions however, the click phenomenon never was observed although the high temperature X-ray camera showed definitely that the phenomenon of delayed unmixing again occurred. It can now be concluded that the audible sound observed simultaneously with the click phenomenon is caused by the sudden shattering of the relatively large solid solution crystals obtained directly from the melt. The white mass resulting from the delayed unmixing of these large crystals was found to be made up of extremely fine crystals[3] of Pm3m cesium chloride and residual Fm3m solid solution and the extreme brittleness of the white mass (described above) obviously is due to this mixture of fine crystals. Heating these small crystals to a temperature above curve A forms only small crystals of the Fm3m solid solution which crystals do not produce an audible click as they unmix upon cooling.

Working with a 90:10 mixture of these small crystals it was found possible to delay greatly the beginning of unmixing by rapid cooling in a capillary tube. The 90:10 mixture was first heated in the high temperature X-ray camera to a few degrees above curve A (423°—Table I) until re-formation of Fm3m solid solution was complete after which the sample was cooled to a series of successively lower and lower temperatures (with reheating to 423° between each test) until the appearance of the low temperature (Pm3m) form of cesium chloride was first observed at 68° (La-30). This long delay in unmixing was avoided by beginning the cooling from just below curve A at which point the mixture still contained a trace of the low temperature cesium chloride (La-41).

(2) In 1910, S. Zemczuzny and F. Rambach reported (*Z. anorg. Chem.*, **65**, 418 (1910)) freezing curves for small additions of either potassium chloride or rubidium chloride to cesium chloride in rough approximate agreement with the first part of curve A rather than curve B. This report would seem to indicate that rapid cooling might be required to cause a delayed Fm3m-Pm3m transition as represented by curve B.

(3) A small amount of an 85:15 molar mixture of cesium chloride and rubidium chloride was melted and drawn into a capillary sample tube where it was allowed to freeze and then cool through the click temperature range to room temperature. Even though the sample was not ground and screened as is usually done, satisfactory X-ray lines were nevertheless obtained which showed clearly that the unmixing of the solid solution associated with the click phenomenon produced a mixture of very fine powders.

HEATS OF FORMATION OF α-PHASE SILVER-INDIUM ALLOYS[1]

BY RAYMOND L. ORR AND RALPH HULTGREN

Department of Mineral Technology, University of California, Berkeley, California

Received July 29, 1960

Heats of formation of the Ag-rich terminal α-solid solutions of Cd, In, Sn and Sb in Ag at 723° K. have been measured by Kleppa.[2–4] The trend in the experimental values showed the heats of formation to become less exothermic with increasing atomic number of the solute except for In, which forms a more exothermic solution than any of the others. This could be interpreted as indicating an anomalously high affinity between Ag and In. However, in other criteria of bond strength such as the effect of solutes on the lattice constant of silver, In falls in a normal sequence between Cd and Sn.

It therefore seemed worthwhile to independently measure heats of formation of solid solutions of In in Ag. This has been done as reported in this paper. The relationship between heats of formation and bond strengths also is discussed.

(1) This work sponsored by Office of Ordnance Research, U. S. Army.

(2) O. J. Kleppa, *J. Am. Chem. Soc.*, **76**, 6028 (1954).

(3) O. J. Kleppa, *Acta Met.*, **3**, 255 (1955).

(4) O. J. Kleppa, THIS JOURNAL, **60**, 846 (1956).

Experimental

Preparation of Alloys.—Four Ag–In alloys containing 5.0, 9.0, 15.0 and 17.0 at. % In, all in the f.c.c. α-solid solution range, were prepared by melting the pure metals together in sealed evacuated Vycor tubes and homogenizing about 50° below the respective solidus temperatures for two weeks. The Ag and In used in the preparations and also for measurements on the pure metals were of 99.9 + % purity.

Sharp well-resolved X-ray diffraction lines obtained from annealed filings taken from both ends of each ingot indicated the alloys to be homogeneous. Measured lattice constants were in good agreement with published data.[5,6]

Apparatus and Methods.—Heats of solution in liquid Sn of Ag, In and the alloys were measured using the calorimetric apparatus and methods described previously.[7,8] Samples were dropped from an initial temperature, T_i, near 317° K., into the tin bath at temperature T_f, near 700°K. The heat capacity of the calorimeter was determined by dropping specimens of pure Sn. The balanced heat effect method, described previously,[7] was used to reduce the magnitudes of the measured heat effects and the associated heat transfer corrections. Heats of formation at temperature T_i were obtained by subtracting the heats of solution of the alloys from the heats of solution of corresponding amounts of the pure metals. During the runs the concentration of solute metals in the liquid Sn bath never exceeded 2 at. %. Within this dilute range any concentration effects were negligible within the experimental uncertainty.

Results

Results for the pure metals are given in Table I. From the measured values together with known heat content data,[9] the relative partial molar heats of solution of Ag(s) and In(s) in Sn(l) for $x_{Sn} \approx 1$ at 700°K. were evaluated and are given in the last column. Results for the alloys are given in Table II. The heats of formation have been referred to a common temperature, 317°K., the mean value of T_i for the alloys.

The heats of formation are plotted in Fig. 1 together with those of Kleppa[4] whose values at 723° K. were measured with respect to Ag(s) and In(l). For purposes of comparison, the values plotted have been recalculated to refer to superheated In(s) at 723°K., using 780 cal./g.-atom for the heat of fusion of In.[9]

TABLE I

HEATS OF SOLUTION OF PURE METALS IN LIQUID TIN

Run no.	Solute	T_i, °K.	T_f, °K.	$\Delta H_{meas.}$, cal./g.-atom	$\Delta H_{soln.,\ 700°K.}$, cal./g.-atom
45-3	Ag	317.9	698.5	6271	3865
45-11	Ag	319.2	698.5	6238	3838
46-4	Ag	314.2	700.3	6303	3863
46-12	Ag	315.0	700.4	6273	3836
	Ag			Av.	3850
45-4	In	317.9	698.6	3267	−185
45-12	In	319.3	699.0	3186	−260
46-11	In	314.7	700.4	3254	−232
	In			Av.	−226

Discussion

The presently reported data and those of Kleppa are in excellent agreement. Kleppa's values at 19 at. % In have been included in Fig. 1, even though they were thought by that author to be well within ($\alpha + \zeta$) two phase region. The recent evaluation of Hansen[10] indicates that the α-phase extends to 19.5 at. % In at Kleppa's temperature of measurement, 723°K.

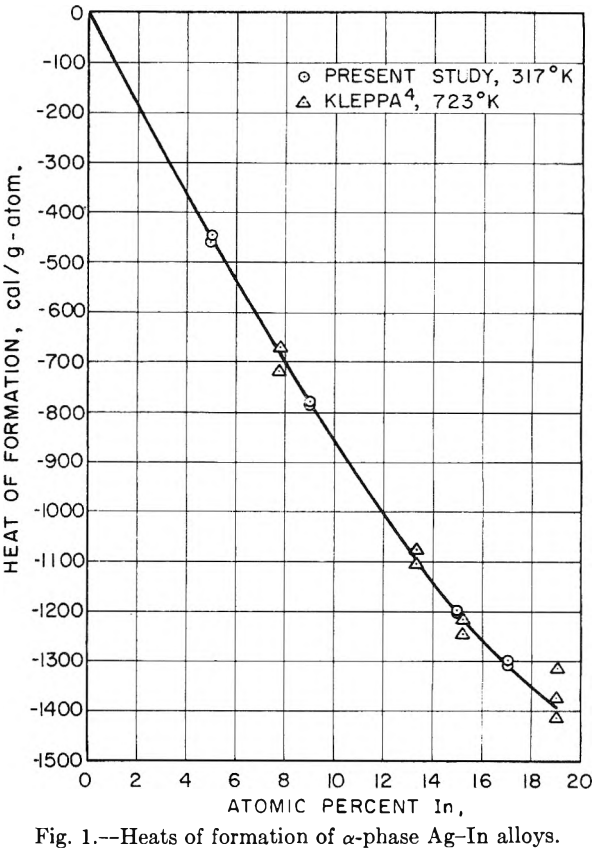

Fig. 1.—Heats of formation of α-phase Ag–In alloys.

TABLE II

HEATS OF FORMATION OF Ag–In ALLOYS AT 317°K.

Run no.	Alloy comp., at. % In	T_i, °K.	T_f, °K.	$\Delta H_{soln.}$, cal./g.-atom	$\Delta H_{form.,317°K.}$, cal./g.-atom
45-6	5.0	319.3	698.7	6559	− 461
46-10	5.0	314.8	700.3	6584	− 448
45-7	9.0	318.7	698.7	6763	− 783
46-8	9.0	314.9	700.3	6795	− 782
45-8	15.0	318.8	698.7	7004	−1206
46-7	15.0	314.5	700.3	7038	−1203
45-10	17.0	318.9	698.8	7041	−1304
46-6	17.0	314.6	700.3	7082	−1309

The present data are well represented by the equation

$$\frac{\Delta H}{x_{In}} = -9100 + 49000x^2_{In}$$

shown by the curve in Fig. 1, with an average deviation of less than 4 cal./g.-atom. The value of $\Delta\bar{H}_{In}$ at $x_{Ag} = 1$ is thus −9100 cal./g.-atom. Because of the extremely small scatter in the present results and their unusually excellent agreement with those of an independent investigation, the uncertainty in the selected curve is thought to be only about ±10 cal./g.-atom.

(5) E. A. Owen and E. W. Roberts, *Phil. Mag.*, **27**, 294 (1939).

(6) W. Hume-Rothery, G. F. Lewin and P. W. Reynolds, *Proc. Roy. Soc. (London)*, **A157**, 167 (1936).

(7) R. L. Orr, A. Goldberg and R. Hultgren, *Rev. Sci. Instr.*, **28**, 767 (1957).

(8) R. L. Orr, A. Goldberg and R. Hultgren, THIS JOURNAL, **62**, 325 (1958).

(9) K. K. Kelley, U. S. Bur. Mines Bull. 584, 1960.

(10) M. Hansen and K. Anderko, "Constitution of Binary Alloys," 2nd Edition, McGraw-Hill Book Co., Inc., New York, N. Y., 1958.

The exact agreement between the heats of formation at 317 and 723°K. indicates that $\Delta C_p = 0$ for the α-phase alloys within this temperature range. The same observation was made for the α-phase Ag–Cd alloys,[8] where close agreement with Kleppa's data also was obtained. The solid solution of In in Ag is indeed more exothermically formed than that of Cd in Ag.

Calculations by Kleppa[4] based on a method by Friedel do predict that the limiting heat of solution of In in Ag should be more exothermic than those of Cd, Sn and Sb, resulting from the relatively low first ionization potential for In. The quantitative agreement however is poor due to the approximations involved in the model. For one thing it seems unlikely that In, or the other solute metals, would contribute only one valence electron to the conduction band of Ag as that model assumes. For this series of alloys the concentration limits of α-phase stability decrease regularly with solute metal valence, and the electron to atom ratio at those limits is relatively constant (1.2–1.4 at room temperature) in accord with Brillouin-zone theory. This suggests that all the valence electrons of the solute atoms enter the Ag conduction band.

Heats of formation are not, however, an absolute measure of bond strength. Rather, they represent the difference between total bond energies of products and reactants, and thus for alloys are relative to the bond strengths of the pure component metals. The highly exothermic result for the reaction $(1 - x)Ag_{(s)} + xIn_{(s)} = Ag_{1-x}In_{x(\alpha)}$ need not be taken as indicating an anomalously high stability for the alloy; it might just as well arise from an anomalously low stability for elementary In. Such considerations must always be kept in mind in attempts to relate intermetallic bond strengths to heats of formation.

FORMATION CONSTANTS OF 6-METHYL-2-PICOLYLMETHYLAMINE WITH SOME COMMON METAL IONS[1]

By Rodney E. Reichard and W. Conard Fernelius

Department of Chemistry, The Pennsylvania State University, University Park, Pennsylvania

Received August 10, 1960

Formation constants for the association of some common divalent metal ions with 2-picolylamine, 2-picolylmethylamine, 2-aminoethylpyridine,[2] and 6-methyl-2-picolylamine[3] have been published. These studies are now extended to include 6-methyl-2-picolylmethylamine and 2-methylaminoethylpyridine with incidental observations on 2-(N-pyrrolodino)- and 2-(N-piperidino)-ethylamine.

Experimental

The amines were commercial products which were first distilled under vacuum and then dissolved in triply-distilled, air-free water. Boiling points and neutral equivalents are reported in Table I. The monopicrate of 2-(2-methylaminoethyl)-pyridine was prepared, m.p. 140°, literature[4] 138–139°,[4] as well as a dipicrate, m.p. 192°, literature[5] 192.8–195.2°.

The preparation of solutions of metal ions, measurements and calculations were performed as described previously.[2] The results are assembled in Tables II and III. Attempts to obtain values for Zn^{++} and Cd^{++} at 10° with 6-methyl-2-picolylmethylamine indicate that the complexes are too unstable for measurement. With Ag^+ at 30° the calculated K's are not constant. With both 2-(N-piperidino)- and 2-(N-pyrrolidino)-ethylamine, in combination with Co^{++}, Zn^{++} and Mn^{++}, the formation of precipitates prevented the determination of any constants. With 2-(2-methylaminoethyl)-pyridine no consistent constants could be obtained for Cu^{++} and Ni^{++} while Ag^+, Zn^{++} and Co^{++} yielded precipitates.

Discussion

The compounds under consideration here permit one to make comparisons with compounds which have less steric hindrance to coördination. The compounds 2-picolylamine, 2-picolylmethylamine, 6-methyl-2-picolylamine and 6-methyl-2-picolylmethylamine show only slight differences in basicity (pK_1 at 30° = 8.51–8.8). The effect of substitution of hydrogen is to increase basicity slightly, more when substitution is on the primary amine group than on the pyridine nucleus. (Substitution has little or no effect on pK_2.) However, the formation constants of the copper derivatives decrease in the order in which the amines are listed log $K_{1 \text{ and } 2}$ at 30°: 9.45, 7.80; 9.27, 6.55; 6.81, 5.65; 6.48, 4.94. The effect of methyl substitution is to decrease stability. For 2-picolylmethylamine the decrease is slight for the coördination of the first ligand and large for the second ligand. For the amines with substitution in the 6-position on the pyridine ring the decrease is large for the coördination of both ligands and slightly more so for the coördination of the first ligand than for the second. The changes in the heat of formation follow those in log K (or free energy). The same statements hold for coördination with Ni^{++} except here the presence of the methyl group in the 6-position on the pyridine nucleus blocks the coördination of the third ligand molecule.

The relation between 2-(2-aminoethyl)-pyridine and 2-(2-methylaminoethyl)-pyridine parallels that between the corresponding picolyl compounds. Methyl substitution on the primary amine group increases pK_1 slightly and decreases pK_2 slightly. However, due to the general lowering of stability by the increased size of chelate ring, the complexes of the methyl-substituted compound are too small for detection by the potentiometric method.

The N-piperidino- and N-pyrrolidino compounds are cyclic substitution products of ethylenediamine ($pK_{1 \text{ and } 2}$ at 30° = 9.81 and 6.79).[8] Here the effect of substitution is to increase slightly the pK_1 for a

(1) This investigation was carried out under contract AT(30-1)-907 between The Pennsylvania State University and the U. S. Atomic Energy Commission.

(2) D. E. Goldberg and W. C. Fernelius, This Journal, **63**, 1246 (1959).

(3) H. R. Weimer and W. C. Fernelius, *ibid.*, **64**, 1951 (1960).

(4) K. Löffler, *Ber.*, **37**, 161 (1904).

(5) H. E. Reich and R. Levine, *J. Am. Chem. Soc.*, **77**, 4913 (1955).

(6) J. Van Alphen, *Rec. trav. chim.*, **58**, 1105 (1939).

(7) E. Munch and O. Schlichting, German Patent 561,136, Dec. 19, 1930; *C. A.*, **27**, 995[9] (1933).

(8) G. H. McIntyre, Jr., B. P. Block and W. C. Fernelius, *J. Am. Chem. Soc.*, **81**, 529 (1959).

TABLE I

	B.p., °C.	Lit. B.p., °C.	Ref.	Neut. equiv.
6-Methyl-2-picolylmethylamine (Aldrich Chemical Co.)	54 (3 mm.)			133.43 (136.19)
	58 (4 mm.)			135.18 (136.19)
	125 (25 mm.)			138.8 (136.19)
2-(2-Methylaminoethyl)-pyridine (Sapon Laboratories)	66 (4.5 mm.)			131.8 (136.19)
	58 (2 mm.)			133.8 (136.19)
2-(N-Pyrrolidino)-ethylamine (Sapon Laboratories)	60 (8.5 mm.)	55–57 (10 mm.)	6	
	47 (4 mm.)			
2-(N-Piperidino)-ethylamine (Sapon Laboratories)	76 (17 mm.)	65–70 (10 mm.)	7	133.64 (128.21)

TABLE II

VALUES FOR THE THERMODYNAMIC QUANTITIES LOG K_n, $-\Delta F_n^0$, $-\Delta H_n^0$ AND ΔS_n^0 INVOLVED IN THE REACTION AT 10, 20, 30 AND 40° AND AT IONIC STRENGTH $\mu \rightarrow 0$ OF BIVALENT METALS IONS WITH 6-METHYL-2-PICOLYLMETHYLAMINE TOGETHER WITH VALUES FOR LOG K_n FOR 2-(N-PIPERIDINO)- AND 2-(N-PYRROLIDINO)-ETHYLAMINE

t, °C.	H^+	Cu^{++}	Ni^{++}	Co^{++}	H^+	Cu^{++}	Ni^{++}	Co^{++}
	6-Methyl-2-picolylmethylamine							
	log K_1					log K_2		
10	9.26 ± 0.01	6.96 ± 0.04	5.45 ± 0.04	3.77 ± 0.10	2.97 ± 0.16	5.41 ± 0.02	3.60 ± 0.10	3.01 ± 0.07
20	8.84 ± .02	6.62 ± .07	4.63 ± .08		3.17 ± .37	5.11 ± .02		
30	8.79 ± .08	6.48 ± .06	4.58 ± .08	3.41 ± .10	2.96 ± .20	4.94 ± .09		
40	8.43 ± .02	6.13 ± .04	4.31 ± .03	3.36 ± .05	2.90 ± .12	4.93 ± .03		
		$-\Delta F_1^0$ (kcal./mole)				$-\Delta F_2^0$ (kcal./mole)		
30	12.14	8.95	6.30	4.71		6.82		
		$-\Delta H_1^0$ (kcal./mole)				$-\Delta H_1^0$ (kcal./mole)		
10–40	4.21	6.98	7.10	3.86		4.37		
		ΔS_1^0 (cal./mole-deg.)				ΔS_2^0 (cal./mole-deg.)		
30	3	7	−3	3		8		
	2-(N-Piperidino)-ethylamine							
	log K_1					log K_2		
30	9.89 ± 0.05	7.77 ± 0.02	4.30 ± 0.02		6.38 ± 0.01	5.83 ± 0.03		
40	9.46 ± 0.02				6.17 ± 0.06			
	2-(N-Pyrrolidino)-ethylamine							
	log K_1					log K_2		
30	9.74 ± 0.04	8.77 ± 0.02	5.36 ± 0.01		6.56 ± 0.04	6.05 ± 0.04	3.16 ± 0.02	

TABLE III

VALUES FOR THE THERMODYNAMIC QUANTITIES pK_n, $-\Delta F_n^0$, $-\Delta H_n^0$ AND ΔS_n^0 AT IONIC STRENGTH $\mu \rightarrow 0$ FOR THE ASSOCIATION OF PROTONS WITH 2-(2-METHYLAMINOETHYL)-PYRIDINE

	10°	20°	30°	40°
pK_1	10.13 ± 0.02	9.78 ± 0.01	9.65 ± 0.02	9.49 ± 0.03
pK_2	3.57 ± 0.03	3.46 ± 0.01	3.58 ± 0.08	3.38 ± 0.05
$-\Delta F_1^0$ (kcal./mole)	13.2	13.2	13.3	13.7
$-\Delta F_2^0$	4.65	4.65	5.0	4.9
$-\Delta H_1^0$ (kcal./mole)		10.1		
$-\Delta H_2^0$		2.4		
ΔS_1^0 (cal./mole-deg.)	11	11	11	11
ΔS_2^0	8	8	8	8

6-membered ring and decrease it slightly for a 5-membered ring. The effect is to decrease slightly the pK_2 in both cases. However, the interference in both cases is to noticeably decrease the stability of the Cu^{++} and Ni^{++} complexes, more so in the case of the 6-membered ring than in the case of the 5-membered ring. The coördination of a third ligand is blocked in the case of Ni^{++} and even a second ligand for the N-piperidino compound. The other ions (Co^{++}, Zn^{++}, Cd^{++}) which form stable compounds with ethylenediamine do not form complexes with the substituted amines in aqueous solution.

SINGLET–TRIPLET ABSORPTION OF ANTHRACENE DUE TO MAGNETIC PERTURBATION

BY FRANKLIN J. WRIGHT

Central Basic Research Laboratory, Esso Research and Engineering Company, P. O. Box 51, Linden, New Jersey

Received August 2, 1960

Recently Chaudhuri and Basu[1] reported that in the presence of the acetylacetonates of copper and iron they had observed a number of absorption

(1) J. N. Chaudhuri and S. Basu, *Trans. Faraday Soc.*, **54**, 1605 (1958).

bands in chloroform solutions of naphthalene, anthracene, phenanthrene and pyrene. They attributed the origin of these bands to singlet–triplet transitions resulting from magnetic perturbations arising from the paramagnetic nature of the chelates. Such transitions can occur with fairly high probabilities when, as a result of the inhomogeneous field of a heavy atom, spin and orbital angular momentum interact with each other. The perturbing effect of a heavy atom or of a paramagnetic ion has been observed even when these are supplied by the solvent.[2]

More recently Evans[3] re-examined the systems studied by Chaudhuri and Basu and found no traces of any bands even where increased concentrations of hydrocarbon or metal complex were used.

We also have obtained the absorption spectrum of anthracene in chloroform solutions containing the acetylacetonates of a number of transition metals: *i.e.*, ferric, cupric, manganous, cobalt, nickel, vanadium, aluminum, chromium and zirconium. No evidence of the bands described by Chaudhuri and Basu as appearing in the spectral region 5000 to 7000 Å. could be detected. In view of this further confirmation of Evans' findings, it must be concluded that the bands which were observed by Chaudhuri and Basu are indeed spurious. Their origin is, however, obscure.

J. T. Baker C.P. chloroform was used as solvent. The stabilizer ($\sim 1\%$ ethanol) was removed by percolation through an alumina column. The presence of this stabilizer proved, however, to have no effect on the absorption spectra.

The chelates were obtained from Mackenzie Chemical Works, Inc., and were dried by heating overnight at 110°.

The anthracene (Eastman Organic Chemicals) was of the blue-violet fluorescence quality and was not further purified.

The absorption spectra were measured between 5000 and 7000 Å. in a Cary recording spectrophotometer using a 5 cm. silica cell. The chelates were present in 10^{-3} M concentrations while the concentration of anthracene was 10^{-2} M. A number of spectra were also obtained at higher concentrations.

In all cases the optical density of the chelate–anthracene solutions increased steeply at the shorter wave lengths. It was also observed that the concentration of the chelate as measured by its absorption between 5000 and 7000 Å. was in all cases reduced by a small but definite amount on adding the anthracene. The most likely explanation for these observations is that a charge-transfer transition is involved. Whether a definite complex between the anthracene and the chelate is formed or whether the charge-transfer transition occurs between two adjacent molecules in the absence of true complex formation has not been ascertained. In view of the apparent decrease in the chelate concentration in the presence of anthracene, it is probable, however, that definite complexes are formed.

(2) M. Kasha, *J. Chem. Phys.*, **20**, 71 (1952).
(3) D. F. Evans, *Proc. Roy. Soc.* (*London*), **A255**, 55 (1960).

COMMUNICATION TO THE EDITOR

ON THE RETENTION OF SOLVENT IN MONOLAYERS OF FATTY ACIDS SPREAD ON WATER SURFACES

Sir:

It has been suggested that volatile solvents may be retained in monolayers spread on aqueous surfaces with the aid of such solvents, and it has been shown that there are indeed differences in the π-A isotherms obtained when different solvents are used.[1,2] Some recent experiments with stearic acid monolayers containing relatively nonvolatile non-polar materials may shed light on this problem. Using the previously described techniques,[3] we have spread mixtures of stearic acid with *n*-hexadecane, 2,6,10,14-tetramethylpentadecane, or bicyclohexyl, on water freshly redistilled in quartz. Purified *n*-hexane was used to aid spreading, and the ratio of this volatile solvent to the stearic acid was held constant (2.0 ml. per mg. of stearic acid). The area of the film at constant surface pressure was measured as a function of time; typical results are shown in Fig. 1 and 2. It is apparent from the figures that, at sufficiently long times after spreading of the mixed film, the observed area per stearic acid molecule becomes constant and equal to that in films initially containing only stearic acid and *n*-hexane. When the films were allowed to stand at low pressures (1–4 dynes/cm.) until this constant area was reached, and a film compression experiment then was performed in the usual way, the π-A curves were identical with those for films containing no added hydrocarbon.

The time required for evaporation of the amount of hydrocarbon in the film can be estimated from the evaporation rate per unit area of free hydrocarbon surface in air; such estimates have been made and the observed times required for the films to reach constant area can be interpreted reasonably in terms of them. We conclude, as did Myers and Harkins,[4] that these hydrocarbons evaporate practically completely from the stearic acid films at low surface pressure. The evaporation process, however, is complicated, and further studies of this phenomenon are planned.

If non-polar hydrocarbon molecules were retained in monolayers as a result of chain–chain interactions with the non-polar part of the film-

(1) H. D. Cook and H. E. Ries, Jr., *J. Phys. Chem.*, **60**, 1533 (1956).
(2) M. L. Robbins and V. K. LaMer, *J. Colloid Sci.*, **15**, 123 (1960).
(3) G. L. Gaines, Jr., *J. Phys. Chem.*, **63**, 1322 (1959).
(4) R. J. Myers and W. D. Harkins, *J. Phys. Chem.*, **40**, 959 (1936).

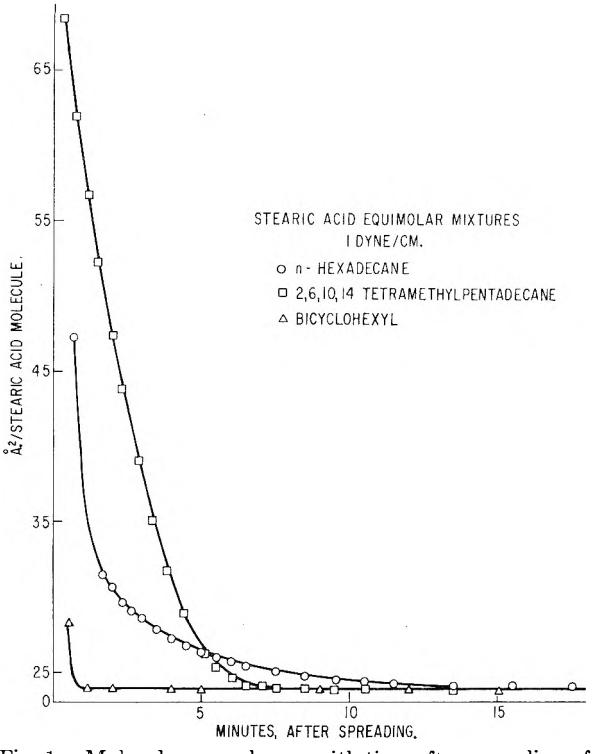

Fig. 1.—Molecular area change with time after spreading of mixed films of stearic acid and hydrocarbons.

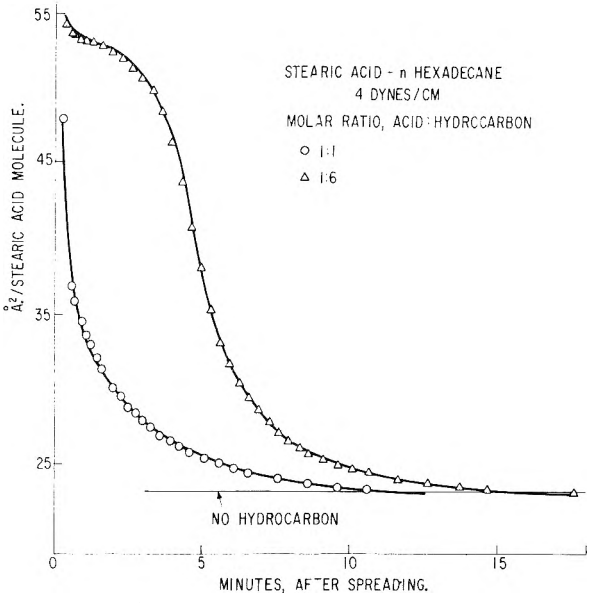

Fig. 2.—Effect of increasing amount of hydrocarbon in mixed films on molecular area change with time after spreading.

forming molecules, we should expect *n*-hexadecane to be strongly retained by stearic acid. Robbins and LaMer[2] have suggested, however, that solubility and diffusion in the subphase may be involved in the observed differences in π-A isotherms obtained with different spreading solvents. The extreme insolubility of the hydrocarbons which we have examined would then account for their lack of effect on the properties of the monolayer.

In the π-A isotherms for fatty acid films on water or dilute acids, two fairly linear portions are observed. The lower pressure linear portion of the π-A curve, which for stearic acid extends from about 25 to 20Å.²/molecule, and therefore includes the region of concern to us, has been the subject of much speculation. Hydration of the carboxyl groups,[5] rotational freedom,[6] and other effects have been suggested to account for the larger areas at low pressure. These all depend, however, on the behavior of the polar head-groups immersed in the aqueous surface. Changes in the π-A diagram should result if spreading solvent can affect the environment or behavior of the polar heads. The differences observed by Robbins and LaMer between stearic acid and octadecanol films, therefore, may be explainable solely on the basis of the difference between the behavior of carboxyl and alcohol groups.

Verification of these ideas may be possible through monolayer experiments in which the nature of the subphase is altered. Such studies are in progress.

GENERAL ELECTRIC RESEARCH LABORATORY
SCHENECTADY, NEW YORK GEORGE L. GAINES, JR.

RECEIVED DECEMBER 28, 1960

(5) I. Langmuir, *J. Chem. Phys.*, **1**, 756 (1933).
(6) M. J. Vold, *J. Colloid Sci.*, **7**, 196 (1952).

WILEY BOOKS

PHYSICAL CHEMISTRY, Second Edition

By FARRINGTON DANIELS, *Emeritus Professor of Chemistry, and* ROBERT A. ALBERTY, *Professor of Chemistry; both of the University of Wisconsin.*

When it first appeared in 1955, Daniels and Alberty's *Physical Chemistry* was immediately recognized as one of the finest and most teachable elementary textbooks in the field. Its clear explanations of fundamentals, its logical organization, and its broad coverage of the subject led to its use in more than 400 leading colleges and universities. Since 1955, however, great progress has been made in the study of physical chemistry. Moreover, students are now receiving better mathematical preparation and are being taught more physical chemistry in their freshman chemistry and analytical chemistry courses. In view of these developments, the second edition of *Physical Chemistry* has been completely rewritten and substantially expanded. It now covers more areas of modern physical chemistry than ever before, and thus affords the instructor a selection with regard to the topics to be included in his course.

Some of the important new features of the second edition of *Physical Chemistry* . . .

- Thermodynamics and its applications in physical chemistry are treated with more exactness than in the previous edition, and greater use is made of the chemical potential μ.
- A new chapter on kinetic theory is used to introduce the subject of chemical kinetics.
- Quantum mechanics is introduced at an earlier point and its applications to the study of molecular structure and of spectroscopy are described in new chapters on these subjects. In addition, an elementary chapter on statistical mechanics has been included which shows how thermodynamics quantities are calculated from spectroscopic theory.
- The authors have included such new topics as "the particle-in-a-box," simple molecular orbital theory, and the mechanical properties of polymers.
- The electromotive forces of cells are discussed in terms of electrode potentials (reduction potentials) in order to simplify the treatment and to bring it into agreement with international usage.
- The authors have made greater use of mathematics in their exposition. Important calculations are illustrated by means of worked out examples, and the Appendix contains a summary of mathematical relations used in physical chemistry and the values of basic physical constants with uncertainty indicated.
- The new edition contains many more problems. Three sets are appended to each chapter, and answers are given in the book for the problems in the first set. *1961. Approx. 776 pages. Prob. $8.75.*

KINETICS and MECHANISM, Second Edition

By ARTHUR A. FROST, *and* RALPH G. PEARSON, *Professors of Chemistry, Northwestern University*

Emphasizes the complexities of chemical reaction . . . .

Like its predecessor, the second edition of *Kinetics and Mechanism* differ from other books on chemical kinetics in this important way: it emphasizes the complexities of chemical reaction and the close relation of kinetics to mechanism. This is a valuable feature, for it enables the student to grasp: (1) exactly how much detail of reaction mechanism can be found from reaction kinetics; and (2) what the limitations of the kinetic method of studying mechanism are. In order to show clearly how kinetics is used to determine the way in which reactions are proceeding, the authors present detailed stereochemical discussions of the reaction steps. The authors' approach is based on fundamental physical principles, with theories such as collision theory and transition state theory used to aid understanding. An unusually complete mathematical treatment of complex reactions is provided. Numerous practical examples of mechanism deduced from kinetics data are used to illustrate the theory. A set of problems at the end of each chapter gives the student valuable experience in applying principles to concrete situations.

In view of remarkable progress recently made on both the theoretical and practical levels in the field of chemical kinetics, the book has been thoroughly revised in order to provide both students and instructors with information which is completely up-to-date. *1961. Approx. 432 pages. Prob. $10.00.*

Send for examination copies.

JOHN WILEY & SONS, Inc. 440 Park Avenue South, New York 16, N.Y.

WILEY BOOKS

PHYSICAL CHEMISTRY OF MACROMOLECULES

By CHARLES TANFORD, *Duke University.* An important new text that covers (in turn) the major areas of physical chemistry: molecular structure, molecular statistics, thermodynamics, transport processes, electrostatics, kinetics. The author presents a summary of the fundamental theory in each of these areas and then shows how the theory may be modified or extended to become applicable to molecules of very high molecular weight. All known varieties of macromolecules are treated. Although the book is organized on the basis of the various major topics of physical chemistry, the secondary theme is the development, on the part of the student, of an increasingly detailed knowledge of the structure and behaviour of individual macromolecules. This is the only book in the field that offers a discussion of all kinds of macromolecules from the *uniform* point of view. A unique feature is the inclusion of chapters on electrostatic forces and on the interaction between macromolecules and small ions. The other chapters of the book, while they do not contain new information per se, are unusual in that they synthesize in one text information which could previously be obtained only by consulting review articles and selected chapters in a variety of books. *1961. In Press.*

VISCOELASTIC PROPERTIES OF POLYMERS

By JOHN D. FERRY, *University of Wisconsin.* In an exacting treatment of the viscoelastic properties and behavior of polymers, the author carefully develops a discussion of the phenomenological theory of viscoelasticity followed by the presentation of a wide variety of experimental methods and a critical appraisal of their applicability to polymeric materials of different characterististics. The existing state of molecular theory is reviewed and the effects of temperature, chemical structure, dilution, and other variables are interpreted in terms of this. *1961. Approx. 496 pages. Prob. $15.00.*

ORGANO-METALLIC COMPOUNDS

By G. E. COATES, *University of Durham.* In 1956 a Methuen Monograph on organo-metallic compounds by Professor Coates was published in Great Britain and the United States. It was as well received in both places and highly praised for its concise, yet thorough treatment of important aspects of a rapidly-developing field. This present book is not simply a revision of the earlier monograph. The author has not only rewritten the original material but has also added a great deal of new material —with the result that this new book is considerably larger in both size and scope. *1961. In Press.*

PROGRESS IN VERY HIGH PRESSURE RESEARCH

Proceedings of an International Conference

Edited by F. P. BUNDY, W. R. HIBBARD, JR., *and* H. M. STRONG, *General Electric Company, Schenectady, New York.* This book is a collection of the very latest research papers presented at an important international conference (held in June 1960 at Bolton Landing, New York) on high pressure research and by a distinguished group of physicists, chemists, and research specialists who have been working very closely with high pressure techniques and methods. The most recent and impressive findings and conclusions in areas of investigation and in respect to apparatus and techniques are brought out. Both theoretical and experimental types of work are presented. *1961. In Press.*

ELECTRODE PROCESSES

Transactions of the Symposium on Electrode Processes, Philadelphia, May 1959.

Edited by ERNEST YEAGER, *Western Reserve University.* Includes all the papers presented at a symposium sponsored by the Electrochemical Society and represents the first time in recent years that the work of so many internationally prominent electrochemists (from ten countries) has been presented in one publication. While virtually all phases of fundamental investigations of electrode processes are covered, emphasis has been placed on new research developments and, more specifically, on hydrogen discharge kinetics, electrodisposition and dissolution of metals, the electrical double layer, adsorption phenomena, and the kinetics of fast electrode processes.

THE FERMI SURFACE

Proceedings of an International Conference

Edited by W. A. HARRISON *and* M. B. WEBB, *General Electric Company, Schenectady, New York.* Participants in this conference held in August 1960 at Cooperstown, New York, were ninety scientists from seven countries, and their papers and discussions offer both general and specific information on the size and shape of Fermi surfaces. Such topics as the importance of many-body effects for both theory and experimentation, theoretical and experimental information on the noble metals, progress in the understanding of polyvalent metals, and the electronic structure of alloys are given special prominence. *1961. 356 pages. $10.00.*

ORGANIC COATING TECHNOLOGY

Volume II, Pigments and Pigmented Coatings

By HENRY FLEMING PAYNE, *University of Florida. 1961. 1363 pages. $17.50.*

Send for examination copies.

JOHN WILEY & SONS, Inc. *440 Park Avenue South, New York 16, N. Y.*

CEC makes the
only medium-priced
MASS SPECTROMETER
FOR ANALYTICAL LABORATORIES
that features human engineered
packaging. This is it...

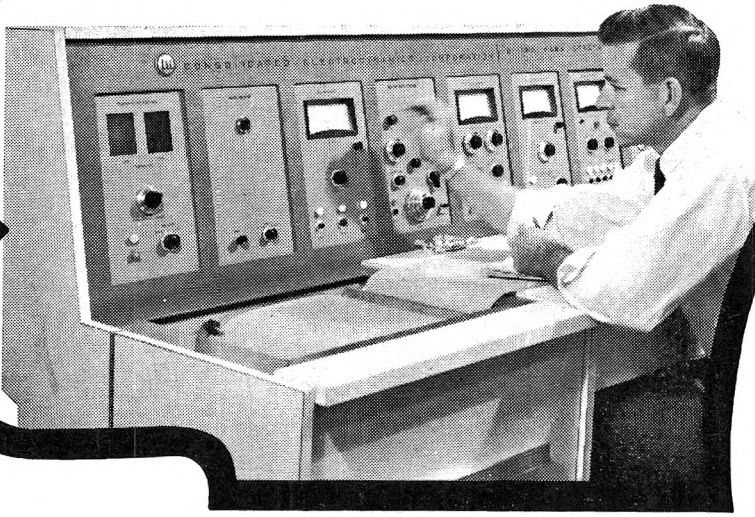

CEC's all-new 21-130 Mass Spectrometer offers the same accuracy, precision, sensitivity and scan speed you'll find only in the largest instruments of its kind.

All this plus a totally new "human" engineered packaging concept that means: Greater accessibility (modular electronics on pull-down chassis)... Convenience in the grouping of operating controls by function, with each operable and adjustable from the front... Lighter weight because it's built on a welded extruded aluminum frame with formica-over-honeycomb cabinet panels.

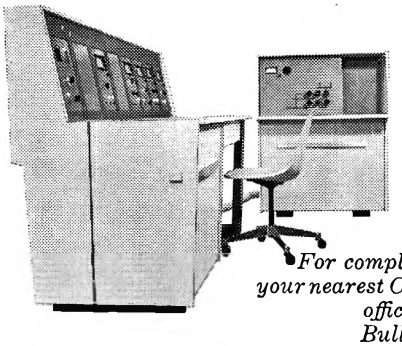

Look at its features: A built-in direct writing oscillograph recording system using five galvanometers... a stainless steel inlet system... a built-in micromanometer. And performance? Mass range from m/e 2 to 230 continuous with unit resolution up to m/e 200.

For complete information call your nearest CEC sales and service office or write today for Bulletin CEC 21130-X3.

Analytical & Control Division CEC

CONSOLIDATED ELECTRODYNAMICS / pasadena, california

A SUBSIDIARY OF **Bell & Howell** · *FINER PRODUCTS THROUGH IMAGINATION*